THE DEVELOPMENT OF THE TURKISH POWER MARKET WITH SPECIAL RESPECT TO RENEWABLE POWER GENERATION IN TURKEY

Dissertation

zur Erlangung des Doktorgrades

der Wirtschaftswissenschaften

vorgelegt von Yusuf Emre Güner, M.Sc.

aus Ankara

genehmigt von der Fakultät für Energie- und Wirtschaftswissenschaften

der Technischen Universität Clausthal

Tag der mündlichen Prüfung: 28.06.2017

Dekan: Prof. Dr. rer. nat. habil. Bernd Lehmann

Vorsitzender der Prüfungskommission: Prof. Dr. rer. pol. habil. Christoph Schwindt

Hauptberichterstatter: Prof. Dr. rer. pol. habil. Mathias Erlei

Mitberichterstatter: Prof. Dr. sc. pol. habil. Roland Menges

EIDESSTATTLICHE ERKLÄRUNGEN

Hiermit erkläre ich an Eides Statt, dass ich die bei der Fakultät für Energie- und Wirtschaftswissenschaften der Technischen Universität Clausthal eingereichte Dissertation selbständig und ohne unerlaubte Hilfe angefertigt habe.
Die benutzten Hilfsmittel sind vollständig angegeben.

Hiermit erkläre ich an Eides Statt, dass ich bisher noch keinen Promotionsversuch unternommen habe.

Entwicklung des türkischen Strommarktes mit spezieller Betrachtung der erneuerbaren Energiegewinnung in der Türkei

KURZFASSUNG

Die türkische Regierung hat eine neue Energiepolitik beschlossen mit dem Ziel die Stromversorgung des Landes durch Ausnutzung noch vorhandener heimischer fossiler Energieträger und erneuerbare Energiequellen zu diversifizieren. Das Hauptziel der in dieser Dissertation behandelten neuen Energiepolitik, genannt „die Energiepolitik 2023“, ist es, den Anteil der erneuerbaren Energien im Energiemix der jährlichen Gesamterzeugung bis zum Jahr 2023 auf mindestens 30% zu erhöhen. Gleichzeitig soll der Anteil der Energieerzeugung aus Erdgas auf maximal 30% reduziert werden. Durch den Ausbau der Zielkapazität von Technologien für erneuerbare Energie (Renewable Energy Technologies - RETs) wird ein Zuwachs des Bruttoinlandsproduktes, eine Senkung der Erdgasimporte und eine Reduktion der CO_2-Emissionen erwartet.

Während sich die regierungspolitischen Analysen der o.g. Energiepolitik hauptsächlich auf die Kosten/Nutzen-Analyse alternativer Nutzungen knapper Ressourcen fokussiert, beschränkt sich die vorliegende Bewertung auf die Analyse der Auswirkungen des Austausches der Gaskraftwerke durch RETs. Diese Dissertation zielt insbesondere auf die Analyse der Entwicklung von RET-Investitionen, die im Rahmen der Energiepolitik 2023 vorgesehen sind, und den damit verbundenen Nettonutzen (net social benefit).

Die Investitionsanalyse wird über die Quantifizierung der Schwellenwerte der Betriebsvolllaststunden (FLHs) für das Auslösen der RET-Investitionen durchgeführt. Hierzu wird die Kapitalwertmethode (NPV) und die Realoptionsanalyse unter Berücksichtigung der entsprechenden Einnahmequellen von Einspeisevergütungen (FiT) und der Großhandelsmarktpreis für Strom verwendet. Die Ergebnisse der Analyse werden mit den FLHs bereits realisierter RET-Projekte in der Türkei verglichen, um beurteilen zu können, ob die Kapazitätsausbauziele erreichbar sind. Die Neuheit dieser Studie liegt in der Anwendung der vorerwähnten Methoden (NPV, Realoption) um die Schwellenwerte der FLHs für die RET-Investitionen zu quantifizieren.

Die Analyse zur Entwicklung der RET-Investitionen zeigen, dass die Ziele für Biomasse, Solar PV und geothermische Kraftwerke unter den gegebenen Annahmen erreichbar erscheinen, während die Erreichung der Ziele für Wasser- und Windkraftwerke davon

abhängig ist, dass die türkische Regierung die entsprechenden FiT-Raten erhöht. Die türkische Regierung hat bereits angekündigt, dass die Einspeisevergütungen erhöht werden können, um die RET-Kapazitätsausbauziele für das Jahr 2023 zu erreichen.

Der Nettonutzen der Energiepolitik 2023 wird relativ gemessen durch die Entwicklung eines Kapazitätsausbau-Modells mit technisch-ökonomischer Analyse des Referenz-Ausbauszenarios (Energiepolitik 2023) verglichen mit alternativen Ausbauszenarien. Dementsprechend zeigt der Nettonutzen der Energiepolitik 2023 den Barwert (abgerechnet auf das Jahr 2015) der entgangenen/gewonnenen Einsparungen an Kapital, Brennstoff und externen Kosten im Vergleich zu alternativen Ausbauszenarien. Insgesamt wurden vier alternative Ausbauszenarien aufgebaut; erneuerbare Energien, importierte Steinkohle und Erdgas, jeweils anstelle der heimischen Kohlearten sowie importierte Steinkohle und Erdgas gemeinsam anstelle der heimischen Energieresourcessen im Referenz-Ausbauszenario. Die Neuheit dieser Analyse liegt im entwickelten Kapazitätsausbau-Modell und der durchgeführten technisch-ökonomischen Analyse basierend auf den gleichzeitigen neuen Studien über „The Future Load Duration Curves of Turkey“ und „The Improved Screening Curve Approach“.

Die Ergebnisse der Analyse zeigen, dass das Hauptziel der Energiepolitik 2023 nur durch das Ausbauszenario, das auf Erdgas und importierte Steinkohle basiert, nicht erfüllt werden kann, weil der erreichte Anteil der erneuerbaren Energien geringer als der angestrebte Anteil ist. Die Kosten/Nutzen-Analyse der Energiepolitik 2023 zeigt, dass der gezielte Kapazitätsausbau von RETs nützlicher als der von fossil befeuerten Kraftwerken ist. Im Gegensatz dazu ist der gezielte Kapazitätsausbau basierend auf den heimischen Kohlesorten weniger vorteilhaft als der auf importierter Steinkohle basierende. Außerdem kann er auch weniger vorteilhaft als der Erdgas-basierende sein, wenn mehr Wert auf Gesundheits- und Umweltschutz gelegt wird. Schließlich können die Ausbauszenarien, die auf erneuerbaren Energien oder importer Steinkohle anstelle heimischer Kohlesorten basieren, durch eine Verbesserung der Energiepolitik 2023 mehr Nutzen für die Gesellschaft schaffen.

Die Schlussfolgerung dieser Analyse legt nahe, das die türkische Regierung die gewährte Subventionierung zur Investitionsförderung von RETs nochmals kritisch überdenken und sich nur auf den Kapazitätsausbau von RETs konzentrieren sollte, um den unter Berücksichtigung der etablierten Methode der Kosten/Nutzen-Analyse größtmöglichen Nutzen für den Zeitraum 2015-2023 zu erzielen.

Schlagwörter: Kosten/Nutzen-Analyse, Kapitalwertmethode, Realoptionsanalyse, Lastdauerlinie, Screening Curve Methode

The Development of the Turkish Power Market with special respect to Renewable Power Generation in Turkey

ABSTRACT

The Turkish government has adopted a new energy policy to diversify electricity supply through exploitation of the remaining potential of the domestic fossil fuels and the renewable energy resources. The main goal of the new energy policy, so called “energy policy 2023” in this dissertation, is to increase the share of renewable in energy mix to at least 30% of the annual total generation in 2023; whereas to reduce that of natural gas to at least 30%. Accordingly, the target capacity expansion of renewable energy technologies (RETs) is anticipated to bring gains in gross domestic product, reductions in natural gas imports and CO_2 emissions.

The aforementioned assessments are limited in scope to the analysis of the impacts of substituting combined cycled gas power plants by RETs; although the governmental policies are principally analyzed taking into account their benefits and costs to the society considering alternative utilizations of the scarce resources. Therefore, this dissertation aims to carry out analyses on the energy policy 2023 regarding the development of the investments in RETs and the net social benefit of the proposed capacity expansion targets for the domestic energy resources.

The investment analysis is carried out by quantifying the level of full load hours (FLHs) of operation to trigger investment in RETs by utilizing the net present value (NPV) and the real option methods taking into account the revenue streams from the feed-in tariff (FiT) scheme and the wholesale market price of electricity respectively. The results of the analysis are compared with the resource potential related to the FLHs of RETs in Turkey to discuss whether the capacity expansion targets are reachable or not. The novelty of this study lies in the application of the NPV and the real option methods to quantify threshold FLHs for the aforementioned investment analysis.

The analyses on the development of the investments in RETs indicate that the targets for biomass, solar PV and geothermal power plants are anticipated to be reachable under the given assumptions; whereas the achievement of the targets for hydropower and wind power plants are considered to be dependent on the decision of the Turkish government whether the corresponding FiT rates should be increased. Indeed, the Turkish government has declared

that the rates in FiT scheme can be raised; in order to reach the RET capacity expansion targets for the year 2023.

The net social benefit of adopting energy policy 2023 is relatively measured by developing a capacity expansion model to conduct techno-economic analyses on the reference (i.e. energy policy 2023) and the alternative capacity expansion scenarios. Accordingly, the net social benefit of adopting energy policy 2023 indicates the 2015 present value of foregone/gained savings in capital, fuel and external costs in comparison to an alternative capacity expansion scenario. In total, four alternative capacity expansion scenarios are constructed dependent on renewable, imported hard coal and natural gas substituting for domestic types of coal and also on both imported hard coal and natural gas substituting for domestic energy resources in the reference scenario. The novelty of this analysis lies in the developed capacity expansion model and the techno-economic assessments based on the concurrent novel studies on the future load duration curves of Turkey and the improved screening curve approach.

The results of the analyses indicate that the main goal of the energy policy 2023 cannot be fulfilled only by the capacity expansion scenario solely dependent on natural gas and imported hard coal due to having a share of renewable less than the targeted one. The social cost-benefit analysis of the energy policy 2023 indicates that the targeted capacity expansion of RETs is more beneficial than that of fossil fuel fired power plants. In contrast, the targeted capacity expansion based on domestic coal types are less beneficial than that of imported hard coal and can also be less beneficial than that of natural gas through attaching more value to the health and environmental concerns. Finally, the capacity expansion scenarios, which are based on renewable resources or imported hard coal in the place of domestic types of coal, can provide more benefits to the society by improving the energy policy 2023.

In conclusion, the Turkish government should review the granted subsidizations to promote investments in RETs and should consider solely relying on the capacity expansion of RETs to achieve the greatest possible net benefit for the period 2015-2023 according to the established method of cost-benefit analysis.

Key Words: Social cost-benefit analysis, real option analysis, net present value method, load duration curves, screening curve method

ACKNOWLEDGEMENTS

I want to express my deepest gratitude to my Ph.D. supervisor, Prof. Dr. Mathias Erlei, who trusted me for realising my ambitions since the first day we met. I am also thankful for his interest and support for my research throughout my study. In particular, I am in debt for his generosity to spend his valuable time for discussions on my studies even for one day long.

I am greatly indebted to my parents Gülsen & Hulusi Güner for supporting my education starting from the nursery school to the end of doctoral study.

I would like to thank to Prof. Dr. Roland Menges, Prof. Dr. Heike Y. Schenk-Mathes and the participants of the PhD seminars who were present on Wednesdays to discuss and to make suggestions about my dissertation.

I am grateful to my friends with whom I studied or worked or shared flats during my doctoral study. I would like to thank Julian Hess for being patient and interested in supporting and reviewing my studies. In particular, I am thankful for his replies during the night times for my paper requests. I want to also mention his motivating feedbacks by which I got familiarized with the word “anspruchsvoll”. I would like to thank Erol Kahraman for sharing his knowledge about financial options and his cooperation. I would like to thank João Nunes Correia for supporting me with his IT skills and also for being an enjoyable flatmate. I am thankful to Emre Seyrek for providing me publications. I thank Bugra Borasoy for his support to continue studying PhD after finishing my master thesis. I thank Wolfgang Gödde for being helpful and spending time together as one of my long time flatmates in Karlsruhe.

I would like to thank Yuanjing Li and Susanne Koschker for giving me feedbacks about my dissertation during Young Energy Economists and Engineers Seminar in Dresden.

Last but not least, I would like to express my gratitude for Atatürk, “The Father of the Turks”, who not only liberated but also enlightened his people through his revolutions. Thanks to his ideology “The truest mentor in life is science”.

[PAGE INTENTIONALLY LEFT BLANK]

TABLE OF CONTENTS

LIST OF FIGURES

LIST OF TABLES

LIST OF ABBREVIATIONS

1E-05	10^{-5}
$	US-Dollar
%/a	Percent per Annum
AACC	Annual Average Cost of Capacity
AACE	Annual Average Cost of Energy
ACF	Autocorrelation Function
AIC	Akaike's Information Criterion
AICc	Corrected Akaike's Information Criterion
ANN	Artificial Neural Network
AR(p)	Autoregressive Model of Order p
AR(P)	Seasonal Autoregressive Model of Order P
ARIMA	Autoregressive Integrated Moving Average
ARIMA	Autoregressive Integrated Moving Average Model
ARMA(p,q)	Mixed Autoregressive Moving Average Model of Order p and q
BEPC-EEE	Beijing Electric Power Corporation
BIC	Schwarz's Bayesian Criterion
BOO	Build Own Operate
BOT	Build Operate Transfer
BOTAS	Petroleum Pipeline Company
Cap	Installed Capacity
CAPEX	Capital Expenditure
CC	Combined Cycle Gas Turbine
cdd	cooling degree days
CF	Capacity Factor
CIRRs	Commercial Interest Reference Rates
CIRRs	Commercial Interest Reference Rates
CO_2	Carbon Dioxide
COAL	Coal Fired Power Plant
CSP	Concentrating Solar Power
df	Degrees of Freedom
DSI	General Directorate of State Hydraulic Works
EEE-RTS	Institute of Electrical and Electronics Engineers- Reliability Test System
EIE	Directorate General of Energy Affairs
EML	Electricity Market Law
EPDK	Energy Market Regulatory Authority
EPIAS	Energy Markets Operating Corporation
EUAS	The Electricity Generation Company
Ex-Im Bank	Export-Import Bank of the United States
exp	Linear exponential function
FC	Fixed Cost
FERC	Federal Energy Regulatory Commission
FiT	Feed-in Tariff

FLHs	Full Load Hours
FLM	Fuzzy Logic Methodology
FOM or Fixed O&M	Fixed Operating and Maintenance Costs
FYEGCP	Five Year Electricity Generation Capacity Projection
GAM	Genetic Algorithm Method
GBM	Geometric Brownian Motion
GDP	Gross domestic product
GNP	Gross National Product
GPRM	Grey Prediction Method
GT	Open Cycle Gas Turbine
GWel	Gigawatt Electric
H_0	Null Hypothesis
H_1	Alternative Hypothesis
hdd	heating degree days
IAEA	International Atomic Energy Agency
IDE	Integrated Development Environment
IEA	International Energy Agency
inc	income of consumers
Inf	Infinity
IREA	International Renewable Energy Agency
KKT	Karush-Kuhn-Tucker
LDC	Load Duration Curve
LDC	Load Duration Curve
LNG	Liquefied Natural Gas
Log	Logarithm
m/s	Meter per Second
MA(q)	Moving Average Model of Order q
MA(Q)	Seasonal Moving Average Model of Order Q
MAED	Model for Analysis of Energy Demand
MAPE	Mean Absolute Percentage Error
MARE	Mean Absolute Relative Error
$MARE_{HLD}$	MARE in approximating hourly load demand (HLD) in a considered year
$MAREs_{AGD}$	MAREs in approximating annual gross electricity demand
$MAREs_{APD}$	MAREs in approximating annual peak load demand
MASE	Mean Absolute Scaled Error
Max	Maximum
MENR	Ministry of Energy and Natural Resources of Turkey
Min	Minimum
MLE	Maximum Likelihood Estimates
MMSE	Minimum Mean Square Error
MW_{el}	Megawatt Electric
NEA	Nuclear Energy Agency
NPV	Net Present Value
NREAP	National Renewable Energy Action Plan for Turkey

NSB	The Net Social Benefit
O&M	Operation and Maintenance Costs
OECD	Organisation for Economic Cooperation and Development
PACF	Partial Autocorrelation Function
PMUM	Market Financial Reconciliation Center
prc	price of electrical energy
PV	Photovoltaic
p or pp	Page(s)
p-value	Probability Value
Q-Q plot	Quantile-Quantile Plot
$\mathbb{R}$	Real Numbers
R^2	Coefficient of Determination
R^2_{adj}	Adjusted R^2
RE	Relative Error
RE_{AGD}	RE in approximating annual gross electricity demand (AGD) in a considered year
RE_{APD}	RE in approximating annual peak load demand (APD) in a considered year
RegMS	Regression Mean Square
RegS	The regression sum of squares
RET	Renewable Energy Technology
RMS	Residual Mean Square
RSS	Residual Sum of Squares
SARIMA	Seasonal Autoregressive Integrated Moving Average Model
SSE	Sum of Squares of Error for Linear Regression
SSE_{NL}	Sum of Squares of Error Function for Nonlinear Regression
STSM	Structural Time Series Method
SVM	Support Vector Machines
TCSCM	The Classical Screening Curve Methodology
TEAS	Turkish Electricity Generation and Transmission Company
TEDAS	Turkish Electricity Distribution Company
TEIAS	Turkish Electricity Transmission Corporation
TEIAS	The Turkish Electricity Transmission Company
TEK	Turkish Electricity Authority
TETAS	Turkey Electricity Trading and Contracting Company
TISCM	The Improved Screening Curve Methodology
TKI	Turkey Coal Enterprises Authority
TL	Turkish Lira
TOOR	Transfer of Operating Rights
TSA	Time Series Analysis
TSC	Total Social cost of Supplying Electricity
TSS	Total Sum of Squares
TTK	Turkish Hard Coal Enterprise Institution
TTSAT	Total Sum of the Area of all Trapezoids
TWh_{el}	Terawatt Hours Electric

UEDT	Underlying Energy Demand Trend
VAT	Value Added Tax
VC	Variable Cost
VIF	Variance Inflation Factor
VOM or Variable O&M	Variable Operating and Maintenance Costs
w.r.t.	with respect to
WRSS	Weighted Residual Sum of Squares
WTI	West Texas Intermediate
y	Year
$\mathbb{Z}^+$	Positive Integer Numbers

1 INTRODUCTION OF THE DISSERTATION

Turkey is the 17th largest economy in the world and distinguishes itself from European countries by its increasing young population, fast growing urbanization and industrialization. The Turkish economy has experienced a remarkable mean economic growth of 4.1%/a in the period 2000-2014; despite the financial crisis of Turkey in 2001 and the global financial crisis in 2009. In the same period, the annual gross electricity demand[1] rose from 128 TWh_{el} to 257 TWh_{el} with a mean growth rate of 5.2%/a. As the Turkish economy rapidly developed, Turkey became a growing energy importer by depending on imported fossil fuels[2] for more than 50% of the annual total electricity generation (see Figure 1).

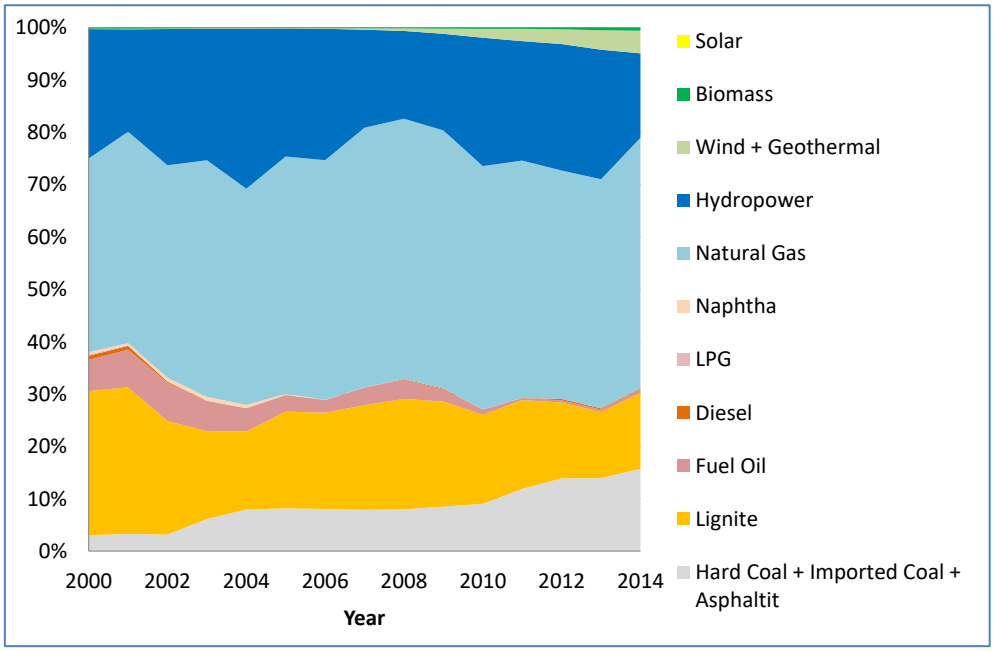

Figure 1- The annual development of the amount of electricity generated by resources (own illustration according to TEIAS[3])

In the period 2000-2014, 70% to 83% of the annual total electricity generation is supplied by thermal power plants (see Figure 1). In particular, the annual supplied amount of electricity by natural gas fired power plants is the highest among all other power plants and lies in the range of 40% to 50% of the total generation in the mentioned period. Further, the second highest amount of electricity is supplied by hydropower plants and their share lies in the range of 16% to 31% of the total generation in the mentioned period. Overall, the supplied amount of

[1] The gross electricity demand equals to the sum of national electricity generation and imported amount of electricity subtracted exported amount of electricity.
[2] They are natural gas, imported hard coal, oil and its derivatives.
[3] The Turkish Electricity Transmission Corporation

electricity by natural gas fired and hydropower plants accounts for 60% of the total generation in the mentioned period. The remaining share belongs to the fossil fuel fired power plants (i.e. lignite, hard coal, asphaltite[4], oil) and other renewable energy based technologies (i.e. wind, solar, geothermal and biomass).

With regard to capacity expansion, the total installed capacity of power plants rose from 27264 MW_{el} to 69519 MW_{el} with a mean growth rate of 7%/a in the period 2000-2014 (see Figure 2). In the mentioned period, about 60% of the total installed capacity is composed of thermal power plants. In particular, the installed capacity of the natural gas fired power plants, which rose from 7044 MW_{el} to 25632 MW_{el}, is observed to be indicating the highest capacity expansion among all other type of power plants. The second highest capacity expansion is observed to be in the installed capacity of the hydropower plants which rose from 11175 MW_{el} to 23664 MW_{el}. Overall, the share of domestic resource based power plants in the total installed capacity decreased from 66% to 54% in the mentioned period and has been indicating a downward trend for the future.

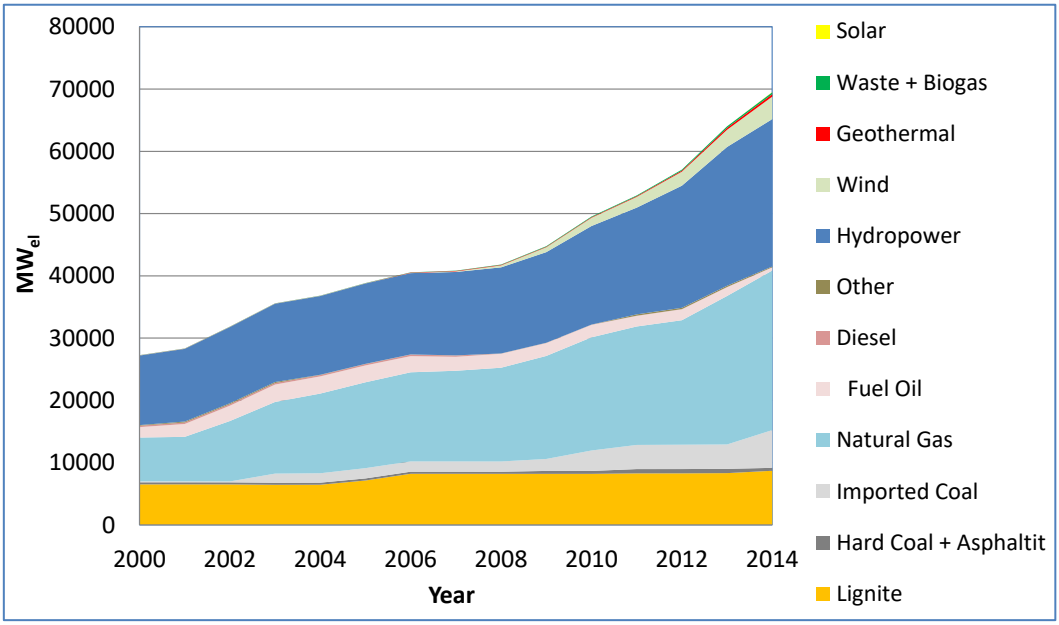

Figure 2- The annual development of the installed capacity by power plant types (own illustration according to TEIAS)

[4] According to the definition given by TEIAS, asphaltite is a kind of coal which originates from oil. The oil in the older layers of a geological formation fills the cracks in the upper layers which occurred as a result of the tectonic events. Further, volatile and fluid substances leave the cracks and finally, the oil waste material in the cracks forms this type of coal.

The imported resource dependency, which emerged through the rapid capacity expansion of the Turkish power plant park, is observed to be originating from the issues given below:

- Turkey's geopolitical location as an energy corridor enables low effort in reaching imported fossil fuels.
- Starting from the 1990s, the quickest and low cost solution to cover the increasing demand for electricity is considered to be installing natural gas fired power plants.
- The Turkish government did not consider the dependence on imported energy resources as a risk until the mid-2000s.
- Since the mid-2000s and the liberalization of the Turkish electricity market; the private investors continue investing in imported fossil fuel fired power plants in hope for more profits relative to the other resources.

The high level of imported resource dependency has been causing adverse effects on Turkey's economic development due to the risks linked with the supplies from other countries and the volatility of the fuel prices. Hence, the diversification of energy supply through exploitation of the remaining potential of the domestic energy resources has been gaining importance in building up a new framework for the national energy policy. In the year 2009, the guidelines to the new energy policy was published in "Turkey Electricity Energy Market and Supply Security Strategy Paper" by the council of ministers of the Republic of Turkey. Based on this cabinet decision, the ministry of energy and natural resources introduced the "National Renewable Energy Action Plan for Turkey" (NREAP) in the year 2014 to promote the use of energy from renewable resources for the purposes of electricity generation, transportation, heating-cooling and energy efficiency in the period 2013-2023. In addition, Turkey's NREAP serves as a commitment for the European Union membership during the accession process. Turkey's NREAP is based on the Renewable Energy Directive 2009/28/EC[5] of the European Parliament and of the Council of 23 April 2009 (The Ministry of Energy and Natural Resources, 2014, p. 8).

[5] Accordingly, the member states of the European Union will reach a 20% share of energy from renewable sources by 2020 and a 10% share of renewable energy specifically in the transport sector.

The set targets[6] for the year 2023, which are published in the Turkey Electricity Energy Market and Supply Security Strategy Paper (2009, p. 12) and in the NREAP (2014, p. 22), are as follows:

- The target year is determined to be the year 2023 as the milestone, as it is the 100th anniversary year of the Turkish Republic.
- Until the year 2023, the share of renewable energy in energy mix is planned to be increased to at least 30% of the annual total generation; whereas the share of natural gas is planned to be reduced to at least 30% of the annual total generation.
- The targeted level of installed capacities until the year 2023 are given below:
    - 34000 MW_{el} hydropower plant
    - 20000 MW_{el} wind power plant (onshore)
    - 1000 MW_{el} geothermal power plant[7]
    - 5000 MW_{el} solar PV power plant at least
    - 1000 MW_{el} biomass power plant
- All proven lignite and domestic hard coal resources[8] will be utilized for power generation.
- Capacity expansion of imported hard coal fired power plants can be enabled considering the supply security of electricity and the developments in utilization of such resources.
- The share of the nuclear energy in energy mix is planned to be increased up to 5% at least by the year 2020 and to increase it even further in the longer run.

The nuclear energy target is the only controversial target among the mentioned ones to mitigate imported resource dependency; since neither the fuel nor the nuclear power plant technology can be domestically provided. Indeed, the aim of the Turkish government is to mitigate the natural gas dependency through the diversification of the energy supply. Accordingly, the first nuclear power plant of Turkey will be the Akkuyu nuclear power plant and will have a total installed capacity of 4800 MW_{el}. The construction of the power plant

[6] Note that the covered topics, which are not directly related to the capacity expansion of power plants, are out of the scope of this study and therefore, further information will not be provided.

[7] In NREAP, the target is set to 600 MW_{el}; however it is also noted that 1000 MW_{el} installed capacity might be surpassed considering the actual developments.

[8] Note that the proven fossil fuel reserves in Turkey are sufficient for up to 25426 MW_{el} installed capacity of lignite fired power plant, up to 1400 MW_{el} installed capacity of domestic hard coal fired power plant and up to 675 MW_{el} installed capacity of asphaltite fired power plant (see p. 30 for more information).

takes place in the period 2011-2023. The power plant is comprised of four 1200 MW_{el} blocks which are scheduled to be successively commissioned starting from the year 2020 until the year 2023 (Akkuyu NGS AS, 2013). In addition, TEIAS has committed itself to a medium term capacity expansion of transmission infrastructure for the period 2015-2020, considering the forecasted penetration of renewable energy technologies (RETs).

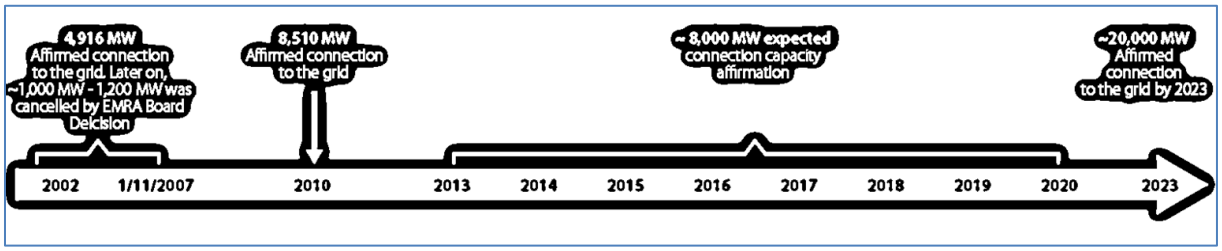

Figure 3-The transmission infrastructure commitment of TEIAS (adapted from NREAP (p. 44))

In this study, the mentioned targets for the year 2023 are gathered under the title "energy policy 2023". The corresponding capacity expansion of power plant types starting from the base year 2014 is represented in Table 1.

Table 1- The target capacity expansion of the power plant types according to the energy policy 2023 (own illustration)

Resource	Installed Capacity in 2014 [MW_{el}]	Target Installed Capacity in 2023 [MW_{el}]
Lignite	8693	25426
Hard Coal	335	1400
Asphaltite	135	675
Hydropower	23664	34000
Wind	3612	20000
Solar	40	5000
Geothermal	405	1000
Biomass	288	1000
Nuclear	0	4800
Total	37172	93301

The target capacity expansion of RETs is anticipated to bring following gains by the year 2023 according to the conducted analysis in NREAP[9] (pp. 71-72):

- The annual reduction of natural gas imports and the corresponding total savings will amount to 21 billion m^3 and \$4 billion[10] respectively.

[9] The details of the assessments can be found in the corresponding publication.
[10] The natural gas price is taken as $\$_{2010}$ 5/Btu according to the US Department of Energy Organization.

- The annual reduction of CO_2 emission and the corresponding economic impact will amount to 47 million ton[11] and $1.2 billion[12] respectively.
- The impact on the Turkish GDP[13] during the investment phase (2013-2023) and by the year 2023 will amount to $6.3 billion and $1.7 billion respectively.

The aforementioned assessments are limited in scope to the analysis of the impacts of substituting combined cycled gas power plants by RETs; although governmental policies are principally analyzed taking into account their benefits and costs to the society considering alternative utilizations of the scarce resources (land, labor, capital, etc.). Most importantly, the Turkish government has declared in NREAP that the energy policy 2023 will be implemented by all means. Accordingly, the adoption of the energy policy 2023 brings a new perspective to the resource allocation problem; since not only it is important to lessen the dependency on the imported energy resources but also the scarce resources should be allocated efficiently among different power generation technologies. Therefore, the energy policy 2023 should be examined to reveal whether the targeted exploitation of the remaining potential of the domestic energy resources produces benefits for the society greater than its costs through mitigating dependency on the imported energy resources.

1.1 Objectives of the Dissertation and Research Questions

The objective of this dissertation is to anticipate the development of the investments in RETs and to appraise[14] the net social benefit of the proposed capacity expansion targets in the energy policy 2023.

The investment analyses are conducted by utilizing the method of net present value (NPV) and the real option analysis taking into account the revenue streams from the feed-in tariff (FiT) scheme and the wholesale market price of electricity respectively.

The appraisal of the energy policy 2023 is carried out with respect to (w.r.t.) the proposed alternative developments of the power plant park of Turkey by utilizing the method of social cost-benefit analysis. In particular, the alternative capacity expansion scenarios are created based on more ambitious utilization of renewable and imported energy resources in

[11] The emission factor for combined cycle gas power plants is assumed to be 0.37 ton/MWh_{el}.
[12] The cost of CO_2 emission is assumed to be 20 €/ton according to the European Union CO_2 emission allowance.
[13] Gross domestic product
[14] It means to analyze in prospective sense.

comparison to the energy policy 2023. In this manner, tradeoff analyses[15] are conducted between the energy policy 2023 and the alternative capacity expansion scenarios in terms of capital, fuel and external costs of electricity generation. In addition, the capacity expansion scenarios are based on the type of power plants but not on specific projects. Accordingly, the official targets for capacity expansion of power plants (see Table 1) are substituted by the proposed alternative targets. Therefore, the net social benefit of adopting energy policy 2023 is relatively measured and dependent on the capacity expansion of the power plant types considered in the alternative capacity expansion scenarios.

The study seeks answers to the following questions:

- How do the FiT rates and the wholesale market price of electricity influence the investments on RETs?
- What is the net social benefit of capacity expansion based on the energy policy 2023 relative to the alternative one solely based on the RETs?
- What is the net social benefit of the targeted capacity expansion based on the domestic fossil resources relative to the alternative ones based on the imported resources?
- What is the net social benefit of the targeted capacity expansion based on the domestic resources relative to the alternative one based on the imported resources?
- What are the pros and cons of adopting energy policy 2023 according to the results of the social cost-benefit analysis?
- Are there any other alternatives for providing more benefits to the society by improving energy policy 2023?

1.2 Methodologies of the Dissertation

In this dissertation, two different analyses in scope are carried out on the energy policy 2023. The first analysis is carried out on the development of the investments in RETs; whereas the second one is carried out on the net social benefit of the proposed capacity expansion targets in the energy policy 2023.

In the first analysis, the investments in RETs are evaluated w.r.t. the immediate investment decisions based on the NPV method and the flexible investment decisions based on the real option method. The mentioned methods are utilized by taking into account the revenue

[15] For example, the society may incur more capital cost for the capacity expansion of RETs relative to that of natural gas fired power plants; in order to avoid fuel costs to some extent.

streams from the FiT scheme and the electricity market respectively. The mentioned methods are traditionally utilized for quantifying the investment trigger prices. In this study, threshold values for annual full load hours[16] (FLHs) of operation, which are necessary to trigger investments, are calculated for immediate and flexible investment decisions by varying the discount rate. Based on the NPV method, the threshold value for FLHs (i.e. so called threshold FLHs in this study) of operation indicates the level above/below which investments should be made/not be made given the FiT rates for RETs. Based on the real option method, the threshold FLHs of operation indicates the level above/below which investments should be made/postponed given the expected market price of electricity. Accordingly, the level of FLHs of operation to trigger investment in RETs is quantified and compared with the resource potential related to the FLHs of RETs in Turkey. Finally, the results of the analyses are discussed whether the capacity expansion targets are reachable or not w.r.t. the mentioned degrees of flexibilities and the cost of capital. The novelty[17] of this study lies in the application of the NPV and the real option methods to quantify threshold FLHs for the aforementioned investment analysis.

In the second analysis, the net social benefit of the energy policy 2023 is appraised by developing a capacity expansion model. The term "model" is defined as an abstract depiction of the real system under consideration and serves the intended purpose of its modeller (Möst, Fichtner, & Grunwald, 2009, p. 12). A model portrays behaviour and interdependencies of the system elements in a qualitative and quantitative way. Möst and Fichtner states that "the basic idea in the formulation of a (scientific) model is the reduction of complexity and abstraction (or negligence) of certain features." It is also noted that the suitable method for the model supported analysis should be selected based on the tradeoff between the benefit and the effort in significant contribution to the decision support.

In this study, the capacity expansion model is developed as a means of quantitative thinking to support appraisal of the energy policy 2023 on well-informed basis; however its objective is not to forecast the future. More specifically, the aimed future in the energy policy 2023 is mathematically described according to the officially targeted capacity expansions and the

[16] It can be calculated by dividing the average annual amount of electricity generation by the corresponding power plant's installed capacity (i.e. rated power capacity).

[17] The fundamentals of this approach were first introduced by the author during the PhD Seminar at TU Clausthal on the 23rd of November in 2011. Later, this approach was utilized in another study "Investment prospects of renewable and non-renewable power generation in China" by Yuanjing Li and the author. The mentioned study was presented in "2015 International Symposium on Energy and Finance Issues" on the 20th of March in 2015 in France.

related parameters. By the same token, alternative futures are created by substituting the official targets with the proposed alternative targets. In this respect, the energy policy is analyzed through a broader perspective than in NREAP and by utilizing the similar methodological approaches in NREAP (e.g. "with-and-without" approach).

The capacity expansion model, which is implemented based on the bottom-up approach, consists of three components so called inputs, process and outputs as represented in Figure 4. Accordingly, the model submits the results of the social cost-benefit analysis by carrying out techno-economic analyses on the given inputs.

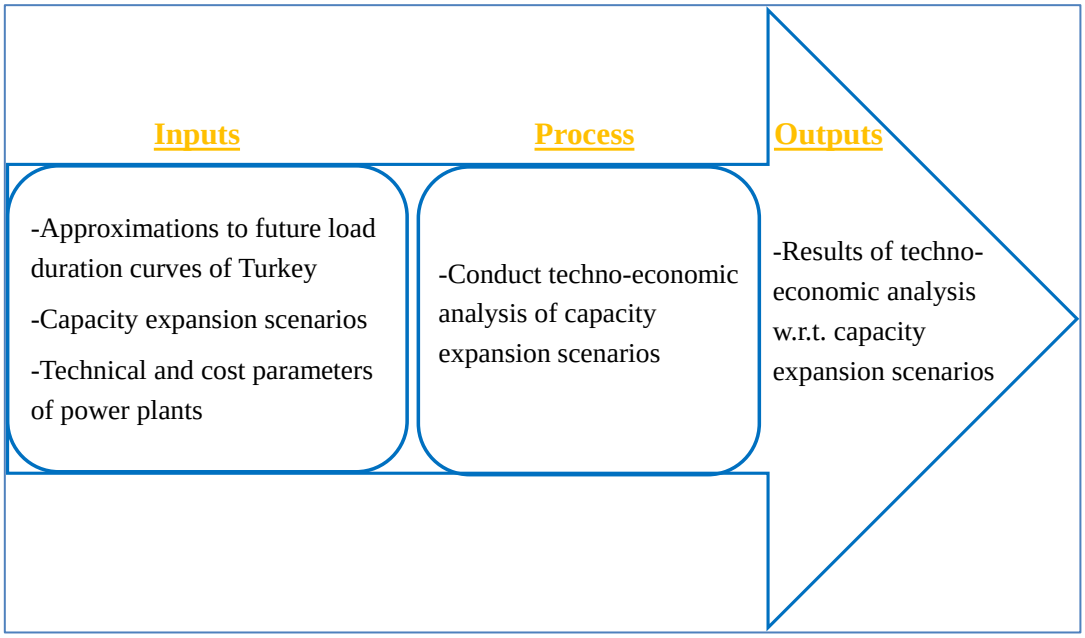

Figure 4- The components of the developed capacity expansion model (own illustration)

The inputs of the model related to the technical parameters, the cost parameters and the fuel price forecasts are obtained from official publications and previous studies to project[18] domestic fuel prices; whereas the approximations to future load duration curves[19] (LDCs) of Turkey and the capacity expansion scenarios are developed during the course of this dissertation. Namely, a study is carried out under the title "A Concept on Obtaining Functional Approximations to Future Load Duration Curves: A Case Study on Turkey". Through the development of this concept, the functional approximations to future LDCs of

[18] The domestic prices for all types of fuels are scaled based on the assumption that the change in fuel prices in the domestic energy market of Turkey are perfectly correlated with the price changes in the international energy markets. See p. 318 for more information.

[19] A load duration curve indicates the duration during which a considered level of load demanded is equaled or exceeded.

Turkey is obtained by determining the adequate[20] functional approximations to the past LDCs of Turkey and by forecasting the functional parameters of the approximated past LDCs respectively. The econometric methods such as regression and univariate time series analysis are utilized for approximating and forecasting the functional parameters of the LDCs respectively. The novelty of this study lies in the developed concept and the performed analysis during the course of the approximation analyses. With regard to inputs related to the capacity expansion scenarios, the energy policy 2023 is considered as the reference scenario; whereas the constructed capacity expansion scenarios are considered as the alternative ones. In total five capacity expansion scenarios are constructed based on the research questions as listed below:

- Reference scenario (high dependency on domestic types of coal and renewable resources)
- Green scenario (high dependency on RETs)
- Grey scenario (high dependency on imported hard coal)
- Blue scenario (high dependency on natural gas)
- Blue-grey scenario (high dependency on imported fossil fuels)

The scenarios are constructed based on their dependency on the domestic and the imported energy resources for the capacity expansion of power plant types. Correspondingly, the scenarios are constructed to carry out tradeoff analyses between the reference and the alternative capacity expansion scenarios in terms of capital, fuel and external costs of electricity generation. In addition, all considered scenarios are assessed for their reliability of supplying electricity to meet power demand at all times with an acceptably high probability.

The techno-economic analysis encompasses the technical and the economic assessments of the energy policy 2023 w.r.t. the alternative capacity expansion scenarios for the period 2015-2023. In particular, the former analysis encompasses the calculation of the amount of electricity generated by all types of power plants and CO_2 emission caused by thermal, geothermal and biomass power plants. The latter analysis encompasses the calculation of the social cost of supplying electricity in each year of the mentioned period. Note that the techno-

[20] In this study, an adequate functional approximation to a LDC is defined to be a parsimonious functional approximation to a LDC with least possible inaccuracy in approximating annual gross electricity demand, annual peak load demand and hourly load demand among other alternatives.

economic analysis is conducted to value the avoided costs[21] for adopting the energy policy 2023 but not to maximize them. Such optimization process is not conducted; since the capacity expansion targets in all scenarios are created in comparison to the energy policy 2023. On the other hand, it is assumed that the short-run competitive equilibrium provides the least cost supply of electricity in the period 2015-2023. Accordingly, the residual load demand[22] is met by starting from the thermal power plant with the least variable cost to the highest one by adjusting the output of the considered type of thermal plants. The corresponding calculations are based on the study "The Improved Screening Curve Method Regarding Existing Units" which is conducted during the course of this dissertation. The novelty of this study lies in its efficient and straightforward geometrical solution process to evaluate a static capacity expansion problem considering both existing and candidate power plants in comparison to the previous works for the similar type of improvements.

The social cost-benefit analysis on the energy policy 2023 is based on the "with-and-without" approach associated with the concept of opportunity cost. Correspondingly, the benefit of adopting energy policy 2023 is measured relative to the savings which would have been foregone/gained by utilizing the scarce resources in an alternative capacity expansion scenario. Further, the social cost-benefit analyses are grounded on the measure of relative change in economic welfare as partial equilibrium analyses. Hence, the impact of capacity expansion of power plant park of Turkey is restricted to the electricity market by assuming that the wider economic environment remains unchanged. Finally, the best policy among others is defined to be the one which theoretically creates more benefits to the society. Therefore, the greatest possible net benefit (i.e. welfare) is the criterion to choose from among the constructed capacity expansion scenarios according to the established method of cost-benefit analysis.

The net social benefit of adopting energy policy 2023 is determined by calculating the difference in the total social cost of supplying electricity in the period 2015-2023 due to not adopting and adopting the energy policy 2023. The total social cost of supplying electricity indicates the present value of annually incurred social costs which are discounted to the year 2015. If the total social cost of supplying electricity arising from the latter case is less than the former case, then the adoption of energy policy 2023 is calculated to be indicating a positive

[21] It is defined to be the savings in fixed, variable and external costs of electricity generation for adopting energy policy 2023 w.r.t. an alternative capacity expansion scenario.

[22] The residual load demand is obtained by subtracting the amount of power generated by RETs from load demand.

net social benefit. By the same token, if the total social cost of supplying electricity arising from the latter case is higher than the former case, a negative net social benefit is indicated due to adopting the energy policy 2023. Thus, the gains/losses in welfare with and without the adoption of the energy policy 2023 are relatively measured.

The social cost of supplying electricity is composed of fixed, variable and external costs. Further, the fixed costs consist of capital and fixed operation and maintenance costs (O&M). Furthermore, the variable costs consist of fuel and variable O&M costs. Moreover, the external costs originate from the environmental and health damages due to supplying electricity. More specifically, the variable and external costs are dependent on the amount of electricity generated; whereas the fixed costs are dependent on the installed capacity of the power plants. Finally, the net social benefit of adopting energy policy indicates the present value of avoided costs for capital, fixed O&M, variable O&M, fuel and externalities which are discounted to the year 2015.

The external cost of electricity generation is included in the total supply cost of electricity to compare the social costs of different technologies based not only on the internal costs but also on the environmental and the health impacts of electricity generation. In particular, the external cost of electricity generation is internalized; in order to account for the damages/benefits associated with different capacity expansion plans and to assess the tradeoffs between not only the domestic and the imported energy resources but also the thermal and the renewable energy power plants. There is neither market value nor published specific value to external effects of electricity generation in Turkey. The social cost-benefit analysis of the energy policy 2023 basically requires the order of the magnitude of the specific impacts per generated amount of electricity by the considered type of technologies; since the "with-and-without" approach is utilized for the aforementioned appraisal. Thus, the values are obtained from two different studies which utilize two different approaches to quantify external costs. Accordingly, a bandwidth of the external costs is formed w.r.t. the considered technologies (see Table 68). Namely, the set of values for the low end of the bandwidth is obtained from the study by Rafaj and Kypreos (2007) in which the corresponding values are derived from the outcomes of "ExternE Project" of the European Commission (EC). The set of values for the high end of the bandwidth is obtained from the study "Subsidies and costs of EU energy" by Ecofys (2014) (ordered by EC). The details of those studies are given in Section 22.3.

Finally, the results of the net social benefit analysis are submitted based on the results of the aforementioned computations.

1.3 Previous Studies on Social Cost-Benefit Analysis

The novelty of this dissertation lies in the developed capacity expansion model, the conducted techno-economic assessments and the aforementioned studies on investments in RETs, future LDCs of Turkey and improved screening curve approach; in order to analyze the energy policy 2023 according to the research objectives and questions.

Kennedy (2003) developed a valuation model to analyze the net social benefit of the potential offshore wind power development to the south of Long Island, New York. The wind power's social benefit is quantified by calculating the amount of thermal generation capacity with and without any installed wind power capacity. Anh and Bhattacharyya (2011) investigated the integration of renewable electricity into the UK system in 2020 to find the optimal wind generation that can be integrated based on the total social cost of electricity supply or at an acceptable electricity price to the consumers. The analyses are based on the tradeoff between conventional power and wind power in terms of costs and environmental considerations. Sheridan (2013) quantified the total or 'social' cost of various electricity generation technologies for new and existing plants found within the PJM Interconnection[23] service territory. Melikoglu (2013) analyzed the amount of incurred total investment cost, caused total CO_2 emission and incurred total carbon tax for covering 30% of Turkey's total electricity demand at the year 2023 by wind, solar, geothermal and hydropower plants in comparison to covering it by coal fired, natural gas fired and hydropower plants. Frank (2014) estimated the net benefits of electricity generated by wind, solar, hydro, nuclear and combined cycle gas fired power plants according to a methodology based on avoided emissions and avoided costs.

[23] PJM interconnection is a regional transmission organization (RTO) that coordinates the movement of wholesale electricity in all or parts of Delaware, Illinois, Indiana, Kentucky, Maryland, Michigan, New Jersey, North Carolina, Ohio, Pennsylvania, Tennessee, Virginia, West Virginia and the District of Columbia (Kato, Zhou, Kang, & Yokoyama, 2011).

1.4 Organization of the Dissertation

This dissertation is organized into four parts according to the conducted studies during this dissertation. The objective and the organization of each part are provided in the corresponding part.

In PART A, the study on the development of the investments in renewable energy technologies in Turkey is provided. In PART B, the study on the approximations to future load duration curves of Turkey, the results of which are utilized as an input to the capacity expansion model, is provided. In PART C, the study on the improved screening curve method regarding existing units, which forms the basis of the techno-economic analysis, is provided. In PART D, the study on the techno-economic assessment of the energy policy 2023, which is conducted by utilizing the capacity expansion model, is provided.

PART A THE DEVELOPMENT OF THE INVESTMENTS IN RENEWABLE ENERGY TECHNOLOGIES IN TURKEY

2 INTRODUCTION

The energy policy of the Turkish government is supported by several incentives to promote investments on RETs[24]; in order to mitigate dependency on natural gas for the generation of electricity. The major incentive is the technology specific feed-in tariff (FiT) scheme which is based on a fixed price per kWh_{el} electricity generated by the corresponding technologies. In Table 2, the introduced FiT scheme is tabulated. Accordingly, a generator is entitled to benefit from the base tariff during the first 10 years[25] of operation. In addition, local equipment bonus is granted for the domestically manufactured mechanical and/or electromechanical equipment during the first five years of operation.

Table 2- The FiT for RETs (own illustration according to the Ministry of Energy and Natural Resources, 2014, pp. 54-55)

Feed-in Tariff ($cent/$kWh_{el}$)			
Type of Technology	Base Tariff (only for 10 years)	Maximum Domestic Manufacture Contribution (only for 5 years)	Total
Hydropower	7.3	2.3	9.6
Wind Power	7.3	3.7	11.0
Solar PV Power	13.3	6.7	20.0
Concentrated Solar Power	13.3	9.2	22.5
Geothermal Power	10.5	2.7	13.2
Biomass	13.3	5.6	18.9

The FiT is granted to those facilities which are commissioned until the year 2020. In NREAP[26], it is mentioned that the council of ministers will determine the FiT applicable to facilities commissioned after December 31, 2020; however it is also emphasized that the FiT cannot exceed the rates represented above. In NREAP, it is pointed out that if the penetration target were fulfilled before the end of the period, a lower feed-in tariff scheme would be adopted for the rest of the period and the next. On the contrary, if the penetration target were not fulfilled before the end of the period, an equal or higher feed-in tariff scheme would be adopted for the rest of the period and the next. Note that the enrollment in the FiT scheme is not compulsory rather optional. In addition, a generator has also the right to sell electricity through a bilateral agreement or in the day-ahead market.

[24] RET refers to the hydropower, wind power (on shore), solar pv power, geothermal power and biomass power plants.
[25] The prolongation of FiT over 10 years is still unclear for RETs with installed capacities under 1 MW_{el}.
[26] National Renewable Energy Action Plan for Turkey

Other provided incentives for achieving renewable energy targets of Turkey are listed below:

- Within the framework of "General Investment Incentive Program", investments on RETs are entitled to exemption for value-added tax, customs duty and income tax withholding allowance (only for investments in Region 6[27]).
- Any type of RET with an installed capacity up to 1 MW_{el} is exempted from the requirement to hold a generation license. Nevertheless, the board of ministers is authorized to increase it to up to 5 MW_{el} for specific projects.
- RET investors are required to pay only one hundredth of the license fee and are freed from the obligation to pay the annual license fee during the first eight years of operation.
- The research and development (R&D) concerning the renewable energies is supported through income tax withholding allowance, social security premium allowance (employer's share) and stamp duty exemption.

The investor perspective on the incentives for promoting renewable energy investments has been investigated by Özcan (2014). The survey study is conducted through face-to-face interviews with 18 investors who have investments in RETs in Turkey. The survey participants are composed of 4 hydropower, 9 wind, 3 geothermal and 2 biomass power plant investors. The findings of the survey provide following insights into investor views:

- The investors are motivated to make investments on RETs due to their profitability and environmental sustainability.
- 2 wind power investors, 2 geothermal power investors, and 2 biomass power investors benefit from the FiT. The majority of the participants stated that the earnings from FiT are low.
- None of the investors benefits from bonus for domestically manufactured equipment, R&D income tax withholding allowance and social security premium allowance.
- 17 investors benefited from the VAT[28] exemption and customs duty exemption.
- All of the participants stated that their investment costs are high and foreign exchange risks substantially affect the profitability of their investments.

[27] Except Bozcaada and Gökçeada (in the west of Turkey), the region six is composed of the cities in the east and south-east Anatolia (Ağrı, Ardahan, Batman, Bingöl, Bitlis, Diyarbakır, Hakkari, Iğdır, Kars, Mardin, Muş, Siirt, Şanlıurfa, Şırnak and Van).

[28] Value Added Tax

- The foreign investors see the global economic situation and the position of the Turkish economy as the major risk for their investments.
- The difficulties related to the grid connection have been experienced by all investors.
- The grid contribution fees paid for getting the right to access grids are considered to be high.
- The investors share the opinion that banks have a very positive point of view in terms of providing credit to RET projects.

The energy policy 2023 is an ambitious target to which the Turkish government has committed itself by providing incentives for its realization; however the downward trend in the wholesale market price of electricity may cause delays in reaching the target until the year 2023 (see Figure 5). It can be inferred from Figure 5 that the annual average wholesale market price of electricity decreased from 122 $/MWh_{el}$ to 53 $/MWh_{el}$ in the period 2008-2015. Accordingly, enrolling in the base FiT scheme has become more profitable than the wholesale market price of electricity (see Table 2). One of the major reasons for the downward trend is the devaluation of the Turkish Lira (TL) against $ (also true for Euro) since the year 2008. In the year 2008, 1.3 TL equaled to about 1 $; however at the end of year 2015, 2.9 TL equaled to about 1 $. Further, the devaluation of TL can be considered to be continuing in the next decade; since the US central bank may continue to raise its interest rate for $ according to the announcements at the end of 2015. In addition, the decreasing global price for fossil fuels and the increasing penetration level of RETs can be considered as other reasons for the corresponding trend.

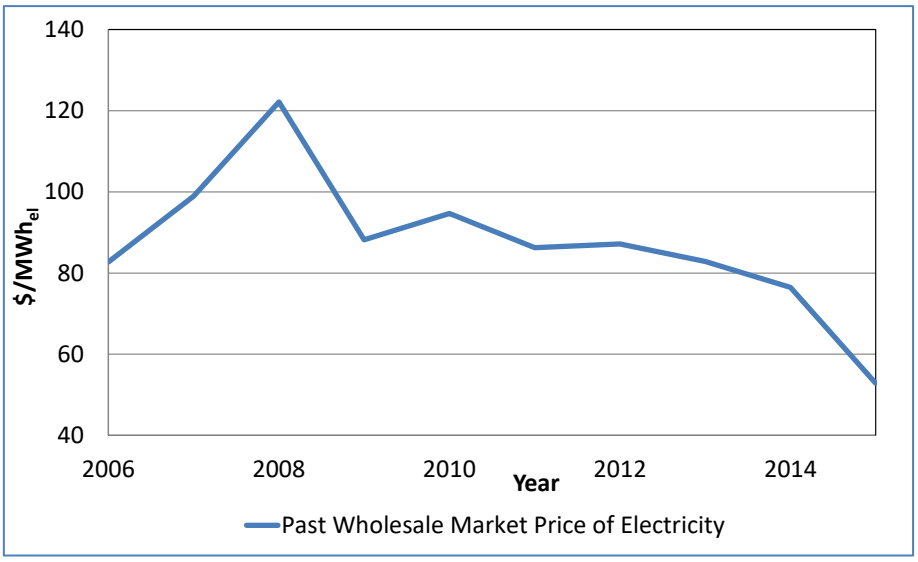

Figure 5- The development of the annual average wholesale market price of electricity in the period 2006-2015 (own illustration according to TEIAS)

The mentioned downward trend in the market price of electricity led to an increase in the number of RETs which are enrolled in FiT scheme as tabulated in Table 3. It can be inferred from the table that the number of enrollments for the year 2016 is the highest among the others. In the year 2015, the installed capacity of RETs amount to 28 GW_{el} and more than half of that amount is enrolled in FiT scheme in the year 2016. Thus, the potential RET investments faces great uncertainty given the market conditions; since the FiT can be provided only for a limited time span (see Table 2) and the economic lifetime of RETs are in the range of 20-50 years.

Table 3- The development of the installed capacities of RETs enrolled in FiT scheme (own illustration according to EPDK[29])

Type of Power Plant	Installed Capacity [MW]					
	2011	2012	2013	2014	2015	2016
Hydropower	21	930	217	598	2116	9960
Wind Power	469	685	76	825	2775	4320
Geothermal Power	72	72	140	228	390	599
Biomass	45	73	101	147	185	204
Total	607	1760	534	1798	5466	15083

Considering the uncertainty in revenues, investors face the dilemma of investing immediately by enrolling in the FiT scheme or postponing investments by waiting until the resolution of the uncertainty. Once the uncertainty is resolved, an immediate investment decision may be advantageous for being able to owning a project which is rare in renewable energy resource quality (e.g. high wind potential). On the other hand, it may also be disadvantageous; since investments on RETs are irreversible (i.e. sunk cost) and investment opportunity in a later time is foregone (i.e. flexibility in investing).

2.1 Objective of the Study

In this study, the energy policy 2023 is analyzed to discuss whether the capacity expansion targets are reachable or not w.r.t. the mentioned degrees of flexibility (i.e. immediate and flexible decisions) and the cost of capital. The aim of the analysis is to anticipate the development of the RET investments in the period 2016-2023 by quantifying the levels of annual full load hours[30] (FLHs) of operation to trigger investments in RETs and then, compare it with the resource potential related to the FLHs of RETs in Turkey. Hence, the term

[29] Energy Market Regulatory Authority

[30] It can be calculated by dividing the average annual amount of electricity generation by the corresponding power plant's installed capacity (i.e. rated power capacity).

FLHs is utilized as a measure of the resource quality of renewable energy resources. The resource potential related to the FLHs of RETs is based on the realized projects in Turkey and the study on the resource quality of renewable energy resources in Turkey which is conducted in the course of the European Union project "Better".

In this respect, uncertainty is considered only for revenue streams; however not for the intermittent generation of electricity by RETs. According to Bjerksund and Ekern (1990, p. 3), "the spot price of the output turns out to be a sufficient statistic for valuation and the relevant state variable for decision rules". Instead of taking into account the corresponding uncertainty in electricity generation, the distribution of RETs in Turkey w.r.t. their FLHs of operation are taken into consideration. The distribution of FLHs of operation is based on the average annual amount of electricity generation[31] and the installed capacity of RETs as indicated in the generation license of the corresponding power plants. In addition, the categorized FLHs of operation, which is based on the resource quality of renewable (i.e. the results of the project Better), is also considered for the analysis. With regard to the different degrees of flexibility and the cost of capital, different investment decision rules and levels of discount rates are taken into account for quantifying the levels of FLHs of operation to trigger investment in RETs.

2.2 Methodology of the Study

Investment opportunities to acquire real assets are called real options (Dixit & Pindyck, 1994, p. 7). The three common features that are shared by most of the investments are given as follows (p. 3):

- The initial costs of investments are partially or completely irreversible.
- There are uncertainties over the future rewards from the investments.
- Investments can be postponed to get more information about the future.

A firm with an opportunity to invest is holding an option analogous to a financial option (p. 6). In particular, a financial call option gives the holder the right but not the obligation to pay an exercise price[32] until a given date and in return receive an asset that has some value (p. 9). Further, once the option is exercised, it is irreversible. Although the asset can be sold to another investor, one cannot retrieve the option or the money that was paid to exercise.

[31] The information is obtained from the publications of EPDK for licensed RETs over 1 MW_{el} installed capacity.
[32] It is also called the strike price.

Similarly, a firm has the option to pay for irreversible investment expenditure (i.e. similar to exercise price) now or in the future, in return for a real asset (e.g. ownership of a hydropower plant) of some value. In analogy to the financial assets, the real assets can be sold to another firm; nevertheless the investment expenditures are irreversible. By exercising the option to invest, the firm forgoes the possibility of resolved uncertainty in the next period which might affect the desirability or timing of the expenditure.

A firm's option to invest is flexibility by being able to postpone an investment and has a value that is not accounted for in net present value analysis (NPV). The NPV of an investment is the difference between the present value of cash inflows (i.e. income) and the present value of the cash outflows (i.e. fixed costs, variable costs, etc.) including the investment cost (see Figure 6 for discrete time NPV analysis). If the NPV of an investment is greater than zero, then the investment should be made and if it is vice versa, the investment should not be made. Hence, the NPV analysis provides a deterministic evaluation of an investment opportunity without considering the value of waiting as an option. This lost option value is an opportunity cost that can be accounted for as part of the investment cost by utilizing the method of real options.

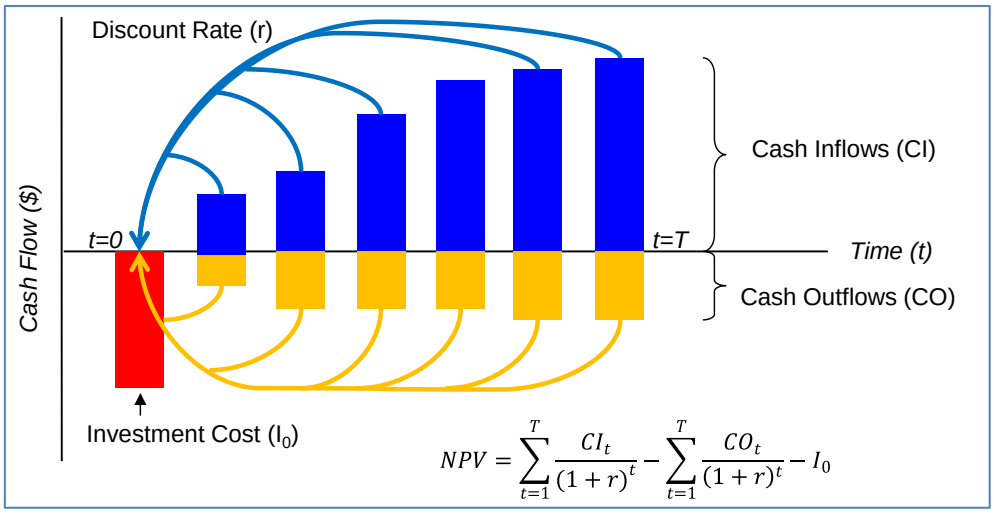

Figure 6- The discrete time NPV analysis (own illustration)

In this study, the level of FLHs of operation to trigger investment in RETs are quantified w.r.t. the different degrees of flexibility (i.e. immediate and flexible decisions) and different levels of discount rate. By using the NPV approach, the break-even price of an investor's immediate investment decision can be calculated by equating the present value of the revenues to the total cost and then by solving for the break-even price[33] (also can be called

[33] In the Chapter 5, detailed information is given about the calculations.

trigger/threshold price). Accordingly, the decision rule is to invest, if the FiT rate exceeds the calculated breakeven price without taking into account the uncertainty in revenues after the expiration of enrollment in the FiT scheme. In analogy, threshold values for FLHs of operation, which are necessary to trigger investments, can be calculated due to an immediate investment decision. A threshold value for FLHs (i.e. called threshold FLHs) of operation indicates the level above/below which investments should be made/not be made given the FiT rates for RETs. In this respect, the threshold FLHs of operation of a considered technology corresponds to the break-even price which is set as high as the corresponding FiT rate.

By utilizing the real options method, the level of FLHs of operation to trigger investment in RETs can be quantified by taking into account the uncertainty in the wholesale market price of electricity. The type of real option, which is utilized for the analysis, is the option "to postpone an investment", with the objective of maximizing the profits from investment opportunities in RETs. By using this general approach, the investment trigger price corresponding to the FLHs of operation of a project can be calculated taking into account the uncertainty and then, the calculated price can be compared with the expected market price[34] whether to initiate an investment or not. More specifically, the risk adjusted break-even prices are calculated indicating a trigger level below which firms are considered to wait further; even though the NPV based break-even prices may indicate the opposite. Accordingly, the decision rule is to invest the first time the expected market price of electricity exceeds a risk adjusted breakeven price. In analogy to the general approach, threshold FLHs of operation indicates the level above/below which investments should be made/postponed given the expected market price of electricity. In this respect, the threshold FLHs of operation of a considered technology corresponds to the investment trigger price which is set as high as the expected market price of electricity.

To sum up, the results of the mentioned analyses indicate above which level of FLHs to initiate an investment and below which level not to invest on RETs in the period 2016-2023. Accordingly, a discussion on the energy policy 2023 is carried out whether the capacity expansion targets are reachable or not by comparing the calculated threshold FLHs of operation of RETs with the resource quality of renewable energy resources in Turkey.

[34] It refers to the expected annual average wholesale market price of electricity. Note that the expected market price of electricity in the period 2016-2023 is simulated by utilizing the Monte Carlo simulation approach prior to the analysis.

The assumptions for the calculation of the trigger prices and also the threshold FLHs are given below:

- The investments on RETs are irreversible.
- The uncertainty in the value of the project arises from annual average price of electricity in the spot market, while all other inputs are deterministic. Also, no fuel costs are incurred for electricity generation.
- The value of the project underlying the real option follows an exogenously specified stochastic process (i.e. geometric Brownian motion).
- The geometric Brownian motion is claimed to be not leading to large errors without considering short term mean reversion (on the order of 5%), since it is indicated that the short-term mean reversion has minor influence for the long-term investment decision rules (Pindyck, 1999, pp. 24-25).
- The due date of an investment initiation (i.e. due to license obligation) can be extended or a new license can be acquired; in order to enable an investment opportunity that does not expire (i.e. in analogy to a perpetual call option).

The novelty[35] of this study lies in the application of the NPV and the real option analysis to calculate threshold FLHs of operation w.r.t. the different degrees of flexibility and different levels of discount rate. The NPV and the real option analyses have been previously applied on the evaluation of the power plants investments in the Nordic region and Turkey.

Fleten et al. (2007) applied real option method for evaluating investments in decentralized renewable power generation under price uncertainty by assessing the value of option to postpone an investment in Nordic markets. Further, Bøckman et al. (2008) applied real option method on three different Norwegian small hydropower projects for making optimal investment decision by assessing the value of option to postpone an investment. Furtmore, Fleten and Ringen (2009) applied real option method for analyzing the path of the expansion of wind power farms and small hydropower plants in Norway. Moreover, Boomsma et al. (2012) analyzed investment timing and capacity choice for renewable energy projects according to feed-in tariffs and renewable energy certificate trading in the Nordic region. Finally, Nygård (2013) analyzed the effect of introducing renewable energy certificates on small hydropower plant investments in Norway.

[35] See footnote 17 on page 8 for detailed information concerning the novelty of this approach.

Kumbaroglu et al. (2005) analyzed the development of the power plant investments in the period 2008-2025 in Turkey by using a real option based investment planning model. In addition, the learning curve information of renewable power generation technologies was integrated into a dynamic programming formulation. Further, Madlener and Stoverink (2010) evaluated the economic feasibility of constructing a 560 MW coal-fired power plant in Turkey by calculating the real options values as a sequential investment. Furthermore, Yılmaz (2014) analyzed uncertainty-investment relationship for coal fired power plant investments in Turkey. Finally, Onar and Kılavuz (2015) analyzed wind power plant investments in Turkey as a put option created through the feed-in tariffs for the wind power plant investments.

2.3 Organization of the Study

This study is organized into 6 chapters.

In Chapter 3, an insight into the electricity sector of Turkey is provided with the emphasis on the basic regulatory framework and the participants. In Chapter 4, information about the fossil fuel reserves and the potential of renewable resources for electricity generation is given. In Chapter 5, theoretical information is provided about the dynamic programming approach for quantifying the investment trigger prices. In Chapter 6, simulation of the expected market price of electricity in the period 2016-2023 is carried out by utilizing the Monte Carlo approach. In Chapter 7, assessments related to the investments on RETs are conducted. In Chapter 8, a conclusion is provided for summarizing the purpose and discussing the results of the assessments.

3 THE BASIC REGULATORY FRAMEWORK OF THE TURKISH ELECTRICITY MARKET

In the 1970s, the Turkish electricity sector was considered as a natural monopoly and all sectoral activities other than distribution (duty of municipalities until 1982) were carried out by Turkish Electricity Authority (TEK). TEK, established in 1970, retained its public monopoly status until the year 1984 (Atiyas, Çetin, & Gülen, 2012, p. 20). Since the 1980s, Turkey carried out regulatory reforms for the electricity sector to enhance competition and efficiency under the consideration of supply security and reliability. Through the implementation of several reforms, the electricity sector was institutionally restructured (see Figure 7) and the participation of private investors is enabled through various ownership models.

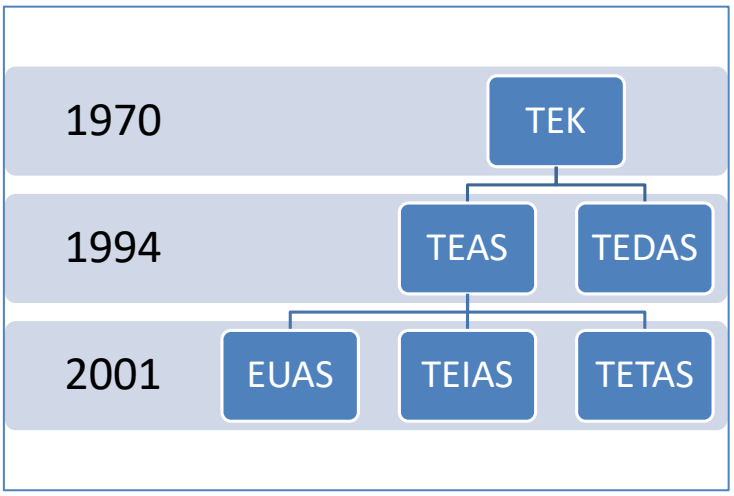

Figure 7- The institutional development of the Turkish electricity sector (own illustration)

In 1994, TEK was split into two corporatized entities, the Turkish Electricity Generation and Transmission Company (TEAS) and the Turkish Electricity Distribution Company (TEDAS). TEAS was in charge of both electricity generation and transmission, and TEDAS carried out the distribution and retail sale activities (Atiyas, Çetin, & Gülen, 2012, p. 21). In the year 2001, the Electricity Market Law (EML, Law No. 4628) was enacted to initiate liberalization of both electricity supply and demand and the establishment of an independent regulatory authority (Bagdadioglu & Odyakmaz, 2009, pp. 145-146). The company TEAS was split into three companies which have been active in different sub-sectors of electricity as follows:

- The Electricity Generation Company (EUAS) owns and operates both thermal and renewable energy power plants.
- The Turkish Electricity Transmission Company (TEIAS) is the sole transmission system operator.
- Turkey Electricity Trading and Contracting Company (TETAS) carries out trading business in wholesale electricity market.

Note that the companies EUAS, TEDAS, TEIAS, TETAS are public corporations and are managed by the Turkish government. TEDAS exists as a corporation but it does not take part in distribution and retail sale activities since the privatization of the electricity grids in the distribution regions.

Through the introduction of EML, Energy Market Regulatory Authority (EPDK) was established. EPDK, which is an autonomous public institution, is responsible for the regulation of the electricity, the natural gas and the petroleum markets. In order to participate in the energy sector, an enterprise has to obtain a license for the desired sectoral activity (e.g. license for electricity generation, trading, distribution, retailing, etc.). The licenses are granted for minimum of 10 years and for maximum of 49 years (Bagdadioglu & Odyakmaz, 2009, p. 146). According to EML, an enterprise can have a maximum market share of 20% in electricity generation.

EPDK is also in charge of regulating transmission tariffs, distribution tariffs, grid connection and use tariffs, retail tariffs for non-eligible consumers (Atiyas, Çetin, & Gülen, 2012, p. 12). The liberalization of the demand side proceeds by lowering the threshold level of consumption every year such that consumers with annual consumption exceeding that level is designated as ‘‘eligible consumers’’. The eligible consumers have the right to choose their own suppliers; whereas the non-eligible consumers do not have. The limit for being an eligible customer has been decreased from 7.8 GWh_{el} to 4000 kWh_{el} in the period 2004-2015 (Turkey Electricity Trading and Contracting Company, 2015, p. 12). In year 2014, 85% of the consumers were categorized as eligible customers; however in practice, only 45% of the consumers used their rights.

Starting from the year 1984, private investors are entitled to participate in the electricity sector through different types of concession contracts such as Build-Operate-Transfer (BOT) for power plants and Transfer of Operating Rights (TOOR) for existing generation and

distribution facilities (Atiyas, Çetin, & Gülen, p. 21). The main reasons for introducing such concessions were the lack of investments in the industry with the increasing electricity demand and the inefficiency of state enterprises.

Through BOT concession contract, a private investor can build and operate a generation plant for 49 years and then has to transfer the plant to the state at no cost (Atiyas, Çetin, & Gülen, p. 21). Further, TOOR contracts give a private investor the right to operate a government owned facility for a specified period of time and oblige to rehabilitate it, if necessary. In year 1994, tax exemptions and guarantees are provided by the ratification of the Law No. 3996. In the year 1997, Build-Own-Operate (BOO) contract was introduced and the corresponding types of private investments are also granted treasury guarantees by the enactment of the Law No. 4283. BOO model allows private investors to retain ownership at the end of the contract period.

Most importantly, the mentioned concessions encompass purchase agreements (take-or-pay obligations) between the private company and the buyer (TETAS). Correspondingly, the buyer is required to purchase a specified amount of electricity at pre-specified prices or price formulas over duration of 15–30 years (Atiyas, Çetin, & Gülen, p. 22). By the early 2000s Turkey had pledged to IMF[36] to end treasury guarantees to enhance competition; however treasury guarantees are still granted by the Turkish government. Namely, Akkuyu (4800 MW_{el}) and Sinop (4480 MW_{el}) nuclear power plants are granted treasury guarantees for 15 and 20 years respectively. The electricity generated by those power plants will be purchased by TETAS for the specified durations (Turkey Electricity Trading and Contracting Company, p. 22).

At the end of 2014, the total installed capacity of power plants reached 69520 MW_{el}. The share of EUAS and its affiliates in total installed capacity was approximately 32%, whereas the share of private generators (including independent power producers, auto-producers[37], and unlicensed generators) amounts to around 55%. The total installed capacity of the plants, which operate under the TOR, BOO and BOT models, was about 13%. Thus, the competition on the supply side of the Turkish electricity market has not been achieved yet. The portfolio of EUAS is under privatization with the ongoing liberalization process. It is planned that the thermal power plants (about 9 GW_{el} in total) and the smaller hydro plants will be privatized;

[36] International Monetary Fund

[37] An autoproducer and autoproducer group are legal entities engaged in electricity generation primarily for their own needs.

whereas the major hydro plants with higher installed capacities (about 6 GW_{el} in total) will remain in its portfolio to reduce the impact of stranded costs on electricity price due to the BOO, BOT and TOR contracts.

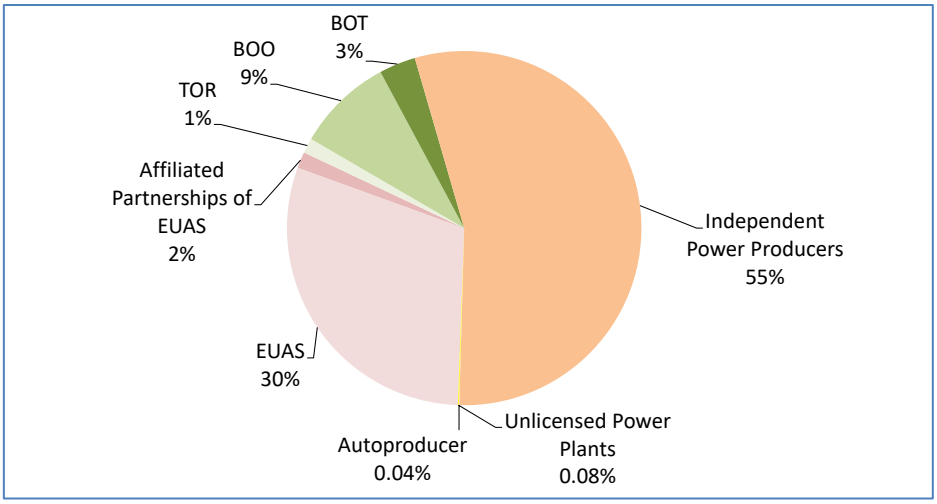

Figure 8- The distribution of Turkey's installed capacity w.r.t. the electricity utilities in the year 2014 (own illustration according to TEIAS)

The total amount of electricity generated by all types of power plants reached about 252 TWh_{el} at the end of 2014. The share of EUAS and its affiliates in total generation was approximately 28%, whereas the share of private generators amounts to around 48%. The total generation of the plants, which operate under the TOR, BOO and BOT models, was about 24%.

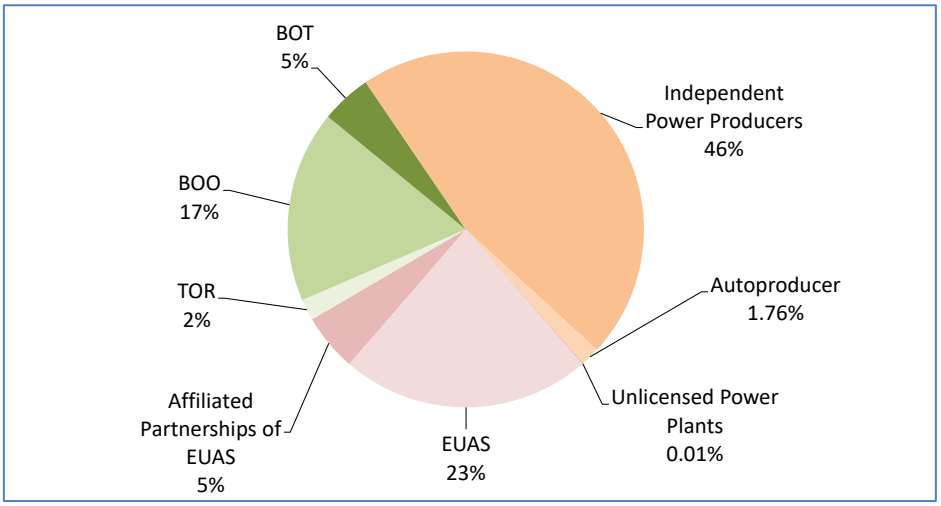

Figure 9- The distribution of Turkey's electricity generation by the electricity utilities in year 2014 (own illustration according to TEIAS)

The Turkish wholesale electricity market is composed of a spot and a bilateral contracting market. The participants of the spot market are generation, autoproducer, wholesale and retail licensees. Energy Markets Operating Corporation (EPIAS) is established on the 12.03.2015 and took over the market operation from PMUM[38] on the 01.09.2015. EPIAS is a market for energy and energy related products through which day ahead, intra-day spot transactions are carried out at the moment. The shareholders of EPIAS are TEİAS (30%), Istanbul Stock Exchange (30%) and the remaining 40% share is open for licensees in the electricity sector; however a licensee is entitled to purchase %4 of shares at most for avoiding monopolization (Herdem, 2015). There have been 97 applications for purchasing shares. Note that EPIAS is in its infant stage compared to European Power Exchange.

The wholesale electricity market of Turkey is dominated by EUAS and TETAS by having a market share of around 52% in generation (see Figure 9). Note that TETAS plays the role of both seller and buyer in the wholesale electricity market. More specifically, TETAS buys electricity from EUAS, from the power plants which operate under the model of BOO, BOT and TOR and also carries out import and export of electricity. The share of TETAS in total electricity consumption has been diminishing since the year 2006. In the year 2006, the corresponding market share of TETAS was 68%; whereas it decreased to 48% in the year 2014 (Turkey Electricity Trading and Contracting Company, p. 17). In the year 2014, TETAS sell 97% of its capacity to retailers and to distribution companies; whereas only 3% of it in PMUM and via bilateral contracts. The number of licensed companies operating in the wholesale market rose from 89 to 172 in the period 2010-2014. The increase in the number of participants is due to the increasing number of eligible customers which can freely choose their own supplier. It will take some years for the Turkish electricity market to be liberalized.

In summary, the Turkish electricity market is still in the transitional phase to a fully liberalized market. It has been observed that a fully liberalized market may take a decade or more under the status quo. Although the total market share of EUAS and TETAS is still high; the ongoing privatization of the state-owned generation portfolio, high renewable energy potential and the increasing demand for electricity make the Turkish electricity sector attractive for new entry in different business activities.

[38] PMUM (Market Financial Reconciliation Center), which was a transitory market to EPIAS, had started its operation on the 01.12.2009 and was operated by TEIAS. The participants were able submit hourly bids/offers in the day ahead market, in the balancing market and for ancillary services.

4 THE POTENTIAL OF DOMESTIC ENERGY RESOURCES OF TURKEY

In Turkey, electricity is generated from various domestic and imported energy resources. The domestic fossil energy resources utilized for electricity generation are lignite, hard coal and asphaltite[39]; whereas the imported fossil energy resources are hard coal, natural gas and oil. As for renewable energy resources, electricity is generated from hydropower, wind, geothermal, solar and biomass energy. In the next sections, information about the fossil fuel reserves and the potential of renewable resources for electricity generation is given.

4.1 The Fossil Fuel Reserves of Turkey for Electricity Generation

The growing electricity demand and the importance of electricity supply security have turned attention towards fossil fuel reserves of Turkey. Coal is one of the plentiful and widely distributed primary energy resources in Turkey. The major coal fields of Turkey are depicted in Figure 10. Lignite reserves make up the major coal reserves of Turkey; whereas hard coal is available only north-west Black Sea coast in the provinces of Zonguldak and Bartin. Asphaltite is located only in the south-east of Turkey in the province of Şırnak.

Figure 10- The major coal fields in Turkey (Turkish Coal Enterprises Institution, 2015, p. 23)

[39] See Footnote 4 on p. 2 for information about asphaltite.

Lignite Reserves of Turkey

According to the coal sector report by Turkey Coal Enterprises Authority (TKI), the total lignite reserves have reached 14.2 billion tons in year 2014 (Turkish Coal Enterprises Institution, p. 32). The majority of the lignite reserves are in Afsin- Elbistan basin (marked as red color in Figure 10) which accounts for 38% (about 4.8 billion tons) of the total deposits of Turkey (Electricity Generation Company, 2015, p. 17). Although the amount of Afsin-Elbistan lignite reserve is quiet high, the lignite has low calorific value and contains relatively high amounts of ash, moisture and sulfur. The other major basins are in Konya-Karapınar (1.8 billion tons), Afyon-Dinar (941 million tons), Eskisehir-Alpu (902 million tons), Manisa-Soma (720 million tons) and Ankara-Cayırhan (366 million tons).

In Turkey, approximately 71% of the total reserves have calorific value below 1500 kcal/kg and 90% of total reserves have calorific value below 3000 kcal/kg (Electricity Generation Company, p. 17). The share of good quality lignite, which is over 3000 kcal/kg, is only 10%. Besides, more than half of the reserves contain moisture over 20%. The majority of the lignite resources having low calorific value are utilized in thermal power plants. Good quality resources are utilized in the industry sector and for heating residences. In Table 4, the lignite fields of Turkey and their potential for power plant capacities are listed. The potentials are calculated according to the producible reserve of lignite reserves, existing power plant capacity and capacity under construction in the corresponding fields in the year 2013. In addition, it is assumed that the calorific value of the lignite is 2200 kcal/kg for every considered field and the power plants operate at 6500 full load hours per year for 30 years (World Energy Council Turkish Committee, 2014, p. 53).

Table 4- The potential of the lignite fields for the installation of power plants in the year 2013 (World Energy Council Turkish Committee, 2014, p. 53)

Lignite Coal Field	Existing Installed Capacity	Capacity under Construction	Remaining Capacity	Total
		MW_{el}		
Afsin-Elbistan	2795	–	8455	11250
Adana-Tufanbeyli	–	450	600	1050
Adıyaman-Gölbaşı	–	–	150	150
Ankara-Çayırhan	620	–	500	1120
Bingöl- Karlıova	-	–	150	150
Bolu-Göynük	–	2x135	–	270
Bursa-Orhanbeyli,Keles,Davraz	210	–	270	480
Çanakkale-Çan	320	–	–	320
Çankırı-Orta	–	–	135	135
Eskişehir-Mihalıççık	–	290	–	290
Konya–Ilgın	–	–	500	500
Konya–Karapınar	–	–	3900	3900
Kütahya-Tunçbilek	365	–	300	665
Kütahya-Seyitömer	600	–	150	750
Manisa-Soma	1034	–	1050	2084
Muğla-Milas	1050	–	–	1050
Muğla-Yatağan	630	–	–	630
Tekirdağ-Saray	–	–	175	175
Sivas-Kangal	457	-	–	457
Total	8081	1010	16335	25426

The lignite reserves of Turkey are owned by the EUAS (53.4%), the TKI (25.8%), the General Directorate of Mineral Research and Exploration (8.5%) and are operated by private sector (12.3%) (Turkish Coal Enterprises Institution, p. 32). The private sector can lease coal fields of the public institutions through tendering procedures. The private companies, which win the tenders, are granted to right to produce coal for a specified time by paying royalty fees to the state. According to TKI, the total share of private companies in the domestic coal market of Turkey is envisaged to surpass 40% and the total share of EUAS and its affiliates will decrease up to 30% (Turkish Coal Enterprises Institution, p. 23). At of the end of 2014, the installed capacity of lignite fired power plants has reached 8693 MW_{el} which corresponds to 34% of the above mentioned potential. The electricity generation from lignite fired power plants amounts to 36615 GWh_{el} at the end of 2014.

Hard Coal Reserves of Turkey

Hard coal is mined only in Zonguldak coal basin in the north-west Black Sea coast. The geological reserves of the basin, calculated down to 1 200 metre under sea level, are about 1.3

billion ton of which accounts for 38% (506 Million ton) of the proven reserves (Turkish Hard Coal Enterprise Institution, 2015, p. 20). The calorific value of the coal varies between 6200 and 7250 kcal/kg (Turkish Hard Coal Enterprise Institution, p. 21). Several types of hard coal are suitable for use as coking coal. Zonguldak hard coal is mainly consumed by the Catalağzı thermal power plant[40] and heavy industry plants. Around 72% of the hard coal production is carried out by Turkish Hard Coal Enterprise Institution (TTK) which is a state owned company. In Zonguldak, the production amount is decreasing with the decreasing amount of producible reserves and there is not any potential for the construction of new capacity. In Bartin-Amasra, there exists potential for 1100 MW_{el} capacity. A private company initiated the legal procedures for the construction of a power plant in Amasra; however the state court declined the power plant project due to the environmental concerns. The future of the project is unclear.

Table 5- The potential of the hard coal fields for the installation of power plants in the year 2013 (World Energy Council Turkish Committee, p. 53)

Hard Coal Field	Existing Installed Capacity	Capacity under Construction	Remaining Capacity	Total
	MW_{el}			
Zonguldak	335	-	-	335
Bartin-Amasra	-	-	1100	1100
Total	335	-	1100	1435

At the end of 2014, the installed capacity of hard coal fired power plants is same as in the year 2013 which corresponds to 24% of the above mentioned potential.

Asphaltite Reserves of Turkey

The asphaltite basins are located only in the province of Şırnak in the southeast of Turkey (see Figure 10). The total asphaltite reserves are estimated to be around 71 million tons (Turkish Coal Enterprises Institution, p. 30). The calorific value of asphaltite is in the range of 5500-5800 kcal/kg. The asphaltite reserves are utilized as fuel in the thermal power plant of Şırnak-Silopi which is owned by a private company (see Table 6). There exist enough reserves to install an additional capacity of 540 MW_{el}.

[40] The hard coal, which is burnt in the Catalagzi power plant, has calorific value of 3300 Kcal/kg.

Table 6- The potential of the asphaltite fields for the installation of power plants in the year 2013 (World Energy Council Turkish Committee, p. 53)

Asphaltite Field	Existing Installed Capacity	Capacity under Construction	Remaining Capacity	Total
		MW_{el}		
Şırnak	135	-	540	675

At the end of 2014, the installed capacity of asphaltite fired power plants is same as in the year 2013 which corresponds to 20% of the above mentioned potential.

Oil and Natural Gas Reserves of Turkey

Turkey is a poor country in terms of oil and natural gas resources. The total recoverable oil reserves of Turkey have reached 45.5 million tons at the end of 2014 (Directorate General of Petroleum Affairs, 2015, p. 18); however 33.8 million tons of oil was consumed in year 2014 and 32.6 million tons of oil was imported (British Petroleum, 2015). Iraq, Iran and Russian Federation are the major countries from which 45% of the total imports were made. At the end of 2014, the installed capacity of diesel and fuel oil fired power plants is 652 MW_{el} which corresponds to about 1% of the total installed capacity. The electricity generation from diesel and fuel oil fired power plants amount to around 2 TWh_{el} at the end of 2014.

The total recoverable natural gas reserves of Turkey have reached 5 billion cubic meters (bcm) at the end of 2014 (Directorate General of Petroleum Affairs, 2015, p. 20). In the year 2014, the consumption of natural gas is about 48.7 bcm and only about 1% of it is met from domestic gas production (Energy Market Regulatory Authority, 2015, p. 5). Further, Turkey exports about 0.6 bcm of natural gas to Greece. Furthermore, Turkey imported about 49.3 bcm of natural gas in total and around 55% of the total natural gas is imported from Russia (around 27 bcm). In Figure 11, the breakdown of total natural gas import of Turkey is illustrated w.r.t. the countries. Note that the label "Others" indicates the imports from spot markets of Qatar, Spain, Norway, Trinidad and Tobago and Nigeria. Moreover, Turkey imported about 85% of its gas needs via pipeline and the remaining in the form of LNG[41]. Finally, about 80% of the natural gas is imported by state owned Petroleum Pipeline Company (BOTAS) and the Turkish natural gas market is in the transition phase to a liberalized market.

[41] Liquefied natural gas

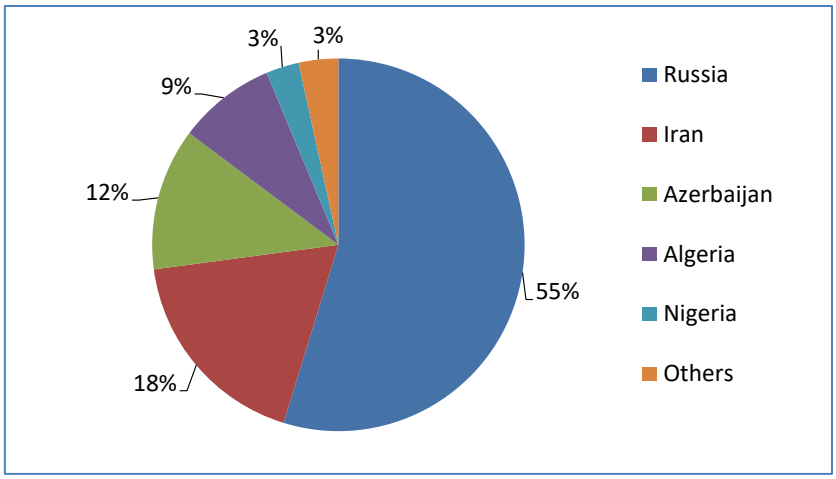

Figure 11- The breakdown of the natural gas imports of Turkey by countries in the year 2014 (own illustration according to EPDK)

4.2 Renewable Energy Potential of Turkey

In the next subsections, information is given about the potential of hydropower, wind power, solar power, geothermal power and biomass in Turkey.

Hydropower Energy Potential of Turkey

Hydropower plays a key role in sustainable energy development of countries where it is abundant. In Figure 12, the hydropower potential of the countries in Europe and Russia are illustrated. It can be inferred from the figure that Russia, Norway, Turkey, France and Italy possess much of the gross hypothetical hydropower energy potential varying in the range of 200-2300 TWh_{el}/a. In Europe, Norway possess the highest theoretical hydropower energy potential of 560 TWh_{el}/a and Turkey takes the second place with a potential of 433 TWh/a.

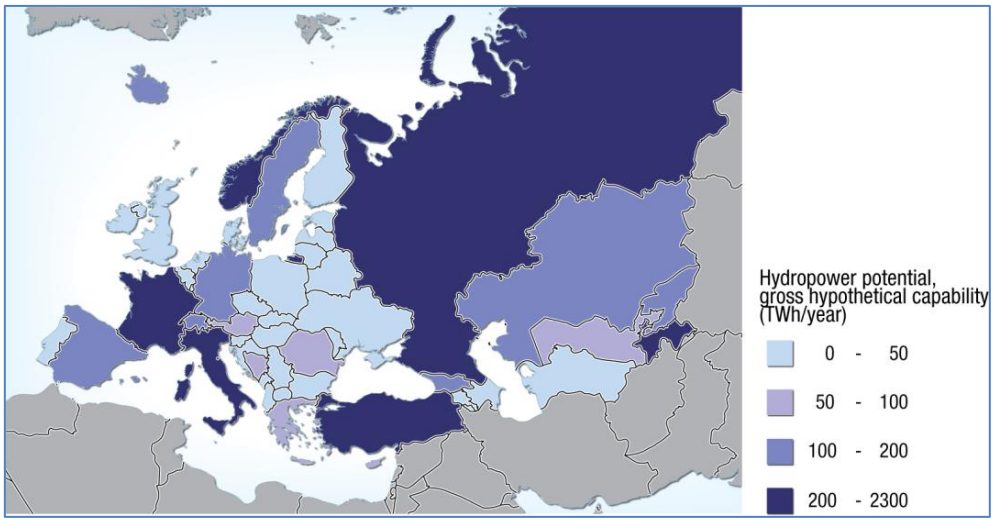

Figure 12- The hydropower potential in Europe and Russia (GRID-Arendal, 2015)

The technical hydroelectric potential of Turkey is about 215 TWh_{el}/a (Directorate General of Renewable Energy, 2015). The technical hydroelectric potential is limited practically with the available technology and unavoidable losses at water fall, during water flow and during conversion. The further limitations which may lead to reduce the technical potential are impoundment of large settlements, industrial estates and agricultural lands. The economical hydroelectric potential of Turkey is about 140 TWh/y (corresponds to 36000 MW_{el}); however this potential does fluctuate considering the changes in energy prices, cost of electricity generation with alternative resources, world's and country's economic situation. Therefore, the potential resources which are not economic at a time can become economic in the future.

At the end of 2014, installed hydropower plants has reached 23664 MW_{el} which correspond to 70% of the above mentioned potential. In addition, the electricity generation by the corresponding power plants amounts to 41 TWh_{el}.

Wind Energy Potential of Turkey

Electricity generation from wind power brings about security of energy supply in terms of reducing dependency on imported energy resources; however it is an intermittent energy resource and its contribution to the electricity supply reliability is relative low. The most favorable areas for high wind energy potentials are at coastal lines, at open spaces, hills and at the mountains (see Figure 13). The highest average speed of wind is observed along the west cost of Turkey, around the Marmara Sea and along the Mediterranean cost in a number of cities such as Mersin and Hatay. In the wind atlas of Turkey, wind resources are categorized into 7 classes for power generation according to their annual average wind speeds (see Figure 13). The quality of wind resources increases from class 1 (ineligible resource with annual average speed lower than 3 m/s) to class 7 (perfect resource with annual average speed higher than 9.5 m/s).

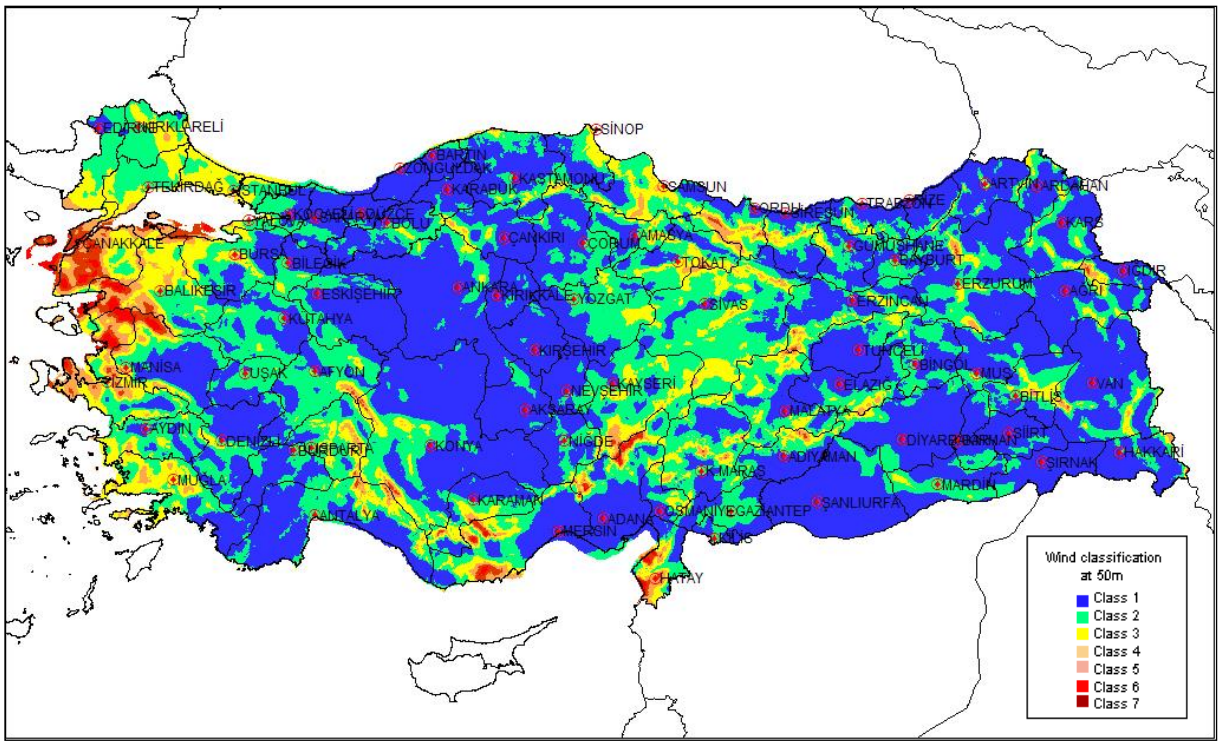

Figure 13- The classification of wind speed at an altitude 50 m (Caliskan, 2011, p. 12)

In the wind atlas of Turkey, it is mentioned that the economical wind power potential encompasses the localities where annual average wind speed is 7 m/s and higher. In the light of the defined wind classification criteria, the wind power potential of Turkey is 47,899.44 MW_{el}, if the wind classes from 4 up to 7 are considered (see Table 7). In particular, the onshore and the offshore potentials are 37,386.16 MW_{el} at 50 altitude and 10,463.28 at up to 50 m water depth respectively. Including class 3 on the other hand, the potential of wind power increases to 131,756.30 MW_{el} (Caliskan, p. 23). The corresponding onshore and offshore potential are 114,363.20 MW_{el} and 17393.1 MW_{el}.

Table 7- The power potential of onshore and offshore wind resources considering the classes 4 and 7 (own illustration according to Caliskan, p. 23)

Quality of Wind Resource	Wind Class [-]	Wind speed at 50 m [m/s]	Installable Capacity [MW]
Good	4	7.5 – 8.1	29259
Perfect	5	8.1 – 8.6	12994
Perfect	6	8.6 - 9.5	5400
Perfect	7	> 9.5	196
		Total	47849

At the end of 2014, installed capacity of onshore wind power plants has reached 3612 MW_{el} which correspond to 7.5% of the above mentioned potential. In addition, the electricity generation by wind and geothermal power plants amounts to 11 TWh_{el}.

Solar Energy Potential of Turkey

Solar energy, which is the most abundant energy resource on earth, has gained importance with the increasing scarcity of fossil energy resources. Turkey is one of the countries in Europe that can benefit from its high solar energy potential to cope with the problem of secure supply of energy in the future. Turkey has a solar energy potential of about 10^{15} kWh/y and this potential is about four thousand times the amount of electricity generated in Turkey in year 2014 (World Energy Council Turkish Committee, 2007, p. 8). The solar energy potential evaluations made by Directorate General of Energy Affairs (EIE) revealed that average annual solar radiation in Turkey is about 1311 kWh/m²-year and the annual average total irradiation duration is about 2640 hours (Ozturk & Yuksel, 2016, p. 1264). In Figure 14, the solar energy potential atlas of Turkey is illustrated. It can be inferred from the figure that more than 60% of Turkey's total surface area has solar energy potential above 1500 kWh/m²-year. The high potential areas are generally on the south and to the south east of the country. The south east Anatolia has the highest solar energy potential (1460 kWh/m²-year) and sunshine duration (2993 hours) compared to other locations. The Black Sea region has the lowest solar energy potential (1120 kWh/m²-year) and sunshine duration (1971 hours) which are close to the values of Germany. The provinces of Antalya, Konya, Karaman and Van are a few of the high solar energy potential possessing cities in Turkey.

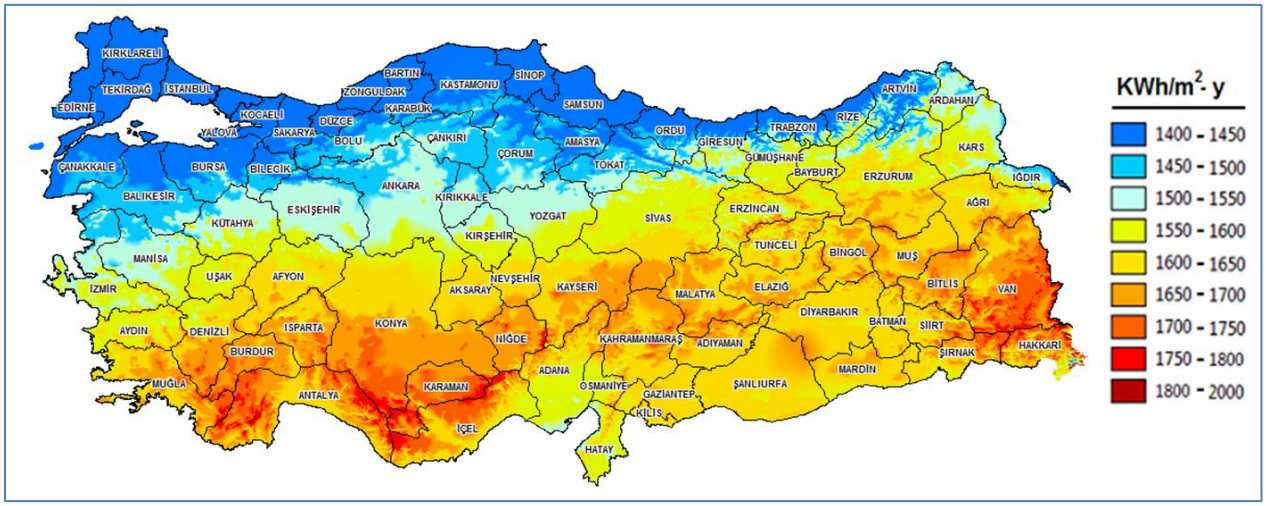

Figure 14- The solar energy atlas of Turkey (Directorate General of Renewable Energy , 2015)

At the end of 2014, installed capacity of solar PV (Photovoltaic) systems has reached 40 MW_{el} which correspond to 0.2% of the above mentioned potential. In addition, the electricity generation by solar PV systems amounts to 17 GWh_{el}.

Geothermal Energy Potential of Turkey

Turkey has significant potential of geothermal power production, possessing one-eighth of the world's total geothermal potential (Balat, 2008, p. 1655). Turkey's geothermal energy potential is ranked as 7th highest potential in the world (Directorate General of Mineral Research and Exploration, 2015, p. 103) and as the highest potential in the Europe (see Figure 15). In Turkey, geothermal resources are utilized for both power generation and district heating. The estimated geothermal power and heating potential are about 1500 MW_{el} and 31,500MW_{th} respectively (Directorate General of Renewable Energy, 2015). Geothermal resources exist all over the country; however more than 80% of the resources is located in the western part of Turkey. The corresponding geothermal fields are mostly high temperature geothermal fields and are suitable for power generation. The geothermal fields on the eastern part of Turkey have temperatures in the range of 40°C-60°C and are not favorable for electricity generation.

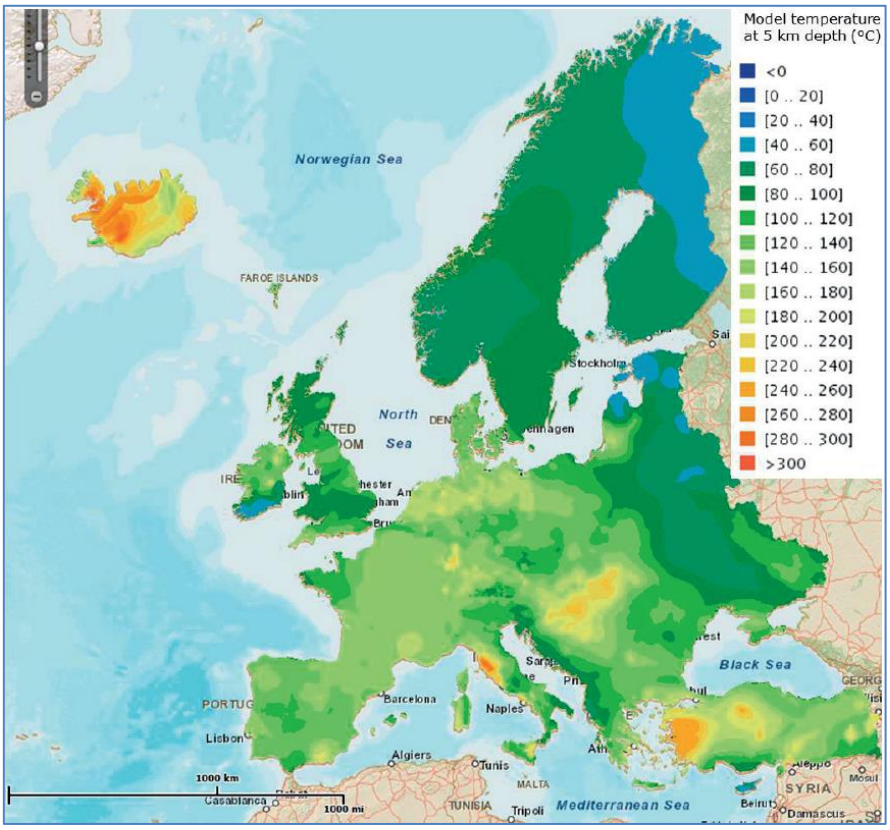

Figure 15- The modelled temperature for geothermal energy at 5 km depth in Europe (European Commission, 2015, p. 12)

At the end of 2014, installed capacity of geothermal power plants has reached 405 MW_{el} which correspond to 27% of the above mentioned potential.

Biomass Energy Potential of Turkey

Turkey is one of the developing countries which have various agricultural byproducts to be utilized as biomass or to produce biogas. Various agricultural residues such as grain dust, wheat straw, hazelnut shell etc. and wastes from livestock farming are available countrywide. In addition, landfill gas, municipal and industry wastes, forestry and wood processing residues have been recently utilized for electricity generation. The biomass and biogas potential of Turkey is estimated to be around 4000 MW_{el} (Investment Support and Promotion Agency, 2013, p. 10). The gasification capacity of forestry waste amounts to 600 MW_{el} of the total potential (Investment Support and Promotion Agency, p. 34).

At the end of 2014, installed capacity of biogas and waste fired power plants has reached 288 MW_{el} which correspond to about 7% of the above mentioned potential. In addition, the electricity generation by the corresponding power plants amounts to 1.4 TWh_{el}.

4.3 A Summary on the Domestic Energy Resources of Turkey

The aforementioned information on the domestic energy resources of Turkey is tabulated in Table 8. Accordingly, the potential of domestic energy resources is categorized into utilized installed capacity in the year 2014, targeted installed capacity in the year 2023 and the total potential. It can be inferred that about 51 GW_{el} installed capacity of new power plants is targeted to be commissioned until the year 2023. Therefore, the energy policy 2023 is an ambitious target to which the Turkish government has committed itself.

Table 8- The utilized, targeted and potential installed capacity of domestic energy resources of Turkey (own illustration)

Domestic Resource	Installed Capacity in 2014 [MW_{el}]	Target Installed Capacity in 2023 [MW_{el}]	Total Potential [MW_{el}]
Lignite	8693	25426	25426
Hard Coal	335	1400	1400
Asphaltite	135	675	675
Hydropower	23664	34000	36000
Wind	3612	20000	48000
Solar	40	5000	10^{15} kWh/a
Geothermal	405	1000	1500
Biomass	288	1000	4000
Total	37172	88501	

5 THE QUANTIFICATION OF THE TRIGGER PRICES FOR INVESTMENTS

In this chapter, information is given about the dynamic programming approach for quantifying the investment trigger prices. The given information is based on the text book "Investment under Uncertainty" by Dixit and Pindyck (1994) and the article "Investment and Hysteresis" by Dixit (1992) as the main references. Detailed information can be found in the Chapters 4 and 5 of the corresponding book and in the corresponding journal.

The trigger price for an investor's flexible investment decision is defined to be indicating the price which is sufficient to make an investment decision considering the value of the project to be uncertain; whereas the investment costs, operational costs and the expected amount of annual electricity generation by RETs are assumed to be deterministic. The value of the RET projects are uncertain due to the uncertainty in the annual average wholesale market price of electricity which is assumed to follow a geometric Brownian motion (GBM):

$$dS_t = \alpha_s S_t \, dt + \sigma_s S_t \, dz \tag{4.3.1}$$

The symbol "S_t" indicates the annual average market price of electricity in year t. The symbols "α_s" and "σ_s" are constants and represent the drift rate and the volatility of the corresponding electricity price respectively. In Eq. (4.3.1), the last term indicates the standard Brownian motion and is explicitly expressed in Eq. (4.3.2). The term "ϵ_t" is considered to be a normally distributed random variable with a mean of zero and a standard deviation of one. The term "dt" denotes the time increment.

$$dz = \epsilon_t \sqrt{dt} \tag{4.3.2}$$

The expected present value of the project (V) is a linear function of the expected market price of electricity following GBM and is discounted by utilizing continuously compounding rate factor (ρ) as represented below:

$$V(S) = G_{el} \int_0^T (S_0 \, e^{\alpha_s \, t}) e^{-\rho t} dt \tag{4.3.3}$$

After taking the integral, the Eq. (4.3.3) can be expressed as follows:

$$V(S) = G_{el} \cdot S_0 \cdot \frac{e^{(\alpha_s - \rho)T} - 1}{\alpha_s - \rho} \tag{4.3.4}$$

In Eq. (4.3.4), the symbols, "S_0", "G_{el}" and "T" denote the annual average market price of electricity in the first year of operation, the expected amount of annual electricity generation[42] and the economic lifetime of the RET respectively. In Eq. (4.3.4), the future cash inflows are discounted with the required rate of return ρ of the project. The revenue streams continue for T years, after commissioning of the power plant. The expected NPV of the project ($\Omega(S_0)$) can then be calculated by taking the difference between the expected revenues and the total costs as expressed below:

$$\Omega(S) = V(S_0) - TC \tag{4.3.5}$$

The total cost of electricity generation by each type of power plant is composed of investment cost (I), discounted total fixed cost of operation and maintenance ($TFC_{O\&M}$) and discounted total variable cost of O&M ($TVC_{O\&M}$) as indicated below:

$$TC = I + TFC_{O\&M} + TVC_{O\&M} \tag{4.3.6}$$

It is assumed that the fixed cost of operation and maintenance ($fc_{O\&M}$) and the variable cost of O&M ($vc_{O\&M}$) develop w.r.t. the given growth/decline rate i[43] and are discounted back to time zero w.r.t. the risk free rate of interest r as indicated below for the calculation of $TFC_{O\&M}$:

$$TFC_{O\&M} = \int_0^T (fc_{O\&M}\, e^{i\,t}) e^{-rt} dt \tag{4.3.7}$$

After taking the integral, the Eq. (4.3.7) can be expressed as follows:

$$TFC_{O\&M} = fc_{O\&M} \cdot \frac{e^{(i-r)T} - 1}{i - r} \tag{4.3.8}$$

[42] Note that the investment analyses are carried out for 1 MW_{el} installed capacity. Therefore, the expected amount of annual electricity generation equals to the annual FLHs of operation.

[43] This rate is considered; in order to take into account the developments in the corresponding costs depending on the technological prospects.

The $TVC_{O\&M}$ of a power plant can be calculated as follows:

$$TVC_{O\&M} = G_{el} \int_0^T (vc_{O\&M}\, e^{i\,t}) e^{-rt} dt \tag{4.3.9}$$

After taking the integral, the Eq. (4.3.9) can be expressed as follows:

$$TVC_{O\&M} = G_{el} \cdot vc_{O\&M} \cdot \frac{e^{(i-r)T} - 1}{i - r} \tag{4.3.10}$$

If an investment opportunity on a RET is a now or never decision, an investor must give an immediate decision whether to invest now or not at all. According to the Marshall' s analysis of long run equilibrium under competitive condition, if the market price exceeds long run average cost, investments are triggered not only for new entry but also for capacity expansion. The trigger price (or break-even price) for an investor's immediate investment decision ($S_{immediate}$) can be calculated by equating the expected present value of the revenues to the total cost and then by solving for $S_{immediate}$ as expressed below:

$$G_{el} \int_0^T (S_{immediate}\, e^{\alpha_s\, t}) e^{-\rho t} dt = TC \tag{4.3.11}$$

After taking the integral and rearranging, the Eq. (4.3.11) can be expressed as follows:

$$S_{immediate} = \frac{TC\ (\alpha_s - \rho)}{G_{el}\ (e^{(\alpha_s - \rho)T} - 1)} \tag{4.3.12}$$

Accordingly, the investment rule is to invest now, if $S_0 > S_{immediate}$ and otherwise reject the investment proposition. Note that in this context, S_0 equals to the FiT rate of the considered RET. In analogy to the general approach, the threshold values for FLHs of operation, which are necessary to trigger investments, can be calculated due to an immediate investment decision. In this respect, the threshold FLHs of operation of a considered technology corresponds to the break-even price which is set as high as the corresponding FiT rate. The corresponding rearrangement of the Eq. (4.3.12) is expressed below:

$$G_{el} = \frac{TC\ (\alpha_s - \rho)}{S_{immediate}\ (e^{(\alpha_s - \rho)T} - 1)} \tag{4.3.13}$$

After rearrangement, the term "G_{el}" in Eq. (4.3.13) is redefined as the threshold FLHs of operation above/below which investments should be made/not be made given the FiT rates for RETs substituting for $S_{immediate}$.

An investment opportunity on a RET is considered to be a perpetual call option and an investor can decide whether to invest or to keep the option alive. Therefore, the dynamic programming approach is utilized for the comparison of the present value that results from the immediate investment decision and from waiting. The corresponding Bellman equation is expressed below:

$$F(S) = max\left\{V(S) - TC, \frac{1}{1+\rho dt} E[F(S+dS)|S]\right\} \tag{4.3.14}$$

The value of the investment opportunity (F) is conditional on S and equals to the maximum value among the termination value (i.e. the left term in the curly braces) and the continuation value (i.e. the right term in the curly braces). By using the dynamic programming approach, a whole sequence of decisions is divided into two components such as the immediate decision and the valuation function. The valuation function is utilized for evaluating the consequences of all subsequent decisions, starting with the state that arises from the immediate decision. The optimal decision can be found by carrying out sequence of computations by initiating from the last decision.

If the payoff from the immediate investment is higher than the one from waiting, then the option is exercised and the investment opportunity equals the termination value. If the value of waiting is higher than the immediate payoff, then the option is held and the value of the investment opportunity equals to the continuation value as indicated below.

$$F(S) = \frac{1}{1+\rho dt} E[F(S+dS)] \tag{4.3.15}$$

In particular, the continuation value equals to the discounted expected value of all future optimal decisions according to considered stochastic process. The Eq. (4.3.15) can be expressed in rearranged form as follows:

$$\rho F(S)dt = E[dF] \tag{4.3.16}$$

Accordingly, over a short period of time dt, the total expected return on the investment opportunity, $\rho F(S)dt$, is equal to its expected rate of capital appreciation (i.e. its expected change in value) (Dixit & Pindyck, 1994, p. 140). It can be inferred from Eq. (4.3.16) that the investment opportunity (i.e. holding an option to invest) is supposed to yield no profits until the investment is under taken. The only return from holding it is its capital appreciation. The term "dF" can be expanded by using Ito's Lemma as follows:

$$dF = \frac{\partial F}{\partial S} dS + \frac{1}{2} \frac{\partial^2 F}{\partial S^2} dS^2 \tag{4.3.17}$$

After substituting Eq. (4.3.1) for dS, the Eq. (4.3.17) takes the rearranged form as indicated below (note that $E(dz) = 0$):

$$dF = \left(\alpha S \frac{\partial F}{\partial S} + \frac{1}{2} \sigma^2 S^2 \frac{\partial^2 F}{\partial S^2} \right) dt + \sigma S \frac{\partial F}{\partial S} dz \tag{4.3.18}$$

After dividing the Eq. (4.3.18) by dt and then rearranging it (considering Eq. (4.3.16)) yields a differential equation which is independent of time but depends on the current start price in the spot market (i.e. so called perpetual call option).

$$\frac{1}{2} \sigma^2 S^2 \frac{\partial^2 F}{\partial S^2} + \alpha S \frac{\partial F}{\partial S} - \rho F = 0 \tag{4.3.19}$$

The solution for $F(S)$ in Eq. (4.3.19) can be computed subject to the three boundary conditions as expressed below:

$$F(0) = 0 \tag{4.3.20}$$

$$F(S_{perpetual}) = V(S_{perpetual}) - I - TC \tag{4.3.21}$$

$$\frac{\partial F(S_{perpetual})}{\partial S_{perpetual}} = 1 \tag{4.3.22}$$

The first boundary condition requires that if S goes to zero, the option to invest will have a zero value as implied by the stochastic process for S (see Eq. (4.3.1)). The second boundary condition is the value-matching condition. The value matching condition requires that upon investing, the firm receives a net pay-off which equals to expected net present value depending on the critical (trigger) price "$S_{perpetual}$". The price $S_{perpetual}$ is the price above

which it is optimal to invest according to the expected market price of electricity. The expected market price of electricity is simulated by utilizing the Monte Carlo simulation approach as explained in the next chapter. The third boundary condition is called the smooth pasting condition. The smooth pasting condition states that if $F(S_{perpetual})$ were not continuous and smooth at the price $S_{perpetual}$, one could do better by exercising at a different point. The third boundary condition helps in finding the position of the second boundary by equating the slopes of the value of waiting and the value of investing at the price $S_{perpetual}$ (see Figure 16).

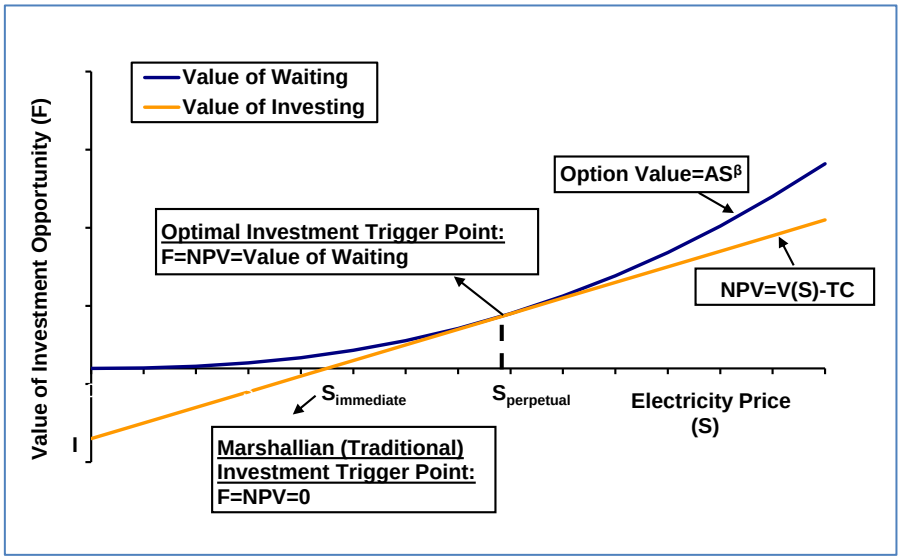

Figure 16- The investment trigger prices w.r.t. the immediate decision and the decision at any time (own illustration according to Dixit (1992, p. 114))

The Eq. (4.3.19) is a second order partial differential equation (PDE) of Cauchy Euler type and a possible solution to it is assumed to have the form $F(S) = S^x$. The so called fundamental quadratic can be obtained by substituting $F(S)$ with S^x and then through rearranging the PDE as represented below:

$$\frac{1}{2}\sigma^2 x(x-1) + \alpha x - \rho = 0 \tag{4.3.23}$$

The left-hand side of the Eq. (4.3.23) is negative at $x = 0$ when $\rho > 0$ and is also negative when $x = 1$ provided $\rho > \alpha$, which is assumed to ensure convergence of the expected discounted present value of the revenues. Accordingly, one root of it exceeds 1 (β); whereas the other one is negative (i.e. γ). The general solution of the PDE can be expressed as follows:

$$F(S) = AS^{\beta} + BS^{\gamma} \tag{4.3.24}$$

In Eq. (4.3.24), the terms A and B are constants to be computed. The value of waiting should go to zero as S goes to zero; since γ has a negative non-zero value, the constant B must consequently be set to zero. Correspondingly, the solution to the Bellman equation takes the form as represented below:

$$F(S) = AS^{\beta} \tag{4.3.25}$$

The root β of the quadratic equation, Eq. (4.3.23), is represented below:

$$\beta = \frac{1}{2} - \frac{\alpha}{\sigma^2} + \sqrt{\left(\frac{\alpha}{\sigma^2} - \frac{1}{2}\right)^2 + \frac{2\rho}{\sigma^2}} \quad > 1 \tag{4.3.26}$$

As a result, A is determined by substituting Eq. (4.3.25) into Eq. (4.3.21) and $S_{perpetual}$ is consequently determined by taking the derivative according to Eq. (4.3.22) and then rearranging as represented below respectively:

$$A = \frac{(V(S^*) - (I + TC))}{\left(S_{perpetual}\right)^{\beta}} \tag{4.3.27}$$

$$S_{perpetual} = \frac{\beta}{\beta - 1} \cdot \frac{(I + TC)}{G_{el} \int_0^T e^{(\alpha_s - \rho)t}\, dt} \tag{4.3.28}$$

Accordingly, the derived Eqs. (4.3.27) and (4.3.28) are utilized for calculating the value of $F(S)$ and $S_{perpetual}$. In this respect, the investment rule is to invest now, if $S_0 > S_{perpetual}$ and otherwise wait. Note that in this context, S_0 equals to the expected market price of electricity. In Eq. (4.3.28), the term $\beta/(\beta - 1)$ acts as a factor for the adjustment of the uncertainty (i.e. risk premium) which is not considered for the calculation of $S_{immediate}$. It can be inferred that as σ increases, β decreases and as a consequence $\beta/(\beta - 1)$ increases. Thus, the greater is the amount of uncertainty over future values of $V(S)$, the larger is the wedge between $V(S^*)$ and $I + TC$, that is, the higher the excess rate of return which is demanded by firms. In addition, as ρ increases, β decreases, so a higher ρ implies a larger wedge between $V(S^*)$ and $I + TC$ which increases value of waiting.

In analogy to the general approach, the threshold values for FLHs of operation, which are necessary to trigger investments, can be calculated for a flexible investment decision. In this respect, the threshold FLHs of operation of a considered technology corresponds to the break-even price which is set as high as the expected market price of electricity. The corresponding rearrangement of the Eq. (4.3.28) is expressed below:

$$G_{el} = \frac{\beta}{\beta - 1} \cdot \frac{(I + TC)}{S_{perpetual} \int_0^T e^{(\alpha_s - \rho)t}\, dt} \tag{4.3.29}$$

After rearrangement, the term "G_{el}" in Eq. (4.3.29) is redefined as the threshold FLHs of operation above/below which investments should be made/not be made given the simulated market price of electricity substituting for $S_{perpetual}$.

6 SIMULATING ANNUAL AVERAGE WHOLESALE MARKET PRICE OF ELECTRICITY

In this study, it is assumed that the annual average wholesale market price of electricity follows a GBM. Through this assumption, the annual average wholesale market price of electricity in the period 2016-2025 is simulated according to the estimated drift rate and volatility from the corresponding price of electricity in the period 2006-2015. The same approach was also utilized by Kumbaroglu et al. (2005, p. 10) and Onar and Kılavuz (2015, p. 1236) in their real option analyses on Turkish electricity market. The simulation of the future prices is carried out by using MATLAB® R2011a function "normrnd" for Monte Carlo simulation approach. In this approach, the random variable ϵ_t is a simulated variable and follows a normal distribution with a mean of zero and a variance of one. In order to calculate the parameters for GBM, n number of past average prices is converted into a return series by taking the logarithm of the ratio of the two consecutive prices as represented below:

$$r_i = \ln\left(\frac{S_{i+1}}{S_i}\right) \quad 1 \leq i \leq n \tag{4.3.30}$$

The drift rate (μ) is estimated by taking the average of $n-1$ number of past returns as follows:

$$\mu = \frac{1}{n-1}\sum_{i=1}^{n-1} r_i \tag{4.3.31}$$

The volatility (σ) is estimated by calculating the standard deviation w.r.t. the past returns as expressed below:

$$\sigma = \sqrt{\frac{1}{n-2}\sum_{i=1}^{n-1}(r_i - \mu)^2} \tag{4.3.32}$$

Accordingly, the drift and volatility parameters are estimated to be -2.2% and 8.7%. In total, 50000 paths are simulated for the annual average wholesale market price of electricity in the period 2016-2023 and 255 of them are displayed in Figure 17. By taking the average of

simulated prices for each corresponding year in the period 2016-2025, the annual average wholesale market price of electricity is calculated as displayed in Figure 18.

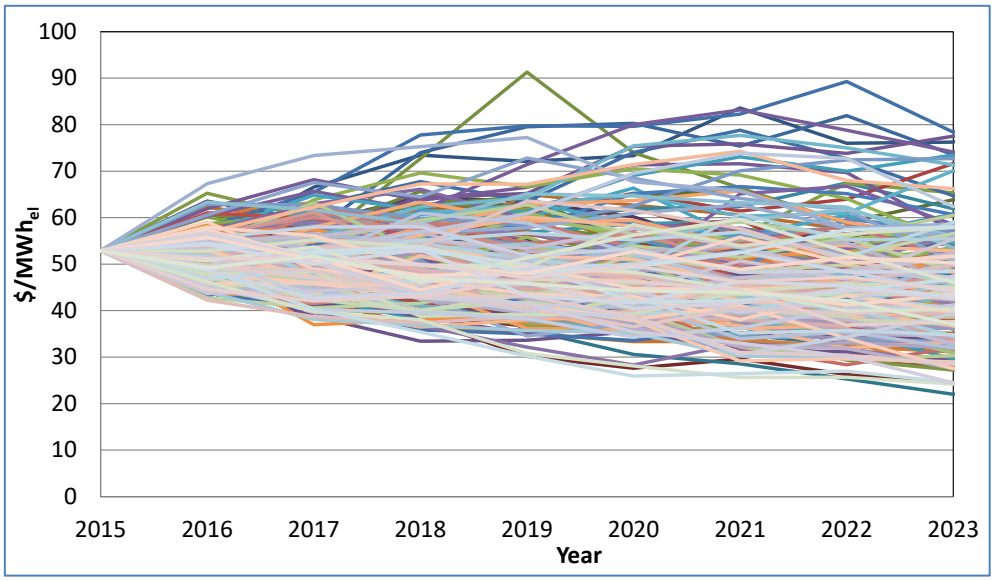

Figure 17- The simulated paths for the annual average wholesale market price of electricity in Turkey (own calculation & illustration)

It can be inferred from Figure 18 that the annual average price for electricity decreases from 2015 level of 53 $/MWh$_{el}$ to 2023 level of 45 $/MWh$_{el}$. This is due to the fact that the electricity price has been in downward trend since the year 2008 which leads to a negative drift rate (see Figure 5 on p. 18 for the reasons of the downward trend).

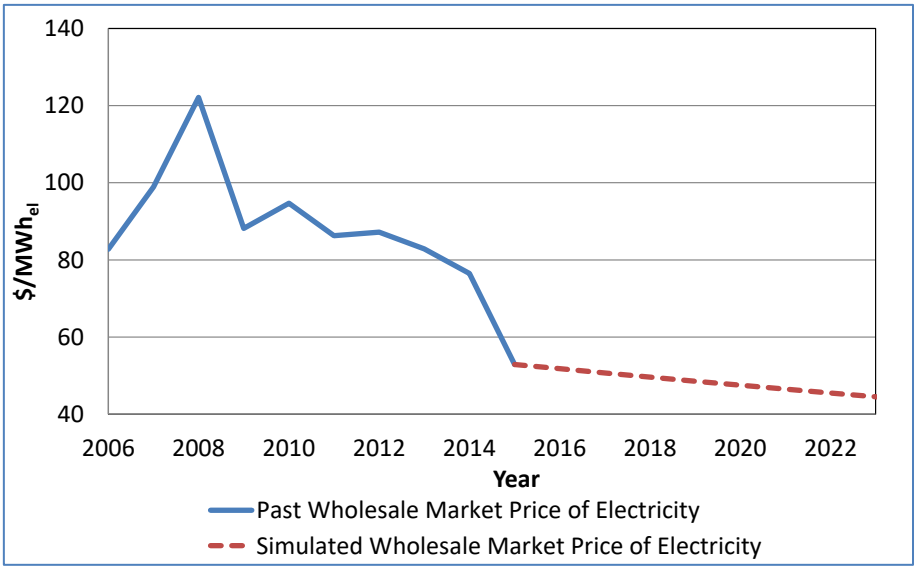

Figure 18- The past and the simulated annual average wholesale market price of electricity in Turkey (own calculation & illustration)

7 ASSESSMENT OF INVESTMENTS ON RENEWABLE ENERGY TECHNOLOGIES

In this chapter, the threshold FLHs of operation to trigger investment in RETs are quantified w.r.t. the different degrees of flexibility (i.e. immediate and flexible decisions) and different levels of discount rate. The threshold FLHs indicate the level above which an investment should be initiated and below which vice versa. In particular, the degree of flexibility in investing is quantified as investment trigger prices for immediate decision (i.e. in analogy to NPV) and decision at any time (i.e. in analogy to perpetual call option). For immediate investment decision, the threshold FLHs of operation of a considered technology corresponds to the NPV break-even price which is set as high as the corresponding FiT rate. For flexible investment decision, the threshold FLHs of operation of a considered technology corresponds to the risk adjusted break-even price which is set as high as the market price of electricity.

The impact of ρ on trigger prices is analyzed by setting ρ at 2%[44], 5% and 8%. The cost of capital is assumed to be 5%[45] for the corresponding investments and the other rates are taken into account as sensitivity analysis. In the report "Projected Costs of Generating Electricity 2015 Edition" (NEA, IEA, OECD, 2015, pp. 143-145), the costs of capital are mentioned to be varying between 3% and 10% and have an average of 7% according to the given responses to the conducted questionnaires in the member countries of OECD. In particular, in this study, all calculations are carried out in US $ and the cost of capital in the USA is also indicated to be 5% (see the corresponding report for more details).

The analyses are carried out considering investment costs[46] and the resource potential related to the FLHs of RETs in Turkey. The related data for each RET such as specific investment, fixed O&M, variable O&M costs and economic life time are tabulated in Table 9 (see Table 11 for the corresponding costs in the Europe and the USA). In the next subsections, detailed information about the represented costs is given.

[44] Note that the weighted average interest rate for US $ by banks in Turkey is about 2% at the end of 2015 (i.e. considered as risk free interest rate in this study).

[45]The minimum Commercial Interest Reference Rates (CIRRs) rates for all direct loans including nuclear power, renewable energies, and hydro is given to be 3.5% for up to 18 repayment years by Export-Import Bank of the United States (Ex-Im Bank) (2016). In addition, IEA also assumes 5% rate for analyzing investments on power plants as mentioned by Grausz (2011, p. 7).

[46] The related costs for all RETs are obtained from the environmental impact assessment reports of those projects. In addition, the name of the projects will not be published due to the data privacy.

Table 9- The cost data utilized in the analysis (own illustration)

Renewable Energy Technology	Specific Investment Cost [$/kW$_{el}$]	Fixed O&M Cost [$/MW$_{el}$-y]	Variable O&M Cost [$/MWh$_{el}$]	Economic Lifetime [Year]
Hydro	2127	53,175	-	50
Wind	1764	49,000	14.3	25
Solar PV	1102	24,813	16.3	25
Geothermal	2197	110,000	-	25
Biomass	1614	32,280	5	25

Note that the represented costs in Table 9 do not include administrative costs (e.g. license fee, grid connection and grid contribution fees) which are paid to the public institutions. The administrative costs are added to the fixed or variable costs of corresponding RETs depending on the officially determined payment structure. Namely, all type of RETs must pay an annual fee for generation license and grid connection which are paid to EPDK and TEIAS respectively. The annual fee for generation license is composed of fixed and variable components. The fixed component is paid only once and amounts to 1935 $/MW$_{el}$ (i.e. 5800 TL/MW$_{el}$ for installed capacity less than or equal to 10 MW$_{el}$). The variable component of the license fee amounts to about 0.01 $/MWh$_{el}$. (0.003 kurus[47]/kWh$_{el}$).

Furthermore, the grid connection fee has two components such as system utilization fee and system operation fee which are paid in TL per MW per annum (TL/MW-y). The system utilization fee[48] differs w.r.t. the transmission regions in Turkey and amounts to 9892 $/MW$_{el}$-y (29692 TL/MW$_{el}$-y) in average. The system operation fee is same in all transmission regions and amounts to 3603 $/MW$_{el}$-y (10814 TL/MW$_{el}$-y).

Finally, hydroelectric resource contribution fee[49], wind power grid contribution fee[50] and solar power grid contribution fee which amount to around 868,697 $/MW$_{el}$ (i.e. 2,714,508

[47] 1 TL equals to 100 kurus.

[48] For RET, only 50% of it is paid for the first five years of operation.

[49] In order to get a generation license from EPDK, water utilization right agreement for the relevant river basin must be signed with the General Directorate of State Hydraulic Works (DSI). The water utilization right is granted to the company which wins the tender. The bids are in TL/MW and must be paid in 3 years and in equal amounts after commissioning of the plant. In this study, the given value is the average value of the tender results and indicates the discounted value of the corresponding equal amounts. See official website of DSI for more information and the tender results.

[50] In order to get a generation license from EPDK, wind and solar projects, which apply for the same transformation center for grid connection, are required to pay contribution fees to TEIAS. The bids are in TL/MW$_{el}$ and must be paid in 3 years and in equal amounts after commissioning of the plant. Note that the given value here is the average value of the previous tender results for wind power plants which were based on kurus/kWh$_{el}$ that is paid during the plant lifetime (i.e. according to the previous tender system).

TL/MW_{el}), 11 \$/MWh_{el} (1.91 kurus/kWh_{el}) and 628,024 \$/MW_{el} (1,884,997 TL/MW_{el}) respectively, are taken into account for the analysis. Note that the analysis is conducted according to the status quo of the regulations during the completion of this study (i.e. in the June 2016). Any regulatory changes, which may be put into effect in the later years, cannot be considered.

A number of studies are examined to anticipate the development of the costs for RETs; since there are not any specific values available for Turkey and especially for the period 2016-2023. Several energy market models and their input data sets are examined by Tidball et al. (2010, p. 43) for the annual change in the specific investment costs of the RETs in the period 2015-2030. Accordingly, it can be inferred from Table 10 that there is not any consensus for the corresponding annual changes due to their modelling approaches and the studied countries/regions. In particular, the decrease in the mentioned costs is due to the developments depending on the corresponding technological prospects. According to the given information in the report "Renewable Power Generation Costs in 2014" by International Renewable Energy Agency (2015, p. 21), the long-term support policies increase the scale of the deployments and the competitiveness of the markets for RETs. In addition, through doubling in cumulative capacity of a RET, the costs can decline by as much as 18% to 22% for solar PV and 10% for wind (i.e. due to high learning rates).

Table 10- The energy market models and the utilized decline rates for specific investment costs of RETs (own illustration according to Tidball et al. (2010, p. 43))

Renewable Energy Technology	Name of Model					
	NEMS[51]	MARKAL[52]	ReEDS [53]	MiniCAM[54]	IPM [55]	MERGE[56]
Wind (onshore)	-1.6%	-1.1%	-0.5%	-0.5%	no change	no change
Solar PV	-3.1%	-2.1%	-3.4%	-3.8%	no change	no change
Geothermal	-2.3%	-0.6%	no change	-0.4%	no change	N/A*
Biomass	-2.7%	N/A	no change	-0.3%	-0.9%	no change

*Technology not included

[51] National Energy Modeling System (NEMS) owned by Energy Information Administration (EIA)
[52] Market Allocation (MARKAL) owned by International Energy Agency and Brookhaven National Laboratory
[53] Regional Energy Deployment System (ReEDS) owned by National Renewable Energy Laboratory (NREL)
[54] Mini Climate Assessment Model (MiniCAM) owned by Pacific Northwest National Laboratory (PNNL)
[55] Integrated Planning Model (IPM) owned by ICF International
[56] Model for Estimating the Regional and Global Effects of Greenhouse Gas Reductions (MERGE) owned by Electric Power Research Institute (EPRI)

Further, the costs for RETs in the Europe and the USA, which are based on the assumed learning rates[57] for the report "World Energy Investment Outlook 2014" (WEIO 2014) by IEA (2014), mostly indicate decline in costs as tabulated in Table 11.

Table 11- The cost assumptions for RETs at regional level in WEIO 2014 (own illustration according to IEA)

Renewable Energy Technology	Region	Specific Investment Cost			O&M Cost		
		Year 2012	Year 2035	Mean Change	Year 2012	Year 2035	Mean Change
		[$/kW$_{el}$]		[%/a]	[$/kW$_{el}$]		[%/a]
Hydro (Large Scale)	Europe	2270	2890	1%	53	67	1%
	United States	2510	2500	0%	62	61	0%
Wind	Europe	1790	1630	-0.4%	46	41	-0.5%
	United States	1890	1710	-0.5%	47	42.8	-0.5%
Solar PV (Large Scale)	Europe	2490	1440	-3%	25	22	-1%
	United States	3000	1730	-3%	32	28	-1%
Geothermal	Europe	2980	2820	-0.2%	60	56	-0.3%
	United States	2090	1890	-0.5%	42	38	-0.5%
Biomass	Europe	2380	2170	-0.4%	83	76	-0.4%
	United States	2500	2320	-0.3%	87	81	-0.3%

In this study, the specific investment, fixed and variable O&M costs of hydropower plants are assumed to be not changing in the period 2016-2023; since hydropower is a mature technology (NEA, IEA, OECD, 2015, p. 157). The related costs of remaining RETs are assumed to be decreasing at a moderate decline rate of 1%/a in the period 2017-2023, considering the technological prospects in the examined studies.

In the following sections, the results of the corresponding analyses on hydropower, wind power, solar pv power, geothermal power and biomass power plants are discussed respectively. All computations are carried out by Excel® 2010 based tool according to the given algorithms in Chapter 5.

7.1 Assessment on Hydropower Plants

The given investment cost for the analysis of the hydropower plant investments (in Table 9) is based on the examples of the hydropower projects in Turkey as tabulated in Table 12. It can be inferred from the table that the installed capacities of the example projects range from 2 MW_{el} to 170 MW_{el} and the specific investment costs of them are in the range of 1575-2500 $/$kW_{el}$. Further, the average specific investment cost of them amounts to 2127 $/$kW_{el}$.

[57] The values are available in the corresponding study.

Furthermore, the fixed O&M[58] cost of hydropower plant is taken as 2.5% of the of the average specific investment cost (i.e. 53175 $/MW$_{el}$-y) according to the given information in the report "Renewable Power Generation Costs in 2014" by International Renewable Energy Agency (2015, p. 118). Finally, the economic life time is taken as 50 years.

Table 12- The examples of realized hydropower investments in Turkey (own illustration)

Hydropower Plant Project	Installed Capacity [MW_{el}]	Specific Investment Cost [$/$kW_{el}$]
HPP 1	2	2500
HPP 2	7	1762
HPP 3	19	1575
HPP 4	60	2393
HPP 5	170	2403
	Average	2127

In Figure 19, the distribution of the hydropower plants in Turkey w.r.t. their FLHs of operation are illustrated. The distribution of the FLHs is based on the annual average amount of electricity generation and the installed capacity of power plants as indicated in the generation license of the corresponding power plants. In the figure, the count of FLHs corresponds to the number of FLHs which lies in the same given range. In total 358 hydropower plants are considered for the analysis and the majority of them lie in the range of 3000-3500 FLHs of operation. Further, about 41% of them can operate in the range of 3000-4000 FLHs and around 30% of them can operate at more than 4000 FLHs. The difference in the magnitude of the FLHs of the corresponding power plants is not only related to the amount of annual precipitation but also related to the size of their reservoirs. The hydropower plants with large reservoirs can operate at higher FLHs than the ones having relative less or even no water storage capability.

[58] For hydropower plant, the fixed O&M cost per MW per year is given as the aggregation of the fixed and the variable O&M costs per annum (i.e. called O&M).

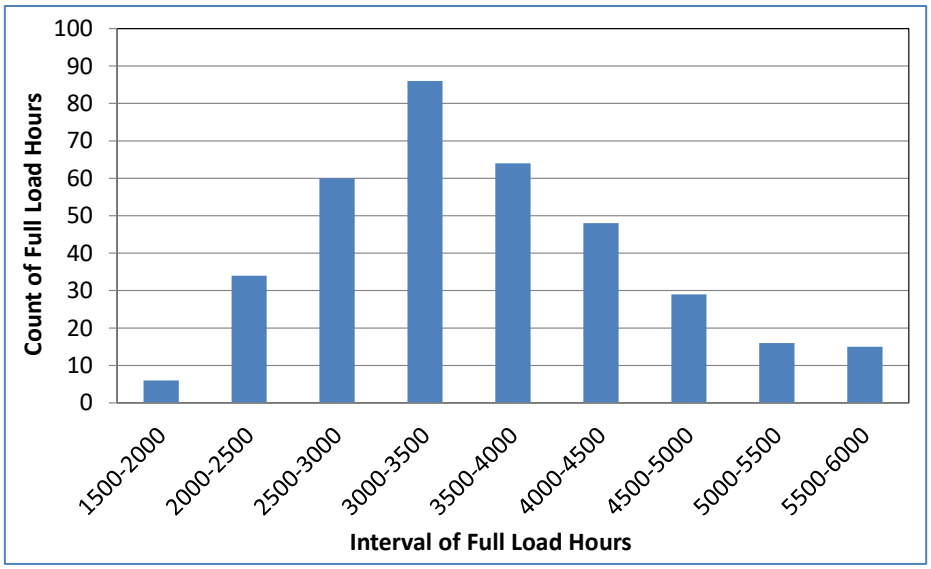

Figure 19- The distribution of the hydropower plants in Turkey w.r.t. their FLHs of operation (own calculation & illustration according to EPDK)

In Figure 20, the results of the analysis[59] on the technical[60] hydropower potential and the related categorized FLHs are represented for Turkey and some of other examined countries. The corresponding analysis is carried out through the simulation of the hydropower generation which is dependent on the simulated daily hydro discharge data[61] for different rivers (Resch, et al., 2015, p. 42). Accordingly, Turkey possesses the highest technical hydropower potential among the examined countries; however the quality of the hydropower resources is especially lower than in Norway (NO) and in Sweden (SE) due to the variation in hydrological conditions in different seasons. More specifically, about 30% of the technical potential is estimated to lie in the range of 2992-3846 FLHs of operation and about 70% of it is estimated to lie in the range of 2138-2992 FLHs. The represented analyses in Figure 19 and in Figure 20 indicate different ranges of FLHs of operation; since the corresponding analyses are dependent on different type of assessments and data set for hydropower generation; however it can be inferred from both of the analyses that hydropower plants operating more than 4000 FLHs depend on rare high quality resources.

[59] The analyses are conducted by the energy economics group of Vienna University of Technology, in the course of the aforementioned project Better. The analyses are conducted based on the hydrological conditions and the technical capability of available hydropower technologies. The details of the study can be found in the report "Bringing Europe and Third countries closer together through renewable Energies" by Resch et al. (2015) and also in the workshop presentation by Ortner (2014).

[60] See subsection "Hydropower Energy Potential of Turkey" for more information on the technical hydropower potential.

[61] The data is mentioned to be obtained by the E-HYPE 2.1 tool of the Swedish Meteorological and Hydrological Institute.

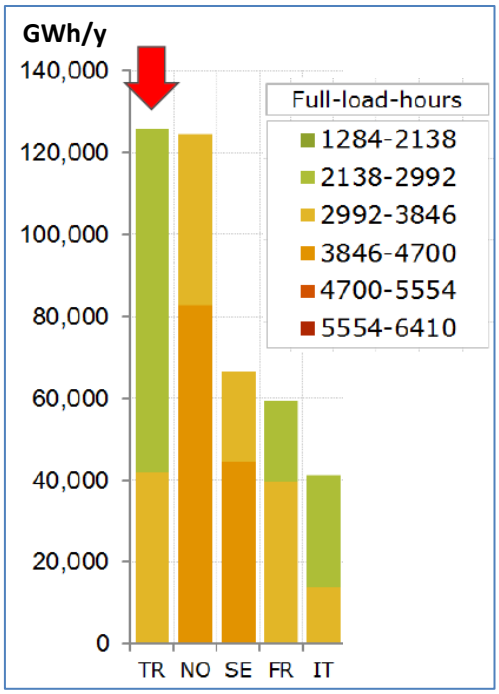

Figure 20- The technical hydropower potential and its categorized FLHs in Turkey (TR), Norway (NO), Sweden (SE), France (FR) and Italy (IT) (Ortner, 2014, p. 9)

In Figure 21, the relation[62] between investment trigger prices and FLHs is displayed for hydropower plant investments in the period 2016-2023, considering different degrees of flexibility and levels of discount rate. Note that the related power plant costs are assumed to be not changing in the mentioned period. In the figure, the dashed and the continuous curves represent the investment trigger prices for immediate decision ($S_{immediate}$, the NPV break-even price) and decision at any time ($S_{perpetual}$, risk adjusted break-even price) respectively. Further, it can be inferred from the figure that the investment trigger prices decrease as the FLHs of operation increase; whereas they increase as ρ increases. Hence, the increase in investment trigger prices relative to the FiT rates and the expected (simulated) market price of electricity hinders the realization of the potential RET investments due to the scarcity of high quality hydropower potential. For the sake of simplicity, the FiT rates are not represented in the graphic; however all relevant threshold FLHs are tabulated in Table 13.

[62] It is implemented by calculating investment trigger prices according to a given theoretical range of FLHs of operation to the Eqs. (4.3.12) and (4.3.28) w.r.t. the different degrees of flexibility and different levels of discount rate.

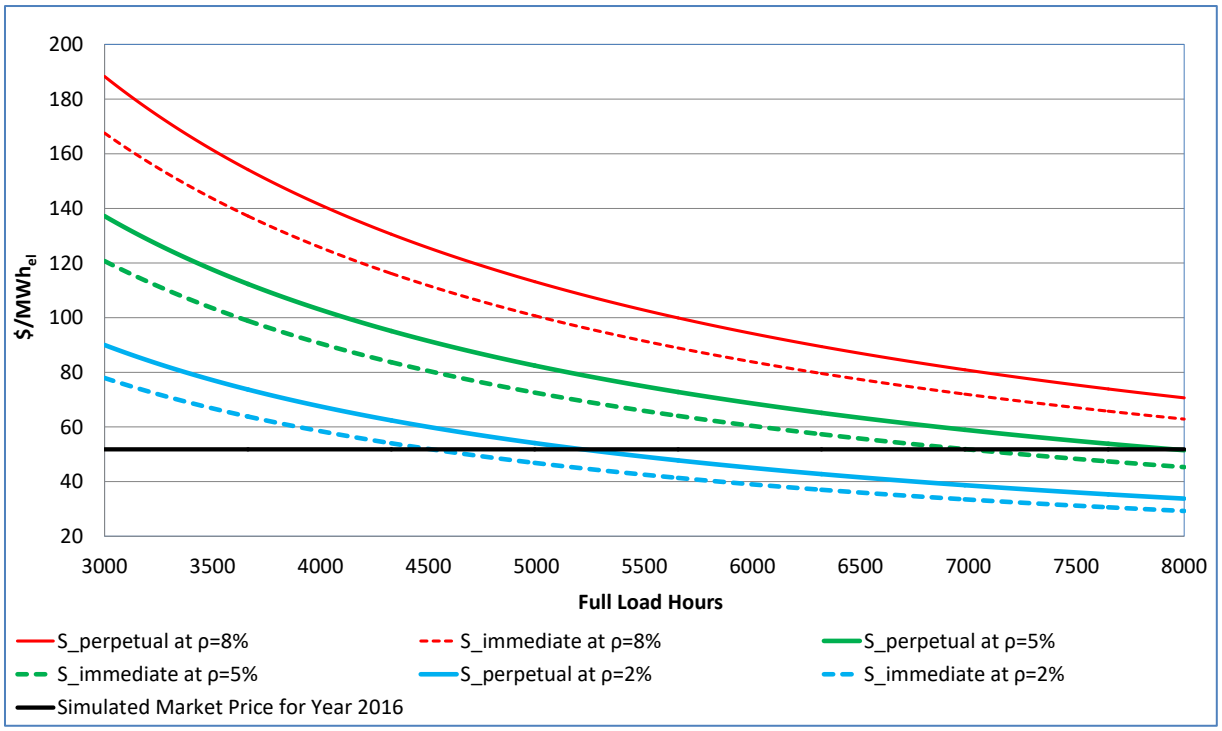

Figure 21- The comparison of the investment trigger prices for hydropower investments as a function of full load hours and w.r.t. the different levels of discount rate and degrees of flexibility (own calculation & illustration)

In Table 13, the threshold FLHs of operation for hydropower plants corresponding to the immediate investment decision is tabulated as obtained from Figure 21. The calculated values for $S_{immediate}$ based on $\rho = 5\%$ indicate that an investment on a hydropower plant project should be initiated, if a hydropower plant is capable of operating more than 4962 FLHs per year (i.e. threshold FLHs), considering the base FiT rate of 73 $/MWh_{el}$. According to the conducted analysis in Figure 19, around 9% of the hydropower plants can operate at FLHs higher than the calculated threshold FLHs. Nevertheless, in Turkey, all most all of the hydropower projects with large reservoirs are made. Further, $S_{immediate}$ based on the maximum FiT rate of 96 $/MWh_{el}$ indicates 3773 threshold FLHs of operation and around 37% of the analyzed hydropower plants can operate above that level. Note that none of the investors benefits from bonus for domestically manufactured equipment according to the participants of the survey conducted by Özcan (2014). To sum up, it can be deduced that the FiT scheme is observed to be not sufficient to trigger immediate investment decisions for about 8.1 GW_{el} capacity which nearly amounts to 30% of the hydropower installed capacity in the year 2015 (i.e. 25.9 GW_{el}); since the remaining hydropower potential, enabling more than 4000 FLHs of operation, is not available for the targeted amount of capacity expansion.

Table 13- The threshold FLHs for hydropower plants w.r.t. the different means of revenue and discount rates (own calculation & illustration)

Investment Trigger Prices	Threshold FLHs at		
	ρ=2%	ρ=5%	ρ=8%
$S_{immediate}$=Base FiT Rate=73 $/MWh$_{el}$	3202	4962	6889
$S_{immediate}$=Maximum FiT Rate=96 $/MWh$_{el}$	2435	3773	5238
$S_{perpetual}$=Expected Market Price in 2016=51.8 $/MWh$_{el}$	5213	7949	>8760

The calculated value for $S_{perpetual}$ based on $\rho = 5\%$ indicates that an investment on a hydropower plant project should be initiated, if a hydropower plant is capable of operating more than 7949 FLHs per year considering the simulated electricity market price for the year 2016 (see Table 13). It is practically an infeasible situation in Turkey to construct a hydropower plant which can operate at a level which is higher than the calculated threshold FLHs. Moreover, the threshold FLHs gets even higher considering the downward trend in the wholesale market price of electricity in the period 2016-2023 (see Figure 18). Accordingly, the uncertainty and the downward trend in the wholesale market price of electricity can lead to postponement of the potential hydropower plant investments.

In summary, the analysis on the FLHs of operation of hydropower plant projects indicates that the FiT rates and the market price of electricity in the period 2016-2023 are not sufficient to reach the capacity expansion target set by the government.

7.2 Assessment on Wind Power Plants

The given investment cost for the analysis of the onshore wind power plant investments (in Table 9) is based on the examples of wind power projects in Turkey as tabulated in Table 14. It can be inferred from the table that the installed capacities of the example projects range from 10 MW_{el} to 72 MW_{el} and the specific investment costs of them are in the range of 1293-2207 $/kW_{el}$. Further, the average specific investment cost of them amounts to 1764 $/kW_{el}$. Furthermore, the fixed and the variable O&M costs of wind power plant are taken as 49,000 $/MW_{el}$-y and 14.3 $/MWh_{el}$ respectively as given in the report "Projected Costs of Generating Electricity 2015 Edition" (NEA, IEA, OECD, 2015, p. 113). Finally, the economic life time of the power plant is taken as 25 years.

Table 14- The examples of realized wind power investments in Turkey (own illustration)

Wind Power Project	Installed Capacity [MW_{el}]	Specific Investment Cost [$/$kW_{el}$]
WPP 1	10	2207
WPP 2	23	1951
WPP 3	39	1293
WPP 4	63	1425
WPP 5	72	1942
	Average	1764

In Figure 22, the distribution of the wind power plants in Turkey w.r.t. their FLHs of operation are illustrated. In total 82 wind power plants are considered for the analysis and about 60% of them can operate in the range of 2000-3000 FLHs per year. Also, around 41% of them can operate more than 2500 FLHs per year.

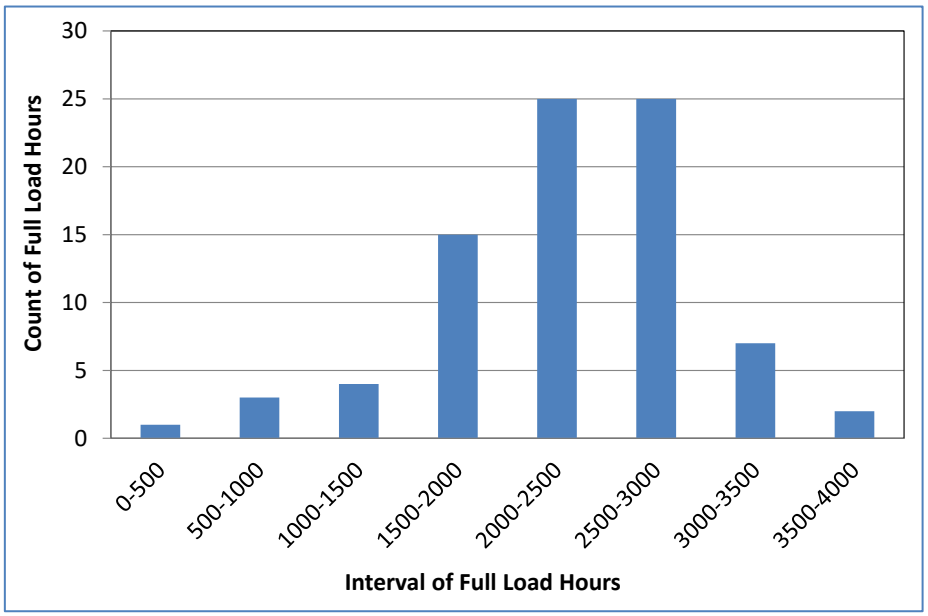

Figure 22- The distribution of the wind power plants in Turkey w.r.t. their FLHs of operation (own calculation & illustration according to EPDK)

In Figure 23, the results of the analysis[63] on the technical[64] wind power potential and the related categorized FLHs are represented for Turkey and some of other examined countries. The corresponding analyses are carried out through the simulation of the wind power generation, which is dependent on the simulated hourly wind speed data (Resch, et al., 2015, p. 42). Accordingly, Turkey possesses the fourth highest technical wind power potential among the examined countries. The quality of the wind power resources is especially lower than in France (FR) and United Kingdom (UK). More specifically, about 4% of the technical potential is estimated to lie in the range of 2635-2910 FLHs of operation and about 77% of it is estimated to operate less than 1860 FLHs. The represented analyses in Figure 22 and in Figure 23 indicate different ranges of FLHs of operation; since the corresponding analyses are dependent on different type of assessments and data set for wind power generation; however it can be inferred from both of the analyses that wind power plants operating more than 3000 FLHs depend on rare high quality resources.

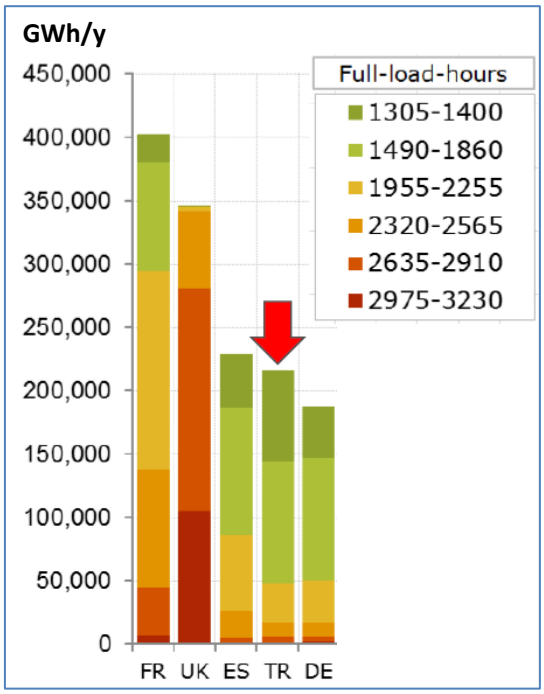

Figure 23- The technical wind power potential and its categorized FLHs in France (FR), United Kingdom (UK), Spain (ES), Turkey (TR) and Germany (DE) (Ortner, 2014, p. 7)

[63] See Footnote 59 on p. 56 for more information about the study.

[64] The analyses are conducted based on the wind conditions and the technical capability of available wind power technologies.

In Figure 24, the relation between investment trigger prices and FLHs is displayed for wind power plant investments in the year 2016, considering different degrees of flexibility and levels of discount rate.

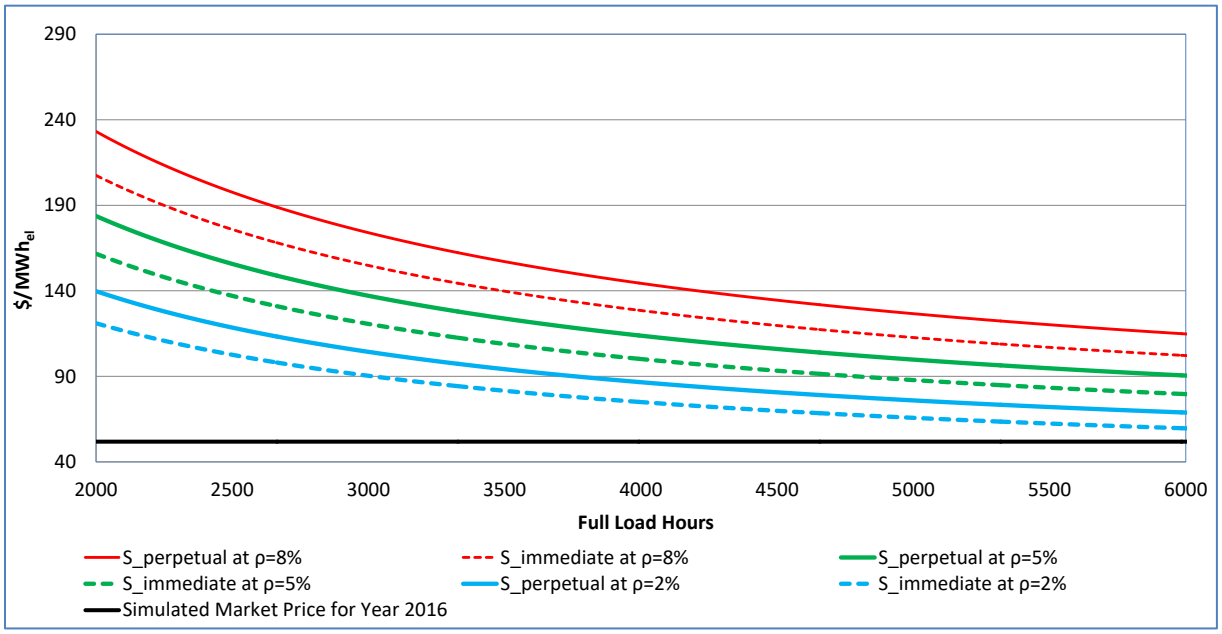

Figure 24- The comparison of the investment trigger prices for wind power investments as a function of full load hours and w.r.t. the different levels of discount rate and degrees of flexibility (own calculation & illustration)

In Table 15, the threshold FLHs of operation for wind power plants corresponding to the immediate investment decision is tabulated as obtained from Figure 24. The calculated values for $S_{immediate}$ based on $\rho = 5\%$ indicate that an investment on a wind power plant project should be initiated, if a wind power plant is capable of operating more than 7149 FLHs per year considering the base FiT rate of 73 $/MWh$_{el}$. Further, the corresponding threshold FLHs decreases to 6337 FLHs until the year 2023 by taking into account the decline rate of 1% in the related costs. It is practically an infeasible situation to construct a wind power plant which can operate at a level which is higher than the calculated threshold FLHs. Furthermore, $S_{immediate}$ based on the maximum FiT rate of 110 $/MWh$_{el}$ indicates 3446 threshold FLHs of operation; however a wind power plant which can operate at a level, which is higher than the calculated threshold FLHs, is rare. In addition, the corresponding threshold FLHs decreases to 3130 FLHs until the year 2023 by taking into account the decline rate of 1% in the related costs. To sum up, it can be deduced that the FiT scheme is not sufficient to trigger immediate investment decisions for about 15.5 GW$_{el}$ capacity which nearly amounts to 3.5 times the wind power installed capacity in the year 2015 (i.e. 4.5 GW$_{el}$); since the remaining wind power potential enabling more than 3000 FLHs of operation is not available for the targeted amount of capacity expansion.

Table 15- The threshold FLHs for wind power plants w.r.t. the different means of revenue and discount rates (own calculation & illustration)

Investment Trigger Prices	Threshold FLHs at		
	ρ=2%	ρ=5%	ρ=8%
$S_{immediate}$=Base FiT Rate=73 \$/MWh$_{el}$	4176	7149	>8760
$S_{immediate}$=Maximum FiT Rate=110 \$/MWh$_{el}$	2272	3446	5221
$S_{perpetual}$=Expected Market Price in 2016=51.8 \$/MWh$_{el}$	>8760	>8760	>8760

The calculated value for $S_{perpetual}$ based on $\rho = 5\%$ (see Table 15) indicates that an investment on a wind power plant project should be initiated, if a wind power plant is capable of operating more than 8760 FLHs per year, considering the simulated electricity market price for the period 2016-2023 (see Figure 18). This is a practically infeasible situation, also by taking into account the decline rate of 1% in the related costs. Accordingly, the uncertainty and the downward trend in the wholesale market price of electricity can lead to postponement of the potential wind power plant investments.

In summary, the analysis on the FLHs of operation of wind power plant projects indicates that the FiT rates and the wholesale market price of electricity in the period 2016-2023 are not sufficient to reach the capacity expansion target set by the government.

7.3 Assessment on Solar PV Power Plants

The given investment cost for the analysis of the solar PV power plant investments (in Table 9) is based on the examples of solar PV projects in Turkey as tabulated in Table 16. It can be inferred from the table that the installed capacities of the example projects range from 2 MW_{el} to 10 MW_{el} and the corresponding power plants are capable of operating at FLHs ranging from 1600 to1800. Further, the average FLHs of operation and the average specific investment cost of the projects amount to 1670 hours and 1102 \$/kW_{el} respectively. Furthermore, the fixed and variable O&M cost of solar PV power plants are taken as 24,813 \$/MW_{el}-y and 16.3 \$/MWh_{el} respectively as given in the Projected Costs of Generating Electricity 2015 Edition (NEA, IEA, OECD, 2015, p. 112). Finally, the economic life time of the power plant is taken as 25 years.

Table 16- The examples of realized solar PV power investments in Turkey (own illustration)

Solar PV Project	Installed Capacity [MW_{el}]	Annual Average Generation [GWh_{el}]	Full Load Hours [Hour]	Specific Investment Cost [$/$kW_{el}$]
PV 1	2	3	1600	1293
PV 2	3	5	1800	1109
PV 3	4	6	1616	840
PV 4	5	8	1680	770
PV 5	10	17	1652	1500
		Average	1670	1102

In Figure 25, the results of the analysis[65] on the technical[66] solar PV power potential and its categorized FLHs in Turkey and in some of other examined countries are represented. The corresponding analyses are carried out through the simulation of the solar power generation which is dependent on the simulated hourly solar irradiation data[67] (Resch, et al., 2015, p. 42). Accordingly, Turkey possesses the highest technical solar PV power potential among the examined countries; however the quality of the resources is especially lower than in Spain (ES). More specifically, about 70% of the technical potential is estimated to lie in the range of 1250-1392 FLHs of operation and about 30% of it is estimated to lie in the range of 1108-1250 FLHs. The represented analyses in Table 16 and in Figure 25 indicate different ranges of FLHs of operation; since the corresponding analyses are dependent on different type of assessments and data set for solar power generation; however it can be inferred from Figure 25 that solar PV power plants operating more than 1400 FLHs are constructed in locations with rare high quality solar irradiation.

[65] See Footnote 59 on p. 56 for more information about the study.
[66] The analyses are conducted based on the weather conditions and the technical capability of available solar PV power technologies.
[67] The data is mentioned to be obtained from Meteosat satellites as provided by HelioCLIM.

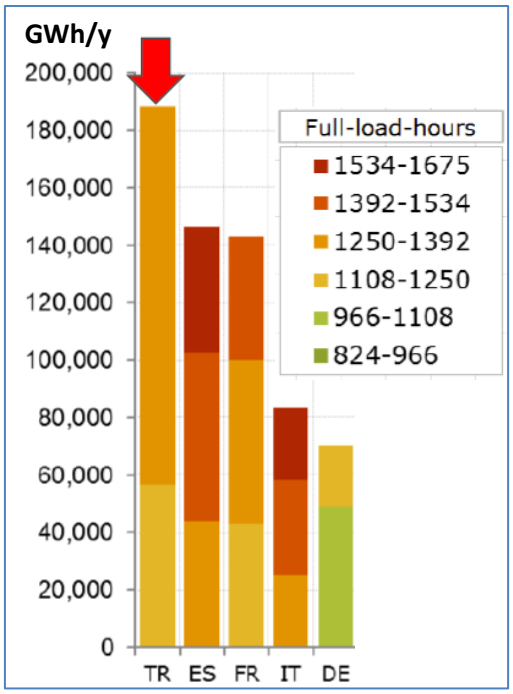

Figure 25- The technical solar PV power potential and its categorized FLHs in Turkey (TR), Spain (ES), France (FR), Italy (IT) and Germany (DE) (Ortner, 2014, p. 8)

In Figure 26, the relation between investment trigger prices and FLHs is displayed for solar PV power plant investments in the year 2016, considering different degrees of flexibility and levels of discount rate.

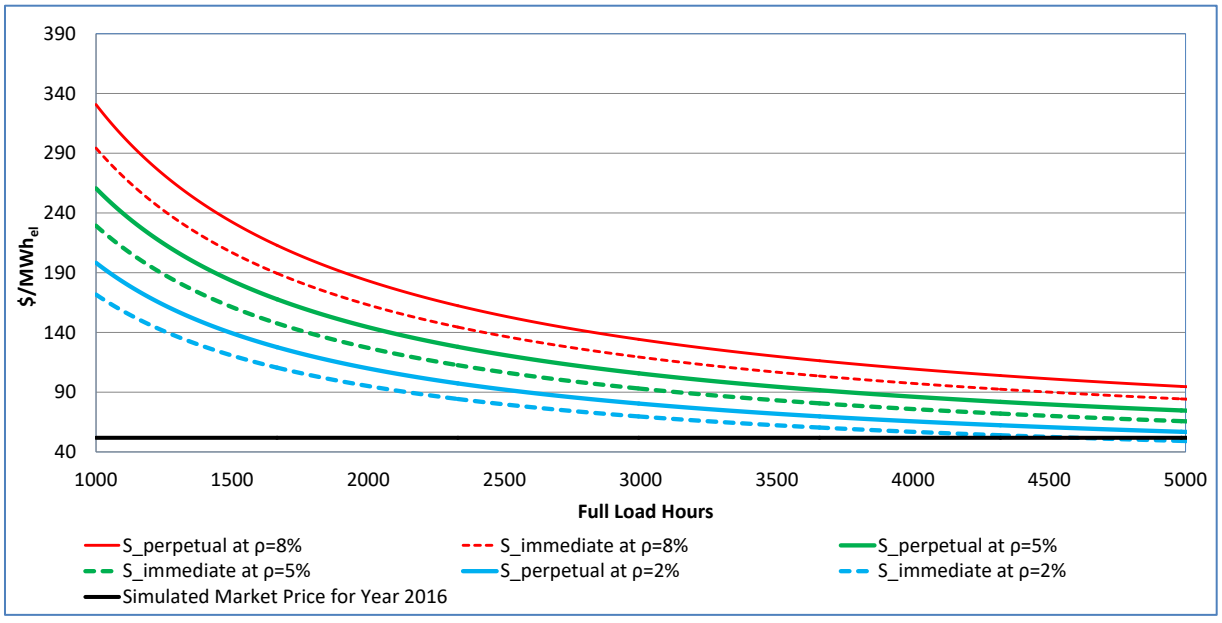

Figure 26- The comparison of the investment trigger prices for solar PV power investments as a function of full load hours and w.r.t. the different levels of discount rate and degrees of flexibility (own calculation & illustration)

In Table 17, the threshold FLHs of operation for solar PV power plants corresponding to the immediate investment decision and decision at any time is tabulated as obtained from Figure 26.

Table 17- The threshold FLHs for solar PV power plants w.r.t. the different means of revenue and discount rates (own calculation & illustration)

Investment Trigger Prices	Threshold FLHs at		
	ρ=2%	ρ=5%	ρ=8%
$S_{immediate}$=Base FiT Rate=133 \$/MWh$_{el}$	1337	1889	2591
$S_{immediate}$=Maximum FiT Rate=200 \$/MWh$_{el}$	840	1167	1559
$S_{perpetual}$=Expected Market Price in 2016=51.8 \$/MWh$_{el}$	5806	>8760	>8760

The calculated values for $S_{immediate}$ based on $\rho = 5\%$ indicate that an investment on a solar PV power plant project should be initiated, if a solar PV power plant is capable of operating more than 1889 FLHs per year, considering the base FiT rate of 133 \$/MWh$_{el}$. According to the FLHs of example projects in Table 16, none of them can operate at FLHs higher than the threshold FLHs. Further, the corresponding threshold FLHs decreases to 1762 FLHs until the year 2023 by taking into account the decline rate of 1% in the related costs. Furthermore, $S_{immediate}$ based on the maximum FiT rate of 200 \$/MWh$_{el}$ indicates 1167 threshold FLHs. In addition, the corresponding threshold FLHs decreases to 1096 FLHs until the year 2023 by taking into account the decline rate of 1% in costs. Although the analysis considering the example projects may seem insufficient to trigger immediate investment decision for about 4.8 GW$_{el}$ capacity, the capacity expansion target may be reached by solely depending on the base FiT rate due to the reasons given below:

- The number of considered projects is not enough considering the geography of Turkey. In Turkey, the sunshine duration is 2993 hours in the South East Anatolia and 1971 hours in the Black Sea region.
- Most of the high quality solar PV power potential[68] has not been exploited yet; although Turkey possesses the highest solar PV power potential in Europe.
- The analysis does not consider rooftop solar PV systems which enable more revenues through avoiding grid contribution fee (see Table 18) and allowing own consumption (i.e. based on retail price).

[68] The installed capacity of solar PV, which is 249 MW$_{el}$ at the end of 2015, stays far behind that of Germany and Spain.

In Table 18, the threshold FLHs of operation for rooftop solar PV systems are tabulated for the immediate investment decision and decision at any time in the year 2016. It can be inferred that an investment on a rooftop solar PV system should be initiated, if a rooftop solar PV system is capable of operating more than 1220 FLHs per year, considering the base FiT rate of 133 $/MWh$_{el}$. In addition, the corresponding threshold FLHs decreases to 1106 FLHs until the year 2023 by taking into account the decline rate of 1% in the related costs. Regarding the calculated values for $S_{perpetual}$, a practically infeasible situation is indicated, also by taking into account the decrease in the related costs. To sum up, it can be deduced that the FiT scheme can be sufficient to trigger immediate investment for 4.8 GW$_{el}$ rooftop solar PV systems. This is due to the fact that the remaining solar PV power potential, which can enable more than 1220 FLHs of operation, is examined to be available for the targeted amount of capacity expansion.

Table 18- The threshold FLHs for rooftop solar PV systems w.r.t. the different means of revenue and discount rates (own calculation & illustration)

Investment Trigger Prices	Threshold FLHs at		
	ρ=2%	ρ=5%	ρ=8%
$S_{immediate}$=Base FiT Rate=133 $/MWh$_{el}$	864	1220	1673
$S_{immediate}$=Maximum FiT Rate=200 $/MWh$_{el}$	545	754	1007
$S_{perpetual}$=Expected Market Price in 2016=51.8 $/MWh$_{el}$	3749	6314	>8760

The calculated value for $S_{perpetual}$ based on $\rho = 5\%$ (see Table 17) indicates that an investment on a solar PV power plant project should be initiated, if a solar PV power plant is capable of operating more than 8760 FLHs per year, considering the simulated electricity market price for the period 2016-2023 (see Figure 18). This is a practically infeasible situation, also by taking into account the decline rate of 1% in the related costs. Accordingly, the uncertainty and the downward trend in the wholesale market price of electricity can lead to postponement of the potential solar PV power plant investments.

In summary, the analysis on the FLHs of operation of solar PV power plants in Turkey indicates that the FiT rates can be sufficient to reach the capacity expansion target; whereas the downward trend in wholesale market price of electricity indicates that the option to invest on solar PV power plant projects should be kept alive by postponing the decision to invest in the period 2016-2023.

7.4 Assessment on Geothermal Power Plants

The investment cost for the analysis of the geothermal power plant investments (in Table 9) is based on the examples of geothermal power projects in Turkey as tabulated in Table 19. It can be inferred from the table that the installed capacities of the example projects range from 10 MW_{el} to 100 MW_{el}. Further, the average specific investment cost of the projects amount to 2197 $/$kW_{el}$. Furthermore, the O&M cost of geothermal power plants is taken as 110,000 $/$MW_{el}$-y according to the information given in Renewable Power Generation Costs in 2014 by International Renewable Energy Agency (2015, p. 142). Finally, the economic life time of the power plant is taken as 25 years.

Table 19- The examples of realized geothermal power investments in Turkey (own illustration)

Geothermal Power Project	Installed Capacity [MW_{el}]	Specific Investment Cost [$/$kW_{el}$]
GPP 1	10	2104
GPP 2	24	1828
GPP 3	34	2009
GPP 4	45	2444
GPP 5	100	2600
	Average	2197

In Figure 27, the distribution of the geothermal power plants in Turkey w.r.t. their FLHs of operation are illustrated.

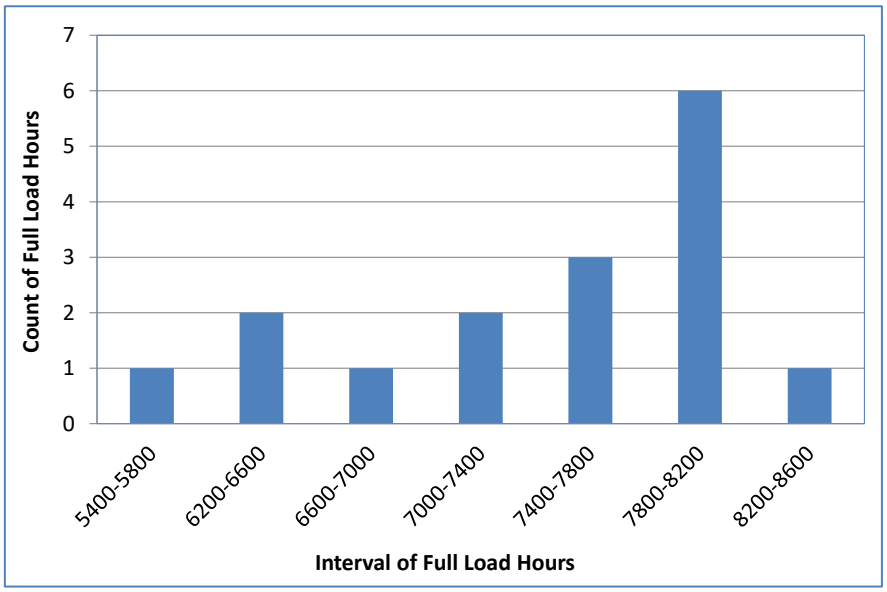

Figure 27- The distribution of the geothermal power plants in Turkey w.r.t. their full load hours of operation (own calculation & illustration according to EPDK)

In total 16 geothermal power plants are considered for the analysis and about 38% of them can operate in the range of 7800-8200 FLHs per year (see Figure 27). In addition, about 75% of them can operate more than 7000 FLHs per year. Note that the average FLHS of geothermal electricity generation in Europe (including Turkey) amounts to 6300 FLHs according to Kaltschmitt and Frick (2006, p. 17).

In Figure 28, the relation between investment trigger prices and FLHs is displayed for geothermal power plant investments in the year 2016, considering different degrees of flexibility and levels of discount rate.

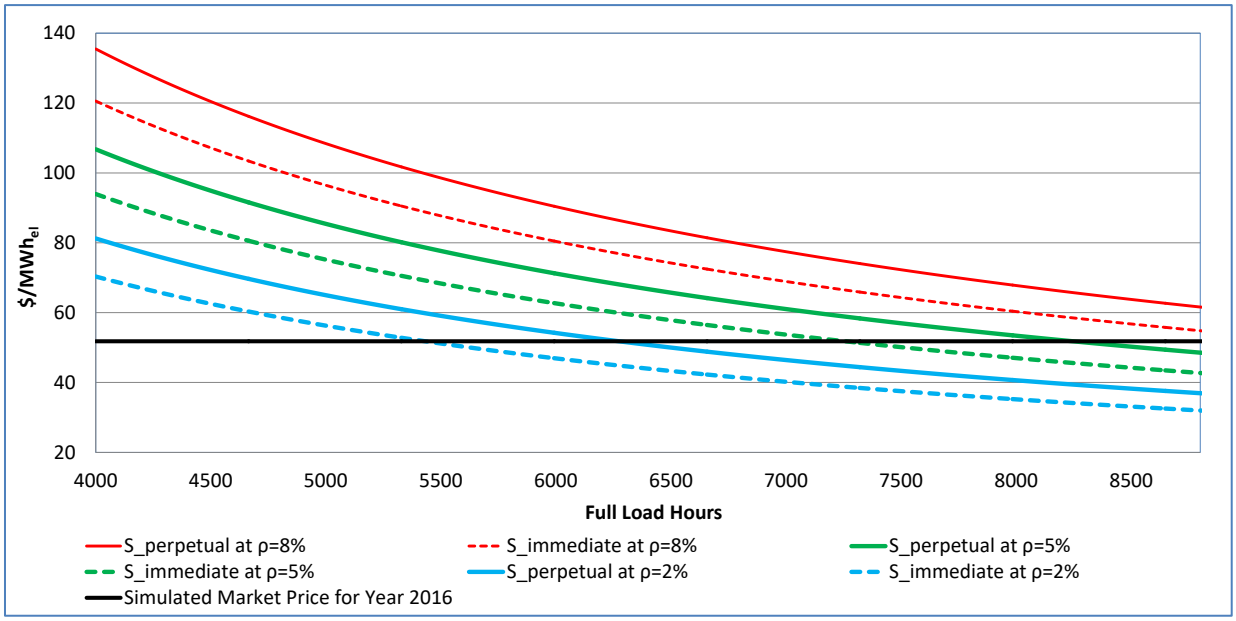

Figure 28- The comparison of the investment trigger prices for geothermal power investments as a function of full load hours and w.r.t. the different levels of discount rate and degrees of flexibility (own calculation & illustration)

In Table 20, the threshold FLHs of operation for geothermal power plants corresponding to the immediate investment decision is tabulated as obtained from Figure 28. The calculated values for $S_{immediate}$ based on $\rho = 5\%$ indicate that an investment on a geothermal power plant project should be initiated, if a geothermal power plant is capable of operating more than 3580 FLHs per year, considering the base FiT rate of 105 \$/MWh$_{el}$. Further, the corresponding threshold FLHs decreases to 3317 FLHs until the year 2023 by taking into account the decline rate of 1% in the related costs. Moreover, $S_{immediate}$ based on the maximum FiT rate of 132 \$/MWh$_{el}$ indicates 2850 threshold FLHs of operation. In addition, the corresponding threshold FLHs decreases to 2638 FLHs until the year 2023 by taking into account the decline rate of 1% in the related costs. According to the conducted analysis in Figure 27, all of the considered power plants can operate at FLHs higher than the calculated threshold FLHs. To sum up, it can be deduced that the FiT scheme is sufficient to trigger

immediate investment decisions for about 376 MW_{el} capacity which is nearly half of the geothermal power installed capacity in the year 2015 (i.e. 624 MW_{el}).

Table 20- The threshold FLHs for geothermal power plants w.r.t. the different means of revenue and discount rates (own calculation & illustration)

Investment Trigger Prices	Threshold FLHs at		
	ρ=2%	ρ=5%	ρ=8%
$S_{immediate}$=Base FiT Rate=105 \$/MWh_{el}	2680	3580	4593
$S_{immediate}$=Maximum FiT Rate=132 \$/MWh_{el}	2130	2850	3655
$S_{perpetual}$=Expected Market Price in 2016=51.8 \$/MWh_{el}	6273	8246	>8760

The calculated value for $S_{perpetual}$ based on $\rho = 5\%$ indicates that an investment on a geothermal plant project should be initiated, if a geothermal power plant is capable of operating more than 8246 FLHs per year considering the simulated electricity market price for the year 2016 (see Table 20). According to the conducted analysis in Figure 27; only one of the considered power plants (as given in Figure 27) can operate more than the threshold FLHs. In addition, the corresponding threshold FLHs gets higher considering the downward trend in the wholesale market price of electricity in the period 2016-2023 (see Figure 18); although the related costs decrease at a rate of 1%/a. Correspondingly, the uncertainty and the downward trend in the wholesale market price of electricity can lead to postponement of the potential geothermal power plant investments, considering 6300 FLHs of operation in average.

In summary, the analysis on the FLHs of operation of geothermal power plants in Turkey indicates that the FiT rates can be sufficient to reach the capacity expansion target; whereas the downward trend in wholesale market price of electricity indicates that the option to invest on geothermal power plant projects should be kept alive by postponing the decision to invest in the period 2016-2023.

7.5 Assessment on Biomass Power Plants

In Turkey, biomass power plants are based on different types of feedstock such as municipal, agricultural, animal and vegetable oil wastes. There is a wide range of type of technologies for the corresponding technologies such as direct combustion in stoker boilers, low-percentage co-firing, anaerobic digestion, pyrolysis, municipal solid waste incineration, landfill gas and combined heat and power. Accordingly, annual average cost of electricity generation from biomass is specific to each individual project dependent on the costs of feedstocks (e.g. collection and transport costs) and infrastructure costs. For the analysis, it is assumed that the feedstock costs are zero due to being onsite at industrial facilities (e.g. municipal dump area, livestock and poultry).

The given investment cost for the analysis of the biomass power plant investments (in Table 9) is based on the examples of biomass power projects in Turkey as tabulated in Table 21. It can be inferred from the table that the installed capacities of the example projects range from 2 MW_{el} to 14 MW_{el} and the specific investment costs of them are in the range of 865-3101 $\$/kW_{el}$. Further, the average specific investment cost of the projects amount to 1614 $\$/kW_{el}$. Furthermore, the fixed O&M cost of biomass power plants is taken as 2% of the of the average specific investment cost (i.e. 32,280 $\$/MW_{el}$-y) and the variable O&M cost of them is taken as 5 $\$/MWh_{el}$ according to the information given in Renewable Power Generation Costs in 2014 by International Renewable Energy Agency (2015, p. 132). Finally, the economic life time of the power plants is taken as 25 years.

Table 21- The examples of realized biomass power plant investments in Turkey (own illustration)

Biomass Power Plant Project	Installed Capacity [MW_{el}]	Specific Investment Cost [$\$/kW_{el}$]
BPP 1	2	2308
BPP 2	5	883
BPP 3	10	914
BPP 4	12	865
BPP 5	14	3101
	Average	1614

In Figure 29, the distribution of the biomass power plants in Turkey w.r.t. their FLHs of operation are illustrated. In total 33 biomass power plants are considered for the analysis and about 67% of them can operate in the interval 7000-75000 FLHs. In addition, around 90% of them can operate at higher than 7000 FLHs.

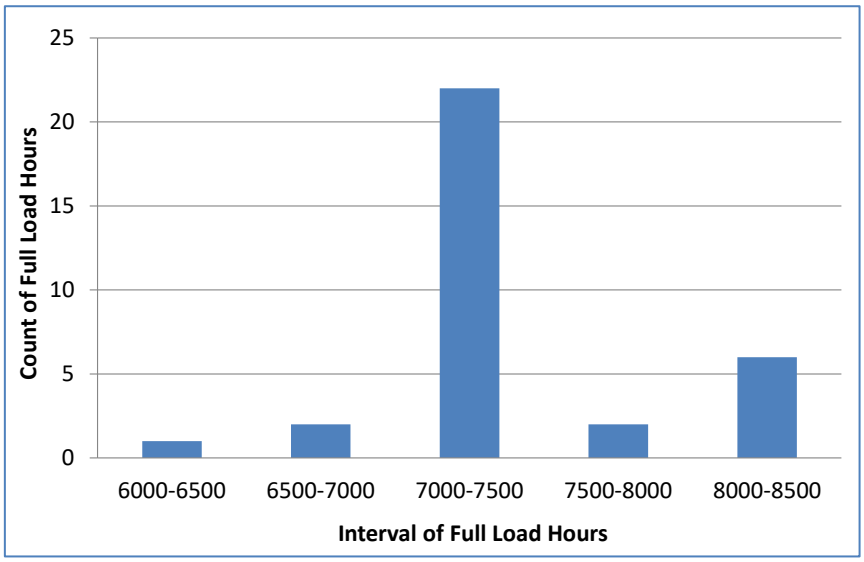

Figure 29- The distribution of the biomass power plants in Turkey w.r.t. their FLHs of operation (own illustration according to EPDK)

In Figure 30, the relation between investment trigger prices and FLHs is displayed for biomass power plant investments in the year 2016, considering different degrees of flexibility and levels of discount rate.

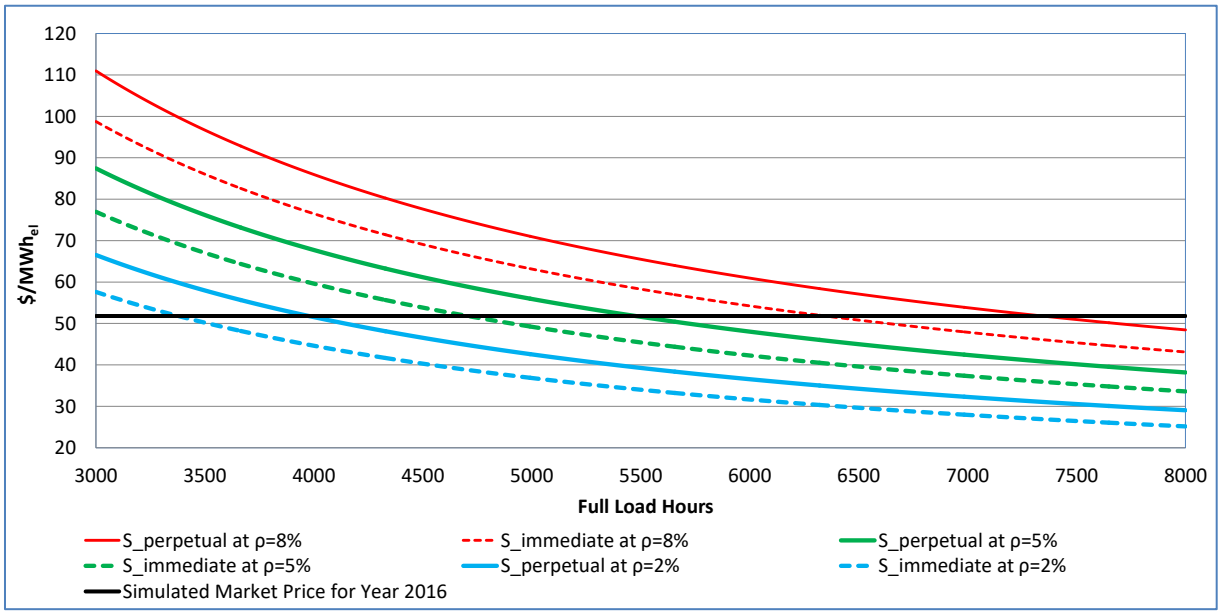

Figure 30- The comparison of the investment trigger prices for biomass investments as a function of full load hours and w.r.t. the different levels of discount rate and degrees of flexibility (own calculation & illustration)

In Table 22, the threshold FLHs of operation for biomass power plants corresponding to the immediate investment decision is tabulated as obtained from Figure 28. The calculated values for $S_{immediate}$ based on $\rho = 5\%$ indicate that an investment on a biomass power plant project should be initiated, if a biomass power plant is capable of operating more than 1659 FLHs per year, considering the base FiT rate of 133 \$/MWh$_{el}$. Further, the corresponding threshold FLHs decreases to 1536 FLHs until the year 2023 by taking into account the decline rate of 1% in the related costs. Furthermore, $S_{immediate}$ based on the maximum FiT rate of 189 \$/MWh$_{el}$ indicates 1145 threshold FLHs of operation. According to the conducted analysis in Figure 29, all of the corresponding power plants can operate at FLHs higher than the calculated threshold FLHs. In addition, the corresponding threshold FLHs decreases to 1063 FLHs until the year 2023 by taking into account the decline rate of 1% in the related costs. To sum up, it can be deduced that the FiT scheme is sufficient to trigger immediate investment decisions for 655 MW$_{el}$ capacity which is nearly 1.9 times the biomass power installed capacity in the year 2015 (i.e. 345 MW$_{el}$).

Table 22- The threshold FLHs for biomass power plants w.r.t. the different means of revenue and discount rates (own calculation & illustration)

Investment Trigger Prices	Threshold FLHs at		
	ρ=2%	ρ=5%	ρ=8%
$S_{immediate}$=Base FiT Rate=133 \$/MWh$_{el}$	1224	1659	2166
$S_{immediate}$=Maximum FiT Rate=189 \$/MWh$_{el}$	850	1145	1490
$S_{perpetual}$=Expected Market Price in 2016=51.8 \$/MWh$_{el}$	3976	5475	7344

The calculated value for $S_{perpetual}$ based on $\rho = 5\%$ indicates that an investment on a biomass plant project should be initiated, if a biomass power plant is capable of operating more than 5475 FLHs per year considering the simulated electricity market price for the year 2016 (see Table 22). According to the conducted analysis in Figure 29, all of the corresponding power plants in Turkey can operate at FLHs higher than the calculated threshold FLHs. In addition, the corresponding threshold FLHs increases to 6015 FLHs considering the downward trend in the wholesale market price of electricity in the period 2016-2023; although the related costs decrease at a rate of 1%/a. Nonetheless, the wholesale market price of electricity can trigger flexible investment decisions for reaching the set targets.

In summary, the analysis on the FLHs of operation of biomass power plants indicates that the FiT rates and wholesale market price of electricity are sufficient to reach the capacity expansion target for biomass power plants.

8 CONCLUSION

The investment analyses are conducted to anticipate the development of the investments in RETs based on the revenue streams from the FiT scheme and the electricity market, FLHs of operation and cost of capital. Accordingly, the level of FLHs of operation to trigger investment in RETs is quantified and compared with the resource potential related to the FLHs of RETs in Turkey. The analyses are carried out taking into account immediate and flexible decisions, and different levels of discount rate. The novelty of this study lies in the application of the NPV and the real option methods for the aforementioned investment analysis.

The Turkish government has committed itself for the installation of about 8.1 GW_{el} more hydropower plant capacity until the year 2023 which nearly amounts to 30% of the hydropower installed capacity in the year 2015 (i.e. 25.9 GW_{el}). The current FiT scheme and the downward trend in the wholesale market price of electricity can lead to delays in reaching the targets for hydropower plants until the year 2023. This is due to the fact that around 15% of the analyzed hydropower plants can operate at FLHs higher than the calculated threshold FLHs based on the corresponding base FiT rate. In addition, the remaining hydropower potential, enabling more than 4000 FLHs of operation, is not available for the targeted amount of capacity expansion. Further, all most all of the hydropower projects with large reservoirs are made until the year 2015. With regard to getting maximum FiT rate, it is considered as a rare occasion; since none of the investors benefit from bonus for domestically manufactured equipment according to the participants of the survey conducted by Özcan. Furthermore, practically infeasible FLHs of operation is indicated by the calculated threshold FLHs based on the wholesale market price of electricity. Finally, the downward trend in the wholesale market price of electricity alleviates the profitability and the attractiveness of the investments in RETs.

The installation of about 15.5 GW_{el} more wind power plant capacity, which is targeted for the year 2023, nearly amounts to 3.5 times the wind power installed capacity in the year 2015 (4.5 GW_{el}). The analysis on the FLHs of operation of wind power plant projects indicates that the FiT rates and the wholesale market price of electricity in the period 2016-2023 are not sufficient to reach the capacity expansion target set by the government. More specifically, practically infeasible FLHs of operation for Turkey are indicated by the calculated threshold FLHs based on the both means of revenue.

About 4.8 GW_{el} more solar PV power plant capacity is targeted for installation until the year 2023 (249 MW_{el} in the year 2015). The analysis on the FLHs of operation for rooftop solar PV systems indicates that the FiT rates can be sufficient to reach the capacity expansion target; however the investors must undertake the market risks after the expiration of the right to enroll in the FiT scheme. Further, the investments in solar PV power plants in Turkey have taken attention since a few years and the amount of investments are behind that in countries such as Germany or Spain. In those countries, the rooftop solar PV systems play an important role for the corresponding capacity expansion supported by the revenues from FiT schemes. In addition, the rooftop solar PV systems enable more revenues through avoiding grid contribution fee and allowing own consumption (i.e. based on retail price). Nevertheless, the downward trend in wholesale market price of electricity indicates the opposite according to the calculated practically infeasible FLHs of operation.

The installation of about 376 MW_{el} more geothermal power plant capacity, which is targeted for the year 2023, nearly amounts to half of the geothermal power installed capacity in the year 2015 (624 MW_{el}). The analysis on the FLHs of operation of geothermal power plants indicates that the FiT rates can be sufficient to reach the capacity expansion target; since the FLHs of all realized projects and also the average FLHs of operation of the geothermal power plants in Europe are observed to be higher than the corresponding calculated threshold FLHs. Nonetheless, the downward trend in wholesale market price of electricity indicates the opposite according to the calculated practically infeasible FLHs of operation.

The installation of about 655 MW_{el} more capacity of biomass power plant, which is targeted for the year 2023, nearly amounts to 1.9 times the biomass power installed capacity in the year 2015 (345 MW_{el}). The analysis on the FLHs of operation of biomass power plants indicates that both the FiT rates and the wholesale market price of electricity are sufficient to reach the corresponding capacity expansion target; since all realized projects are observed to be capable of operating at FLHs higher than the corresponding calculated threshold FLHs.

The energy policy 2023 is an ambitious target to which the Turkish government has committed itself; however the analyses indicate that only the set target for biomass power plants can be reachable based on both mentioned means of revenue. This is mainly due to the fact that biomass power plants can operate at higher average FLHs compared to the other RETs. In addition, it is considered that biomass power plants incur no feedstock costs and no contribution fees. The contribution fees, which are incurred by hydropower, wind and solar PV power plant projects (for installed capacities over 1 MW_{el}) according to the status quo of

the regulations, make those investments less profitable. The capacity expansion targets set for solar PV and geothermal power plants can only be reached according to the immediate investment decision analyses; however the investors must undertake the market risks after the expiration of the right to enroll in the FiT scheme. Neither immediate investment decision analyses nor flexible investment decision analyses indicate that the targets for hydropower and wind power plants can be reachable under the given assumptions and according to the resource potential related to the FLHs. Nevertheless, the Turkish government has also declared that the rates in FiT scheme can be raised; in order to reach the RET capacity expansion targets for the year 2023. In conclusion, the targets for biomass, solar PV and geothermal are anticipated to be reachable under the given assumptions; whereas the achievement of the targets for hydropower and wind power plants are considered to be dependent on the decision of the Turkish government whether the corresponding FiT rates should be increased.

For future research, the analysis can be extended by conducting locational analysis of renewable energy potentials and FLHs of operation of RETs.

PART B A CONCEPT ON OBTAINING FUNCTIONAL APPROXIMATIONS TO FUTURE LOAD DURATION CURVES: A CASE STUDY ON TURKEY

9 INTRODUCTION

The commodity electricity is an essential need of everyday life with its distinct properties. First of all, electricity cannot be stored on a large scale. The generation and consumption of electricity must be balanced on real time basis. Secondly, electricity cannot always be consumed where it is generated. Electricity should be transported to where it is demanded through an electricity grid. Finally, forecasting of electricity demand should be carried out as accurate as possible; in order to be able to reliably and economically operate a power system.

Electricity demand forecasts are carried out for planning horizons of short-term, midterm and long-term. Further, short-term demand forecasts are made to schedule power plants to run economically (e.g. one day-ahead) and to adjust power flow in an electricity grid. Furthermore, mid-term demand forecasts are carried out for a period of up to one year ahead and are utilized for scheduling maintenance of power plants or allocating fuel. Finally, long-term demand forecasts are made at least for one year ahead; in order to plan both the capacity expansion of the power plant park[69] and the electricity grid of a power system. The former topic is the main objective of this study.

The capacity expansion planning of a power plant park is primarily analyzed for determining the required amount of power; in order to cover the load demands in each hour of the years considered in a planning period (especially the annual peak load demands[70]). In particular, a capacity expansion model is utilized for planning the type, the size and the commissioning time of the power plants to be installed in a considered power system.

In this study, the improved screening curve methodology (TISCM) is considered for analyzing the capacity expansion of the power plant park of Turkey in the period 2015-2023. TISCM provides the optimal solution to meet the increasing demand for electricity by minimizing the capital and operational costs of both existing and candidate[71] power plants depending on the given load duration curves (LDCs). Therefore, TISCM requires the future LDCs of each year considered in the planning period as an input to the capacity expansion model of Turkey.

[69] The term “power plant park” encompasses all installed thermal and renewable energy power plants in a power system.

[70] It is the maximum magnitude of load demand occurring in a single hour period across the course of a year.

[71] The candidate units are the new units which are going to be commissioned, if they are found out to be economical during the evaluation process.

LDCs indicate the duration during which a considered level of load demanded is equaled or exceeded. LDCs are constructed by sorting the hourly loads in a descending order of their magnitudes with respect to (w.r.t.) their frequency of occurrences in a cumulative way (i.e. the duration). Hence, the future LDCs can be obtained by forecasting either LDCs per se (i.e. through itself) or hourly load demands in the form of load curves for the considered planning period. A load curve indicates the variation of load demands over a given period of time w.r.t. a chronological order.

In the following two sections, general information about LDCs and load curves, so called "the key constructs in power system economics" are given. At the end of each section, discussions are also made about the effort and accuracy in obtaining the future LDCs of Turkey by forecasting LDCs per se or hourly load demands.

9.1 Load Duration Curves

LDCs indicate the duration during which a considered level of load demanded is equaled or exceeded. The duration can be represented both as a fraction of time total time or number of hours. LDCs are different from load curves in non-chronological representation of hourly load demand through a day, a week or a year. LDCs are plotted by ordering of the load demanded in each hour of a given period of time, according to its magnitude from the hour of highest demand to the lowest (placed on the ordinate) and by cumulating the number of hours of occurrence (placed on the abscissa). In Figure 31, the representative construction of a LDC from a daily load curve is illustrated. In the same manner, an annual LDC can be constructed by utilizing the data comprised of hourly load demand during a year.

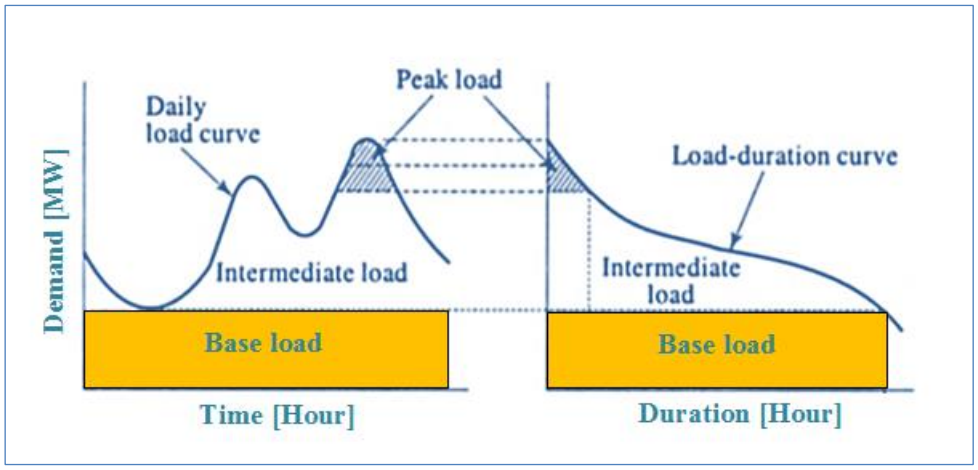

Figure 31- The representative construction of a LDC from a load curve (adapted from Nag (2008, p. 9))

The area under an annual LDC equals to the total amount of electricity supplied during that year. It is usually divided into three segments according to the frequency in occurrence of corresponding load levels.

First of all, the base load, which occurs in the range from 70% to 100% of the time, constitutes the bottom segment of the LDC in Figure 31. The typical examples of power plants (so called base load power plants) operating in the corresponding range are hydropower plants with large reservoirs, nuclear, lignite fired and hard coal fired power plants. Base load power plants inherit high fixed costs (i.e. capital cost intensive); however variable costs incurred during operation are low (i.e. mainly due to low/no fuel costs) (Chandra, 2006, p. 83). In contrast with the hydropower plants with large reservoirs, the thermal base load power plants, which have a low load change capability (i.e. a range between 70% and 100% of its rated power[72]), are started-up or shut down a few times in a year (Spliethoff, 2010, p. 95).

Secondly, the peak load, which occurs at maximum around 20% of the time, is located at the top segment of the LDC in Figure 31. The examples for the types of peak load power plants are pumped-storage hydropower, open cycle gas turbine and diesel fired power plants. They have relatively low fixed costs; however variable costs incurred during operations are relatively higher (i.e. mainly due to high fuel costs, excluding pumped-storage hydropower) (Chandra, 2006, p. 83). These plants have a high load change capability (quick start-up and shut-down times), which enables them to be utilized for instantaneous load variation (Spliethoff, 2010, p. 95).

Finally, the intermediate (also called cycling) load represents the remaining segment between the two previously mentioned segments in Figure 31. It occurs in the range from 20% to 70% of the time. The intermediate load power plants are the hard coal fired, the fuel-oil fired and the combined-cycle gas fired power plants. They have relatively moderate fixed and variable costs (Chandra, 2006, p. 83). The mentioned features enable them to be flexibly operated in a range of about 30% to 100% of its rated power with daily start-ups/shutdowns for peak load operation as well as long operating periods at full/partial capacity for base load operations (Spliethoff, 2010, p. 95).

In Figure 32, the development of the annual LDCs of Turkey in the period 2000-2014 is represented. It can be deduced from the figure that the annual LDCs of Turkey generally shift

[72] It defines the power output of a power plant under specified nominal operating conditions.

upwards year by year owing to the increasing hourly demands in each year. In addition, the shapes of the corresponding LDCs mainly change towards the peak and minimum load demands indicating more curvature; however the intermediate parts of the LDCs are approximately linear for every observed year. This is due to the fact that the increase in hourly load demands towards the peak and minimum load demands are non-linear; whereas the increase in the intermediate load demands is approximately linear for every observed year. In this respect, a mathematical function can be determined to account for the changes in the shape of the past LDCs of Turkey over years.

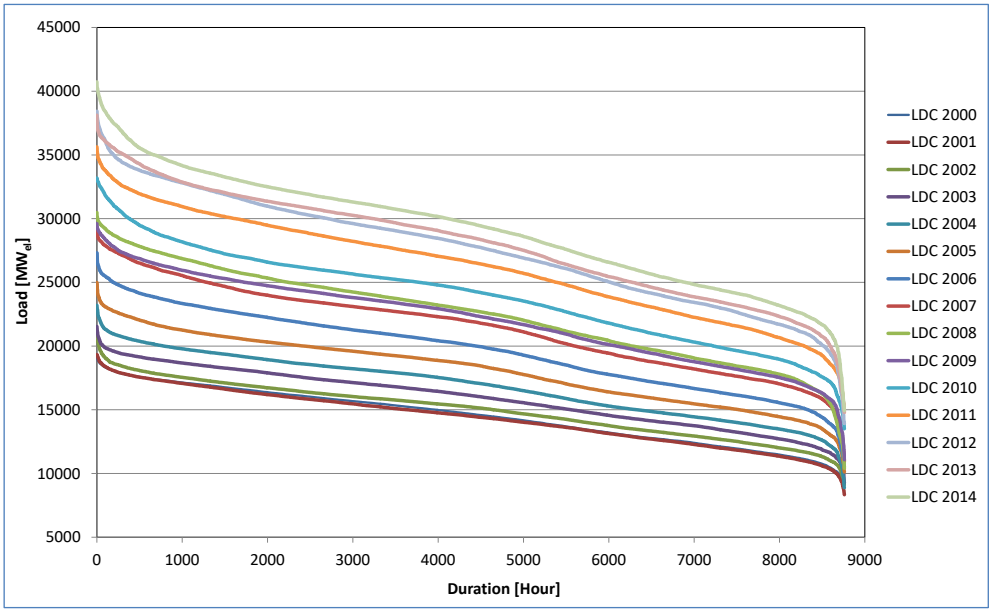

Figure 32- The development of the annual LDCs of Turkey in the period 2000-2014 (own illustration according to data from TEIAS)

Accordingly, the future annual LDCs of Turkey can be obtained by an approximating function whose parameters evolve in time w.r.t. the changes in the shape of the LDCs. Hence, the development in base, intermediate and peak load demands can be implicitly taken into account with relatively low effort and relatively better accuracy.

9.2 Load Curves

A load curve is utilized for indicating the variation of load demanded over a given period of time by plotting the hourly load demand w.r.t. time in chronological order. A load curve can be plotted for observing load variations in a day, a month or a year. The daily load curves are utilized for planning the required units which can generate electricity at least cost during a considered day. In general, a monthly load curve is utilized for determining the rates of

energy (Tewari, 2003, pp. 686-687). An annual load curve is generally utilized for calculating the annual load factor[73].

A daily load curve can be obtained by plotting the load variations during a whole day w.r.t. the corresponding time of occurrences. Daily load curves represent the characteristics of an electricity system; since they differ from day-to-day and season-to-season. In order to illustrate the variations from hour to hour and from day to day in Turkey, a typical winter week (14.01.2013-20.01.2013) is exhibited in Figure 33. At first glance by looking at the figure, it is recognized that the total[74] and peak electricity demands were typically higher during weekdays than during the weekend. This is due to the fact that the industrial sector is more active during the weekdays in comparison to the weekends. During the weekdays the minimum demand occurred at 5 a.m.; whereas the peak demand occurred at 6 p.m. due to the increasing level of activity in the residential sector. The minimum demand on Saturday and on Sunday occurred at 5 a.m. and at 8 a.m. respectively; whereas the peak demand occurred at 6 p.m. and 12 p.m. respectively.

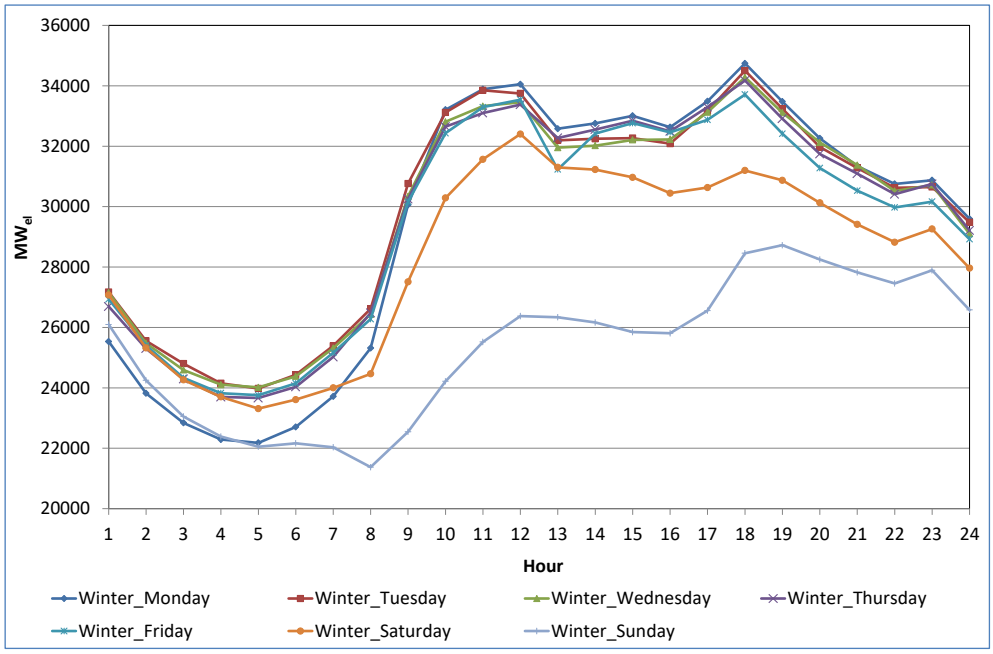

Figure 33- The load variation in the days of a representative winter week (own illustration according to data from TEIAS)

[73] Annual Load Factor [-] = Average Load Demanded in a Year [MW_{el}] / Maximum Load Demanded in a Year [MW_{el}]

[74] In this study, the daily total electricity demand is defined to be equal to the sum of hourly load demands in 24 hours.

It can be inferred from the figure that the hourly demands vary depending on the day of the week and the level of activity in different sectors. The corresponding variations should be taken into account during forecasting the hourly load demand for obtaining the future annual LDCs of Turkey.

In Figure 34, the daily load curves exhibit the annual peak and the annual minimum load demands in Turkey in the period 2011-2014. The annual peak load demands occurred on Thursday 28.07.2011 at 3 p.m. (35634 MW_{el}), on Friday 27.07.2012 at 3 p.m. (38431 MW_{el}), on Thursday 29.08.2013 at 3 p.m. (38116 MW_{el}), on Thursday 14.08.2014 at 3 p.m. (40734 MW_{el}); whereas the annual minimum load demands occurred on Monday 07.11.2011 at 7 a.m. (14822 MW_{el}), on Friday 26.10.2012 at 8 a.m. (13922 MW_{el}), on Wednesday 16.10.2013 at 8 a.m. (14800 MW_{el}), on Saturday 04.10.2014 at 5 a.m. (15387 MW_{el}). It can be inferred from this information that in Turkey, the peak load demands occurred during hot weekdays and summer afternoons (because of vast switching on of air conditioners); whereas the minimum load demands occurred during the second day of every sacrifice fest [75] before noon (because of low activity during an official holiday). Further, although the annual minimum load demand did not change much, the annual peak demand increased substantially.

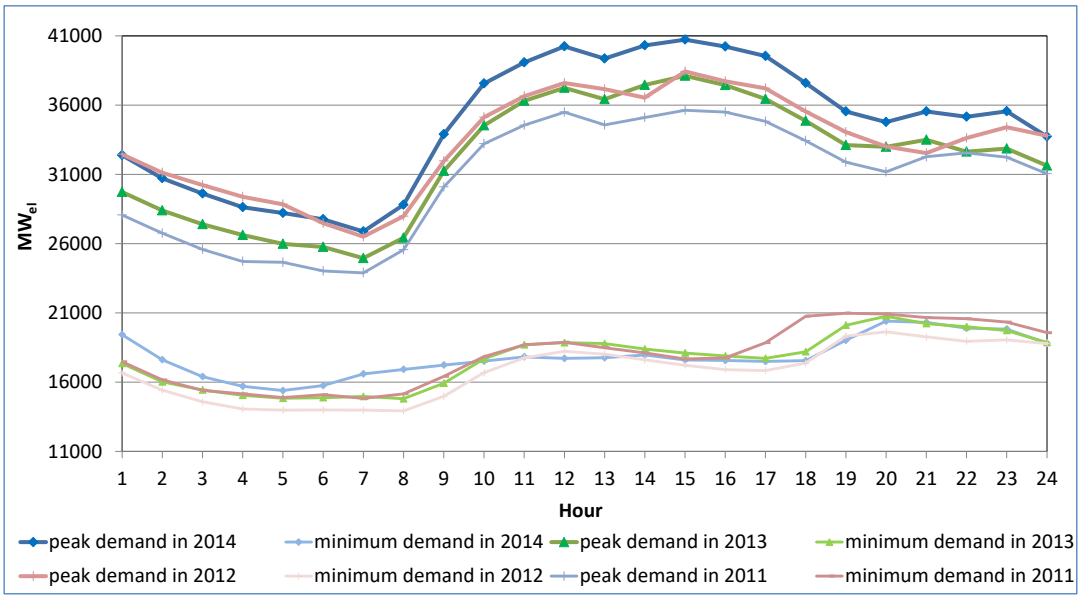

Figure 34- The annual peak and minimum load demand in Turkey in years 2011, 2012, 2013 and 2014 (own illustration according to the data from TEIAS)

It can be inferred from the figure that the annual peak and minimum load demands vary mainly depending on the temperature, the consumer behavior and the income of consumers.

[75] In Turkey, sacrifice fest is celebrated for four days and every year about ten days prior w.r.t. the previous year, in order to keep in track of moon calendar.

Therefore, the corresponding variations should also be taken into account during forecasting hourly load demand for obtaining future annual LDCs of Turkey.

Correspondingly, forecasting load curves requires high effort in relating the chronological variations in hourly load demands (i.e. the annual, weekly and daily cycles and trends) with the variations in the energy prices, the consumer behavior, economic and climatic variables in long term. In addition, the accuracy of long-term forecasts diminishes as more uncertainty is present due to the states of the mentioned factors in the future. As a consequence, the long-term forecasting of annual load curves is not preferred for obtaining the future LDCs of Turkey. Instead, obtaining forecasts of future LDCs per se is preferred.

9.3 Objective of This Study

In this study, a concept on obtaining functional approximations to future LDCs of Turkey is introduced for the first time. This concept is based on the previous study conducted by Uri and Maybee (1980) implemented at the Federal Energy Regulatory Commission (FERC) region level[76] in the USA. In their approach, the functional approximations to future LDCs are obtained from the forecasted functional parameters of the approximated past LDCs. Their approach is briefly described as follows:

- First of all, the hourly load demands in each year are divided by the corresponding annual gross electricity demand[77] of each year yielding normalized hourly demands. Then, from the normalized hourly demands corresponding normalized LDCs with unit areas are constructed[78].
- Secondly, the LDCs are approximated by using linear-exponential functions (see Eq. (12.1.14) p. 190). Correspondingly, a sequence comprised of all the estimated functional parameters is formed.
- Thirdly, the obtained sequence of parameters is analyzed by using the Box-Jenkins method of univariate time series analysis[79] (TSA); in order to find the adequate TSA model[80] that fits to the values of the sequence.

[76] In particular, the FERC region 5 consists of the power transmission systems in New Mexico, Texas, Louisiana, Arkansas, Oklahoma, Kansas, and parts of Missouri and Mississippi (Maybee & Uri, p. 306).
[77] The annual gross electricity demand equals to the sum of national electricity generation and imported amount of electricity subtracted exported amount of electricity.
[78] Note that the normalized hourly load demands should be sorted in a descending order of their magnitudes during the construction of the LDCs.
[79] See Section 10.2 for background information on TSA.

- Finally, the functional parameters of the future LDCs are forecasted by using the determined adequate TSA model and the areas under the approximated future LDCs are validated by checking for any considerable deviation from unit area.

Further, their approach is based on the assumption that the short and long term variations in hourly load demands are inherited in the functional parameters through the functional approximations of the considered LDCs. In particular, the functional parameters evolve over time w.r.t. the mentioned factors affecting the hourly demand. Hence, by utilizing their approach, the aforementioned difficulties (see Section 9.2) in obtaining future LDCs of Turkey can be surpassed. Consequently, the future LDCs of Turkey can be obtained with relatively less effort and relatively better accuracy.

In this study, the functional approximations to future LDCs are obtained in four stages as different from the approach of Uri and Maybee. The four stages are listed as follows:

- Data preparation for functional approximation analysis,
- Determination of adequate functional approximations to past LDCs,
- Forecasting functional approximations to future LDCs,
- Validation of functional approximations to future LDCs.

Although the authors described the solution process of their approach, they did not group the computations as different stages of the solution process. In Figure 35, the four stage solution process and the corresponding computations are illustrated in a vertical chevron list.

[80] An adequate econometric model (e.g. TSA model) is defined to be a model whose statistical assumptions are validated through diagnostic tests. See Chapter 10 for the considered econometric models in this study and their corresponding model assumptions.

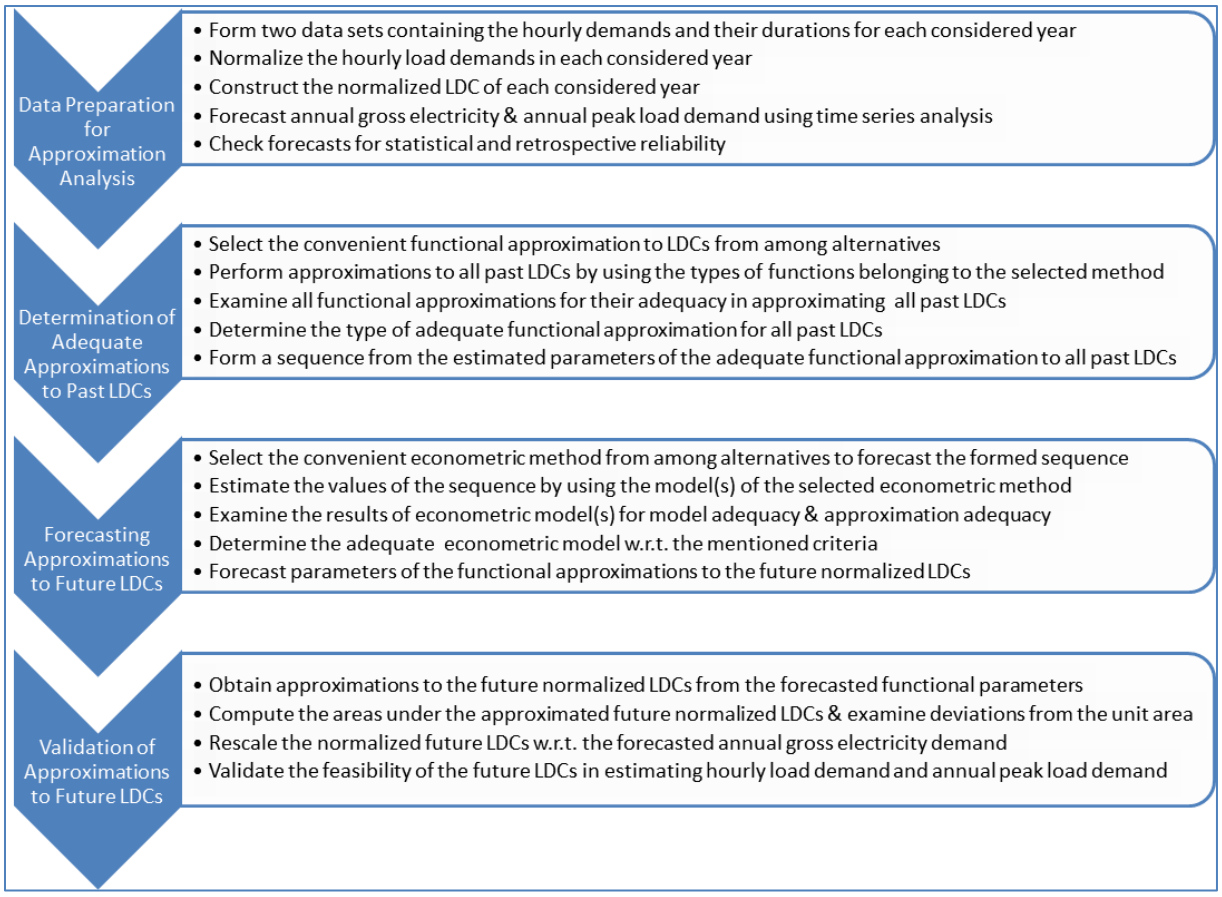

Figure 35- The concept on obtaining functional approximations to future LDCs of Turkey (own illustration)

First of all, the solution procedure is initiated through the data preparation stage. In particular, the past LDCs of Turkey are constructed from the two formed data sets containing the normalized hourly load demands and their durations for each year. Furthermore, the annual gross electricity and annual peak load demand are forecasted by utilizing TSA; in order to be utilized for rescaling and validation of the functional approximations to future LDCs of Turkey respectively (i.e. at the fourth stage). During forecasting, care is taken for achieving statistically and retrospectively reliable forecasts w.r.t. the statistical model assumptions and the corresponding past developments respectively.

In the second stage, the constructed each LDC is approximated by utilizing a functional method; in order to determine the type of mathematical function which adequately approximates the considered LDCs. In particular, the convenient functional method is selected based on the tradeoff between the effort and the accuracy among the methods utilized for approximating LDCs in the previous studies such as discrete, optimal and smooth functional approximations to LDCs (see Chapter 12). The types of mathematical functions, which belong to the selected functional method, are analyzed for adequacy in approximating the past LDCs

to determine the adequate one among others (e.g. polynomial and nonlinear types of functions belonging to smooth functional approximations). In this study, an adequate functional approximation to a LDC is defined to be a parsimonious functional[81] approximation to a LDC with least possible inaccuracy in approximating annual gross electricity demand, annual peak load demand and hourly load demand among other alternatives. Accordingly, the adequate functional approximation to all past LDCs is the functional approximation that overall holds true to its adequacy. At the end of this stage, a sequence is formed from the estimated parameters of the adequate functional approximations to the considered LDCs.

In the third stage, the formed sequence of estimated parameters is analyzed by using a convenient econometric method. The convenient econometric method is selected based on the least effort and the highest accuracy among the methods utilized for obtaining future approximations to LDCs in the previous studies such as regression analysis[82] or TSA (see Chapter 13). The regression analysis requires the values of the sequence to be related with the price of electrical energy, income and climatic variables by utilizing an adequate regression model; whereas the TSA requires an adequate model to be determined from a number of stochastic models fitted to the sequence itself (see Chapter 13). Accordingly, the values of the sequence are predicted by the model of the selected econometric method. Subsequently, the corresponding model is examined not only for model adequacy in statistical terms but also for adequacy of approximations to LDCs. In particular, the annual gross electricity demand, the annual peak load demand and the hourly load demand for each year are estimated by using the predicted (i.e. also called fitted) functional parameters from the selected econometric model. After finding an adequate econometric model based on the mentioned methods and criteria, the functional parameters of the approximations to future normalized LDCs are forecasted.

In the final stage, the approximations to future LDCs are examined for their feasibility in approximating the annual gross electricity demand, reflecting the changes in hourly load demands (i.e. through the shape of the LDCs) and the annual peak load demand in the period 2015-2025. The approximations to future LDCs can be used as an input to the capacity expansion model of Turkey, if the approximations to future LDCs are validated w.r.t. the

[81] The term "parsimonious function" refers to the simplest function which has the smallest possible number of parameters to adequately explain the variation in the dependent variable (i.e. hourly load demand) using independent variable (i.e. duration). Note that the more parameters considered for approximation of LDCs, the more uncertainty will be present in the forecasts of the corresponding parameters which are used for obtaining approximations to future LDCs.

[82] See Section 10.1 for the relevant background information.

mentioned criteria. Accordingly, the approximations to normalized future LDCs are obtained from the forecasted functional parameters in the previous stage. In order to examine deviations from unit area, the areas under the corresponding curves are computed. Any deviation from unity, which is higher than 1%, is considered to be infeasible. Further, the normalized future LDCs are rescaled w.r.t. the forecasted annual gross electricity demand and graphically examined for any infeasible discrepancy in the shape of the approximations to future LDCs w.r.t. the past LDCs. Lastly, the feasibility of the future LDCs in estimating future annual peak load demand[83] is examined for any discrepancy in growth rate w.r.t. the past development and forecasted development of the peak load demand during the first stage.

9.4 Organization of This Study

This study is organized into six chapters.

In Chapter 10, relevant background information on the econometric methods is provided. In particular, information is given about the regression analysis and the TSA in Section 10.1 and in Section 10.2 respectively. The regression analysis, such as linear and nonlinear regression analysis, is utilized for approximating the past LDCs of Turkey in the period 2000-2014. Further, the TSA is utilized for forecasting the annual gross electricity demand, annual peak load demand and also for forecasting the parameters of the approximating functions of the LDCs in the period 2015-2025.

In Chapter 11, detailed information about data preparation for approximation analysis is given (i.e. the 1st stage of the introduced concept). In Section 11.1, information is provided about constructing past LDCs of Turkey. In Section 11.2, an overview is given on the demand for electricity in Turkey in the period 2000-2014. In the final Section 11.3, the analysis on the future development of annual gross electricity demand and annual peak load demand are explained.

In Chapter 12, comprehensive information is provided on the determination of adequate functional approximations to LDCs of Turkey in the period 2000-2014 (i.e. the 2nd stage of the introduced concept). In Section 12.1, detailed information about the methods on functional approximations to LDCs is provided, such as ad hoc and optimal discrete approximations and smooth functional approximations to LDCs. At the end of the section, a summary on the corresponding methods is given and a discussion is carried out for selecting the convenient

[83] The estimated annual peak load demand is obtained from rescaling of the approximated future LDCs.

method for approximating the LDCs of Turkey. In the final Section 12.2, information is given about determining the adequate functional approximation to past LDCs of Turkey among the smooth functional approximations (i.e. polynomial and non-linear functions).

In Chapter 13, comprehensive information is provided on obtaining functional approximations to future LDCs of Turkey in the period 2015-2025 (i.e. the 3rd stage of the introduced concept). In Section 13.1, comprehensive information on the type of methods for forecasting functional approximations to LDCs are provided, such as using regression analysis and TSA. At the end of the section, a summary on the type of forecasting methods for approximations to LDCs is given and a discussion is carried out for selecting the convenient type of method for obtaining future approximations to the LDCs of Turkey. In the final Section 13.2, information is given about the analysis on obtaining approximations to LDCs of Turkey for the period 2015-2025.

In Chapter 14, information is provided about the examination on feasibility of the approximations to future LDCs in approximating annual gross electricity demand, reflecting the changes in hourly load demands (i.e. through the shape of the LDCs) and annual peak load demand for the forecasted period (i.e. the final stage of the introduced concept).

In Chapter 15, a conclusion is provided for summarizing the purpose and novelty of the introduced concept for obtaining functional approximations to future LDCs of Turkey for the period 2015-2025. In particular, the results and findings of all analysis are summarized. Finally, an insight into the opportunities for further research is provided.

10 RELEVANT BACKGROUND INFORMATION ON ECONOMETRIC METHODS

In this chapter, relevant background information on the econometric methods is provided. In particular, information is given about the regression analysis and the TSA in Section 10.1 and 10.2 respectively. The regression analysis, such as linear and nonlinear regression analysis, is utilized for approximating the past LDCs of Turkey in the period 2000-2014. Further, the TSA is utilized for forecasting the annual gross electricity demand, the annual peak load demand and also for forecasting the parameters of the approximating functions of the LDCs in the period 2015-2025.

10.1 Regression Analysis

The linear and nonlinear regression methods are utilized for analyzing the mathematical relationship between the hourly load demand (i.e. dependent variable) and the duration (i.e. independent variable) forming LDCs. The mathematical relationship is determined by estimating unknown regression parameters of the regression functions under certain assumptions. A model is classified as linear or non-linear according to the linearity or non-linearity in the regression parameters. A linear regression model is utilized for estimating the regression parameters according to the assumed linear relationship between the dependent and independent variable; whereas a nonlinear regression model is based on the nonlinear relationship of the corresponding variables. In the next subsections, comprehensive information about the linear and nonlinear regression is given.

10.1.1 Linear Regression

The general linear model is analytically represented as expressed below (Fox, 2008, p. 187):

$$y_i = \beta_0 + \beta_1 x_{i,1} + \beta_2 x_{i,2} + \cdots + \beta_k x_{i,k} + \epsilon_i \qquad i = 1,2 \dots, n \tag{10.1.1}$$

In the model, the random variable y_i is called the dependent (also called the response) variable representing the values for each i^{th} observation from a sample size of n (i.e. $i = 1,2 \dots, n$). The dependent variable is composed of a deterministic and a stochastic part. The deterministic part is expressed by the multiplication of the regression parameters $\beta_0, \beta_1, \beta_2 \dots \beta_k$ with the corresponding independent (also called the predictor) variables

$\boldsymbol{x} = (x_{i,1}, x_{i,2}, \dots, x_{i,k})$. The symbol $x_{i,k}$ indicates i^{th} observation of the k^{th} independent variable. The stochastic part, represented by the random variable $\boldsymbol{\epsilon} = (\epsilon_1, \epsilon_2 \dots \epsilon_n)$, is a stochastic disturbance, considered for taking into account the variation in the dependent variable. The general model can also be expressed in matrix form (Fox, p. 187) as follows:

$$\boldsymbol{y} = \boldsymbol{X\beta} + \boldsymbol{\epsilon} \tag{10.1.2}$$

where

$$\boldsymbol{y} = \begin{bmatrix} y_1 \\ y_2 \\ \vdots \\ y_n \end{bmatrix}, \boldsymbol{X} = \begin{bmatrix} 1 & x_{1,1} & x_{1,2} & \cdots & x_{1,k} \\ 1 & x_{2,1} & x_{2,2} & \cdots & x_{2,k} \\ \vdots & \vdots & \vdots & & \vdots \\ 1 & x_{n,1} & x_{n,2} & \cdots & x_{n,k} \end{bmatrix}, \boldsymbol{\beta} = \begin{bmatrix} \beta_0 \\ \beta_1 \\ \vdots \\ \beta_k \end{bmatrix} \text{ and } \boldsymbol{\epsilon} = \begin{bmatrix} \epsilon_1 \\ \epsilon_2 \\ \vdots \\ \epsilon_n \end{bmatrix}.$$

In the above representation, $\boldsymbol{y}$ is a $(n \times 1)$ vector of the dependent variables, $\boldsymbol{X}$ is a $(n \times k + 1)$ matrix of the predictor variables. In the design matrix, $\boldsymbol{X}$, each n^{th} row corresponds to an observation and each k^{th} column after the first corresponds to an independent variable. The first column of $\boldsymbol{X}$ is composed of ones (i.e. called a dummy variable) for the calculation of intercept β_0. The vector $\boldsymbol{\beta}$ is a $(k \times 1)$ vector of the regression parameters, and $\boldsymbol{\epsilon}$ is a $(n \times 1)$ vector of random errors. From here on, matrices and vectors are denoted with bold notations.

Note that in linear regression, the errors ϵ_i are assumed to be independent and normally distributed (N) with mean zero and constant variance (Var) $\sigma_{\boldsymbol{\epsilon}}^2$ (Fox, p. 188), i.e.

$$E[\boldsymbol{\epsilon}] = \boldsymbol{0} \tag{10.1.3}$$

$$Var[\boldsymbol{\epsilon}] = E[\boldsymbol{\epsilon\epsilon}'] = \sigma_{\boldsymbol{\epsilon}}^2 \boldsymbol{I_n} \tag{10.1.4}$$

The symbol "$\boldsymbol{I_n}$" is an $n \times n$ identity matrix and the superscript " $'$ " denotes the transpose of the matrix. The assumptions can be written in compact form as shown below:

$$\boldsymbol{\epsilon} \sim N_n(\boldsymbol{0}, \sigma_{\boldsymbol{\epsilon}}^2 \boldsymbol{I_n}) \quad \forall i: i = 1,2, \dots, n \tag{10.1.5}$$

According to the assumptions, the expectation function of the regression model can be represented as shown below (Bates & Watts, 1988, p. 2):

$$E[\boldsymbol{y}] = \boldsymbol{X\beta} \tag{10.1.6}$$

Further, the joint probability density function $p(\boldsymbol{y}|\boldsymbol{\beta}, \sigma_{\epsilon}^2)$ for $\boldsymbol{y}$, given $\boldsymbol{\beta}$ and the variance σ_{ϵ}^2 can be written as represented below (Bates & Watts, p. 2):

$$p(\boldsymbol{y}|\boldsymbol{\beta}, \sigma_{\epsilon}^2) = (2\pi\sigma_{\epsilon}^2)^{-n/2}\, exp\left[\frac{-(\boldsymbol{y}-\boldsymbol{X\beta})'(\boldsymbol{y}-\boldsymbol{X\beta})}{2\sigma_{\epsilon}^2}\right] \tag{10.1.7}$$
$$= (2\pi\sigma_{\epsilon}^2)^{-n/2}\, exp\left[\frac{-\|\boldsymbol{y}-\boldsymbol{X\beta}\|^2}{2\sigma_{\epsilon}^2}\right]$$

Note that the double vertical bars denote the length of the vectors. Furthermore, the likelihood function $l(\boldsymbol{\beta}, \sigma_{\epsilon}^2|\boldsymbol{y})$ differs from $p(\boldsymbol{y}|\boldsymbol{\beta}, \sigma_{\epsilon}^2)$ due to being a function of $\boldsymbol{\beta}$, σ_{ϵ}^2 and also conditional on $\boldsymbol{y}$. By suppressing the constant $(2\pi)^{-n/2}$, it can be seen that $l(\boldsymbol{\beta}, \sigma|\boldsymbol{y})$ is proportional ($\propto$) to the remaining terms as indicated below (Bates & Watts, p. 4):

$$l(\boldsymbol{\beta}, \sigma|\boldsymbol{y}) \propto \sigma_{\epsilon}^{-n}\, exp\left[\frac{-\|\boldsymbol{y}-\boldsymbol{X\beta}\|^2}{2\sigma_{\epsilon}^2}\right] \tag{10.1.8}$$

Thus, the objective is to maximize the likelihood w.r.t. $\boldsymbol{\beta}$ when the sum of squares of error ($SSE(\boldsymbol{\beta})$) is at minimum as represented below (Fox, p. 193):

$$SSE(\boldsymbol{\beta}) = \boldsymbol{\epsilon}'\boldsymbol{\epsilon} = \|\boldsymbol{y}-\boldsymbol{X\beta}\|^2 = (\boldsymbol{y}-\boldsymbol{X\beta})'(\boldsymbol{y}-\boldsymbol{X\beta}) \tag{10.1.9}$$

Hence, the minimum of SSE can be achieved by finding the maximum likelihood estimate $\widehat{\boldsymbol{\beta}}$ of $\boldsymbol{\beta}$. It should be noted that the maximum likelihood estimator $\widehat{\boldsymbol{\beta}}$ is same as the least square estimator of $\boldsymbol{\beta}$ under the assumptions of the linear model (Fox, p. 197). From here on, $\widehat{\boldsymbol{\beta}}$ is called the least squares estimate and the minimization is carried out for residual sum of squares ($RSS(\widehat{\boldsymbol{\beta}})$) expressed below:

$$RSS(\widehat{\boldsymbol{\beta}}) = \boldsymbol{e}'\boldsymbol{e} = (\boldsymbol{y}-\boldsymbol{X}\widehat{\boldsymbol{\beta}})'(\boldsymbol{y}-\boldsymbol{X}\widehat{\boldsymbol{\beta}}) \tag{10.1.10}$$

RSS is a function of $\widehat{\boldsymbol{\beta}}$ and the symbol "$\boldsymbol{e}$" denotes the vector of residuals. The difference between the observation y_i and the fitted (also called the predicted) value $\hat{y}_i$ is a residual and represented below in $n \times 1$ vector form for n number of fitted values:

$$\boldsymbol{e} = \boldsymbol{y} - \hat{\boldsymbol{y}} \tag{10.1.11}$$

The unknown values of $\widehat{\boldsymbol{\beta}}$ can be found by taking the first vector partial derivatives of $RSS(\widehat{\boldsymbol{\beta}})$ w.r.t. each unknown parameter as indicated below in vector form (Fox, p. 193):

$$\frac{\partial RSS(\widehat{\boldsymbol{\beta}})}{\partial \widehat{\boldsymbol{\beta}}} = \mathbf{0} - 2\boldsymbol{X}'\boldsymbol{y} + 2\boldsymbol{X}'\boldsymbol{X}\widehat{\boldsymbol{\beta}} \tag{10.1.12}$$

After that these derivatives are set to zero yielding the normal equations, and then solving the normal equations provides the first order necessary conditions for an optimum. It should be noted that for linear models, derivatives w.r.t. any of the parameters are independent of all other parameters (i.e. due to linearity). In matrix form, the normal equations can be expressed as shown below (Fox, p. 193):

$$\boldsymbol{X}'\boldsymbol{X}\widehat{\boldsymbol{\beta}} = \boldsymbol{X}'\boldsymbol{y} \tag{10.1.13}$$

To solve the normal equations, both sides of Eq. (10.1.13) are multiplied by the inverse of $\boldsymbol{X}'\boldsymbol{X}$ yielding the (ordinary) least squares estimate of $\boldsymbol{\beta}$ in matrix form (Fox, p. 193):

$$\widehat{\boldsymbol{\beta}} = (\boldsymbol{X}'\boldsymbol{X})^{-1}\boldsymbol{X}'\boldsymbol{y} \tag{10.1.14}$$

Remark that there are $p = k + 1$ normal equations for $p = k + 1$ unknowns (the values of $\hat{\beta}_0, \hat{\beta}_1, \hat{\beta}_2, \dots, \hat{\beta}_k$) and the matrix $\boldsymbol{X}'\boldsymbol{X}$ is assumed to be always invertible[84]. The details of computing the derivatives of above given equations can be found in Fox (pp. 192-194). In matrix notation, the fitted model can be expressed as indicated below:

$$\widehat{\boldsymbol{y}} = \boldsymbol{X}\widehat{\boldsymbol{\beta}} \tag{10.1.15}$$

The unbiased estimate of $\sigma_{\boldsymbol{\epsilon}}^2$, i.e. $\hat{\sigma}_{\boldsymbol{\epsilon}}^2$,can be obtained by the given equation below (Fox, p. 198):

$$\hat{\sigma}_{\boldsymbol{e}}^2 = \frac{RSS}{n-p} = \frac{\boldsymbol{e}'\boldsymbol{e}}{n-p} = \frac{\sum_{i=1}^{n} e_i^2}{n-p} \tag{10.1.16}$$

In the given above equation, the denominator $n - p$ is the residual degrees of freedom (df).

10.1.1.1 Properties of the Linear Least Squares Estimators

1. The least squares estimator $\widehat{\boldsymbol{\beta}}$ is normally distributed and unbiased estimator of $\boldsymbol{\beta}$. Note that the $\widehat{\boldsymbol{\beta}}$ is a linear function of $\boldsymbol{y}$, which in turn is a linear function of $\boldsymbol{\epsilon}$. Hence it can be written that

[84] In linear algebra, an n-by-n square matrix is called invertible.

$$E(\widehat{\boldsymbol{\beta}}) = E[(\boldsymbol{X}'\boldsymbol{X})^{-1}\boldsymbol{X}'\boldsymbol{y}] = E[(\boldsymbol{X}'\boldsymbol{X})^{-1}\boldsymbol{X}'(\boldsymbol{X}\boldsymbol{\beta} + \boldsymbol{\epsilon})] = \boldsymbol{\beta} \quad (10.1.17)$$

since $E(\boldsymbol{\epsilon}) = \mathbf{0}$ and$(\boldsymbol{X}'\boldsymbol{X})^{-1}\boldsymbol{X}'\boldsymbol{X} = \boldsymbol{I}$ (Fox, p. 195).

2. The covariance matrix of the least squares estimator

$$Var[\widehat{\boldsymbol{\beta}}] = \hat{\sigma}_{\epsilon}^2(\boldsymbol{X}'\boldsymbol{X})^{-1} \quad (10.1.18)$$

depends on the variance of the disturbances and on the design matrix $\boldsymbol{X}$ (Fox, p. 195). The diagonal elements of $\hat{\sigma}_{\epsilon}^2(\boldsymbol{X}'\boldsymbol{X})^{-1}$ are the variances of $\hat{\beta}_0, \hat{\beta}_1, \hat{\beta}_2, \ldots, \hat{\beta}_k$and the off-diagonal elements of this matrix are the covariances.

3. Let $E[\widehat{\boldsymbol{y}}]$ be the least square estimate of $E[\boldsymbol{y}] = \boldsymbol{X}\boldsymbol{\beta}$ and $\boldsymbol{c}$ be the vector of constants, then $\boldsymbol{c}'E[\widehat{\boldsymbol{y}}]$ is the unique estimate (i.e. so called the Best Linear Unbiased Estimate, or BLUE) with the minimum variance among the class of linear unbiased estimates $\boldsymbol{c}'E[\boldsymbol{y}]$ (Fox, p. 196).

10.1.1.2 Statistical Inference for Linear Regression Analysis

Statistical inference is based on the laws of probability, and provides a basis for inferring conclusions about a given population using data from a sample of it. In this subsection, brief information about performing hypothesis tests and constructing confidence intervals on the regression parameters is given.

10.1.1.2.1 The Coefficient of Determination

The coefficient of determination, R^2, is utilized for the assessment of how good a mathematical relation fits to the considered sample data. In particular, the goodness of a fit can be measured by the percentages of variation in the dependent variable explained jointly by the independent variables (Huang, 1970, p. 81). Therefore, a calculated value of high R^2 represents a good fit of the considered relation, whereas a low value of R^2 a poor fit.

The variation in dependent variable, so called the total sum of squares (TSS), is decomposable into "explained" and "unexplained" components so called the regression sum of squares ($RegSS$) and RSS respectively (Fox, p. 92):

$$TSS = RegSS + RSS \quad (10.1.19)$$

Where

$$TSS = \sum (y_i - \bar{y})^2 \tag{10.1.20}$$

$$RegSS = \sum (\hat{y}_i - \bar{y})^2 \tag{10.1.21}$$

$$RSS = \sum (y_i - \hat{y}_i)^2 = \sum e_i^2 \tag{10.1.22}$$

The given above decomposition is called the analysis of variance for the regression. Subsequently, R^2 can be represented as the ratio of the explained variation in dependent variable to the total variation (Fox, p. 93):

$$R^2 = \frac{RegSS}{TSS} = 1 - \frac{RSS}{TSS} \tag{10.1.23}$$

Note that the smaller the number of variables in a relation, the more preferable the relation becomes (Huang, 1970, p. 81). In the light of this remark, an adjusted R^2 statistic (R^2_{adj}) is suggested to be utilized in prevention of over-fitting due to over-parameterization. R^2_{adj} measures the contribution of additional variables to the goodness of fit of a regression model (Fox, p. 94):

$$R^2_{adj} = 1 - \frac{RSS/(n-p)}{TSS/(n-1)} \tag{10.1.24}$$

This is due to the reason that the denominator of the term is a constant and R^2_{adj} can only increase, if the new added variable reduces RSS.

10.1.1.2.2 Hypothesis Test for Significance of a Regression Model

The test for significance of a regression model is a test for examining the global significance of a model. The examination reveals whether a linear relationship exists between the dependent variable and the independent variables. By applying a global F-test for the null hypothesis (H_0), it is tested whether all the regression parameters are different from 0 (Fox, p. 107):

$$H_0: \beta_1 = \beta_2 \ldots = \beta_k = 0 \tag{10.1.25}$$

H_0 is a hypothesis which is tried to be disproved or rejected based on a statistical evidence; whereas the alternative hypothesis

$$H_1: \beta_j \neq 0 \; for \; at \; least \; one \; j \tag{10.1.26}$$

indicates that at least one of the independent variables $x_1, x_2, \dots, x_k$ is significant and related to the dependent variable. H_1 is the conclusion, if the test indicates that H_0 is false. The test statistic for H_0, so called F-statistic (denoted as F_0), can be calculated as represented below (Fox, p. 108):

$$F_0 = \frac{RegSS/k}{RSS/(n-k-1)} = \frac{RegMS}{RMS} \tag{10.1.27}$$

A test statistic is a random variable whose outcome can be obtained by computing the statistic for a given sample. F_0 is calculated from the analysis of the variance of the regression and has an F distribution with $k \; df$ (due to $RegSS$) and $n-k-1 \; df$ (due to RSS) (Fox, p. 108). The residual mean square, RMS, represents the estimated error variance $\hat{\sigma}_\epsilon^2$. In case the null hypothesis cannot be rejected, the regression mean square ($RegMS$) is able to provide an independent estimate of the error variance implying the ratio of the two mean squares to be close to 1 (Fox, p. 108). Alternatively, if the null hypothesis is rejected, the RegMS estimates the error variance plus a positive quantity that depend on the βs (Fox, p. 108). Thus, the global null hypothesis can be rejected for values of F_0 that are sufficiently larger than 1. Formally, H_0 is rejected if

$$F_0 > F_{k,n-k-1}^{\alpha} \tag{10.1.28}$$

The critical value for F-Test ($F_{k,n-k-1}^{\alpha}$) can be found in tabulated form in statistical tables considering the dependence on α (the significance level), k (the df of the numerator), and $n-k-1$, (the df of the denominator). The critical value for a hypothesis test is a threshold which is compared with the calculated test statistic to investigate whether the null hypothesis can be rejected based on statistical evidences. A significance level is defined to be the probability of rejecting H_0 given that H_0 is true (so called Type I error). Hence, H_0 can be rejected in favor of H_1 at level α when $F \geq F_{k,n-k-1}^{\alpha}$. If H_0 is rejected, it can be concluded

that $x_1, x_2, \dots, x_k$ are jointly statistically significant, at the selected α level. Common chosen values by practitioners for α are 0.10, 0.05 and 0.01.

A probability value (so called a p-value) can also be computed for testing hypothesis together with an F-statistic. A p-value can be defined as the lowest significance level at which a null hypothesis can be rejected. Subsequently, the null hypothesis can be rejected for any H_0 when $\alpha \geq p$-value, whereas the null hypothesis cannot be rejected when $\alpha < p$-value.

10.1.1.3 Hypothesis Test on Individual Regression Coefficients and Confidence Intervals

A significance test can be applied on a single regression parameter β_j to investigate whether the independent variable x_j has an effect on $\boldsymbol{y}$ once the effects of $x_2, x_3, \dots, x_{j-1}, x_{j+1}, \dots, x_k$ on $\boldsymbol{y}$ have been accounted for. Therefore, the hypotheses for testing the significance of any individual regression coefficient can be proposed as follows:

$$H_0: \beta_j = 0 \tag{10.1.29}$$

$$H_1: \beta_j \neq 0 \tag{10.1.30}$$

The test statistic for the mentioned hypothesis can be calculated as a t-statistic (t_0) (Fox, p. 104):

$$t_0 = \frac{\hat{\beta}_j - \beta_j}{se(\hat{\beta}_j)} \tag{10.1.31}$$

Note that β_j is set to zero for H_0. The standard error of $\hat{\beta}_j$ ($se(\hat{\beta}_j)$) can be expressed in scalar form (Fox, p. 107):

$$se(\hat{\beta}_j) = \frac{1}{\sqrt{1 - R_j^2}} \cdot \frac{\hat{\sigma}_e}{\sqrt{\sum (x_{ij} - \bar{x}_j)^2}} \tag{10.1.32}$$

The symbol "R_j^2" is the squared multiple correlation from the regression of x_j on all the other $x's$ as indicated below (Fox, p. 106):

$$R_j^2 = \frac{\sum_{i=1}^{n}(\hat{x}_{ij} - \bar{x}_j)^2}{\sum_{i=1}^{n}(x_{ij} - \bar{x}_j)^2} \tag{10.1.33}$$

Hence, H_0 is rejected if $|t_0| \geq t_{n-k-1}^{\alpha/2}$. The critical value for t-test ($t_{n-k-1}^{\alpha/2}$) corresponds to the upper $\alpha/2$ quantile[85] for Student's t-distribution with $-k-1$ df. Alternatively, H_0 is rejected for any level of significance, if $\alpha \geq p - value$; whereas H_0 is not rejected, if $\alpha < p - value$. If H_0 is not rejected, the regressor x_j can be ignored for the model.

A $100(1-\alpha)\%$ confidence interval for β_j can be introduced with lower and upper bounds by using the below given relation (Fox, p. 104):

$$\beta_j = \hat{\beta}_j \pm t_{n-k-1}^{\alpha/2} \cdot se(\hat{\beta}_j) \tag{10.1.34}$$

10.1.1.4 Tests on Subsets of Regression Coefficients

A significance test can also be applied on a subset of regression parameters to test the null hypothesis

$$H_0: \beta_1 = \beta_2 = \cdots = \beta_q = 0 \;\; \forall q: 1 \leq q \leq k \tag{10.1.35}$$

against the alternative hypothesis

$$H_1: H_0 \; is \; not \; true \tag{10.1.36}$$

The F-test of H_0 is based on the first q coefficients of a regression model with k coefficients. The resulting model subset is called the null model. The model including all independent variables is called the full model. Let RSS_0 and $RegSS_0$ represent the residual and regression sums of squares for the null model; similarly RSS_1 and $RegSS_1$ are the corresponding parameters for the full model. The F-statistic (F_0) for testing the corresponding null hypothesis is given below (Fox, p. 109):

$$F_0 = \frac{(RegSS_1 - RegSS_0)/q}{RSS_1/(n-k-1)} = \frac{n-k-1}{q} \cdot \frac{R_1^2 - R_0^2}{1 - R_1^2} \tag{10.1.37}$$

[85] Quantiles are statistics that describe various subdivisions of a probability distribution into equal intervals.

The terms R_1^2 and R_0^2 represent the squared multiple correlations from the full and null models respectively. Under the null hypothesis, F_0 has an F-distribution with q and $-k-1\ df$. H_0 is rejected if

$$F_0 > F_{q,n-k-1}^{\alpha} \tag{10.1.38}$$

Alternatively, the null hypothesis is rejected for any H_0 $\alpha \geq p$-value, whereas the null hypothesis is not rejected when $\alpha < p$-value.

10.1.1.5 Linear Regression Diagnostics

A series of assumptions are aforementioned; in order to fit a regression model to a considered set of data. The assumptions should have to be tested whether the fitted model is appropriate (i.e. also called adequate) and the conclusions based upon it are valid. Note that forecasting can be performed by using a considered model, only if the validity of the assumptions is achieved. This can be carried out by a series of tools known as regression diagnostics to measure model adequacy. In this section, several important testing procedures for linear regression assumptions are accordingly described.

10.1.1.5.1 Residual Analysis

Residuals can be analyzed to test whether a proposed model is a valid model for exhibiting an adequate fit to the data under the given assumptions. Thus, the plots of standardized residuals can be visually examined for assessing the magnitude of the residuals to identify unusual values (Fox, p. 246):

$$E_i = \frac{e_i}{\sqrt{\hat{\sigma}_{\boldsymbol{e}}(1-h_{i,i})}}\ i = 1,2,\dots,n \tag{10.1.39}$$

The term "$h_{i,i}$" is called a hat value and is the i^{th} diagonal element of the "hat" matrix $\boldsymbol{H}$ (Fox, p. 261):

$$\boldsymbol{H} = \boldsymbol{X}(\boldsymbol{X}'\boldsymbol{X})^{-1}\boldsymbol{X}' \tag{10.1.40}$$

By using the weight in i^{th} row and j^{th} row ($h_{i,j}$) of $\boldsymbol{H}$, the fitted value $\hat{y}_j$ (also called y-hat) can be expressed in terms of the observed values y_i (Fox, p. 244):

$$\hat{y}_j = h_{1,j}y_1 + h_{2,j}y_2 + \cdots + h_{j,j}y_j + \cdots + h_{n,j}y_n = \sum_{i=1}^{n} h_{i,j}y_i \qquad (10.1.41)$$

It can be inferred that the hat values measure the potential influence (the leverage) of y_i on all fitted values. For example, if h_{ij} is large, the i^{th} observation exerts a considerable impact on the j^{th} fitted value. The-hat values are defined in the interval $1/n \leq h_{i,i} \leq 1$ (Fox, p. 244).

Another approach for identifying unusual values is to compute studentized residuals as expressed below (Fox, p. 246):

$$E_i^* = \frac{\hat{\sigma}_{\boldsymbol{\epsilon}}}{\hat{\sigma}_{\boldsymbol{e}(-i)}\sqrt{1 - h_{i,i}}} \qquad (10.1.42)$$

The studentized residuals is calculated by refitting the model after removing the i^{th} observation, and then obtaining an estimate $\hat{\sigma}_{\boldsymbol{e}(-i)}$ of $\sigma_{\boldsymbol{\epsilon}}$ that is based on the remaining $n - 1$ observations.

The listed features below can be observed in a plot of E_i (or E_i^*) versus any predictor or fitted values, if a valid model has been fit to the considered data (Sheather, 2009, p. 155):

- A random scatter of points around the horizontal axis, since the mean function of e_i is zero when a valid model has been fit,
- Constant variability along the horizontal axis. Remark that the residuals do not have equal variances unlike it is assumed for the errors as follows:

$$Var(e_i) = \sigma_{\boldsymbol{\epsilon}}^2\left(1 - h_{i,i}\right) \quad i = 1,2,\ldots,n \qquad (10.1.43)$$

If any pattern in a plot of standardized residuals can be recognized, it can be concluded that an invalid model has been fit to the data. Subsequently, the residuals should be checked for the model assumptions for normality, homoscedasticity, correlation of errors and linear relationship among the observations.

The normality of the errors can be assessed by constructing a probability plot (Quantile-Quantile plot, i.e. Q-Q plot) and/or a histogram of E_i or E_i^* (Fox, p. 268). A normal probability plot of the E_i or E_i^*can be constructed by plotting the ordered E_i or E_i^* on the ordinate against the ordered statistics from a standard normal distribution on the abscissa. By

using the corresponding plot, the quantiles from E_i or E_i^* (sample quantiles) are compared with the quantiles from a normal distribution (theoretical quantiles) to examine whether they match with each other. If these match, the graph will indicate a line which seems close to a straight line. The observed departures from linearity are the evidence for non-normality (Sheather, 2009, p. 70). Shapiro-Wilk test or Anderson-Darling-Test (A^2-test) can also be utilized as a supplement to the Q-Q plot. By using Wilk-Shapiro test, it can be checked whether the residuals are normally distributed. The W-statistic (W_0) is calculated as follows (Wetherill, 1986, p. 182):

$$W_0 = \left\{\sum_{i=1}^{n} a_i e_{(i)}\right\}^2 / \left\{\sum_{i=1}^{n} (e_i - \mu_{\boldsymbol{e}})^2\right\} \tag{10.1.44}$$

The term a_i is a constant (i.e. a tabulated value by Shapiro and Wilk) together with a significance level α. The term "$e_{(i)}$" denotes the i^{th} order statistic[86] that is the i^{th}smallest number in ordered form of the residuals. The term "$\mu_{\boldsymbol{e}}$" denotes the mean of residuals. H_0 of this test assumes that the population is normally distributed (whereas H_1 indicates the opposite). Hence, H_0 is rejected if the p-value is less than the chosen α-level. This test is suitable for $n \leq 50$ (Wetherill, p. 182). Anderson-Darling-Test (A^2-test) is another test for checking normality for $n \geq 10$. Wetherill (p. 183) remarks that the Shapiro-Wilk test is more powerful than the A^2-test up to a sample size of 50. The A^2-test is recommended to be applied on sample with large sample sizes (Wetherill, p. 183). The A^2-test has the form as follows (Wetherill, p. 182):

$$A^2 = -n^{-1} \sum_{i=1}^{n} (2i-1)[1 + ln\{z_i(1 - z_{n+1-i})\}] \tag{10.1.45}$$

Where

$$z_i = \Phi\{(e_{(i)} - \mu_e)/\hat{\sigma}_{\boldsymbol{e}}\} \tag{10.1.46}$$

It should be noted that $e_{(i)}$ are order statistic with the specified cumulative distribution function Φ. H_0 of this test indicates that the data follow a specified distribution which is in

[86] An i^{th} order statistic is an indexed statistic representing the i^{th} lowest value in a statistical sample.

this case a normal distribution assumed for residuals (whereas H_1 indicates the opposite). Hence, H_0 is rejected if the p-value is less than the chosen α-level.

Heavy-tailed or highly skewed error distributions generate outliers causing the least square estimates to be inaccurate (Fox, p. 268). In general, these problems can be avoided by transforming the data. The Box-Cox transformation approach can be utilized by selecting a power of transformation of $\boldsymbol{y}$ to normalize the errors in the form (Bates & Watts, p. 28):

$$\boldsymbol{y}^{(\lambda)} = \begin{cases} \dfrac{\boldsymbol{y}^{(\lambda)} - 1}{\lambda} & \lambda \neq 0 \\ ln\boldsymbol{y} & \lambda = 0 \end{cases} \tag{10.1.47}$$

In this procedure, variances are calculated and plotted versus $\boldsymbol{y}^{(\lambda)}$, $\lambda = 0, \pm 0.5 \pm 1, \ldots$ and the value of λ (so called the transformation parameter), which makes the variance stable, is selected.

During the analysis of residuals plotted against fitted values, there can be a pattern detected indicating the increase in the variance of the residuals with the level of the response variable. This patter can be considered as an evidence of non-constant error variance ("heteroscedasticity") (Fox, p. 277). Fox proposes a rough rule for the least squares estimates to be in accurate due to presence of heteroscedasticity, when the ratio of the largest to smallest variance is about 10 or more (or more conservatively about 4 or more). The ignorance of the non-constant variance leads to invalid inferences about hypothesis tests and confidence intervals. Fox states that the non-constant error variance can be overcome by the transformation of $\boldsymbol{y}$ to stabilize the variance or by the substitution of weighted-least-squares estimation with ordinary least squares. The weighted-least-squares estimation method is a type of generalized least squares method. As opposed to the least squares method, the generalized least squares method is utilized in such situations when the covariance matrix of errors is any positive definite matrix rather than an identity matrix (Fox, p. 274):

$$Var(\epsilon) = \sigma_{\boldsymbol{\epsilon}}^2 \Omega \tag{10.1.48}$$

The term Ω is considered to be a known $n \times n$ symmetric and positive definite matrix[87] (Huang, p. 128). When Ω is a diagonal matrix, it indicates unequal variances. When Ω has

[87] Ω is defined to be a positive definite and symmetric matrix, since $\boldsymbol{a}'\Omega\boldsymbol{a} > 0$ for any non-zero column vector $\boldsymbol{a} \in \mathbb{R}^n$.

nonzero off-diagonal elements, it indicates presence of correlated errors. As distinct from the least squares method, each term in weighted least squares method is assigned a weight (w_i) reflecting the uncertainty in each observation of the dataset influencing the final parameter estimates (Huang, p. 128) as shown below:

$$Var(\boldsymbol{\epsilon}) = \sigma^2 \begin{bmatrix} \frac{1}{w_1} & 0 & 0 & \cdots & 0 \\ 0 & \frac{1}{w_2} & 0 & \cdots & 0 \\ \vdots & \vdots & \vdots & \ddots & \vdots \\ 0 & 0 & 0 & \cdots & \frac{1}{w_n} \end{bmatrix} \tag{10.1.49}$$

In practice, the weighted least squares criterion for minimizing the weighted residual sum of squares ($WRSS$) can be expressed as follows (Sheather, p. 115):

$$WRSS = \sum_{i=1}^{n} w_i (y_i - \hat{y}_i)^2 = w_i \cdot e_i^2 \tag{10.1.50}$$

In theory, the weight w_i is considered to be a function of the variance of the i^{th} observation σ_i^2 (Fox, p. 274):

$$w_i^2 = \frac{\sigma_{\boldsymbol{\epsilon}}^2}{\sigma_{\epsilon_i}^2} \tag{10.1.51}$$

Note that the term "$\sigma_{\epsilon_i}^2$" denotes the variance of ϵ_i. It can be deduced that observations with smaller variance are multiplied with greater weights. More information on the estimation of w_i can be found in Fox (pp. 274-275).

The plot of residuals against time index can also be analyzed for any pattern indicating correlation of the residuals with each other (i.e. autocorrelation). The residuals vary randomly around zero line, if there is no correlation among the residuals. In addition, the Durbin–Watson statistic (DW)

$$DW = \frac{\sum_{t=2}^{n} (e_t - e_{t-1})^2}{\sum_{t=1}^{n} e_t^2} \tag{10.1.52}$$

can also be computed as a supplement to the residual plot (Fox, p. 442). The range of DW is from 0 to 4. It is assumed for H_0 of the Durbin–Watson test that no autocorrelation exists

between consecutive residuals. H_0 cannot be rejected for the values of DW close to 2. If DW is substantially less/more than 2, there is evidence for positive/negative autocorrelation. If autocorrelation is identified (i.e. Ω has nonzero off-diagonal elements), the generalized least squares method can be applied on the data to avoid the autocorrelation. More information on the estimation of w_i can be found in (pp. 428-429).

The analysis of the residual plots may also indicate non-linearity. In general, nonlinearity can be prevented by the transformation of considered variables or by increasing the order of the terms for the considered dependent variables (e.g. including a quadratic term).

10.1.1.5.2 Influential Data Analysis

Once the linear models are estimated by least squares, they should also be examined for unusual data influencing the results of the regression analysis. The used data should be analyzed for distinguishing among high-leverage observations, regression outliers, and influential observations (Fox, p. 244). These observations may cause the considered model to fail in capturing important features of the data; however they may also indicate results which are consistent with the rest of the data.

The leverage points are the data points whose x-values have unusual large impacts on the regression model by affecting the accuracy in estimation of the regression coefficients. These points are extreme values and are distant from the rest of the data. A point is a bad leverage point (i.e. called an outlier) if its $y - value$ does not follow the pattern set by the other points (Sheather, p. 52). A high leverage point which is in line with the rest of the data (indicating low discrepancy) is not an outlier, since this observation has no influence on the regression coefficients. The given formula below by Fox (p. 242) serves for distinguishing among the three concepts: Influence, leverage, and discrepancy (i.e. also called outlyingness).

$$Influence\ on\ coefficients = Leverage \cdot Discrepancy \tag{10.1.53}$$

It can be inferred that the observations with high leverage and large studentized residual cause substantial influence on the regression coefficients. The influence on the coefficients can be measured by using Cook's D statistic (Fox, p. 250). The Cook's D statistic is used for measuring the impact on each coefficient $\boldsymbol{\beta}$ by removing each i^{th} observation and calculating $\widehat{\boldsymbol{\beta}}_{(i)}$ after each removal of i^{th} observation. The Cook's D statistic (D_i) can simply be computed using the equation given below (Fox, p. 250):

$$D_i = \frac{E_i^2}{k+1} \cdot \frac{h_{i,i}}{1-h_{i,i}}, \quad i = 1,2,\dots,n \tag{10.1.54}$$

The first quotient in the formula indicates a measure of discrepancy, while the second is a measure of leverage. If the i^{th} observation is influential, its removal will result in a large value of D_i. A rough cutoff value for identifying highly influential points of D_i is when $D_i > 4/(n-k-1)$ (Fox, p. 266). If any highly influential points are identified, they should be checked whether any error occurred during the data entry or measurement taking. Further, it is convenient to temporarily remove observations one at a time and then refitting the model at each step to reexamine the resulting changes in Cook's distances. The permanent removal of the identified highly influential points as outliers depends on the judgment of practitioners.

10.1.1.5.3 Multicollinearity

The multiple regression models are based on the dependencies between the dependent variable in $\boldsymbol{y}$ and the independent variables in $\boldsymbol{x}$. On the contrary, dependencies can also be observed among independent variables indicating multicollinearity. The existence of perfect collinearity causes the least-squares coefficients to be not unique (Fox, p. 331). The existence of strong collinearity increases the sampling variances of the least-squares coefficients and makes them useless as estimators for forecasting (Fox, p. 309). The variance-inflation factor (VIF)

$$IF(\beta_j) = \frac{1}{(1-R_j^2)} \quad j = 1,2,\dots,k \tag{10.1.55}$$

is utilized for measuring impact of collinearity on the precision of the estimate β_j (Fox, p. 309). The term R_j^2 is the squared multiple correlation for the regression of x_j on the other x's. The higher the value of VIF the greater is the degree of collinearity. The precision of the

estimate is halved as R_j approaches 0.9 which corresponds to a VIF value of about 5 (Fox, p. 308).

10.1.2 Nonlinear Regression

A nonlinear regression model, which is non-linear in regression parameters $\boldsymbol{\theta} = (\theta_0, \theta_1, \theta_2 \dots \theta_k)$, is utilized for estimating $\boldsymbol{\theta}$ based on the assumed non-linear relationship between $\boldsymbol{y}$ and $\boldsymbol{x}_i$. The relation can be expressed in general form by the set of regression equations for a sample size of n observations as expressed below (Gallant, 1975, p. 73):

$$y_i = f(\boldsymbol{x}_i, \boldsymbol{\theta}) + \epsilon_i \quad \forall i: i = 1,2, \dots, n \tag{10.1.56}$$

The term y_i is the value of the dependent variable for the i^{th} of n observations, $f(\boldsymbol{x}, \boldsymbol{\theta})$ represents the expectation function, $\boldsymbol{x}_i$ is the $k+1$ dimensional row vector of i^{th} inputs (i.e. inclusive a constant), $\boldsymbol{\theta}$ is a $k+1$ dimensional vector of unknown parameters, and ϵ_i is the error term for the i^{th} observation with the same properties as in the linear regression (i.e. $\boldsymbol{\epsilon} \sim N_n(\boldsymbol{0}, \sigma_\epsilon^2 \boldsymbol{I}_n)$). The general non-linear model can also be expressed in matrix form as follows (Gallant, p. 73):

$$\boldsymbol{y} = f(\boldsymbol{x}, \boldsymbol{\theta}) + \boldsymbol{\epsilon} \tag{10.1.57}$$

Where

$$\boldsymbol{y}' = (y_1, y_2, \dots, y_n) \tag{10.1.58}$$

$$f'(\boldsymbol{\theta}) = [f(\boldsymbol{x}_1, \boldsymbol{\theta}), f(\boldsymbol{x}_2, \boldsymbol{\theta}), \dots, f(\boldsymbol{x}_n, \boldsymbol{\theta})] \tag{10.1.59}$$

$$\boldsymbol{\epsilon}' = (\epsilon_1, \epsilon_2, \dots, \epsilon_n) \tag{10.1.60}$$

The likelihood of the general nonlinear model $l(\boldsymbol{\theta}, \sigma_\epsilon^2)$ can be represented as shown below (Fox, p. 463):

$$l(\boldsymbol{\theta}, \sigma_\epsilon^2) = \frac{1}{(2\pi\sigma_\epsilon^2)^{n/2}} exp\left[-\frac{1}{2\sigma_\epsilon^2} SSE(\boldsymbol{\theta})\right] \tag{10.1.61}$$

The function $SSE_{NL}(\boldsymbol{\theta})$[88] denotes the sum of squares of error function for nonlinear regression and can be explicitly expressed as follows (Fox, p. 463):

$$SSE_{NL}(\boldsymbol{\theta}) = \sum_{i=1}^{n} \left[y_i - f(\boldsymbol{x}_i, \boldsymbol{\theta})\right]^2 = [\boldsymbol{y} - f(\boldsymbol{\theta})]'[\boldsymbol{y} - f(\boldsymbol{\theta})] = \|\boldsymbol{y} - f(\boldsymbol{\theta})\|^2 \qquad (10.1.62)$$

As in the case of the general linear model, the objective is to maximize $l(\boldsymbol{\theta}, \sigma_{\boldsymbol{\epsilon}}^2)$ by minimizing SSE_{NL}. Subsequently, SSE_{NL} can be differentiated to derive normal equations as indicated below (Fox, p. 464):

$$\frac{\partial SSE_{NL}(\boldsymbol{\theta})}{\partial \boldsymbol{\theta}} = -2 \sum [y_i - f(x_i, \boldsymbol{\theta})] \frac{\partial f(x_i, \boldsymbol{\theta})}{\partial \boldsymbol{\theta}} \qquad (10.1.63)$$

The normal equations can be achieved by setting these partial derivatives to 0, and replacing the unknown parameters $\boldsymbol{\theta}$ with the vector of non-linear least squares estimates $\widehat{\boldsymbol{\theta}}$. The normal equations can also be represented in matrix form as follows (Fox, p. 464):

$$\left[\boldsymbol{F}(\widehat{\boldsymbol{\theta}}, \boldsymbol{x})\right]' \left[\boldsymbol{y} - f\left(\widehat{\boldsymbol{\theta}}, \boldsymbol{x}\right)\right] = 0 \qquad (10.1.64)$$

The term $\boldsymbol{F}(\widehat{\boldsymbol{\theta}}, \boldsymbol{X})$ is the matrix of derivatives with i^{th} row and j^{th} column entry (Fox, p. 464):

$$F_{i,j} = \frac{\partial f\left(\widehat{\boldsymbol{\theta}}, x_i\right)}{\partial \hat{\theta}_j} \qquad (10.1.65)$$

In nonlinear regression models, the derivatives of expectation functions w.r.t. the parameters in $\widehat{\boldsymbol{\theta}}$ depend on at least one of the parameters in $\widehat{\boldsymbol{\theta}}$. Note that in linear regression the derivatives are not functions of $\boldsymbol{\beta}$'s. Therefore, in nonlinear regression more advanced methods are required for the computation of $\widehat{\boldsymbol{\theta}}$. In the following subsection, information on the methods of estimating $\boldsymbol{\theta}$ is given.

10.1.2.1.1 Methods of Computing Nonlinear Least Squares Estimators

The procedure for the computation of the nonlinear normal equations starts through linearization of the nonlinear function and then continues with the application of the least-squares method on the linearized relation. The linearization of the expectation function is

[88] The subscript "NL" in SSE_{NL} stands for nonlinear regression, in order to distinguish with SSE previously mentioned in Subsection 10.1.1 for the linear regression.

achieved by using the Taylor series expansion of $f(\boldsymbol{x}_t, \boldsymbol{\theta})$ about the point $\boldsymbol{\theta}_0' = [\theta_{1,0}, \theta_{2,0}, \dots, \theta_{p,0}]$ without the second and higher order terms of the series as shown below (Draper & Smith, 1981, p. 462):

$$f(\boldsymbol{x}_i, \boldsymbol{\theta}) = f(\boldsymbol{x}_i, \boldsymbol{\theta}_0) + \sum_{j=1}^{k+1} \left[\frac{\partial f(\boldsymbol{x}_i, \boldsymbol{\theta})}{\partial \theta_j}\right]_{\boldsymbol{\theta}=\boldsymbol{\theta}_0} \left(\theta_j - \theta_{j,0}\right) \quad \forall i: i = 1,2, \dots, n \tag{10.1.66}$$

The zero subscript of $\boldsymbol{\theta}_0$**,** in Eq. (10.1.66), indicates the initial (zeroth) iteration for the chosen starting value of $\boldsymbol{\theta}$.

The common methods of computing non-linear least squares estimators are stated to be Hartley's modified Gauss-Newton method and Marquardt's algorithm (Gallant, p. 76). The information given in this section encompasses the idea of linearization and iterative process in a routine computer calculation.

Hartley's modified Gauss-Newton method

The Gauss-Newton method is based on the substitution of the first-order Taylor series expansion of $f(\boldsymbol{\theta})$ about a trial (T) parameter value $\boldsymbol{\theta}_T$ in the formula for $SSE_{NL}(\boldsymbol{\theta})$ (Gallant, p. 76):

$$SSE_{NL}(\boldsymbol{\theta}_T) = \|\boldsymbol{y} - f(\boldsymbol{\theta}_T) - F(\boldsymbol{\theta}_T)(\boldsymbol{\theta} - \boldsymbol{\theta}_T)\|^2 \tag{10.1.67}$$

The approximating sum of squares obtained from Eq. (10.1.67) can be minimized by linear least squares. This opportunity can be attained by substituting the terms in general non-regression model with the below given corresponding terms for $\boldsymbol{\theta}_0$ (Draper & Smith, p. 462):

$$f_i^0 = f(\boldsymbol{x}_i, \boldsymbol{\theta}_0) \tag{10.1.68}$$

$$b_j^0 = \theta_j - \theta_{j0} \tag{10.1.69}$$

$$F_{i,j}^0 = \left[\frac{\partial f(\boldsymbol{x}_i, \boldsymbol{\theta})}{\partial \theta_j}\right]_{\boldsymbol{\theta}=\boldsymbol{\theta}_0} \tag{10.1.70}$$

Subsequently, the substitution results in approximated form of a linear regression model as represented below (Draper & Smith, p. 463):

$$y_t - f_t^0 = \sum_{j=1}^{p} b_j^0 F_{t,j}^0 + \epsilon_t, \quad t = 1,2,\dots,n \tag{10.1.71}$$

or in vector form as

$$\boldsymbol{y}_0 = \boldsymbol{F}_0 \boldsymbol{b}_0 + \boldsymbol{\epsilon} \tag{10.1.72}$$

Hence, the estimate of $\boldsymbol{b_0}$, i.e. "$\widehat{\boldsymbol{b}}_{\boldsymbol{0}}$", can be computed using least squares method as follows (Draper & Smith, p. 463):

$$\widehat{\boldsymbol{b}}_{\boldsymbol{0}} = (\boldsymbol{F}_0'\boldsymbol{F}_0)^{-\boldsymbol{1}}\boldsymbol{F}_0'\boldsymbol{y}_0 \tag{10.1.73}$$

$$= (\boldsymbol{F}_0'\boldsymbol{F}_0)^{-\boldsymbol{1}}\boldsymbol{F}_0'(\boldsymbol{y} - \boldsymbol{f}_0)$$

The value of the parameter $\boldsymbol{\theta}_M$ minimizing the approximating sum of squares following T iterations can be expressed as given below (Gallant, p. 76) in Eqs.(10.1.74) and (10.1.75):

$$\boldsymbol{\theta}_M = \boldsymbol{\theta}_T + \widehat{\boldsymbol{b}}_T \tag{10.1.74}$$

$$\boldsymbol{\theta}_M = \boldsymbol{\theta}_T + [F'(\boldsymbol{\theta}_T)F(\boldsymbol{\theta}_T)]^{-1}F'(\boldsymbol{\theta}_T)[\boldsymbol{y} - f(\boldsymbol{\theta}_T)] \tag{10.1.75}$$

The iterative solution process for the approximating sum of squares proposed by Hartley proceeds as follows (Gallant, p. 76):

1. 0^{th} Iteration: Choose a starting estimate $\boldsymbol{\theta}_0$ and compute

$$\boldsymbol{D}_0 = [F'(\boldsymbol{\theta}_0)F(\boldsymbol{\theta}_0)]^{-1}F'(\boldsymbol{\theta}_0)[\boldsymbol{y} - f(\boldsymbol{\theta}_0)] \tag{10.1.76}$$

   Then, find a λ_0 between 0 and 1 such that

$$SSE_{NL}(\boldsymbol{\theta}_0 + \lambda_0 \boldsymbol{D}_0) \leq SSE_{NL}(\boldsymbol{\theta}_0) \tag{10.1.77}$$

2. 1^{st} Iteration: Let $\boldsymbol{\theta}_1 = \boldsymbol{\theta}_0 + \lambda_0 \boldsymbol{D}_0$ and compute

$$\boldsymbol{D}_1 = [F'(\boldsymbol{\theta}_1)F(\boldsymbol{\theta}_1)]^{-1}F'(\boldsymbol{\theta}_1)[\boldsymbol{y} - f(\boldsymbol{\theta}_1)] \tag{10.1.78}$$

   Then, find a $\boldsymbol{\lambda}_1$ between 0 and 1 such that

$$SSE_{NL}(\boldsymbol{\theta}_1 + \lambda_1 \boldsymbol{D}_1) \leq SSE_{NL}(\boldsymbol{\theta}_1) \tag{10.1.79}$$

3. 2nd Iteration: Let $\boldsymbol{\theta}_2 = \boldsymbol{\theta}_1 + \lambda_1 \boldsymbol{D}_1$

⋮

A practical method for choosing the step length λ_l at each iteration (l) is by picking up the largest number in the sequence $a_q = (.8)^q \; q = (0,1,2, \dots)$ for which $SSE_{NL}(\boldsymbol{\theta}_i + a_q \boldsymbol{D}_i) < SSE(\boldsymbol{\theta}_i)$ (Gallant, p.76). See Gallant (p. 76) for other methods for choosing λ_l. The iterative solution process can be continued until the termination by a stopping rule such as

$$\|\boldsymbol{\theta}_l - \boldsymbol{\theta}_{l+1}\| < \varepsilon(\|\boldsymbol{\theta}_l\| + \tau) \tag{10.1.80}$$

and simultaneously

$$|SSE_{NL}(\boldsymbol{\theta}_l) - SSE_{NL}(\boldsymbol{\theta}_{l+1})| < \varepsilon(SSE_{NL}(\boldsymbol{\theta}_l) + \tau) \tag{10.1.81}$$

where $\varepsilon > 0$ and $\tau > 0$ are preset tolerance limits, e.g. $\varepsilon = 10^{-5}$ and $\tau = 10^{-3}$ (Gallant, p. 76).

Marquardt's algorithm

Marquardt's algorithm is another method providing solution to $SSE_{NL}(\boldsymbol{\theta}_T)$ by approximation as shown below (Gallant, p. 77):

$$\boldsymbol{\theta}_\delta = [F'(\boldsymbol{\theta}_T)F(\boldsymbol{\theta}_T) + \delta \boldsymbol{I}]^{-1} F'(\boldsymbol{\theta}_T)[\boldsymbol{y} - f(\boldsymbol{\theta}_T)] \tag{10.1.82}$$

The basis of the Marquardt's algorithm is formed by the fact that for all δ sufficiently large, $\boldsymbol{\theta}_\delta$ is an improvement such that $SSE_{NL}(\boldsymbol{\theta}_\delta)$ is smaller than $SSE_{NL}(\boldsymbol{\theta}_T)$ under appropriate conditions (Gallant, p. 77). The initial value of δ_0 is commonly set to some small number, e.g. 10^{-8} (Fox, p. 466). If $l + 1^{th}$ iteration results in $SSE_{NL}(\boldsymbol{\theta}_{k+1}) < SSE_{NL}(\boldsymbol{\theta}_k)$, then the new value of $\boldsymbol{\theta}_{l+1}$ is accepted and the next iteration is initiated with $\delta_{l+2} = \delta_{l+1}/10$; if however, $SSE_{NL}(\boldsymbol{\theta}_{l+1}) > SSE_{NL}(\boldsymbol{\theta}_l)$, then δ_l is increased by a factor of ten and tried again (Fox, p. 466). The Marquardt procedure seems similar to Gauss-Newton; when δ is small. Note that Marquardt algorithm is stated to be more difficult to implement than the Gauss-Newton, since both the conditioning factor δ and step factor λ must be manipulated (Bates & Watts, p. 81). See Bates and Watts (p. 81) for more information.

Gallant (p. 78) notes that using either method may not lead to convergence to $\boldsymbol{\theta}_M$ from a starting value. The reasons for not being able to achieving a convergence may depend both on the distance of the starting value from the correct answer and on the extent of over-parameterization in the response function relative to the data. In case of a failure of convergence, it is recommended to find better starting values or to use a similar response function with fewer parameters. Further, in case of a convergence, it is suggested to check for several reasonable starting values to see whether the iterations converge to the same answer for each starting value.

10.1.2.1.2 Statistical Properties of Nonlinear Least Squares Estimators

Nonlinear regression inference is carried out through the linear approximation of non-linearity (i.e. discussed in Subsection 10.1.2.1.1) to reduce the condition to the linear case and then, by analogy use linear model inference results (Bates & Watts, p. 52). Note that the use of approximation leads to approximate (asymptotic) results rather than exact ones. It should be emphasized that the standard error can be exact, when the sample size is infinitely large. In case of a finite sample size, the calculated standard error is only an approximation which improves itself as sample size gets larger.

The two of the non-linear model inferences, which can be considered in analogy with linear model inferences, are mentioned in the following. See Gallant (pp. 78-81) for more information about hypothesis testing and confidence intervals of nonlinear regression models and see Subsection 10.1.1.2 for linear model inferences for analogy.

An approximate $100(1-\alpha)\%$ confidence interval for θ_j with an approximate standard deviation ($ASE(\hat{\theta}_j)$) can be expressed by the confidence statement given below (Graybill & Iyer, 1994, p. 610):

$$C\left[\hat{\theta}_j - t_{n-k-1}^{1-\alpha/2} ASE(\hat{\theta}_j) \leq \theta_j \leq \hat{\theta}_j + t_{n-k-1}^{1-\alpha/2} ASE(\hat{\theta}_j)\right] \approx 1-\alpha \tag{10.1.83}$$

An approximate hypothesis test for α level of significance can be written as represented below:

$$H_0: \theta_j = c \tag{10.1.84}$$

$$H_1: \theta_j \neq c \tag{10.1.85}$$

where c is any specified number. The test can be performed as follows (Graybill & Iyer, p. 610):

1. Compute $t_0 = \frac{\widehat{\theta}_j - q}{ASE(\widehat{\theta}_j)}$,
2. Reject H_0 if $|t_0| > t_{n-k-1}^{\alpha/2}$.

10.1.2.2 Nonlinear Regression Diagnostics

Similar to the case of the linear regression, the assumptions underlying a nonlinear regression should also be checked for their validity. The assumptions in nonlinear regression models are listed below (Ritz & Streibig, 2008, p. 55):

1. The mean function is correct,
2. The variance of the errors are homoscedastic,
3. The errors are normally distributed,
4. The errors are not auto correlated.

It can be inferred that the previously mentioned techniques in linear regression diagnostics can be similarly applied on nonlinear regression. See Chapter 5 and Chapter 6 (73-91) for information on the corresponding diagnostic tests and remedies for model violations in nonlinear regression models in Ritz and Strebig (pp. 55-70) respectively.

10.2 The Box-Jenkins Method of Time Series Analysis

In this study, the TSA is conducted for identifying an adequate stochastic model for the time series formed by the annual gross electricity demand, the annual peak load demand and also for the sequence formed by the parameters of the adequate function approximating the past LDCs of Turkey. In this respect, the development of annual gross electricity demand and annual peak load demand are forecasted for the period 2015-2025. In addition, the parameters of the adequate function approximating the future LDCs are forecasted to obtain the future LDCs of Turkey in the period 2015-2025.

A stochastic model or process is a probability model that describes the evolution of a system in time according to the laws of probability (Box & Jenkins, 1976, p. 7). The TSA utilize the inherent dependency or correlation in observations of a time series rendering the chronology of the observations to be important. Hence, the TSA is performed to describe the stochastic processes generating the time series and to forecast future observations by utilizing the stochastic models proposed in Box-Jenkins method.

An important class of stochastic models is introduced to be the stationary models. Stationary models are assumed to be defining processes which vary about a fixed constant mean level and with constant variance (Box & Jenkins, p. 7). More information about stationarity is given in the next Subsection. Further, the stationary stochastic processes such as linear filter model, the autoregressive, moving average models and their duality relationship and mixed autoregressive–moving average models are explained in Subsections 10.2.2, 10.2.3, 10.2.4 and 10.2.5, 10.2.6 respectively. Furthermore, information about non-stationary processes called autoregressive integrated moving average (ARIMA) models and seasonal ARIMA models are given in Subsections 10.2.7 and 10.2.8 respectively. Finally, the iterative stages of the Box-Jenkins model building process and forecasting time series models are explained in Subsections 10.2.9 and 10.2.10.

10.2.1 Stationarity of Time Series

A time series is a time-ordered sequence of observed values. Further, a univariate discrete time series (i.e. considered in this study) consists of a single set of "n" successive observations $(z_1, z_2, \dots z_n)$ recorded sequentially over equal time increments "t". A stochastic process represents the evolution of a series of random variables $\{Z_t: t = 0, \pm 1, \pm 2, \dots\}$ from which $z_1, z_2, \dots z_n$ originate according to probabilistic laws. Therefore, the observations are

assumed to be representative of the corresponding infinite population which originates from the same stochastic process (Box & Jenkins, p. 7).

Consequently, the statistical distribution functions[89] of a random variable Z_t for each t can be theoretically determined by using the observations which are assumed to be generated from a stationary stochastic process. The assumption is due to the fact that a single set of observations cannot provide precise information about the population. Hence to overcome this problem, it is assumed that a weakly (covariance) stationary process has a population mean[90] (μ), and population variance[91] ($\gamma_0 \; or \; \sigma^2$) which do not vary over time (Hamilton, 1994, p. 45). Furthermore, the population covariance[92] (γ_k) between values of the process at two time points depends only on "k", the length of the time separating these points (i.e. called the time lag), not on time itself (Hamilton, 1994, p. 46). The mentioned assumptions are analytically expressed in Eq. (10.2.1) and Eq. (10.2.2) respectively.

$$E[Z_t] = \mu \; for \; all \; t \tag{10.2.1}$$

$$E[(Z_t - \mu)(Z_{t-k} - \mu)] = \gamma_k \; for \; all \; t \; and \; any \; k \tag{10.2.2}$$

Further, the magnitude of γ_k is same for any chosen value of t. Finally, for any covariance stationary process γ_k is equal to γ_{-k} (Hamilton, 1994, p. 46):

$$\gamma_k = E\big[(Z_{t+k} - \mu)\big(Z_{[t+k]-j} - \mu\big)\big] = E[(Z_{t+k} - \mu)(Z_t - \mu)] = E[(Z_t - \mu)(Z_{t+k} - \mu)] \tag{10.2.3}$$

Furthermore, a process is proposed to be strictly stationary, if for any values of $k_1, k_2, k_3, \dots, k_n$ the joint distribution of $\left(Z_t, Z_{t+k_1}, Z_{t+k_2}, \dots, Z_{t+k_n}\right)$ depend only on the time lags separating the dates $k_1, k_2, k_3, \dots, k_n$ and not on the date itself (Hamilton, 1994, p. 46). It should be note that a strictly stationary process must be covariance stationary; however a covariance stationary process must not be strictly stationary. In addition, a covariance stationary Gaussian process is at the same time strictly stationary, since the mean and variance are all that are needed to parameterize a multivariate Gaussian distribution completely (Hamilton, 1994, p. 46).

[89] E.g. probability and cumulative distribution functions.
[90] The average value of a variable computed from all members of a population.
[91] It is defined as the average of sum of squares of deviations from mean for each member in a population.
[92] It is the covariance of all possible values of a variable against its own k-lagged values.

Moreover, another assumption on the stationary time series analysis is that the process be μ and σ^2 ergodic. It is assumed that the values of the process, which are sufficiently far apart in time, are almost uncorrelated. Correspondingly, by averaging $(z_1, z_2, \dots z_n)$ through time, new and useful information to the average is continually added to make better estimates of the corresponding process (Kirchgässner & Wolters, 2007, p. 13). Thus, the sample average (see Eq. (10.2.4)) is an unbiased and consistent estimate of the population mean when the variance of $\bar{z}_n$ approaches to zero as $n \to \infty$ and the expectation $E[Z_t] = \mu$ is constant for all t (Kirchgässner & Wolters, p. 13).

$$\lim_{n\to\infty} E\left[\left(\frac{1}{n}\sum_{t=1}^{n} z_t - \mu\right)^2\right] = 0 \tag{10.2.4}$$

Similarly, the variance of the observations can be interpreted for all t as follows (Kirchgässner & Wolters, p. 13):

$$\lim_{n\to\infty} E\left[\left(\frac{1}{n}\sum_{t=1}^{n} (z_t - \mu)^2 - \sigma^2\right)^2\right] = 0 \tag{10.2.5}$$

In conclusion, the mean, variance, autocovariances and autocorrelations ($\rho_k = \gamma_k/\gamma_0$) of the stochastic process can be estimated from the observations under the mentioned assumptions. Given below are the formulas which can be used for calculating the sample mean ($\bar{z}$), sample variance ($\hat{\sigma}_z^2$), sample autocovariances (c_k) and sample autocorrelations ($\hat{\rho}_k$) respectively (Box & Jenkins, 1976, pp. 26,32):

$$\bar{z} = \sum_{t=1}^{n} \frac{z_t}{n} \tag{10.2.6}$$

$$\hat{\sigma}_z^2 = \sum_{t=1}^{n} \frac{(z_t - \bar{z})^2}{n} \tag{10.2.7}$$

$$c_k = \sum_{t=1}^{n-k} \frac{(z_t - \bar{z})(z_{t-k} - \bar{z})}{n}, k = 0,1,2 \dots, K \tag{10.2.8}$$

$$\hat{\rho}_k = \frac{c_k}{c_0}, k = 0,1,2 \dots, K \tag{10.2.9}$$

Note that the symbol "K" denotes the total number of lags considered for autocorrelation analysis. The autocorrelations are measured quantities showing the length and strength of the "memory" of a stochastic process, i.e. the extent to which one value of the stochastic process is correlated with previous values (Mills, 1990, p. 65). The plot of $\hat{\rho}_k$ against the corresponding $k's$ is called a correlogram and is utilized for characterizing the properties of a considered process.

10.2.2 Linear Filter Model

A general property of the stationary stochastic processes is the Wold's decomposition (Wold, 1938). According to the Wold's decomposition, every covariance stationary, purely non deterministic, stochastic process can be expressed as a linear combination of series of independent shocks (also called white noise) "a_t" (Mills, 1990, p. 67). The a_t's are assumed to be random drawings from a fixed distribution and also normally distributed with zero mean and constant variance as represented in Eq. (10.2.10). By purely non nondeterministic, it is meant that any linearly deterministic components (μ) have been subtracted from z_t so that the process ($z_t - \mu = \tilde{z}_t$) is proposed to vary about the mean.

$$E[a_t] = 0 \ \wedge \ E[a_t a_{t+k}] = \begin{cases} \sigma_a^2 & k = 0 \\ 0 & k \neq 0 \end{cases} \tag{10.2.10}$$

The utilized stochastic models for TSA are based on the high dependency of successive $z_t's$ with each other which are considered to be generated from a white noise series (Box & Jenkins, p. 8). Hence, the white noise process a_t is supposed to be transformed to the observable time series z_t by using a linear filter as shown in Figure 36.

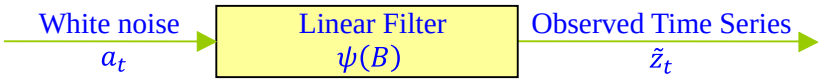

Figure 36- The transformation of a white noise process to an observed time series by a linear filter (Box & Jenkins, p. 8)

The linear filtering operation takes a weighted sum of the present and past values of a_t as indicated below (Box & Jenkins, p. 46):

$$\tilde{z}_t = a_t + \psi_1 a_{t-1} + \psi_2 a_{t-2} + \cdots = a_t + \sum_{j=1}^{\infty} \psi_j a_{t-j} \tag{10.2.11}$$

Given below is the linear operator "$\psi(B)$", so-called the transfer function of the filter, that transforms a_t into $\tilde{z}_t$ (Box & Jenkins, p. 9).

$$\psi(B) = 1 + \psi_1 B + \psi_2 B^2 + \cdots = \sum_{j=0}^{\infty} \psi_j B^j \tag{10.2.12}$$

The backward shift operator "B" provides the means for shifting to a previous observation (i.e. $B^m \tilde{z}_t = \tilde{z}_{t-m}$). The coefficients ψ_j in the linear filter are called ψ (psi)-weights whose number can theoretically be finite or infinite.

The number of the corresponding weights can be infinite under the proposition that the weights converge absolutely $\left(\sum|\psi_j| < \infty\right)$. This proposition implies that $\tilde{z}_t$ is stationary, and guarantees that all moments[93] exist and are independent of time (Mills, pp. 68-69).

The $E(z_t) = \mu$ is valid w.r.t. the stationarity restriction since

$$E[z_t - \mu_t] = E\left[\sum_{j=0}^{\infty} \psi_j a_{t-j}\right] = \sum_{j=0}^{\infty} \psi_j \, E\left[a_{t-j}\right] = 0 \tag{10.2.13}$$

(Kirchgässner & Wolters, 2007, p. 21). Further, the variance can be calculated as follows (Mills, p. 68):

$$\gamma_0 = \sigma_z^2 = E(z_t - \mu)^2 \tag{10.2.14}$$

$$= E(a_t + \psi_1 a_{t-1} + \psi_2 a_{t-2} + \cdots)^2 \tag{10.2.15}$$

$$= E(a_t^2) + \psi_1^2 E(a_{t-1}^2) + \psi_2^2 E(a_{t-2}^2) + \cdots \tag{10.2.16}$$

$$= \sigma_a^2 + \psi_1^2 \sigma_a^2 + \psi_2^2 \sigma_a^2 + \cdots \tag{10.2.17}$$

[93] Moments are the population parameters used for describing probability distributions such as mean, variance, etc.

$$= \sigma_a^2 \sum_{j=0}^{\infty} \psi_j^2 \tag{10.2.18}$$

Therefore, the variance is finite and independent of time. Correspondingly, the time independent autocovariances with $k > 0$ can be calculated by using the result that $E(a_{t-i}a_{t-j}) = 0 \ \ for\ i \neq j$ as indicated below (Mills, p. 68):

$$\gamma_k = E(z_t - \mu)(z_{t-k} - \mu) \tag{10.2.19}$$

$$= E(a_t + \psi_1 a_{t-1} + \cdots + \psi_k a_{t-k} + \psi_{k+1} a_{t-k-1} + \cdots) \cdot (a_{t-k} + \psi_1 a_{t-k-1} + \cdots) \tag{10.2.20}$$

$$= \sigma_a^2 (1 \cdot \psi_k + \psi_1 \psi_{k+1} + \psi_2 \psi_{k+2} + \cdots) \tag{10.2.21}$$

$$= \sigma_a^2 \sum_{j=0}^{\infty} \psi_j \psi_{j+k} \tag{10.2.22}$$

It can be inferred that the autocovariances are only functions of the time difference (i.e. the distance between two random variables) through fulfilling all conditions of covariance stationarity. The autocorrelation function is accordingly expressed below (Mills, p. 68):

$$\rho_k = \frac{\sum_{j=0}^{\infty} \psi_j \psi_{j+k}}{\sum_{j=0}^{\infty} \psi_j^2} \tag{10.2.23}$$

10.2.3 The General Autoregressive Models

A general autoregressive model can be utilized for describing a univariate time series by regressing the current deviation $\tilde{z}_t$ on past deviations $(\tilde{z}_{t-1}, \tilde{z}_{t-2}, ...,)$ of the corresponding stochastic process. Correspondingly, the representation of $\tilde{z}_t$ as a weighted sum of past values plus an added shock is given below (Box & Jenkins, p. 47):

$$\tilde{z}_t = \pi_1 \tilde{z}_{t-1} + \pi_2 \tilde{z}_{t-2} + \cdots + a_t = \sum_{j=1}^{\infty} \pi_j \tilde{z}_{t-j} + a_t \tag{10.2.24}$$

The coefficients π_j in the linear filter are called π (pi)-weights whose number is infinite and relates $\tilde{z}_t$ to past deviations together with a_t. The corresponding operator, $\pi(B)$, which is utilized in establishing the mentioned relations is indicated below:

$$\pi(B) = 1 - \pi_1 B - \pi_2 B^2 - \cdots \tag{10.2.25}$$

Thus, the Eq. (10.2.24) can be written in compact form as follows (Box & Jenkins, p. 51):

$$\pi(B)\tilde{z}_t = a_t \tag{10.2.26}$$

The π-weights can be derived from the linear filter model according to the relationship $\pi(B) = \psi^{-1}(B)$ and by using the known values of the ψ-weights (Box & Jenkins, p. 48). The relationship between both weights can be derived, after multiplying both sides of the above Eq. (10.2.26) by $\psi(B)$ and cancelling $\tilde{z}_t$'s on both sides, which results in Eq. (10.2.27) as shown below (Box & Jenkins, p. 48):

$$\psi(B)a_t = \tilde{z}_t \tag{10.2.27}$$

A stochastic process can be considered as a general autoregressive model of order p (i.e. abbreviated as $AR(p)$), if only a finite number of π weights are non-zero, i.e. $\pi_1 = \phi_1, \pi_2 = \phi_2, \dots, \pi_p = \phi_p$ and $\pi_k = 0$ for $k > p$ as expressed below (Box & Jenkins, p. 51):

$$\tilde{z}_t = \phi_1\tilde{z}_{t-1} + \phi_2\tilde{z}_{t-2} + \cdots + \phi_p\tilde{z}_{t-p} + a_t \tag{10.2.28}$$

The autoregressive operator of order p can be subsequently expressed as follows (Box & Jenkins, p. 51):

$$\phi(B) = 1 - \phi_1 B - \phi_2 B^2 \dots - \phi_p B^p \tag{10.2.29}$$

A p^{th} order autoregressive model can be indicated in parsimonious form as follows:

$$\phi(B)\tilde{z}_t = a_t \tag{10.2.30}$$

The corresponding $AR(p)$ characteristic equation can be expressed as indicated below (Cryer & Chan, 2008, p. 76):

$$1 - \phi_1 B - \phi_2 B^2 - \phi_p B^p = 0 \tag{10.2.31}$$

The stationarity of an $AR(p)$ model, i.e. the convergence of the ψ-weights, is ensured by the requirement of the roots of the characteristic equation to lie outside of the unit circle[94] (Box & Jenkins, p. 54). As indicated below in Eq. (10.2.32), polynomial factorization of the characteristic equation is needed to be carried out for finding the roots of the characteristic polynomial. It is such that $|G_i| < 1$ for $i = 1,2, \dots p$, or the roots G_i^{-1} all lie outside the unit circle (Box & Jenkins, p. 54):

$$\phi(B) = (1 - G_1 B)(1 - G_2 B) \dots \left(1 - G_p B\right) = 0 \tag{10.2.32}$$

An autoregressive model is considered to be always invertible (i.e. $\pi(B) = \psi^{-1}(B)$ is always valid), since $\sum_{j=1}^{\infty}|\pi_j| = \sum_{j=1}^{p}|\phi_j| < \infty$ (Wei, 2006, p. 33). In addition, the model contains p+2 unknown parameters $\mu, \phi_1, \phi_2, \dots, \phi_p, \sigma_a^2$, which can be estimated from the observations (Box & Jenkins, p. 9).

10.2.3.1 Autocorrelation function of $AR(p)$ processes

The autocovariance function of a general AR process, indicated in Eq. (10.2.33), can be obtained by multiplying Eq. (10.2.28) by $\tilde{z}_t$, and then taking the expectations (Wei, p. 45). Note that $E(a_t \tilde{z}_t) = E(a_t^2) = \sigma_a^2$.

$$\gamma_k = \phi_1 \gamma_{k-1} + \phi_2 \gamma_{k-2} + \cdots + \phi_p \gamma_{k-p}, \qquad k > 0 \tag{10.2.33}$$

Hence the autocorrelation function (ACF), represented in Eq. (10.2.34) as ρ_k, can be found through dividing the Eq. (10.2.33) by γ_0 (Wei, p. 46).

$$\rho_k = \phi_1 \rho_{k-1} + \phi_2 \rho_{k-2} + \cdots + \phi_p \rho_{k-p}, \qquad k > 0 \tag{10.2.34}$$

The Eq. (10.2.34) can be written in parsimonious form as follows (Box & Jenkins, p. 55):

$$\phi(B)\rho_k = 0 \tag{10.2.35}$$

In Eq. (10.2.35), B now backshifts k and not t. Further, the polynomial factorization of the equation $\phi(B)$ can be written as given below (Box & Jenkins, p. 55):

$$\phi(B) = \prod_{i=1}^{p}(1 - G_i B) \tag{10.2.36}$$

[94] Unit circle is a circle with radius equaling to 1.

The general solution of the Eq. (10.2.34) is then

$$\rho_k = A_1 G_1^k + A_2 G_2^k + \cdots + A_p G_p^k \tag{10.2.37}$$

where $G_1^{-1}, G_2^{-1}, \ldots, G_p^{-1}$ are the roots of the characteristic equation (Box & Jenkins, p. 55).

For a stationary $AR(p)$ process (i.e. $|G_i| < 1$), there can arise two situations, if it is assumed that the roots G_i are distinct (Box & Jenkins, p. 55):

1) If a root G_i is real, the ACF of the general $AR(p)$ geometrically decays (i.e. called damped exponential) to zero as k increases.
2) If a pair of roots G_i, G_j, is complex, the ACF follows a damped sine wave.

The general Yule-Walker equations, indicates the recursive relationship for ρ_k, can be obtained by setting $k = 1,2, \ldots, p$ in Eq. (10.2.34) to form a set of equations as follows (Box & Jenkins, p. 55):

$$\begin{array}{lll} \rho_1 = \phi_1 & +\phi_2 \rho_1 & +\cdots+\phi_p \rho_{p-1} \\ \rho_2 = \phi_1 \rho_1 & +\phi_2 & +\cdots+\phi_p \rho_{p-2} \\ \vdots \quad \vdots & \vdots & \ldots \ \vdots \\ \rho_p = \phi_1 \rho_{p-1} & +\phi_2 \rho_{p-2} & +\cdots+\phi_p \end{array} \tag{10.2.38}$$

It should be noted that $\rho_0 = 1$ and $\rho_k = \rho_{-k}$. Once the values for $\phi_1, \phi_2, \ldots, \phi_p$ are found, the set of linear equations can be solved recursively to obtain numerical values for ρ_k at any number of higher lags (Box & Jenkins, p. 55). The so called "Yule-Walker estimates" of the parameters can be calculated by replacing ρ_k with $\hat{\rho}_k$.

The sample autocorrelations should be tested for statistical significance. Therefore, it is investigated whether $\hat{\rho}_k$'s lie outside the confidence interval $\pm 1.96/\sqrt{n}$ at a 5% level of significance (i.e. $H_0: \rho = 0$). Note that to test for uncorrelated observations ($\rho_k = 0 \ \forall k: k \neq 0$), the corresponding standard error of $\hat{\rho}_k$ can be approximated with $1/\sqrt{n}$. Further, the large lag standard error "S_{r_k}" is used for approximating standard error of $\hat{\rho}_k$ for large lags $k > q$, i.e. for ρ_k's which are tested to be zero beyond $k = q$. $S_{\hat{\rho}_k}$ can be calculated as follows (Box & Jenkins, p. 35):

$$S_{\hat{\rho}_k} \simeq \sqrt{\frac{1}{n}(1 + 2\rho_1^2 + \cdots + 2\rho_{k-1}^2)} \quad k > q \tag{10.2.39}$$

10.2.3.2 The partial autocorrelation function of general AR(p) Processes

The partial autocorrelation function (PACF) provides the means for distinguishing between different orders of $AR(p)$ models, since ACFs of all $AR(p)$ models damp out. The PACF measures the correlation between $\tilde{z}_t$ and $\tilde{z}_{t-k}$ after removing the effect of intermediate variables $\tilde{z}_{t-1}, \tilde{z}_{t-2}, \dots, \tilde{z}_{t-k-1}$. In general, the correlation between two random variables is often due to both variables being correlated with a third variable. Namely, $\tilde{z}_{t-2}$ involves $\{a_{t-2}, a_{t-3}, \dots\}$ which are all uncorrelated with a_t, a_{t-1}. Since $\tilde{z}_t$ is dependent on $\tilde{z}_{t-2}$ through $\tilde{z}_{t-1}$, a correlation between $\tilde{z}_t$ and $\tilde{z}_{t-2}$ exists. The PACF indicates the correlation between $\tilde{z}_t$ and $\tilde{z}_{t-2}$ with the removed linear dependence of $\tilde{z}_{t-1}$. The lag k partial autocorrelation is the last coefficient $\phi_{k,k}$ in the k^{th} order autoregression as shown below (Mills, p. 78):

$$\tilde{z}_t = \phi_{k,1}\tilde{z}_{t-1} + \phi_{k,2}\tilde{z}_{t-2} + \cdots + \phi_{k,k}\tilde{z}_{t-k} + a_t \tag{10.2.40}$$

The term, $\phi_{k,j}$, denotes the j^{th} coefficient in an autoregressive process of order k (Mills, p. 78).

The partial autocorrelation can be estimated using least squares method for fitting successive autoregressive processes of orders 1,2,3, ... and choosing the estimates $\hat{\phi}_{1,1}, \hat{\phi}_{2,2}, \hat{\phi}_{3,3}, \dots$ which are the last coefficient fitted at each stage (Box & Jenkins, p. 65). Alternatively, a recursive method, by Durbin (1960), can also be utilized to find the estimates of the partial autocorrelations and the estimates of coefficients $\hat{\phi}_{k,j}$ (Mills, p. 80):

$$\hat{\phi}_{k,k} = \frac{\hat{\rho}_k - \sum_{j=1}^{k-1} \hat{\phi}_{k-1,j}\ \hat{\rho}_{k-j}}{1 - \sum_{j=1}^{k-1} \hat{\phi}_{k-1,j}\ \hat{\rho}_j} \tag{10.2.41}$$

$$\hat{\phi}_{k,j} = \hat{\phi}_{k-1,j} - \hat{\phi}_{k,k}\hat{\phi}_{k-1,k-j} \quad j = 1,2, \dots, k-1 \tag{10.2.42}$$

The partial autocorrelation function of an autoregressive process of order p, $\phi_{k,k}$, will be non-zero for k less than or equal to p and zero for k greater than p ($i.e. \phi_{k,k} = 0\ for\ k > p$). Hence, its correlogram of partial autocorrelations cuts off after lag p. The estimates of the partial autocorrelations should also be tested for statistical significance at 5% level ($H_0; \phi_{k,k} = 0$). The standard error of the sample PACF "$S_{\hat{\phi}_{k,k}}$" can be calculated as follows (Box & Jenkins, p. 65):

$$S_{\hat{\phi}_{k,k}} \simeq \sqrt{\frac{1}{n}} \quad k \geq p+1 \tag{10.2.43}$$

10.2.4 Moving Average Models

The linear filter model possessing a finite number of non-zero ψ-weights is called a moving average model of order q (i.e. $\psi_1 = -\theta_1, \psi_2 = -\theta_2, \dots, \psi_q = -\theta_q$ and $\psi_k = 0,$ for k $> q$) and is denoted as $MA(q)$. The terms $-\theta_1, -\theta_2, \dots, -\theta_q$ indicate the finite set of weight parameters for the first q of ψ-weights of the linear filter model. In this model, $\tilde{z}_t$'s are linearly dependent on a finite number of previous random shocks as represented below (Box & Jenkins, p. 10):

$$\tilde{z}_t = a_t - \theta_1 a_{t-1} - \theta_2 a_{t-2} - \cdots - \theta_q a_{t-q} \tag{10.2.44}$$

It should be noted that the weights need to be neither unity nor positive in total. The moving average operator of order q can be indicated as indicated below (Box & Jenkins, p. 10):

$$\theta(B) = \left(1 - \theta_1 B - \theta_2 B^2 - \cdots - \theta_q B^q\right) \tag{10.2.45}$$

The general $MA(q)$. model can subsequently be expressed in parsimonious form by using the moving average operator of order q (Box & Jenkins, p. 10):

$$\tilde{z}_t = \theta(B) a_t \tag{10.2.46}$$

The general $MA(q)$. model contains $q + 2$ unknown parameters $\mu, \theta_1, \theta_2, \dots, \theta_q, \sigma_a^2$ which are in practice estimated from the data.

10.2.4.1 The stationarity and invertibility conditions of general $MA(q)$ model

A finite moving average process is always stationary; since $1 + \theta_1^2 + \cdots + \theta_q^2 < \infty$ (see linear filter assumptions). Further, the process is invertible, if the roots of $\theta(B) = 0$ lie outside of the unit circle (Wei, p. 47).

10.2.4.2 Autocorrelation function of general moving average processes

The autocovariance function of a general $MA(q)$ model process can be calculated by multiplying Eq. (10.2.44) with its lagged form and then taking the expectation (Box & Jenkins, p. 68):

$$\gamma_k = E\left[\left(a_t - \theta_1 a_{t-1} - \cdots - \theta_q a_{t-q}\right)\left(a_{t-k} - \theta_1 a_{t-k-1} - \cdots - \theta_q a_{t-k-q}\right)\right] \quad (10.2.47)$$

Hence from the Eq. (10.2.47), variance, autocovariance and autocorrelation of a general $MA(q)$ model can be derived as follows (Box & Jenkins, p. 68):

$$\gamma_0 = 1 + \sigma_a^2 \sum_{j=1}^{q} \theta_j^2 \quad (10.2.48)$$

$$\gamma_k = \begin{Bmatrix} \sigma_a^2\left(-\theta_k + \theta_1\theta_{k+1} + \cdots + \theta_{q-k}\theta_q\right) & k = 1,2,\ldots,q \\ 0 & k > q \end{Bmatrix} \quad (10.2.49)$$

$$\rho_k = \begin{Bmatrix} \dfrac{-\theta_k + \theta_1\theta_{k+1} + \cdots + \theta_{q-k}\theta_q}{1 + \theta_1^2 + \cdots + \theta_q^2} & k = 1,2,\ldots,q \\ 0 & k > q \end{Bmatrix} \quad (10.2.50)$$

It can be inferred from Eq. (10.2.50) that the ACF of the general $MA(q)$ model cuts off after lag q. The corresponding property is used for identifying whether a considered time series is a moving average process. If it is true, the order of the $MA(q)$ process can be subsequently determined from it (Wei, p. 52).

10.2.4.3 The partial autocorrelation function of general $MA(q)$ models

The theoretical partial autocorrelation function of a general moving average process is given below (Box & Jenkins, p. 70):

$$\phi_{kk} = -\theta_1^k\{1 - \theta_1^2\}/\left\{1 - \theta_1^{2(k+1)}\right\} \quad (10.2.51)$$

On the contrary to the ACF of $MA(q)$ models, their partial autocorrelation functions (PACFs) tail off. Depending on the nature of the roots of characteristic equation (see Eq. (10.2.52)), their PACFs generally exhibit combinations of exponential decays (for the presence of real roots) and/or damped sine waves (for the presence of complex roots) (Mills, p. 84).

$$\left(1 - \theta_1 B - \theta_2 B^2 - \cdots - \theta_q B^q\right) = 0 \tag{10.2.52}$$

10.2.5 The Dual Relationship between AR(p) and MA(q) Models

The duality relationship between the $AR(p)$ and $MA(q)$ models are utilized in identifying the presence and order of the AR and/or MA models when building time series models. The corresponding important aspects are listed below (Box & Jenkins, pp. 72-73):

(1) A stationary AR model of order p can be expressed as an infinite and converging weighted sum of past a's.

$$\tilde{z}_t = \phi^{-1}(B) a_t \tag{10.2.53}$$

(2) An invertible moving average process of order q can be expressed as an infinite and converging weighted sum of past $\tilde{z}$'s.

$$a_t = \theta^{-1}(B) \tilde{z}_t \tag{10.2.54}$$

(3) The finite MA model has an autocorrelation function which cuts off beyond a certain order, but since it corresponds to an infinite order AR model, its partial autocorrelation function is infinite in extent and its partial autocorrelations tails off.

(4) Conversely, the finite AR model has a partial autocorrelation function which cuts off beyond a certain order; however its autocorrelation function is infinite in extent (i.e. corresponds to an infinite order AR model) and exhibits a mixture of damped exponentials and/or damped sine waves.

(5) The parameters of an autoregressive model of finite order p, are required to satisfy stationarity condition but not invertibility. On the other hand, the parameters of the MA model are required to satisfy invertibility condition but not stationarity.

10.2.6 Mixed Autoregressive-Moving Average Models

During building a time series model, both autoregressive and moving average terms can be included in a stationary time series model as represented below (Box & Jenkins, p. 74):

$$\tilde{z}_t = \phi_1 \tilde{z}_{t-1} + \cdots + \phi_p \tilde{z}_{t-p} + a_t - \theta_1 a_{t-1} - \cdots - \theta_q a_{t-q} \tag{10.2.55}$$

These types of models are called mixed autoregressive moving average models ($ARMA$), in which p and q indicate the orders of the corresponding autoregressive and moving average models respectively (Box & Jenkins, p. 74). The general $ARMA$ model can also be parsimoniously represented as indicated below in Eqs. (10.2.56) and (10.2.57) respectively (Box & Jenkins, p. 74):

$$\left(1 - \phi_1 B - \cdots - \phi_p B^p\right)\tilde{z}_t = (1 - \theta_1 B - \cdots - \theta_q B^q)a_t \tag{10.2.56}$$

$$\phi(B)\tilde{z}_t = \theta(B)a_t \tag{10.2.57}$$

The general $ARMA$ model has $p + q + 2$ unknown parameters $\mu; \phi_1, \dots, \phi_p; \theta_1, \dots, \theta_q; \sigma_a^2$ which can be estimated from the data. In practice, the order of most used $ARMA$ models is not greater than 2 and often less than 2 (Box & Jenkins, p. 11).

If an $ARMA(p, q)$ model is defined to be invertible, then the roots of the characteristic equation $\theta_q(B) = 0$ should lie outside the unit circle. Further, if an $ARMA(p, q)$ model is defined to be a stationary process, then the roots of $\phi_p(B) = 0$ should lie outside the unit circle. Finally, the roots of the characteristic equations $\theta_q(B) = 0$ and $\phi_p(B) = 0$ are required to share no common roots (Wei, p. 57).

10.2.6.1 Autocorrelation Function of General ARMA(p, q) Model

The autocovariance function of a general $ARMA(p, q)$ model can be derived through multiplying Eq. (10.2.55) by $\tilde{z}_{t-k}$ on both sides and then taking the expectations (Wei, p. 58):

$$\begin{aligned}\gamma_k &= \phi_1\gamma_{k-1} + \cdots + \phi_p\gamma_{k-p} + E(\tilde{z}_{t-k}a_t) - \theta_1 E(\tilde{z}_{t-k}a_{t-1}) - \cdots \\ &\quad - \theta_q E\left(\tilde{z}_{t-k}a_{t-q}\right)\end{aligned} \tag{10.2.58}$$

Since $E(\tilde{z}_{t-k}a_{t-i}) = 0$ for $k > i$ due to the dependence of $\tilde{z}_{t-k}$ on shocks which have occurred up to time $t - k$, the Eq. (10.2.58) becomes as follows:

$$\gamma_k = \phi_1\gamma_{k-1} + \phi_2\gamma_{k-2} + \cdots + \phi_p\gamma_{k-p} \qquad k \geq (q + 1) \tag{10.2.59}$$

The variance of the process when $k = 0$ is

$$\gamma_0 = \phi_1\gamma_1 + \cdots + \phi_p\gamma_p + \sigma_a^2 - \theta_1\gamma_{z,a}(-1) - \cdots \theta_q\gamma_{z,a}(-q) \tag{10.2.60}$$

where $\gamma_{z,a}(k) = E(\tilde{z}_{t-k}a_t)$ is the cross covariance function between z and a (Box & Jenkins, p. 75). Hence, the autocorrelation function can be represented as given below (p. 75):

$$\rho_k = \phi_1\rho_{k-1} + \cdots + \phi_p\rho_{k-p} \qquad k \geq (q+1) \tag{10.2.61}$$

It can be inferred that the autocorrelation function of the general $ARMA(p,q)$ model tails off after lag q similar to a general $AR(p)$ process. Moreover, the first q autocorrelations $\rho_q, \rho_{q-1}, \dots, \rho_1$ depend on both autoregressive and moving average parameters in the model, which can be used as a guide in identification of the most appropriate time series model (Wei, p. 59).

10.2.6.2 Partial Autocorrelation Function of the General $ARMA(p,q)$ Model

Since the MA model is incorporated in the $ARMA$ model as a special case, it shows similar patterns like the PACF of a general moving average model. Hence, the PAFC of an $ARMA(p,q)$ model will exhibit a mixture of exponential decays and/or damped sine waves depending on the roots of $\theta_q(B) = 0$ and $\phi_p(B) = 0$ (Wei, p. 59).

10.2.7 Linear Non-Stationary Models

A linear stochastic process, which exhibits non-stationary behavior through not fluctuating around a fixed mean, can be reduced to a stationary series by taking a suitable difference of the considered time series. This is due to the fact that the fluctuations can exhibit homogeneous patterns in the broad behavior of the series after differencing, in comparison to their patterns in general behavior without differencing (Box & Jenkins, p. 11). Consequently, a difference operation can be applied on a covariance stationary time series; in order to transform it into a mean stationary series.

The homogenous non-stationary behavior of a time series can be inferred from one/more of the root(s) of the polynomial $\varphi(B) = 0$ which is/are unity. The operator $\varphi(B)$ is defined to be the non-stationary operator of a generalized autoregressive process. The relation of it with the stationary operator $\phi(B)$ of a generalized autoregressive process is expressed below (Box & Jenkins, p. 11):

$$\varphi(B) = \nabla^d \phi(B) \tag{10.2.62}$$

In Eq. (10.2.62), the symbol "∇" denotes the backward difference operator which can also be written in terms of backward shift operator B as shown below:

$$\nabla^d = (1 - B)^d \tag{10.2.63}$$

In practice, the d^{th} difference of the process is usually chosen to be 0, 1, or at most 2 (Box & Jenkins, p. 11). Hence the general model, which can represent homogenous non-stationary behavior, is called an autoregressive integrated moving average $(ARIMA)$ model of order (p, d, q) (Box & Jenkins, p. 88):

$$\varphi(B)\tilde{z}_t = \phi(B)\nabla^d \tilde{z}_t = \theta(B)a_t \tag{10.2.64}$$

After differencing, the stationary process can be represented as

$$w_t = \phi_1 w_{t-1} + \cdots + \phi_p w_{t-p} + a_t - \theta_1 a_{t-1} - \cdots - \theta_q a_{t-q} \tag{10.2.65}$$

where $w_t = \nabla^d \tilde{z}_t$ (Box & Jenkins, p. 12).The above expression can be written in parsimonious form as shown below (Box & Jenkins, p. 11):

$$\phi(B)w_t = \theta(B)a_t \tag{10.2.66}$$

An alternative way of representing the above given model in the form of a stationary invertible $ARMA$ process can be represented as follows (Box & Jenkins, p.92):

$$\phi(B)\tilde{w}_t = \theta(B)a_t \quad where\ \tilde{w}_t = w_t - \mu_w \tag{10.2.67}$$

According to Box and Jenkins (p. 92), the mean of series $\boldsymbol{w}$ can be assumed to be zero, unless such an assumption is contradicted by the used data through exhibiting physical reasons for a deterministic component to exist.

Listed below are the corresponding features of a general $ARIMA$ model (Box-Jenkins, p.92):

1. The autoregressive operator$\phi(B)$ is assumed to be stationary with the roots of $\phi(B) = 0$ lie outside the unit circle.
2. $\varphi(B) = \nabla^d \phi(B)$ is defined to be the generalized autoregressive operator which is non-stationary with d roots of $\varphi(B) = 0$ equal to unity.

3. The moving average operator $\theta(B)$ is assumed to be invertible with the roots of $\theta(B) = 0$ lie outside the unit circle.
4. Hence, a generalized $ARIMA$ model is assumed to be corresponding to the d^{th} difference of the series which can be expressed by a stationary, invertible $ARMA$ process.

The represented general model is without a constant term "θ_0" and can represent series which has stochastic trends due to random changes in the level and slope of the series (Box-Jenkins, p.92). A constant ($\theta_0 > 0$) can also be included in the general $ARIMA$ model for a deterministic trend as represented below:

$$\varphi(B)z_t = \phi(B)\nabla^d \tilde{z}_t = \theta_0 + \theta(B)a_t \tag{10.2.68}$$

In the next subsection, information is given about Box-Cox power transformation to stabilize the variance of a considered time series; since a difference operation can be applied on a covariance stationary time series.

10.2.7.1 Variance Stabilizing Transformation

The non-stationarity of a time series in variance can be eliminated by applying the power transformation by Box and Cox (1964). The transformation function "T" with the transformation parameter "λ" is represented below (Wei, p. 85):

$$T(\tilde{z}_t) = \tilde{z}_t^{(\lambda)} = \frac{\tilde{z}_t^{\lambda} - 1}{\lambda} \tag{10.2.69}$$

Listed below are some important remarks about the power transformation (Wei, pp. 85-86):

1. The transformation to a stabilized variance can be carried out only for positive series. The transformation can be applied on a time series possessing negative values, after adding a constant to the series without affecting the correlation structure of it.
2. The transformation should be carried out before differencing, if unstable variance is present.
3. λ can be estimated from the observed series by using the method of maximum likelihood method.

4. The objective is to find the maximum likelihood estimate of λ which minimizes the residual sum of squares of errors calculated from the fitted model. Given below in Table 1 are the empirical values of λ which are commonly utilized by practitioners.

Table 23- The commonly used values of λ and their associated transformations (Wei, p. 85)

Values of lambda	Transformation
-1.0	$\frac{1}{\tilde{z}_t}$
-0.5	$\frac{1}{\sqrt{\tilde{z}_t}}$
0.0	$ln\tilde{z}_t$
0.5	$\sqrt{\tilde{z}_t}$
1.0	$\tilde{z}_t$

5. In practice, the transformation is observed to be not only stabilizing the variance, but also improving the approximation of the distribution by a normal distribution.

10.2.8 The Seasonal ARIMA Models

The seasonal ARIMA models are special forms of ARIMA models and can be built for time series containing seasonal phenomenon that repeats itself in seasonal periods. For example, the annual peak demands for electricity which occur in the month of August in every year (i.e. a seasonal period of 12 months abbreviated as $s = 12$) depending on the highest ambient temperature of the year.

The seasonal ARIMA models are based on the assumption that the considered time series has a stochastic seasonal component, which is correlated with non-seasonal components (Wei, p. 164). To explain it in general terms, let the series $\{z_t\}$ be a seasonal time series with a seasonal period of s. Hence, the series contains relationships between periods (i.e. correlation among $\dots, z_{t-2s}, z_{t-s}, z_t, z_{t+s}, z_{t+2s}, \dots$) (Wei, p. 164).

It can be inferred from the given information that there exits non-stationarity in the series $z_t, z_{t-s}, z_{t-2s}, \dots$; since the observations s interval apart are similar. Subsequently, the considered series should be differenced in order to achieve stationarity i.e. $\nabla_s z_t = (1 - B^s)z_t = z_t - z_{t-s}$. Note that the seasonal differencing operator is denoted by ∇_s. Thus, the relation between periods can be expressed as an $ARIMA(P, D, Q)$ model as follows (Wei, p. 166):

$$\Phi_P(B^s)(1-B^s)^D z_t = \Theta_Q(B^s)a_t \tag{10.2.70}$$

The polynomials, $\Phi_P(B^s)$ and $\Theta_Q(B^s)$, are called the seasonal autoregressive and moving average characteristic polynomials as represented in Eq. (10.2.71) and Eq. (10.2.72) respectively. Both polynomials are functions of B^s with no common roots and the roots of both polynomials lie outside of the unit circle (Wei, p. 166).

$$\Phi_P(B^s) = 1 - \Phi_1 B^s - \Phi_2 B^{2s} - \cdots - \Phi_P B^{Ps} \tag{10.2.71}$$

$$\Theta_Q(B^s) = 1 - \Theta_1 B^s - \Theta_2 B^{2s} - \cdots - \Theta_Q B^{Qs} \tag{10.2.72}$$

A general seasonal autoregressive model of order P ($AR(P)$) with seasonal period s is expressed below (Cryer & Chan, 2008, p. 230):

$$\tilde{z}_t = \Phi_1 \tilde{z}_{t-s} + \Phi_2 \tilde{z}_{t-2s} \ldots + \Phi_P \tilde{z}_{t-Ps} + a_t \tag{10.2.73}$$

In order the stationarity condition to be satisfied, the roots of $\Phi(x) = 0$ must be greater than 1 in absolute value. The Eq. (10.2.73) can also be seen similar to a special case of a regular $AR(p)$ model of order $p = P\ s$ with non-zero ϕ-coefficients only at the seasonal lags of s, $2s$, $3s$,…, Ps (Cryer & Chan, 2008, p. 230).

The autocorrelation function "$\rho_{k,s}$" of the general seasonal $AR(p)$ model is non-zero only at lags s, $2s$, $3s$,… and behaves like a combination of decaying exponentials and damped sine waves (Cryer & Chan, 2008, p. 230).

$$\rho_{k,s} = \Phi^k \ for\ k = 1,2, \ldots \tag{10.2.74}$$

Further, a general seasonal $MA(Q)$ model of order Q with seasonal period "s" can be written as indicated below (Cryer & Chan, 2008, p. 229):

$$z_t = a_t - \Theta_1 a_{t-s} - \Theta_2 a_{t-2s} - \cdots - \Theta_Q a_{t-Qs} \tag{10.2.75}$$

The general seasonal $MA(Q)$ is always stationary and its $\rho_{k,s}$ will be nonzero only at the seasonal lags of s, $2s$, $3s$,… , Qs as indicated below (Cryer & Chan, 2008, p. 229):

$$\rho_{k,s} = \frac{-\Theta_k + \Theta_1\Theta_{k+1} + \Theta_2\Theta_{k+2} + \cdots + \Theta_{Q-k}\Theta_Q}{1 + \Theta_1^2 + \Theta_2^2 + \cdots + \Theta_Q^2} \qquad for\ k = 1,2,\ldots,Q \qquad (10.2.76)$$

Furthermore, the MA model is invertible, if all the roots of the $\Theta(x) = 0$ exceed 1 in absolute value. The seasonal $MA(Q)$ model can also be considered as a special case of a regular MA model of order $q = Qs$ with all θ-values being equal to zero except at the seasonal lags s, $2s$, $3s$,… Qs (Cryer & Chan, 2008, p. 229).

Moreover, it has been emphasized that the seasonal and non-seasonal autoregressive components have their PACF cutting of at the seasonal or non-seasonal lags. However, the seasonal and non-seasonal moving average components possess PACF which show exponential decays or damped sine waves at the seasonal and non-seasonal lags. (Wei, p. 169)

Given below in Eqs. (10.2.77) and (10.2.78) are the parsimonious representations of the Box-Jenkins multiplicative seasonal ARIMA model without a constant term (Wei, p. 166):

$$\Phi_P(B^s)\phi_p(B)(1-B)^d(1-B^s)^D\tilde{z}_t = \theta_q(B)\Theta_Q(B^s)a_t \qquad (10.2.77)$$

$$\Phi_P(B^s)\phi_p(B)\nabla^d\nabla_s^D\tilde{z}_t = \theta_q(B)\Theta_Q(B^s)a_t \qquad (10.2.78)$$

The model is composed of both seasonal and non-seasonal components and can also be denoted as ARIMA(p, d, q) X (P, D, Q)$_s$ with non-seasonal orders (i.e. p, d and q), seasonal orders (i.e. P, D and Q) and seasonal period s.

10.2.9 Steps in Analyzing Data and Identifying ARIMA Models

In this section, information about the three-stage iterative ARIMA model building process by using the Box-Jenkins method is given. Identification, estimation and diagnostic checking are the three successive stages in model building as illustrated in double framed rectangles in Figure 37.

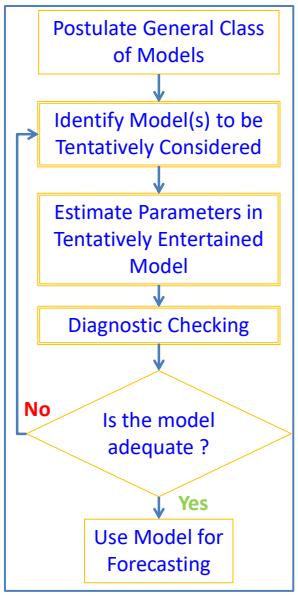

Figure 37- The steps in the iterative approach of Box-Jenkins model building (Box & Jenkins, p. 19)

Since seasonal multiplicative ARIMA models are special forms of the ARIMA models, their model building process is similar to the general ARIMA models and are not exclusively explained in this study.

10.2.9.1 Stage 1- Identification of the order of the ARIMA model

The aim of the model identification stage is to determine appropriate subclass of models from the general $ARIMA(p,d,q)$ family (i.e. w.r.t. the considered orders p, d and q) by matching the patterns in $\hat{\rho}_k$ and $\hat{\phi}_{k,k}$ plots with the known patterns of the ρ_k and $\phi_{k,k}$ as summarized in Table 24 given below.

Table 24- The characteristics of the theoretical ACF and PACF for stationary processes (Wei, p. 109)

Process	ACF	PACF
AR(p)	Tails off toward 0 as exponential decay or damped sine wave	Cuts off to 0 after lag p
MA(q)	Cuts off to 0 after lag q	Tails off to 0 as exponential decay or damped sine wave
ARMA(p,q)	Tails off toward 0 after the first (q-p) lag	Tails off toward 0 after the first (p-q) lag

By using the correlogram of the considered time series, it can be investigated whether each lag's individual autocorrelation coefficient is significantly different from zero or not. If a spike lies outside the estimated 95% confidence interval, the correlation at that lag is significant.

The model identification process can be carried out in four stages as listed below (Wei, pp. 108-111):

1. During the first stage of the identification process, the time series z_t is plotted against t; in order to examine it for a trend, seasonality, outliers, non-constant variances, non-normal and non-stationary phenomena. The examinations reveal whether any data transformation is needed. In general, the variance-stabilizing transformation (i.e. Box-Cox's power transformation) and/or differencing are commonly applied on the considered time series due to the presence of non-stationarity.
2. During the second stage of the identification process, $\hat{\rho}_k$ and $\hat{\phi}_{k,k}$ of the original series are computed and examined for any further need of differencing transformations so that the differenced series is mean stationary. A slow decaying $\hat{\rho}_k$ (i.e. the spikes, at high lag orders, remain statistically significant) and a $\hat{\phi}_{k,k}$ cutting off after lag 1 indicate the need of differencing to eliminate non-stationarity in mean. The required order of differencing determines d. If non-stationarity is observed, the first order differencing $(1-B)z_t$ or higher higher-order differencing $(1-B)^d z_t$ for $d > 1$ can be performed to remove the non-stationarity. In most cases, d is either $0{,}1\ or\ 2$.
3. During the third stage of the identification process, the orders of the p and q is identified by matching the patterns in the sample ACF and PACF with the theoretical patterns of known models . Often, the needed orders of p and q are less than or equal to 3.
4. During the fourth stage of the identification process, the transformed series can be tested for deterministic trend mean θ_0. If the preliminary estimation result is not significant, it can be then discarded at the final model estimation.

10.2.9.2 Stage 2- Estimation of the model parameters:

At the end of the identification process, one or more tentative models of the considered time series are determined; in order to obtain the most efficient estimates of the model parameters. The most efficient estimates of the model parameters are considered to be the ones which minimize the squared difference between the true parameter value and the estimate (Nelson, 1973, p. 92). Nelson (p. 92) states that the statistical theory is not capable of determining which alternative estimates to be efficient in all situations. However he emphasizes that maximizing the value of the likelihood function can show what values of the model parameters likely to have given rise to those observations, if the number of observations is

large. Furthermore, the computation of maximum likelihood estimates (MLE) is recommended by Nelson for its calculatory procedure in determining the parameter estimates for any ARIMA model regardless of the data or the particular values of p, d, q.

The Maximum likelihood method

The following information on the maximum likelihood method is based on Nelson (pp. 92-94).

Let a sequence of observations $z_1, \dots, z_n$ be drawn from a joint distribution $(\boldsymbol{w}|\boldsymbol{\phi}, \boldsymbol{\theta}, \theta_0, \sigma_a^2)$ as follows:

a) The term "$p()$" is the probability density function,
b) The symbol "$\boldsymbol{w}$" indicates the sequence of observations on the stationary difference of the $z's$,
c) The symbols "$\boldsymbol{\phi}$" and "$\boldsymbol{\theta}$" denote the vector of ϕ's and the vector of θ's respectively,
d) The symbol θ_0 is the deterministic trend and the vertical line "|" means given.

Hence, the corresponding joint distribution is defined by the identified particular ARIMA(p, d, q) model and its unknown parameters $\phi_1, \dots, \phi_p$; $\theta_1, \dots, \theta_q$; θ_0;and σ_a^2. By using the method of maximum likelihood, the set of values of the model parameters, which maximizes the likelihood function "$L(\boldsymbol{\phi}, \boldsymbol{\theta}, \theta_0, \sigma_a^2|w)$", can be determined. Note that the likelihood function treats parameters as the variables and the observations as given.

Subsequently, the distribution function of a normally distributed single random shock a_t can be represented as indicated below:

$$p(a_t|\sigma_a^2) = (2\pi\sigma_a^2)^{-\frac{1}{2}} \exp(\frac{-a_t^2}{2\sigma_a^2}) \tag{10.2.79}$$

Since a_t's are independent and identically distributed, their joint distribution can be expressed as the product of their marginal distributions as indicated below:

$$p(a_1, \dots, a_n|\sigma_a^2) = (2\pi\sigma_a^2)^{-\frac{n}{2}} \exp(\frac{-1}{2\sigma_a^2}\sum_{t=1}^{n} a_t^2) \tag{10.2.80}$$

It should be note that each a_t may be represented in terms of observations **w**; parameters $\boldsymbol{\phi}, \boldsymbol{\theta}, \theta_0,$ and σ_a^2; and previous disturbances as follows:

$$a_t = w_t - \phi_1 w_{t-1} - \cdots - \phi_p w_{t-p} - \theta_0 + \theta_1 a_{t-1} + \cdots + \theta_q a_{t-q} \tag{10.2.81}$$

The above given equation can be considered as a recursive relationship between successive a_t's, given the parameters and observations. Consequently, the value of any a_t is computable as a function of the observations and the parameters. Hence, the joint density of the **w** can be obtained by substituting Eq. (10.2.81) in Eq. (10.2.80) as shown below:

$$\begin{aligned} &p(\boldsymbol{w}|\boldsymbol{\phi}, \boldsymbol{\theta}, \theta_0, \sigma_a^2) \\ &= (2\pi\sigma_a^2)^{-\frac{n}{2}} \exp\left[\frac{-1}{2\sigma_a^2}\sum_{t=1}^{n}\left(w_t - \cdots - \phi_p w_{t-p} - \theta_0 + \theta_1 a_{t-1} + \cdots + \theta_q a_{t-q}\right)^2\right] \end{aligned} \tag{10.2.82}$$

Hence, the likelihood function for the parameters given the data can be expressed as indicated in Eq. (10.2.83) by using Eq. (10.2.82). The term $\hat{a}(\boldsymbol{\phi}, \boldsymbol{\theta}, \theta_0)_t$ indicates the estimated value of a_t from Eq.(10.2.81) as a function of the unknown parameters and the observations.

$$L(\boldsymbol{\phi}, \boldsymbol{\theta}, \theta_0, \sigma_a^2|\boldsymbol{w}) = (2\pi\,\sigma_a^2)^{-\frac{n}{2}} \exp\left[\frac{-1}{2\sigma_a^2}\sum_{t=1}^{n}\hat{a}(\boldsymbol{\phi}, \boldsymbol{\theta}, \theta_0)_t^2\right] \tag{10.2.83}$$

In general, it suffices to consider the log of the likelihood as shown in Eq. (10.2.84); since the interest is in the relative magnitudes of the likelihood.

$$l(\boldsymbol{\phi}, \boldsymbol{\theta}, \theta_0, \sigma_a^2|\boldsymbol{w}) = -n\,ln\sigma_a - \frac{S(\boldsymbol{\phi}, \boldsymbol{\theta}, \theta_0)}{2\sigma_a^2} \tag{10.2.84}$$

The term "$S(\boldsymbol{\phi}, \boldsymbol{\theta}, \theta_0)$" in Eq. (10.2.84) denotes the sum-of-squares function.

$$S(\boldsymbol{\phi}, \boldsymbol{\theta}, \theta_0) = \sum_{t=1}^{n}\hat{a}(\boldsymbol{\phi}, \boldsymbol{\theta}, \theta_0)_t^2 \tag{10.2.85}$$

In order to maximize the likelihood, the sum of squares function over the values of the parameter should be minimized (i.e. $\boldsymbol{\phi}, \boldsymbol{\theta},$ and θ_0). After determining MLE of those parameters, the MLE of σ_a^2 can be calculated by the below given equation in which $\hat{\boldsymbol{\phi}}, \hat{\boldsymbol{\theta}},$ and $\hat{\theta}_0$ represent MLE of those parameters.

$$\sigma_a^2 = \frac{S(\hat{\boldsymbol{\phi}}, \hat{\boldsymbol{\theta}}, \hat{\theta}_0)}{n} \tag{10.2.86}$$

10.2.9.3 Stage 3- Diagnostic Checking of the Residuals

Once one or more tentative models are identified and their parameters are estimated; diagnostic checking of the residuals should be carried out in order to verify whether the model assumptions are validated. Remark the basic assumption that a_t's are uncorrelated random shocks with zero mean and constant variance. Consequently, for any tentative model the estimated residual series $\{\hat{a}_t\}$ of white noise series $\{a_t\}$ should be analyzed for filling the considered conditions. In particular, the given tests below should be carried out (Wei, pp. 152-153):

1. The assumption of normally distributed white noise series can be checked by constructing a histogram of the standardized residuals and compare it with the standard normal distribution.
2. The assumption of constant variance can be checked by examining the plot of residuals.
3. The assumption of white noise series can be checked by examining the sample ACF and PACF plot of the residuals. There should not be any recognized pattern in the sample ACF and PACF and they should all be statistically insignificant, e.g. at significance level $\alpha = 0.05$.
4. In addition, the Ljung-Box Q-statistic can be calculated to take into account the magnitudes of the residual sample ACF's as a group. In this portmanteau lack of fit test, it is assumed that the first K autocorrelations are considered to be jointly zero for H_0:

$$H_0: \rho_1 = \rho_2 = \cdots = \rho_K = 0 \tag{10.2.87}$$

The Q-statistic can be computed as shown below:

$$Q = n(n+2)\sum_{k=1}^{K}(n-k)^{-1}\hat{\rho}_k^2. \tag{10.2.88}$$

In Eq. (10.2.88), the symbol "n" denotes the number of residuals, "k" is the order of residual autocorrelation, "K" is the number of autocorrelations (i.e. also number of lags) included in the test. If the calculated Q-statistic exceeds the tabulated value

$\chi^2_{\alpha,df}$, then the null hypothesis is rejected. Note that "$\chi^2_{\alpha,df}$" represents the chi-squared distribution with $df = K - p - q$ at α-level of significance.

10.2.9.4 Stage 4- Model Selection Criteria

In TSA, several tentative models can be identified as adequate models by using identification tools such as ACF, and PACF. Further, the examinations of residuals from all tentative models can result in white noise series and thus, the models can be indistinguishable. Therefore, tests for model adequacy such as the Akaike's information criterion (AIC), the corrected AIC (AIC_c), and Schwarz's Bayesian Criterion (BIC) should be applied on the tentative models to select the model exhibiting a curve fitting which is statistically better than the others.

1. The AIC:

   This criterion was introduced by Akaike (1973); in order to assess the quality of several model fittings and to select the model yielding the lowest value among others as shown below (Cryer & Chan, p. 130):

$$AIC(\boldsymbol{\phi}, \boldsymbol{\theta}) = -2\ln(maximum\ likelihood) + 2M \tag{10.2.89}$$

   In the above given equation, the symbol "M" indicates the number of parameters in the considered model. The log likelihood value is the maximized value of the log likelihood function for the considered model. If the model contains a constant then $M = p + q + 1$; whereas $M = p + q$ without a constant. The addition of the term $2(p + q + 1)$ or $2(p + q)$ is considered to be serving as a "penalty function" to help ensure in selection of parsimonious models.

2. The AIC_c:

   Hurvich and Tsai (1989) have represented a bias-corrected version of the AIC by adding another non-stochastic penalty term to the AIC resulting in the corrected AIC (AIC_c) as follows (Brockwell & Davis, 2006, p. 287):

$$AIC_C(\boldsymbol{\phi}, \boldsymbol{\theta}) = -2\ln(maximum\ likelihood) + \frac{2 \cdot M \cdot n}{n - M - 1} \tag{10.2.90}$$

   In the above given equation, the symbol "n" denotes the number of observations that is equivalent to the number of residuals that can be calculated.

3. BIC:

   Schwarz (1978) proposed his Bayesian criterion of model selection, which has been called the Schwarz's Bayesian Criterion (BIC). This criterion penalizes the free parameters of the models more than AIC and the model which yields the lowest value of the Eq. (10.2.91), is selected (Cryer & Chan, p. 131).

$$BIC(\boldsymbol{\phi}, \boldsymbol{\theta}) = -2\ln(maximum\ likelihood) + M\ln(n) \tag{10.2.91}$$

It can be inferred from the above given equations that all methods require performing maximum likelihood estimates. It has been noted that if the true process follows an ARMA(p, q) model, the selected model with the minimum BIC has consistent orders (i.e $p\ and\ q$) approaching the true orders as the sample size increases (Cryer & Chan, p. 130). On the other hand, if the true process is not a finite-order ARMA process, the selected model with the minimum AIC has consistent orders leading to an optimal ARMA model which is closest to the true process among other alternatives (Cryer & Chan, p. 130). Various simulation studies by McQuarrie and Tsai (1998) have shown that BIC is usually better in selection of the correct order in larger samples (Shumway & Stoffer, 2011, p. 53). However, the AICc is usually superior in smaller samples where the relative number of parameters is large (Shumway & Stoffer, p. 53).

10.2.10 Forecasting Time Series Using ARIMA Models

Once an adequate model is determined and fitted to the considered time series, the future values of the corresponding series can be forecasted. Let the observations $(z_1, z_2, \dots, z_n)$ be generated from the general $ARIMA(p, d, q)$ model as represented below:

$$\phi(B)\nabla^d z_t = \theta(B)a_t \tag{10.2.92}$$

The objective of the time series analysis is to forecast the value z_{n+l} $(l \geq 1)$, which is to be made at origin "n" (i.e. current time) for lead lime l given $(z_n, z_{n-1}, \dots)$. The linear filter representation of z_{n+l} is

$$z_{n+l} = a_{n+l} + \psi_1 a_{n+l-1} + \cdots + \psi_{l-1}a_{n+1} + \psi_l a_n + \psi_{l+1}a_{n-1} + \cdots \tag{10.2.93}$$

where $\psi(B) = \phi^{-1}(B)\nabla^{-d}\theta(B)$ (Mills, p. 104).

The best forecast "$\hat{z}_n(l)$" of z_{n+l} is

$$\hat{z}_n(l) = \psi_l^* a_n + \psi_{l+1}^* a_{n-1} + \psi_{l+2}^* a_{n-2} + \cdots \tag{10.2.94}$$

and is a linear function of current and previous shocks $(a_n, a_{n-1}, a_{n-2}, \dots)$ where the weights ψ_l^*, ψ_{l+1}^* ... are to be determined (Box & Jenkins, pp. 127-128). Then, the mean square error forecast can expressed as

$$E[z_{n+l} - \hat{z}_n(l)]^2 = (1 + \psi_1^2 + \cdots + \psi_{l-1}^2)\sigma_a^2 + \sum_{j=0}^{\infty} \{\psi_{l+j} - \psi_{l+j}^*\}^2 \sigma_a^2 \tag{10.2.95}$$

which can be minimized by setting $\psi_{l+j}^* = \psi_{l+j}$ (Box & Jenkins, p. 128). Consequently,

$$z_{n+l} = (a_{n+l} + \psi_1 a_{n+l-1} + \cdots + \psi_{l-1} a_{n+1}) + (\psi_l a_n + \psi_{l+1} a_{n-1} + \cdots) \tag{10.2.96}$$

$$= e_n(l) + \hat{z}_n(l) \tag{10.2.97}$$

where $e_n(l)$ is the error of the forecast $\hat{z}_t(l)$ at lead time *l* (Box & Jenkins, p. 128). Note that current and past values of a_{n+j} (i.e. $j \leq 0$) are known, and future values have zero expectation as indicated below (Mills, p. 105):

$$E\left(a_{n+j} \middle| z_t, z_{t-1}, \dots\right) = \begin{cases} a_{n+j}, & j \leq 0 \\ 0, & j > 0 \end{cases} \tag{10.2.98}$$

Hence, the minimum mean square error forecast at origin n and for lead time l is the conditional expectation of z_{n+l} given the observations up to time n as represented below (Box & Jenkins, p. 128):

$$\hat{z}_n(l) = \psi_l a_n + \psi_{l+1} a_{n-1} + \cdots + \psi_{l+2} a_{n-2} + \cdots = E(z_{n+l} | z_n, z_{n-1}, \dots) \tag{10.2.99}$$

Note that $\hat{z}_n(l)$ can also be regarded as the forecast function for origin n which is a function of l for fixed n.

Some important facts about minimum mean square error (MMSE) forecasts are listed below (Box & Jenkins, pp. 128-129):

1. Any linear function $\sum_{l=1}^{L} w_l \hat{z}_n(l)$ of the forecasts will be a MMSE forecast of the corresponding linear function $\sum_{l=1}^{L} w_l z_n(l)$ of future observations. The symbol "w" can be considered as a weight given to a forecast or a future observation.
2. The l-step ahead forecast error for origin n is shown below:

$$e_n(l) = a_{n+l} + \psi_1 a_{n+l-1} + \cdots + \psi_{l-1} a_{n+1} \tag{10.2.100}$$

   Accordingly, the forecast is an unbiased forecast, since $\mathrm{E}(e_n(l)|z_n, z_{n-1}, \ldots) = 0$. The variance of the forecast error is then

$$\sigma^2_{e_t(l)} = \sigma_a^2(1 + \psi_1^2 + \psi_2^2 + \cdots + \psi_{l-1}^2) \tag{10.2.101}$$

3. The one-step ahead forecast error ($l = 1$) is

$$e_n(l) = z_n(l) - \hat{z}_n(l) = a_{n+1} \tag{10.2.102}$$

   Thus, for a MMSE forecast, the one-step ahead forecast errors must be uncorrelated, since a_{n+1} is assumed to be a random variable. However, in general, a correlation can be observed between the forecast errors, $e_n(l)$ and $e_{n-j}(l)$, made at the same lead time l but from the different origins n and $n - j$.
4. In addition, the forecast errors $e_n(l)$ and $e_n(l + j)$,which are made at different lead times but from the same origin n, are correlated. The derivations and the general expressions of the corresponding correlations can be found in Box and Jenkins Appendix A5.1.1 (p. 158) and Appendix A5.1.2 (p. 159). It has been remarked that there will often be a tendency for the forecast function to lie either wholly above or below the values of the series when they finally become observable.

A general procedure for computing forecasts

In this subsection, a general procedure for computing forecasts with general ARIMA models is explained on the basis of Mills (pp. 106-107) and Box and Jenkins (p. 156).

Consider the general $ARIMA(p, d, q)$ model including a constant as expressed below:

$$\phi(B)\nabla^d z_t = \theta_0 + \theta(B)a_{n+h} \tag{10.2.103}$$

Let the terms $\phi(B)$ and ∇^d be represented in parsimonious form as follows:

$$\upsilon(B) = \phi(B)\nabla^d = (1 - \upsilon_1 B - \upsilon_2 B^2 - \cdots - -\upsilon_{p+d} B^{p+d}) \tag{10.2.104}$$

Then, the value z_{n+l} in terms of difference equation can be written as follows:

$$\begin{aligned} & z_{n+l} \\ & = \upsilon_1 z_{n+l-1} + \upsilon_2 z_{n+l-2} + \cdots + \upsilon_{p+d} z_{n+l-p-d} + \theta_0 + a_{n+l} - \theta_1 a_{n+l-1} - \cdots \\ & \qquad -\theta_q a_{n+l-q} \end{aligned} \tag{10.2.105}$$

The forecast $z_n(l)$ of z_{n+l} can be represented as conditional expectation of current and past values as follows:

$$\begin{aligned} & z_n(l) \\ & = E\{\upsilon_1 z_{n+l-1} + \upsilon_2 z_{n+l-2} + \cdots + \upsilon_{p+d} z_{n+l-p-d} + \theta_0 + a_{n+l} - \theta_1 a_{n+l-1} \\ & \qquad\qquad\qquad\qquad\qquad\qquad\qquad\qquad\qquad\qquad\qquad\qquad - \cdots \\ & \qquad -\theta_q a_{n+l-q} | z_n, z_{n-1}, \ldots \} \end{aligned} \tag{10.2.106}$$

It can be inferred from Eqs. (10.2.107) and (10.2.108) that to evaluate $\hat{z}_n(l)$, past expectations $(for\ j \leq 0)$ should be replaced by known values, z_{n+j}, and a_{n+j}. Also, future expectations $(for\ j > 0)$ should be replaced by forecast values, $z_n(l + j)$ and 0, i.e.

$$E\big(z_{n+j} | z_n, z_{n-1}, \ldots\big) = \begin{cases} z_{n+j}, & j \leq 0 \\ z_n(l + j), & j > 0 \end{cases} \tag{10.2.107}$$

$$E\big(a_{n+j} | z_n, z_{n-1}, \ldots\big) = \begin{cases} a_{n+j}, & j \leq 0 \\ 0 & j > 0 \end{cases} \tag{10.2.108}$$

The forecast limits $100(1-\alpha)\%$ for each desired level of significance α and for each lead time l can be built by substituting in

$$z_{n+l}(\pm) = \hat{z}_n(l) \pm u_{\alpha/2}\left(1 + \sum_{j=1}^{l-1} \psi_j^2\right)^{1/2} \sigma_a \tag{10.2.109}$$

where σ_a is replaced by an estimate $\hat{\sigma}_a$, and $u_{\alpha/2}$ is the standard normal deviate exceeded by a proportion $\alpha/2$ of the unit normal distribution such that $P(u > u_{\alpha/2}) = \alpha/2$ (Box & Jenkins, p. 156).

11 DATA PREPARATION FOR APPROXIMATION ANALYSIS (1st STAGE)

In this chapter, detailed information about data preparation for approximation analysis is given (i.e. the 1st stage of the introduced concept). In particular, information is provided about constructing past LDCs of Turkey in the next section. Further in Section 11.2, an overview is given on the demand for electricity in Turkey in the period 2000-2014. Furthermore in Section 11.3, the analysis on the future development of annual gross electricity and the annual peak load demand is explained. Note that the annual gross electricity and the annual peak load demand are forecasted; in order to be utilized for rescaling and validation of the functional approximations to future LDCs of Turkey respectively (i.e. at the fourth stage).

11.1 Construction of Load Duration Curves of Turkey in the Period 2000-2014

First of all, the approximation analysis is initiated by forming two data sets containing the hourly loads demands and the corresponding durations of the hourly load demands for each year. Secondly, the hourly load demands in the first data set[95] are sorted w.r.t. their magnitudes from the highest hourly load demands to the lowest. Subsequently, the second data set is formed by cumulating the number of occurrence of each load in the first data set according to its magnitude. Thirdly, the hourly loads are divided by the corresponding year's gross electricity demand to normalize[96] the areas under the approximated LDCs to unity. Finally, the LDCs are formed by pairing the data in the two data sets according to the one-to-one relationship existing between them. The number of data pairs (i.e. also the sample size) for each year is given in Table 25.

[95] Note that the approximation of LDCs, only by using the inverse of Hill's function, requires an ascending order arrangement of hourly load demands w.r.t. the increasing values of duration (see Section 12.1.3).

[96] Note that the normalization is carried out for evaluating the inaccuracy in both approximated and forecasted LDCs.

Table 25- The number of data pairs forming the historical LDC of each year (own illustration)

Years	Number of Data Pairs
2000	5287
2001	5529
2002	5269
2003	5446
2004	5606
2005	5750
2006	5995
2007	6182
2008	6507
2009	6229
2010	6390
2011	7220
2012	8300
2013	8689
2014	8750

In this study, the functional approximations to past LDCs are carried out by utilizing experimental data rather than observational ones. The underlying reason is that the causal inferences are justified in experiments, where the independent variables are under the direct control of the researcher (Fox, 2008, p. 4). During the formation of the second data set, the independent variable (duration) is measured without any error by utilizing the ordered hourly load data. If the process were to be replicated, the values of the corresponding variable would remain the same and the full range of values taken by the variable would be covered (i.e. from 1 to 8760 or to 8784 hours for regular years and for leap years respectively). This is due to the fact that the values are deterministic (i.e. not sampled). For more information about the topic see Fox (p. 101).

In addition, the formation of the first data set is also designed to be deterministic by ordering the sequence of hourly loads in a decreasing order (i.e. non-randomized). Since the values of the independent variable are assigned by the researcher, along with the values of the dependent variable (the "effect"), the causal inferences are justified through the design of the experiment (Fox, 2008, p. 4). In an experimental research, in which the causal relationship is exact, trials of the experiment are points on the deterministic function rather than a sample drawn from the probability distribution centered on that function; because there is no sampling error if the dependent variable is not stochastic (Lewis-Beck, Bryman, & Liao, 2004, p. 1084).

11.2 An Overview of the Demand for Electricity in Turkey in the Period 2000-2014

Turkey has a total area of about 783,562 km^2 possessing various abundant energy resources (wind, solar and hydropower etc.). Turkey is situated at the meeting point of three continents Asia, Europe and Africa. Turkey's geographical location makes it an important energy corridor between Europe and the energy-rich countries in the Middle East and in the south eastern Asia. In the period 2000-2014, the population of Turkey increased from 65 to 77 million inhabitants with an annual mean growth rate[97] of 1.3% as illustrated in Figure 38.

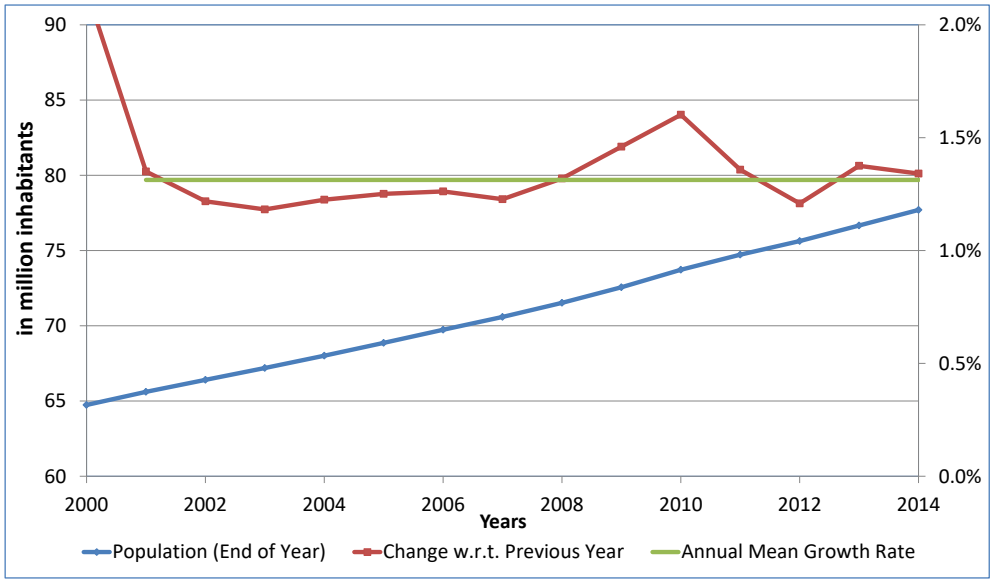

Figure 38- The total population of Turkey in the period 2000-2014 (own illustration according to Turkish Statistical Institute (2015))

In the period 2000-2014, the Turkish economy has experienced a remarkable economic growth; despite the financial crisis of Turkey in 2001 and the global financial crisis in the year 2009 as depicted in Figure 39. In the period 2000-2014, the gross domestic product[98] (GDP) of Turkey increased from 72 to 126 billion Turkish Lira (i.e. abbreviated as TL and 3 TL~1 Euro in July 2015) with an annual mean growth rate of 4.1%.

[97] It equals to the mean of changes (e.g. in population, electricity demand, etc.) w.r.t. the previous years. In addition, it is used interchangeably with average growth per annum (/a) in a mentioned period.

[98] According to World Bank, the GDP at purchaser's prices is the sum of gross value added by all resident producers in the economy plus any product taxes and minus any subsidies not included in the value of the products. The GDP is calculated based on the production approach and in constant 1998 TL.

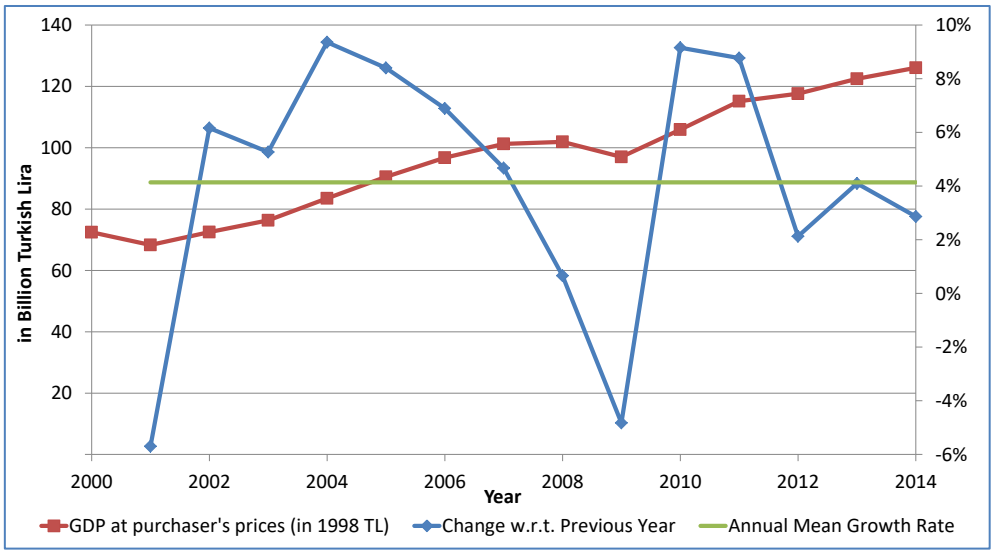

Figure 39- The economic development of Turkey in the period 2000-2014 (own illustration according to Turkish Statistical Institute (2015))

The energy demand of the country grows with increasing young population, fast growing urbanization and economic development. From the year 2000 until 2014 the annual gross electricity demand[99] rose from 128 to 257 TWh_{el} which corresponds to an annual mean growth rate of 5.2% (see Figure 40). The demand decrease in the years 2001 and 2009 are due to the mentioned financial crisis.

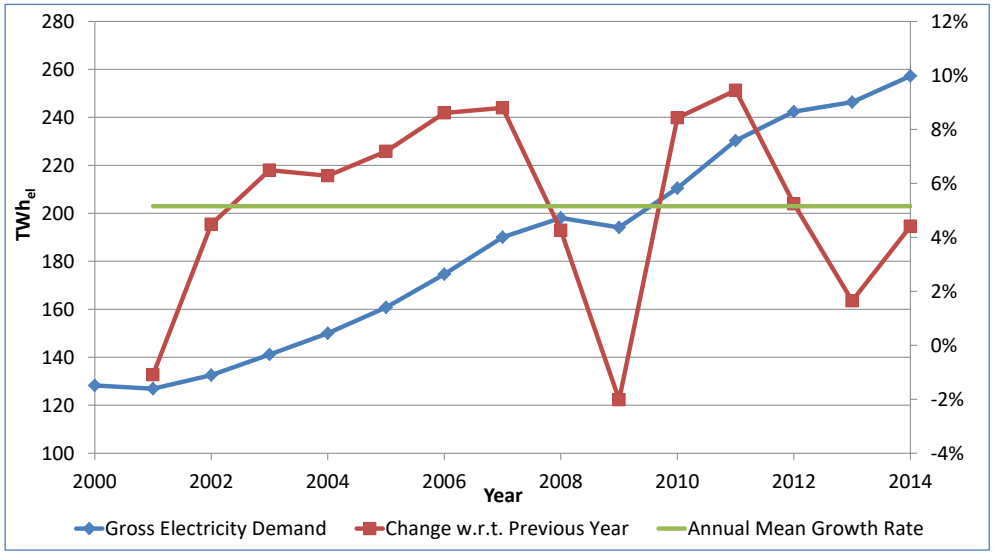

Figure 40- The development of the annual gross electricity demand in the period 2000-2014 (own illustration according to TEIAS (2015))

In the period 2000-2014, the demand for annual peak load demand also rose from 19390 to 40734 MW_{el} which corresponds to an annual mean growth rate of 5.5% as displayed below.

[99] The gross electricity demand equals to the sum of national electricity generation and imported amount of electricity subtracted exported amount of electricity.

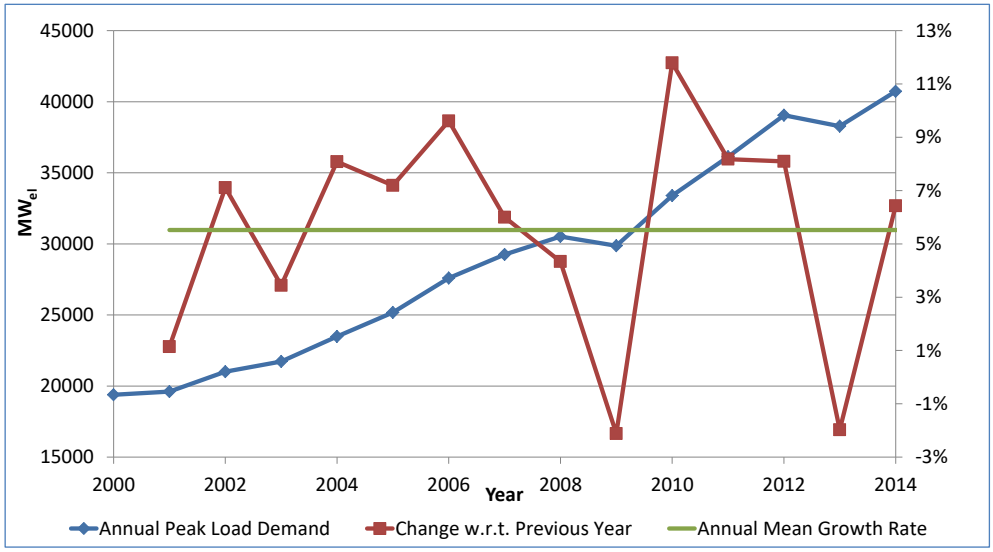

Figure 41- The development of the annual peak load demand in the period 2000-2014 (own illustration according to TEIAS (2015))

In Figure 42, the distribution of net electricity consumption[100] is illustrated according to sectors. In the period 2000-2013, the net electricity consumption rose from 98 to 198 TWh_{el} which corresponds to an annual mean growth rate of 5.6%. In Turkey, the highest net electricity consumption is in industrial sector (e.g. textile, automobile, steel industry) and increased from 49 to 93 TWh_{el} in the period 2000-2013. In that period, the demand rose in average 5.2%/a; although there were two financial crises with -3.8% and -5.9% decrease in the years 2001 and 2009 respectively.

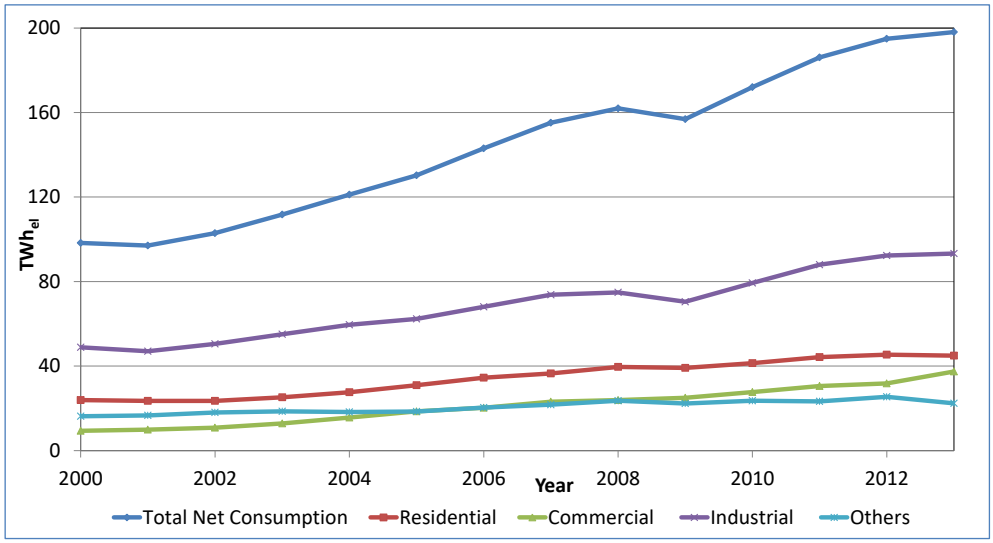

Figure 42- The distribution of the net electricity consumption by sectors for the period 2000-2012 (own illustration according to Turkish Statistical Institute (2015))

[100]Net Electricity Consumption = Gross Electricity Generation - Internal Consumption of Power Plants + Imports - Exports- Network Losses (due to Transmission and Distribution)

Further, the net electricity consumption in the residential sector increased from 24 to 45 TWh_{el} in the period 2000-2013 (see Figure 42). The residential sector mainly needs electricity for using household appliances and air conditioning. In that period, the demand rose in average 5.1%/a; although there were two financial crises with -1.4% and -1.1% decrease in the years 2001 and 2009 respectively.

Furthermore, the net electricity consumption in the commercial sector increased from 9 to 38 TWh_{el} in the period 2000-2013 (see Figure 42). The commercial sector requires electricity for providing service in shopping malls, restaurants, offices, restaurants, etc. As opposed to the residential and industrial sectors influenced by the financial crisis, the demand in commercial sector continuously rose in average 11.4%/a.

Finally, the net electricity consumption in the sector defined as "others" which indicates the aggregate net electricity consumption in public[101], agriculture, livestock, and fishery sectors of Turkey, increased from 16 to 22 TWh_{el} in the period 2000-2013 (see Figure 42). In that period, only the consumption for illumination (for streets, highways etc.) decreased from 4.6 to 3.9 TWh_{el} (i.e. in average -1.2%/a due to transition to automation); whereas the net consumption in public, agriculture sector, etc. increased.

11.3 The Future Development of Demand for Electricity in Turkey

In this section, the analysis on the future development of annual gross electricity and annual peak load demand is explained. Further in the next subsection, information is given about the previous studies on the gross electricity demand of Turkey. Furthermore in Subsection 11.3.2, information is given about the computation of forecasting the annual gross electricity demand of Turkey for the period 2015-2025. In the final Subsection 11.3.3, information is given about the computation of forecasting the annual peak load demand of Turkey for the period 2015-2025.

11.3.1 Previous Studies on the Gross Electricity Demand of Turkey

The Turkish Electricity Transmission Corporation (TEIAS) annually publishes a report on five-year electricity generation capacity projection[102] (FYEGCP) by using demand projections

[101] The public sector needs electricity for services, illumination, water supply and drainage.

[102] The objective of the study is to guide electricity market participants to indicate the time of required new capacity to meet the demand safely, i.e. with a suitable reserve. Note that until the year 2012 ten-year generation capacity projections were made; however starting from the year 2013 projections for five-year are made.

estimated by the Ministry of Energy and Natural Resources (MENR). MENR utilizes a mathematical model so called "Model for Analysis of Energy Demand" (MAED) developed by the International Atomic Energy Agency (IAEA). MAED[103] helps in evaluating future energy demands based on scenarios considering the influence of socioeconomic, technological and demographic developments. MENR conducts demand analysis according to the macroeconomic targets set by the Turkish government.

In FYEGCP of the period 2014-2018, the demand forecasts for the period 2014-2023 are published; however the assumed economic parameters are not explicitly specified. In the analysis, it is assumed that no change occurs in the annual load curve characteristics during the period 2014-2023 (Turkish Electricity Transmission Corporation, 2014, p. 12). In addition, the annual peak load demand is scaled by using growth rates for the forecasted period.

Accordingly, the annual gross electricity demand is forecasted w.r.t. the low, the reference and the high demand scenarios as depicted in Figure 43. Starting from the base year 2013 (246 TWh_{el}), the electricity demand is forecasted to be amounting to 381 TWh_{el} in the year 2023 w.r.t. the low demand scenario (i.e. a mean increase of 4.4%/a). For the reference demand scenario, the electricity demand is forecasted to be amounting to 416 TWh_{el} in the year 2023 (i.e. a mean increase of 5.3%/a). For the high demand scenario, the electricity demand is forecasted to be amounting to 463 TWh_{el} in the year 2023 (i.e. a mean increase of 6.4%/a).

[103] MAED is an excel based tool which can evaluate sectorial energy demand according to the given categorized services or production of certain goods for end-use. The corresponding demand for services or goods is a function of several determining factors such as national priorities for the development of certain industries or economic sectors, population growth, number of inhabitants per dwelling, type and number of electrical appliances used in households, mobility, efficiency etc. (International Atomic Energy Agency, 2006, p. 3).

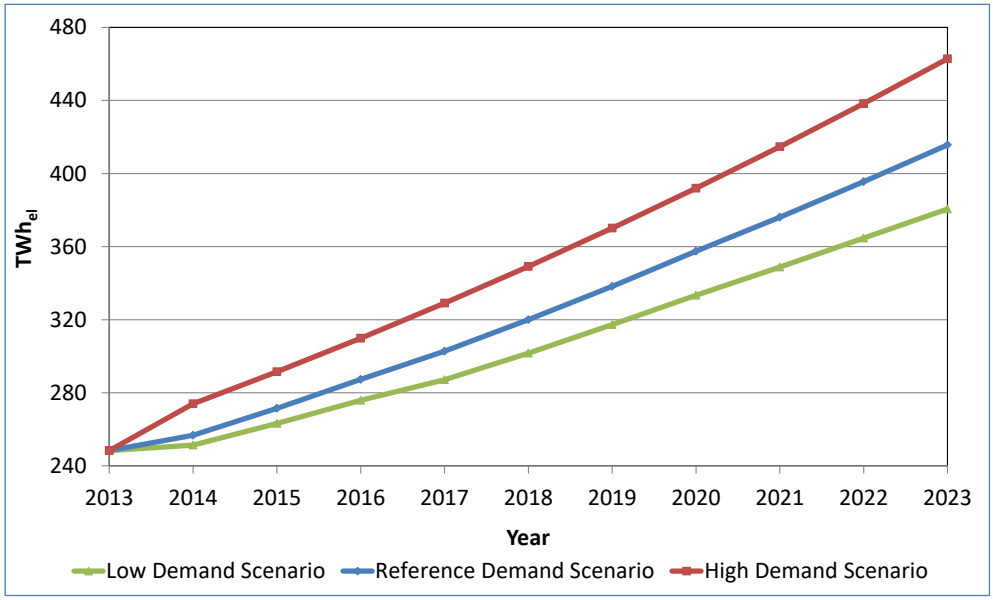

Figure 43- The forecasted scenarios of gross electricity demand for the period 2014-2023 (own illustration according to TEIAS (2014, pp. 14-16))

Similarly, the annual peak demand is also forecasted w.r.t. the low, the reference and the high demand scenarios as depicted in Figure 44. Starting from the base year 2013 (38274 MW_{el}), the peak load demand is forecasted to be amounting to 58630 MW_{el} in the year 2023 w.r.t. the low demand scenario (i.e. a mean increase of 4.4%/a). For the reference demand scenario, the electricity demand is forecasted to be amounting to 64040 MW_{el} in the year 2023 (i.e. a mean increase of 5.3%/a). For the high demand scenario, the electricity demand is forecasted to be amounting to 71300 MW_{el} in the year 2023 (i.e. a mean increase of 6.4%/a).

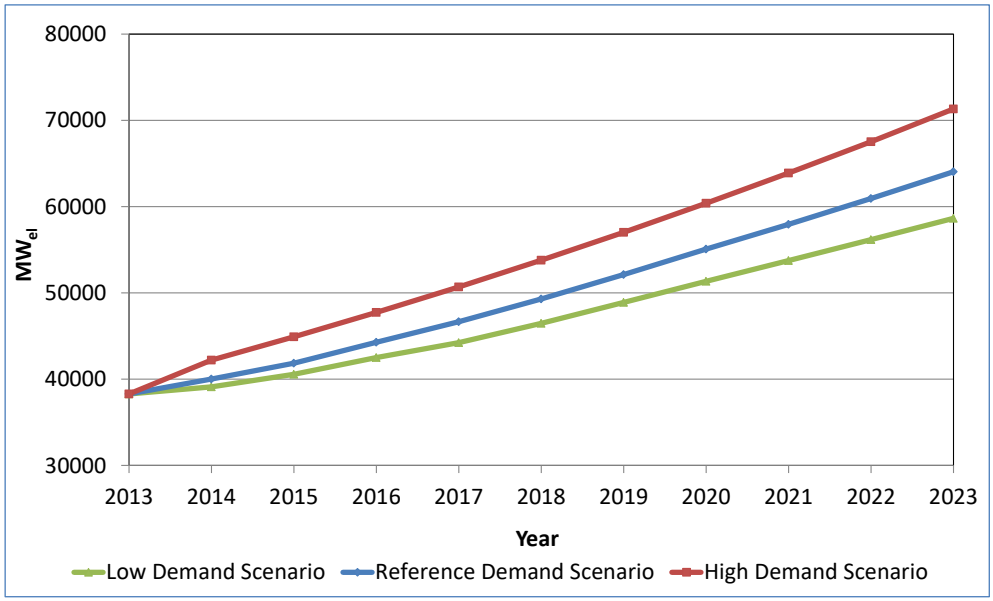

Figure 44- The forecasted scenarios of annual peak load demand for the period 2014-2023 (own illustration according to TEIAS (2014, pp. 14-16))

TEIAS publishes the inaccuracy of the former forecasts of annual gross electricity demand in comparison to the realized values as deviation ratios (see Table 26). The deviation ratios indicate that as the lead time increases, the accuracy of the forecasts substantially decrease. For example, the demand forecast made in the year 2000 indicates an increasing deviation ratio ranging from -1% to 44% from the forecasted year 2000 to 2013. In comparison to the all published demand forecasts, only the forecasts published in year 2010 represents a relatively good best practice example for the period 2011-2013; since the deviation ratios remain under the 5% level of inaccuracy.

Table 26- The inaccuracy in the former annual gross electricity demand forecasts as deviation ratios (own illustration according to TEIAS (2014, p. 13))

Forecasted Year	The Publication year of Generation Capacity Projections							
	2000	2002/1	2002/2	2004	2008	2010	2012	2013
2000	-1%	-	-	-	-	-	-	-
2001	9%	0.3%	-	-	-	-	-	-
2002	14%	1%	-0.2%	-	-	-	-	-
2003	17%	7%	1%	-	-	-	-	-
2004	20%	15%	6%	-	-	-	-	-
2005	22%	22%	9%	-0.2%	-	-	-	-
2006	22%	21%	9%	1%	-	-	-	-
2007	22%	20%	9%	0.4%	-	-	-	-
2008	27%	24%	14%	4%	3%	-	-	-
2009	40%	37%	26%	15%	13%	-	-	-
2010	40%	36%	26%	15%	12%	-	-	-
2011	37%	34%	24%	14%	11%	-4%	-	-
2012	38%	36%	26%	17%	13%	-3%	1%	-
2013	44%	42%	31%	23%	18%	2%	6%	3%

The accuracy of corresponding forecasts is influenced by the considered planning horizon and the uncertainty in the economic and climatic variables as well as consumer behavior. The uncertainty in the corresponding factors is inherent, since they also must be forecasted; in order to be utilized in a long-term load forecasting process. For example, the peak load demand is usually triggered by an increase in the temperature and as the lead time of forecasts increase; the accuracy in predicting the temperature as well as the peak load demand deteriorates. Further, if income of consumers were also to be accounted for, the accuracy might get lower due to introducing more uncertainty in forecasting. The lower the level of forecasting accuracy, the higher the incurred cost of electricity supply and vice versa.

The growth of the Turkish economy and the electricity demand indicate a relatively similar pattern; however the fluctuations in the growth rate of economy is more sharper as illustrated

in Figure 45. In the period 2001-2014, the mean economic growth[104] of the Turkish economy is 4.1%/a which is 1% less than the mean growth rate of electricity in the same period.

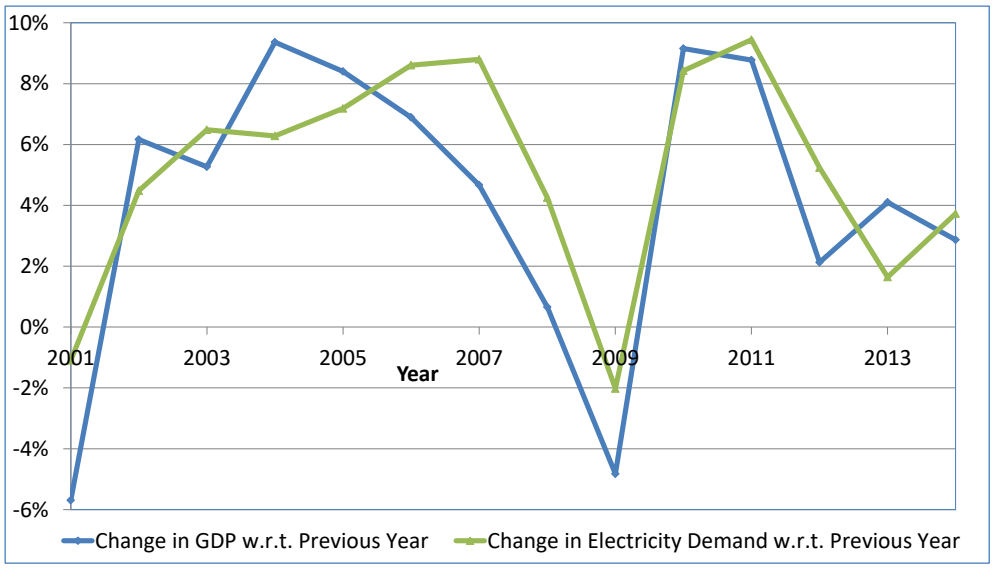

Figure 45- The change in GDP at purchaser's prices (in 1998 TL) and in electricity demand in the period 2000-2014 (own illustration according to TEIAS (2015) and Turkish Statistical Institute (2014))

The assumed rate of economic growth is the major input influencing the accuracy of the long term forecasts for electricity demand in Turkey. A good proof is the assumptions for the electricity demand forecasts of the period 2008-2017 which are tabulated in Table 27. An average increase of 4.2%/a was realized in the period 2005-2010 which is below the considered level for both high and low demand scenarios. Moreover, the economic growth in year 2008 and 2009 were 0.7% and -4.8% respectively due to the global financial crisis. Consequently, the average increase in economic growth was 3.3%/a in the period 2008-2013. Since the assumptions for economic growth was not accurate, the deviation ratio of demand forecasts ranges from 3% to 18% in the period 2008-2013 (see Table 26). Also, it can be expected that the deviations are going to increase until the latest forecast year 2017.

Table 27- The economic growth rate assumptions for the demand scenarios of electricity (own illustration according to TEIAS (2008, p. 12))

The growth rate of economy		
Period	Reference demand scenario	Low demand scenario
2005-2010	5.8%/a	5.3%/a
2010-2015	5.5%/a	4.5%/a
2015-2030	5.5%/a	4.5%/a

[104] The rates are based on the changes in the gross domestic product (in Turkish Lira) which are calculated based on the production approach and in purchasers' price (see Figure 39 for the absolute values).

It should be noted that the other assumptions made by TEIAS such as no dynamic changes occur in annual load curve characteristics or projecting annual peak power demands by a considered growth rate also lower the accuracy of long-term forecasts. The corresponding assumptions are abstract; since different end-use sectors exhibit different consumption characteristics in the long-term (see Figure 42) due to the difference in sectoral purposes of electricity utilization, developments in sectoral growth rate, achievements in implementing energy efficiency, etc.

In Table 28, the studies focusing on the development of annual gross electricity demand in Turkey are represented. It can be deduced that all studies are conducted by using the econometric methods. Comprehensive information about the mentioned methods can be found in APPENDIX A.

Table 28- The studies on the development of electricity demand in Turkey (own illustration)

Author(s)	Publication Year	Method(s)	Forecasted Period
Özturk & Ceylan	2005	Genetic Algorithm	2004-2020
Akay & Atak	2007	Grey Prediction with Rolling Mechanism	2006-2015
Kücükdeniz	2010	Artificial Neural Network & Support Vector Machines	2009-2025
Kücükali & Baris	2010	Fuzzy Logic	2010-2014
Dilaver & Hunt	2011	Structural Time Series Analysis	2009-2020
Polater	2013	Artificial Neural Network & Time Series Analysis	2013-2023
Yavuzdemir & Gökgöz	2015	Regression, Fuzzy Logic & Time Series Analysis	2013-2018

Ozturk and Ceylan (2005) utilize the genetic algorithm method (GAM) to analyze the relationship of annual gross electricity demand with population, national imports and exports and gross national product (GNP) in the period 1980 to 2003. Correspondingly, the electricity demand is forecasted w.r.t. the low and the high growth scenarios of the mentioned variables. For the low growth scenario, it is assumed that the average growth rate for GNP is 4%, for population 0.15%, for imports 4% and for exports 4% for the period of 2004–2020. For the high growth scenario, it is assumed that the average growth rate for GNP is 5%, for population 0.18%, for imports 5% and for exports 5% in the period of 2004–2020. The electricity demand in 2020 is forecasted to be about 462 TWh_{el} (w.r.t. the low growth scenario) and 500 TWh_{el} (w.r.t. the high growth scenario).

Akay and Atak analyze the gross electricity demand in the period 1970-2004 by utilizing the grey prediction method (GPRM) with rolling mechanism (based on Grey Theory). After

building a model based on the method, the annual gross electricity demand is forecasted to be about 266 TWh_{el} in year 2015.

Kücükdeniz (2010) developed models based on artificial neural network (ANN) and support vector machines (SVV) to analyze the electricity demand in the period 1980-2000 (data for the period 2001-2008 is used for testing.). The gross electricity demand is forecasted to be about 294 TWh_{el} (i.e. the result by using ANN) and 321 TWh_{el} (i.e. the result by using SVM) in year 2025.

Kücükali and Baris (2010) utilize fuzzy logic methodology (FLM) and classical regression approach to forecast short term electricity demand; according to its relation with the GDP (based on purchasing power parity) of Turkey in the period 1980-2009. The gross electricity demand is forecasted to be about 230 TWh_{el} (i.e. the result by using FLM) and 247 TWh_{el} (i.e. the result by using regression method) in year 2014.

Dilaver and Hunt (2011) estimated a so called "aggregate electricity demand[105] function" for Turkey by applying the structural time series method (STSM) to annual data over the period 1960 to 2008. According to Dilaver and Hunt, STSM decomposes a time series into independent variables, a stochastic trend and a random component. The demand function relates the aggregate electricity demand with GDP, electricity prices and underlying energy demand trend (UEDT). An estimated stochastic UEDT is considered to be accounting for unobserved components due to the electricity demand behavior of consumers (environmental regulations, economic structure, etc.). In the reference case, the average real electricity prices are assumed to increase by 1%/a, the GDP increases 2%/a in average and the slope of the UEDT is projected to decrease 0.001 per annum in the period. In the low case scenario, the average real electricity prices are assumed to increase 2%/a, the GDP increases 1.5%/a in average and the slope of the UEDT is projected to decrease 0.003 per annum in the period. In high case scenario, average real electricity prices are assumed to increase by only 0.5%/a, the GDP increases 2.5%/a in average and the slope of the UEDT is projected to increase 0.003 per annum in the period. It is forecasted that the Turkish annual gross electricity demand will be somewhere between 259 TWh and 368 TWh in 2020.

Polater (2013) analyzed the development of the annual gross electricity demand in the period 1980-2012 utilizing ANN and TSA. The electricity demand is forecasted to be about 454 TWh_{el} (by using ANN), and 440 TWh (by using TSA) in the year 2023. Nevertheless, the

[105] Aggregate electricity demand implies annual gross electricity demand.

ARIMA(2,2,0) model utilized by Polater cannot be an adequate model for forecasting the electricity demand. In particular, he did not recognize that the analyzed data were heteroscedastic as it can be deduced from the cone-shaped pattern (indicated as green dashed lines) in the plots of first order differenced data (left panel) and second order differenced data (right panel) of his work. Further, he did not also apply diagnostic tests on the residuals of the mentioned model. Furthermore, he chose the mentioned model based on the lowest MAPE (i.e. 6.1%).

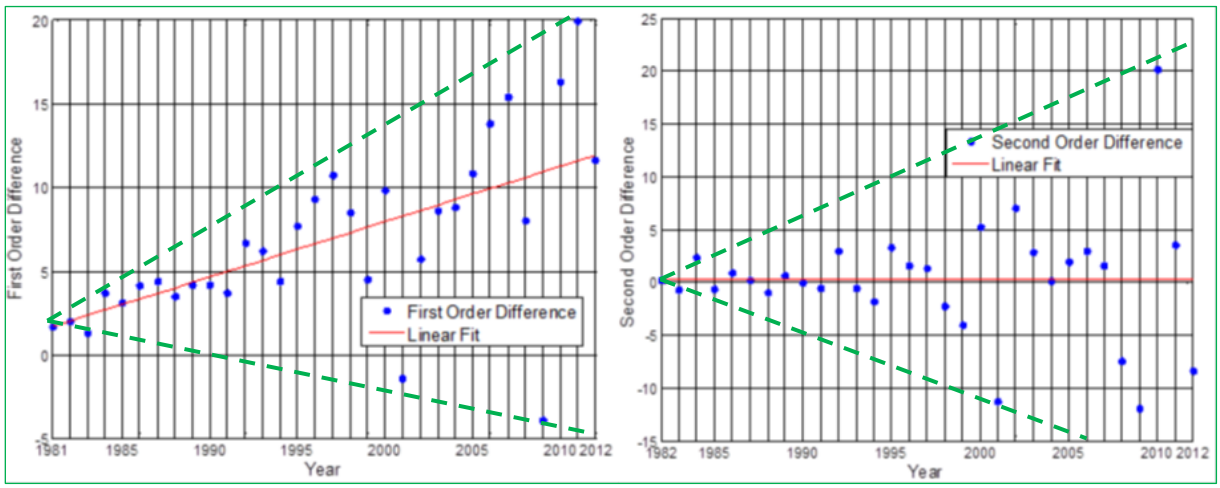

Figure 46- The disregarded heteroscedasticity in the TSA of Polater (modified illustration from Polater, p. 60)

As in the case of forecasting annual gross electricity demand with an inadequate model, the ARIMA(1,2,0) model utilized by Polater is also observed to be an inadequate model for forecasting the annual peak load demand. In particular, he did not recognize that the analyzed data were heteroscedastic (i.e. indicated as cone-shaped pattern in green dashed lines) as it can be observed from the plots of first order (left panel) and second order differenced data (right panel) of his work. Further, he did not also apply diagnostic tests on the residuals of the mentioned model. Furthermore, he chose the mentioned model based on the lowest MAPE (i.e. 7.9%).

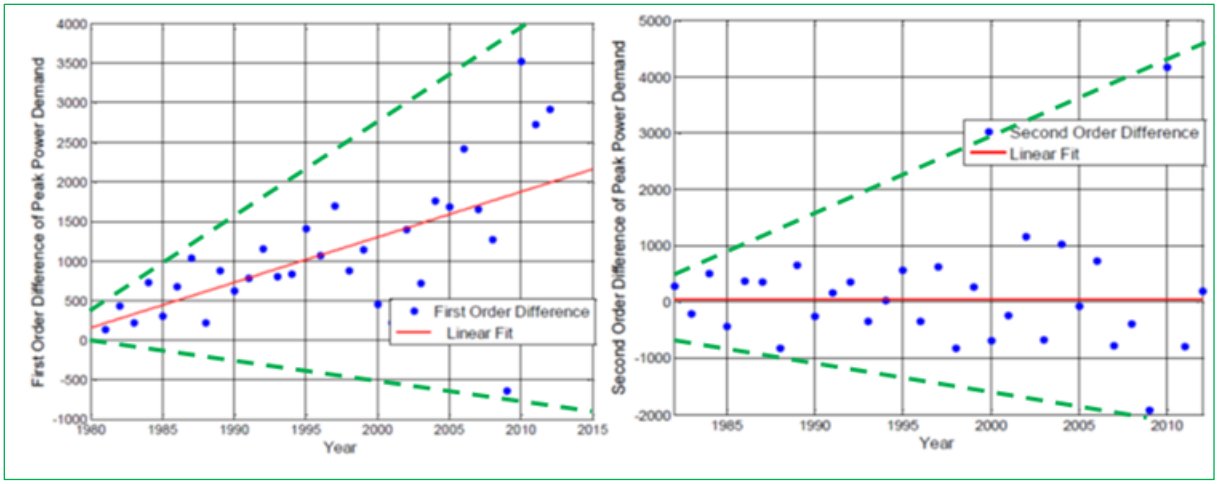

Figure 47- The disregarded heteroscedasticity in the TSA of Polater (modified illustration from Polater, p. 67)

Yavuzdemir and Gökgöz (2015) apply fuzzy logic and regression approaches by relating energy demand to GDP (purchasing power parity) in the period 1980-2012. In addition, the TSA is also applied for the same period. The demand in electricity demand is forecasted to be 356 TWh_{el} (using regression approach), 352 TWh_{el} (using FLM) and 309 TWh_{el} (using TSA) in year 2018.

In Table 29, the forecasts made in the previous studies are compared based on the inaccuracy in forecasting annual gross electricity demand in the year 2014.

Table 29- The comparison of inaccuracy in forecasting annual gross electricity demand for the year 2014 (own illustration)

Author(s)	Method	Method/Scenario	Forecast for the Year 2014 (TWh_{el})	Forecast Error
TEIAS (2014)	Econometric Analysis	Low Demand Scenario	251	-2.0%
		Reference Demand Scenario	257	0.4%
		High Demand Scenario	273	6.6%
Özturk & Ceylan (2005)	GAM	Low Case	330	28.9%
		High Case	380	48.4%
Akay & Atak (2007)	GPRM	-	249	-2.7%
Kücükdeniz (2010)	ANN	-	213	-16.8%
	SVM		203	-20.7%
Kücükali & Baris (2010)	FLM	-	230	-10.2%
	Regression		247	-3.5%
Dilaver & Hunt (2011)	STSA	Low Case	213	-16.8%
		Reference Case	224	-12.5%
		High Case	235	-8.2%
Polater (2013)	ANN	-	272	6.3%
	TSA		274	7.0%
Yavuzdemir & Gökgöz (2015)	Regression	-	276	7.8%
	FLM		279	9.0%
	TSA		259	1.2%

Accordingly, it can be deduced that the reference case forecast by TEIAS indicates the least inaccuracy among the others (in particular compared to Yavuzdemir and Gökgöz); however the advantage of its publication year compared to the earlier studies cannot be disregarded. Further, the study by Özturk and Ceylan indicates the highest inaccuracy among the others;

nevertheless it is the earliest considered publication. In addition, any particular method has not been observed for being significantly accurate for the long-term forecasting of annual gross electricity demand of Turkey.

The development of the annual gross electricity demand depends primarily on the energy prices, the consumer behavior, economic and climatic variables. In addition, the accuracy of long-term forecasts diminishes as more uncertainty is present due to the states of the mentioned factors in the future. Therefore, Box-Jenkins method of univariate time series analysis is considered for forecasting the development of the annual gross electricity demand and the annual peak load demand for the period 2015-2025.

11.3.2 Forecasting Annual Gross Electricity Demand of Turkey in the Period 2015-2025

In this section, an adequate ARIMA model of order[106] p, d and q is determined for the time series which consists of the annual gross electricity demand of Turkey in the period 1970-2014. The relation of the ARIMA model with the corresponding time series is achieved by a three-stage iterative procedure based on identification, estimation, and diagnostic checking (i.e the Box-Jenkins model building process mentioned in Subsection 10.2.8). In the 4th fourth stage, the annual gross electricity demand of Turkey in the period 2015-2025 is forecasted by utilizing the determined adequate model.

The analysis is carried out by using the license free statistical software R (version 3.1.2) and also by using the RStudio IDE (Integrated Development Environment, Version 0.98.1102) which is a license free user interface for R.

The 1st Stage- Model Identification

During this stage, the subclasses of parsimonious models are specified according to how the considered data were generated. In particular, the objective is to obtain some tentative values of p, d and q orders needed in the general linear ARIMA model building process.

First of all, the annual gross electricity demand of Turkey in the period 1970-2014 (i.e. composed of 45 observations) is plotted against time and visually examined for non-

[106] Note that the orders p, d and q indicate the order of autoregressive component, differencing and moving average component of a general ARIMA model respectively.

stationarity (see Figure 48). It can be inferred from the figure that the non-linear upward trend is evident for the presence of non-stationarity in the time series.

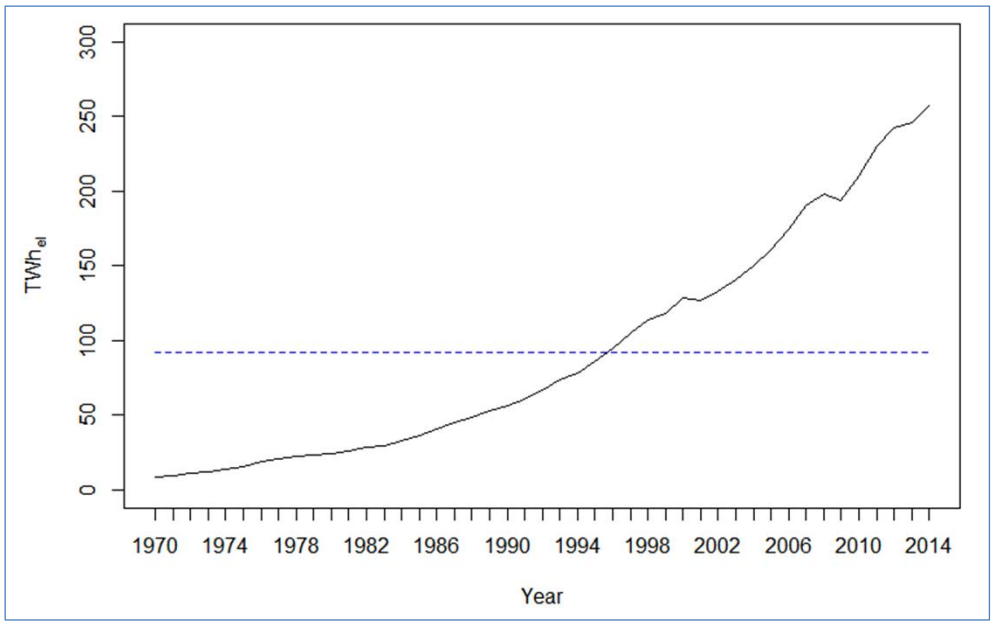

Figure 48- The annual gross electricity demand in the period 1980-2014 (continuous line) and its mean (dashed line) (own illustration according to TEIAS (2015)

The sample autocorrelation function (ACF) of the time series also indicates non-stationarity by showing large autocorrelations that diminish very slowly as lags increase (see Figure 49). Therefore, it is necessary to transform the data into a stationary time series by differencing.

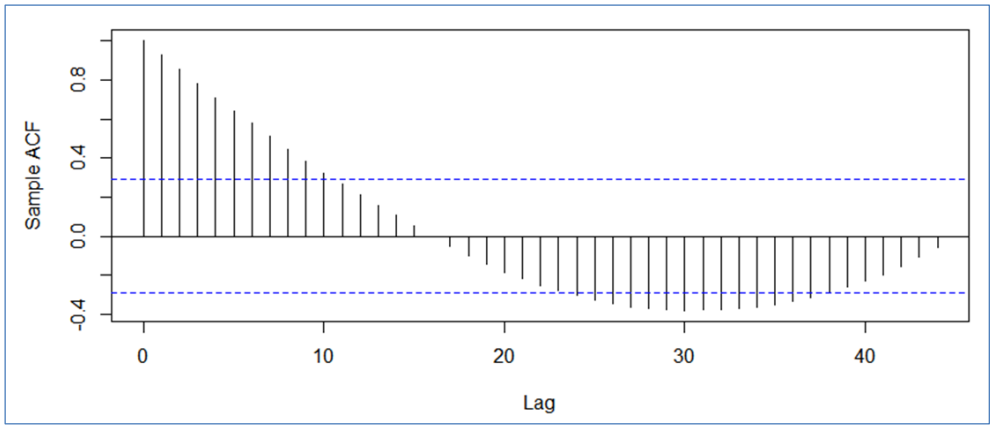

Figure 49- The sample ACF of the annual gross electricity demand series (own calculation & illustration)

In Figure 50, the first order difference of the time series is displayed. The general upward trend is alleviated and it is also observed that as the lags increase, the dispersion in the series increase. In the figure, the cone-shaped pattern (i.e. depicted as dotted green dashed lines) indicates variance instability (i.e. heteroscedasticity). The variance of the data should also be stable (homoscedastic); in order to validate the stationarity condition. Consequently, the

second order difference should be taken; in order to make the observations vary around their mean.

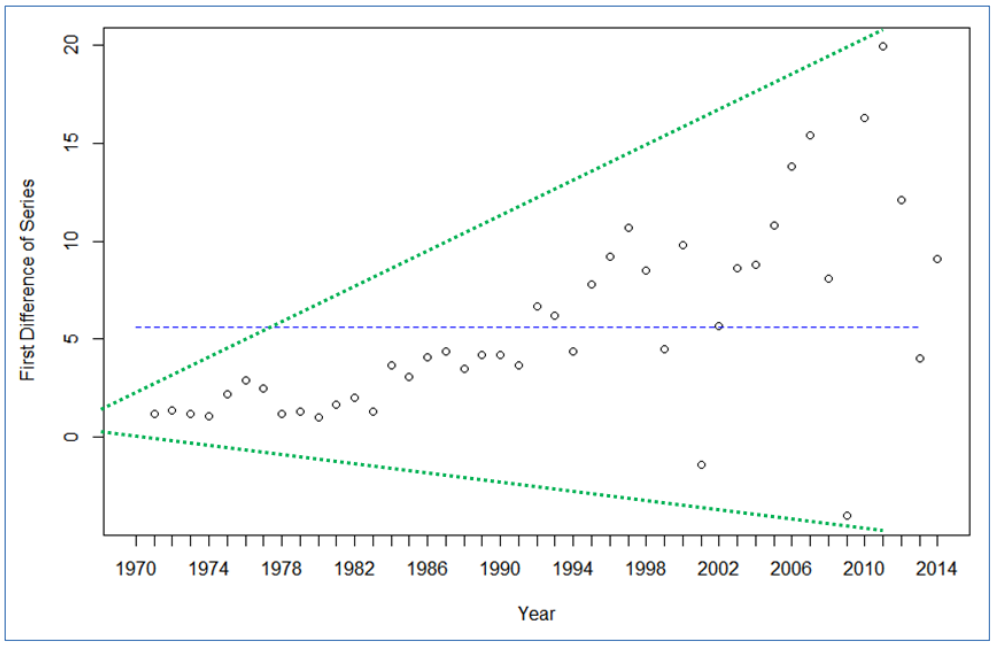

Figure 50- The scatter plot of the first order difference of the annual gross electricity demand series (circle) and its mean (dashed line) (own calculation & illustration)

The sample ACF of the once differenced series also suggests that differencing is required by indicating non-stationarity through displaying a recurrent pattern which decays slowly (see Figure 51).

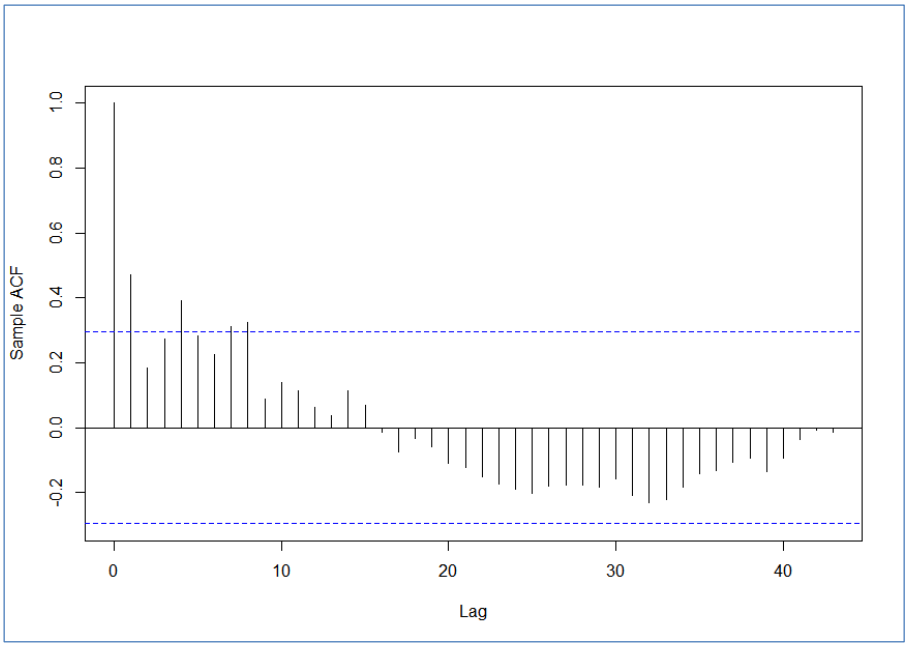

Figure 51- The sample ACF of first order difference of gross annual electricity demand series (own calculation & illustration)

In Figure 52, the second order difference of the time series is displayed. It can be inferred that the general upward trend has disappeared and the observations vary around their mean; however the heteroscedasticity still recurs (i.e. depicted as dotted green dashed lines). Subsequently, the data should be transformed according to the Box-Cox power transformation technique before fitting any tentative models. The Box-Cox technique of data transformation is utilized for determining a power transformation of the data to stabilize the variance of the series (see Subsection 10.2.7.1 for information).

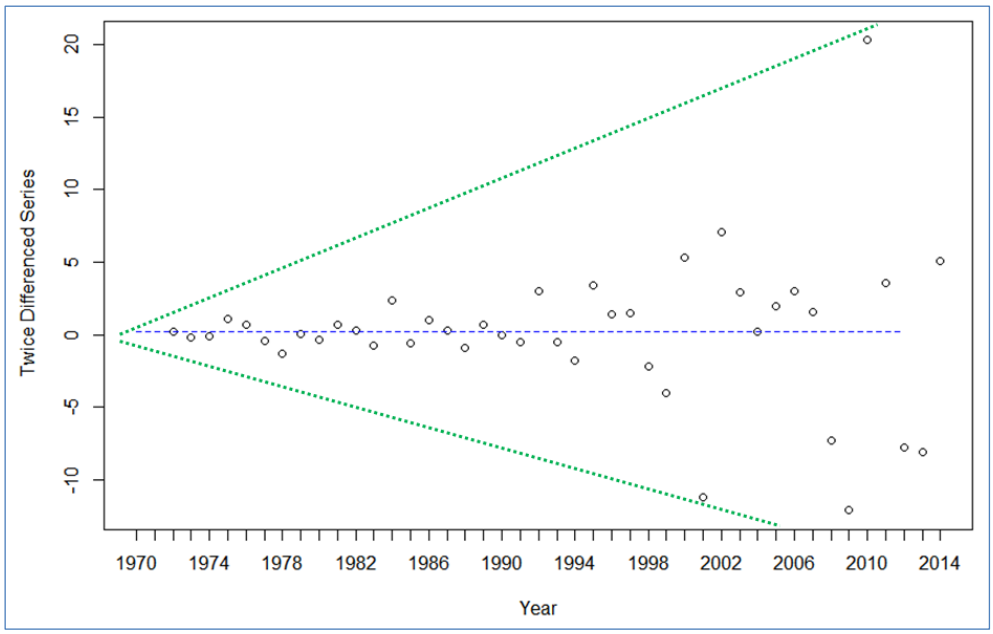

Figure 52- The scatter plot of the second order difference of the annual gross electricity demand series (circle) and its mean (dashed line) (own calculation & illustration)

The "BoxCox" function (in package "FitAR" version 1.94) is applied on the original series and the transformation parameter (λ) is estimated by maximizing the relative likelihood ($R(\lambda)$) of the series. The estimated transformation parameter ($\hat{\lambda}$) is computed as -0.049 (see Figure 53). Subsequently, the original series is transformed by using the computed $\hat{\lambda}$ and then twice differenced. The sample ACF and the sample PACF of the resulting series are displayed in Figure 54.

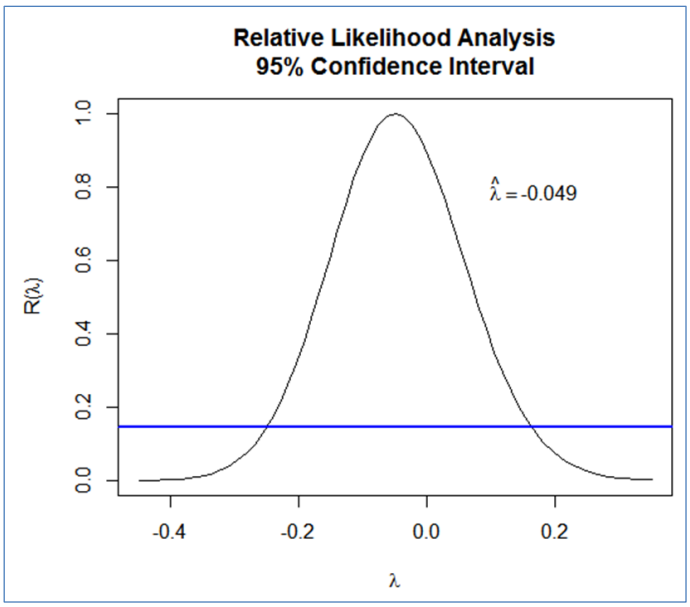

Figure 53- The plot of Box-Cox transformation analysis of the original series (own calculation & illustration)

In Figure 54, the sample ACF of the transformed and the twice differenced series indicates that the stationarity is achieved with the Box-Cox transformation of the series. The sample ACF of the corresponding series indicates no spikes (i.e. randomness); whereas the sample PACF (partial autocorrelation function) indicates only one significant spike at lag 2. Both patterns in sample ACF and sample PACF do not indicate a specific tentative model according to the tabulated theoretical patterns in Table 24 on p. 133. In particular, the patterns indicate an ARIMA model which is especially difficult to identify. In order to analyze all possible tentative ARIMA(p,d,q) models, the auto.arima function (in package "forecast" Version 6.1) is applied on the corresponding series. Note that the number of times the data have been differenced to become stationary (i.e. d) equals to 2. During the next stage, the parameter estimation process is carried out according to the possible tentative models.

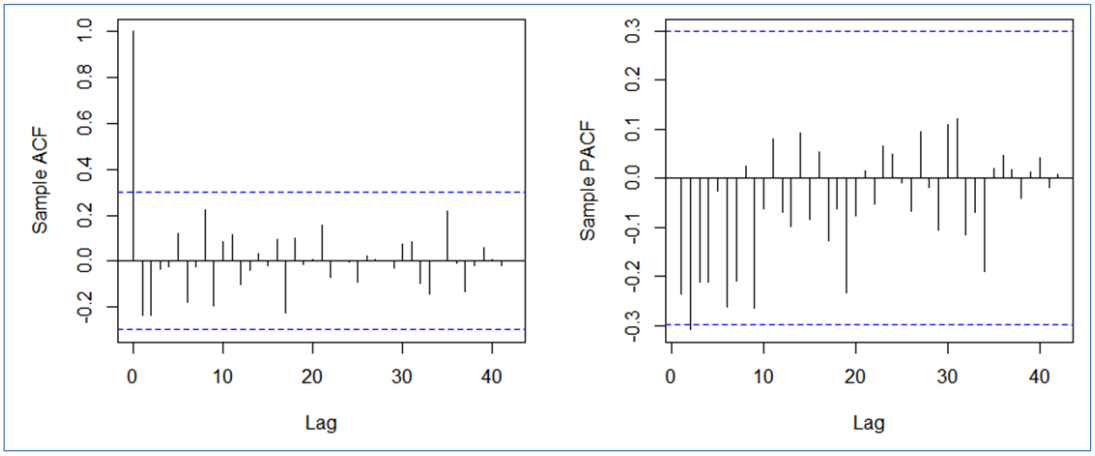

Figure 54- The sample ACF and the sample PACF of the Box-Cox transformed and the twice differenced annual gross electricity demand series (own calculation & illustration)

The 2nd Stage- Parameter Estimation

During the second stage of the time series modelling, the parameters of the possible tentative models are estimated and the corresponding models are compared based on their corrected AIC criterion[107] (AICc). The AICc criterion is considered for comparing the tentative models; since the AICc is usually superior in smaller samples where the relative number of parameters is large (Shumway & Stoffer, p. 53).

The "auto.arima" function in R is utilized for automatically fitting a number of tentative models by varying the assigned starting values of the orders (i.e. p and q). In contrast, the order of differencing is once given, cannot be varied. The utilized function increases the assigned starting values in a stepwise manner and finally returns the tentative model with the lowest magnitude of the selected information criterion. During the analysis, the starting values of p and q are set to zero, while the order of differencing is set to 2. Note that the value of p and q can be automatically raised to 5 at maximum during computations. The maximum likelihood method is preferred for fitting the models to the time series data.

The result of the model fitting analysis is tabulated below in Table 30. In total seven different ARIMA models are analyzed (the first model is calculated twice). Note that due to having positive log-likelihoods, the analyzed tentative models have negative AICc values (e.g. see APPENDIX B for the summary statistics of the selected model). The best model is selected to be the ARIMA(1,2,1) model; however this is not the adequate model selected to be representing the process generating the considered time series.

Table 30- The output from the auto.arima function for the analyzed tentative models (own calculation & illustration)

Time Series Model	AICc Value
ARIMA(0,2,0)	-175.17
ARIMA(0,2,0)	-175.17
ARIMA(1,2,0)	-175.27
ARIMA(0,2,1)	-179.58
ARIMA(1,2,1)	-180.76
ARIMA(1,2,2)	-179.16
ARIMA(2,2,2)	-176.64
ARIMA(2,2,1)	-179.21
Best model: ARIMA(1,2,1)	

[107] See Subsection 10.2.9.4 on p. 138 for more information.

The best model, which is returned after the computation, indicates the selected tentative model based on the lowest magnitude of AICc criterion among others. The selected tentative model can be an adequate model as a mathematical representation of the linear stochastic process under study, after being validated for its adequacy through running diagnostic tests on its residuals. If the selected tentative model is found to be inadequate, the next model on the lowest rank of AICc criterion is considered for diagnostic checking.

The coefficients of the ARIMA(1,2,1) model and their standard errors are tabulated in Table 31. The error measures of the fitted model are observed to be at an acceptable level; especially the mean absolute percentage error (MAPE) of 2.52% (see APPENDIX B for the detailed summary statistics).

Table 31- The brief summary statistics of the ARIMA(1,2,1) model (own calculation & illustration)

	AR(1)	MA(1)
Coefficients	0.3558	-0.8482
Standard Error	0.1797	0.0969

The ARIMA(1,2,1) model can be expressed in general form as follows:

$$\nabla^2(1-\phi_1 B)\, z_t = (1-\theta_1 B)a_t \tag{11.3.1}$$

$$(1-\phi_1 B - 2B + 2\phi_1 B^2 + B^2 - \phi_1 B^3)\, z_t = (1-\theta_1 B)a_t \tag{11.3.2}$$

$$z_t = (2+\phi_1)z_{t-1} - (1+2\phi_1)z_{t-2} + \phi_1 z_{t-3} + a_t - \theta_1 a_{t-1} \tag{11.3.3}$$

In the general form, the symbol "∇" represents the difference operator and indicates that the series is differenced twice $\nabla^2 = (1-B)^2$. The symbol "B" is the back shift operator. The symbol "z_t" indicates the gross electricity demand at time t. The symbol "ϕ" represents the autoregressive parameter; whereas the symbol "θ" indicates the moving average parameter. The random shock at time t is represented as "a_t" respectively. The model can be expressed in equation form with the computed parameters as shown below:

$$(1-\mathrm{B})^2(1-0.3558B)z_t = (1+0.8482B)a_t \tag{11.3.4}$$

$$z_t = (2+0.3558)z_{t-1} - (1+2\cdot 0.3558)z_{t-2} + 0.3558 z_{t-3} + a_t + 0.8482 a_{t-1} \tag{11.3.5}$$

$$z_t = 2.3558z_{t-1} - 1.7116z_{t-2} + 0.3558z_{t-3} + a_t + 0.8482a_{t-1} \qquad (11.3.6)$$

The goodness of the fitted model ARIMA(1,2,1) can also be visually examined by plotting the predicted values versus the observed values as displayed in Figure 55. The plot indicates a successful fit to the data by substantially overlapping green and red circles representing the observed and the predicted values respectively.

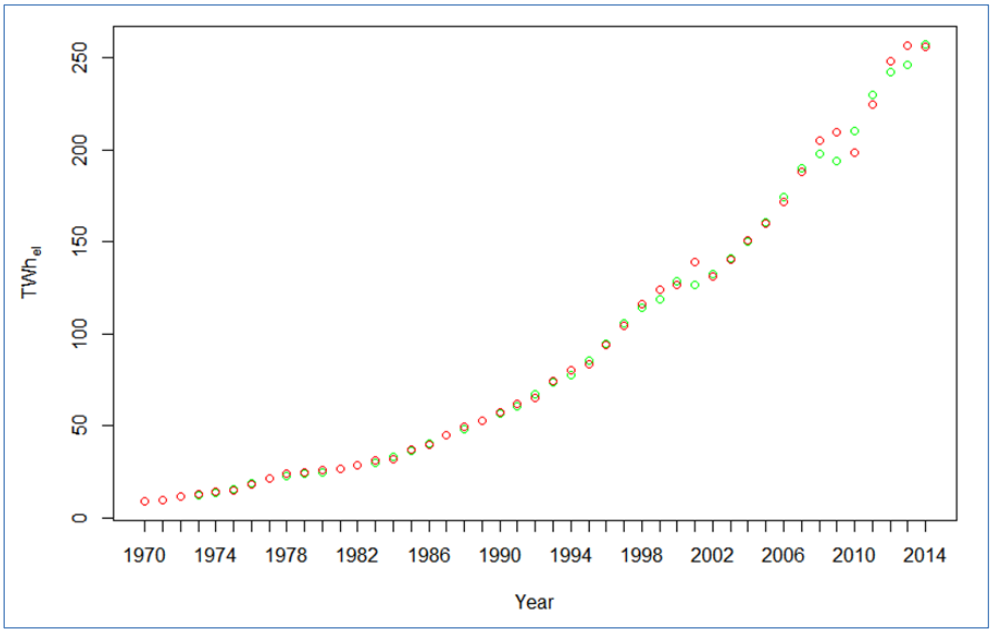

Figure 55- The scatter plot of the observed values (green circles) and the predicted values from ARIMA(1,2,1) model (red circles) (own calculation & illustration)

The 3rd Stage- Diagnostic Checking of Residuals

During the third stage of the time series modelling, the residuals of the ARIMA(1,2,1) model is tested for normality and randomness by both graphical and analytical methods. See Subsection 10.1.1.5.1 on p. 99 for more information about the analysis of residuals.

The Quantile-Quantile (Q-Q) plot of the residuals from the ARIMA (1,2,1) model is represented in Figure 56 to examine whether the residuals are normally distributed. The "qqnorm" function (in package stats version 3.1.2) is used for plotting the residuals. Further, the function "qqline" adds a line (so called Q-Q line) to a normal Q-Q plot which passes through the first and third quartiles. Although there exits deviations at the tails of the Q-Q line; most of the values are close to it. Hence, the residuals are considered to be normally distributed.

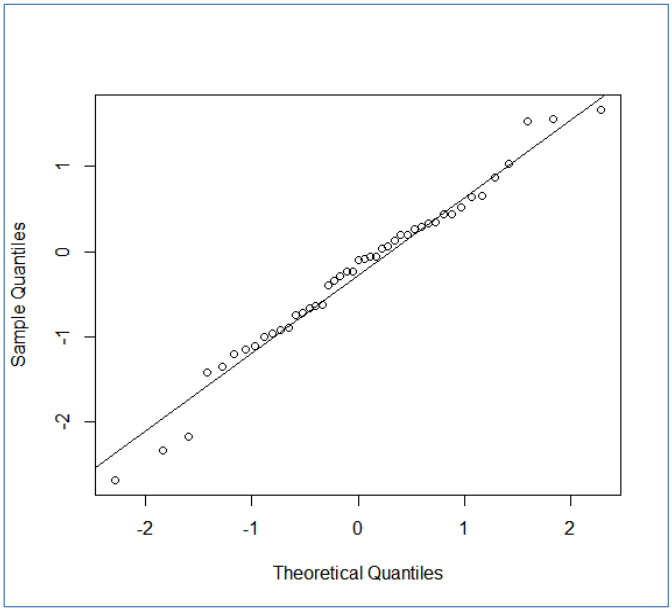

Figure 56- The Q-Q plot of the residuals from ARIMA(1,2,1) model (own calculation & illustration)

In addition to the examination of the Q-Q plot, the function "shapiro.test" (in package stats) is applied on the data to analytically examine the normality according to the shapiro-wilk test of normality. The value of the test statistic W and p-value are computed to be 0.98 and 0.50 respectively. Accordingly, there is not enough evidence to reject the null hypothesis which states that the residuals are from a normally distributed population at an alpha level of 5% (i.e. a p-value higher than 5%).

The standardized residuals of the model, displayed in Figure 57, resemble identically and independently distributed white noise series by varying around the zero horizontal level (i.e. mean of the series). There are three unusual residuals with magnitudes higher than 2; however these residuals are caused by the abrupt change in the demand growth rate originating from the financial crisis of 1978 and 2001 in Turkey and the global financial crisis of 2009 respectively.

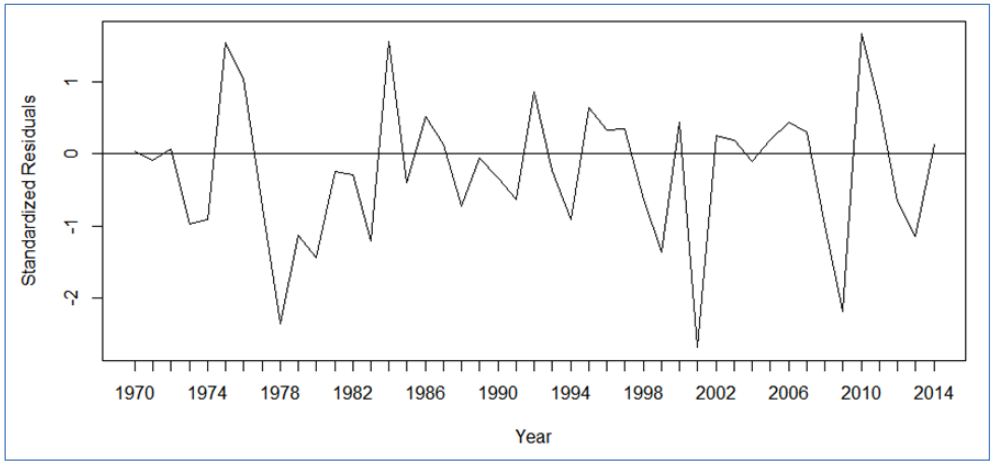

Figure 57- The standardized residuals from ARIMA(1,2,1) model (own calculation & illustration)

The sample ACF and the sample PACF of the residuals from ARIMA(1,2,1) model can be examined for correlation at each individual lag as displayed in Figure 58. In both of the plots, there is not any statistically significant spike indicating correlation.

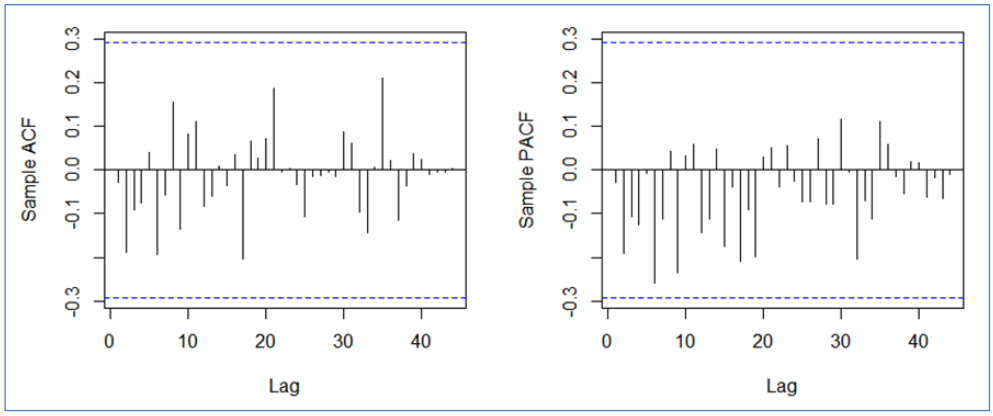

Figure 58- The sample ACF and the PACF plot of the residuals from ARIMA(1,2,1) model (own calculation & illustration)

In addition to examining residual correlations at individual lags, it is also useful to carry out Ljung-Box test that takes into account the magnitudes of autocorrelations as a group. Note that the number of lags to be tested is required to be given by the practitioner. According to the analysis conducted by Hyndman and Athanasopoulos (2014, p. 56), the number of lags to be jointly tested can be practically considered as the result of the function "f" for a given sample size "n".

$$f(n) = \min(10, n/5) \tag{11.3.7}$$

Thus, the number of lags for analysis is set to 9; since $n = 45$. By applying Ljung-Box test function (in package "stats" version 3.1.2), the value of the test statistic Q and p-value are

computed to be 7.3 and 0.4 respectively (for 7 degrees of freedom). The examination of the residuals indicates that there is not enough evidence to reject the null hypothesis of independently distributed series at an alpha level of 5% (i.e. considering a p-value higher than 5%).

To sum up, The ARIMA (1,2,1) is validated through all diagnostic tests and is determined to be an adequate model representing the stochastic process generating the time series data. Hence, the model can be utilized for forecasting the annual gross electricity demand of Turkey.

The 4th Stage- Forecasting Annual Gross Electricity Demand of Turkey

After validating the adequacy of the ARIMA(1,2,1) model, the annual gross electricity demand of Turkey is forecasted for the period 2015-2025 by utilizing the function "forecast" (in package "forecast"). The confidence level for forecast intervals is set to 95%. The computed forecasts and their corresponding forecast intervals are displayed in Figure 59. According to the results of forecasting, the annual gross electricity demand increases from 270 TWh_{el} to 456 TWh_{el} in the mentioned period. The corresponding annual mean growth rate is determined to be 5.3% per annum (see Table 32). Note that forecasting is recursively carried out by utilizing time series models. Accordingly, the uncertainty in forecasts rises as the forecast horizon rises; as it can be deduced from the displayed forecast intervals.

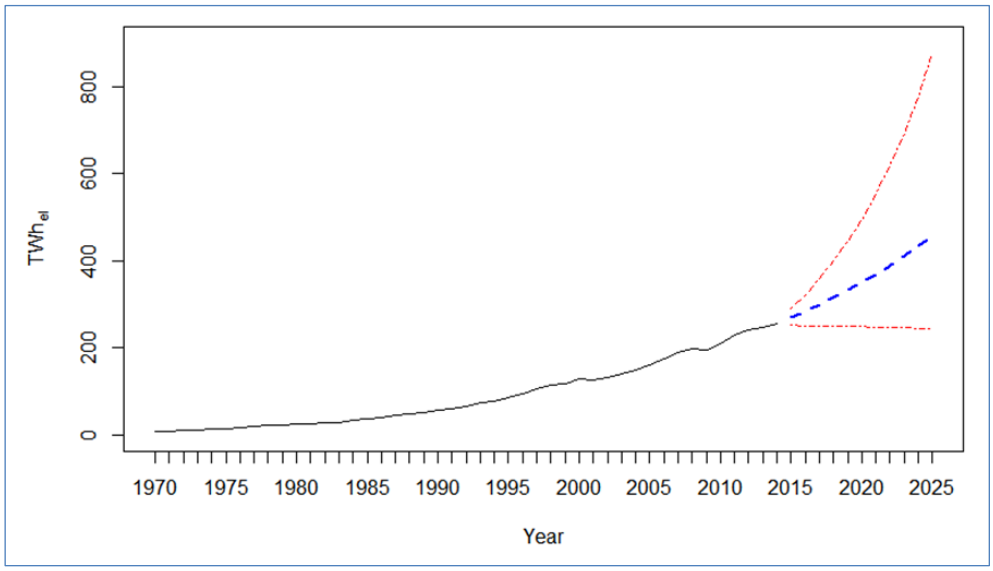

Figure 59- The historical gross electricity demand (solid black line), corresponding forecasts (dashed blue line) and forecast limits (dotted dashed red lines) (own calculation & illustration)

In Table 32, the results of forecasting including the change in annual gross electricity demand w.r.t. the previous years are tabulated.

Table 32- The forecasted annual gross electricity demand by using ARIMA(1,2,1) model (own calculation & illustration)

Year	Forecasted Gross Electricity Demand (TWh_{el})	Lower Limit of Forecast Interval (TWh_{el})	Upper Limit of Forecast Interval (TWh_{el})	Change w.r.t. Previous Year (per annum)
2015	270	252	290	5.0%
2016	284	250	323	5.2%
2017	299	250	359	5.3%
2018	315	249	399	5.4%
2019	332	249	444	5.4%
2020	350	249	495	5.4%
2021	369	249	552	5.4%
2022	389	248	617	5.4%
2023	410	247	691	5.4%
2024	433	245	776	5.5%
2025	456	244	872	5.5%
			Annual Mean Growth Rate	5.3%

In order to retrospectively check the feasibility of forecasting, the forecasted period is compared to the historical development in the period 2000-2014 as displayed in Figure 60. In the figure, the historical data are represented as solid lines; whereas the forecasts are represented as dashed lines. The forecasted annual gross electricity demand exhibits an increasing trend roughly similar to the one in the period 2000-2014, if the sudden falls in demand are ignored. In particular, the annual mean growth rate for the forecasted period is about the same as the corresponding growth rate in the period 2000-2014 (i.e. 5.2%/a).

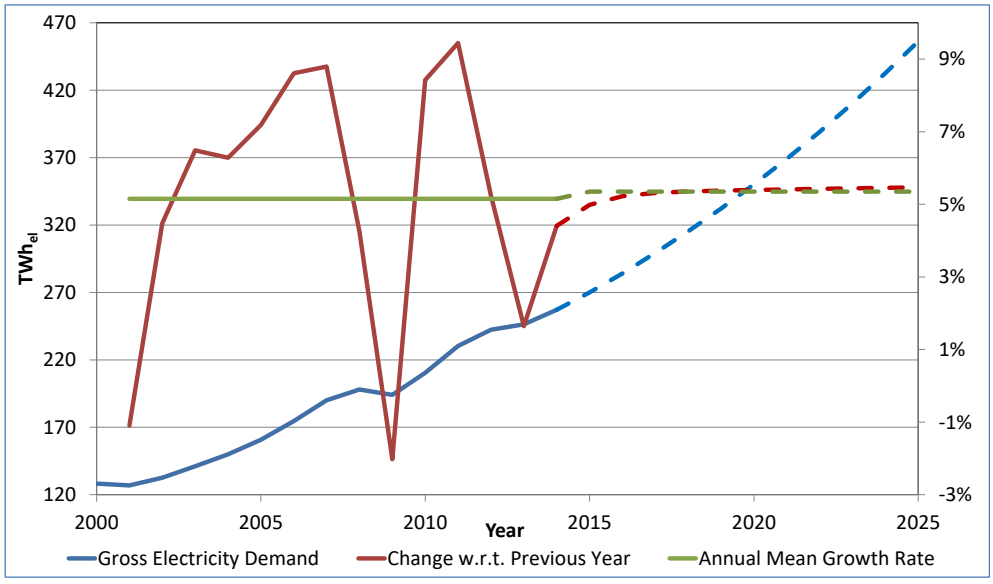

Figure 60- The development of the annual gross electricity demand in the period 2000-2014 and in the forecasted period 2015-2025 (own calculation & illustration)

In Table 33, the forecasts made in the previous studies are represented and compared with the forecasts of this study. Note that the forecasts indicate the latest forecasted year in the corresponding studies. See Subsection 11.3.1 for more information about the previous studies.

Table 33- The comparison of the forecasts from the previous studies and this study (own illustration)

Author(s)	Method	Method/Scenario	Latest Year Forecasted	Forecast of the Latest Year (TWh_{el})	Forecast of This Study (TWh_{el})
TEIAS (2014)	Econometric Analysis	Low Case	2023	381	410
		Reference Case		416	
		High Case		463	
Özturk & Ceylan (2005)	GAM	Low Case	2020	462	350
		High Case		500	
Akay & Atak (2007)	GPRM	-	2015	266	270
Kücükdeniz (2010)	ANN	-	2025	294	456
	SVM			321	
Dilaver & Hunt (2011)	STSA	Low Case	2020	259	350
		Reference Case		310	
		High Case		368	
Polater (2013)	ANN	-	2023	454	410
	TSA			440	
Yavuzdemir & Gökgöz (2015)	Regression	-	2018	356	315
	FLM			352	
	TSA			309	

The results of forecasting in this study are observed to be different from the presented results in previous studies. Namely, the forecasted year 2023 of this study is observed to be between the low case and reference case scenarios of TEIAS. Further, the forecasted year 2020 is seen to be well below the low case scenario of the study by Özturk and Ceylan. Furthermore, the forecasted year 2025 is seen to be well above the both forecasts using ANN and SVM by Kücükdeniz. Moreover, the forecasted year 2020 is observed to be between the reference case and the high case scenarios of the study by Dilaver and Hunt.

Nevertheless, the forecasts of this study are observed to be close to the two previous studies by Akay and Atak and by Yavuzdemir and Gökgöz (i.e. true only for forecasting by using TSA). Note that Yavuzdemir and Gökgöz did not provide any information about their model adequacy rather indicated a MAPE of 2.75% (i.e. 2.52% for this study). Although Polater also used TSA, his forecast for the year 2023 is higher than the forecast in this study. However the ARIMA(2,2,0) model utilized by Polater cannot be an adequate model for forecasting the annual gross electricity demand (see p. 156).

In conclusion, the statistical evidences and historical data examination revealed that the forecasted time series using ARIMA(1,2,1) model adequately reflects the development of the annual gross electricity demand of Turkey for the period 2015-2025. In addition, the conducted analysis is statistically more reliable than the mentioned previous studies utilizing TSA for forecasting.

11.3.3 Forecasting Peak Load Demand of Turkey in the Period 2015-2025

In this section, an adequate ARIMA model of order p, d and q is determined for the time series which consists of the annual peak load demand of Turkey in the period 1970-2014. The relation of the ARIMA model with the corresponding time series is achieved by a three-stage iterative procedure based on identification, estimation, and diagnostic checking (i.e. the Box-Jenkins model building process mentioned in Subsection 10.2.8). In the 4th fourth stage, the annual peak load demand of Turkey in the period 2015-2025 is forecasted by utilizing the determined adequate model.

The analysis is carried out by using the license free statistical software R (version 3.1.2) and also by using the RStudio IDE (Integrated Development Environment, Version 0.98.1102) which is a license free user interface for R.

1st Stage- Model Identification

During this stage, subclasses of parsimonious models are specified according to how the considered data were generated. In particular, the objective is to obtain some tentative values of p, d and q orders needed in the general linear ARIMA model building process.

First of all, the annual peak load demand of Turkey in the period 1970-2014 (i.e. a sample size of 45 observations) is plotted against time and visually examined for non-stationarity. It can be inferred from Figure 61 that the non-linear upward trend is evident for the presence of non-stationarity in the time series. In this respect, the development of the annual peak load demand is similar to the development of the annual gross electricity demand.

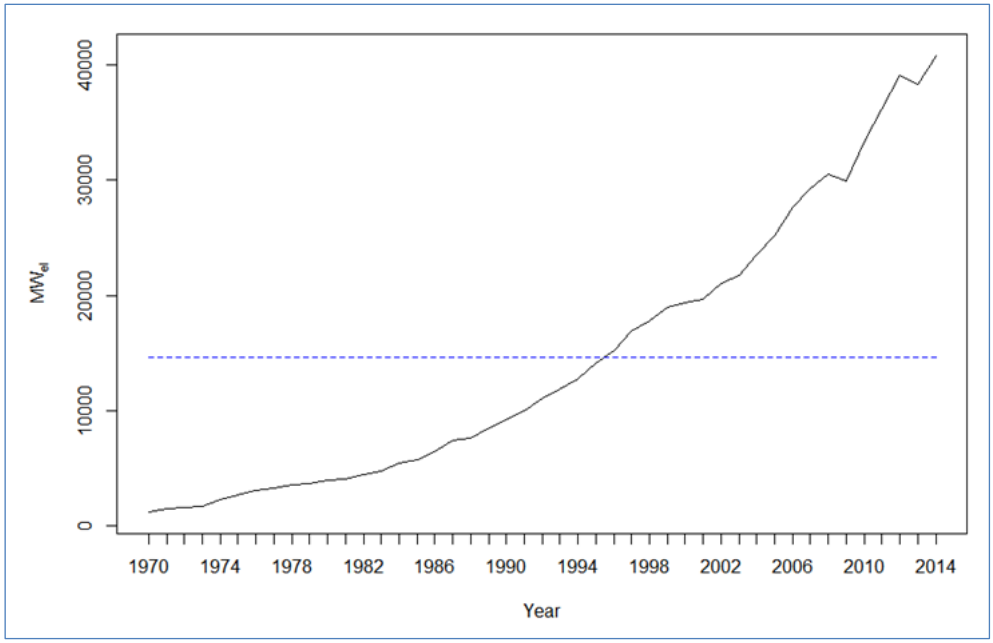

Figure 61-The annual peak load demand in the period 1980-2014 (continuous line) and its mean (dashed line) (own illustration according to TEIAS (2015)

The sample ACF of the time series also indicates non-stationarity by showing large autocorrelations that diminish slowly at large lags as represented in Figure 62. Therefore, it is necessary to transform the data into a stationary series by differencing.

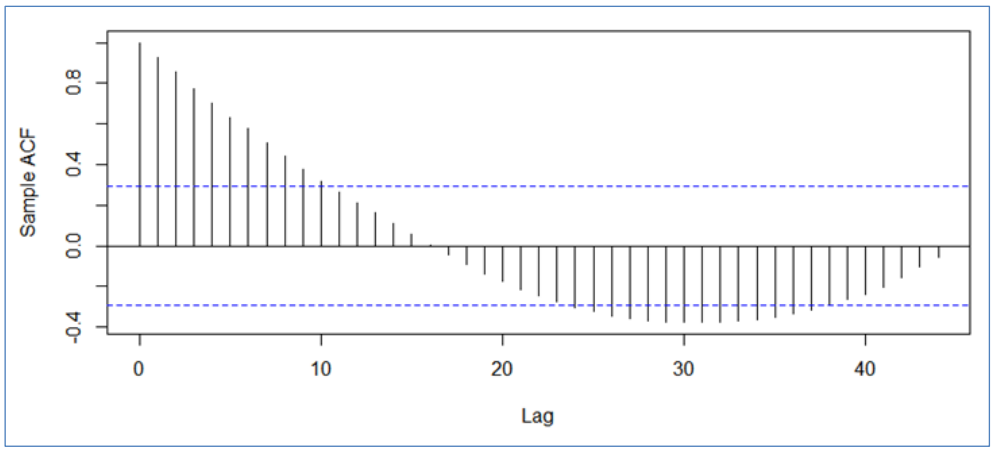

Figure 62- The sample ACF and the sample PACF of the annual peak load demand series (own calculation & illustration)

In Figure 63, the first order difference of the time series is displayed. The general upward trend is alleviated and it is also realized that as the lags increase, the dispersion in the time series increases. In the figure, the cone-shaped pattern (i.e. depicted as dotted green dashed lines) indicates heteroscedasticity. The variance of the data should also be homoscedastic; in order to validate the stationarity condition. Consequently, the second order difference should be taken; in order to make the observations vary around their mean.

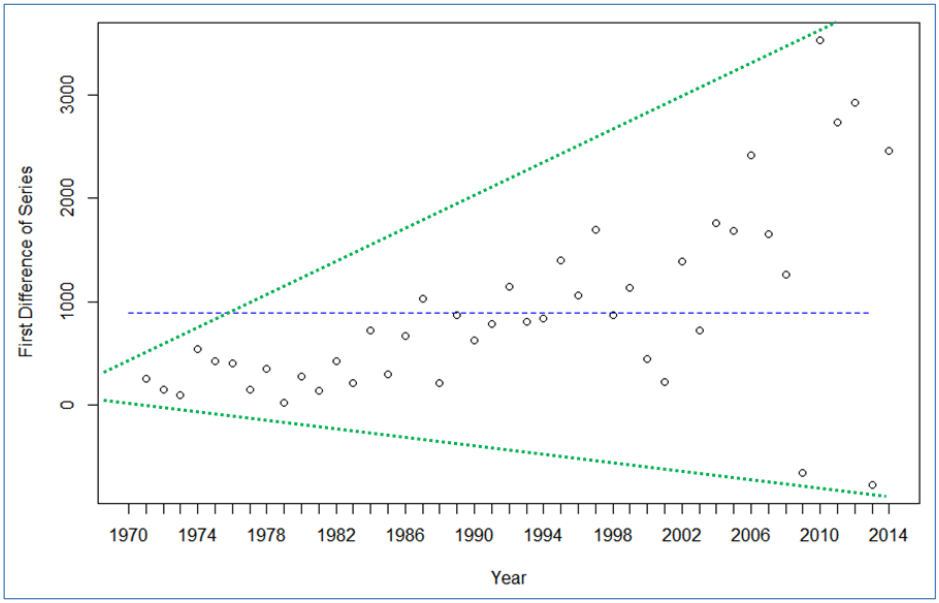

Figure 63- The scatter plot of the first order difference of annual peak electricity demand series (circle) and its mean (dashed line) (own calculation & illustration)

In Figure 64, the sample ACF of the once differenced series also suggests that twice differencing is required due to the presence of a recurrent pattern which decays slowly.

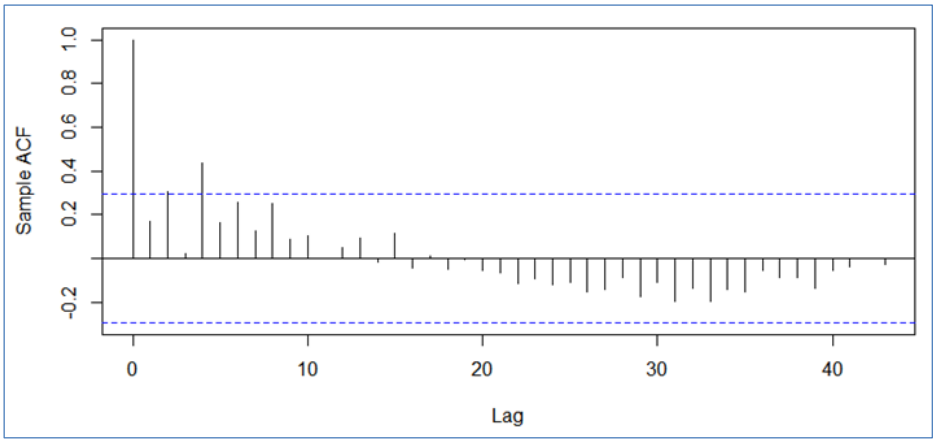

Figure 64- The sample ACF of first order difference of the annual peak electricity demand series (own calculation & illustration)

In Figure 65, the second order difference of the time series is displayed. It can be inferred that the general upward trend has disappeared and the observations vary around their mean; however the heteroscedasticity still recurs (i.e. depicted as dotted green dashed lines). Subsequently, the series should be transformed according to the Box-Cox power transformation technique before fitting any tentative models (see Subsection 10.2.7.1 for information).

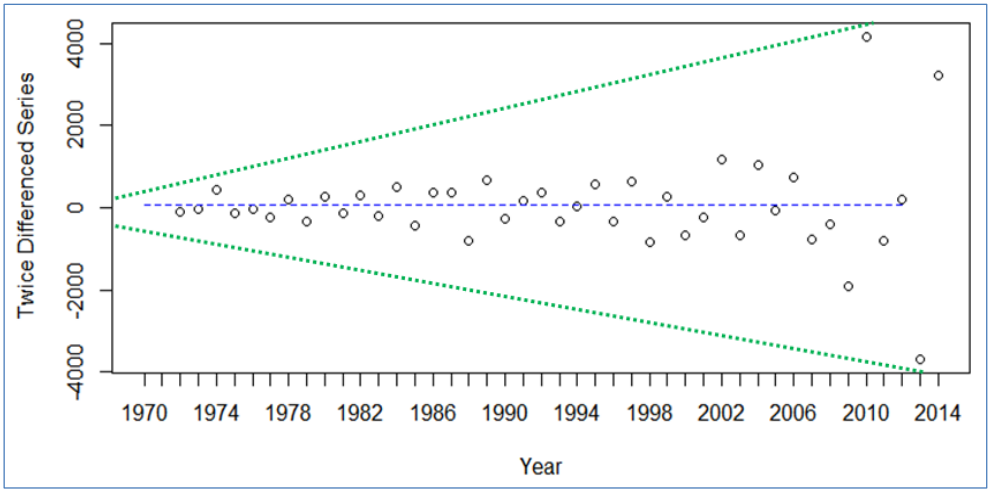

Figure 65- The scatter plot of twice difference of the annual peak load demand series (circle) and its mean (dashed line) (own calculation & illustration)

The "BoxCox" function (in package "FitAR version" 1.94) is applied on the considered twice difference series and the transformation parameter λ is estimated by maximizing the relative likelihood $R(\lambda)$ of the series. The estimated transformation parameter $\hat{\lambda}$ is computed to be 0.203 (see Figure 66). Subsequently, the original series is transformed by using the computed $\hat{\lambda}$ and then twice differenced. The sample ACF and the sample PACF of the resulting series are displayed in Figure 67.

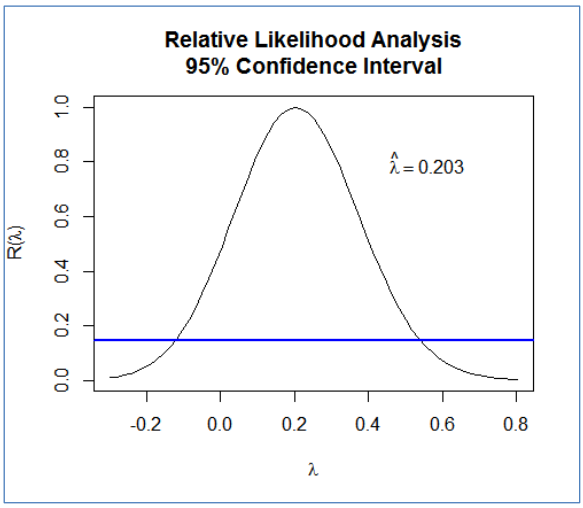

Figure 66- The plot of Box-Cox transformation analysis of the considered data (own calculation & illustration)

In Figure 67, the sample ACF of the transformed and the twice differenced series indicates that the stationarity is achieved with the Box-Cox transformation of the series. Accordingly, the sample ACF and the sample PACF indicate highly significant spikes at 1st lag. In addition, the sample ACF displays a significant spike at lag 14; whereas the sample PACF indicates a significant spike at lag 3. The pattern in the sample ACF suggests a moving average model of

order q equals to 1; while the spikes in the sample PACF indicates an autoregressive model of order p equals to 1 or 2 or 3 at maximum. Another possible model is an ARIMA(1,2,1) model. Note that the number of times the data have been differenced to become stationary equals to two (i.e. $d = 2$). During the next stage, the parameter estimation process is carried out according to the possible tentative models.

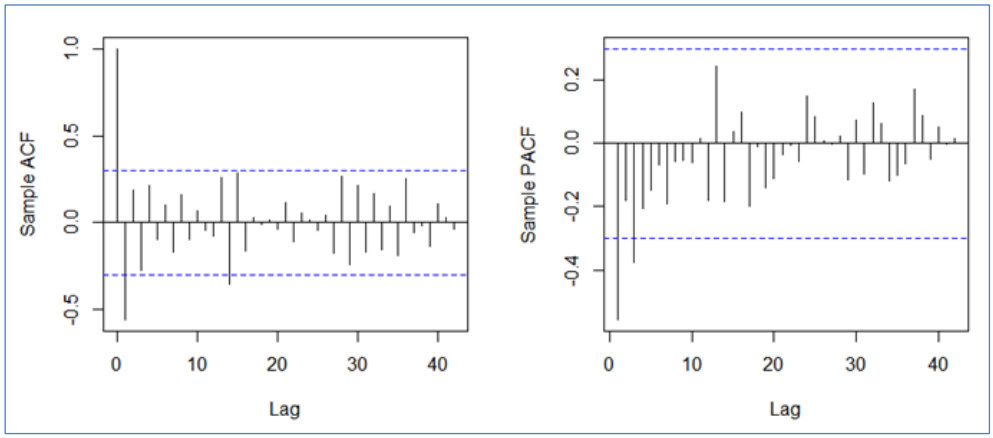

Figure 67- The sample ACF and the sample PACF of the twice differenced annual peak electricity demand series (own calculation & illustration)

The 2nd Stage- Parameter Estimation

During the second stage of the time series modelling, the parameters of the possible tentative models are estimated and the corresponding models are compared based on their AICc.

The computations are carried out by utilizing the auto.arima function in R. The maximum likelihood method is preferred for fitting the models to the series. The result of the model fitting analysis is tabulated in Table 34. In total eight different ARIMA models are analyzed (the first model is calculated twice) and the model with the lowest AICc value is determined to be the ARIMA(1,2,1) model.

Table 34- The output from the auto.arima function for the analyzed tentative models (own calculation & illustration)

Time Series Model	AICc Value
ARIMA(0,2,0)	49.26
ARIMA(0,2,0)	49.26
ARIMA(1,2,0)	34.08
ARIMA(0,2,1)	Inf
ARIMA(2,2,0)	34.99
ARIMA(1,2,1)	24.71
ARIMA(2,2,2)	Inf *
ARIMA(2,2,1)	Inf
ARIMA(1,2,2)	26.00
Best model: ARIMA(1,2,1)	

Note that the output "Inf" is returned when the likelihood of the model turns out to be infinity or when the lowest root in the characteristic polynomial of the model is lower than 1.001 (i.e. if non-stationarity emerges due to the magnitude parameters). Also, "Inf*" is reported when the ARIMA model couldn't be fitted and an error is returned.

The coefficients of the ARIMA(1,2,1) model and their standard errors are tabulated in Table 35. The error measures of the fitted model are observed to be at an acceptable level; especially the MAPE of 3.4% (see APPENDIX B for the detailed summary statistics).

Table 35- The brief summary statistics of the ARIMA(1,2,1) model (own calculation & illustration)

	AR(1)	MA(1)
Coefficients	-0.0654	-0.9854
Standard Error	0.1591	0.2245

The ARIMA(1,2,1) model can be expressed in general form as follows:

$$s_t = (2 + \phi_1)s_{t-1} - (1 + 2\phi_1)s_{t-2} + \phi_1 s_{t-3} + a_t - \theta_1 a_{t-1} \tag{11.3.8}$$

The above represented general form is derived similar to the Eq. (11.3.3) on p. 164. Here, the symbol "s_t" indicates the annual peak load demand at time t. The symbol "ϕ" represents the autoregressive parameter; whereas the symbol "θ" indicates the moving average parameter. The random shock at time t is represented as "a_t" respectively. The model can be expressed in equation form with the computed parameters as shown below:

$$(1 - \mathrm{B})^2(1 + 0.0654B)s_t = (1 + 0.9854B)a_t \tag{11.3.9}$$

$$s_t = 1.9346s_{t-1} - 0.8692s_{t-2} - 0.0654s_{t-3} + a_t + 0.9854a_{t-1} \tag{11.3.10}$$

Note that in Eq. (11.3.9) the symbol "*B*" represents the back shift operator.

The goodness of the fitted model ARIMA(1,2,1) can also be visually examined by plotting the predicted values versus the observed values as depicted in Figure 68. The plot indicates a successful fit to the data by generally overlapping green and red circles representing the observed and fitted values respectively.

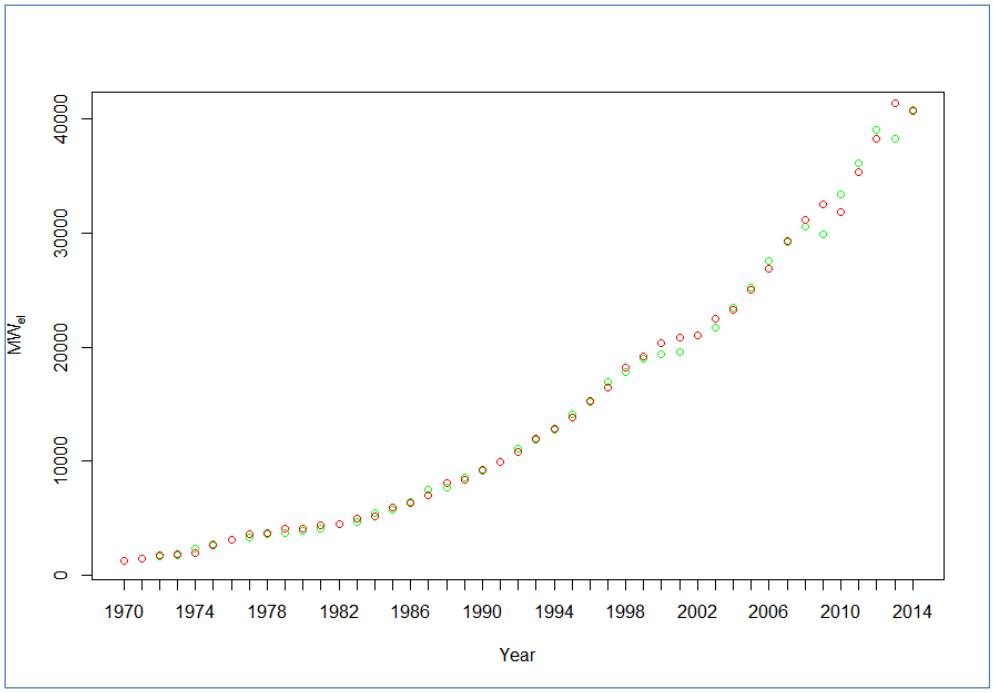

Figure 68- The scatter plot of the observed values (green circles) and the predicted values from ARIMA(1,2,1) model (red circles) (own calculation & illustration)

The 3rd Stage-Diagnostic Checking

During the third stage of the time series modelling, the residuals of the ARIMA(1,2,1) model is tested for normality and randomness by both graphical and analytical methods. See Subsection 10.1.1.5.1 on p. 99 for more information about residual analysis.

The Q-Q plot of the residuals from the ARIMA model is represented in Figure 69 to examine whether the residuals are normally distributed. Although there exits deviations at the tails of the Q-Q line; most of the values are close to the Q-Q line. Hence, the residuals are considered to be normally distributed.

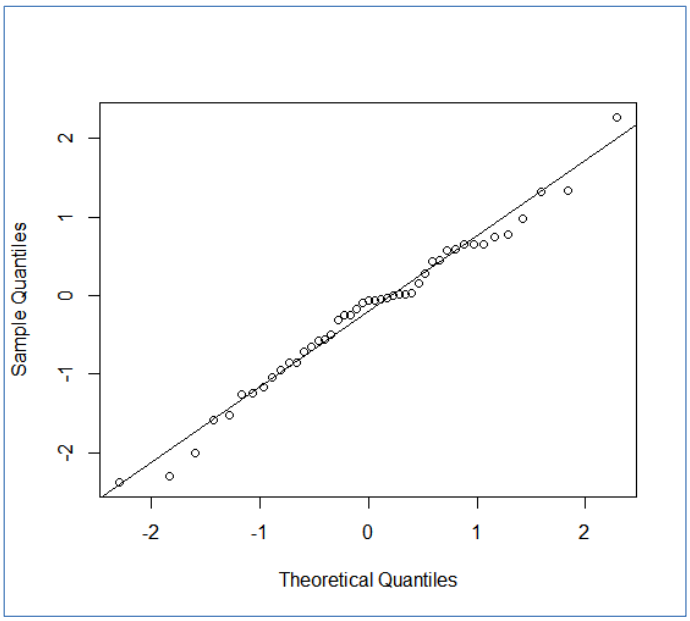

Figure 69- The Q-Q plot of the residuals from ARIMA(1,2,1) model (own calculation & illustration)

In addition to the examination of Q-Q plot, the shapiro-wilk test of normality is carried out by using the function shapiro.test. The value of the test statistic W and p-value are computed to be 0.98 and 0.8 respectively. The examination of residuals indicates that there is not enough evidence to reject the null hypothesis which states that the residuals are from a normally distributed population at an alpha level of 5% (i.e. a p-value higher than 5%).

The standardized residuals of the model, which are displayed in Figure 70, resemble independent and identically distributed white noise series by varying around the zero horizontal level (i.e. mean of the series). There are two unusual residuals with magnitudes higher than 2; however these residuals are caused by the abrupt change in the demand growth rate originating from the financial crisis of 2001 in Turkey and the global financial crisis of 2009 respectively.

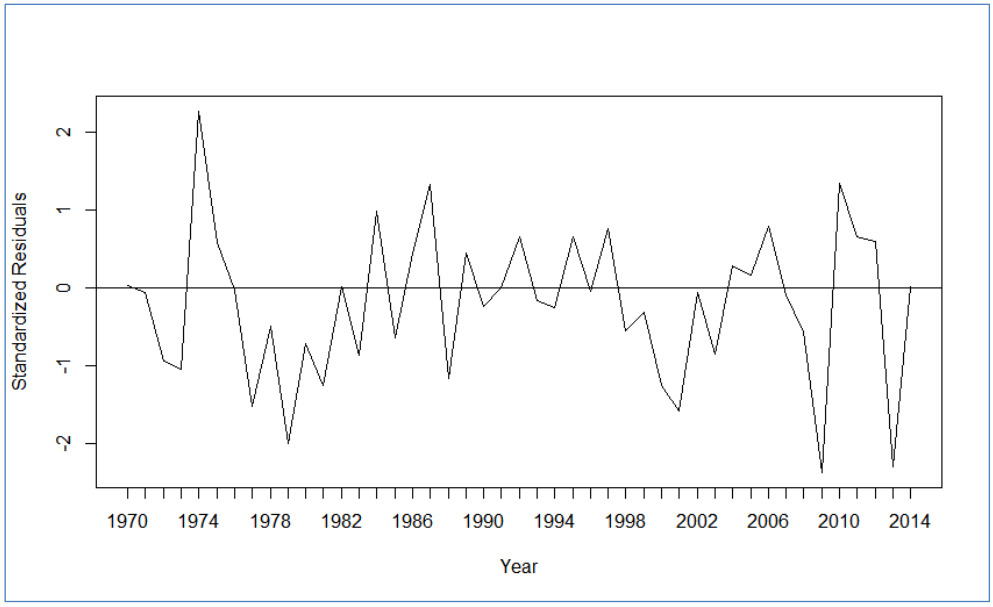

Figure 70- The standardized residuals from ARIMA(1,2,1) model (own calculation & illustration)

The sample ACF and the sample PACF of the residuals from ARIMA(1,2,1) model can be examined for correlation at each individual lag as displayed in Figure 71. There is not any significant spike in the sample ACF; whereas there is a significant at lag 14 in the sample PACF. The spike at lag 14 is considered to be ignorable; since it emerges in the sample PACF and also at a high lag (i.e. its inconvenient effect is negligible).

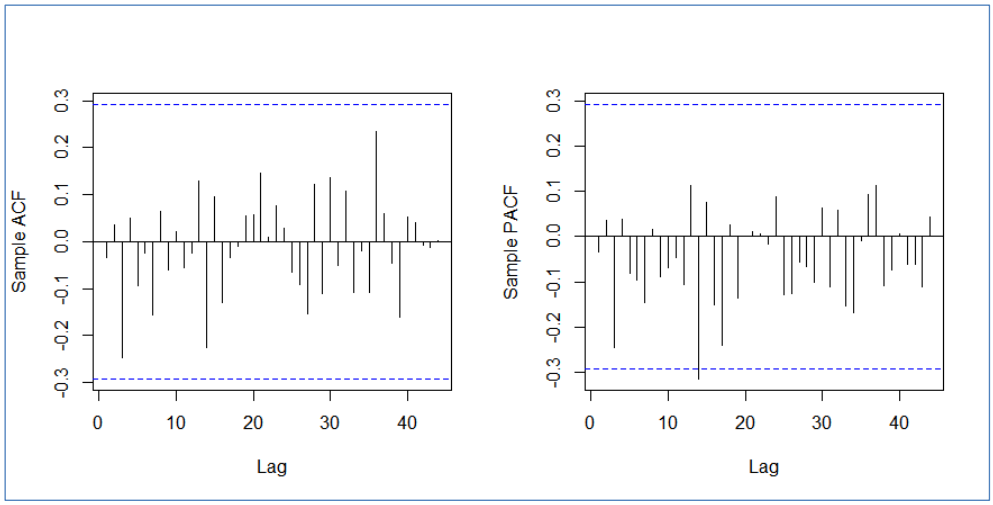

Figure 71- The sample ACF and the sample PACF plot of the residuals from ARIMA(1,2,1) model (own calculation & illustration)

In addition to examining residual correlations at individual lags, it is also useful to carry out Ljung-Box test that takes into account the magnitudes of autocorrelations as a group. The number of lags for analysis is set to 9; since n=45 (see p. 167 for information on selecting of number of lags). By applying Ljung-Box test function, the value of the test statistic Q and p-

value are computed to be 5.6 and 0.6 respectively (for 7 degrees of freedom). The examination of the residuals indicates that there is not enough evidence to reject the null hypothesis of independently distributed series at an alpha level of 5% (i.e. considering a p-value higher than 5%).

To sum up, The ARIMA (1,2,1) is validated through all diagnostic tests and is determined to be an adequate model representing the stochastic process generating the time series. Therefore, the model can be utilized for forecasting the annual peak load demand of Turkey.

The 4th Stage- Forecasting Annual Peak Demand of Turkey

After validating the adequacy of the ARIMA(1,2,1) model, the annual peak load demand of Turkey is forecasted for the period 2015-2025 by utilizing the function "forecast" in R. The confidence level for forecast intervals is set to 95%. The computed forecasts and their corresponding forecast intervals are displayed in Figure 72. According to the results of forecasting, the annual peak load demand increases from 43069 MW_{el} to 73059 MW_{el} in the mentioned period. The annual mean growth rate is determined to be 5.5%/a. In addition, the uncertainty in forecasts rises as the forecast horizon rises; as it can be deduced from the displayed forecast intervals.

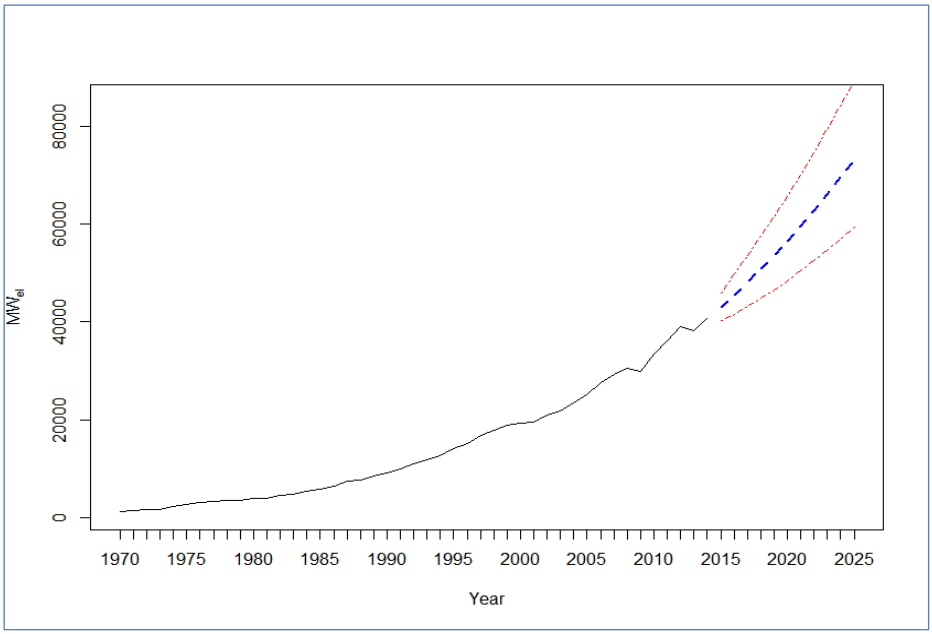

Figure 72- The past annual peak load demand (solid black line), corresponding forecasts (dashed blue line) and forecast limits (dotted dashed red line) (own calculation & illustration)

The results of forecasting and the change in annual peak electricity demand w.r.t. previous year are tabulated in Table 36.

Table 36- The forecasted annual peak load demand by using ARIMA(1,2,1) model (own calculation & illustration)

Year	Forecasted Annual Peak Demand (MW_{el})	Lower Limit of Forecast Interval (MW_{el})	Upper Limit of Forecast Interval (MW_{el})	Change w.r.t. Previous Year (per annum)
2015	43069	40346	45937	5.7%
2016	45527	41620	49721	5.7%
2017	48094	43120	53514	5.6%
2018	50775	44775	57398	5.6%
2019	53573	46551	61415	5.5%
2020	56494	48434	65588	5.5%
2021	59540	50415	69935	5.4%
2022	62715	52490	74468	5.3%
2023	66024	54657	79200	5.3%
2024	69470	56915	84140	5.2%
2025	73059	59264	89300	5.2%
			Annual Mean Growth Rate	5.5%

In order to check the accuracy of forecasting; the forecasted period is compared to the past development in the period 2000-2014 as displayed in Figure 73. In the figure, the historical data are represented as solid lines; whereas the forecasts are represented as dashed lines. The forecasted annual peak load demand exhibits an increasing trend roughly similar to the one in the period 2000-2014, if the sudden falls in demand are ignored. In particular, the annual mean growth rate for the forecasted period is same as the corresponding annual mean growth rate in the period 2000-2014.

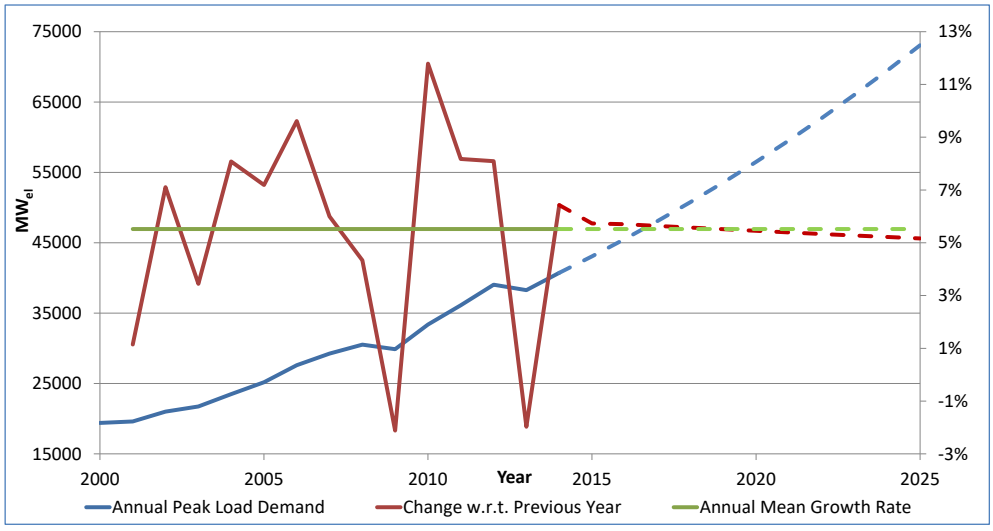

Figure 73- The development of the annual peak load demand in the period 2000-2014 and in the forecasted period 2015-2025 (own calculation & illustration)

In Table 37, the forecasts made in the previous studies are represented and compared with the forecasts of this study. Note that the forecasts indicate the latest forecasted year in the corresponding studies. See Subsection 11.3.1 for more information about the previous studies.

Table 37- The comparison of the forecasts from the previous studies and this study (own illustration)

Author(s)	Method	Method/Scenario	Latest Year Forecasted	Forecast of the Latest Year (MW_{el})	Forecast of This Study (MW_{el})
TEIAS (2014)	Econometric Analysis	Low Case	2023	58630	66024
		Reference Case		64040	
		High Case		71300	
Polater (2013)	ANN	-	2023	74138	
	TSA			74803	

The results of forecasting in this study are observed to be different from the results in previous studies. Namely, the forecasted year 2023 of this study is observed to be between the reference case and high case scenarios of TEIAS. Further, the forecasted year 2023 is seen to be well below the both forecasts using ANN and TSA by Polater. Although Polater also used TSA, his forecast for the year 2023 is higher than the forecast in this study. As in the case of forecasting annual gross electricity demand with an inadequate model, the ARIMA(1,2,0) model utilized by Polater cannot be an adequate model for forecasting the annual peak load demand (see p. 156).

In conclusion, the statistical evidences and historical data examination revealed that the forecasted time series using ARIMA(1,2,1) model adequately reflects the development of the annual peak load demand of Turkey for the period 2015-2025. In addition, the conducted analysis is statistically more reliable than the mentioned previous work utilizing TSA for forecasting.

12 DETERMINATION OF ADEQUATE APPROXIMATIONS TO PAST LOAD DURATION CURVES (2nd STAGE)

In this chapter, comprehensive information is provided on the determination of the adequate functional approximations to LDCs of Turkey in the period 2000-2014 (i.e. the 2nd stage of the introduced concept). In Section 12.1, detailed information about the methods on functional approximations to LDCs is provided, such as ad hoc and optimal discrete approximations and smooth functional approximations to LDCs. At the end of the section, a summary on the corresponding methods is given and a discussion is carried out for selecting the convenient method for approximating the LDCs of Turkey. In the final Section 12.2, information is given about determining the adequate functional approximation to past LDCs of Turkey among the smooth functional approximations (i.e. polynomial and non-linear functions).

12.1 The Functional Methods for Approximating Load Duration Curves

The second step in forecasting annual LDCs requires an approximation to it. Annual LDCs can be approximated by utilizing either discrete functional or smooth functional approximation approaches. The discrete functional approximations are carried out by using stepwise linear functions[108] which have all slopes equal to 0; whereas the smooth functional approximations are carried out using continuous functions[109] which are differentiable up to a desired order. LDCs can be approximated by using discrete stepwise functions according to ad hoc or optimal segmentation of their abscissa (see Subsection 12.1.1 and 12.1.2 respectively). The smooth approximations to LDCs can be carried out by using polynomial and non-linear functions (see Subsection 12.1.3).

In all mentioned methods of approximations to LDCs, the approximation processes are initiated after the normalization of the areas under the LDCs to unity. The normalization is carried out by dividing the hourly loads "Z_t" at time "t" (i.e. on the ordinate of LDCs) by the

[108] A step function has its domain and range comprised of discrete set of values.
[109] A continuous function has its domain and range comprised of continuous set of values in an interval in $\mathbb{R}$.

corresponding year's annual gross electricity demand yielding normalized values of hourly loads "Z_t^*" at time t (Uri & Maybee, 1978; Maybee & Uri, 1978; Maybee & Uri, 1979).

The normalization allows for checking the accuracy in approximation of the areas under the LDCs by examining whether any significant deviations from unity occur. It should be note that all mentioned methods of approximations assume that the actual LDCs "$F(t)$" are continuous functions of time"t" and are not known in advance; however some values in its range corresponding to the values in its domain are known (i.e. measured level of demand at hourly intervals and their durations are known).

In the next subsections, the corresponding approximation methods are explained based on the mentioned assumptions.

12.1.1 Ad Hoc Discrete Functional Approximations to Load Duration Curves

Uri and Maybee (1978), Maybee and Uri (1978) and (1979)[110] introduced stepwise linear functions to approximate annual LDCs. This type of discrete function approximation is based upon empirically chosen steps on abscissa[111] of LDCs to significantly represent the load shares for all types of generation (e.g. peak, intermediate, and base loads). The most often used number of steps to approximate a LDC is by partitioning the abscissa in six steps, i.e. in hourly intervals coinciding with 200, 800, 2000, 4000, 6000, and 8760 hours (see Figure 74). The chosen steps are then used for estimating the corresponding heights of the steps (also called the lengths of the vertical line segments of the steps) to approximate LDCs.

[110] Maybee and Uri published in 1979 their article "Time Series Forecasting of Utility Load Duration Curves" which is same as the previous study in 1978 "Forecasting the Load Duration Curve Using Box-Jenkins Time Series Analysis" by Uri and Maybee in a different journal with a different title.

[111] The intervals for twenty segments are 100, 200, 400,600, 800, 1100, 1400, 1700, 2000, 2500, 3000, 3500, 4000, 4500, 5000, 5500, 6000, 7000, 8000, and 8760. The intervals for fifty segments are 25, 50, 75, 100, 125, 150, 175, 200, 250, 300, 350, 400, 450, 500, 550, 600, 650, 700, 750, 800, 900, 1000, 1100, 1200, 1300, 1400, 1500, 1600, 1700, 1800, 1900, 2000, 2250, 2500, 2750, 3000, 3250, 3500, 3750, 4000, 4250, 4500, 4750, 5000, 5250, 5500, 6000, 7000, 8000, 8760.

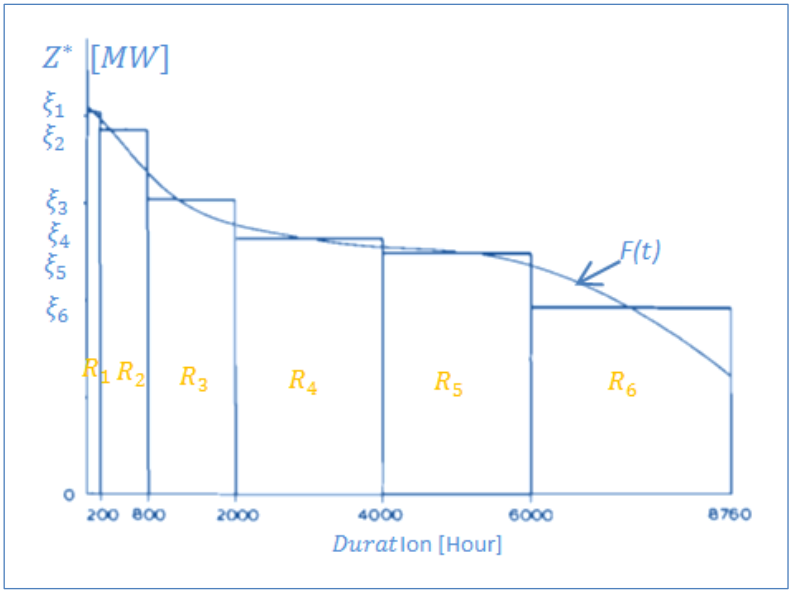

Figure 74- A representative LDC with six-step approximations adapted from Uri & Maybee (1978, p. 194)

Uri and Maybee (1978), Maybee and Uri (1979), Elrazaz, Al-Mohawes, and Mazi (1988) investigated discrete approximations to LDCs by segmenting their abscissas into six, twenty, or fifty steps to determine the adequate number of steps for feasible long-term forecasting. It was concluded that while a larger number of approximations performed marginally better, there is nothing to mitigate using only a six-step approximations. The authors also recommend the use of a finite number of average hourly load demands to approximate LDCs (e.g. 876 average loads by averaging every 10th load measurement from 8760 hours of measurement); since it is found out that 8760 hours of load measurement involve more detail than is needed for long run forecasting.

The objective of the discrete approximations to LDCs requires the height of the k^{th} step (ξ_k) in each interval be chosen in such a way that the area of the resulting rectangle "R_k" is equal to the area under the curve in the corresponding interval (see Figure 74). These rectangular areas are denoted as $R_1, R_2, \dots, R_6$ and are computed using the trapezoidal rule for numerical quadrature[112]. Then the height ξ_k can be calculated as indicated below:

$$\xi_k = R_k/(\tau_k - \tau_{k-1}) \qquad (12.1.1)$$

[112] The trapezoidal rule for numerical quadrature is used for approximation of the definite integral of the LDC function $F(t)$ in the interval $[\tau_{k-1}, \tau_k]$, then $R_k = (\tau_k - \tau_{k-1})\frac{|F(\tau_k-1)+F(\tau_k)|}{2}$.

The symbols "τ_k" and "τ_{k-1}" are the right-hand and the left-hand side break points (i.e. end points of the considered time intervals) of the considered k^{th} step respectively. Thus, the first height is $R_1/200$, the second $R_2/600$, etc.

The represented results of performed six-step approximations by Maybee and Uri[113] (1978, p. 130) are considered to be at an acceptable level of accuracy as observed in Table 38. The area under the approximated curve for the year 1973 is 1.0002 with a deviation of 0.02% from unity; whereas 0.9978 for the approximated curve of the year 1972 with a deviation of -0.02% from unity.

Table 38- The accuracy results of the ad hoc discrete approximations to LDCs by Maybee and Uri (p. 130) (own illustration)

Year	Area under the Approximated Curve	% Deviation
1973	1.0002	0.02%
1974	0.9998	-0.02%

For more information on the accuracy results of six, twenty and fifty step ad hoc approximations of LDCs can be found in Uri and Maybee (1978, p. 198) or Maybee and Uri (1979, p. 7). Although Elrazaz, Al-Mohawes and Mazi[114] (1988) carry out six and twenty step ad hoc approximations to LDCs, any information about the inaccuracy in approximations is not provided.

During forecasting LDCs, the heights of the N line segments (i.e. for N-steps) are estimated on an annual basis over η years with the same time duration steps (i.e. hourly intervals) forming a sequence of estimates $\hat{\xi}_k$ for each ξ_k represented in $(n \times 1)$ vector "$\hat{\boldsymbol{\xi}}$" as follows:

$$\hat{\boldsymbol{\xi}} = \left(\hat{\xi}_1(1), \hat{\xi}_2(1), \cdots, \hat{\xi}_N(1), \cdots, \hat{\xi}_1(\eta), \hat{\xi}_2(\eta), \cdots, \hat{\xi}_N(\eta)\right) \qquad (12.1.2)$$

The symbol "$\hat{\xi}_k(j)$" denotes the estimated height corresponding to the k^{th} step in LDC of the j^{th} considered year ($j = 1, \ldots, \eta$). It is assumed that the heights will vary through time and the corresponding variation in the sequence can be determined by using econometric methods

[113] The results are based on hourly load data for Federal Power Commission (FPC) Region 5 consisting of New Mexico, Texas, Louisiana, Arkansas, Oklahoma, Kansas, and parts of Missouri and Mississippi for the period 1965 through 1974.

[114] The results are based on hourly load data of the Eastern Region of Saudi Arabia (SCECO-E) for the period 1980 through 1984.

such as regression analysis (Maybee & Uri, 1978) or TSA (Uri & Maybee, 1978; Maybee & Uri, 1979; Elrazaz, Al-Mohawes, & Mazi, 1988).

12.1.2 Optimal Discrete Functional Approximations to Load Duration Curves

The aforementioned method of discrete approximations to LDCs is carried out in an ad hoc manner. Maybee, Randolph and Uri (1979) presented an objective approach for finding the right-hand and the left-hand side of the break points (e.g. $T_1$and T_2 in Figure 75) to construct an optimal N-step approximations to LDCs. In their concept, a presumed electric utility has to provide adequate supply of electrical energy for its service area and is supposed to optimally approximate the LDC of its service area by using a dynamic programming algorithm. The utility is assumed to be subject to a penalty not only for failing to provide adequate energy, but also for generating excess amount of it. In Figure 75, the concept is illustrated in a representative LDC with a typical three-step approximation; however it can be utilized for any intended number of steps of approximation.

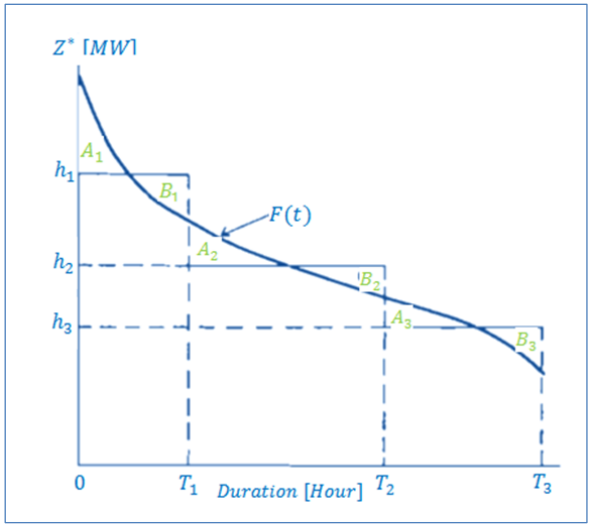

Figure 75- A representative LDC with three-step approximation adapted from Maybee, Randolph and Uri (p. 90)

The LDC represented in Figure 75 is defined over the interval $[0, T_3]$. The symbol "T_3" equals the total number of hours considered in a year (i.e. 8760 hours for regular or 8784 hours for leap years). It can be inferred from the figure that the break point T_1 for the first step should be determined in such a way that neither a deficiency in electricity generation (as represented by the area A_1) nor an excess generation (as represented by the area B_1) occurs. In the same way, the areas A_2, B_2, A_3, B_3 in correspondence with their time intervals can be interpreted. Therefore, the area under the approximating step function should be equal to the

area under F for each step. Accordingly, each height of the step "h" as a function of T_1 and T_2 are subject to the given below conditions (Maybee, Randolph, & Uri, p. 90):

$$h_1 = \frac{1}{T_1}\int_0^{T_1} F(t)\,dt \tag{12.1.3}$$

$$h_2 = \frac{1}{T_2 - T_1}\int_{T_1}^{T_2} F(t)\,dt \tag{12.1.4}$$

$$h_3 = \frac{1}{T_3 - T_2}\int_{T_2}^{T_3} F(t)\,dt \tag{12.1.5}$$

Thus, the break points of the step function "$s(t)$" (i.e. at a given time $t \in [0, T_3]$) should be determined in such a way that the costs of incurred mismatches, for which the utility is subject to, are minimized. After that, h_i can be derived from the calculated break points. The function $s(t)$, which comprises of the break points T_1 and T_2 on the abscissa with the corresponding heights h_1, h_2 and h_3 on the ordinate, is expressed as follows (Maybee, Randolph, & Uri, p. 91):

$$s(t) = \begin{cases} h_1 \;\; for \;\; 0 \le t \le T_1 \\ h_2 \;\; for \;\; T_1 \le t \le T_2 \\ h_3 \;\; for \;\; T_2 \le t \le T_3 \end{cases} \tag{12.1.6}$$

The amount of mismatch at given time t is defined by the function "$e(t)$" as indicated below (Maybee, Randolph, & Uri, p. 91):

$$e(t) = |F(t) - s(t)| \tag{12.1.7}$$

A penalty function $p\big(e(t)\big)$ is defined for relating per unit of mismatch at given time t. The objective is to choose break points such that the total penalty "P" is minimized as shown below (Maybee, Randolph, & Uri, p. 91):

$$min\, P = \int_0^{T_3} p\big(e(t)\big)e(t)\,dt \tag{12.1.8}$$

It is assumed that the penalty is equal to the mismatch ($p\big(e(t)\big) = e(t)$), so that the total penalty for a three-step function can then be simply represented as follows (Maybee, Randolph, & Uri, p. 91):

$$min\, P = \int_0^{T_3} \big(F(t) - s(t)\big)^2\, dt \tag{12.1.9}$$

The minimization problem, formulated in dynamic programming, is expressed in Eq. (12.1.10). The function f_m is the minimal penalty from an m-step process given that the starting point for the process is at the point v whereas the ending point is at w in the domain of F. For details of the algorithm see Maybee, Randolph and Uri (pp. 91-93).

$$f_m(v) = \min_{v \le w \le \mathrm{H}} \left(\sum_{i=v}^{w} p\big(e(i)\big)e(i) + f_{m-1}(w) \right) \quad m = 1, \dots, N \tag{12.1.10}$$

The represented results of performed six-step approximations by Uri and Maybee[115] (1980, p. 205) are considered to be at an acceptable level of accuracy (see Table 39). The areas under the approximated curves, for both of the years 1973 and 1974, amount to 0.9999 with a deviation of -0.01% from unity.

Table 39- The accuracy results of the optimal discrete approximations to LDCs by Uri & Maybee (own illustration)

Year	Area under the Approximated Curve	% Deviation
1973	0.9999	-0.01%
1974	0.9999	-0.01%

In other publications, Uri (1979, p. 382) or Uri and Maybee (1980, p. 347)[116] presented a 100% accuracy for the approximated curves of the year 1974 with same data of FERC Region 1.

[115] The results are based on hourly load data for Federal Regulatory Commission (FERC) Region 1 consisting of the states of Connecticut, Maine, Massachusetts, New Hampshire, Rhode Island and Vermont for the period 1965 through 1974.

[116] Uri and Maybee published in 1980 their article "Long-Term Forecasts of Optimal Approximations to the Load Duration Curve" which is same as the previous study in 1979 "Mid-range forecasting of the load duration curve" by Uri in a different journal with a different title.

During forecasting LDCs, the heights of the N line segments (i.e. for N-steps) are estimated on an annual basis over η years with the same time duration steps (i.e. hourly intervals) forming a sequence of estimates $\hat{h}_k$ for each h_k represented in $(n \times 1)$ vector "$\hat{\boldsymbol{h}}$" as follows:

$$\hat{\boldsymbol{h}} = \left(\hat{h}_1(1), \hat{h}_2(1), \cdots, \hat{h}_N(1), \cdots, \hat{h}_1(\eta), \hat{h}_2(\eta), \cdots, \hat{h}_N(\eta)\right) \tag{12.1.11}$$

The symbol "$\hat{h}_k(j)$" denotes the estimated height corresponding to the k^{th} step in LDC of the j^{th} considered year ($j = 1, \ldots, \eta$). It is assumed that the heights will vary through time and the corresponding variation in the sequence can be determined by econometric methods such as regression analysis (Uri & Maybee, 1980) or TSA (Uri N. D., 1979; Uri & Maybee, 1980).

In the previous studies, it has been emphasized that the forecasts of the heights provide better results than forecasting the break points; therefore a suitable transfer function is proposed for determining the breaking points from the forecasted heights (Uri N. D., 1979, p. 382; Uri & Maybee, 1980, p. 346) as follows.

$$e^{T_i} = \alpha_{0i} + \alpha_{1i} h_i + \alpha_{2i} h_{i+1} + \varepsilon_i \; for \; 1 \leq i \leq 5 \tag{12.1.12}$$

Note that only 5 break points are needed to be determined for six-step approximations and the coefficients of the function should have to be estimated from the data by using regression.

12.1.3 Smooth Functional Approximations of Load Duration Curves

The smooth functional approximations to LDCs have been carried out with N^{th} degree polynomials, linear exponential functions (represented below as "exp") and the inverse of Hill's function as expressed below respectively:

$$Z_t^* = \beta_0 + \sum_{k=1}^{N} \beta_k \, (t)^k + \epsilon_t \tag{12.1.13}$$

$$Z_t^* = \theta_0 + \theta_1 \exp(\theta_2 t) + \theta_3 t + \varepsilon_t \tag{12.1.14}$$

$$Z_t^* = Z_{min}^* + \frac{c}{(b/t - 1)^{1/m}} + \mathfrak{E}_t, \;\; b > 1 \tag{12.1.15}$$

In the above given equations, the normalized load at hour t is denoted by Z_t^*, where $t \in \mathbb{R} \wedge 1 \leq t \leq 8760 \; or \; 8784$. The terms "$\beta_0$", "$\theta_0$" and "$Z_{min}^*$" (i.e. the minimum value of hourly load demand in any considered year) are the constants in the corresponding functions. The

other terms are the parameters of the independent variable t and are the random shocks ϵ_t, ε_t and $\mathcal{E}_t$ at time t in the corresponding functions.

Uri (1977, p. 406) experimented with polynomial regression models to determine the order of N in Eq. (12.1.13) by using maximum likelihood method and concluded that the 5^{th} degree polynomial approximations to LDCs is the best alternative among other degree of polynomials.

Further, Uri and Maybee (1978, p. 256) examined smooth functional approximations to LDCs by using polynomials of degree $N \leq 5$ and the exponential function in Eq. (12.1.14) to fit them to 876 data points of each considered LDC (i.e. by sampling every 10^{th} point on a LDC). The approximations are carried out by using ordinary least squares and non-linear least squares method respectively. The results of the examinations indicate that the statistical properties of the polynomial degrees of $N = 4$ or 5 are both viable to be used in approximating LDCs. Similarly, the results of the linear-exponential function indicate also viable statistical properties to be an eligible function to approximate LDCs.

In addition to examining smooth functional approximations for statistical significance, Uri and Maybee (1978, p. 256) evaluated the accuracy of the models using two tests. The first test is carried out to examine whether the areas under the approximated LDCS are close to unity. During the first test, it is observed that both the polynomials and the linear-exponential function possess an area close to unity (e.g. the fourth degree polynomial fitted to the 1973 data has an area of 1.00151). The second test is conducted to calculate the maximum error[117] (max. error) as represented below (Uri & Maybee, 1978, p. 256):

$$max.error = max_{0 \leq i \leq 8760} |l(t_i) - F(t_i)| \tag{12.1.16}$$

In Eq. (12.1.16), the approximated and the actual function of the considered LDCs are represented as "l"and "F" respectively. The symbol "t_i" indicates the i^{th} value of the duration on the abscissa. Further, $l(t_i)$ indicates the approximated load value on the ordinate of the approximated LDC corresponding to t_i. Finally, $F(t_i)$ is the actual load value on the ordinate of the actual LDC corresponding to t_i.

[117] In the examined all LDC approximation methods, the maximum error test was conducted only for smooth approximations; however this test can also provide important accuracy results for discrete approximations.

The results of the second test for all functions are presented to be satisfactory (e.g. maximum error of linear-exponential function is $0.57463X10^{-5}$). Overall, the polynomial approximations are stated to be vastly inferior to the linear-exponential approximations because the intercept of the function essentially determines the shape of the curve (e.g. the location of the peak load). Further, the polynomial approximations are extremely sensitive to variations in the coefficients causing instability for forecasting. On the other hand, the linear-exponential function is observed to be stable from year to year providing a better forecasting opportunity.

The accuracy results of the exponential function approximation to LDCs (see Table 40), which are the only represented results by Uri and Maybee[118] (1978, p. 258), indicate that the area under the approximated curve for the year 1973 is 1.0116 with a deviation of 1.16%; whereas 0.9890 for the approximated curve of the year 1974 with a deviation of -1.10% from unity.

Table 40- The accuracy results of the exponential function approximations to LDCs by Uri & Maybee (own illustration)

Year	Area under the Approximated Curve	% Deviation
1973	1.0116	1.16%
1974	0.9890	-1.10%

Kato et al. (2011) introduced the inverse of Hill's function[119] as an approximating function of LDCs. As opposed to the other mentioned functions, the hourly demanded must be arranged in an ascending order w.r.t. the increasing duration for this function. Due to this configuration of approximated LDCs, the screening curve methodology must be accordingly adapted to be able to be utilized during capacity expansion planning (see Figure 76). In this configuration, the LDC indicates the fraction of the time or the duration a considered level of load is equaled or fallen behind.

[118] The results are based on hourly load data for FPC Region 5 consisting of New Mexico, Texas, Louisiana, Arkansas, Oklahoma, Kansas, and parts of Missouri and Mississippi for the period 1965 through 1974.

[119] The Hill function, introduced by, Archibald Hill (1910), is a function commonly used in biochemistry or ecology (e.g. to approximate the dissociation curves of hemoglobin) (Kato, Zhou, Kang, & Yokoyama, p. 309).

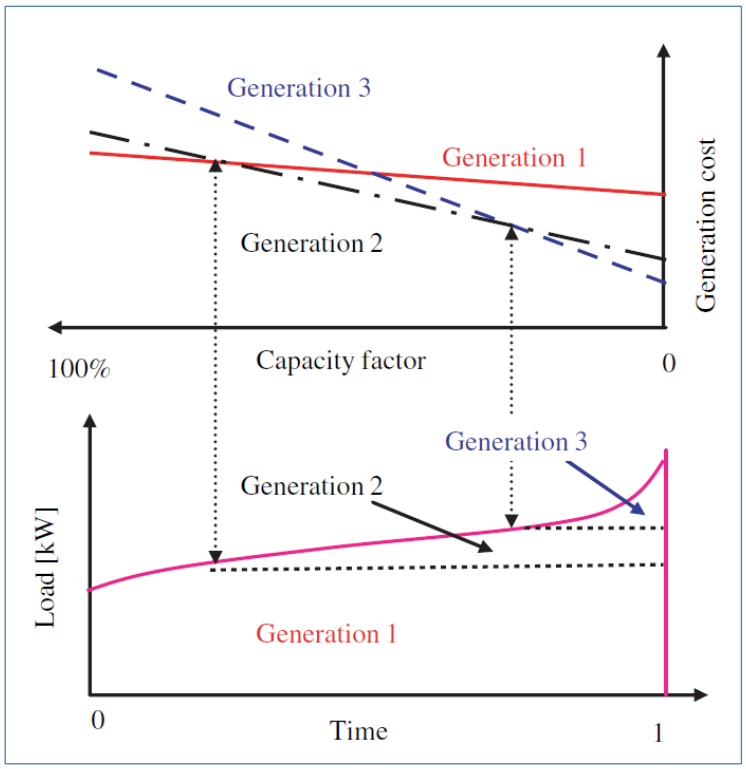

Figure 76- The screening curve methodology adapted to the approximated LDC for using Inverse of Hill's Function (Kato, Zhou, Kang, & Yokoyama, p. 308)

After approximating LDCs, parameters of the inverse Hill's function have also been proposed to be adjusted; in order to minimize the error in predicting the peak load. The first proposed adjustment is on parameter "m" (so called model-m). The change in parameter m (i.e. Δm) is related to the change in load factor by using 2nd degree polynomial; since m is defined to representing a slope of the Hill's curve. The other parameters can be recursively adjusted with the introduced mathematical relations (see p. 306 of the relevant article for more information).

The second proposed adjustment is on the parameter "b" (so called the model-b). The parameter b is defined to be an index which represents sharpness of the peak of LDC. Accordingly, LDC is devoted into two parts representing the peak period part (in the duration interval 1 to $t_1 = 0.98$) and thereafter the base period part (in the duration interval from t_1 to 0). The peak period part is adjusted according to given mathematical relations based on Z_{max} and Z_{min} (see p. 307 of the relevant article for more information); whereas the base period part is not modified (i.e. the estimated values of the parameters in the original approximation are kept unchanged).

Three sets of load data from IEEE-RTS[120] and PJM[121] in the year 2006 (hourly day-ahead demand bid data) and BEPC[122] in the year 2002 are used to test the original model as shown below:

Table 41- The inaccuracy in approximating LDCs by utilizing the Hill's Function (Kato, Zhou, Kang, & Yokoyama, p. 306)

		Total demand (GWh)	Peak load (GW)	RMS
IEEE-RTS	Actual load	15 297	2.85	—
	Original model	15 290	2.58	—
	Error	−0.047%	−9.56%	0.86%
	Model-*m*	15 300	2.85	—
	Error	0.018%	0.000%	4.92%
	Model-*b*	15 295	2.84	0.82%
	Error	−0.01%	−0.09%	
PJM-2006	Actual load	69 5871	137.1	—
	Original model	69 6604	129.3	—
	Error	0.11%	−5.74%	2.13%
	Model-*m*	69 5020	137.0	—
	Error	−0.12%	−0.10%	2.54%
	Model-*b*	69 7063	136.9	—
	Error	0.17%	−0.17%	2.13%
BJ-2002	Actual load	41 568	8.18	—
	Original model	41 600	7.12	—
	Error	0.08%	−12.96%	1.91%
	Model-*m*	41 697	8.15	—
	Error	0.31%	−0.28%	6.28%
	Model-*b*	41 677	8.17	—
	Error	0.26%	−0.13%	1.72%

In Table 41, the root mean square of error of hourly load demand is denoted as "RMS" and can be calculated as expressed below:

$$RMS = \sqrt{\frac{\left(l(t_i) - F(t_i)\right)}{n}}, \qquad 1 \leq i \leq 8760 \; or \; 8784 \tag{12.1.17}$$

In this study, the model-m and the model-b of the modified inverse of Hill's function are not considered for approximating the past LDCs of Turkey. It has been observed that the modification generally minimizes the error in peak load; however in some cases the modifications causes decrease in accuracy of the prediction of the hourly load demands (e.g. model-m of IEEE-RTS). Further, any modification of the functional parameters conflicts with the underlying basis of the analysis in study; since it is considered that the parameters evolve over time w.r.t. the short and the long term variations in hourly load demands. Accordingly,

[120] EEE-RTS (Institute of Electrical and Electronics Engineers- Reliability Test System) comprises a load model, generation system and transmission network which can be used to test or compare methods for reliability analysis of power systems (Kato, Zhou, Kang, & Yokoyama).

[121] See Footnote 23 on p. 13 for information about PJM interconnection.

[122] Beijing Electric Power Corporation (BEPC) is responsible for the electricity supply to the capital city. There are 18 districts or counties (Kato, Zhou, Kang, & Yokoyama).

any modification to any parameter is actually affecting the results of the analysis of the sequence which is formed by the modified and unmodified parameters of the corresponding function.

During forecasting LDCs, the parameters of a considered approximating functions (e.g. polynomial function) are estimated on an annual basis over η years forming a sequence of estimates $\hat{\beta}_k$ for each β_k represented in $(n \times 1)$ vector "$\boldsymbol{B}$" as follows:

$$\boldsymbol{B} = \left(\hat{\beta}_0(1), \hat{\beta}_1(1), \cdots, \hat{\beta}_N(1), \cdots, \hat{\beta}_0(j), \hat{\beta}_1(j), \cdots, \hat{\beta}_N(j), \cdots, \hat{\beta}_0(\eta), \hat{\beta}_1(\eta), \cdots, \hat{\beta}_N(\eta)\right) \quad (12.1.18)$$

The symbol "$\hat{\beta}_k(j)$" denotes the estimated k^{th} coefficient of Eq. (12.1.13) calculated for the estimation of LDC in the j^{th} considered year ($j = 1, \ldots, \eta$). It is assumed that the parameters vary through time and the corresponding variation in the sequence can be determined by econometric methods such as regression analysis (Uri N. D., 1977; Uri & Maybee, 1978) or TSA (Uri & Maybee, 1980).

12.1.4 A Summary on the Approximation Methods of LDCs

The proposed methods for approximations to LDCs in the previous studies exhibit advantages and disadvantages in praxis as follows:

- Ad hoc discrete approximations to LDCs are relatively easier to apply than the optimal approximations to LDCs in which the approximation problem is solved by dynamic programming approach. In addition, their accuracy in approximating LDCs is observed to be as good as the accuracy in optimal approximations to LDCs.
- In ad hoc discrete approximations to LDCs, an implicit assumption is made that the forecasted k^{th} height of a LDC in a future year corresponds again to the same ad hoc defined time interval.
- In optimal discrete approximations to LDCs, a suitable transfer function is proposed for determining the breaking points from the forecasted heights. Although this seems more accurate, the parameters of the transfer function should also have to be estimated from the data by using regression analysis.
- In both of the discrete approximation methods, the heights of the step functions are used for forecasting LDCs.

- The accuracy of the discrete approximations to LDCs gets better as the number of steps is increased and so the effort.
- The smooth functional approximations to LDCs are relatively easier to apply and need less effort than the both mentioned discrete approximation approaches.
- The smooth functional approximations to LDCs are observed to be less accurate than the discrete approximations to LDCs; however the inaccuracies are considered to be at acceptable levels to be used as approximations to LDCs.
- In order to approximate LDCs at an acceptable level of inaccuracy, a convenient smooth function should be identified among alternatives.

In this study, the smooth functional approach is considered for approximating LDCs of Turkey due to the given reasons below:

- First of all, the effort in discrete functional approximations is relatively high in comparison to the effort in smooth functional approximations.
- Secondly, the LDCs of Turkey are in the form of a continuous monotone decreasing function (see Figure 32); hence the discretization of the corresponding LDCs can cause unacceptable level of inaccuracies for capacity expansion planning.
- Finally, the computation of hourly load demands w.r.t. the given values of duration requires less effort and can be carried out with lower inaccuracies than using discrete approximations.

12.2 Approximating Load Duration Curves of Turkey

In this section, the LDCs of Turkey in the period 2000-2014 are analyzed to determine a mathematical function which adequately approximates the corresponding curves among other alternatives. In this study, an adequate functional approximation to a LDC is defined to be a parsimonious functional[123] approximation to a LDC with least possible inaccuracy in

[123] The term “parsimonious function” refers to the simplest function which has the smallest possible number of parameters to adequately explain the variation in the dependent variable (i.e. hourly load demand) using independent variable (i.e. duration). Note that the more parameters considered for approximation of LDCs, the more uncertainty will be present in the forecasts of the corresponding parameters which are used for obtaining approximations to future LDCs. Box, Jenkins and Reinsel (2008, p. 16) state that "Our objective, then, must be to obtain adequate but parsimonious models. Forecasting and control procedures could be seriously deficient if these models were either inadequate or unnecessarily prodigal in the use of parameters. Care and effort is needed in selecting the model."

approximating annual gross electricity demand, annual peak load demand and hourly load demand among other alternatives.

The functional approximations of LDCs are carried out; in order to use them for computing hourly load demands corresponding to given values of duration or vice versa during capacity expansion planning. In particular, the approximations are conducted only in the observed range of the duration from 0 to 8760 hours (or 8784 hours). Accordingly, any approximation or forecast out of the corresponding range of values will not be carried out.

In this study, a functional approximation approach is pursued; since the actual function of the historical LDCs are not known and cannot be precisely determined by utilizing the available data. Further, the actual functions of all LDCs are considered to be continuous functions of duration "t" ($t \in \mathbb{R} \wedge 1 \leq t \leq 8760\ or\ 8784$). Furthermore, the pursued approach is based on the Weierstrass approximation theorem (1885). According to Weierstrass (as cited in Hoffman, 2001, p.191), if $f(x)$ is any continuous function of "x" defined in the domain $a \leq x \leq b$, then for every $\varepsilon > 0$ there exists an n^{th} degree polynomial function "$P_n(x)$" approximating $f(x)$, where the value of n depends on the intended value of ε, i.e.

$$|P_n(x) - f(x)| < \varepsilon \tag{12.2.1}$$

In relation (12.2.1), $P_n(x)$ and $f(x)$ are both deterministic functions of the variable x. $P_n(x)$ resembles the approximate value and the $f(x)$ indicates the actual value corresponding to x. The term ε indicates the intended level of inaccuracy for the approximation in the interval $a \leq x \leq b$. Hence, any continuous function can be approximated depending on the intended accuracy utilizing a polynomial of high enough degree. Note that a polynomial of degree n is supposed to be unique, if it passes through $n + 1$ discrete points.

Any conducted functional approximation in a considered domain yields an approximation error for each approximated value. Any obtained approximation error is supposed to be non-stochastic; since the error will be identical on repeated applications. The two different types of measurements for approximation errors are introduced (Hoffman, 2001, p. 62):

$$Absolute\ approximation\ error = Approximate\ value - Actual\ value \tag{12.2.2}$$

$$Relative\ approximation\ error = \frac{Absolute\ approximation\ error}{Actual\ Value} \quad (12.2.3)$$

Note that absolute approximation error may be positive or negative and is not the absolute value of that error. The relative error can be represented as a decimal number or as a percentage. From here on, approximation error is practically called as error.

In analogy to Weierstrass approximation theorem, any analytical function can be reasonably applied on a dataset as an approximating function (Hoffman, 2001, p. 189). In this study, the given below functions in general form are utilized for approximating LDCs:

$$Z_t^* = \beta_0 + \sum_{k=1}^{N} \beta_k\,(t)^k + \epsilon_t \quad (12.2.4)$$

$$Z_t^* = \theta_0 + \theta_1 \exp(\theta_2 t) + \theta_3 t + \varepsilon_t \quad (12.2.5)$$

$$Z_t^* = \alpha_0 + \alpha_1 log\frac{t + \alpha_2}{\alpha_2 + \alpha_3 - t} + e_t \quad (12.2.6)$$

$$Z_t^* = Z_{min}^* + \frac{c}{(b/t - 1)^{1/m}} + \mathfrak{E}_t,\ \ b > 1 \quad (12.2.7)$$

In the above given Eqs. (12.2.4), (12.2.5), (12.2.6) and (12.2.7), the normalized load at hour t is denoted by Z_t^*, where $t = 1, \cdots, n$ and n is the number of observations. The terms "β_0", "θ_0", "α_0" and "Z_{min}^*" (i.e. the minimum value of load demand in any considered year) are the constants in the corresponding functions. The other terms are the parameters of the dependent variable t and are the random shocks ϵ_t, ε_t, e_t and $\mathfrak{E}_t$ at time t in the corresponding functions. Note that for the first three functions, the normalized hourly loads must be arranged in a descending order w.r.t. the increasing values of duration; whereas for the last one (i.e. the inverse of Hill's function) the arrangement must be made in an ascending order. The represented functions in Eqs. (12.2.4), (12.2.5), (12.2.7) are previously utilized for approximating LDCs (see Subsection 12.1.3 for more information); however the represented function in Eq. (12.2.6) is utilized for functional approximations to LDCs for the first time in this study. The nonlinear function in Eq. (12.2.6) is a four-parameter logarithmic function introduced in Ratkowsky (1990, p. 145).

During functional approximation, an approximate fit to a dataset is carried out according to the method of least squares approximation which can be utilized in analogy to the application

of least squares in statistics. In the case of functional approximation, the best approximation is the approximation which yields the minimum sum of difference between the discrete values of approximating and the actual function in absolute value given the domain of x as represented below for general polynomial approximation (Rao, 2007, p. 289):

$$\min_{a \leq x \leq b} \sum |P_n(x) - f(x)| \tag{12.2.8}$$

The above given optimization problem can be solved by least squares approximation through minimizing the sum of squares of errors given the domain of x as indicated below (Rao, p. 289):

$$\min_{a \leq x \leq b} \sum [P_n(x) - f(x)]^2 \tag{12.2.9}$$

For functional approximation, the magnitudes of the errors are taken into account for determining the adequate approximation rather than assessing the validity of a model's underlying statistical assumptions (i.e. the mentioned regression diagnostics in Subsection 10.1.1.5). The diagnostic tests for the assumptions of the errors for the non-autocorrelation, normal distribution, homoscedasticity cannot be conducted; since the errors are non-stochastic. Apart from the corresponding diagnostic tests, the inaccuracy in approximation of any LDC is assessed by utilizing the below given measures:

1. The relative error (RE) in approximating annual gross electricity demand (AGD) in a considered year (RE_{AGD}),
2. The relative error in approximating annual peak load demand (APD) in a considered year (RE_{APD}),
3. The mean absolute relative error ($MARE$) in approximating hourly load demand (HLD) in a considered year ($MARE_{HLD}$),
4. The mean of absolute relative errors ($MAREs$), the periodical mean of relative errors, in approximating annual gross electricity demand ($MAREs_{AGD}$), annual peak load demand ($MAREs_{APD}$) and the mean of $MAREs_{HLD}$ for the period 2000-2014.

The RE_{AGD} is utilized for determining the adequate functional approximation to annual gross electricity demand among other considered type of functional approximations. Further, it is calculated by taking the difference between the area under approximated LDC (A_{App}) and the

actual annual gross electricity demand (A_{Act}) in the considered year and then dividing by A_{Act} as shown below:

$$RE_{AGD} = \frac{A_{App} - A_{Act}}{A_{Act}} \cdot 100 \tag{12.2.10}$$

Note that the area under any LDC equals to the total annual electricity demand and is calculated as represented below:

$$A_{App} = \int_{1}^{8760} L(x)\, dx \tag{12.2.11}$$

Note that "$L(t)$" denotes any smooth function utilized for approximating a LDC and is a function of duration "t". In addition, the upper limit of the definite integral can also be equal to 8784, if a leap year is under consideration.

Similarly, the RE_{APD} is utilized for determining the adequate functional approximation to annual peak load demand among other considered type of functional approximations. Further, it is calculated by taking the difference between the approximated annual peak load demand ($L_{App,peak}$) and the actual annual peak load demand ($L_{Act,peak}$) of a considered year and then dividing by $L_{Act,peak}$ as shown below:

$$RE_{APD} = \frac{L_{App,peak} - L_{Act,peak}}{L_{Act,peak}} \cdot 100 \tag{12.2.12}$$

For capacity expansion planning, the magnitude of RE_{APD} indicates the accuracy in determining the installed capacities of new power plants to be commissioned and also the required capacity of power plant reserves in a power system.

In the same manner, the $MARE_{HLD}$ is utilized for determining the adequate functional approximation to hourly load demand among other considered type of functional approximations. Further, it is the mean absolute percentage error for each the i^{th} approximated hourly load demand ($L_{App,i}$) minus the i^{th} actual hourly load demand ($L_{Act,i}$) of a considered year divided by $L_{Act,i}$ as indicated below:

$$MARE_{HLD} = \frac{1}{n-d} \sum_{i=1}^{n} \left| \frac{L_{App,i} - L_{Act,i}}{L_{Act,i}} \right| \cdot 100, \quad 1 \le i \le n \ \wedge \ n = 8760 \ or \ 8784 \tag{12.2.13}$$

Note that the mean is taken w.r.t. the degrees of freedom which equal to $n - d$. The term"n" represents the number of observations (see Table 25) and the term "d" indicates the total number of parameters possessed by the considered function. Furthermore, the magnitude of $MARE_{HLD}$ indicates the accuracy in determining the installed capacities of new units to be commissioned and also whether to set the existing units to run at full capacity or partial capacity during capacity expansion planning. In this respect, the lower the inaccuracy in $MARE_{HLD}$, the better the planning of capacity expansion of power plants.

In addition to the above mentioned inaccuracy measures, the inaccuracy in approximation of LDCs can be further assessed by calculating $MARES_{AGD}$, $MARES_{APD}$ and the mean of $MARES_{HLD}$ for the period 2000-2014 for each type of functional approximation. The corresponding measures are expressed for n^{th} degree polynomials as given below respectively:

$$MARES_{AGD}\ for\ n^{th}\ order\ polynomial = \frac{|RE_{AGD}^{2000}| + \cdots + |RE_{AGD}^{2014}|}{15} \tag{12.2.14}$$

$$MARES_{APD}\ for\ n^{th}\ order\ polynomial = \frac{|RE_{APD}^{2000}| + \cdots + |RE_{APD}^{2014}|}{15} \tag{12.2.15}$$

$$Mean\ of\ MARES_{HLD}\ for\ n^{th}\ order\ polynomial = \frac{MARE_{HLD}^{2000} + \cdots MARE_{HLD}^{2014}}{15} \tag{12.2.16}$$

The above mentioned relative measures of inaccuracy are used in assessing the overall inaccuracy of all considered type of functional approximations to past LDCs of Turkey. Therefore, maximum acceptable levels for measures of overall inaccuracy are set; in order to compare and determine the adequate functional approximation to past LDCs among alternatives. In analogy with the statements of Taper and Lele (2004, p. 537) on statistical models, a functional approximation is supposed to be adequate for a researcher's purposes; if the estimated discrepancy between a LDC and its approximation is less than some arbitrary but meaningful level. The maximum acceptable level of inaccuracy for the $MARES_{AGD}$ and the $mean\ of\ MARES_{HLD}$ is assigned to be 1% for all considered type of functional approximations to LDCs. The corresponding level of inaccuracy is considered according to the presented results of the inaccuracy of the functional approximations to LDCs in the mentioned previous studies (see Table 38, Table 39, Table 40 and Table 41).

The maximum level of inaccuracy for the $MARES_{APD}$ is assigned to be 5% for all types of functional approximations to LDCs. The corresponding error level is analyzed to be not endangering the long term supply reliability of the Turkish power system in the period 2015-2025. The analysis is carried out by taking into account the following points:

1. The development of the total installed capacity of the power plants and the annual peak load demand in Turkey in the period 2000-2014,
2. The availability[124] of power plants during the occurrence of the annual peak load demand in year 2014,
3. The assigned maximum level of inaccuracy (i.e. 5%) for the $MARES_{APD}$.

The analysis is based on the below given assumptions and relations:

1. The total installed capacity of power plants in year 2014 (Cap) is projected to be increasing at a rate of 7%/a (i.e. same as in the period 2000-2014) yielding projected total installed capacity of power plants ($Projected\ Cap_i$) for each i^{th} year in the period 2015-2025 as represented below:

$$Projected\ Cap_i = Cap \cdot (1 + 7\%)^{(i-2014)}, \quad \forall\, i: i \in \mathbb{Z}^+ \wedge\ 2015 \leq \mathrm{i} \leq 2025 \tag{12.2.17}$$

2. The demand for annual peak load in year 2014 (APD) is projected to be increasing at a rate of 5.5%/a (i.e. same as in the period 2000-2014) yielding projected annual peak load demand ($Projected\ APD_i$) for each i^{th} year in the period as represented below:

$$Projected\ APD_i = APD \cdot (1 + 5.5\%)^{(i-2014)}, \quad \forall\, i: i \in \mathbb{Z}^+ \wedge\ 2015 \leq \mathrm{i} \leq 2025 \tag{12.2.18}$$

3. The $Projected\ Cap_i$ in the period 2015-2025 is derated according to the availability factor "a" yielding "$Derated\ Cap_i$" as expressed below:

$$Derated\ Cap_i = Projected\ Cap_i \cdot a, \quad \forall\, i: i \in \mathbb{Z}^+ \wedge\ 2015 \leq \mathrm{i} \leq 2025 \tag{12.2.19}$$

[124] In capacity expansion planning, the forced outages and maintenance requirements of the power plants are taken into account in a deterministic manner by derating the total installed capacity of power plants with an availability factor "a" ($0 \leq a \leq 1$).

The value of a is assigned to be 65.5% which equals to the value of a during the occurrence of the annual peak load demand in year 2014.

4. The $Derated\ Cap_i$ in the period 2015-2025 is reduced according to the maximum acceptable level of inaccuracy for the $MARES_{APD}$ (i.e. set to 5%) yielding $Reduced\ Cap_i$ as indicated below:

$$Reduced\ Cap_i = Derated\ Cap_i \cdot 95\%, \quad \forall\, i: i \in \mathbb{Z}^+ \wedge\ 2015 \leq \mathrm{i} \leq 2025 \tag{12.2.20}$$

The result of the analysis is depicted in Figure 77. Accordingly, any electricity supply deficit is not observed w.r.t. the $Reduced\ Cap_i$; since it is higher than the projected annual peak load in the period 2015-2025.

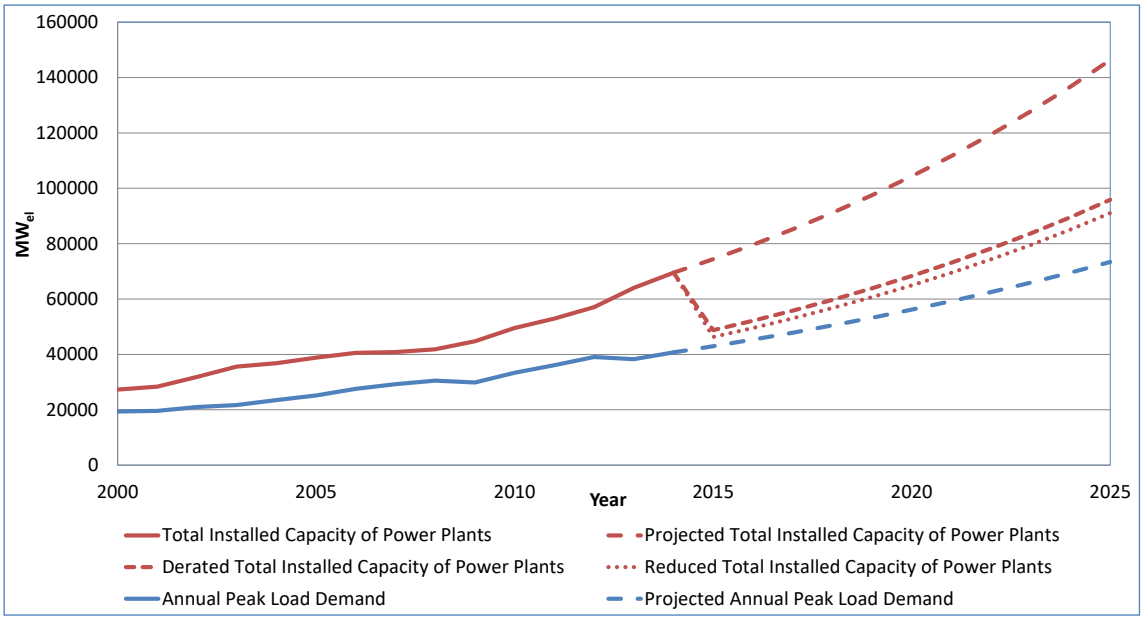

Figure 77- The analysis on the development of the annual peak load demand w.r.t. the long term supply reliability (own calculation & illustration)

In particular, it is also assumed that an effective decrease in inaccuracy should be at least 1% for possessing an additional functional parameter, if two different types of functional approximations have different total number of parameters (see the definition of parsimonious function in Footnote 123). Note that the total number of parameters in polynomials equals to one more than their polynomial degree. Further, the exponential function, logarithmic function and the inverse of Hill's function possess 4, 4 and 3 parameters in total respectively.

During the determination of the adequate functional approximation to past LDCs of Turkey, all considered functional approximations are initially examined for fulfillment of the

maximum acceptable level of inaccuracy for the $MARES_{AGD}$, the $MARES_{APD}$ and the mean of $MARES_{HLD}$. Subsequently, the functional approximations, which indicate acceptable levels of corresponding inaccuracies, are further investigated for the parsimony of the total number of possessed parameters according to the aforementioned criterion.

In the following subsections, the polynomial and nonlinear approximations to LDCs are carried out to determine the function which adequately approximates the past LDCs among others based on the mentioned criteria.

12.2.1 Polynomial Function Approximation to Load Duration Curves of Turkey

In this section, the past LDCs of Turkey are approximated using polynomial functions of degrees[125] ranging from 4^{th} to 12^{th}. The objective of the analysis is to determine the parsimonious polynomial function which adequately approximates the considered LDCs based on the $MARES_{AGD}$, $MARES_{APD}$ and the mean of $MARES_{HLD}$.

The analysis for the functional approximation of LDCs are carried out by using the license free statistical software R (version 3.1.2) and also by using the RStudio IDE (Integrated Development Environment, Version 0.98.1102) which is a license free user interface for R. The polynomial approximations are applied on the corresponding data by using the "lm" function (in package "stats" version 3.1.2) to solve linear least squares problems (see Subsection 10.1.1).

The first approximation analysis is carried out for examining whether the polynomials with intercepts or without intercepts are better in approximating past LDCs of Turkey. It is observed that the polynomials without intercepts cannot be used in capacity expansion planning; since they are not useful as depicted in Figure 78[126].

[125] The polynomials with degrees higher than 12^{th} possess some parameters which are not available (i.e. not estimable) in the output of approximation analysis. This is due to the fact that the multicollinearity increases with the increasing degree of the polynomials causing exact multicollinearity (an exact linear relationship among some of the independent variables); which results in a singular matrix during the calculations that cannot be inverted (Kennedy P. , 2008, p. 192).

[126] The unit of y-axis indicates normalized hourly load values w.r.t. annual energy demand (i.e. load per unit energy demand).

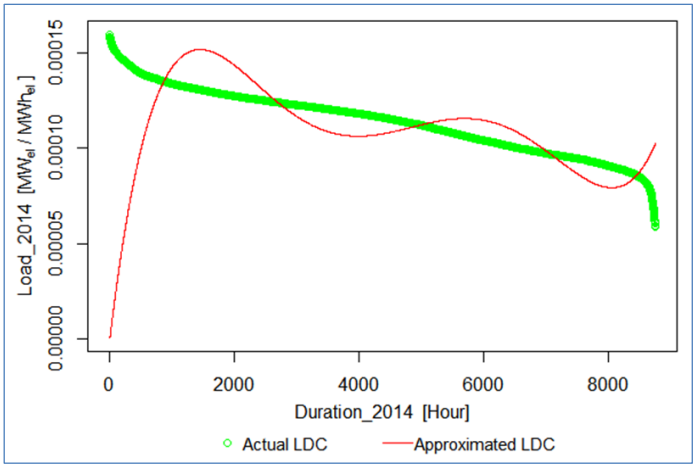

Figure 78- The approximated LDC of the year 2014 by using 5th degree polynomial without intercept (own calculation & illustration)

The second analysis for approximation of past LDCs is carried out by using polynomials with intercepts. In Figure 79, the relative error in approximating annual gross electricity demand (RE_{AGD}) w.r.t. the different degrees of polynomials for each considered year is depicted.

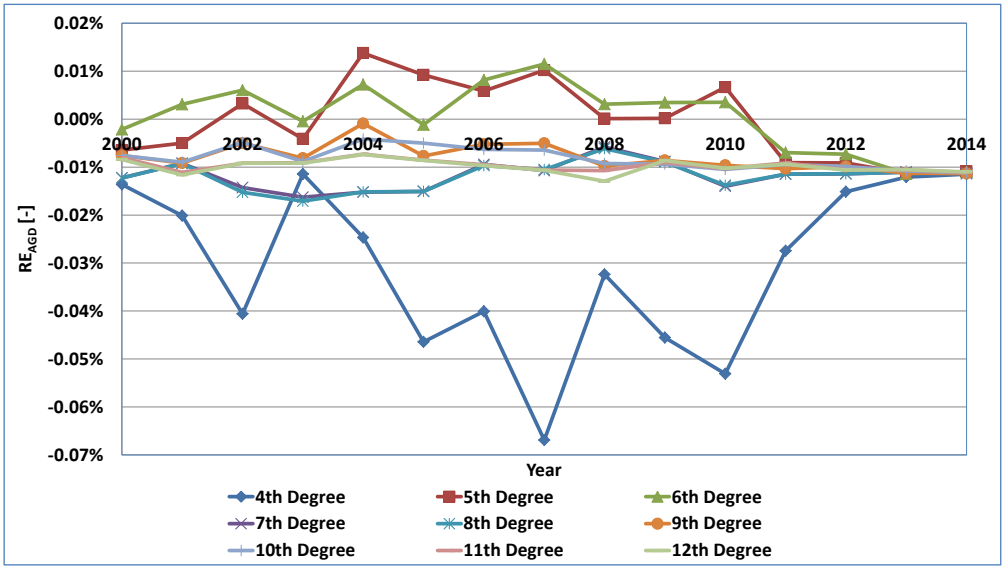

Figure 79- The RE_{AGD} for approximated LDCs in the period 2000-2014 (own calculation & illustration)

It can be inferred from Figure 79 that as the degree of the polynomials is increased, the RE_{AGD} generally decreases. The RE_{AGD} is observed to be not continuously decreasing with the increasing degree of polynomials; since the functional approximations are carried out by minimizing the difference between the hourly load demand values of the actual function and the approximating function (see Eq. (12.2.9)). Accordingly, a minimization of the error in approximating the area under the approximating function w.r.t. the actual function is not taken into account. Note that LDCs are approximated as smooth functions from data composed of hourly load demands which are recorded in discrete time intervals. In this respect, the values

lying between any two approximated values are obtained by interpolation using the approximating function. Therefore, the inaccuracy of the interpolated values cannot be measured; since the actual data corresponding to the interpolated values are not available. In addition, the areas under the LDCs are calculated by taking the integral (see Eq. (12.2.11)) in the continuous interval [0, 8760] or [0, 8784] constituting the approximated and the interpolated hourly load demand values. Therefore, it should be expected that the RE_{AGD} cannot be continuously decreasing with the increasing degree of polynomials.

Further, the $MARES_{AGD}$ is observed to be under 1% for all considered functional approximations to past LDCs of Turkey (see also Figure 83). Correspondingly, the maximum acceptable level for $MARES_{AGD}$ is not exceeded for all considered functional approximations. Furthermore, the 4th degree polynomial approximations are observed to be the least accurate of them all and have the least number of parameters in total. The polynomials with degrees higher than four mainly overestimate the annual gross electricity demand; however the corresponding inaccuracies are less than 0.02% for each considered year. If the approximations are individually examined for each year (see Figure 79 and Figure 83), most of the time an odd degree polynomial indicates a slightly less $MARES_{AGD}$ compared to a consecutive even degree polynomial for the same year (e.g. the 5th and the 6th degree polynomials). Accordingly, the overall inaccuracy in the 11th degree polynomial approximations is the lowest. However the achieved level of accuracy is not effective w.r.t. the 4th degree polynomial approximations; since the decrease in inaccuracy is less than 1% per each additionally possessed parameter. In particular, an effective decrease in inaccuracy (i.e. at least 1%) w.r.t. the 4th degree polynomial approximations is also not achieved by other polynomial approximations possessing additional functional parameter(s).

Here, the effectiveness of the decrease in RE_{AGD} cannot be measured by both adjusted R^2 (see p. 94 for definition) or any mentioned information criteria (see p. 138 for the types); since the former mainly depends on the minimization of the sum of the squared residuals[127] (i.e. least squares approximation) and the latter mainly depends on the maximization of the probability of the observed data (i.e. maximum likelihood). Hence, both of the model adequacy measures cannot account for the interpolated hourly load demand values which are considered in the calculation of the areas under the approximated LDCs.

[127] They are the deviations of approximated hourly load demand from the actual ones (i.e. the observed data).

In Table 42, the adjusted R^2 of the polynomial approximations generally indicate only infinitesimal increase with the increasing degree of polynomials. Note that in Table 42 only for the three of the values marked as bold italic, the adjusted R^2 indicates infinitesimal decrease as the degree of polynomials is increased from 7^{th} to 8^{th} for the corresponding years. Although the adjusted R^2 generally increases with the increasing degree of polynomials, it contradicts with the RE_{AGD} (see Figure 79) due to the aforementioned reason. For example, the 5^{th} degree polynomial approximation to LDC of the year 2014 indicates a RE_{AGD} of 1.09106E-04 in absolute value; whereas the 6^{th} degree polynomial approximation for the same year indicates a RE_{AGD} of 1.09723E-04 in absolute value (see Figure 79). However the value of adjusted R^2 for 6^{th} degree polynomial approximation is higher than 5^{th} degree polynomial approximation favoring the 6^{th} degree polynomial approximation with higher RE_{AGD} in absolute value and higher total number of parameters.

Table 42- The adjusted R^2 of the polynomial approximations to LDCs of Turkey in the period 2000-2014 (own calculation & illustration)

Years	Degree of Polynomial								
	4^{th}	5^{th}	6^{th}	7^{th}	8^{th}	9^{th}	10^{th}	11^{th}	12^{th}
2000	0.9964957	0.9986096	0.9988057	0.9995095	0.9995279	0.9997812	0.9997929	0.9999301	0.9999334
2001	0.9955821	0.9973793	0.9976422	0.9988874	0.9988956	0.9993151	0.9993303	0.9996451	0.9996664
2002	0.9925051	0.9960448	0.9962332	0.9979375	0.9980137	0.9988175	0.9988292	0.9993657	0.9993665
2003	0.9942450	0.9971365	0.9974399	0.9983933	0.9984077	0.9990146	0.9990640	0.9993910	0.9993916
2004	0.9880755	0.9942634	0.9953996	0.9970314	***0.9970309***	0.9982095	0.9984193	0.9990289	0.9990568
2005	0.9895715	0.9957644	0.9971464	0.9981934	***0.9981932***	0.9986992	0.9990102	0.9994122	0.9994142
2006	0.9900253	0.9949980	0.9964189	0.9982280	0.9982347	0.9987972	0.9990798	0.9994930	0.9995120
2007	0.9900667	0.9942457	0.9970016	0.9980677	0.9981048	0.9986756	0.9989931	0.9993865	0.9994561
2008	0.9873896	0.9923854	0.9952908	0.9975462	0.9978969	0.9987141	0.9990128	0.9994867	0.9995848
2009	0.9899569	0.9947771	0.9959627	0.9977401	0.9978348	0.9985401	0.9987189	0.9991352	0.9992448
2010	0.9914896	0.9967355	0.9973906	0.9989670	0.9989715	0.9993679	0.9994412	0.9996554	0.9997149
2011	0.9941143	0.9971238	0.9976082	0.9990522	***0.9990521***	0.9993265	0.9993936	0.9996785	0.9997007
2012	0.9900616	0.9939486	0.9949675	0.9973661	0.9973663	0.9985047	0.9985761	0.9992595	0.9993965
2013	0.9891504	0.9951318	0.9967627	0.9980911	0.9983063	0.9986313	0.9990174	0.9993996	0.9995207
2014	0.9880240	0.9946300	0.9952880	0.9975879	0.9976100	0.9982980	0.9985243	0.9989733	0.9991945

In Table 43, the AICc values of the polynomial approximations generally decrease with the increasing degree of polynomials. Note that in Table 43 only for the four of the values marked as bold italic, the AICc values increase as the degree of polynomials is increased from 7^{th} to 8^{th} for the corresponding years. Although, the AICc values generally decrease with the increasing degree of polynomials, it contradicts with the RE_{AGD} (see Figure 79) due to the aforementioned reason. In particular, the value of AICc for 6^{th} degree polynomial approximation is lower than 5^{th} degree polynomial approximation (see Table 43) favoring the 6^{th} degree polynomial approximation with higher RE_{AGD} and higher total number of parameters. Also, the BIC of the polynomial approximations indicate the same situation (see

APPENDIX B). Hence, the mentioned model adequacy measures cannot specifically account for the selection of the degree of the adequate polynomial approximation to LDCs based on the RE_{AGD}. To sum up, the adequate functional approximations (see Footnote 123 for the details of the corresponding definition) to annual gross electricity demands are observed to be realized by the 4th degree polynomial approximations among other considered polynomial approximations.

Table 43- The AICc values of the polynomial approximations to LDCs of Turkey in the period 2000-2014 (own calculation & illustration)

Years	Degree of Polynomial								
	4th	5th	6th	7th	8th	9th	10th	11th	12th
2000	-130657.0	-135543.4	-136346.1	-141049.4	-141250.7	-145315.5	-145606.3	-151349.1	-151599.7
2001	-135137.0	-138023.3	-138606.8	-142758.1	-142798.1	-145438.5	-145561.9	-149072.3	-149413.7
2002	-126527.7	-129894.5	-130150.7	-133323.3	-133520.7	-136252.5	-136303.8	-139532.2	-139537.7
2003	-132294.4	-136094.8	-136703.9	-139240.0	-139287.8	-141900.6	-142179.4	-144519.6	-144523.5
2004	-131754.8	-135855.9	-137092.2	-139547.0	***-139545.0***	-142379.4	-143077.0	-145807.2	-145969.6
2005	-135845.8	-141025.7	-143295.6	-145923.0	***-145921.6***	-147809.7	-149379.9	-152375.3	-152393.9
2006	-141312.8	-145449.6	-147452.0	-151668.9	-151690.6	-153989.9	-155594.0	-159167.1	-159395.2
2007	-145768.1	-149142.0	-153170.9	-155886.1	-156004.9	-158219.5	-159912.6	-162975.1	-163718.1
2008	-151636.2	-154917.7	-158043.6	-162284.3	-163286.8	-166487.1	-168206.0	-172460.6	-173839.2
2009	-147304.3	-151376.1	-152978.9	-156592.2	-156857.9	-159312.0	-160124.9	-162571.8	-163414.9
2010	-151754.4	-157876.1	-159306.4	-165226.9	-165253.9	-168362.9	-169150.2	-172237.7	-173449.1
2011	-174707.8	-179876.8	-181207.4	-187889.8	***-187887.8***	-190354.8	-191110.6	-195691.6	-196205.9
2012	-196407.4	-200524.2	-202053.5	-207426.3	***-207425.8***	-212123.4	-212528.5	-217954.2	-219650.8
2013	-205588.2	-212550.6	-216094.7	-220683.1	-221721.6	-223571.9	-226450.5	-230729.8	-232685.7
2014	-206140.4	-213157.6	-214300.4	-220158.5	-220238.0	-223207.7	-224454.6	-227628.1	-229749.9

In Figure 80, the relative error in approximating annual peak load demand (RE_{APD}) w.r.t. the different degrees of polynomials are depicted for each considered year.

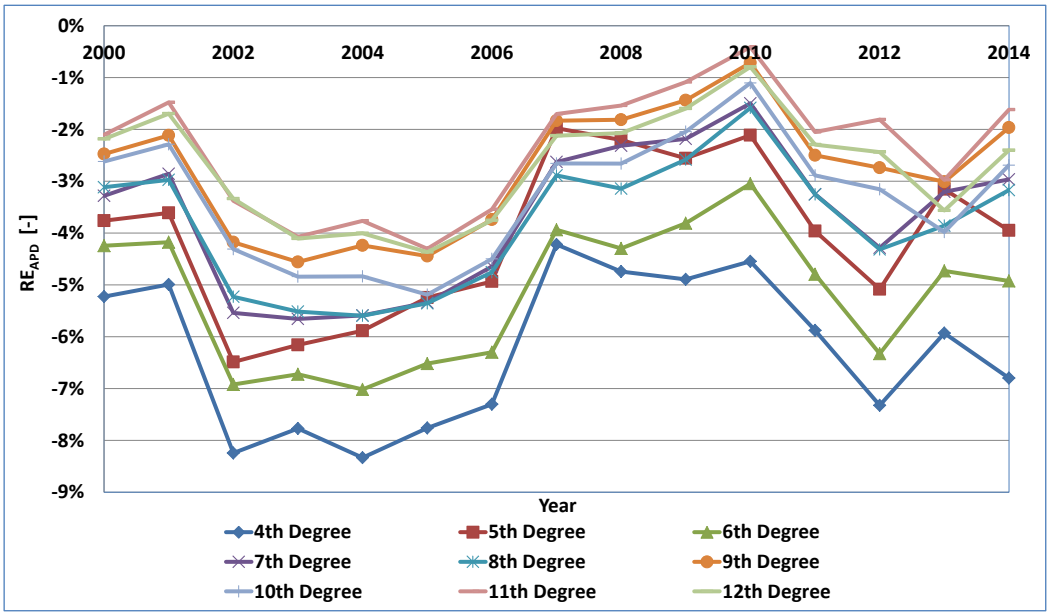

Figure 80- The RE_{APD} for approximated LDCs in the period 2000-2014 (own calculation & illustration)

It can be inferred from Figure 80 that the RE_{APD} is higher than RE_{AGD} for each considered year. Further, the RE_{APD} generally decreases with the increasing degree of the polynomials. Note that all considered polynomials underestimate the annual peak load demand. Furthermore, the 4th degree polynomial approximations are observed to be indicating the highest inaccuracy of them all. Moreover, the $MARES_{APD}$ is observed to be under 5% for all considered functional approximations excluding the 4th and 6th degree polynomial approximations (see also Figure 83). Correspondingly, the maximum acceptable level of inaccuracy for the $MARES_{APD}$ is not exceeded for all polynomial approximations excluding the 4th and 6th degree polynomials. In particular, the 5th degree polynomial approximations are more effective than the 4th degree polynomial approximations; since the overall decrease in inaccuracy (i.e. from -6.3% to -4.1%) is more than 1% for an additionally possessed parameter (see Figure 83). Overall, the 11th degree polynomials indicate the least possible inaccuracy in approximating annual peak load demands (see Figure 83).

In order to analyze the effectiveness of selecting 11th degree polynomials for approximating annual peak load demands, a comparison is made with 5th degree polynomials. Correspondingly, the LDC of the year 2002 is examined for both 5th and 11th degree polynomial approximations as depicted in left and right panels of Figure 81 respectively. See APPENDIX D for the plots of all approximated LDCs by using polynomials in the period 2000-2014. The comparison is based on the LDC of the year 2002; since it is the year for which the highest RE_{APD} is observed for using 5th degree polynomial approximations (i.e. -6.5%). For the same year, the RE_{APD} of approximation for using 11th degree polynomial is -3.4%; however 6 more parameters are needed to achieve this level of intended inaccuracy. The reduction in inaccuracy is not effective; since it is about 0.5% per each added parameter and also a 100% accuracy level cannot be achieved. As a matter of fact, the reduction in overall inaccuracy for the other years in the period 2000-2014 is much more less than this level by using 11th degree polynomial approximations (see Figure 80). In particular, an effective decrease in $MARES_{APD}$ (i.e. at least 1%) is also not achieved w.r.t. the 5th degree polynomial approximations by other polynomial approximations possessing additional functional parameter(s).

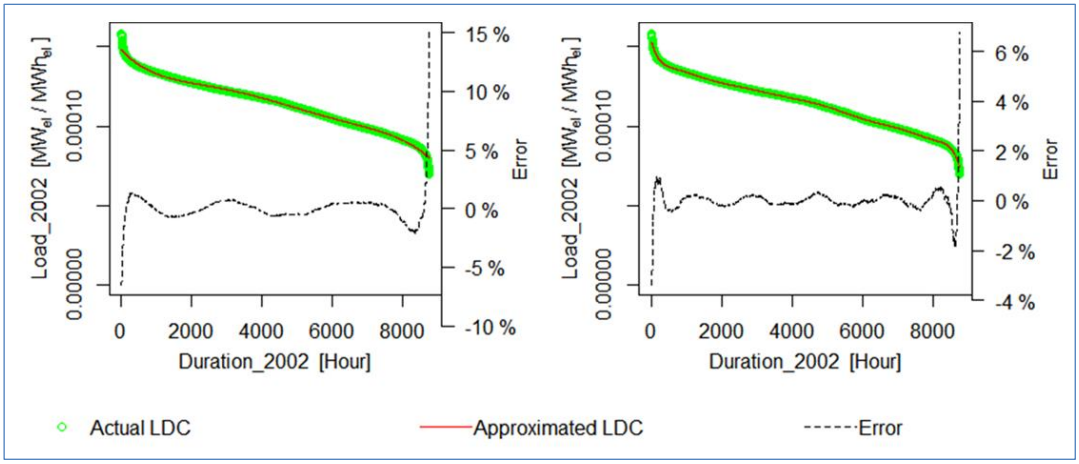

Figure 81- The comparison of the 5th degree polynomial approximation (left panel) to 11th degree polynomial approximation (right panel) (own calculation & illustration)

Also here, the effectiveness of the decrease in RE_{APD} cannot be assessed by both adjusted R^2 or any mentioned information criteria; since all of them account for the overall model adequacy but not for the inaccuracy in approximating a specific observation (i.e. annual peak load demand). Although the adjusted R^2 (see Table 42) generally increases with the increasing degree of polynomials (see Figure 80), it contradicts with the decrease in RE_{APD}. For example, the 5th degree polynomial approximation to LDC of the year 2014 indicates a RE_{APD} of -3.9%; whereas the 6th degree polynomial approximation for the same year indicates a RE_{APD} of -4.9% (see Figure 80). However the value of adjusted R^2 for 6th degree polynomial approximation is higher than 5th degree polynomial approximation (see Table 42) favoring the 6th degree polynomial approximation with higher RE_{APD} and higher total number of parameters. In the same manner, the value of AICc for 6th degree polynomial approximation is lower than 5th degree polynomial approximation (see Table 43) favoring the 6th degree polynomial approximation with higher RE_{APD} and higher total number of parameters. Hence, both of the model adequacy measures cannot specifically account for the selection of the degree of the adequate polynomial approximation to LDCs based on the RE_{APD}. To sum up, the adequate functional approximations to annual peak load demands are observed to be realized by the 5th degree polynomials among other considered polynomial approximations.

Note that the inaccuracy in approximating hourly loads increases toward the end of the duration as depicted in Figure 81. In particular, this causes overestimation of minimum magnitude of load demanded for the duration of 8760 hours or 8784 hours in a year. Although the minimum magnitude of demanded load is overestimated, neither the reliability of electricity supply nor the capacity expansion of base load power plants is overestimated. This is due to the fact that the base load constitutes the segment on the bottom of LDCs which is

in-between the origin and the highest magnitude of base load demanded (see Figure 31). Accordingly, the installed capacity of base load power plants equals to the highest magnitude of demanded base load. Since the highest magnitude of base load demanded generally occurs about 70% of the time (i.e. towards the mid of LDCs); it is considered that the mentioned inaccuracy do not interfere with the feasibility of capacity expansion planning of power plants.

In Figure 82, the relative error in approximating hourly load demand ($MARE_{HLD}$) w.r.t. the different degrees of polynomials are depicted for each considered year.

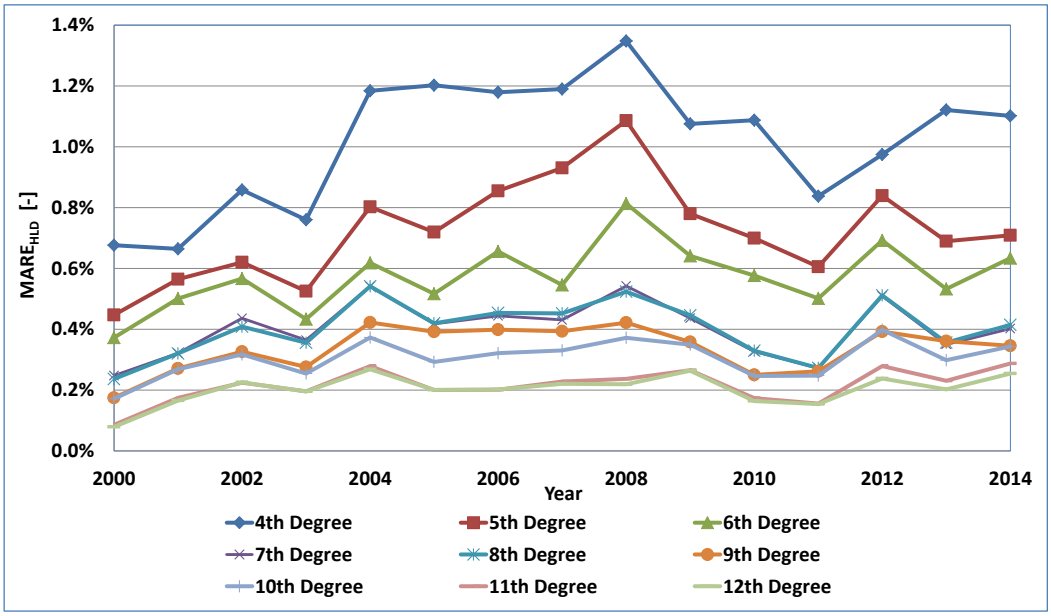

Figure 82- The $MARE_{HLD}$ for the approximated LDCs in the period 2000-2014 (own calculation & illustration)

It can be inferred from Figure 82 that the $MARE_{HLD}$ is higher than the RE_{APD}; whereas lower than the RE_{AGD} for each considered year. Similar to the previous measures of inaccuracy, the $MARE_{HLD}$ generally decreases with the increasing degree of polynomials. Although the residual sum of squares (RSS) decreases with the increasing degree of polynomials, a continuous decrease in $MARE_{HLD}$ is not observed; since it is unrelated to RSS by being a measure of predictive accuracy. For example, the 7th degree polynomial approximation to LDC of the year 2014 indicates a $MARE_{HLD}$ of 4.02E-03 with 5742 degrees of freedom; whereas the 8th degree polynomial approximation for the same year indicates a higher $MARE_{HLD}$ of 4.14E-03 with 5741 degrees of freedom (see Figure 82). This indicates that the 8th degree polynomial approximation is over fitted, and hence its predictive accuracy should be expected to be less than the 7th degree polynomial approximation.

Further, the 4th degree polynomial is observed to be indicating the highest inaccuracy of them all. Furthermore, the mean of $MARES_{HLD}$ is observed to be under 1% for all considered polynomial approximations excluding the 4th degree polynomials (see also Figure 83). Correspondingly, the maximum acceptable level for the mean of $MARES_{HLD}$ is not exceeded for all polynomial approximations excluding the 4th degree polynomial approximations. Moreover, the mean of $MARES_{HLD}$ for the 12th degree polynomial approximations is the lowest (i.e. 0.2%); however the reduction in inaccuracy w.r.t. the 5th degree polynomial approximations (i.e. 0.7%) is not effective; since 7 more parameters are needed to achieve this level of intended inaccuracy. In particular, an effective decrease in inaccuracy (i.e. at least 1%) w.r.t. the 5th degree polynomial approximations is also not achieved by other polynomial approximations possessing additional functional parameter(s).

Here, the effectiveness of the decrease in $MARE_{HLD}$ can also be measured by both adjusted R^2 or any mentioned information criteria; since both of the model adequacy measures mainly depend on the observed hourly load demand values which are also considered in the calculation of the $MARE_{HLD}$. In particular, the adjusted R^2 generally indicates infinitesimal increase as the degree of polynomials is increased (see Table 42); whereas the AICc generally decreases with the increasing degree of polynomials (see Table 43). Hence, both of the model adequacy measures indicate that 12th degree polynomials can adequately approximate the hourly load demand in each considered year. As aforementioned, an effective decrease in inaccuracy w.r.t. the 5th degree polynomial approximations is not achieved by the 12th degree polynomials due to the definition of the parsimonious function in the context of this study (see Footnote 123 on p. 196). The adjusted R^2 and the information criteria measure the adequacy in status quo; however in the next stage of the LDC concept, the parameters considered for approximation of LDCs will be forecasted for obtaining approximations to future LDCs. As per definition, 12th degree polynomials cannot be adequate approximations to past LDCs of Turkey. To sum up, the adequate functional approximations to hourly load demand in each year are observed to be realized by the 5th degree polynomials among other considered degree of polynomials.

In addition to the above mentioned inaccuracy analysis, the inaccuracy in approximation of LDCs is further assessed by calculating the $MARES_{AGD}$, the $MARES_{APD}$ and the mean of $MARES_{HLD}$ for the period 2000-2014 (see below).

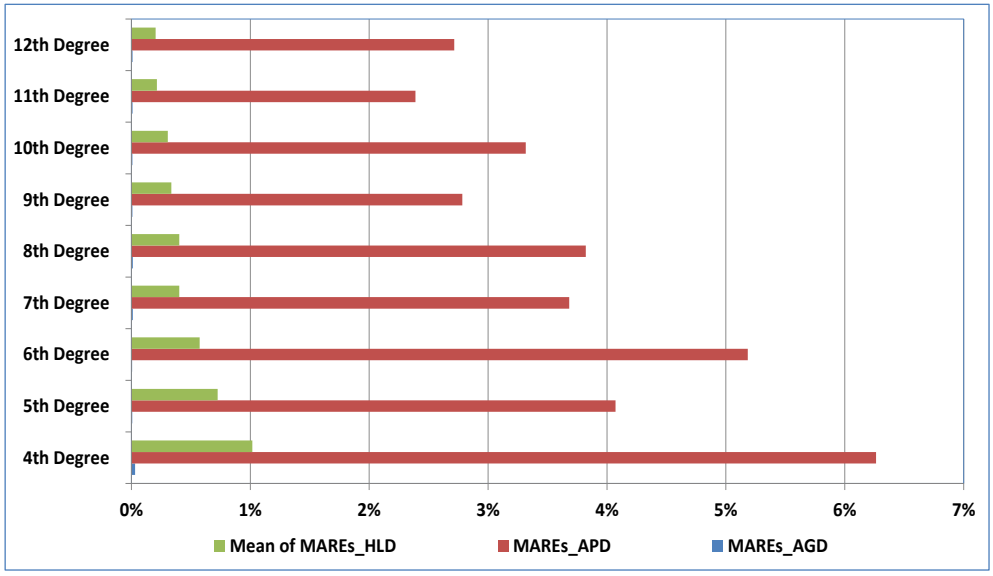

Figure 83- The $MARES_{AGD}$, the $MARES_{APD}$ and the mean of $MARES_{HLD}$ for the approximated LDCs in the period 2000-2014 (own calculation & illustration)

The $MARES_{AGD}$'s are nearly zero for all degree of polynomials making the approximations indistinguishable for determining the adequate functional approximation to past LDCs of Turkey. Further, the $MARES_{APD}$ ranges from 2.4% (for the 11th degree) to 6.3% (for the 4th degree) for the considered degree of polynomial approximations. Note that the maximum acceptable level of inaccuracy for the $MARES_{APD}$ is not exceeded for all polynomial approximations excluding the 4th and the 6th degree polynomials. The mean of $MARES_{HLD}$ ranges from 0.2% (for the 12th degree) to 1.02% (for the 4th degree) for the considered degree of polynomial approximations. Also, the $MARES_{HLD}$ indicates that the approximations are indistinguishable for determining the adequate functional approximation among the degrees of polynomials ranging from the 5th to the 12th degree. In addition, the mean of $MARES_{HLD}$ is observed to be under 1% for all considered polynomial approximations excluding the 4th degree polynomials. According to the assigned maximum acceptable level of inaccuracy for the $MARES_{AGD}$, the $MARES_{APD}$ and the mean of $MARES_{HLD}$, the adequate functional approximation to past LDCs of Turkey should be determined among the degree of polynomial functions ranging from the 5th to the 12th degree excluding the 6th degree. Hence, it has been observed that the desired level of inaccuracy in approximating annual peak load demand and the total number of parameters are the essential criteria for the selection of the adequate approximating function among polynomials. Subsequently, the mentioned polynomial approximations are further examined for observing whether an effective decrease in the $MARES_{APD}$ occurs for possessing additional functional parameter(s).

Here, the effectiveness of the decrease in $MARES_{APD}$ cannot be assessed by both adjusted R^2 or any mentioned information criteria; since $MARES_{APD}$ is an average value of all calculated $MARE_{APD}$ in the period 2000-2014 (see Eq. (12.2.15)); whereas all mentioned model adequacy measures can account for the overall model adequacy of a functional approximation in a year of the period 2000-2014. Therefore, it is aforementioned that an effective decrease in $MARES_{APD}$ should be at least 1% for possessing an additional functional parameter, if two different types of functional approximations have different total number of parameters.

Accordingly, the least overall approximation inaccuracy for annual peak demand can be achieved by using 11^{th} degree polynomials; however it is about 1.4% less than the corresponding overall inaccuracy of the 5^{th} degree polynomial approximations (see Figure 83). Nevertheless, the achieved level of accuracy is not effective considering the six more parameters possessed w.r.t. the 5^{th} degree polynomial approximations. In particular, an effective decrease in inaccuracy (i.e. at least 1% per additionally possessed parameter) w.r.t. the 5^{th} degree polynomial approximations is also not achieved by other polynomial approximations possessing additional functional parameter(s). Therefore, the 5^{th} degree polynomial function is selected among other polynomials to be used as an adequate functional approximation to LDCs of Turkey in the period 2000-2014. The result of the 5^{th} degree polynomial approximations to LDCs is tabulated in Table 44. See APPENDIX E for the summary statistics of all analyzed polynomials.

Table 44- The parameters of the 5^{th} degree polynomial approximation to LDCs in the period 2000-2014 (own calculation & illustration)

Year	β_0	β_1	β_2	β_3	β_4	β_5
2000	1.45553736E-04	-1.75698397E-08	8.03088767E-12	-2.24998796E-15	2.75360676E-19	-1.23586211E-23
2001	1.47988583E-04	-1.90436503E-08	8.02271745E-12	-2.14776272E-15	2.60591062E-19	-1.18161963E-23
2002	1.48024554E-04	-2.38797521E-08	1.14921341E-11	-3.03487496E-15	3.57933162E-19	-1.56717916E-23
2003	1.45029201E-04	-1.81550627E-08	8.72731595E-12	-2.48699729E-15	3.09959905E-19	-1.41527157E-23
2004	1.47387974E-04	-2.48575157E-08	1.35314534E-11	-3.83553103E-15	4.71571343E-19	-2.11066860E-23
2005	1.49140515E-04	-2.70437798E-08	1.45678339E-11	-4.03607203E-15	4.87433349E-19	-2.15089321E-23
2006	1.50602074E-04	-2.61687478E-08	1.34892250E-11	-3.74078428E-15	4.55794610E-19	-2.03540121E-23
2007	1.51968581E-04	-2.79472299E-08	1.37237580E-11	-3.62442868E-15	4.27246461E-19	-1.86678041E-23
2008	1.51033529E-04	-2.56648551E-08	1.27810595E-11	-3.57275443E-15	4.46160934E-19	-2.05426691E-23
2009	1.49309929E-04	-2.58866338E-08	1.33147566E-11	-3.62850541E-15	4.35779123E-19	-1.92820199E-23
2010	1.55153698E-04	-3.46540374E-08	1.71421500E-11	-4.32916943E-15	4.91513824E-19	-2.08204185E-23
2011	1.49219849E-04	-2.31434029E-08	1.09109456E-11	-2.90805809E-15	3.45677359E-19	-1.52584441E-23
2012	1.50872331E-04	-2.53675973E-08	1.20845372E-11	-3.24040982E-15	3.90396050E-19	-1.74625906E-23
2013	1.50505754E-04	-2.80863196E-08	1.46305536E-11	-3.98174000E-15	4.78425178E-19	-2.11539594E-23
2014	1.53370735E-04	-3.28308903E-08	1.67830233E-11	-4.39437825E-15	5.14030310E-19	-2.22855299E-23

12.2.2 Nonlinear Functional Approximation to Load Duration Curves of Turkey

In this section, the past LDCs of Turkey are approximated by using the exponential function, logarithmic function and the inverse of Hill's function (see p. 198 for their representations). The nonlinear functional approximations are applied on the corresponding LDCs by using the "nls" function (in package stats in R). The Gauss-Newton algorithm is selected for solving the nonlinear least squares problem (see Subsection 10.1.2.1.1 for more information). Since it is an iterative solution process, the starting values for the parameters must be given; in order to initiate the procedure to find the optimal parameters minimizing the residual sum of squares.

During the course of this study, an approach for finding the starting values for the parameters of exponential and logarithmic functions is proposed as subsequently explained. The initial parameter values, which are considered to be causing non-linearity, are estimated by guessing values (i.e. trial and error) and then linear least squares problems are solved to estimate starting values for the remaining parameters. For instance, the starting values of the exponential function approximations are estimated by guessing values for the parameter θ_2 (e.g. $k = 3.598709\text{E} - 03$) and then linear least squares problems are solved for finding the starting values for θ_0, θ_1 and θ_3 as represented below:

$$Z_t^* = \theta_0 + \theta_1 \exp(k * t) + \theta_3 t + \varepsilon_t, \quad \text{where } 1 \leq t \leq n \ \wedge \ n = 8760 \ or \ 8784 \tag{12.2.21}$$

Once the initial parameter values, which are sufficiently close to the optimal parameter values, are determined; the iteration procedure will be started. The process will stop when the decrease in the residual sum of squares from iteration to iteration is less than a specific amount (i.e. called the tolerance level). The tolerance level and maximum number of iterations are set at 1E-05 and 50 respectively. At the end of the iteration procedure, the optimal parameters are obtained. Similarly, the starting values for the logarithmic functional approximations are estimated by guessing values for the parameters α_2 and α_3 (e.g. $c_1 = 2404.722$ and $c_2 = 7735.391$ respectively) and then linear least squares problems are solved for finding starting values for α_0 and α_1 as represented below:

$$Z_t^* = \alpha_0 + \alpha_1 log \frac{t + c_1}{c_1 + c_2 - t} + e_t, \quad \text{where } 1 \leq t \leq n \ \wedge \ n = 8760 \ or \ 8784 \tag{12.2.22}$$

The starting parameter values for the inverse of Hill's function (i.e. b_0, c_0 and m_0) are determined by the following procedure as introduced by Kato et al. (p. 305):

1. Set $b_0 = 1 + \alpha$, where α is given empirically,
2. $c_0 = Z_0^* - Z_{min}^*$, where Z_0^* is the actual load data when time equals to $b_0/2$,
3. $m_0 = \frac{\log(b_0/t-1)}{\log(c_0/(Z_t^* - Z_{min}^*))}$, where the data pair (Z_t^*, t) is selected from the actual data sets considering the values in the interval defined by $1 \leq t \leq n \ \wedge \ n = 8760 \ or \ 8784$.

Similar to the analysis in the previous subsection, the inaccuracies in nonlinear functional approximations are examined based on the RE_{AGD}, RE_{APD} and $MARE_{HLD}$ for each year in the period 2000-2014. Further, the results of inaccuracies in corresponding approximations are also compared with the inaccuracy in 5th degree polynomial approximations to LDCs.

In Figure 84, the RE_{AGD} w.r.t. the considered nonlinear approximating functions and the 5th degree polynomial are depicted for each considered year.

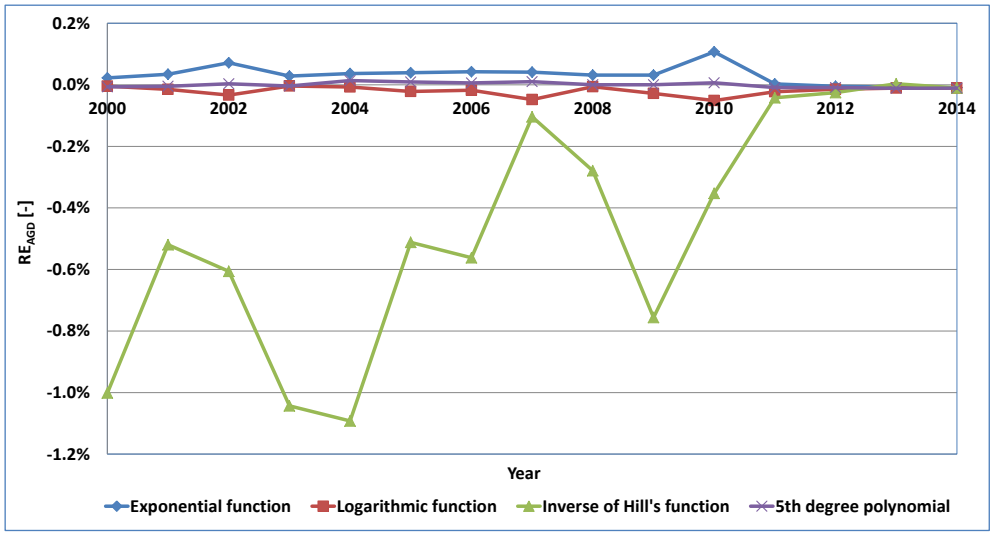

Figure 84- The RE_{AGD} for the approximated LDCs in the period 2000-2014 (own calculation & illustration)

It can be inferred from Figure 84 that the inverse of Hill's function indicates the highest RE_{AGD} among all other functions and has the least number of parameters[128]. The other functions mainly overestimate the gross annual electricity demand; however the corresponding inaccuracies are less than 0.2% for each considered year.

[128] Note that the exponential function, logarithmic function and the inverse of Hill's function possess 4, 4 and 3 parameters in total respectively.

Further, the $MARES_{AGD}$ is observed to be under 1% for all considered functional approximations to past LDCs of Turkey (see also Figure 87). Correspondingly, the maximum acceptable level for the $MARES_{AGD}$ is not exceeded for all considered functional approximations in Figure 84. Accordingly, the inaccuracy in the 5th degree polynomial approximations is the lowest (see also Figure 87). However the achieved level of accuracy is not effective w.r.t. the other approximations; since the decrease in $MARES_{AGD}$ is less than 1% per each additionally possessed parameter. In particular, an effective decrease in $MARES_{AGD}$ is not achieved w.r.t. the inverse of Hill's function which has the least total number of parameters among others. Furthermore, the effectiveness of the decrease in RE_{AGD} cannot be measured both by adjusted R^2 or any mentioned information criteria; since the former is only valid for linear regression analysis and the latter depends on the maximization of the probability of the observed data and does not account for the minimization of the error in approximating the area under the approximating function. To sum up, the adequate functional approximations to annual gross electricity demands are observed to be realized by the approximations using the inverse of Hill's function among other considered functional approximations.

In Figure 85, the RE_{APD} w.r.t. the considered nonlinear approximating functions and the 5th degree polynomial are depicted for each considered year.

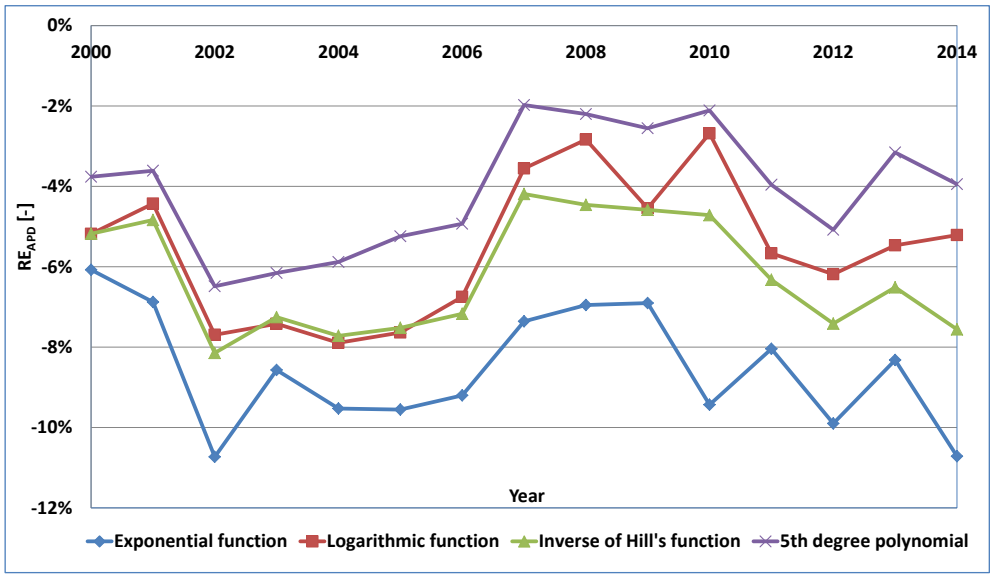

Figure 85- The RE_{APD} for the approximated LDCs in the period 2000-2014 (own calculation & illustration)

It can be inferred from Figure 85 that all considered functions underestimate the annual peak load demand. Further, the exponential functional approximations indicate the highest RE_{APD} among all other considered functions in the figure and relatively ineffective w.r.t. the

logarithmic functional approximations which have the same total number of parameters. Also here, the effectiveness of the decrease in RE_{APD} cannot be assessed both by adjusted R^2 or any mentioned information criteria; since the former is only valid for linear regression analysis and either of them can account for the overall model adequacy but not specifically for the adequacy in approximating annual peak load demand.

Furthermore, the $MARES_{APD}$ is observed to be under 5% only for the 5th degree polynomial approximations (see also Figure 87). Correspondingly, the maximum acceptable level for the $MARES_{APD}$ is exceeded for all considered nonlinear functional approximations and hence, they are considered to be not eligible for approximating annual peak load demand of Turkey. To sum up, the adequate functional approximations to annual peak load demands are observed to be realized by the 5th degree polynomials among other considered functional approximations.

In Figure 86, the $MARE_{HLD}$ w.r.t. the considered nonlinear approximating functions and the 5th degree polynomial are depicted for each considered year.

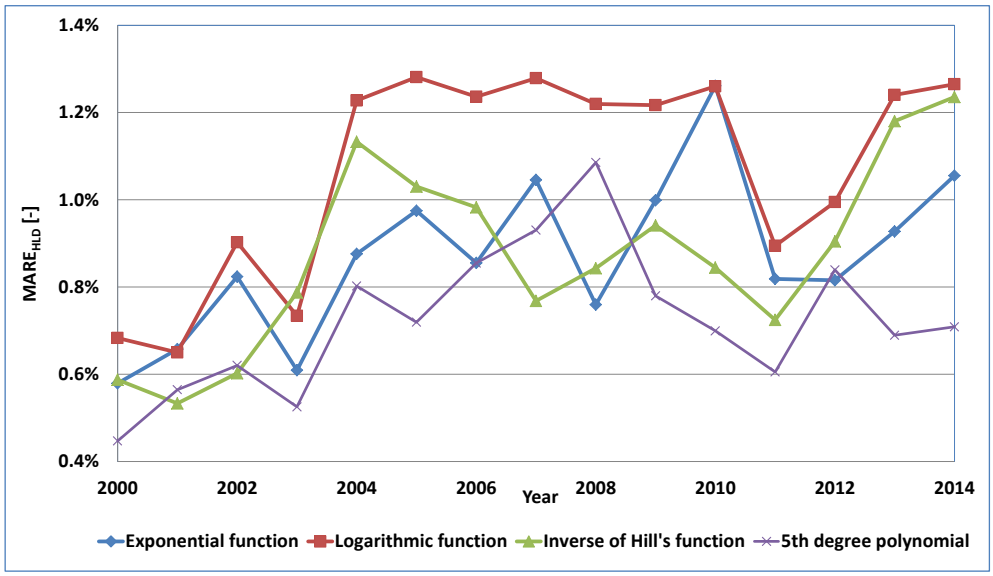

Figure 86- The $MARE_{HLD}$ for the approximated LDCs in the period 2000-2014 (own calculation & illustration)

It can be inferred from Figure 86 that the $MARE_{HLD}$ is higher than the RE_{AGD}; however lower than the RE_{APD}. Further, the logarithmic functional approximations indicate the highest $MARE_{HLD}$ among considered functions in the figure. Furthermore, the mean of $MARES_{HLD}$ is observed to be under 1% for all considered polynomial approximations excluding the logarithmic functional approximations (see also Figure 87). Correspondingly, the maximum acceptable level for the mean of $MARES_{HLD}$ is not exceeded for all considered

approximations excluding the logarithmic functional approximations. Moreover, the 5th degree polynomial approximations indicate the lowest mean of $MARES_{HLD}$ among all other considered functions (i.e. 0.7%). However the reduction in inaccuracy is not effective w.r.t. the exponential functional approximations (i.e. 0.9%) and the inverse of Hill's function (i.e. 0.9%); since 2 and 3 more parameters are needed to achieve this level of intended inaccuracy respectively (i.e. under 1% for each additionally possessed parameter). In particular, an effective decrease in inaccuracy w.r.t. the inverse of Hill's function is not observed; since it possesses the least number of parameters in total.

Here, the effectiveness of the decrease in $MARE_{HLD}$ can be measured by any mentioned information criteria; since they mainly depend on the observed hourly load demand values which are also considered in the calculation of $MARE_{HLD}$. In Table 45, the AICc values of the nonlinear functional and the 5th degree polynomial approximation are tabulated. It can be inferred from Table 45 that the 5th degree polynomial approximations indicate lower AICc values w.r.t. the exponential and the logarithmic polynomial approximations; whereas this is most of the time true for the approximations using the inverse of Hill's function. Note that in Table 45 only for the six of the values marked as bold italic, the AICc values of 5th degree polynomial approximations are higher than the corresponding values for the inverse of Hill's function. In this respect, the AICc is not a consistent criterion for choosing an adequate functional approximation to LDCs which is valid in the period 2000-2014. Also, the BIC of the nonlinear linear functional approximations indicate the same situation (see APPENDIX B). Therefore, the adequate functional approximations to hourly load demands are considered to be realized by the inverse of Hill's function as per definition of the parsimonious function in this study (see Footnote 123 p. 196).

Table 45- The AICc values of the functional approximations to LDCs of Turkey in the period 2000-2014 (own calculation & illustration)

Years	Type of Function			
	Exponential Function	Logarithmic Function	Inverse of Hill's Function	5th Degree Polynomial
2000	-131783.4	-131317.4	-133032.6	-135543.4
2001	-135206.6	-136729.7	-139148.0	***-138023.3***
2002	-125295.6	-127406.2	-129644.3	-129894.5
2003	-134275.6	-133355.5	-134322.8	-136094.8
2004	-134757.9	-132558.2	-134531.2	-135855.9
2005	-137248.3	-136279.3	-139222.1	-141025.7
2006	-144099.8	-142338.7	-145712.7	***-145449.6***
2007	-146248.5	-146741.1	-153300.3	***-149142.0***
2008	-157218.0	-154809.1	-159546.9	***-154917.7***
2009	-148945.8	-148247.9	-152075.4	***-151376.1***
2010	-147011.1	-152673.6	-155791.6	-157876.1
2011	-174310.9	-175791.5	-178478.3	-179876.8
2012	-198701.0	-198721.4	-201325.5	***-200524.2***
2013	-208208.9	-206870.9	-208470.3	-212550.6
2014	-204637.1	-207741.5	-207619.7	-213157.6

In addition to the above mentioned inaccuracy analysis, the inaccuracy in approximation of LDCs is further assessed by calculating the $MARES_{AGD}$, the $MARES_{APD}$ and the mean of $MARES_{HLD}$ for the period 2000-2014 (see below).

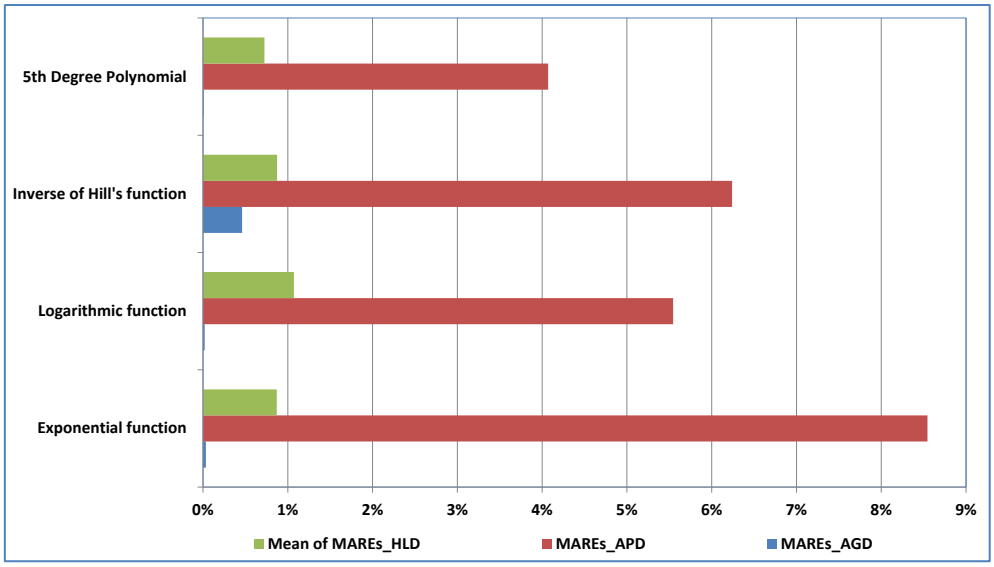

Figure 87- The $MARES_{AGD}$, the $MARES_{APD}$ and the mean of $MARES_{HLD}$ for the approximated LDCs in the period 2000-2014 (own calculation & illustration)

It can be inferred from Figure 87 that the $MARES_{AGD}$ are not exceeded for all considered types of functions. Further, the maximum acceptable level for the $MARES_{APD}$ is not exceeded only for the 5th degree polynomial approximations. Furthermore, the maximum acceptable level for the mean of $MARES_{HLD}$ is not exceeded for all considered approximations excluding the logarithmic functional approximations. Accordingly, the assigned maximum acceptable level of inaccuracy for the $MARES_{APD}$ is observed to be the distinctive criterion; since it is

satisfied only for the 5^{th} degree polynomial approximations. Therefore, the 5^{th} degree functional approximations are determined to be the adequate functional approximations to LDCs of Turkey in the period 2000-2014. The result of the 5^{th} degree polynomial approximations to LDCs is tabulated in Table 44. See APPENDIX D and APPENDIX E for the plots and the summary statistics of all considered functional approximations respectively.

13 FORECASTING APPROXIMATIONS TO FUTURE LOAD DURATION CURVES (3rd STAGE)

In this chapter, comprehensive information is provided on obtaining functional approximations to future LDCs of Turkey in the period 2015-2025 (i.e. the 3rd stage of the introduced concept). In Section 13.1, comprehensive information on the type of methods for forecasting functional approximations to LDCs are provided, such as using regression analysis and TSA. At the end of the section, a summary on the type of forecasting methods for approximations to LDCs is given and a discussion is carried out for selecting the convenient type of method for obtaining future approximations to the LDCs of Turkey. In the final Section 13.2, information is given about the analysis on obtaining approximations to LDCs of Turkey for the period 2015-2025.

13.1 The Methods for Obtaining Functional Approximations to Future Load Duration Curves

The forecasting functional approximations to LDCs can be based on the econometric analysis of the variations in the elements of the sequences represented below:

1. The lengths of the estimated line segments (i.e. the result of the discrete functional approximations to LDCs) as indicated in Eqs. (12.1.2) and (12.1.11).
2. The parameters of the approximating functions (i.e. the result of the smooth functional approximations to LDCs) as indicated in Eq. (12.1.18).

In this study, discrete approximations to LDCs of Turkey are not considered and the information on forecasting using the corresponding sequences will not be given in detail. For more information see the mentioned studies in Subsection 12.1.1 and 12.1.2. In the following subsections, regression analysis and the Box-Jenkins method of univariate time series analysis are discussed for forecasting smooth functional approximations to future LDCs.

13.1.1 Obtaining Functional Approximations to Future Load Duration Curves using Regression Analysis

In this approach, it is assumed that the parameters of the approximating functions of LDCs evolve in time in response to the variations in the price of electrical energy (prc), income (inc) of consumers, heating degree days (hdd), cooling degree days[129] (cdd). This assumption originates from the fact that the consumers adjust their consumption of electrical energy according to the corresponding variables. For example, an increase in the personal income enhances the quality of life by purchasing more of the electronics, which in turn raises the demand for electricity and changes the shape of LDCs. Since the changes in the shape of LDCs are reflected by the approximation functions, the forecasts of the parameters can be utilized for forecasting LDCs (Uri N. D., 1977, p. 405).

Hence, a multiple linear regression model is proposed by Uri (1977), and Uri and Maybee (1978) for forecasting LDCs as indicated in Eq. (13.1.1) in matrix form:

$$\begin{bmatrix} y_k(1) \\ \vdots \\ y_k(j) \\ \vdots \\ y_k(\eta) \end{bmatrix} = \begin{bmatrix} 1 & prc_{1,2} & inc_{1,3} & hdd_{1,4} & cdd_{1,5} \\ 1 & prc_{2,2} & inc_{2,3} & hdd_{2,4} & cdd_{2,5} \\ \vdots & \vdots & \vdots & \vdots & \vdots \\ 1 & prc_{\eta,2} & inc_{\eta,3} & hdd_{\eta,4} & cdd_{\eta,5} \end{bmatrix} \begin{bmatrix} \mathscr{b}_{0,k} \\ \mathscr{b}_{1,k} \\ \mathscr{b}_{2,k} \\ \mathscr{b}_{3,k} \\ \mathscr{b}_{4,k} \end{bmatrix} + \begin{bmatrix} \epsilon_{1,k} \\ \epsilon_{2,k} \\ \epsilon_{3,k} \\ \vdots \\ \epsilon_{\eta,k} \end{bmatrix} \tag{13.1.1}$$

The given above model is composed of a dependent variable "$y_k(j)$" ($j = 1, \dots, \eta$) which is related to four independent variables (i.e. prc, inc, hdd, cdd) through the regression parameters ($\mathscr{b}_{0,k}, \dots, \mathscr{b}_{4,k}$) and the error term ($\epsilon_{i,k}$). The symbol "$k$" denotes the k^{th} height or functional parameter depending on the considered type of approximation function and is defined in the interval $1 \leq k \leq N \ \wedge \ k \in \mathbb{Z}^+$. The symbol "$N$" indicates the total number of steps in a discrete function or the total number of parameters in a smooth function depending on its usage.

The symbol "η" indicates the maximum number of years considered for the analysis. The variable $y_k(j)$ denotes the k^{th} height or functional parameter for the approximated LDC of j^{th} considered year ($j = 1, \dots, \eta$). In particular, $y_k(j)$ can be substituted with $\hat{\xi}_k(j)$, $\hat{h}_k(j)$ or $\hat{\beta}_k(j)$ depending on the chosen method of approximation to LDCs. By using this relation, the

[129] Uri (1977, p. 406) defines a degree day as a unit measuring the extent to which the outdoor mean (average of maximum and minimum) daily dry-bulb temperature fall below (in the case of heating) or rises above (in the case of cooling) a base of 65°F (~18°C).

variation in same k^{th} height or functional parameter during a considered period can be analyzed in response to the past variations in the independent variables and can be forecasted according to the future values of the corresponding variables.

The matrix form of the model can be expressed in parsimonious form as a vector "$\boldsymbol{y}_k$" containing the dependent variable which is related to the design matrix "$\boldsymbol{x}$" composed of the independent variables with the vector "$\boldsymbol{\mathscr{b}}_k$" containing the regression parameters and the vector "$\boldsymbol{\epsilon}_k$" containing the error terms as shown below:

$$\boldsymbol{y}_k = \boldsymbol{x}\boldsymbol{\mathscr{b}}_k + \boldsymbol{\epsilon}_k \tag{13.1.2}$$

Given below in Eq. (13.1.3) are the corresponding parsimonious form of the regression models for each k^{th} height in Eq. (12.1.2) or Eq. (12.1.11) or for each k^{th} functional parameter in Eq. (12.1.18) of the considered type of approximation function (Uri & Maybee, 1978, p. 257).

$$\begin{aligned} \boldsymbol{y}_1 &= \boldsymbol{x}\boldsymbol{\mathscr{b}}_1 + \boldsymbol{\epsilon}_1 \\ &\vdots \\ \boldsymbol{y}_N &= \boldsymbol{x}\boldsymbol{\mathscr{b}}_N + \boldsymbol{\epsilon}_N \end{aligned} \tag{13.1.3}$$

The estimation of the regression parameters for the system of equations in (13.1.3) is stated to be carried out simultaneously rather than an equation-by-equation application of least-squares method. In order the estimates $\widehat{\boldsymbol{\mathscr{b}}}_1$, $\widehat{\boldsymbol{\mathscr{b}}}_2$,..., $\widehat{\boldsymbol{\mathscr{b}}}_N$ to be more efficient, the seemingly unrelated technique of Zellner on the corresponding system of equations is applied (Uri & Maybee, 1978, p. 257). The basis of the Zellner's technique is the simultaneous estimation of regression parameters in all equations by applying Aitken's generalized least-squares (see Eq. (10.1.48) on p. 102 for more information) to the whole system of equations (Zellner, 1962, pp. 348-349). In order to construct such Aitken estimators, the disturbance term's variances and covariances are employed on the basis of the residuals derived from an equation-by-equation application of least-squares method. The estimates of the covariances between $\boldsymbol{\epsilon}_1$,…,$\boldsymbol{\epsilon}_n$ are obtained by the estimated covariances of the elements in $\boldsymbol{y}_1$,…, $\boldsymbol{y}_N$. Zellner states that the gain in efficiency can be quite large if independent variables in different equations are not highly correlated and if disturbance terms in different equations are highly correlated.

During forecasting using the proposed regression method, it is assumed that the future value of y_k in year $\eta + i$ (i.e. $y_k(\eta + i)$ where $i > 0$) can be forecasted by using the estimated parameters ($\widehat{\mathscr{b}}_{0,k}, \dots, \widehat{\mathscr{b}}_{4,k}$) and the forecasted values $prc_{\eta+i,}, inc_{\eta+i,3}, hdd_{\eta+i,4}, cdd_{\eta+i,5}$.

The proposed regression model can be adapted for forecasting the estimated k^{th} functional parameter (i.e. $\hat{\beta}_k(\eta + l)$) in any smooth function approximations to LDCs by substituting $\boldsymbol{y}_k$ with the corresponding parameters of the function. Similarly, the k^{th} height of the step function resulted from ad hoc or optimal approximations to LDCs can be forecasted.

In Table 46, the accuracy results are tabulated for the obtained approximations to future LDCs in the previous studies. Note that although the approximations of LDCs are carried out with different type of smooth functions, the previously mentioned regression approach was used for obtaining the approximations to future LDCs.

Table 46- The comparison of the areas under the forecasted LDCs w.r.t. the chosen method of approximations to LDCs (own illustration)

Year	Smooth Approximations			
	5th Degree Polynomial (Uri, 1977)		Exponential Function (Uri & Maybee, 1978)	
	Area under the Future LDC	% Deviation from Unity	Area under the Future LDC	% Deviation from Unity
1973	1.0217	2.17%	1.0111	1.11%
1974	1.0598	5.98%	1.0591	5.91%

Uri[130] (1977, p. 406) analysed the deviation of the area under the 5th degree polynomial approximations to future LDCs w.r.t. unity. The author indicated that the area under the future LDC for the year 1973 is 1.0217 with a deviation of 2.17% from unity; whereas it is 1.0598 for the future LDC of the year 1974 with a deviation of 5.98% from unity (see Table 46). The future LDC of the year 1974 is observed to be not as accurate as the LDC of the year 1973. It is claimed that the year 1974 is an uncharacteristic year for electric utilities as a result of non-economically induced conservation effects diminishing their sales. Therefore, the regression analysis carried out with the considered independent variables may lack information in explaining untypical circumstances. Nevertheless, the corresponding method of LDC forecasting has a tendency to over-forecast.

Uri and Maybee (1978, p. 259) analysed the deviation of the area under the exponential function approximations to future LDCs w.r.t. unity. The authors indicated that the area under the future LDC of the year 1973 is 1.0111 with a deviation of 1.11% from unity; whereas it is 1.0591 for the future LDC of the year 1974 with a deviation of 5.91% from unity. The future

[130] The results are based on hourly load data for FPC Region 5 consisting of New Mexico, Texas, Louisiana, Arkansas, Oklahoma, Kansas, and parts of Missouri and Mississippi for the period 1965 through 1974.

LDC of the year 1974 is observed to be not as accurate as the LDC of the year 1973. As it is mentioned previously, it is claimed that the year 1974 is an uncharacteristic year for electric utilities and the considered independent variables may lack information in explaining untypical circumstances. Nonetheless, the mentioned method of LDC forecasting is argued to be indicating a tendency to over forecast.

It can be inferred from the results that the lack of accuracy in long term forecasting of independent variables causes lack of accuracy for obtaining approximations to future LDCs. Although the inaccuracy in future LDC is analyzed for only two years; it shows weakness for forecasting over longer periods subject to the limitation of accuracy of such forecasts for independent variables.

13.1.2 Obtaining Functional Approximations to Future Load Duration Curves using Time Series Analysis

In this approach, the approximations to future LDCS are obtained according to the selection of the adequate Box-Jenkins time series model, which can account for the periodicity in the considered sequence of smooth functional parameters. Correspondingly, the general seasonal autoregressive integrated moving average (SARIMA[131]) models are considered for forecasting functional parameters of any considered smooth function.

In the following, forecasting parameters of linear exponential function (see Eq. (12.1.14) on p. 190) is explained; however it can be applied for forecasting the parameters of any considered smooth function. Before forecasting, the parameters of the exponential function are estimated on an annual basis over η years forming a sequence of estimates $\hat{\theta}_k$ for each θ_k represented in $(n \times 1)$ vector "$\boldsymbol{S}$" as follows:

$$\boldsymbol{S} = \left(\hat{\theta}_0(1), \hat{\theta}_1(1), \cdots, \hat{\theta}_N(1), \cdots, \hat{\theta}_0(j), \hat{\theta}_1(j), \cdots, \hat{\theta}_N(j), \cdots, \hat{\theta}_0(\eta), \hat{\theta}_1(\eta), \cdots, \hat{\theta}_N(\eta)\right) \quad (13.1.4)$$

The symbol "$\hat{\theta}_k(j)$" denotes the estimated k^{th} parameter of Eq. (12.1.14) calculated for the estimation of LDC in the j^{th} considered year $(j = 1, \dots, \eta)$. The forecasting of the functional parameters are based on the assumption that the parameters vary through time and the corresponding variation in the sequence can be determined by using Box-Jenkins method of univariate time series analysis (Uri & Maybee, 1980).

[131] See p. 130 for more information.

In order to forecast the parameters, a general ARIMA$(p,d,q)\times(P,D,Q)_4$ model is proposed as given below (Maybee & Uri, 1980, p. 131):

$$\Phi_P(B^4)\nabla_4 x_t = \Theta_Q(B^4)a_t \tag{13.1.5}$$

In the above given general form, the symbol "x_t" denotes the t^{th} parameter in the sequence of parameters (i.e. $x_t = \boldsymbol{S}(t)$). Further, the index "t" is defined in the interval $1 \leq t \leq n \ \wedge \ t \in \mathbb{Z}^+$ and the term "n" equals to the number of elements in $\boldsymbol{S}$. Furthermore, the symbol "B" denotes the back shift operator (i.e. $B^m x_t = x_{t-m}$). Moreover, the symbol "∇_4" represents the seasonal difference operator and indicates that the series is seasonally differenced once $\nabla_4 = (1 - B^4)$. The symbol "Φ" represents the seasonal autoregressive parameter; whereas the symbol "Θ" indicates the seasonal moving average parameter. Finally, the t^{th} random shock is represented as "a_t".

For the periodic data of a four-parameter approximation, the seasonality is considered to be observed through the first estimated value "$\boldsymbol{S}(1)$" to the fifth estimated value "$\boldsymbol{S}(5)$" and so forth (i.e. with a time lag of 4 observations). Namely, the estimated constant of the function $\hat{\theta}_0(1)$ of the LDC in year 1974 (i.e. 1st LDC approximated) is related to $\hat{\theta}_0(2)$ of the LDC of the year 1975 (i.e. 2nd LDC approximated) and so forth. The same analogy can be considered for the other estimated parameters such as $\hat{\theta}_1(1)$ and $\hat{\theta}_1(2)$ for the first parameters in the 1st and 2nd approximated LDCs.

According to the time series analysis of the sequence by Maybee and Uri (1980, p. 131), the adequate model for forecasting LDCs is found to be the model given in Eq. (13.1.6) (i.e. $ARIMA(0,0,0)\times(0,1,1)_4$). Note that the given below representation is the corrected representation of the model, which is given in Maybee and Uri. Although the models are correctly described, their representations are not truly written.

$$(1 - B^4)x_t = (1 - \theta_4 B^4)a_t \tag{13.1.6}$$

The considered model implies that the series is needed to be once seasonally differenced; in order to satisfy the stationarity condition. The model also indicates covariance at lag 4 for which one periodic moving average parameter is determined. The forecasting accuracy of the

proposed model[132] indicates that the area under the forecasted curve for the year 1985 is 1.000289 with a deviation of 0.03% from unity. It has been concluded that the deviation is at an acceptable level of tolerance for long-range forecasting of LDCs (Maybee & Uri, p. 132).

13.1.3 A Summary on Obtaining Functional Approximations to Future Load Duration Curves

The proposed methods for forecasting functional parameters of future LDCs exhibit advantages and disadvantages in practice as follows:

- The accuracy in obtaining approximations to future LDCs by using regression method is highly dependent on the accuracy of the forecasted inputs such as prc, inc, hdd, cdd.
- In addition, it is also observed that the inputs for multiple regression analysis may lack information in explaining untypical circumstances.
- The accuracy in forecasting functional parameters by using univariate time series analysis is observed to be at an acceptable level; however it is a more advanced method compared to the application of the multiple linear regression analysis.

In this study, the Box-Jenkins method of univariate time series analysis is considered for forecasting the functional parameters of the future LDCs of Turkey due to the given reasons below:

- First of all, the level of inaccuracy is observed to be at an acceptable level for using in capacity expansion planning of power plants in Turkey.
- Finally, the application of univariate time series analysis does not make it necessary to be dependent on any inputs to be forecasted for Turkey.

[132] The results are based on hourly load data for Federal Regulatory Commission (FERC) Region 5 consisting of the states of New Mexico, Texas, Louisiana, Arkansas, Oklahoma, Kansas and parts of Missouri and Mississippi for the period 1965 through 1974.

13.2 Obtaining Functional Approximations to Load Duration Curves of Turkey for the Period 2015-2025

In this section, an adequate seasonal ARIMA model of order[133] P, D and Q is determined for the sequence which consists of the functional parameters (see Table 44 on p. 214) from the 5th degree polynomial approximations to LDCs of Turkey in the period 2000-2014. The relation of the seasonal ARIMA model with the corresponding sequence is achieved by a three-stage iterative procedure based on the Box-Jenkins model building process (see Subsection 10.2.8 for more information). In the 4th fourth stage, the functional parameters of the annual LDCs of Turkey in the period 2015-2025 are forecasted. Thus, the approximations to future LDCs are obtained by using the forecasted functional parameters.

The analysis is carried out by using the license free statistical software R (version 3.1.2) and also by using the RStudio IDE (Integrated Development Environment, Version 0.98.1102) which is a license free user interface for R.

The 1st Stage- Model Identification

During this stage, subclasses of parsimonious models are specified according to how the considered data were generated. In particular, the objective is to obtain some tentative values of P, D and Q orders needed in the general seasonal ARIMA model building process.

First of all, the functional parameters of the 5th degree polynomial approximations to all LDCs (i.e. a sample size of 90 observations) are plotted and visually examined for stationarity (see Figure 88). In the figure, the values corresponding to the indices between 1 and 6 represent the functional parameters of the approximated LDC of year 2000. Similarly, the values corresponding to the indices between 7 and 12 represent the functional parameters of the approximated LDC of year 2001 and so on. It can be inferred from the figure that the sequence is non-stationary according to the indicated periodical (also called seasonal) pattern that repeats itself over 6 period (i.e. the frequency of the seasonality with a seasonal lag of 6). The periodical pattern is exhibited by the intercepts of the polynomials with the indices $1,7,\ldots 85$ in the sequence. The other parameters have values close to zero.

[133] Note that the orders P, D and Q indicate the order of seasonal autoregressive component, seasonal differencing and seasonal moving average component of a general seasonal ARIMA model respectively.

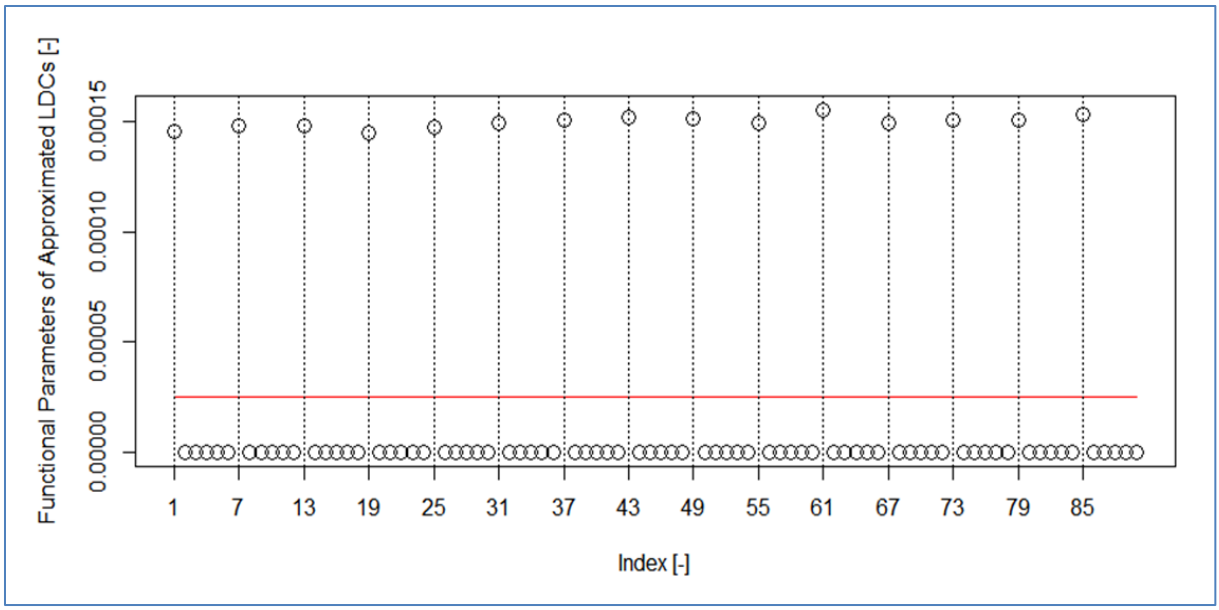

Figure 88- The parameters of the 5th degree polynomials (black circles) and their mean (red line) for the approximated LDCs in the period 2000-2014 (own calculation & illustration)

The sample ACF of the sequence indicates significant spikes at the seasonal lags 6, 12 …66 which decay slowly indicating non-stationary behavior (see Figure 89). A seasonal difference should be taken; in order to remove the periodicity. Nevertheless, the non-seasonal autocorrelations, in between, are much smaller and follow a linear decaying pattern. Correspondingly, any regular differencing is not required.

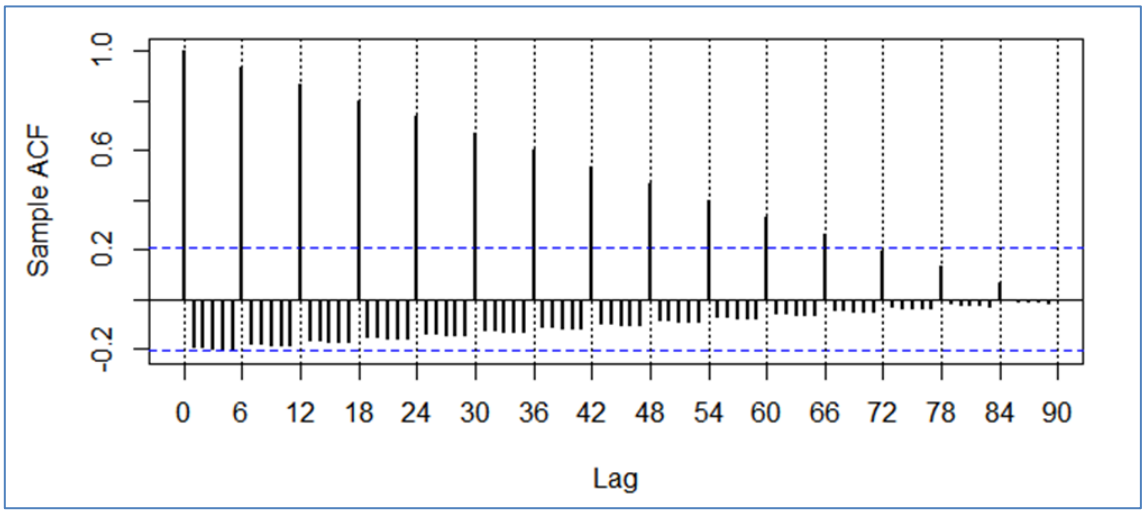

Figure 89- The sample ACF plot of the sequence formed by the functional parameters of the approximated LDCs (own calculation & illustration)

In Figure 90, the first order difference of the sequence is displayed. It can be inferred from the figure that the periodical pattern prevailing in the sequence has disappeared. Most of the values lie close to the mean of the sequence; whereas the others vary randomly around the mean. Note that the randomly varying values results from the seasonally differenced values of

the intercepts; whereas the other parameters do not show any substantial variation as before and after the differencing. Hence, sample ACF and the sample PACF are subsequently analyzed.

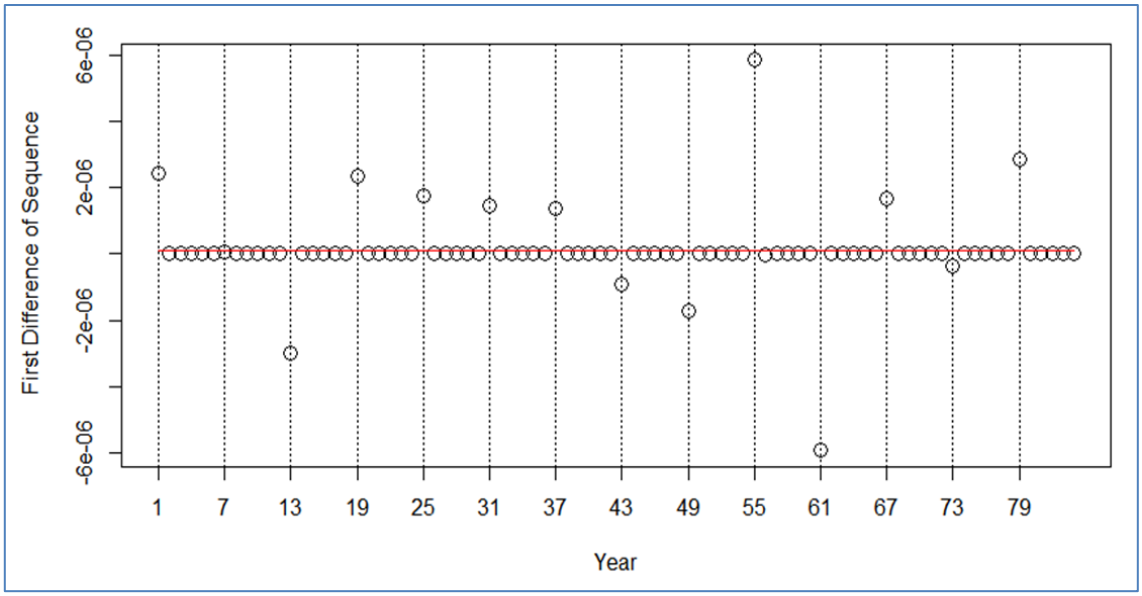

Figure 90- The scatter plot of the first order difference of the sequence (circle) and its mean (dashed line) (own calculation & illustration)

In Figure 91, the sample ACF and the sample PACF plots of the first difference of the sequence is represented. The sample ACF of the once differenced sequence indicates that the stationarity is achieved. Both the sample ACF and the sample PACF indicate highly significant spikes at the 6^{th} lag. In addition, the sample ACF displays a significant spike at lag 42; whereas the sample PACF indicates at lag 54. The pattern in sample ACF suggests a seasonal moving average model of order Q equals to 1; while the spikes in the sample PACF indicates a seasonal autoregressive model of order P equals to 1. Another possible model is a seasonal ARIMA(1,1,1)[6] model. Note that the value in brackets represents the frequency of the periodicity (i.e. 6). In addition, the number of times the data have been seasonally differenced to become stationary equals to one (i.e. D =1). During the next stage, the parameter estimation process is carried out according to the possible tentative models.

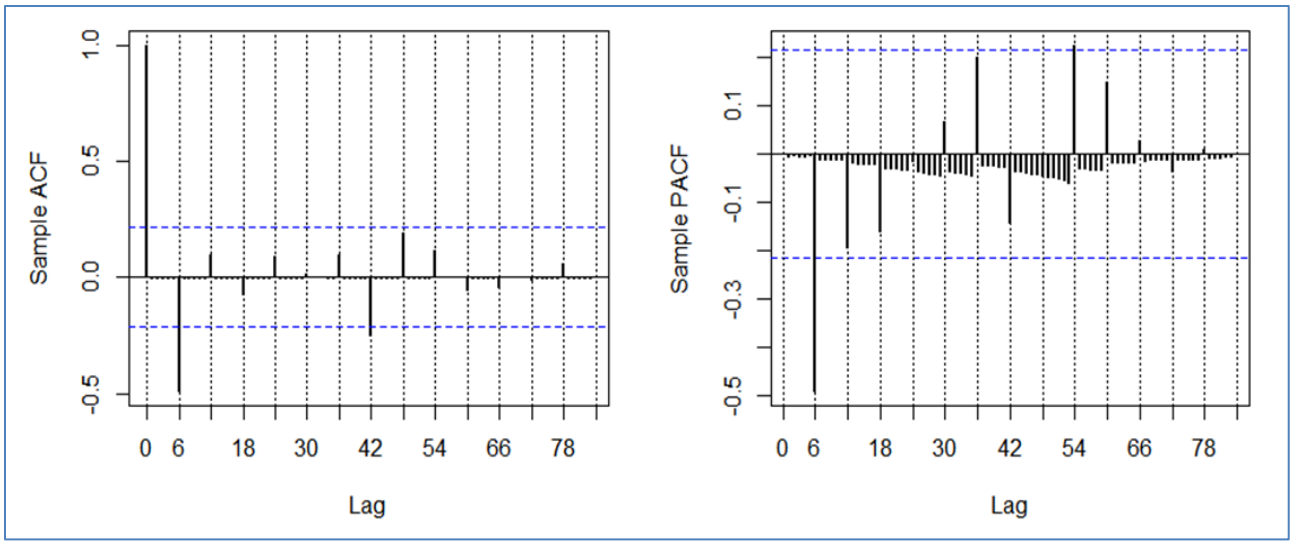

Figure 91- The sample ACF and the sample PACF of the first order seasonal difference of the sequence (own calculation & illustration)

The 2nd Stage- Parameter Estimation

During the second stage, the parameters of the possible tentative models are estimated and the corresponding models are compared based on their AICc.

The computations are carried out by utilizing the auto.arima function. The maximum likelihood method is preferred for fitting the tentative models to the sequence of functional parameters. The result of the model fitting analysis is tabulated in Table 47. In total sixteen different seasonal ARIMA models are analyzed (the first model is calculated twice) and the model with the lowest AICc is determined to be the ARIMA(0,0,0)(1,1,1)[6] model[134]. Note that the output "Inf" is returned when the likelihood of the model turns out to be infinity or when the lowest root in the characteristic polynomial of the model is lower than 1.001 (i.e. if non-stationarity emerges due to the magnitude of parameters).

[134] The values in the first parenthesis indicate the order of regular autoregressive component, regular differencing and regular moving average component of the model respectively; whereas the values in the second parenthesis indicate the corresponding seasonal orders included in the model. Further, the value in brackets represents the frequency of the periodicity

Table 47- The output from auto.arima function for the analyzed tentative models (own calculation & illustration)

Time Series Model	AICc Value
ARIMA(0,0,0)(0,1,0)[6]	-2056.55
ARIMA(0,0,0)(0,1,0)[6]	-2056.55
ARIMA(1,0,0)(1,1,0)[6]	-2076.67
ARIMA(0,0,1)(0,1,1)[6]	-2079.51
ARIMA(0,0,1)(1,1,1)[6]	-2079.75
ARIMA(0,0,1)(1,1,0)[6]	-2076.67
ARIMA(0,0,1)(1,1,2)[6]	-2079.37
ARIMA(0,0,1)(0,1,0)[6]	-2054.45
ARIMA(0,0,1)(2,1,2)[6]	Inf
ARIMA(1,0,1)(1,1,1)[6]	-2077.49
ARIMA(0,0,0)(1,1,1)[6]	-2081.95
ARIMA(0,0,0)(0,1,1)[6]	-2081.66
ARIMA(0,0,0)(2,1,1)[6]	-2080.10
ARIMA(0,0,0)(1,1,0)[6]	-2078.83
ARIMA(0,0,0)(1,1,2)[6]	-2081.63
ARIMA(0,0,0)(2,1,2)[6]	Inf
ARIMA(1,0,0)(1,1,1)[6]	-2079.75
Best model: ARIMA(0,0,0)(1,1,1)[6]	

The coefficients of the ARIMA(0,0,0)(1,1,1)[6] model and their standard errors are tabulated in Table 48. The error measures of the fitted model are observed to be at an acceptable level (see APPENDIX B for the detailed summary statistics).

Table 48- The brief summary statistics of the ARIMA(0,0,0)(1,1,1)[6] model (own calculation & illustration)

	SAR(1)	SMA(1)
Coefficients	-0.2597	-0.4046
Standard Error	0.1562	0.1363

The ARIMA(0,0,0)(1,1,1)[6] model can be expressed in general form as follows:

$$\nabla_6(1-\Phi_1 B^6)\, z_t = (1-\Theta_1 B^6)a_t \tag{13.2.1}$$

$$z_t - \Phi_1 z_{t-6} - z_{t-6} + \Phi_1 z_{t-12} = a_t - \Theta_1 a_{t-6} \tag{13.2.2}$$

$$z_t = (1+\Phi_1) z_{t-6} - \Phi_1 z_{t-12} + a_t - \Theta_1 a_{t-6} \tag{13.2.3}$$

In the general form, the symbol "∇_6" represents the difference operator and indicates that the series is seasonally differenced once $\nabla_6 = (1-B^6)$. The symbol "B" is the back shift operator. The symbol "z_t" denotes the t^{th} parameter in the sequence of parameters. The symbol "Φ" represents the seasonal autoregressive parameter; whereas the symbol "Θ"

indicates the seasonal moving average parameter. The t^{th} random shock is represented as "a_t". The model can be expressed in equation form with the computed parameters as shown below:

$$(1 - B^6)(1 + 0.2597\ B^6)z_t = (1 + 0.4046B^6)a_t \tag{13.2.4}$$

$$z_t = 0.7403z_{t-6} + 0.2597z_{t-12} + a_t + 0.4046a_{t-6} \tag{13.2.5}$$

The goodness of the fitted model ARIMA(0,0,0)(1,1,1)[6] can also be visually examined by plotting the fitted values against the observed values as shown in Figure 92. The plot indicates a successful fit to the data by nearly overlapping green circles and red plus signs representing the observed and fitted values respectively.

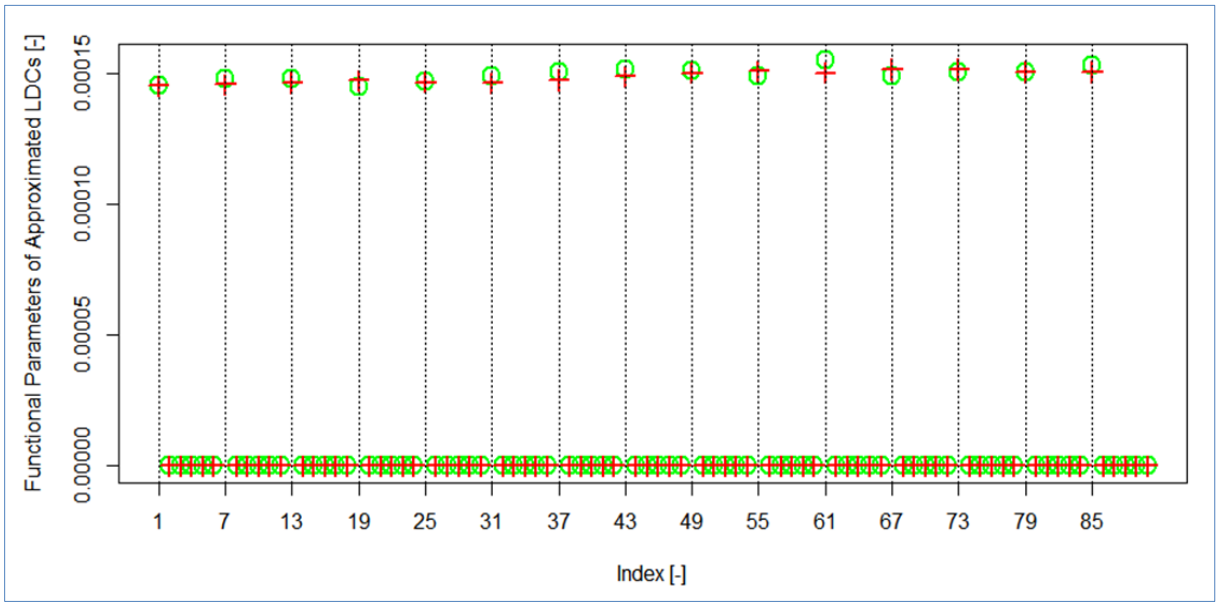

Figure 92- The scatter plot of the observed values (green circles) and the predicted values from ARIMA(0,0,0)(1,1,1)[6] model (red plus signs) (own calculation & illustration)

Moreover, the approximated LDCs from the predicted functional parameters[135] are tested for the relative error in approximating gross electricity demand, annual peak load demand and hourly load demand as depicted in Figure 93 (See Section 12.2 p. 196 for information on measuring relative errors).

[135] The predicted functional parameters result from the fitting of the ARIMA(0,0,0)(1,1,1)[6] model to the sequence of functional parameters formed by the 5th degree polynomial approximations to LDCs tabulated in Table 44.

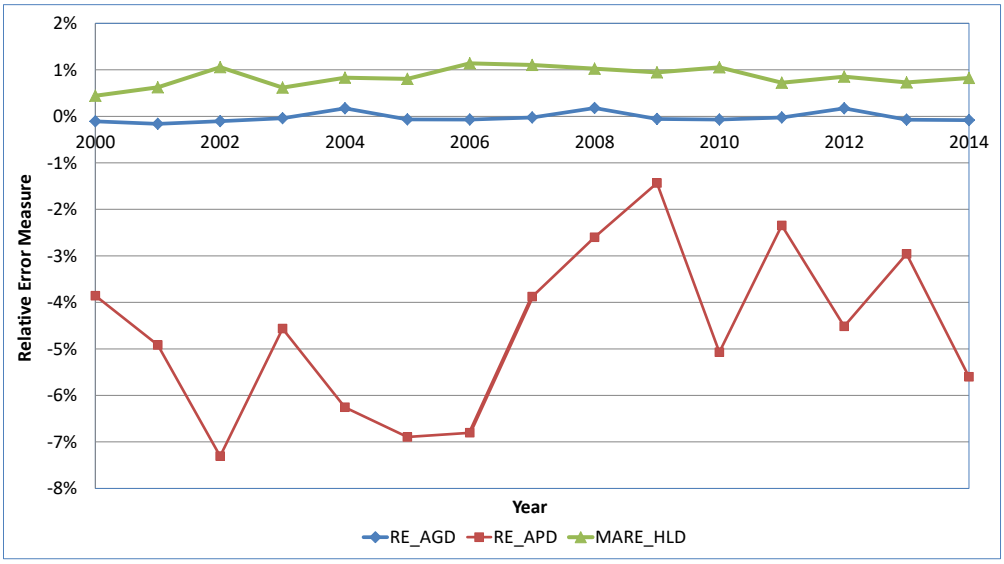

Figure 93- The RE_{AGD}, the RE_{APD} and the $MARE_{HLD}$ of the approximated LDCs from the predicted functional parameters (own calculation & illustration)

It is observed that the inaccuracy in approximating annual gross electricity demand or hourly load demanded is substantially lower than the inaccuracy in approximating annual peak load demand. Although the inaccuracy in annual peak load demand seems relatively higher than the inaccuracies in other aspects, it does not originate from the ARIMA(0,0,0)(1,1,1)[6] model fitted to the sequence of parameters. The relatively high inaccuracy is inherent due to the 5th degree polynomial function which is selected to be adequately approximating the historical LDCs (see Figure 80 on p. 208).

In addition to the above mentioned inaccuracy analysis, the inaccuracy in approximation of LDCs, is further assessed by utilizing $MARES_{AGD}$, $MARES_{APD}$ and the mean of $MARES_{HLD}$ for the period 2000-2014 (see Figure 94). Further, it can be deduced that the $MARES_{APD}$ is relatively high w.r.t. the $MARES_{AGD}$ and the mean of $MARES_{HLD}$; however the relatively high inaccuracy is inherent (see Figure 83 on p. 213). Furthermore, the maximum acceptable level of inaccuracy for the $MARES_{AGD}$ and the mean of $MARES_{HLD}$, which are assigned to be 1%, are observed to be fulfilled by the predicted functional parameters. Moreover, the maximum level of inaccuracy for the $MARES_{APD}$, which is assigned to be 5%, is also observed to be satisfied. Hence, the ARIMA(0,0,0)(1,1,1)[6] model is observed to be adequately predicting the mentioned past LDCs.

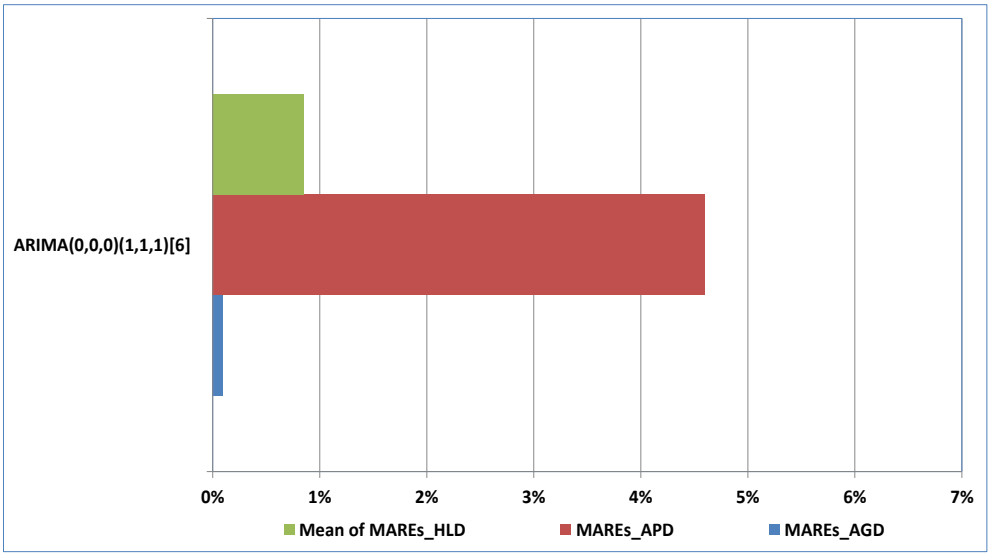

Figure 94- The $MAREs_{AGD}$, the $MAREs_{APD}$ and the mean of $MAREs_{HLD}$ of the approximated LDCs from the predicted functional parameters (own calculation & illustration)

The 3rd Stage- Diagnostic Checking of Residuals

During the third stage of the time series modelling, the residuals of the ARIMA(0,0,0)(1,1,1)[6] model is tested for normal distribution and randomness both by graphical and analytical means. See Subsection 10.1.1.5.1 on p. 99 for more information about residual analysis.

The normality assumption of the residuals is examined by using the Q-Q plot[136] of the standardized residuals. It can be seen from Figure 95 that the sample distribution of the residuals is not normally distributed due to the fact that the most of the values in the data are close to zero and also large deviations occur from the horizontal line. If the observed data had contained positive values rather than values close to zero, normally distributed residuals could be achieved by applying Box-Cox transformation.

[136] The function "qqnorm" (in package stats version 3.1.2) and the function "qqline" are used for plotting the residuals in the Q-Q plot.

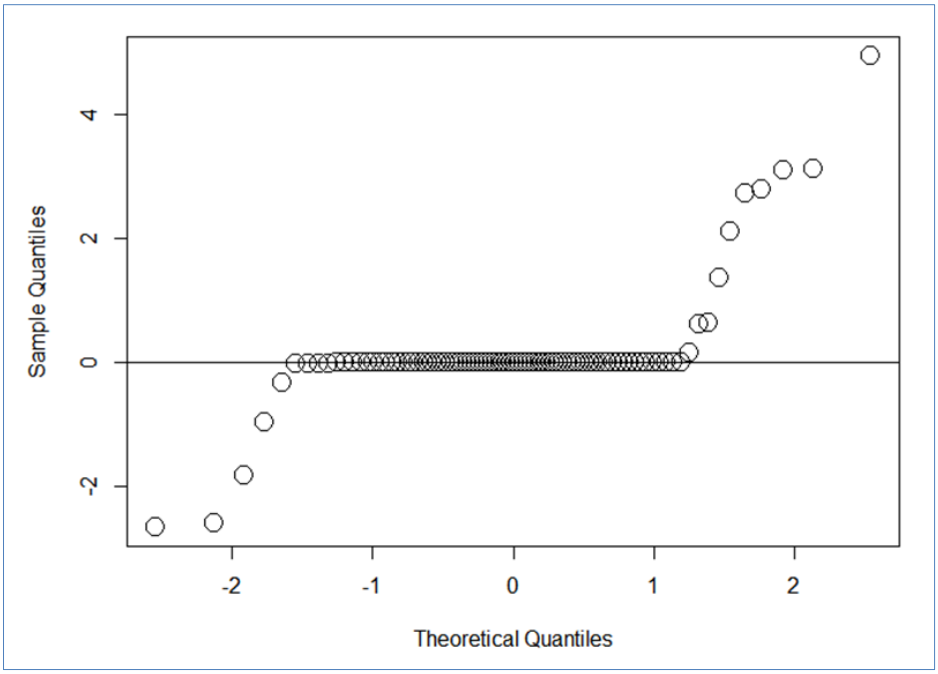

Figure 95- The Q-Q plot of the residuals from ARIMA(0,0,0)(1,1,1)[6] model (own calculation & illustration)

In addition to the examination of the Q-Q plot, the shapiro-wilk test of normality is carried out using the function shapiro.test in R. The value of the test statistic W and p-value are computed to be 0.5 and 5.204e-16 respectively. The examination of residuals indicates that there is enough evidence to reject the null hypothesis which states that the tested data are from a normally distributed population at an alpha level of 5% (i.e. a p-value lower than 5%).

Note that the maximum likelihood method can still be utilized for parameter estimation of ARIMA models, although the assumption of normally distributed residuals is not validated. According to Masani and Wiener (1959), mathematics requires a process be necessarily Gaussian; in order to achieve optimal linear predictors. If the process is non-Gaussian, a better predictor may be given by a non-linear dynamic model (as cited in Ozaki & Iino, 2001, p. 81).

During the model fitting analysis, it is assumed that the maximum likelihood estimation is asymptotically equivalent to least squares estimation. Particularly, the minimization of sum of squared errors does not require the assumption of normally distributed residuals. Further, the non-linear stochastic models are not considered as alternative tentative models; since the non-normality is inherent in the analyzed data and the linear models are observed to be adequate for obtaining future LDCs with relatively less effort as mentioned in previous studies (see Subsection 13.1.2). Therefore, a best fitting stochastic model is sought among a number of tentative linear models by utilizing the maximum likelihood method.

Furthermore, the standardized residuals of the model, displayed in Figure 96, resemble identically and independently distributed white noise series by varying around the zero horizontal level.

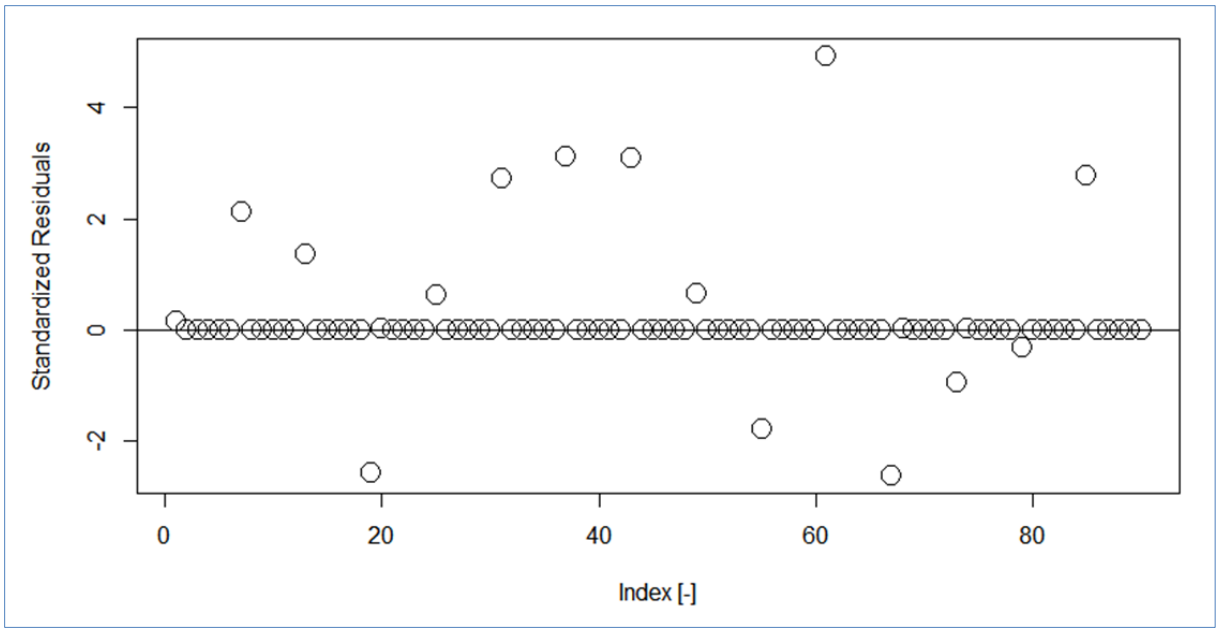

Figure 96- The standardized residuals from the ARIMA(0,0,0)(1,1,1)[6] model (own calculation & illustration)

Moreover, the sample ACF and the sample PACF of the residuals from ARIMA(0,0,0)(1,1,1)[6] model is examined for correlation at each individual lag as displayed in Figure 97. There is not any significant spike observed in both sample ACF and sample PACF indicating any dependency among residuals. Note that the Ljung-Box test cannot be applied on the residuals due to the violation of normality assumption.

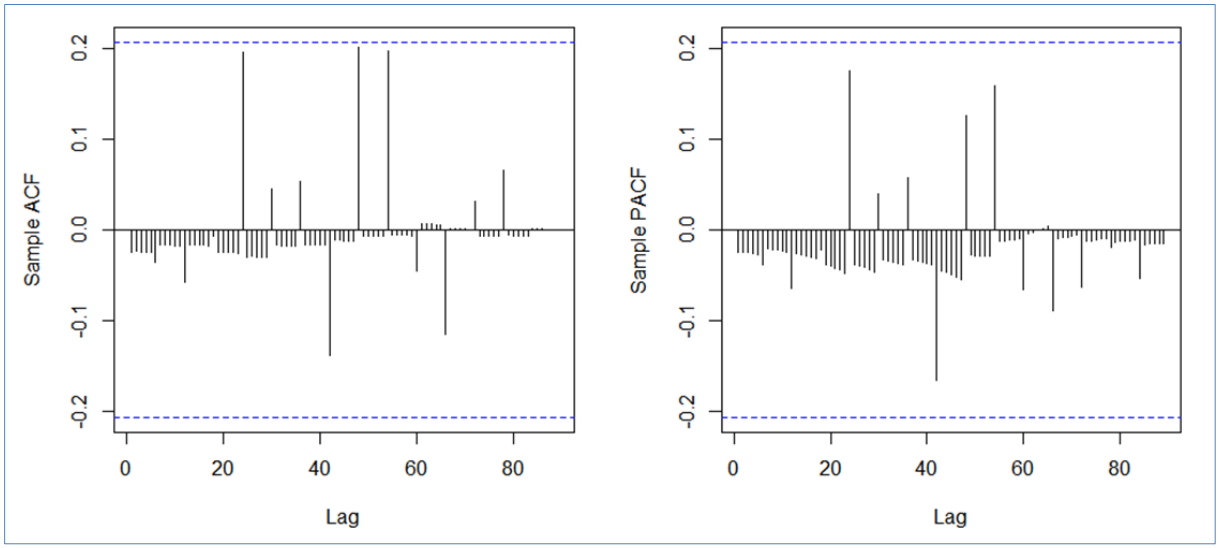

Figure 97- The sample ACF and the sample PACF plot of the residuals from ARIMA(0,0,0)(1,1,1)[6] model (own calculation & illustration)

To sum up, the ARIMA(0,0,0)(1,1,1)[6] is considered to be a convenient[137] model in representing the stochastic process generating the sequence of functional parameters. Subsequently, the model is considered for forecasting the functional parameters of the future LDCs of Turkey.

The 4th Stage- Forecasting Parameters of Load Duration Curves

After determining the ARIMA(0,0,0)(1,1,1)[6] model as an convenient model, the parameters of the 5th degree polynomial approximations to LDCs in the period 2015-2025 are forecasted. The forecast process is carried out by utilizing the function forecast in R. The computed forecasts are displayed in Figure 98. In the figure, the values corresponding to the indices between 91 and 96 represent the parameters of the forecasted LDC of year 2015. Similarly, the values corresponding to the indices between 97 and 102 represent the parameters of the approximated LDC of year 2016 and so on. Note that any forecast limit cannot be considered due to the violation of the normality assumption.

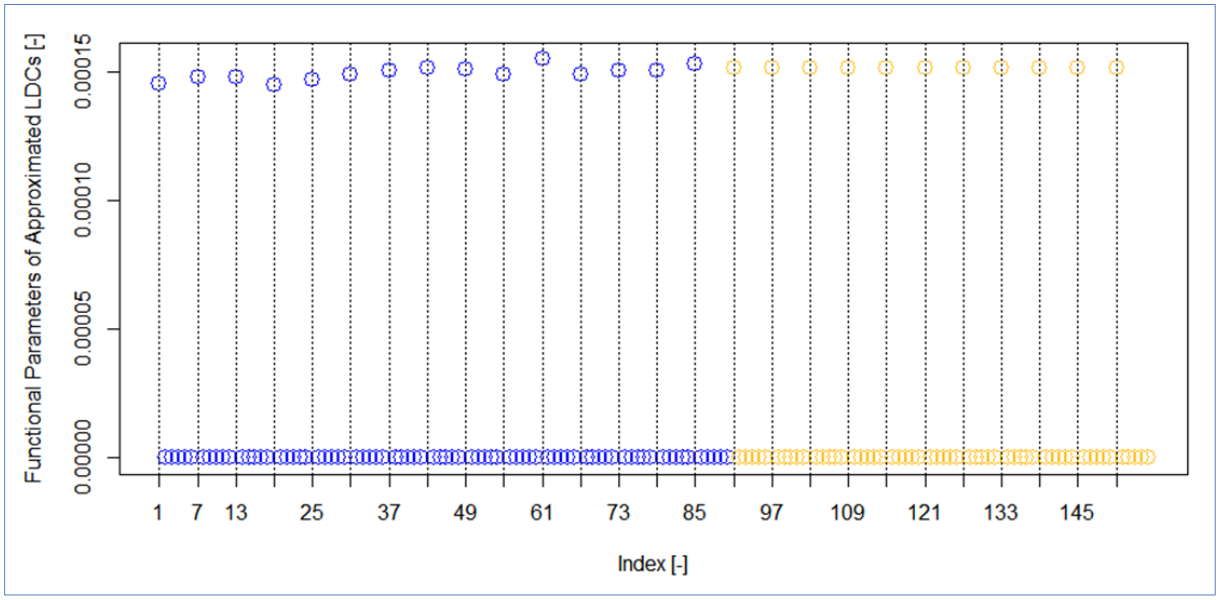

Figure 98- The observed sequence of functional parameters (blue circles) and the forecasts (orange circles) (own calculation & illustration)

[137] The Information criteria (i.e. AIC, AICc and BIC) require the validity of the normality assumption. Since this assumption is violated, the considered ARIMA(0,0,0)(1,1,1)[6] cannot be the adequate model but rather a convenient model representing the stochastic process generating the data.

In Table 49, the forecasted functional parameters of the approximated LDCs for the period 2015-2025 are tabulated.

Table 49- The forecasted parameters of polynomial approximations to LDCs in the period 2015-2025 (own calculation & illustration)

Year	β_0	β_1	β_2	β_3	β_4	β_5
2015	1.51555901E-04	-2.90596270E-08	1.47459808E-11	-3.93484445E-15	4.67335617E-19	-2.05249860E-23
2016	1.52027165E-04	-3.00389247E-08	1.52749471E-11	-4.05417328E-15	4.79460999E-19	-2.09821529E-23
2017	1.51904790E-04	-2.97846269E-08	1.51375885E-11	-4.02318672E-15	4.76312356E-19	-2.08634387E-23
2018	1.51936568E-04	-2.98506613E-08	1.51732569E-11	-4.03123311E-15	4.77129976E-19	-2.08942656E-23
2019	1.51928316E-04	-2.98335139E-08	1.51639947E-11	-4.02914368E-15	4.76917661E-19	-2.08862607E-23
2020	1.51930459E-04	-2.98379667E-08	1.51663999E-11	-4.02968625E-15	4.76972794E-19	-2.08883394E-23
2021	1.51929902E-04	-2.98368104E-08	1.51657753E-11	-4.02954536E-15	4.76958477E-19	-2.08877996E-23
2022	1.51930047E-04	-2.98371107E-08	1.51659375E-11	-4.02958194E-15	4.76962195E-19	-2.08879398E-23
2023	1.51930009E-04	-2.98370327E-08	1.51658954E-11	-4.02957244E-15	4.76961230E-19	-2.08879034E-23
2024	1.51930019E-04	-2.98370529E-08	1.51659063E-11	-4.02957491E-15	4.76961480E-19	-2.08879128E-23
2025	1.51930017E-04	-2.98370477E-08	1.51659035E-11	-4.02957427E-15	4.76961415E-19	-2.08879104E-23

14 VALIDATION OF FUNCTIONAL APPROXIMATIONS TO FUTURE LOAD DURATION CURVES (4th STAGE)

In the final stage of the introduced concept, the approximations to future LDCs are examined for their feasibility in approximating annual gross electricity demand, in representing the development of hourly load demand (i.e. through the shape of the LDCs) and in estimating the annual peak load demand in the period 2015-2025.

The inaccuracy in approximating[138] the future LDCs is evaluated by calculating the deviation of the areas under the future LDCs from unity[139] (i.e. RE_{AGD}) as depicted in Figure 99. It can be inferred that the RE_{AGD} is less than 1% for all approximations in the period 2015-2025. Therefore, the $MARES_{AGD}$[140] is considered to be at an acceptable level (i.e. under 1%) for the adequate approximation of all corresponding future LDCs.

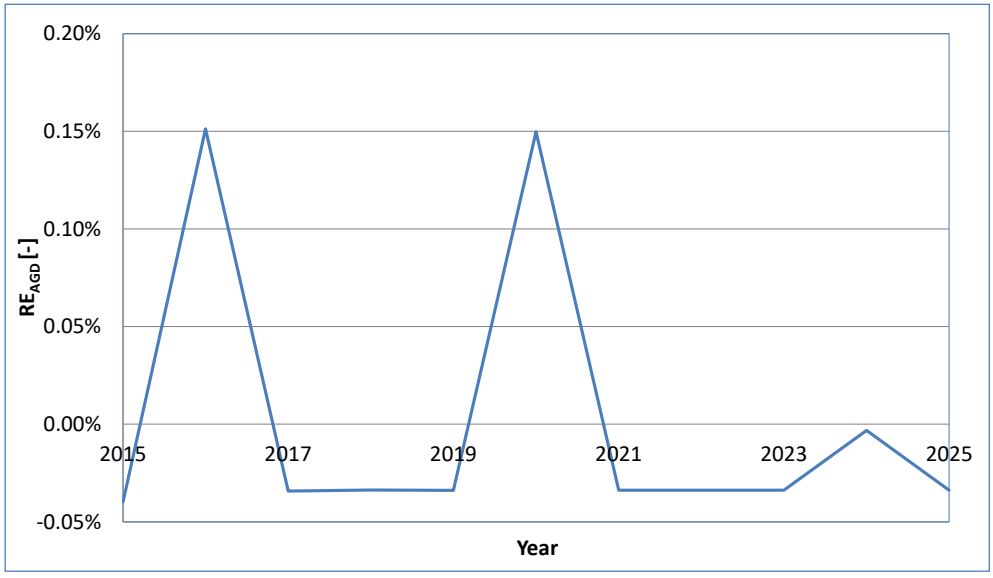

Figure 99- The RE_{AGD} of obtained approximations to future LDCs in the period 2015-2025 (own calculation & illustration)

[138] The future LDCs are approximated by using the forecasted functional parameters.

[139] The area under the approximated future LDCs should ideally amount to unity (i.e. normalized magnitude of annual gross electricity demand); since the areas under the historical LDCs are normalized to unity for functional approximation, before the subsequent forecasting of parameters.

[140] It is called the mean of absolute relative errors in approximating annual gross electricity demand (see p. 201 for more information).

In order to utilize the obtained approximations to future LDCs in capacity expansion planning, they are rescaled by using the forecasted annual gross demand of Turkey[141] for the same period as represented in Figure 100. Namely, the approximating function of each future LDC is rescaled with the corresponding forecasted annual gross electricity demand (F_{AGD}) as expressed below:

$$HLD_t = L(t) \cdot F_{AGD}, \qquad 1 \leq t \leq n \ \wedge \ n = 8760 \ or \ 8784 \tag{13.2.6}$$

Note that "$L(t)$" denotes the 5th degree polynomial function approximating the LDC of a year in the period 2015-2025 and is a function of duration "t". The symbol "HLD_t" denotes the t^{th} hourly load demand in the LDC of the corresponding year.

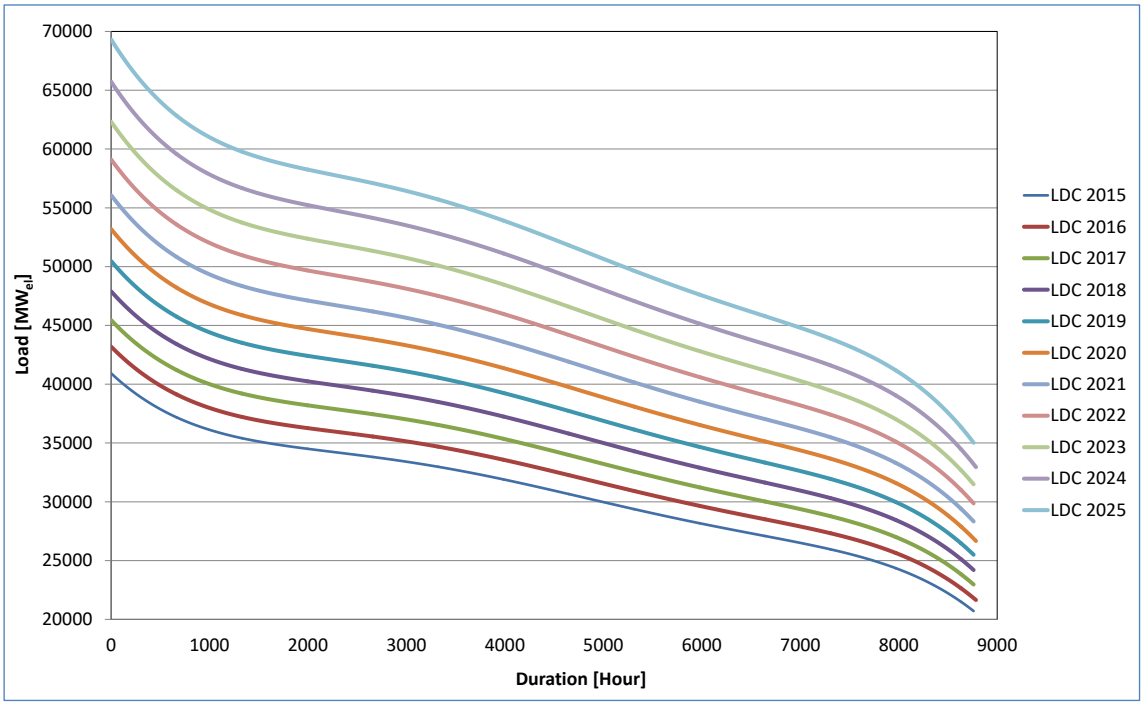

Figure 100- The rescaled future LDCs of Turkey in the period 2015-2025 (own calculation & illustration)

It can be deduced from Figure 100 that the approximated future LDCs are shifted upwards due to the forecasted annual gross electricity demand which increases during the mentioned period (see also Table 32 on p. 169). In this respect, the mentioned future development in the period 2015-2025 resembles the past development in the period 2000-2014 (see Figure 32 on p. 81).

[141] See Subsection 11.3.2 for the related information.

Further, the future development of the annual peak load demand is estimated as a consequence of rescaling as tabulated in Table 50.

Table 50- The estimated value of the annual peak load demand due to the rescaling of future LDCs (own calculation & illustration)

Year	Estimated Annual Peak Demand (MW_{el})	Change w.r.t. Previous Year (per annum)
2015	40919	0.5%
2016	43189	5.5%
2017	45447	5.2%
2018	47890	5.4%
2019	50462	5.4%
2020	53186	5.4%
2021	56063	5.4%
2022	59105	5.4%
2023	62320	5.4%
2024	65720	5.5%
2025	69314	5.5%
Annual Mean Growth Rate		5.0%

It can be deduced from Table 50 that the estimated annual peak load demand is in an increasing trend except for the year 2015. The annual mean growth rate is determined to be 5.0% for the period 2015-2025; however it amounts to 5.4% for the period 2016-2025 which is close to the corresponding annual mean growth rate in the period 2000-2014 (i.e. 5.5%).

The past and future development of the annual peak load demand w.r.t. different analysis is illustrated in Figure 101. In the figure, the forecasted annual peak load demand originates from the TSA of past observations (see Table 36 on p. 181); whereas the estimated annual peak load demand is obtained from rescaling of the approximated future LDCs (see Table 50).

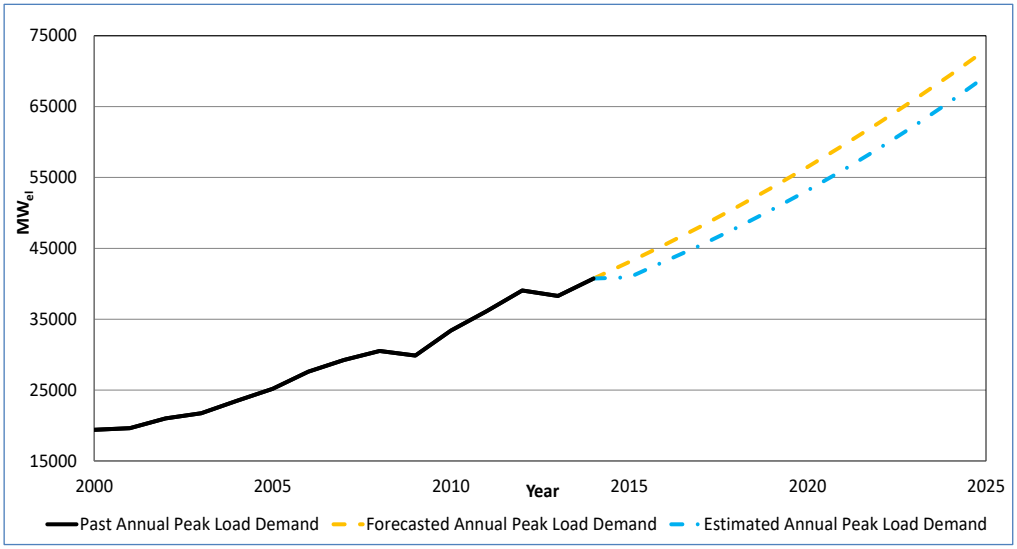

Figure 101- The development of annual peak load demand in the period 2000-2014 and in the forecasted period 2015-2025 w.r.t. different approaches (own calculation & illustration)

It can be inferred from the figure that the forecasted annual peak load demand indicates a steeper trend than the estimated annual peak demand. Also, it does not indicate any sudden fall in the period 2015-2025; whereas the estimated annual peak demand stays at the same level in the year 2015 and then indicates a subsequent increasing trend. However this can be considered as reasonable, since trend changes also took place in the years 2009 and 2013.

In conclusion, the statistical evidences and historical data examination revealed that the obtained approximations to future LDCs can characterize the development of LDCs for Turkey to be utilized as inputs to capacity expansion planning in the period 2015-2025.

15 CONCLUSION

This study is conducted for obtaining approximations to future LDCs of Turkey in the period 2015-2025 to be utilized as inputs to the capacity expansion model of Turkey. Accordingly, a concept on obtaining functional approximations to future LDCs of Turkey is introduced for the first time in this study.

The future LDCs can be obtained by forecasting either LDCs per se or hourly load demands in the form of load curves for the considered planning period. It has been observed that forecasting load curves of Turkey requires high effort in relating the chronological variations in hourly load demands (i.e. the annual, weekly and daily cycles and trends) with the variations in the energy prices, in the consumer behavior, in economic and climatic variables in long term. In addition, the accuracy of the long-term forecasts diminishes as more uncertainty is present due to the states of the mentioned factors in the future as observed in the previous studies. As a consequence, the long-term forecasting of annual load curves is not preferred for obtaining the future LDCs of Turkey. Instead, obtaining the forecasts of the future LDCs per se is preferred.

This concept is based on the previous study conducted by Uri and Maybee (1980) implemented at the FERC region level in the USA. In their approach, the functional approximations to future LDCs are obtained from the forecasted functional parameters of the approximated past LDCs. Their approach is based on the assumption that the short and long term variations in hourly load demands are inherited in the parameters through the functional approximations of the considered LDCs. In particular, the functional parameters evolve over time w.r.t. the mentioned factors affecting the hourly demands. By utilizing their approach, the aforementioned difficulties in obtaining future LDCs of Turkey are surpassed. Consequently, the future LDCs of Turkey are obtained with relatively less effort and relatively better accuracy.

In this study, the functional approximations to future LDCs are obtained in four stages as different from the approach of Uri and Maybee. The four stages are listed as follows:

- Data preparation for functional approximation analysis,
- Determination of adequate functional approximations to past LDCs,
- Forecasting functional approximations to future LDCs,
- Validation of functional approximations to future LDCs.

Although the authors described the solution process of their approach, they did not group the computations as different stages of the solution process. Further, the introduced concept can also be utilized for other power systems in which the annual gross electricity and the annual peak load demand develop similar to Turkey. Furthermore, the novelty of this study lies in the performed analysis during the course of the approximation analysis as listed below:

- The annual gross electricity and peak load demands are forecasted for Turkey in the period 2015-2025 and the forecasts are statistically and retrospectively more reliable than the previous studies utilizing TSA for forecasting.
- Different types of mathematical functions are analyzed to determine the function which adequately approximates the LDCs of Turkey in the period 2000-2014 among others.
- A four-parameter logarithmic function, which is introduced in Ratkowsky (1990, p. 145), is proposed to be utilized for functional approximations to LDCs.
- The functional approximation analyses are based on the Weierstrass approximation theorem (1885).
- A heuristic approach is proposed for finding the starting values for the parameters of exponential and logarithmic functions; in order to initiate the Gauss-Newton algorithm to solve non-linear least squares problem.
- The 5^{th} degree polynomial approximations are determined to be adequately approximating the past LDCs of Turkey and are subsequently utilized for obtaining approximations to future LDCs in the period 2015-2025.
- The validation of the approximations to future load duration curves is not only based on the examinations for considerable deviations from the unit area (as proposed by Uri and Maybee) but also on the feasibility of approximating annual peak load and hourly load demand for the forecasted period.

During the first stage, the past LDCs of Turkey are constructed from the hourly load demands. Further, the annual gross electricity demand and the annual peak load demand are forecasted; in order to be utilized for rescaling and validation of the functional approximations to future LDCs of Turkey respectively (i.e. at the fourth stage). The TSA of the series, which consists of the annual gross electricity demand, yielded an ARIMA(1,2,1) model with the lowest AICc among other tentative models. The considered model is validated through all diagnostic tests and is determined to be an adequate model representing the stochastic process generating the time series with a MAPE of 2.52%. For the period 2015-2025, the annual gross electricity demand is forecasted to be increasing from 270 TWh_{el} to 456 TWh_{el} with an annual mean growth rate of 5.4% which is about the same growth rate as in the period 2000-2014 (i.e. 5.2%).

Similarly, the analysis of the time series data, which consists of the annual peak load demand, yielded an ARIMA(1,2,1) model with the lowest AICc among other tentative models. The model has a MAPE of 3.4% and is determined to be an adequate model through all diagnostic tests. For the period 2015-2025, the annual peak load demand of Turkey is forecasted to be increasing from 43069 MW_{el} to 73059 MW_{el} in the period 2015-2025 with the same corresponding annual mean growth rate as in the period 2000-2014 (i.e. 5.5%). At the end of the both time series analyses, it is observed that the conducted analyses are statistically and retrospectively more reliable than the mentioned previous studies utilizing TSA for forecasting.

In the second stage, the constructed each LDC is approximated by utilizing smooth functional approximations to past LDCs of Turkey. According to the presented results in previous studies, the smooth functional approximations are observed to be demanding the least effort and indicating the highest accuracy among the utilized methods such as discrete and optimal functional approximations. Accordingly, the LDCs of Turkey are approximated utilizing smooth functions such as polynomial and non-linear functions to determine the function which adequately approximates the LDCs in the period 2000-2014. In this study, an adequate functional approximation to a LDC is defined to be a parsimonious functional approximation to a LDC with least possible inaccuracy in approximating annual gross electricity demand, annual peak load demand and hourly load demand among other alternatives.

Therefore, maximum acceptable levels for measures of overall inaccuracy are set; in order to compare and determine the adequate functional approximation to past LDCs among

alternatives. Further, the maximum acceptable level of inaccuracy for the $MARES_{AGD}$ and the $mean\ of\ MARES_{HLD}$ is assigned to be 1% for all considered type of functional approximations to LDCs according to the presented results in previous studies. Furthermore, the maximum level of inaccuracy for the $MARES_{APD}$ is assigned to be 5% for all types of functional approximations to LDCs. The corresponding error level is analyzed to be not endangering the long term supply reliability of the Turkish power system in the period 2015-2025. Finally, it is also assumed that an effective decrease in inaccuracy should be at least 1% for possessing an additional functional parameter, if two different types of functional approximations have different total number of parameters. During the analysis, it is emphasized that the common measures of model adequacy (e.g. R^2, AIC and etc.) cannot be essential criteria for assessing the effectiveness of decrease in inaccuracy as per definition of the adequate approximations to LDCs.

During the analysis of the polynomial approximations to past LDCs of Turkey, it is observed that the polynomials without intercepts are ineffective and cannot be used in capacity expansion planning. Further, the approximations are carried out by using polynomial functions of degrees ranging from minimum 4^{th} to 12^{th} at maximum due to multicollinearity. According to the assigned maximum acceptable level of inaccuracy for the $MARES_{AGD}$, the $MARES_{APD}$ and the mean of $MARES_{HLD}$, the adequate functional approximation to past LDCs of Turkey is determined among the degree of polynomial functions ranging from the 5^{th} to the 12^{th} degree excluding the 6^{th} degree. Also, it has been observed that the desired level of inaccuracy in approximating annual peak load demand and the total number of parameters in the polynomials are the essential criteria for the selection of the adequate approximating function among polynomials. It is observed that an effective decrease in inaccuracy w.r.t. the 5^{th} degree polynomial approximations is not achieved by any polynomial approximations possessing additional functional parameter(s). Therefore, the 5^{th} degree polynomial function is selected among other polynomials to be used as an adequate functional approximation to LDCs of Turkey in the period 2000-2014.

Similar to the analysis for polynomials, the inaccuracies in non-linear functional approximations are analyzed based on the maximum acceptable levels for the measures of overall inaccuracy for each year in the period 2000-2014. Further, the approximations are carried out by utilizing the exponential, logarithmic and the inverse of Hill's function. Furthermore, the results of inaccuracies in corresponding approximations are also compared with the inaccuracy in 5^{th} degree polynomial approximations to LDCs. During the course of

the analysis, an approach for finding the starting values for the parameters of exponential and logarithmic functions is proposed; in order to initiate the Gauss-Newton algorithm. The corresponding overall analyses indicate that the assigned maximum acceptable level of inaccuracy for the $MARES_{APD}$ is observed to be the distinctive criterion; since it is satisfied only for the 5th degree polynomial approximations. Therefore, the 5th degree functional approximations are determined to be the adequate functional approximations to LDCs of Turkey in the period 2000-2014.

In the third stage, the formed sequence of functional parameters, which is obtained from the 5th degree polynomial approximations to past LDCs of Turkey, is analyzed by using TSA. The TSA is observed to be indicating relatively less effort and relatively better accuracy in comparison to the regression analysis which is also utilized in the previous studies.

Therefore, the mentioned sequence is fitted a number of tentative time series models. The model with the lowest AICc is selected to be the ARIMA(0,0,0)(1,1,1)[6] with a MAPE of 11%. Further, the approximated LDCs from the predicted functional parameters are tested for functional adequacy. Accordingly, the maximum acceptable level of inaccuracy for the $MARES_{AGD}$, $MARES_{APD}$, and the mean of $MARES_{HLD}$ are observed to be fulfilled by the predicted functional parameters. Hence, the ARIMA(0,0,0)(1,1,1)[6] model is observed to be adequately predicting the mentioned past LDCs. In addition, the diagnostic tests on the residuals indicate that the selected model can be considered as a convenient model in representing the stochastic process generating the sequence of functional parameters. Therefore, the parameters of the functional approximations to future normalized LDCs are forecasted by using the selected model.

In the final stage, the approximations to future LDCs are examined for their feasibility in approximating the annual gross electricity demand, reflecting the changes in hourly load demands (i.e. through the shape of the LDCs) and in estimating the annual peak load demand in the period 2015-2025. The approximations to future LDCs can be used as an input to the capacity expansion model of Turkey, if the approximations to future LDCs are validated w.r.t. the mentioned criteria. Accordingly, the analysis indicates that the $MARES_{AGD}$ is considered to be at an acceptable level (i.e. under 1%) for the adequacy of approximations to future LDCs.

In order the approximation to future normalized LDCs to be used in capacity expansion planning; they are rescaled by using the forecasted annual gross demand of Turkey in the same period. Subsequently, it is observed that the obtained approximations to future LDCs are shifted upwards due to the forecasted electricity demand which increases during the mentioned period. In this respect, the mentioned future development in the period 2015-2025 resembles the past development in the period 2000-2014.

Further, the future annual peak load demands are estimated as a consequence of rescaling the future normalized LDCs. It is observed that the estimated annual peak load demand is in an increasing trend except for the year 2015. The growth rate per annum is calculated to be 5.0% for the period 2015-2025; however it amounts to 5.4% for the period 2016-2025 which is close to the corresponding annual mean growth rate in the period 2000-2014 (i.e. 5.5%).

Furthermore, the past and the future development of the annual peak load demand is examined for feasibility w.r.t. the forecasted (i.e. originating from the TSA of past observations) and estimated annual peak load demand (i.e. originating from the rescaling of the future normalized LDCs). It is observed that the forecasted annual peak load demand indicates a steeper trend than the estimated annual peak demand and also does not indicate any sudden fall in the period 2015-2025; whereas the estimated annual peak demand stays at the same level in year 2015 and then indicates a subsequent increasing trend. However this can be considered as reasonable, since trend changes also took place in year 2009 and 2013.

In conclusion, the statistical evidences and historical data examination revealed that the obtained approximations to future LDCs can characterize the development of LDCs for Turkey to be utilized as inputs to capacity expansion planning in the period 2015-2023.

For future research, the functional approximation analysis can be extended by examining other nonlinear functions; in order to decrease the inaccuracy in approximating annual peak load demand under 5%. In addition, the functional parameters can also be forecasted by applying other econometric methods such as the artificial neural network, the fuzzy logic method, etc.

PART C THE IMPROVED SCREENING CURVE METHOD REGARDING EXISTING UNITS*

* With permission from Yusuf Emre Güner, The Improved Screening Curve Method regarding Existing Units, European Journal of Operational Research, Volume 264, Issue 1, Pages 310-326, © 2017 Elsevier.
Doi: 10.1016/j.ejor.2017.06.007

16 INTRODUCTION

A capacity expansion model is utilized for planning the type, the size and the commissioning time of the power plants[142] to be installed in a power system. The capacity expansion models can be classified as static or dynamic models. A static capacity expansion model is utilized for the analysis of energy mix in a target year, whereas a dynamic model is utilized for a planning horizon of 2 to 50 years by which an expansion problem is solved simultaneously across all time periods in the planning horizon. A detailed analytical description of the mentioned models and under which conditions they can have similar results can be found in Levin, Tishler and Zehavi (1980, pp. 2-3; 1983, pp. 892-893).

The focus of the recent capacity expansion studies has been the issues related to the increasing penetration of renewable energy sources and the optimal utilization of existing and new generation capacities. One of the important issues is the uncertainties originating from the intermittent power generation from renewable. Parpas and Webster (2014) proposed a stochastic multiscale model to take into account the uncertainties in load demand and in generation availability for capacity expansion planning. Vespucci et al. (2015) introduced a decision support model to take into account the risk associated with the capacity expansion problem originating from the uncertainty of prices and the uncertainty of market share. Pineda and Morales (2016) presented a static mathematical model to investigate capacity expansion planning under the effects of short-term forecast errors of renewable power generation, market design and competition at the investment level.

Another important issue is the power transmission expansion planning with the comissioning of new generation capacity and the dynamic demand response management. Georgiou (2016) introduced a deterministic bottom-up mixed integer linear programming model to determine the least cost combination of electricity generation technologies considering interconnection infrastructures for the long-term energy planning of Greek power system. Sauma et al. (2015) proposed a robust-optimization model for transmission expansion planning to assess the impact of postponing the connection time of some new power plants over the system cost and the optimal network expansion plan.

[142] In this study, a unit or a generator is used as a synonym of the term “power plant”.

Finally, the economic and the environmental evaluation of national or international energy policies and the electricity market design are the other important related issues among the recent studies. Alizamir et al. (2016) proposed optimization models to analyze the dynamic control of remuneration rates (prices) of feed-in tariff policies considering the main market dynamics in the evolution of renewable technologies (i.e. learning and diffusion) and investors' strategic behaviors. Hach et al. (2016) introduced a dynamic capacity investment model to analyze the impact of different capacity market design choices for Great Britain by taking into account ramping costs and constraints, strategic bidding, and price elasticity of demand. Ritzenhofen et al. (2016) presented an agent-based dynamic model to compare the impact of the different renewable energy support schemes on electricity prices, generation portfolios, security of supply and carbon emissions considering the investor behavior and the major characteristics of electricity markets (i.e. in particular for Californian electricity market).

The classical screening curve methodology (TCSCM), a practical methodology, is often utilized in capacity expansion models as considered in the recent studies by Hach et al. (2016) and Ritzenhofen et al. (2016). TCSCM provides the optimal solution to meet the increasing demand for electricity by minimizing the capital and the operational costs of generators. Although it provides initial solutions on a capacity expansion problem, the solutions are guidelines for a detailed analysis. In the next section, detailed information about TCSCM is provided.

16.1 The Classical Screening Curve Methodology

TCSCM is preferred to be utilized during the preliminary investigation of the capacity expansion planning studies to narrow down the technology alternatives for detailed analysis. The method enables the graphical means of constructing and examining the cost curves of all candidate[143] thermal units considered for capacity expansion. An example cost curve of a generator is illustrated in Figure 102 and mathematically expressed in Eq. (16.1.1). A cost curve (or a screening curve) depicts the annual average cost of capacity usage (AACC) or annual revenue requirement of a generator[144], which is composed of fixed (FC) and variable

[143] The candidate units are the new units which are going to be commissioned, if they are found out to be economical during the evaluation process.

[144] A screening curve shows the average cost of using a plant's capacity. It should not be confused with the annual average cost of energy (AACE) supplied, i.e. AACE (in €/MWy) = FC (in €/MWy) / CF +VC (in €/MWy) (Stoft, 2002, pp. 36-39).

costs (VC), and is a function of the capacity factor[145] (CF). The intercept of the curve is the FC of the unit, whereas the slope of the curve is the VC.

$$\text{AACC}^{146}\ [€/\text{MWy}] = \text{FC}\ [€/\text{MWy}] + \text{VC}\ [€/\text{MWy}] \times \text{CF}\ [\text{unitless}] \qquad (16.1.1)$$

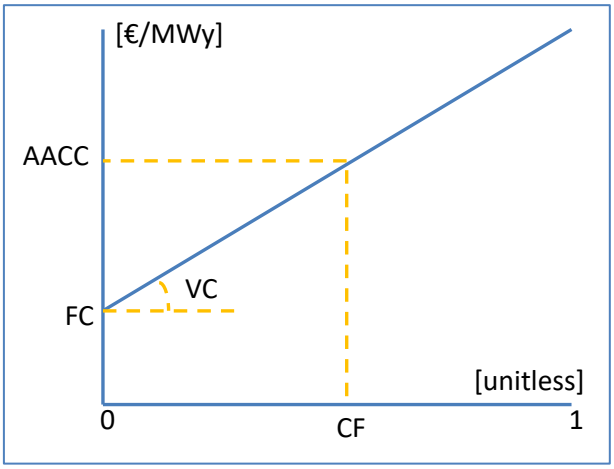

Figure 102- The representation of a generator's cost curve for analysis with TCSCM (own illustration)

The costs can also be represented in €/MWh, if the unit €/MWy is divided by 8760 hours/y. Although energy is measured in MWh, while power and capacity are measured in MW, the price of power, capacity and energy are all priced in €/MWh[147], so are fixed and variable costs (Stoft, 2002, pp. 32-33). For more information about TCSCM refer to Shaalan (2001, pp. 167-204) and Stoft (2002, pp. 30-45).

The annual revenue requirement is the amount of income needed by the generators to cover their annual fixed and variable costs. The annual fixed costs are composed of capital expenditure (CAPEX) and the fixed operating and maintenance costs (FOM). The CAPEX, expressed as specific investment cost in €/MW_{el}, encompasses the costs of erecting the power plant and bringing it to commercial operation and as well as the costs related to interest charges accrued during the construction period. During the calculations, the CAPEX is assumed to be recovered annually (or annuitized as fixed investment charges in €/MWy) over

[145] The fraction of time the capacity of a unit is used.

[146] Throughout this study, the cost accounting terms in IAEA (1984, pp. 151-163) are adapted for the sake of compatibility of terminology with most of the studies on capacity expansion in the literature.

[147] "Power" is the flow of energy (in MW) and "capacity" is the potential to deliver power (in MW). In contrast, energy is a static amount (in MWh). Consequently the price (per unit cost) of power is measured in dollars per hour per MW of power flow ($/h/MW = $/MWh), while the price of energy is measured likewise in dollars per MWh. Stoft (2002, pp. 30-31) states that generation cost data are usually presented in $/kW. This indicates the cost of the flow of capacity produced by a generator over its lifetime, so the true (but unstated) units are in $/kW-lifetime.

the economic life time (t) of the generator by using a capital recovery factor (r). The formula is represented below:

$$The\ Capital\ Cost\ of\ Capaciy\ per\ year = CAPEX \cdot \frac{r \cdot (1+r)^t}{(1+r)^t - 1} \qquad (16.1.2)$$

The FOM costs constitute taxes and insurance, personnel administration costs, etc. The annual fixed costs are independent of the amount of electricity generated, whereas dependent on the size of the generator and whether running or not must be paid.

The variable costs are, dependent on the amount of electricity generated, composed of the variable operating and maintenance costs (VOM) and the fuel costs. The VOM costs include the cost of waste disposal, the cost of unscheduled repairs, etc. The fuel costs are mainly dependent on the type of fuels used by the power plants and their efficiencies.

The first stage of the screening methodology is to construct cost curves for each type of generator according to their fixed and variable costs (see Figure 103). The candidate units are then compared on the basis of their AACC, and the most competitive ones are selected to be operative during the planning horizon. In the graph three types of generators are depicted, namely open cycle gas turbine (GT), combined cycle gas turbine (CC) and coal fired power plant (COAL). In relative terms, the GT generates power at the lowest cost among the other two in CF_3 times 8760 hours per year or less. By the same token, the COAL (the base load plant power plant) is the most economically attractive generator starting from CF_2 times 8760 hours per year or more. Finally, the CC (the medium load power plant) can be cost effectively operated, if it is run at least CF_3 times 8760 hours per year and at most CF_2 times 8760 hours per year.

At the second stage of the process, the cost-effective operation intervals, which are found at the first stage, are projected onto the annual load duration curve[148] to find the optimal capacities for the mentioned power plants (indicated as Cap in Figure 103). The merit order of loading provides the increasing order of variables cost in which the individual units are expected to be called upon to cover the demand in a power system. The marked points on the y-axis of the loading duration curve (expressed as D_{COAL}, D_{CC}, and D_{GT}), are so called the

[148] It is formed by ordering demand in each hour in a year according to its magnitude. Each point on the abscissa denotes the fraction of time (expressed as τ_1, τ_2), during which the corresponding demand on the ordinate is equaled or exceeded. The ordinate is assumed to be normalized to 1.

dispatching[149] (also called the loading) points of units, indicates the load levels starting from which the corresponding units will generate power (see Eq. (17.1.10) for the mathematical representation). In this manner, the cost of power generation is minimized. As illustrated in Figure 103, the base load unit is located at the lowest horizontal slice of the load duration curve, at the next lowest slice medium load unit and at the top slice peak load unit respectively. The area under the load duration curve amounts to the total annual electricity demand.

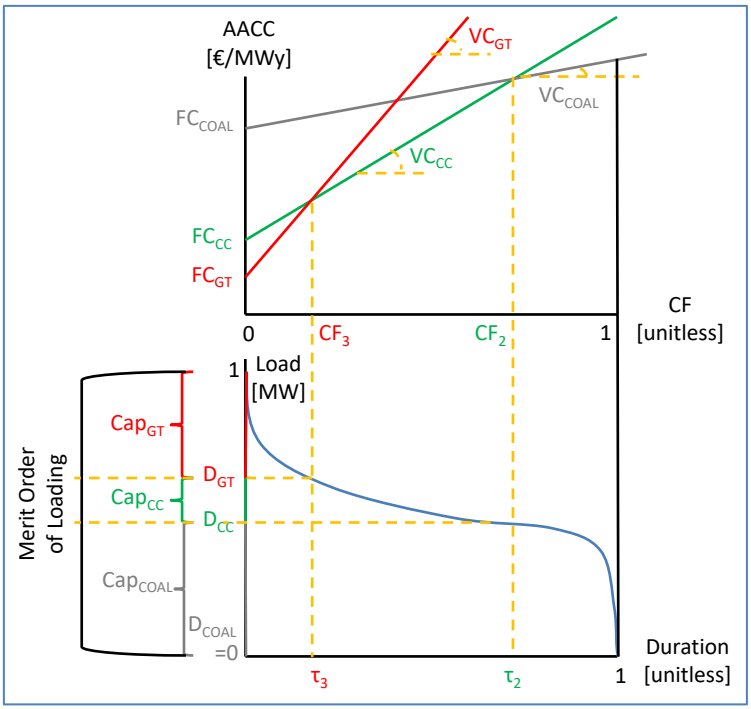

Figure 103- The determination of the optimal capacity expansion by using TCSCM (the top graph) with a load duration curve (the lower graph) (own illustration)

TCSCM requires minimal technical data and effort to account for tradeoffs between the low capital/high fuel costs; high capital/low fuel costs i.e. peak/medium/base load generators in a power system.

The inherent limitations of TCSCM make it a relative approximate approach, when compared to the more sophisticated methods used in comprehensive capacity expansion planning models (Anderson, 1972; Connolly, Lund, Mathiesen, & Leahy, 2010). Listed below are several corresponding shortcomings of TCSCM which cannot be taken into account during the optimization of a capacity expansion planning according to the International Atomic

[149] Dispatching is the process of scheduling power output of units according to the corresponding demand.

Energy Agency (1984, pp. 235-240), Georgakaki et al. (2009, pp. 24-25) and Howells (2011, pp. 16,28).

- It is a static approach which cannot take into account dynamics of a power market such as load changes and fuel price changes in short or long term.
- It can be utilized for thermal only power systems, since it cannot consider non-conventional power plants such as wind and solar power for capacity expansion.
- It is a deterministic approach which cannot account for stochastic events such as fluctuations in demand and renewable power generation (i.e. system reliability), as well as for minimum load constraints, start-up costs of power plants and spinning reserves etc.
- It cannot take into account existing units, while planning the capacity expansion with candidate units to cover the demand.
- It cannot account for the effects of unit unavailability such as scheduled or forced outages on a power market.
- The results of the capacity expansion are not in discrete unit size and adjustments are necessary for the desired allowable unit sizes.
- It does not consider the cost of power transmission.

16.2 Objective and Methodology of the Study

In this study, a new approach is introduced to contribute to the screening curve methodologies which can take into account the candidate and the existing units to determine the least cost capacity expansion of an all-thermal power system. The proposed methodology differs from the previous studies by its geometrical solution process to evaluate a static capacity expansion problem considering both existing and candidate power plants. The geometrical solution process (see Chapter 19) is based on the fundamental idea of TCSCM that the least cost capacity expansion alternative is the lowest combination of the cost curves converging with the primary and the secondary y-axes and the x-axis (see Figure 103). Accordingly, the geometrical solution process can be favored as the common operational research approach; since all scholars agree with this basic idea of TCSCM as it is also explained in all text books related to the energy economics. The basic idea of TCSCM has not been utilized for the consideration of existing units yet; since it entails the input for cost parameters in Eq. (16.1.1)

both for candidate and existing units. Although the candidate units are modeled to have the corresponding parameters, the existing units are modeled to have no fixed costs (i.e. sunk fixed costs). Indeed, the existing units possess shadow prices of their capacity values which can be considered as their fixed costs to be able to utilize Eq. (16.1.1).

The geometrical solution process can be interpreted as minimizing the long run marginal cost of supplying 1 MW_{el} capacity throughout a year by finding the optimal combination of units. The developed method calculates and finds the minimum area by moving along the intersection points of the cost curves to form all feasible[150] trapezoids and then join them to form all feasible cost polygons. In particular, the area of the cost polygon resulting from the combination of the trapezoids amounts to the annual total cost of supplying 1 MW_{el} capacity by the considered units. The intersection points, which are needed to calculate the areas of the cost polygons, are found by using the Karush-Kuhn-Tucker (KKT) conditions in a recursive manner. The areas of the formed cost polygons are calculated to determine the least cost polygon for optimal capacity expansion. Finally, after finding the points through which a lowest cost polygon is defined, the resulting CFs are projected onto the load duration curve to find the optimal capacity expansion. Accordingly, the solution procedure and the algorithms of the geometrical solution process are so developed to determine the least cost capacity expansion alternative among others.

The utilized algorithms are computationally more efficient and straightforward than the ones in previous studies for the similar type of improvements; since it is shown that there are three fundamental solution algorithms for finding the base (i.e. the values corresponding to CF) and the height (i.e. the values corresponding to AACC) of the trapezoids; in order to calculate the area of all possible cost polygons and to find the lowest one (see Section 19.3). In addition, the test[151] of the geometrical solution process against the so called "general mathematical formulation of the capacity expansion problem" (see Chapter 17) resulted in around 43% savings in computational time. Further, the interpretation of the optimal capacity expansion plan is enhanced by explicitly exhibiting the results of all considered capacity expansion alternatives, which is useful for preliminary energy policy analysis. Last but not least,

[150] Feasible trapezoids and cost polygons are analytically formed according to the described solution process in Subsection 19.2 and the given algorithms in Subsection 19.3.

[151] The test is carried out on the given example capacity expansion plan in APPENDIX G by using MATLAB® R2011a with a laptop having Intel Core i7 processor 2.20 GHz, 8192MB (1600MHz) memory and operating system of Windows 10. The elapsed time is 0.402689 seconds for the proposed method; whereas it is 0.699823 seconds for the general method.

scholars can take the advantage of geometrical solution process to introduce advances in TCSCM.

In several studies, TCSCM is directly applied or extended according to the necessities of the relevant research topics. The direct application of TCSCM, without accounting for existing units, has been carried out by substantial number of scholars. The details of those previous studies are given in APPENDIX F.

The extension of TCSCM to account for existing units has been studied by several scholars. Stoughton et al. (1980) recursively solved the non-linear capacity expansion problem by starting with the first candidate unit in the merit order and working upwards towards the last unit analyzing one candidate unit at each time until the demand is covered. Borison and Morris (1984) proposed a dynamic programming approach to solve the static optimization problem by finding the best trajectory through all the stages to arrive at the best state. The stages of the dynamic programming are the type of candidate units and the states are the cumulative capacity of the units. Levin and Zahavi (1984) proposed another iterative approach by which the non-linear optimal mix problem only for the candidate units is initially solved and then the loading points of the existing units are found by solving one dimensional auxiliary problem. In their further study, Levin and Zahavi (1985) improved their previous all-thermal power system to include any number of existing renewable units and one candidate renewable unit. Conejo et al. (1985) used an annual production cost and a static optimal mix capacity expansion model to assess the potential economic and reliability impacts of the integration of solar thermal generation in an electric utility system. The algorithms of the developed capacity expansion model are based on the Kuhn Tucker optimality conditions and can take into account not only existing thermal units but also must-run, hydropower units with reservoir or pumped-storage. Murphy et al. (1987) used feasible directions algorithms to find optimality by evaluating non-linear system of equations according to directional derivatives. Murphy and Weiss (1990) presented another approach to solve the non-linear expansion problem in 3 steps. During the first step, the problem is solved only for the break-even points of candidate units. In the second step, existing units are integrated into the solution of the previous step by loading all considered units starting with the highest variable cost to the lowest variable cost. In the last step, the retirement of existing units are taken into account for the optimal solution of expansion problem. Staffell and Green (2016) utilized the so-called “merit order stack approach” to achieve the optimal generation mix by minimizing the sum of investment and operating costs of power plants. The mentioned cost minimization

process is conducted by linking the capacities and the costs of power plants with their outputs and electricity prices (i.e. obtained as the variable cost of the marginal unit in merit order). Their proposed model considers the short-run equilibrium to minimize the operating cost of given plants and the long-run equilibrium to take online new power plants when each type covers its costs by leaving no further opportunities for profitable entry to the market. Their model is stated to be able to accommodate a so called "brownfield scenario" (i.e. capacity expansion planning considering also existing units) when existing units have to cover only their operating and maintenance costs (i.e. the past investment costs are sunk). In addition, heuristic improvements are added to the mentioned approach by taking into account the start-up cost of thermal units, and introducing a peak-shaving algorithm for hydro scheduling and must-run output requirement. Zhang and Baldick (2016) proposed another approach by which the capacity expansion problem is solved in two steps. In the first step, the load levels corresponding to the optimal operation of only candidate units are determined. In the second step, the load levels corresponding to the optimal operation of existing units are integrated to the previously obtained results by minimizing the total cost of electricity generation. In particular, they took into account the start-up costs of units and the retirement of existing units by considering a chronological load profile.

16.3 Organization of the Study

This study is organized into four chapters.

In Chapter 17, the general formulation of the cost minimization problem with existing units is explained. In Chapters 18 and 19, the lagrangian formulation and the proposed geometrical solution process of the cost minimization problem are explained respectively. In Chapter 20, a conclusion is provided for summarizing the purpose and the novelty of the proposed approach. In APPENDIX F, the studies on the direct application of TCSCM without accounting for existing units are provided. In APPENDIX G, an example on the proposed method is provided to guide practitioners.

17 THE GENERAL MATHEMATICAL FORMULATION OF THE CAPACITY EXPANSION PROBLEM

In this chapter, information is provided about the general mathematical formulation of the capacity expansion problem in previous studies. The general mathematical formulation of the static cost optimization, considering existing units, is previously proposed in Stoughton et al. (1980, pp. 753-754), Levin et al. (1980, p. 14), Levin et al. (1983, pp. 895-897), Levin and Zahavi (1984, p. 955), Conejo et al. (1985, pp. 169-170), Murphy et al. (1987, pp. 20-21), Murphy and Weiss (1990, pp. 830-831). In the following, the proposed concept in the mentioned previous studies is explained.

17.1 The General Mathematical Formulation in Previous Studies

The analysis commences by forming an array which constitutes variable and fixed costs as well as the installed capacities of existing and candidate units. The array is sorted and the elements[152] of it are indexed as indicated by "i" (see relation (17.1.1)) according to the increasing order of variable costs of all units (see relation (17.1.2)), i.e., the merit order of units which enables the least cost dispatch of units. In this way, the candidate units are de facto sorted in decreasing order of fixed costs, since it is assumed that a candidate unit, with a higher rank on the merit order, has a relative lower fixed cost than a candidate unit with a lower rank on the merit order[153] (see relations (17.1.3), (17.1.4), (17.1.5)). On the other hand, it is assumed that the fixed costs of existing units are sunk costs and do not indicate any ordering (see relation (17.1.6)).

$$i = 1, \dots, n \tag{17.1.1}$$

$$VC_1 < VC_2 < \cdots < VC_n \qquad \forall\, i \tag{17.1.2}$$

$$VC_i < VC_j \qquad if\ i < j \tag{17.1.3}$$

$$FC_i > FC_j \qquad if\ i < j\ \wedge\ \forall\, i,j \notin old \tag{17.1.4}$$

$$FC_i > 0 \qquad \forall\, i \notin old \tag{17.1.5}$$

$$FC_i = 0 \qquad \forall\, i \in old \tag{17.1.6}$$

[152] It refers to the considered power plants for the analysis.
[153] If this assumption were not made, a candidate unit i+1 would be inferior to candidate unit i relative to their AACC and could be eliminated without any evaluation process.

There are no start-up costs to bring the units online which are in reality added to variable costs. No economies of scale are taken into account in calculating FC and VC of all type units. The forced outages and maintenance requirements of the generating units are taken into account in a deterministic manner by derating the installed capacity of units (Cap_i) with an availability factor "a_i" ($0 \leq a_i \leq 1$). The indices of existing units are defined to be belonging to an index vector called "*old*" to which the candidate units does not belong. Accordingly, the decision variable "x_i" represents the utilized level of capacity of a candidate unit[154], if the index "i" does not belong to the index vector *old*. It should be noted that the installed capacity of a candidate unit is not known in advance and determined by using Eq. (17.1.7) after finding x_i.

$$Cap_i = \frac{x_i}{a_i} \qquad \forall\, i \notin old \tag{17.1.7}$$

The decision variable "x_i" represents the utilized level of capacity of an existing unit, if the index "i" belongs to *old*. In contrast, the installed capacity of an existing unit is known in advance and it is derated according to a factor a_i. The level of utilized capacity of an existing unit can be set at partial or full capacity (see constraint (17.1.13)).

The objective of the analysis is to minimize the sum of fixed and variable costs subject to the set constraints for all units considered in the capacity expansion planning, $\underline{x} = (\mathrm{x}_1, \ldots, \mathrm{x}_n)$, as expressed below:

$$\min_{\underline{x}} TC(x) = \sum_{i \notin old} FC_i \cdot \frac{x_i}{a_i} + \sum_{i=1}^{N} VC_i \cdot E_i \tag{17.1.8}$$

The energy output of a unit i (E_i) is calculated by using Eq. (17.1.9) according to its loading point on the annual load duration curve. This equation makes the optimization problem a non-linear mathematical programming to find the optimal utilized capacity, $\mathrm{x_i}$. The inverse of the load duration curve is indicated as $L^{-1}(z)$.

[154] Since only a target year can be planned with the method, it is not economical to commission a unit and set it at its partial capacity. Therefore, a commissioned unit is always set to its highest available capacity.

$$E_i = \int_{D_i}^{D_{i+1}} L^{-1}(z)\, dz \tag{17.1.9}$$

The loading point of a unit i (D_i) is found by summing up the utilized capacities of all units, which are prior to the unit i in the merit order, as expressed by Eq. (17.1.10). It can be inferred from the equation that the difference of two consecutive loading points will yield the utilized capacity of unit i (i.e. $x_i = D_{i+1} - D_i$). The last loading point (D_{n+1}) equals to the peak load of the considered year (L^m).

$$\begin{cases} D_1 = 0 & i = 1 \\ D_i = \sum_{j=1}^{i-1} x_j & i = 2, \dots., n+1 \\ D_{n+1} = L^m & \end{cases} \tag{17.1.10}$$

The peak load constraint (17.1.11) provides that the demand is to be satisfied in all hours of a year. The sum of x_i is set to be at least as high as the L^m. The L^m as well as the demand is considered to be normalized to 1 throughout this study.

$$\sum_{i=1}^{n} x_i \geq L^m \tag{17.1.11}$$

The non-negativity constraint (17.1.12) does not allow the utilization of an existing or a candidate unit to be determined as negative.

$$x_i \geq 0 \;\; \forall i \tag{17.1.12}$$

The existing unit constraint (17.1.13) limits the maximum allowable power generation capacity of an existing unit to its availability derated installed capacity.

$$x_i \leq a_i \cdot Cap_i \;\; \forall\, i \in old \tag{17.1.13}$$

18 THE LAGRANGIAN FORMULATION OF THE CAPACITY EXPANSION PROBLEM

In this chapter, information is provided about the lagrangian formulation of the capacity expansion problem in previous studies. The method of Langrangian multipliers can be utilized for the reformulation of the capacity expansion problem, since it is composed of a non-linear objective function with linear inequality and non-negativity constraints. The corresponding formulation of the static cost optimization, considering existing units, is previously proposed in Stoughton et al. (1980, pp. 753-754), Levin et al. (1980, p. 14). In the following, the proposed concept in the mentioned previous studies is explained.

18.1 The Lagrangian Formulation in Previous Studies

The formulation helps to solve the minimization of the objective function (18.1.1) by controlling the value of the decision variables which are restricted in a feasible region by the set constraints. Every given constraint is associated with an unconstrained multiplier so called a “lagrange multiplier” or “dual variable” or “shadow price”. The multipliers “ρ” “β_i” and “α_i” are associated with the peak load (17.1.11), non-negativity (17.1.12) and existing unit (17.1.13) constraints respectively. It should be noted that this formulation delivers valid results according to the previously introduced assumptions and relations from (17.1.1) to (17.1.7).

$$\min_{\underline{x}} \sum_{i \notin old} FC_i \cdot \frac{x_i}{a_i} + \sum_{i=1}^{N} VC_i \cdot E_i + \rho \left(L^m - \sum_{i=1}^{N} x_i \right) - \sum_{i=1}^{N} \beta_i \cdot x_i + \sum_{j \in old} \alpha_j \cdot \left(x_j - a_j \cdot Cap_j \right) \tag{18.1.1}$$

The non-negativity constraints on the decision variables of the minimization problem require the KKT conditions to be satisfied. If a non-linear optimization problem is constrained by non-negativity restrictions, the solution can be an interior or a boundary solution. This difficulty is overcome by using the KKT conditions. In Eq. (18.1.2), a representative nonlinear differentiable function with a non-negativity restriction is depicted to explain the possible restricted solution to the first quadrant that may arise.

$$\min y = f(z) \;\; s.t. \;\; z \geq 0 \tag{18.1.2}$$

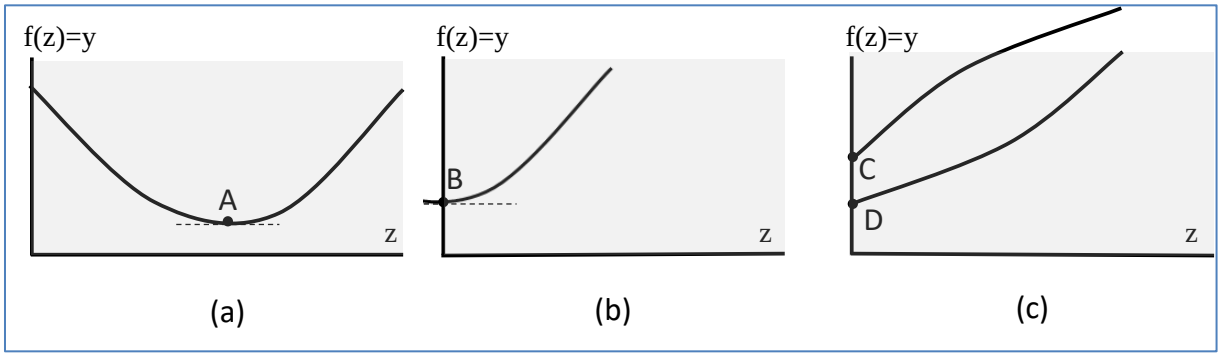

Figure 104- The possible global minimums of the function f with a non-negativity constraint (own illustration)

The panel (a) of Figure 104 depicts the occurrence of an interior solution in the shaded feasible region in which local minimum of $f(z)$ occurs at point A. The first-order condition is $dy/dz = f'(z) = 0$, where $z > 0$. In the panel b, another local minimum solution, which can occur on the boundary of the abscissa at point B, is depicted. In this case, the first order condition is also $dy/dz = f'(z) = 0$, whereas $z = 0$. The third possibility is another boundary solution occurring either on point C or D as depicted in the panel (c). The local minimum is defined by the inequality $f'(z) > 0$ where $z = 0$. These possibilities make up the first order necessary conditions for a value z to give a local minimum of y, namely $f'(z) \geq 0$; $z \geq 0$; $z \cdot f'(z) = 0$. The last condition is the complementary slackness condition indicating at least either the term z or $f'(z)$ must be zero, in order their product to be equal to zero. More information about non-linear programming can be found in Chapter 14 by Hillier & Liebermann (1988, pp. 415-461).

Listed below are the KKT optimality conditions, which are the first order conditions, sufficient for a global maximum and must be satisfied to be certain to get a global solution.

- The objective function $f(z)$ is a convex differentiable function,
- The constraints defines a convex set[155] and are also differentiable,
- The above given conditions assure a convex programming[156] problem for minimization.
- Finally, the corresponding decision variables satisfy the Kuhn Tucker conditions.

[155] A convex set is defined to be a collection of points forming a region inside which the line segments joining any pair of points can accommodate.
[156] A convex programming method is applied for minimizing convex functions over convex sets.

If all KKT conditions are satisfied, the decision variables represent a global minimum of the objective function subject to the constraints.

The capacity expansion problem expressed from Eq. (17.1.1) to Eq. (17.1.13) is stated to be a convex programming problem in Levin (as cited in Levin & Zahavi, 1984, p. 955), Murphy et al. (1987, p. 21), Murphy and Weiss (1990, pp. 837-838), and the derivation will not be repeated in this study. As it is stated by Levin and Zahavi, the necessary conditions for optimality by the KKT conditions are also sufficient conditions for optimality, and any solution that satisfies the KKT conditions also yields a global optimum to the capacity expansion problem.

In connection with the above explained excursus, the lagrangian function (18.1.1) is differentiated w.r.t. each decision variable and each multiplier and then set equal to zero yielding stationary points. The partial derivative of the objective function[157] w.r.t. the decision variable of a candidate unit i is given below:

$$FC_i + Q_i - \beta_i - \rho = 0 \quad \forall\, i \notin old \tag{18.1.3}$$

The derivative of the non-linear energy output function (see Eq. (17.1.9)) for every unit i is explicitly shown below:

$$Q_i \triangleq \sum_{h=i}^{n} (VC_h - VC_{h+1}) \cdot L^{-1}(D_{h+1}) \quad \forall\, i \tag{18.1.4}$$

The partial derivative of the objective function w.r.t. the decision variable of an existing unit i is represented below:

$$\alpha_i + Q_i - \beta_i - \rho = 0 \qquad \forall i \in old \tag{18.1.5}$$

[157] In this derivation, a_i is set to 1 according to the given information in Footnote 154.

The complementary slackness conditions of the peak load (17.1.11), non-negativity (17.1.12) and existing unit (17.1.13) constraints are respectively represented below:

$$\rho \cdot \left(\sum_{i=1}^{n} x_i - L^m \right) = 0 \tag{18.1.6}$$

$$\beta_i \cdot x_i = 0 \qquad \forall\, i \tag{18.1.7}$$

$$\alpha(a_i \cdot Cap_i - x_i) = 0 \qquad \forall\, i \in old \tag{18.1.8}$$

The non-negativity conditions for the dual variables are indicated below:

$$\rho \geq 0 \tag{18.1.9}$$

$$\beta_i \geq 0 \quad \forall\, i \tag{18.1.10}$$

$$\alpha_i \geq 0 \quad \forall\, i \in old \tag{18.1.11}$$

The primal problem of the capacity expansion is a resource allocation problem; on the other hand its lagrangian dual problem is a resource valuation problem. The dual problem is to maximize the value of the capacities supplied by the units. It can be analytically expressed as maximizing the objective function w.r.t. the dual variables on which constraints are set. A dual variable or a shadow price can be interpreted as the marginal cost of providing an additional MW_{el} over the next hour by the corresponding unit. In other words, it is a price for each scarce (or constrained) resource to be received in case of delivery. A shadow price associated with a non-binding constraint, i.e. if the capacity of an existing unit is partially utilized, is set zero due to the complementary slackness. A binding constraint corresponding to a scarce resource, i.e. if the capacity of an existing unit is fully utilized, implies a positive shadow price.

19 THE GEOMETRICAL FORMULATION OF THE CAPACITY EXPANSION PROBLEM

In this chapter, the geometrical formulation of the capacity expansion problem, which is developed during this study, is introduced. The novelty of this approach lies in the geometrical solution process to minimize the long run marginal cost of supplying 1 MW_{el} capacity throughout a year by finding the optimal combination of units. In Section 19.1, brief information about the fundamentals of the geometrical formulation is provided. In Sections 19.2 and 19.3, detailed information about the geometrical formulation regarding the solution process and algorithms is provided respectively.

19.1 The Fundamentals of the Geometrical Formulation

A number of cost polygons can be formed between the primary and the secondary y-axes and the x-axis by joining the line segments through the numbered intersection points in circles (p), as depicted in Figure 105. Example cost polygons can be formed by joining the line segments through the points FC_1 & p_3 or FC_2 & p_3 or FC_2 & p_5 etc., and the mentioned coordinate axes. In this respect, each cost polygon corresponds to a particular capacity expansion alternative consisting of different combination of units through variation in values of AACC and CF. In this example, the cost polygon with the lowest area is formed by the line segments passing through the points FC_3, p_1, p_2, p_3 and the mentioned coordinate axes.

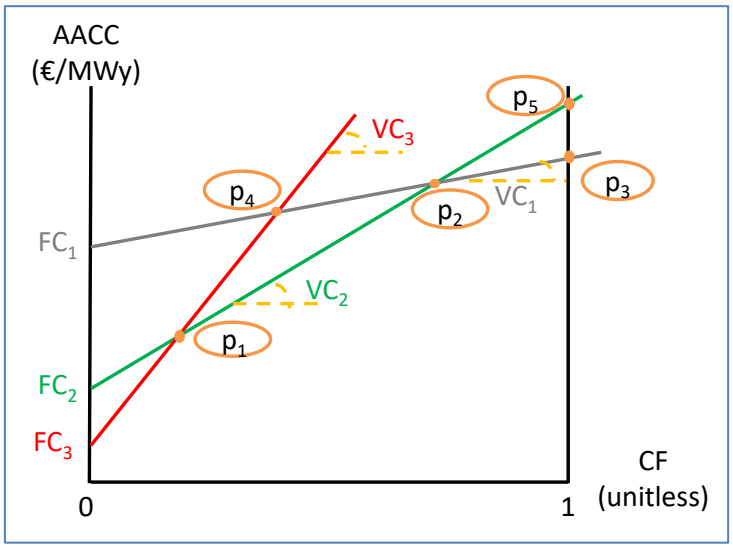

Figure 105- The example cost polygons formed through the points FC_1 & p_3 or FC_2 & p_3 or FC_2 & p_5 together with the coordinate axes (own illustration)

As it can be qualitatively inferred from Figure 105, the lowest cost polygon has the lowest area among others and hence located under all others. The developed geometrical solution process in this study calculates and finds the minimum area by moving along the intersection points of the cost curves to form all feasible[158] trapezoids and then join them to form all feasible cost polygons. The geometrical solution process can be considered in contrast to the solution process of an optimization problem by the simplex algorithm, which begins at a corner point and moves along the edges of the given boundary conditions until it reaches the vertex of the optimum solution.

The total sum of the area of all trapezoids (TTSAT) forming a cost polygon is expressed in Eq. (19.1.1) in general form. Note that FC_i will represent the shadow price α_i, if $i \in old$. Further, any first unit i on the merit order has $CF_i = 1$, since $D_i = 0$ (see Eq. (17.1.10)).

$$\text{TTSAT} = \sum_{i=1}^{n} \frac{AACC_i + AACC_{i+1}}{2} \cdot (CF_i - CF_{i+1}) \qquad (19.1.1)$$

The trapezoids, which form the cost polygon with the lowest area in the above example, are visualized in Figure 106 as numbered from 1 to 3. The areas of the numbered trapezoids indicate the annual cost of supplying 1 MW_{el} capacity by the corresponding units w.r.t. their AACCs and the cost-effective operation intervals (i.e. the range of CFs).

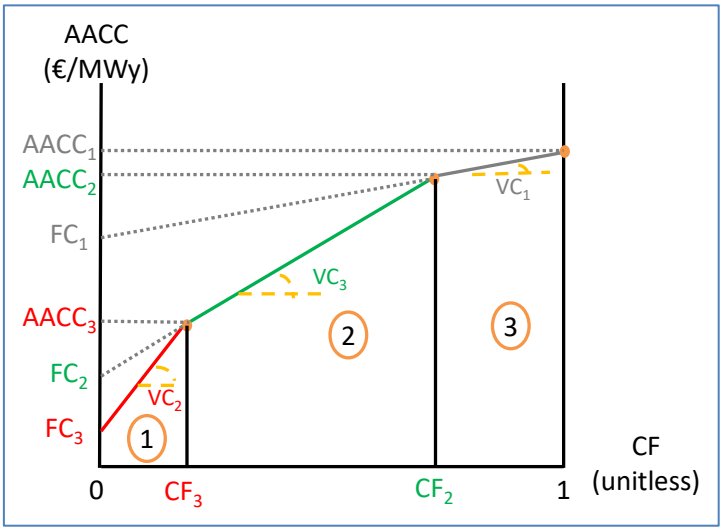

Figure 106- The lowest cost polygon of the above example formed by the numbered trapezoids (own illustration)

[158] Feasible trapezoids and cost polygons are analytically formed according to the described solution process and the given algorithms in the following sections.

For example, the unit 2 (marked in green color) can be cost effectively operated, if it is run at least CF_3 times 8760 hours per year and at most CF_2 times 8760 hours per year. Further, the unit 2 operates CF_2-CF_3 times 8760 hours per year (i.e. the duration of operation) at an average capacity cost range of $AACC_3$-$AACC_2$. Hence, the area of the trapezoid 2 amounts to the annual cost of supplying 1 MW_{el} capacity by the unit 2. Furthermore, the area of the cost polygon resulting from the combination of the numbered trapezoids amounts to the minimum annual total cost of supplying 1 MW_{el} capacity by the units 1, 2, and 3. Thus, the solution process can be interpreted as minimizing the long run marginal cost of supplying 1 MW_{el} capacity throughout a year by finding the optimal combination of units. Finally, after finding the points through which a lowest cost polygon is defined, the resulting CFs are projected onto the load duration curve to find the optimal capacity expansion as described in Section 16.1.

19.2 The Solution Process

In this section, the process of forming feasible cost polygons and the subsequent determination of the cost polygon with the lowest area are described in detail. The details of the algorithms, which are necessary for the corresponding computations, are explained in the next section. A flow chart is presented in Figure 107 to depict the developed solution procedure. The solution procedure is composed of the recursion process that is conducted by using Eq. (19.3.7) (see Subsection 19.3.1 for its derivation) and the scenario based analysis. The scenario based analysis is conducted subsequent to the termination of the recursive process; in order to determine the last unit in the merit order of each analyzed scenario. The determination of the last unit in the merit order of each analyzed scenario means that each feasible cost polygon corresponding to a particular capacity expansion alternative is finally obtained in analogy to the depiction in Figure 105. Afterwards, the cost polygon with the lowest area among the others is determined in analogy to the depiction in Figure 106. Thus, the determination of the least cost capacity expansion alternative is provided by the solution process and the corresponding algorithms.

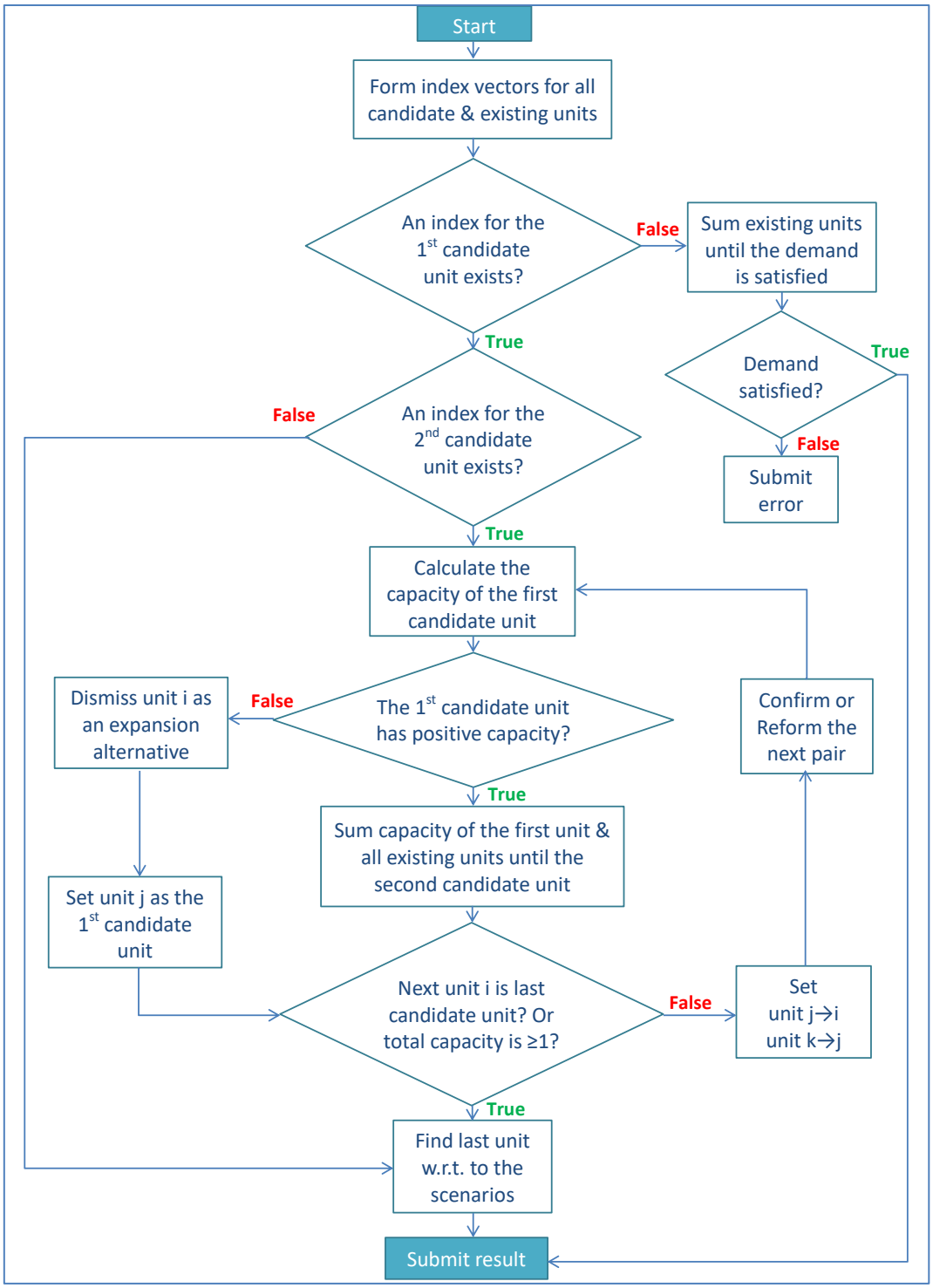

Figure 107- The flow chart representing the solution procedure of the geometrical method (own illustration)

The solution procedure starts by forming two separate index vectors for all considered candidate and existing units. An index vector is composed of the numbers indicating the position of the units in the merit order of dispatching (see Section 17.1 for more information).

The second step[159] is to check whether an index of a first candidate unit (i) exists. If there are not any candidate units, the demand should be satisfied with the existing units according to the merit order formed by them. The solution procedure submits error, if the demand were not to be satisfied. The third step is to check whether an index of a second candidate unit (j) exists. If a candidate unit with an index j does not exist, the process directly skips to the scenario based analysis (as will be later explained in the course of the solution procedure); since the candidate unit i is the single unit available for capacity expansion.

The step 2 and 3 are a validation of forming a pair from candidate units to start conducting a recursive procedure by using Eq. (19.3.7). More specifically, the Eq. (19.3.7) makes it necessary to form a pair of candidate units (i, j) for each computed iteration throughout the recursive procedure. Further, the candidate unit with the lower variable cost is indicated with the index i (i.e. the first candidate unit of a formed pair). Similarly, the unit with the index j (i.e. the second candidate unit of a formed pair) indicates the candidate unit with the higher variable cost according to the position of the paired units in the merit order of dispatching. Furthermore, the index values of each pair (i, j) are assigned according to the stored values in the index vector for candidate units. Moreover, the assumption in derivation of Eq. (19.3.7) makes it necessary not only for both candidate units i and j to have positive installed capacities but also for existing units (i.e. in case of being in the interval $i < \cdots < j$) to be set to operate at their maximum available capacities. Note that only the capacity of unit i is calculated during an iteration. If the result (x_i) is not positive, the candidate unit i will be dismissed from the expansion analysis and its capacity will be set to 0. Subsequently, the candidate unit j will be set to be the first candidate unit of the pair (the next i) which can be formed in the next step under the condition that the recursive process proceeds. If unit i were found out to have a positive capacity from the analysis of the pair $i - j$; also the unit j had to result in a positive capacity from the analysis of the pair $j - k$. The formed pair should be confirmed for the validity of the assumption (in derivation of Eq. (19.3.7)) before the recursion process. If the analysis of the pair $j - k$ does not yield that j has a positive capacity, then the determined capacity for unit i is not valid due to the mentioned assumption. In this situation, the index for the first candidate unit of the pair is set to i, whereas the second

[159] The capacity expansions of all considered type of power plants are exogenously given to the aforementioned capacity expansion model in Chapter 1; since they are based on scenarios for the target year 2023. Accordingly, all types of power plants are treated as existing units for the techno-economic analysis. Thus, only adjustments are carried out for the amount of capacity supplied by thermal power plants; which solely depends on their positions within the corresponding merit order curves and the considered load duration curves. See Chapters 22 and 23 in PART D for more information.

candidate unit of the pair is set to k during the recursive process. The corresponding unit j is dismissed from the expansion alternatives.

In order for the recursive process to end and skip to the scenario based analysis at least one of the below given conditions must be satisfied.

- The next unit i (i.e. the first candidate unit of the next possible pair) should be the last candidate unit available for capacity expansion.
- The total sum of the utilized capacities until the second candidate unit of the formed pair (i.e. the considered unit j) should be equal to or higher than 1.

The term "last candidate unit", which is mentioned in the first condition, means that a single unit is available in the index vector for candidate units and implies that the next pair of candidate units (i, j) cannot be formed in the above given context. If both of the mentioned conditions are not satisfied, the recursive process continues through forming the next candidate unit pair according to the stored values in the index vector for candidate units.

After satisfying both/either of the previously mentioned two conditions, the developed solution process continues with the scenario based analysis to find the last unit in the merit order. The last examined candidate unit, at the termination of the recursive process, is stored as a reference unit for the scenario based analysis and denoted with the index "ℓ". The utilized capacities of the units, which are in the interval $1 \leq ... \leq \ell$ or $1 \leq ... \ell ... <$ j (i.e. in case of existing units in the interval $\ell <...<$ j) in the merit order, are determined and stored before the termination of the recursive process. The last unit in the merit order of dispatching can be a candidate or an existing unit succeeding candidate unit ℓ or even unit ℓ itself. Further, a last existing unit can be a unit, which is set to operate at full capacity or at partial capacity. The scenarios represent the capacity expansion alternatives for finding the last unit in the merit order and are depicted in Figure 108 given below. It can be inferred from the figure that the scenarios are devoted into two according to the level of utilized capacity of the unit $\ell\,(x_l)$. This is necessary, since the recursion is terminated after analyzing the candidate unit ℓ and x_l is found to be positive on the ground that the successor candidate unit has a positive capacity. By setting the capacity of the unit ℓ higher than zero and equal to zero, the last candidate unit pair can be confirmed for the validity of the assumption (in derivation of Eq. (19.3.7)) after the recursion process. For this reason, in the 1st scenario, the unit ℓ or a candidate unit

succeeding the unit ℓ covers the rest demand[160] which results from setting the capacities of the subsequent higher indexed units to zero. In the 2nd and the 3rd scenarios, existing units set at partial or full capacities are considered in addition to the unit ℓ or a candidate unit succeeding the unit ℓ. In the 4th and the 5th scenario, only the existing units which succeed the unit ℓ, are considered. The 4th and the 5th scenario take online the corresponding existing units one by one and work backwards by replacing the capacity of the unit ℓ and the predecessor candidate units respectively. Most importantly, the scenario based analysis does not differentiate its solution process depending on the condition by which the recursion is terminated. In any case, the scenarios yielding negative utilized capacity for the considered unit will not be considered. Accordingly, the scenarios are computed in an iterative manner to calculate the areas under the all feasible cost polygons as explained in the next section.

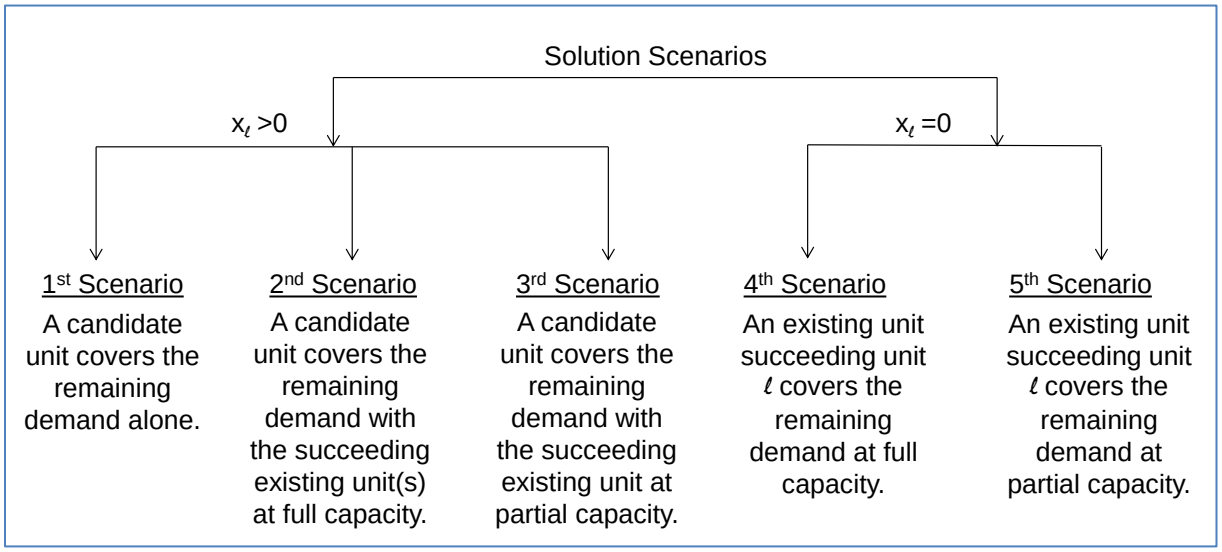

Figure 108- The scenarios for determining the last unit (own illustration)

The scenarios are primarily based on a tradeoff between the candidate units and the existing units following it, if they exist. This basis provides the means to verify whether to construct new power plants (i.e. to incur investment cost) or take the existing units succeeding unit ℓ with relative higher marginal costs online to cover the demand (i.e. to incur higher variable costs). The second tradeoff is grounded on the utilized levels of capacities of existing units to cover the demand with or without the last candidate unit ℓ. This basis provides the means to verify whether it is economical to use an existing unit at full or partial capacity to cover the demand. If an existing unit is operated at full capacity, the shadow price is higher than zero

[160] The mentioned computations are independent of the satisfied condition to terminate the recursive process. The corresponding computations are particularly expressed by Eq. (19.3.6) and the relations from (19.3.9) to (19.3.12).

and this implies that the corresponding unit can gain its capital cost by taking it online. If an existing unit is operated at partial capacity, the shadow price is equal to zero and this implies that the corresponding unit gains nothing by taking it online.

In the same manner, the proposed approach by Stoughton et al. (1980, p. 754) used an identical recursive algorithm through introducing one candidate unit in the merit order at a time and assigning capacity to the ones which fulfill the KKT conditions. The complication of this approach is in finding the last candidate unit and stopping the recursive procedure by satisfying the demand. In their articles, the solution procedure to find the last candidate unit is not analytically explained; however qualitatively described that bounds on the capacity of the last candidate unit are defined by identifying the final existing unit (p. 755). The described solution procedure is prone to complications during implementation. Although it uses forward recursive approach to find the optimal installed capacities of candidate units, it can go backwards to identify the last candidate unit, if the KKT conditions are not met for a final candidate unit in question. Through this operation procedure, the previously assigned capacities to the both candidate and existing units should be again calculated. In this study, the improved solution algorithms are developed to prevent this complication in finding the last unit.

19.3 The Solution Algorithms

In this section, the algorithms which are necessary to determine the last unit in the merit order are derived. The solution algorithms are implemented according to the given conditions by the capacity expansion scenarios. In addition, the results of these scenarios provide the necessary inputs to create cost polygons and calculate the areas of them (i.e. x_i, $AACC_i$, CF_i and α_i). It should be noted that the algorithms deliver valid results according to the aforementioned lagrangian formulation of the capacity expansion problem and the relations from (17.1.1) to (17.1.7), and they will not be repeated for the derivation of the developed methodology.

The solution algorithms are categorized into 3 cases. The 1st case indicates the algorithms for the 1st scenario to determine the last unit which is a candidate unit (see Subsection 19.3.1). Further, the 2nd case indicates the algorithms for the 2nd and 4th scenarios to determine the last unit which is an existing unit set at full operational capacity. Note that the main difference in the 2nd and 4th scenarios is whether the last candidate unit ℓ has a positive capacity as assumed in 2nd scenario or equals to zero as assumed in 4th scenario (see Subsection 19.3.2). Finally, the 3rd case indicates the algorithms for the 3rd and 5th scenarios in which the last unit is an

existing unit set at partial operational capacity (see Subsection 19.3.3). The main difference in the mentioned scenarios is whether the last candidate unit ℓ has a positive capacity as assumed in 3rd scenario or equals to zero as assumed in 5th scenario.

The solution process is iterative and its outer and inner loops are depicted in Figure 109. The main difference between the panel a and b of the figure is the clockwise and the counterclockwise operations of the corresponding outer loops[161] respectively. In contrast, both of the inner loops operate in clockwise direction. According to the aforementioned relations from (17.1.1) to (17.1.6), the clockwise operation of the outer loop leads to the consideration of candidate units with relatively higher variable and lower investment costs for capacity expansion planning. Nevertheless, the counterclockwise operation of the outer loop leads to the consideration of candidate units with relatively lower variable and higher investment costs for capacity expansion planning[162]. The inner loops, operating in clockwise direction, lead to the consideration of existing units with relatively higher variable costs compared to the considered candidate units for capacity expansion planning[163]. As a result, the solution process is implemented based on the two main tradeoffs mentioned for the construction of the scenarios in the previous section. As a matter of fact, all feasible capacity expansion alternatives (i.e. cost polygons) are provided by the solution process and the corresponding algorithms to determine the least cost capacity expansion alternative.

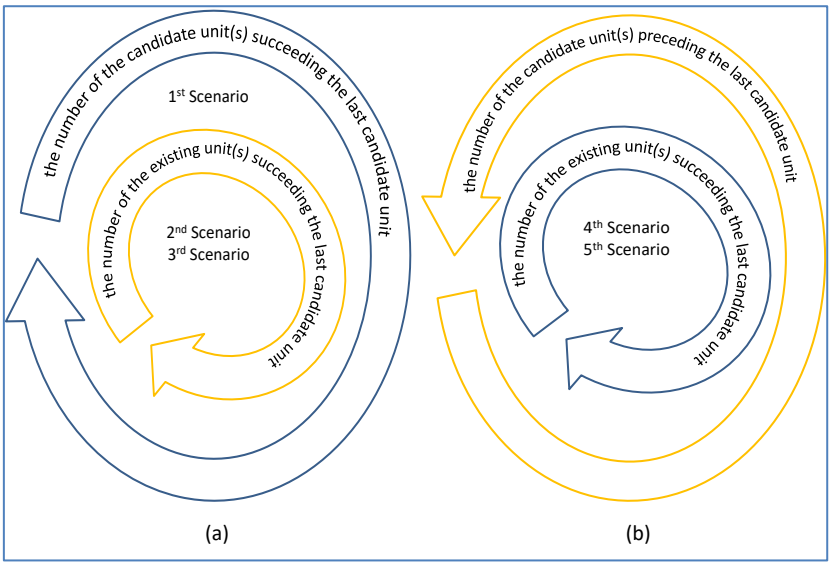

Figure 109- The loops of the solution process w.r.t. the scenarios (own illustration)

[161] This process also makes the 2nd vs. the 4th scenario and the 3rd vs. the 5th scenario different from each other.
[162] The mentioned operations of the outer loops are qualitative descriptions of the tradeoffs between the low capital/high fuel costs and high capital/low fuel costs.
[163] This statement qualitatively describes the tradeoff between incurring investment costs by commissioning candidate units and incurring relatively higher variable costs by taking existing units online.

It can be inferred from the panel a of the Figure 109 that the 1st scenario runs so many times as the number of the candidate unit(s) succeeding the unit ℓ; whereas the 2nd and 3rd scenarios run so many times as the number of the candidate unit(s) and existing unit(s) succeeding the unit ℓ. During each run, the outer loop takes candidate units with higher marginal cost online; whereas the inner loop takes the existing units with higher marginal costs online. In this way, the incurred investment costs are intended to be reduced, however the incurred variable costs are intended to be increased. It can be inferred from panel b that the 4th and 5th scenarios run so many times as the number of the candidate unit(s) preceding and the number of the existing unit(s) succeeding the unit ℓ. During each run, the outer loop takes candidate units with higher marginal cost offline; whereas the inner loop takes the existing units with higher marginal costs online. In this way, the incurred investment costs are intended to be increased, however the incurred variable costs are intended to be reduced relative to the clockwise operation of the outer loop in the panel a of the Figure 109. Note that the 4th or the 5th scenario also contributes to the aforementioned outcome together with the counterclockwise operation of the corresponding outer loop; since the capacity of the last candidate unit ℓ is assigned to be zero without depending on the satisfied condition to terminate the recursive process. Accordingly, the candidate unit(s) preceding unit ℓ with relatively lower variable and higher investment cost(s) is/are taken into account for capacity expansion planning.

The loading points of the existing units operating at full and partial capacities are found analytically similar to Levin and Zahavi (1984, pp. 957-960). Although the utilized algorithms are similar to the ones in Levin and Zahavi, their results are utilized in different solution procedures in comparison to this study. In their solution procedure, the algorithms are utilized to introduce existing-multi-units (i.e. consecutive series of existing units) into the analysis, after solving the problem for only new units. In this way, the previously determined optimal capacities of the new units are adjusted so as to satisfy the existing unit constraints at minimum cost. Although their solution procedure is analytically efficient, the definitions and the assumptions make it quite challenging to implement it and also to interpret the result of the analysis. In addition, the costs of the different expansion alternatives cannot be explicitly provided and a trial and error procedure is applied to find the index of candidate and existing units in the optimal capacity expansion plan. In this study, these complications are overcome by creating cost polygons dependent on the proposed capacity expansion scenarios and finding the cost polygon with the lowest area for optimal capacity expansion. For the sake of simplicity to visualize, the cases are explained in an example power system with only three

units in the next subsections. In addition, the algorithms are also adapted for n number of candidate and existing units for evaluation.

19.3.1 Case 1: One of the candidate units is the last unit

The derivation of this case is same as the derivation of TCSCM which does not consider any existing units in a power system during the evaluation of a capacity expansion problem (see Figure 110). The solution algorithm is derived by excluding the existing unit capacity constraint (17.1.13) and also the corresponding KKT conditions (18.1.5), (18.1.8), and (18.1.11) of the lagrangian formulation. The given below Eq. (19.3.1) is formed by using the KKT condition (18.1.3) and then equating it for two consecutive candidate units i and $i+1$ in the merit order.

$$FC_i - \beta_i + (VC_i - VC_{i+1}) \cdot L^{-1}(D_{i+1}) = FC_{i+1} - \beta_{i+1} \tag{19.3.1}$$

The Eq. (19.3.1) is obtained by assuming both consecutive candidate units to be in the optimal mix solution with positive capacity, i.e. the shadow prices (β_i, β_{i+1}) associated with the non-binding non-negativity constraint (17.1.12) is set equal to 0 for the units i and $i+1$. By substituting $L^{-1}(D_i)$ in Eq. (19.3.1) with CF_{i+1}[164], it results in Eq. (19.3.2) as represented below:

$$FC_i + VC_i \cdot CF_{i+1} = FC_{i+1} + VC_{i+1} \cdot CF_{i+1} \tag{19.3.2}$$

After solving Eq. (19.3.2) for CF_{i+1}, Eq. (19.3.3) is obtained. It should be note that the corresponding FCs and VCs of units are known during the evaluation.

$$CF_{i+1} = \frac{FC_i - FC_{i+1}}{VC_{i+1} - VC_i} \tag{19.3.3}$$

The CFs of all given candidate units can be found recursively by the above derived equation and then through projecting the CFs onto to the LDC by using Eq. (19.3.4). The optimal utilized capacity of the corresponding units $(x_1, x_l \,\&\, x_3)$ can be obtained by finding the corresponding loading points D_l, D_3 (note that $D_1 = 0$) according to Eqs. (19.3.5) and (19.3.6). Furthermore, AACC, Cap and TTSAT of all corresponding units can be determined by using Eq. (16.1.1), (17.1.7) and (19.1.1) respectively. The derived equations are indicated

[164] See Eq. (19.3.8) for CF_{i+1}.

in their general forms, however the unit l in Figure 110 is the same representation used in the general form of the equations to enable a simplified practice of the example.

$$D_i = L(CF_i) \qquad \forall i \tag{19.3.4}$$

$$x_i = D_{i+1} - D_i \qquad \forall i: i \leq l \tag{19.3.5}$$

$$x_i = \left(1 - \sum_{p=1}^{i-1} x_p\right) \qquad \forall i: i > l \ \wedge \ i \notin old \tag{19.3.6}$$

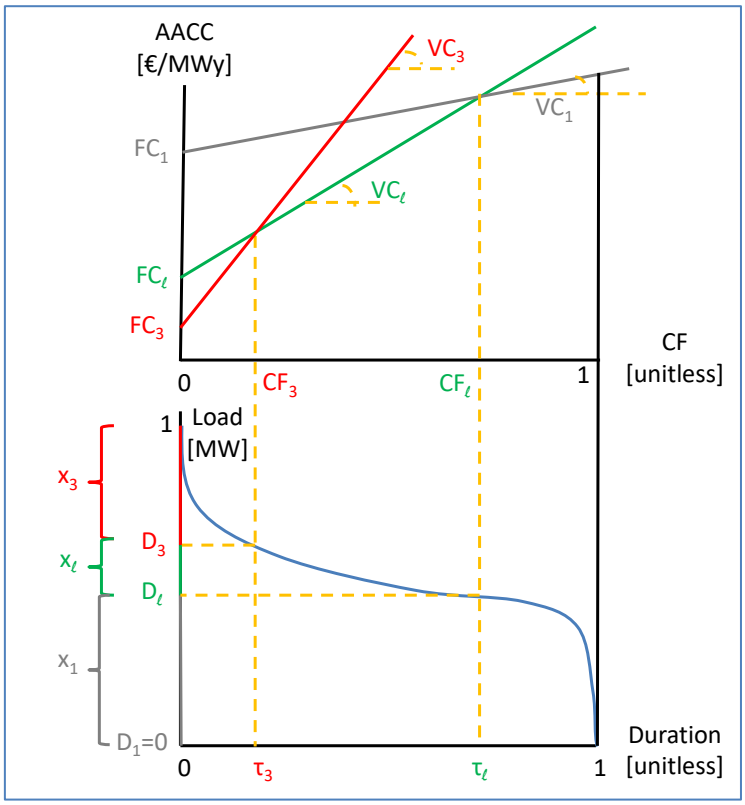

Figure 110- An example power system with three candidate units (own illustration)

If additional units were to exist between the new units in the above diagram, the general form of Eq. (19.3.3) takes the form of Eq. (19.3.7) (also in Stoughton et al., p.754). In Eq. (19.3.7), the index i and j denotes two consecutive candidates in the merit order which in between can constitute existing units (i.e. the indices between $i \leq \cdots \leq j$). Similar to the derivation of Eq. (19.3.2), both consecutive new units, i and j, are initially assumed to have positive capacity and the existing units, between i and j in the loading merit order, are set to operate at their maximum available capacities. This equation is derived by recursively equating the Eq. (19.3.1) for all the units in the above mentioned interval. During the application of Eq. (19.3.7), only the derated installed capacities of the existing units are needed to be used in the

last term, whereas the other parameters of the existing units cancel each other. The Eq. (19.3.7) is solved for x_i ($i \notin old$) and the CFs can be derived by using the given below Eq. (19.3.8) for every index in the interval $1 \leq \cdots \leq j$.

$$FC_i - FC_j = \sum_{a=i}^{j-1} (VC_{a+1} - VC_a) \cdot L^{-1}\left(\sum_{p=1}^{a} x_p\right) \tag{19.3.7}$$

The Eq. (19.3.8) is given in general form and can be used for finding CF_{i+1} in any case, if the utilized levels of capacities in the index interval $1 \leq \cdots \leq i$ are known. Furthermore, AACC, Cap and TTSAT of all corresponding units can be determined by using Eqs. (19.3.8), (16.1.1), (17.1.7) and (19.1.1) respectively.

$$CF_{i+1} = L^{-1}\left(\sum_{p=1}^{i} x_p\right) \tag{19.3.8}$$

The given above equations from (19.3.4) to (19.3.8) are used not only for the recursion process but also for the 1st scenario. In addition, the given constraints below are also considered in the 1st scenario. The last candidate unit ℓ should have a positive capacity as indicated in relation (19.3.9). Further, the considered candidate unit or units, which is/are succeeding the unit ℓ, should also have a positive capacity or capacities during the evaluation of the capacity expansion problem (see relations (19.3.10) and (19.3.11)). These mentioned units are evaluated one by one according to their indexes on the merit order which are stored in the index vector called "cusl"[165]. The elements of the corresponding index vector is specified by the index "o". The loop process is repeated according to the number of candidate units which are higher than the index ℓ, denoted as "ncusl"[166]. In particular, it is for each positive integer value (i.e. $\mathbb{Z}^+$) of o from 1 to ncusl.

$$x_l > 0 \tag{19.3.9}$$

$$cusl(o) \geq l \qquad \forall o: o \in [1, ncusl] \ \wedge \ o \in \mathbb{Z}^+ \tag{19.3.10}$$

$$x_i > 0 \qquad \forall i: i = cusl(o) \tag{19.3.11}$$

[165] "cusl" is an abbreviation for "the candidate unit(s) succeeding the last candidate unit".

[166] "ncusl" is an abbreviation for "the number of the candidate unit(s) succeeding last candidate unit".

During the loop process, the higher indexed candidate and existing units, other than the considered ones, are set 0 as indicated below.

$$x_i = 0 \qquad \forall i: i > cusl(o) \tag{19.3.12}$$

19.3.2 Case 2: One of the existing units, operating at full capacity, is the last unit

In this case, the existing units are taken into account as the last unit in the merit order; however on the condition that all existing units operate at maximum of the available capacity. The Figure 111 depicts an example 3 unit system in which the last unit on the merit order is an existing unit (i.e. unit 3); whereas the other units are candidate units. The VCs of all depicted units are known; whereas the FCs of only candidate units are known. Since the unit 3 is an existing unit, its corresponding shadow price can be determined by using the present information on its derated installed capacity x_3, loading point D_3 (i.e. equal to $1 - x_3$) and the given parameters of the candidate units. Formally, by assuming that the capacity constraint for existing units (17.1.13) is binding (i.e. the existing unit is set at full capacity and $\alpha_{i+1} > 0$) and the KKT conditions (18.1.3) and (18.1.5) for candidate unit i and existing unit $i+1$ can be equated with each other to find α_{i+1}.

$$FC_i - \beta_i + VC_i \cdot L^{-1}(D_{i+1}) = \alpha_{i+1} - \beta_{i+1} + VC_{i+1} \cdot L^{-1}(D_{i+1}) \tag{19.3.13}$$

The given above Eq. (19.3.13) is obtained by assuming both units to be in the optimal mix solution with positive capacity, i.e. the shadow prices (β_i, β_{i+1}) associated with the non-binding non-negativity constraint (17.1.12) is set equal to 0 for the units i and $i+1$. By substituting $L^{-1}(D_i)$ in Eq. (19.3.13) with CF_{i+1}, the given below Eq. (19.3.14) is obtained as represented below:

$$FC_i + VC_i \cdot CF_{i+1} = \alpha_{i+1} + VC_{i+1} \cdot CF_{i+1} \tag{19.3.14}$$

After solving Eq. (19.3.14) for α_{i+1}, Eq. (19.3.15) is obtained. Furthermore, AACC, Cap and TTSAT of all corresponding units can be determined by using Eq. (16.1.1), (17.1.7) and (19.1.1) respectively. The derived equations are indicated in their general forms, however the

unit l in Figure 111 is the same representation used in the general form of the equations to enable a simplified practice of the example.

$$\alpha_{i+1} = FC_i + CF_{i+1} \cdot (VC_i - VC_{i+1}) \tag{19.3.15}$$

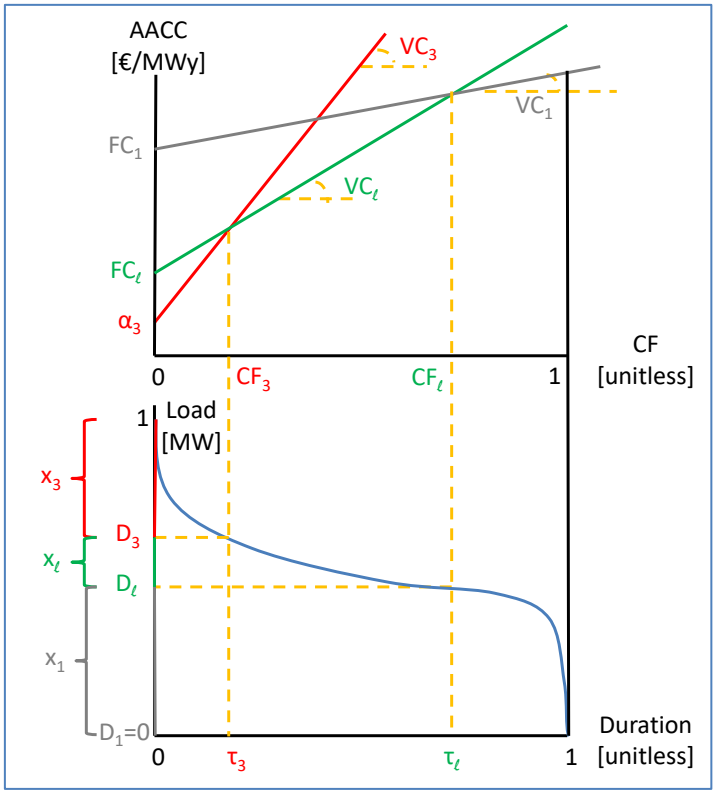

Figure 111- An example power system with an existing last unit operating at full capacity (own illustration)

The algorithms can be recursively extended to find the corresponding parameters of all considered existing units, if there is more than one existing unit present between the unit ℓ and the last existing unit operating at full capacity. In the 2nd and the 4th scenarios, the general solution processes are proposed for the case, if the last unit in the merit order is an existing unit. The two scenarios distinguish their selves from each other by their assumptions about the installed capacity of the unit ℓ. For the 2nd scenario, it is assumed that the unit ℓ has a positive capacity (19.3.16); whereas the opposite for the 4th scenario (19.3.25). The 2nd scenario processes forward by taking online the candidate units according to (19.3.17), (19.3.18) and existing units succeeding unit ℓ one by one according to (19.3.19), (19.3.23); whereas the 4th scenario processes forward by taking online the existing units succeeding ℓ according to (19.3.27), (19.3.33), and backwards taking offline the units preceding unit ℓ one by one according to (19.3.26), (19.3.31).

In the 2nd scenario, the indexes of analyzed existing units, which are higher than the index ℓ, are stored in the index vector called "$eusl$"[167]. The elements of the corresponding index vector are specified by the index "k". It should be noted that the $eusl$ is a proper subset of the index vector old according to (19.3.19). The loop process is repeated according to the number of candidate and existing units which are higher than the index ℓ, denoted as $ncusl$ and "$neusl$"[168] respectively according to (19.3.18), (19.3.19). The loop for candidate units is repeated for each positive integer value of o between 1 to ncusl, whereas for existing units for each integer value of k between 1 to $neusl$. During the loop process, the indexes of the existing units are always higher than the candidate units as expressed in (19.3.20).

$$x_l > 0 \tag{19.3.16}$$

$$x_i > 0 \qquad \forall i: i = cusl(o) \tag{19.3.17}$$

$$cusl(o) \geq l \qquad \forall o: o \in [1, ncusl] \ \wedge \ o \in \mathbb{Z}^+ \tag{19.3.18}$$

$$eusl(k) > l \qquad eusl \subset old \wedge k \in [1, neusl] \wedge k \in \mathbb{Z}^+ \tag{19.3.19}$$

$$cusl(o) < eusl(k) \qquad \forall k \wedge \forall o \tag{19.3.20}$$

During the loop process, the higher indexed candidate and existing units, other than the considered ones, are set 0 as represented in (19.3.21), (19.3.22). The existing units between the unit ℓ and including the last existing unit are set at full load as indicated in (19.3.23).

$$x_i = 0 \qquad \forall i: i \in cusl \ \wedge \ i > cusl(o) \tag{19.3.21}$$

$$x_i = 0 \qquad \forall i: i > eusl(k) \tag{19.3.22}$$

$$x_i = a_i \cdot Cap_i \qquad \forall i: i \in eusl \ \wedge \ cusl(o) < i \leq eusl(k) \tag{19.3.23}$$

The given below Eq. (19.3.24) is solved recursively for all the units in $cusl$ and in $eusl$. Each trial resulting with a positive result is considered for determining the lowest cost polygon. Finally, CF, AACC, Cap and TTSAT of all corresponding units can be determined by using Eqs. (19.3.8), (16.1.1), (17.1.7) and (19.1.1) respectively.

[167] "$eusl$" is an abbreviation for "the existing unit(s) succeeding last candidate unit".
[168] "$neusl$" is an abbreviation for "the number of the existing unit(s) succeeding last candidate unit.

$$x_i = \left(1 - \sum_{h=1}^{i-1} x_i + \sum_{b=1}^{k} x_{eusl(b)}\right) \quad \forall i,k: i \in cusl \ \wedge \ 1 \leq k \leq neusl \tag{19.3.24}$$

In the 4th scenario, the indexes of candidate units, which are lower than the index ℓ, are stored in the index vector called "$cupl$"[169]. The elements of the corresponding index vector are specified by the index "m". The loop process is repeated according to the number of candidate and existing units denoted as "$ncupl$"[170] and $neusl$ respectively according to (19.3.26), (19.3.27). The loop for candidate units is repeated for each integer value of m from 1 to $ncupl$, whereas for existing units for each integer value of k from 1 to $neusl$. During the loop process, the indexes of the existing units are always higher than the candidate units according to (19.3.28). It should be noted that $cupl(m)$ is iterated backwards according to (19.3.29), whereas $eusl(k)$ is iterated forward w.r.t. the merit order according to (19.3.30).

$$x_l = 0 \tag{19.3.25}$$

$$cupl(m) < l \qquad \forall m: m \in [1, ncupl] \ \wedge \ m \in \mathbb{Z}^+ \tag{19.3.26}$$

$$eusl(k) > l \qquad eusl \subset old \wedge k \in [1, neusl] \ \wedge \ k \in \mathbb{Z}^+ \tag{19.3.27}$$

$$cupl(m) < eusl(k) \qquad \forall k \ \wedge \ \forall m \tag{19.3.28}$$

$$cupl(m+1) < cupl(m) \qquad \forall m \tag{19.3.29}$$

$$eusl(k) < eusl(k+1) \qquad \forall k \tag{19.3.30}$$

During the loop process, the higher indexed candidate and existing units, other than the considered ones, are set 0 as expressed in (19.3.31), (19.3.32). The existing units between the unit $cupl(m)$ and including the last existing unit are set at full load as indicated in (19.3.33).

$$x_i = 0 \qquad \forall i: i \in cupl \ \wedge \ i > cupl(m) \tag{19.3.31}$$

$$x_i = 0 \qquad \forall i: i > eusl(k) \tag{19.3.32}$$

$$x_i = a_i \cdot Cap_i \qquad \forall i: i \in eusl \ \wedge \ cupl(m) < i \leq eusl(k) \tag{19.3.33}$$

The given below Eq. (19.3.34) is solved recursively for all the units in $cupl$ and units in $eusl$. Each trial resulting with a positive result is considered for determining the lowest cost

[169] "$cupl$" is an abbreviation for "the candidate unit(s) preceding last candidate unit"

[170] "$ncupl$" is an abbreviation for "the number of the candidate unit(s) succeeding last candidate unit"

polygon. Finally, CF, AACC, Cap and TTSAT of all corresponding units can be determined by using Eqs. (19.3.8), (16.1.1), (17.1.7) and (19.1.1) respectively.

$$x_i = \left(1 - \sum_{h=1}^{i-1} x_i + \sum_{b=1}^{k} x_{eusl(b)}\right) \quad \forall i,k: i \in cupl \ \wedge \ 1 \leq k \leq neusl \tag{19.3.34}$$

19.3.3 Case 3: One of the existing units, operating at partial capacity, is the last unit

In case 3, the existing units are taken into account as the last unit in the merit order; however on the condition that some of the existing units operate at full capacity available. In particular the last existing unit among them operates at partial capacity during the planning year. The Figure 112 depicts an example 3 unit system in which the last unit in the merit order is an existing unit (i.e. unit 3); whereas the other units are the candidate units. The VCs of all depicted units are known; whereas the FCs of only candidate units are known. Since the unit 3 is an existing unit operating at partial capacity; its corresponding shadow price of capacity is 0 and by using these given information, the utilized level of capacity x_3, and the loading point D_3 can be determined. Formally, by assuming that the capacity constraint for existing units (17.1.13) is not binding and the KKT conditions (18.1.3) and (18.1.5) can be equated with each other for candidate unit i and existing unit $i+1$ as shown below:

$$FC_i - \beta_i + VC_i \cdot L^{-1}(D_{i+1}) = \alpha_{i+1} - \beta_{i+1} + VC_{i+1} \cdot L^{-1}(D_{i+1}) \tag{19.3.35}$$

The Eq. (19.3.35) is obtained by assuming both units to be in the optimal mix solution with positive capacity, i.e. the shadow prices (β_i, β_{i+1}) associated with the non-binding non-negativity constraint (17.1.12) are set equal to 0. In addition, the shadow price (α_{i+1}) associated with the non-binding existing unit constraint (17.1.13) is also set to 0. By substituting $L^{-1}(D_{i+1})$ in Eq. (19.3.35) with CF_{i+1}, the given below Eq. is obtained.

$$FC_i + VC_i \cdot CF_{i+1} = VC_{i+1} \cdot CF_{i+1} \tag{19.3.36}$$

After solving Eq. (19.3.36) for CF_{i+1}, Eq. (19.3.37) is obtained. The loading point D_{i+1} can then be found by projecting the CF_{i+1} onto to the LDC by using Eq. (19.3.4). Since $i+1$ is the last unit in the merit order, the capacity x_{i+1} can be found by subtracting D_{i+1} from the peak load, which is normalized to 1 (19.3.38). Furthermore, CF, AACC, Cap and TTSAT of

all corresponding units can be determined by using Eqs. (19.3.8), (16.1.1), (17.1.7) and (19.1.1) respectively. The derived equations are indicated in their general forms, however the unit l in Figure 112 is the same representation used in the general form of the equations to enable a simplified practice of the example.

$$CF_{i+1} = \frac{FC_i}{VC_{i+1} - VC_i} \qquad \forall i+1 : i+1 \in old \tag{19.3.37}$$

$$x_{i+1} = (1 - D_{i+1}) \qquad \forall i+1 : i \in old \ \wedge \ \alpha_{i+1} = 0 \tag{19.3.38}$$

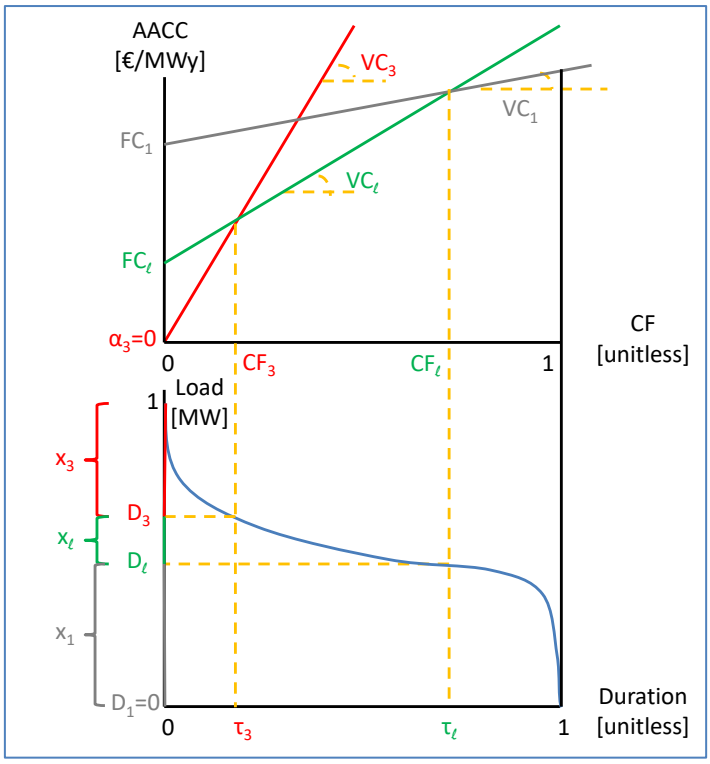

Figure 112- An example power system with an existing last unit operating at partial capacity (own illustration)

The algorithms can be recursively extended to find the corresponding parameters of all considered existing units, if there is more than one existing unit present between the unit ℓ and the last existing unit operating at partial capacity. The 3rd scenario is identical to the 2nd scenario w.r.t. the Eqs. (19.3.16), (19.3.18), (19.3.22). The main difference of the 3rd scenario is the partially utilized capacity of the last existing unit which makes it necessary to replace the constraint (19.3.23) with (19.3.39). The utilized level of capacity of the last existing unit must be smaller than its derated installed capacity as indicated in (19.3.39). The existing units between the last candidate unit and excluding the last existing unit are set at full load according to (19.3.40).

$$x_i < a_i \cdot Cap_i \qquad \forall i: i = eusl(k) \tag{19.3.39}$$

$$x_i = a_i \cdot Cap_i \qquad \forall i: l < i < eusl(k) \tag{19.3.40}$$

The given below Eq. (19.3.41) is in general form and provides solution for every o of $x_{cusl(o)}$ whether there are any existing units present between the units $cusl(o)$ and $eusl(k)$ or not (also in Levin and Zahavi, 1984, p. 959). Finally, CF, AACC, Cap and TTSAT of all corresponding units can be determined by using Eqs. (19.3.8), (16.1.1), (17.1.7) and (19.1.1) respectively.

$$\sum_{b=cusl(o)}^{eusl(k)-1} (VC_b - VC_{b+1}) \cdot L^{-1}(D_{b+1}) + FC_{cusl(o)} = 0 \tag{19.3.41}$$

The 5th scenario is different from the 3rd scenario according to the assumption that $x_l = 0$; whereas identical to the 4th scenario by Eqs. (19.3.25), (19.3.26) and (19.3.32). The main difference of the 5th scenario vs. the 4th is the partially utilized capacity of the last existing unit which makes it necessary to replace the Eq. (19.3.33) with (19.3.42). The utilized amount of capacity of the last existing unit must be smaller than its installed capacity (19.3.42). The existing units between the unit ℓ and excluding the last existing unit are set at full load (19.3.43). The given below Eq. (19.3.44) is similar to Eq. (19.3.41); however the initial and the final values of the summation are different. The Eq. (19.3.44) provides solution for every m of $x_{cupl(m)}$ whether there are any existing units present between the units $cupl(m)$ and $eusl(k)$ or not. Finally, CF, AACC, Cap and TTSAT of all corresponding units can be determined by using Eqs. (19.3.8), (16.1.1), (17.1.7) and (19.1.1) respectively.

$$x_i < a_i \cdot Cap_i \qquad \forall i: i = eusl(k) \tag{19.3.42}$$

$$x_i = a_i \cdot Cap_i \qquad \forall i: l < i < eusl(k) \tag{19.3.43}$$

$$\sum_{b=cupl(m)}^{eusl(k)-1} (VC_b - VC_{b+1}) \cdot L^{-1}(D_{b+1}) + FC_{cupl(m)} = 0 \tag{19.3.44}$$

20 CONCLUSION

The classical screening curve methodology is a practical approach and preferred to be utilized during the preliminary investigation of a capacity expansion planning. The inherent limitations of the method have been overcome in several studies. In this study, a new approach is introduced to contribute to the screening curve methodologies which can take into account the candidate and the existing units to determine the least cost capacity expansion of an all-thermal power plant park. Further, the proposed methodology differs from the previous studies by its geometrical solution process to evaluate a static capacity expansion problem considering both existing and candidate power plants. Furthermore, the algorithms are computationally more efficient and straightforward than the ones in previous studies for the similar type of improvements. Finally, the interpretation of the optimal capacity expansion plan, which is enhanced by explicitly exhibiting the results of all considered capacity expansion alternatives, is useful for preliminary energy policy analysis.

The geometrical solution process can be interpreted as minimizing the long run marginal cost of supplying 1 MW_{el} capacity throughout a year by finding the optimal combination of units. The developed method calculates and finds the minimum area by moving along the intersection points of the cost curves to form all feasible trapezoids and then join them to form all feasible cost polygons. In particular, the area of the cost polygon resulting from the combination of the trapezoids amounts to the annual total cost of supplying 1 MW_{el} capacity by the considered units. The intersection points, which are needed to calculate the areas of the cost polygons, are found by using the KKT conditions in a recursive manner. The proposed approach by Stoughton et al. (1980, p. 754) uses an identical recursive algorithm through introducing one candidate unit on the merit order at a time and assigning capacity to the ones which fulfill the KKT conditions. In this study, the complication of their approach in finding the last candidate unit and stopping the recursive procedure is prevented. The last unit in the merit order of dispatching is determined by scenarios to obtain an optimal capacity expansion plan. The scenarios are primarily based on a tradeoff between the candidate and the succeeding existing. This basis provides the means to verify whether to construct new power plants (i.e. to incur investment costs) or take the existing units succeeding unit ℓ with relatively higher marginal costs online to cover the demand (i.e. to incur higher variable costs). The second tradeoff is grounded on the utilized level of capacity of existing units to cover the demand with or without the last candidate unit ℓ. This basis provides the means to

verify whether it is economical to use an existing unit at full or partial capacity to cover the demand. If an existing unit is operated at full capacity, the shadow price is higher than zero and this implies that the corresponding unit can gain its capital cost by taking it online. If an existing unit is operated at partial capacity, the shadow price is equal to zero and this implies that the corresponding unit gains nothing by taking it online. The solution algorithms of scenario based analysis, which are utilized for finding the loading points of the existing units operating at full and partial capacities, are implemented similar to the study by Levin and Zahavi (1984). According to the conditions which are set by the scenarios, a number of cost polygons are created by using the calculated loading points of the units and then using them to find the corresponding CFs and AACCs of the units on the screening curves. The areas of the formed cost polygons are calculated to determine the least cost polygon for optimal capacity expansion. Finally, after finding the points through which a lowest cost polygon is defined, the resulting CFs are projected onto the load duration curve to find the optimal capacity expansion.

For future research, the geometrical formulation can be extended not only to take into account renewable energy technologies but also to be a dynamic approach.

PART D THE TECHNO-ECONOMIC ASSESSMENT OF THE ENERGY POLICY 2023

21 INTRODUCTION

Turkey became a growing energy importer to meet its growing electricity demand as the Turkish economy rapidly developed. The Turkish government has committed itself to mitigate natural gas dependency according to the published guidelines in "Turkey Electricity Energy Market and Supply Security Strategy Paper" (2009) and in the NREAP[171] (2014). As mentioned in the Chapter 1, the Turkish government expects gains through the capacity expansion of the domestic resource based power plants alternative to the natural gas fired power plants. Most importantly, the Turkish government has declared in the NREAP that the energy policy 2023 will be implemented by all means. Accordingly, the adoption of the energy policy 2023 brings a new perspective to the resource allocation problem; since not only it is important to lessen the dependency on imported resources but also it should be examined to reveal whether the targeted exploitation of the remaining potential of the domestic energy resources produces benefits for the society greater than its costs.

21.1 Objective and Method of this Study

The social cost-benefit analysis is conducted by developing a capacity expansion model (see Figure 4 on p. 9). In this study, the energy policy 2023 is appraised to reveal whether the targeted exploitation of the remaining potential of the domestic energy resources produces benefits for the society w.r.t. the alternative capacity expansion scenarios. Accordingly, tradeoff analyses are conducted between the energy policy 2023 and the alternative capacity expansion scenarios in terms of capital, fuel and external costs of electricity generation. Further, the social cost-benefit analysis of the energy policy 2023 is conducted based on the "with-and-without" approach associated with the concept of opportunity cost. Hence, the benefit of adopting energy policy 2023 is measured relative to the savings which would have been foregone/gained by utilizing scarce resources in an alternative capacity expansion scenario. Furthermore, the gains/losses in welfare (i.e. net social benefit) with and without the adoption of the energy policy 2023 are relatively measured based on partial equilibrium analyses. Thus, the measured change in welfare is restricted to the electricity market by presuming that the broader economic status remains unaffected. Finally, the chosen best policy among other constructed capacity expansion scenarios is the one which can

[171] National Renewable Energy Action Plan for Turkey

theoretically create the greatest possible net benefit to the society according to the established method of cost-benefit analysis.

21.2 Organization of the Study

This study is organized into five chapters.

In Chapter 22, information is provided about the required inputs of the capacity expansion model for the calculation of the social cost of supplying electricity, the annual amount of generated electricity and CO_2 emissions. Namely, information is given about the construction of the capacity expansion scenarios, reliability assessments on the capacity expansion scenarios, technical and cost parameters of all considered type of power plants.

In Chapter 23, theoretical information is given about the definition of the welfare and welfare analysis of electricity market. In addition, detailed information is provided about the techno-economic calculations which are carried out by utilizing the capacity expansion model.

In Chapters 24 and 25, the results of the techno-economic calculations are given.

In Chapter 26, a conclusion is provided for summarizing all conducted analyses on the energy policy 2023 and the corresponding results. In addition, a discussion is carried out on the obtained results and suggestions are made for the improvement of not only the official targets for the year 2023 but also the limitations regarding the techno-economic analysis.

22 Inputs of the Capacity Expansion Model

In this chapter, information is provided about the required inputs of the capacity expansion model for the calculation of the annual amount of electricity generated by all considered types of power plants, CO_2 emissions caused by thermal, geothermal and biomass power plants and the social cost of supplying electricity. In section 22.1, information is given about the construction of the capacity expansion scenarios. In section 22.2, reliability assessments on the capacity expansion scenarios are carried out. In section 22.3, technical and cost parameters of all considered type of power plants are provided.

22.1 Constructing Capacity Expansion Scenarios

The energy policy 2023 is analyzed for its net social benefit relative to the constructed capacity expansion scenarios. The energy policy 2023 is considered as the reference capacity expansion scenario; whereas the constructed capacity expansion scenarios are considered as the alternative ones. The alternative capacity expansion scenarios are created based on more ambitious utilization of renewable and imported energy resources in comparison to the energy policy 2023. Accordingly, the official targets for the year 2023 (see Table 1) are substituted by the proposed alternative targets and the total installed capacity of power plants reaches 131452 MW_{el} in all scenarios. Hence, the capacity expansion scenarios are based on the type of power plants but not on specific projects. In total five capacity expansion scenarios are constructed based on the research questions as listed below:

- Reference scenario (high dependency on domestic types of coal and renewable resources)
- Green scenario (high dependency on RETs)
- Grey scenario (high dependency on imported hard coal)
- Blue scenario (high dependency on natural gas)
- Blue-grey scenario (high dependency on imported hard coal and natural gas)

The alternative scenarios are constructed based on their dependency on the domestic and the imported energy resources for electricity generation. The highest degree of dependence on the domestic energy resources is considered for the green scenario through the ambitious capacity expansion of RETs; whereas the least degree of corresponding dependence is considered for the blue-grey scenario through the ambitious capacity expansion of imported fuel based power plants. With regard to grey and blue scenarios, same degree of dependency on domestic resources is considered through the capacity expansion of imported hard coal and natural gas fired power plants respectively. In this manner, tradeoff analyses are conducted between the energy policy 2023 and the alternative capacity expansion scenarios in terms of capital, fuel and external costs of electricity generation.

The analysis encompasses the long-term capacity expansion plans for the period 2015-2023. In the period 2015-2019, the development of the installed capacities of the power plant types is considered to be same for all scenarios according to the given information in "Turkish Electrical Energy 5-Year Generation Capacity Projection (2015–2019)"[172] by TEIAS (2015, p. 84). Correspondingly, the capacity expansion trajectories of all power plant types are taken into account as close to reality as possible in the period 2015-2019 for all constructed scenarios. In the period 2020-2023, all capacity expansion scenarios differ from each other depending on the proposed targets for the year 2023. More specifically, the development of the installed capacities of the power plant types in the period 2020-2022 are calculated through the linear interpolation[173] of the given values for the installed capacities in the year 2019 and 2023. The linear development of the installed capacities of the power plant types is considered in accordance with the conducted analysis in NREAP as displayed in Figure 113.

[172] In this report, the development of the installed capacities of the power plant types are published taking into account not only the existing power plants but also the power plants which are expected to be in service in the period 2015-2019.

[173] In order to find the installed capacity ($Cap_{i,t}$) of the i^{th} type of power plant in year t, a straight line joining the known coordinates $(2019, Cap_{i,2019})$ and $(2023, Cap_{i,2023})$ is formed. For a given value t in the interval (2019,2023), the value of $Cap_{i,t}$ is calculated by using the relation $\frac{Cap_{i,t}-Cap_{i,2019}}{t-2019} = \frac{Cap_{i,2023}-Cap_{i,2019}}{2023-2019}$.

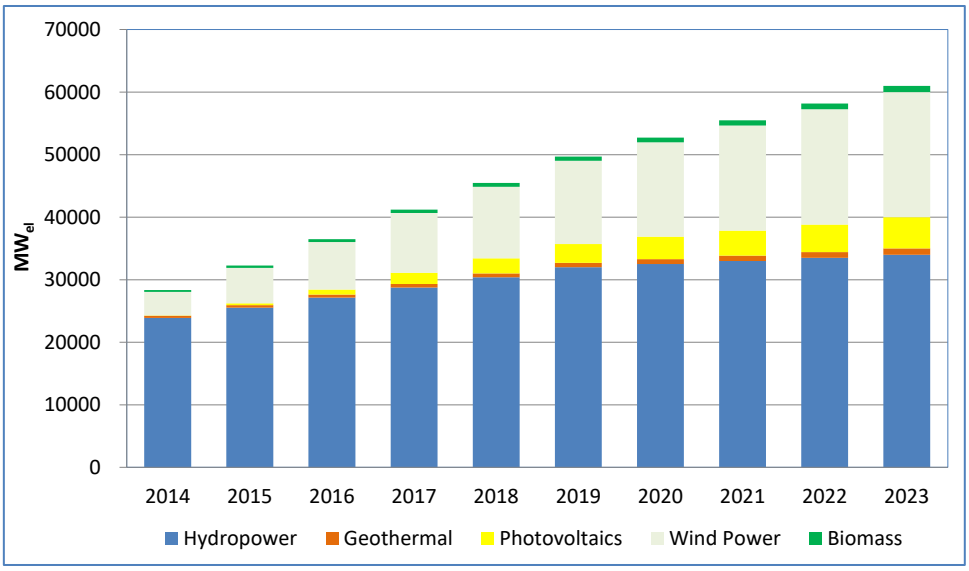

Figure 113- The targeted trajectory for capacity expansion of RETs in NREAP (own illustration according to the Ministry of Energy and Natural Resources, 2014, p. 68)

The represented trajectory, in Figure 113, is based on the development of the electricity demand and the need to meet the established target (The Ministry of Energy and Natural Resources, 2014, p. 67). Hence, any specific investment timing for each year in the period 2015-2023 is not calculated rather exogenously taken into account as tabulated in Table 51. It can be inferred from the table that the higher the targeted capacity expansion for the year 2023 is, the higher the magnitude of the annual capacity expansion is (e.g. hydropower and wind power plants) and vice versa. In particular, the corresponding values for hydropower, biomass and geothermal power plants are observed to be linearized values.

Table 51- The assumed annual capacity expansion of RETs (own illustration according to the Ministry of Energy and Natural Resources, 2014, p. 68)

Year	Hydropower	Geothermal	Photovoltaics	Wind Power	Biomass
			[MW_{el}]		
2015	1618	74	260	1901	77
2016	1619	73	500	1944	76
2017	1618	74	1000	1945	77
2018	1619	73	600	1909	76
2019	1618	74	600	1850	77
2020	500	73	600	1782	76
2021	500	74	400	1710	77
2022	500	73	400	1636	76
2023	500	74	600	1564	88

Further, the system adequacy of each mentioned capacity expansion scenario is assessed based on the development of the electricity demand (see Section 22.2). Furthermore, it is

assumed for all capacity expansion scenarios that the Akkuyu nuclear power plant will be commissioned as officially scheduled[174]. Moreover, the import and the export of electricity between Turkey and the neighbor countries are neglected in accordance with the NREAP. Finally, the annual amount of electricity generated by RETs is calculated through multiplying the installed capacity by the given annual full load hours of operation of the corresponding technologies as assumed in the NREAP. In Table 52, the corresponding full load hours of operation of RETs are tabulated.

Table 52- The assumed full load hours of operation of RETs in the NREAP (own calculation & illustration)

Type of Power Plant	Annual Full Load Hours of Operation
Hydropower	2700
Wind Power	2500
Solar PV Power	1600
Geothermal Power	5100
Biomass Power	4560

In the next subsections, detailed information about the development of the power plant park of Turkey w.r.t. the constructed capacity expansion scenarios is given.

22.1.1 Reference Capacity Expansion Scenario

The reference capacity expansion scenario is built based on the set targets for the year 2023 as explained in the Chapter 1. Accordingly, the development of the installed capacity of the thermal power plant technologies w.r.t. the reference scenario is tabulated in Table 53.

Table 53- The development of the installed capacities of the thermal power plants w.r.t. the reference capacity expansion scenario (own calculation & illustration)

Year	Installed Capacity of Thermal Power Plants [MW_{el}]							Total
	Nuclear	Lignite	D. Hard Coal	Asphaltite	I. Hard Coal	Natural Gas	Fuel Oil	
2014	-	8693	335	135	6063	25632	652	41510
2015	-	8761	895	405	6063	27045	783	43952
2016	-	8761	1345	405	6063	27199	862	44635
2017	-	8761	1345	405	6063	28164	873	45611
2018	-	9961	1480	405	6063	29055	873	47837
2019	-	9961	1480	405	6063	31135	873	49917
2020	1200	13827	1480	473	6063	31135	873	55051
2021	2400	17694	1480	540	6063	31135	873	60185
2022	3600	21560	1480	608	6063	31135	873	65318
2023	4800	25426	1480	675	6063	31135	873	70452

[174] See Chapter 1 for more information.

In the Table 53, the year 2014 is the base year and is not taken into account for capacity expansion analysis. Further, the development of the installed capacities of the power plants in the period 2015-2019 are separated from the subsequent years by a solid line; in order to point out that existing power plants as well as the power plants which are expected to be in service on proposed time are obtained from TEIAS. More specifically, it is expected by TEIAS that all domestic hard coal proven reserves will be exploited until the year 2019. Therefore, further capacity expansion of the corresponding type is not considered for the period 2020-2023 and the corresponding stagnation is indicated in blue color. Furthermore, the development of the installed capacity of the imported fuel fired power plants in the period 2020-2023 is considered to be stagnating due to adopting the energy policy 2023. Moreover, the development of the installed capacities of the lignite and the asphaltite fired power plants in the period 2020-2022 is interpolated through linear interpolation of the corresponding installed capacities of power plants in the year 2019 and 2023. The red colored values indicate the target installed capacities of lignite and asphaltite fired power plants for the year 2023; whereas the orange colored values indicate the values as a result of the mentioned interpolations. Finally, the installed capacities of the diesel (11 MW_{el} in 2014) and the multi-fuel fired (132 MW_{el} in 2014) power plants are categorized together with the fuel oil fired power plants (509 MW_{el} in 2014). In addition, the development of the installed capacities of the corresponding power plants in the period 2020-2023 is considered to be stagnating due to adopting the energy policy 2023.

Similarly, the development of the installed capacities of the RETs is tabulated in Table 54 starting from the base year 2014.

Table 54- The development of the installed capacities of the RETs w.r.t. the reference capacity expansion scenario (own calculation & illustration)

Year	Installed Capacity of Renewable Energy Power Plants [MW_{el}]					Total
	Hydro	Wind	Geothermal	Solar PV	Biomass	
2014	23664	3612	405	40	288	28009
2015	26273	3957	606	640	306	31782
2016	28227	4167	648	1240	311	34593
2017	30254	5841	710	1840	321	38966
2018	31123	5941	710	2440	321	40535
2019	31123	5941	710	3040	321	41135
2020	31842	9456	783	3530	491	46101
2021	32562	12971	855	4020	661	51068
2022	33281	16485	928	4510	830	56034
2023	34000	20000	1000	5000	1000	61000

As a result of the set targets for the year 2023, the total installed capacity of the power plants increases from 2014 level of 69519 MW_{el} to 2023 level of 131452 MW_{el}. In Figure 114, the development of the installed capacities of both thermal and RETs is illustrated.

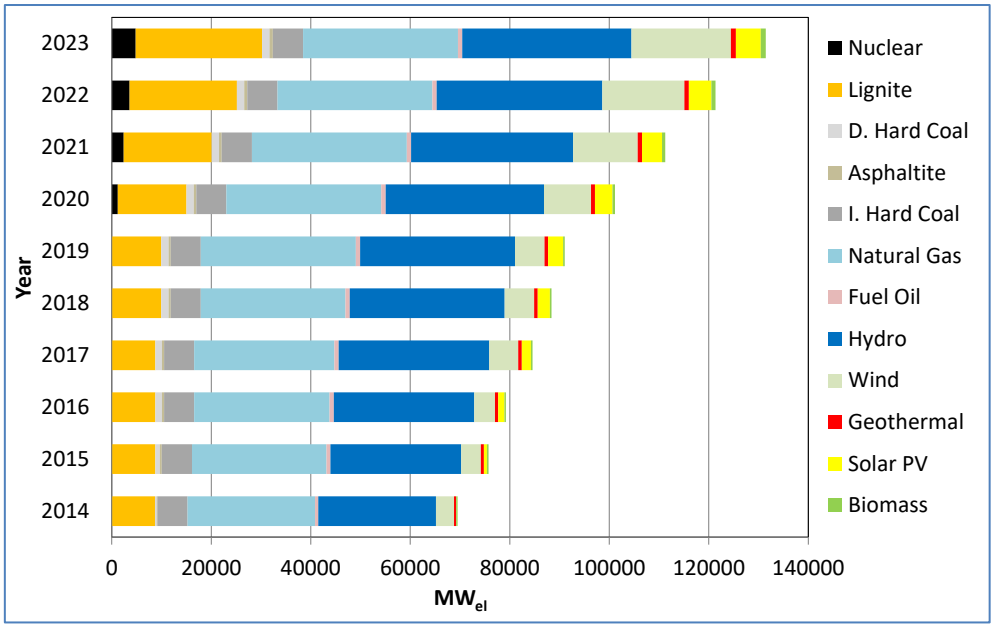

Figure 114- The overview of the reference capacity expansion scenario (own illustration)

22.1.2 Green Capacity Expansion Scenario

The green capacity expansion scenario is constructed based on a special focus on the capacity expansion of RETs in comparison to the reference scenario. In particular, the capacity expansion of power plants in the period 2020-2023 is only proposed for RETs, instead of including capacity expansion of lignite and asphaltite fired power plants. Hence, the green scenario is constructed according to the tradeoff between the domestic fossil fuel and the renewable energy resources in terms of capital, fuel and external costs of electricity generation. Namely, the green scenario focuses on presumably reducing both fuel and external costs at the expense of more capital costs in comparison to the reference scenario.

In Table 55, the development of the installed capacities of the thermal power plants in the green scenario is tabulated starting from the base year 2014. The corresponding development in the period 2015-2019 is obtained from TEIAS and it is considered to be stagnating in the period 2020-2023 as previously mentioned.

Table 55- The development of the installed capacities of the thermal power plants w.r.t. the green capacity expansion scenario (own calculation & illustration)

Year	Installed Capacity of Thermal Power Plants [MW_{el}]							Total
	Nuclear	Lignite	D. Hard Coal	Asphaltite	I. Hard Coal	Natural Gas	Fuel Oil	
2014	-	8693	335	135	6063	25632	652	41510
2015	-	8761	895	405	6063	27045	783	43952
2016	-	8761	1345	405	6063	27199	862	44635
2017	-	8761	1345	405	6063	28164	873	45611
2018	-	9961	1480	405	6063	29055	873	47837
2019	-	9961	1480	405	6063	31135	873	49917
2020	1200	9961	1480	405	6063	31135	873	51117
2021	2400	9961	1480	405	6063	31135	873	52317
2022	3600	9961	1480	405	6063	31135	873	53517
2023	4800	9961	1480	405	6063	31135	873	54717

The capacity expansion of RETs is so planned that in the year 2023, the same level of total installed capacity of power plants is reached as in the case of the reference scenario. Therefore, in the green scenario 15735 MW_{el} more capacity of RETs is considered to be installed in the year 2023; in order to substitute for the capacity expansion of the lignite and the asphaltite fired power plants in the reference scenario. Accordingly, the ambitious capacity expansion of hydropower, wind, geothermal and biomass power plants accounts for substituting 7500 MW_{el} of the corresponding 15735 MW_{el} thermal capacity. Further, the remaining 8235 MW_{el} is considered to be substituted by solar PV power plants.

In Table 56, the development of the installed capacities of the RETs is tabulated starting from the base year 2014. The corresponding development in the period 2014-2019 is obtained from TEIAS and it is calculated for the period 2020-2022 through the linear interpolation of the installed capacities of the RETs in the year 2019 and 2023.

Table 56- The development of the installed capacities of the RETs w.r.t. the green capacity expansion scenario (own calculation & illustration)

Year	Installed Capacity of Renewable Energy Power Plants [MW_{el}]					Total
	Hydro	Wind	Geothermal	Solar PV	Biomass	
2014	23664	3612	405	40	288	28009
2015	26273	3957	606	640	306	31782
2016	28227	4167	648	1240	311	34593
2017	30254	5841	710	1840	321	38966
2018	31123	5941	710	2440	321	40535
2019	31123	5941	710	3040	321	41135
2020	32342	10456	908	5521	741	49968
2021	33562	14971	1105	8003	1161	58800
2022	34781	19485	1303	10484	1580	67633
2023	36000	24000	1500	13235	2000	76735

The priority of capacity expansion is given to the hydropower and geothermal power resources through the exploitation of the economically viable potential[175] of hydropower (i.e. 36000 MW_{el}) and geothermal resources (i.e. 1500 MW_{el}) until the year 2023. Accordingly, 2000 MW_{el} more capacity of hydropower and 500 MW_{el} more capacity of geothermal power plants are proposed in the green scenario in comparison to the reference scenario (see Figure 115). Further, up to half of the economically viable potential of wind power (i.e. 24000 MW_{el}) and biomass resources (i.e. 2000 MW_{el}) are assumed to be exploited until the year 2023. Accordingly, 4000 MW_{el} more capacity of wind power and 1000 MW_{el} more capacity of biomass power plants are proposed for the green scenario in comparison to the reference (see Figure 115). The remaining 8235 MW_{el} of capacity is considered to be substituted by solar PV power through reaching an installed capacity level of 13235 MW_{el} for the target year 2023. In Figure 115, the development of the installed capacities of both thermal and RETs is illustrated.

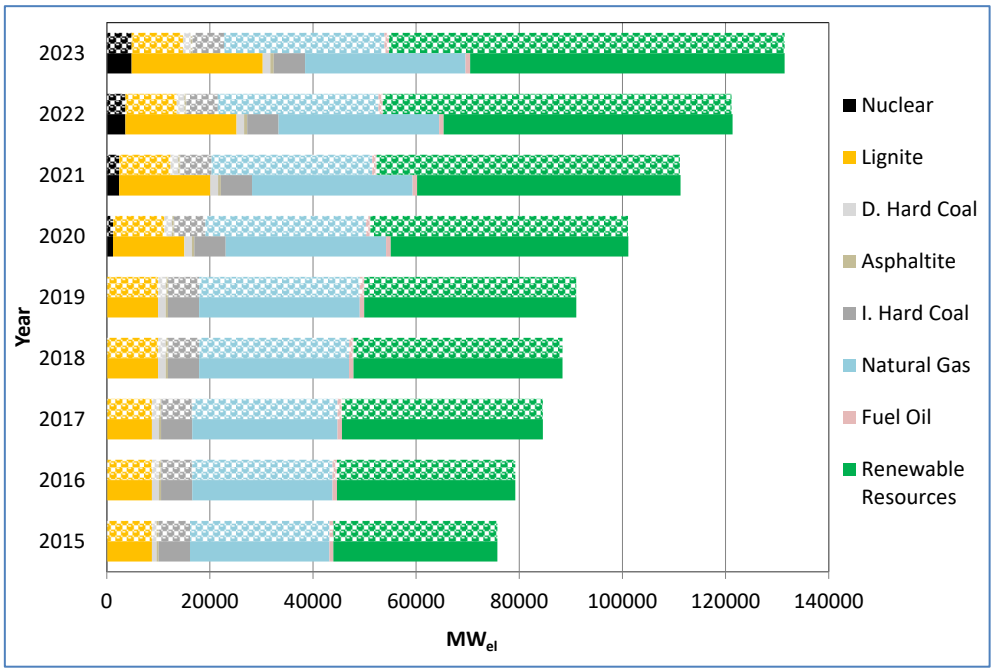

Figure 115- The development of the installed capacities of the power plants w.r.t. the reference (solid bars) and the green (patterned bars) capacity expansion scenarios (own calculation & illustration)

[175] See p. 35 for economically viable potential of renewable energy resources.

22.1.3 Grey Capacity Expansion Scenario

The grey capacity expansion scenario is constructed based on a special focus on the capacity expansion of imported hard coal fired power plants in comparison to the reference scenario. In particular, the capacity expansion of power plants in the period 2020-2023 is only proposed for imported hard coal[176] fired power plants, instead of including also capacity expansion of lignite and asphaltite fired power plants. Consequently, the development of the installed capacities of the RETs in the period 2015-2023 is same in both scenarios. Hence, the grey scenario is constructed according to the tradeoff between the domestic and the imported types of coal in terms of capital, fuel and external costs of electricity generation. Namely, the grey scenario focuses on utilizing imported hard coal with high calorific value at the expense of more fuel cost per ton in comparison to the reference scenario.

In Table 57, the development of the installed capacities of the thermal power plants in the grey scenario is tabulated starting from the base year 2014. The capacity expansion of the imported hard coal fired power plants in the grey scenario is so planned that in the target year 2023, the same level of total thermal installed capacity is reached as in the case of the reference scenario. Therefore, in the grey scenario 15735 MW_{el} more capacity of imported hard coal fired power plant is considered to be installed in the year 2023; in order to substitute for the capacity expansion of the lignite and the asphaltite fired power plants in the reference scenario.

Table 57- The development of the installed capacities of the thermal power plants w.r.t. the grey capacity expansion scenario (own calculation & illustration)

Year	Installed Capacity of Thermal Power Plants [MW_{el}]							Total
	Nuclear	Lignite	D. Hard Coal	Asphaltite	I. Hard Coal	Natural Gas	Fuel Oil	
2014	-	8693	335	135	6063	25632	652	41510
2015	-	8761	895	405	6063	27045	783	43952
2016	-	8761	1345	405	6063	27199	862	44635
2017	-	8761	1345	405	6063	28164	873	45611
2018	-	9961	1480	405	6063	29055	873	47837
2019	-	9961	1480	405	6063	31135	873	49917
2020	1200	9961	1480	405	9997	31135	873	55051
2021	2400	9961	1480	405	13931	31135	873	60185
2022	3600	9961	1480	405	17864	31135	873	65318
2023	4800	9961	1480	405	21798	31135	873	70452

[176] Note that there is not any specific constraint for the capacity expansion of imported hard coal fired power plants (see p. 4).

The development of the installed capacities of the power plants in both scenarios is depicted in Figure 116. It can be inferred from the figure that the total installed capacities of thermal power plants and RETs are equal in the target year 2023 in both scenarios.

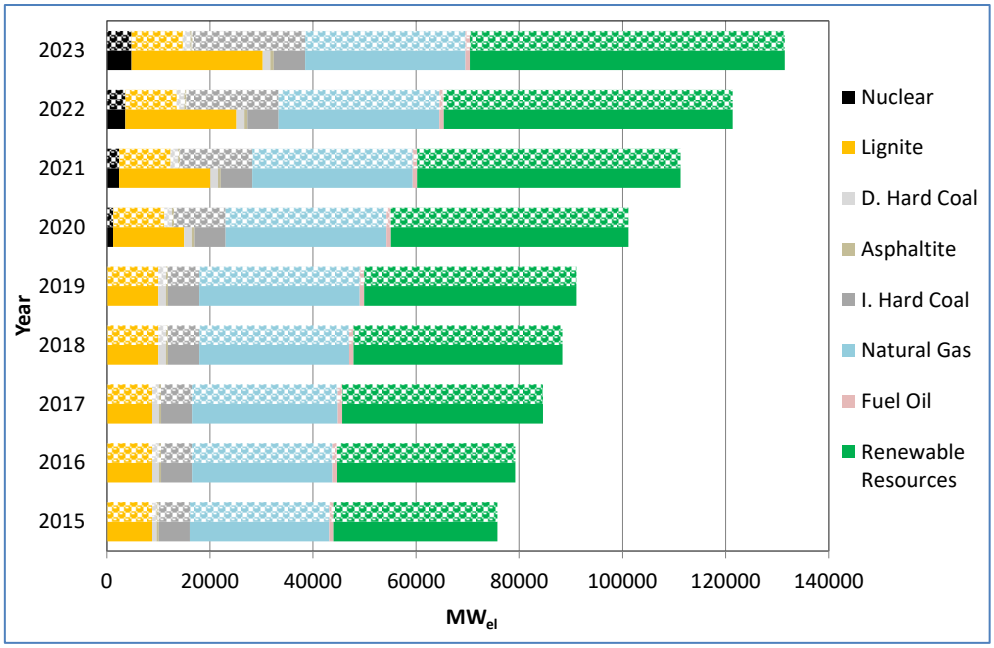

Figure 116- The development of the installed capacities of the power plants w.r.t. the reference (solid bars) and the grey (patterned bars) capacity expansion scenarios (own calculation & illustration)

22.1.4 Blue Capacity expansion scenario

The blue capacity expansion scenario is constructed based on a special focus on the capacity expansion of natural gas fired power plants in comparison to the reference scenario. In particular, the capacity expansion of power plants in the period 2020-2023 is only proposed for natural gas fired power plants, instead of including also capacity expansion of lignite and asphaltite fired power plants. Consequently, the development of the installed capacities of the RETs in the period 2015-2023 is same in both scenarios. Hence, the blue scenario is constructed according to the tradeoff between the domestic types of coal and the natural gas in terms of capital, fuel and external costs of electricity generation. Namely, the blue scenario focuses on presumably reducing capital and external costs at the expense of more fuel costs.

In Table 58, the development of the installed capacities of the thermal power plants in the blue scenario is tabulated starting from the base year 2014. The capacity expansion of the natural gas fired power plants in the blue scenario is so planned that in the target year 2023, the same level of total thermal installed capacity is reached as in the case of energy policy 2023. Therefore, in the blue scenario 15735 MW_{el} more capacity of natural gas fired power

plants is considered to be installed in the year 2023; in order to substitute for the capacity expansion of the lignite and the asphaltite fired power plants in the reference scenario.

Table 58- The development of installed capacities of thermal power plants w.r.t. the blue capacity expansion scenario (own calculation & illustration)

Year	Installed Capacity of Thermal Power Plants [MW_{el}]							Total
	Nuclear	Lignite	D. Hard Coal	Asphaltite	I. Hard Coal	Natural Gas	Fuel Oil	
2014	-	8693	335	135	6063	25632	652	41510
2015	-	8761	895	405	6063	27045	783	43952
2016	-	8761	1345	405	6063	27199	862	44635
2017	-	8761	1345	405	6063	28164	873	45611
2018	-	9961	1480	405	6063	29055	873	47837
2019	-	9961	1480	405	6063	31135	873	49917
2020	1200	9961	1480	405	6063	35069	873	55051
2021	2400	9961	1480	405	6063	39003	873	60185
2022	3600	9961	1480	405	6063	42936	873	65318
2023	4800	9961	1480	405	6063	46870	873	70452

The development of the installed capacities of the power plants in both scenarios is depicted in Figure 117. It can be inferred from the figure that the total installed capacities of thermal power plants and RETs are equal in the target year 2023 in both scenarios.

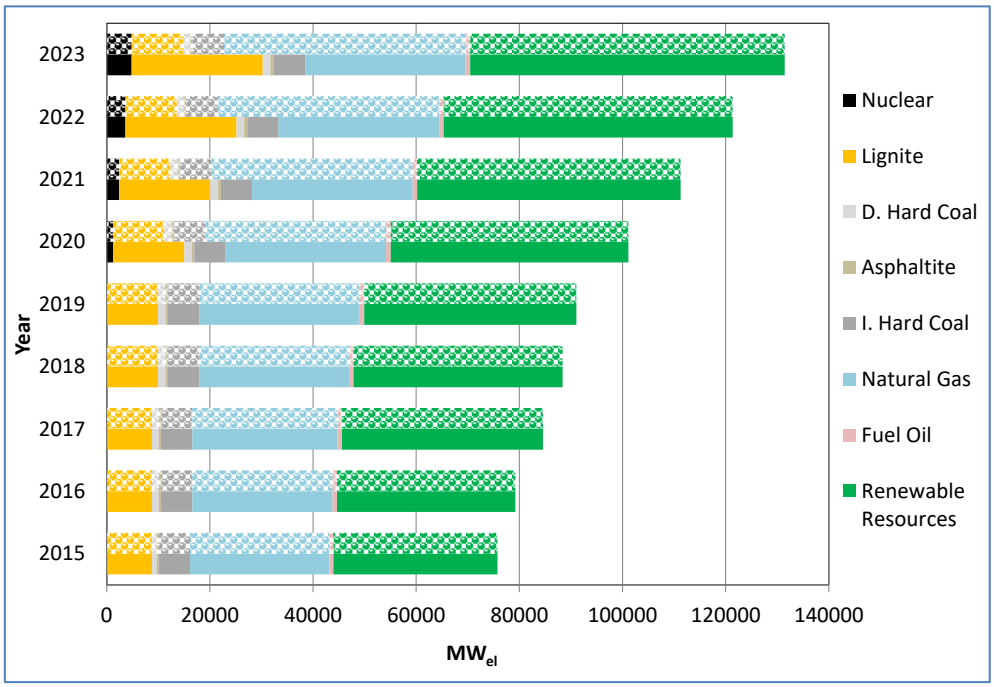

Figure 117- The development of the installed capacities of the power plants w.r.t. the reference (solid bars) and the blue (patterned bars) capacity expansion scenarios (own calculation & illustration)

22.1.5 Blue-Grey Capacity Expansion Scenario

The blue-grey capacity expansion scenario is constructed based on a special focus on the capacity expansion of natural gas and imported hard coal fired power plants in comparison to the reference scenario. In particular, the capacity expansion of power plants in the period 2020-2023 is only proposed for natural gas and imported hard coal fired power plants, instead of including capacity expansion of lignite and asphaltite fired power plants and RETs. Consequently, 35600 MW_{el} more capacity of imported resource based power plants is installed in the blue-grey scenario relative to the reference scenario. Hence, the development of the installed capacities of the RETs in the period 2015-2023 is different in both scenarios. The blue-grey scenario is constructed according to the tradeoff between the domestic energy resources and the imported fossil fuels in terms of capital, fuel and external costs of electricity generation. The blue-grey scenario focuses on presumably reducing capital costs at the expense of more fuel and external costs for substituting the target capacity expansion of RETs with natural gas fired power plants. In addition, it also focuses on utilizing imported hard coal with high calorific value at the expense of more fuel cost per ton for substituting the target capacity expansion of lignite and asphaltite fired power plants in the reference scenario.

In Table 59, the development of the installed capacities of the thermal power plants in the blue-grey scenario is tabulated starting from the base year 2014. The capacity expansions of imported hard coal and natural gas fired power plants are so planned that the same level of total installed capacity of power plants in the target year 2023 is reached as in the case of reference scenario. Therefore, in the blue-grey scenario 15735 MW_{el} more capacity of imported hard coal and 19865 MW_{el} more capacity of natural gas fired power plants are proposed to be installed; in order to substitute for the capacity expansion of the domestic fossil fuel fired power plants and the RETs respectively. Accordingly, the ambitious capacity expansion of imported hard coal fired power plants accounts for the substitution of 15465 MW_{el} installed capacity of lignite and 270 MW_{el} installed capacity of asphaltite fired power plants in the reference scenario. In addition, the ambitious capacity expansion of natural gas fired power plants accounts for the substitution of 2877 MW_{el} installed capacity of hydropower, 14059 MW_{el} installed capacity of wind power, 290 MW_{el} installed capacity of geothermal power, 1960 MW_{el} installed capacity of solar PV power and 679 MW_{el} installed capacity of biomass power plants.

Table 59- The development of the installed capacities of the thermal power plants w.r.t. the blue-grey capacity expansion scenario (own calculation & illustration)

Year	Installed Capacity of Thermal Power Plants [MW_{el}]							Total
	Nuclear	Lignite	D. Hard Coal	Asphaltite	I. Hard Coal	Natural Gas	Fuel Oil	
2014	-	8693	335	135	6063	25632	652	41510
2015	-	8761	895	405	6063	27045	783	43952
2016	-	8761	1345	405	6063	27199	862	44635
2017	-	8761	1345	405	6063	28164	873	45611
2018	-	9961	1480	405	6063	29055	873	47837
2019	-	9961	1480	405	6063	31135	873	49917
2020	1200	9961	1480	405	9997	36101	873	60017
2021	2400	9961	1480	405	13931	41068	873	70117
2022	3600	9961	1480	405	17864	46034	873	80217
2023	4800	9961	1480	405	21798	51000	873	90317

In Table 60, the development of the installed capacities of the RETs is tabulated starting from the base year 2014. The corresponding development in the period 2014-2019 is obtained from TEIAS and is considered to be stagnating in the period 2020-2023 as previously mentioned.

Table 60- The development of the installed capacities of the RETs w.r.t. the blue-grey capacity expansion scenario (own calculation & illustration)

Year	Installed Capacity of Renewable Energy Power Plants [MW_{el}]					Total
	Hydro	Wind	Geothermal	Solar PV	Biomass	
2014	23664	3612	405	40	288	28009
2015	26273	3957	606	640	306	31782
2016	28227	4167	648	1240	311	34593
2017	30254	5841	710	1840	321	38966
2018	31123	5941	710	2440	321	40535
2019	31123	5941	710	3040	321	41135
2020	31123	5941	710	3040	321	41135
2021	31123	5941	710	3040	321	41135
2022	31123	5941	710	3040	321	41135
2023	31123	5941	710	3040	321	41135

In Figure 118, the development of the installed capacities of the power plants in both scenarios is depicted. It can be inferred from the figure that the total installed capacities of thermal power plants and RETs are different in the target year 2023 in both scenarios.

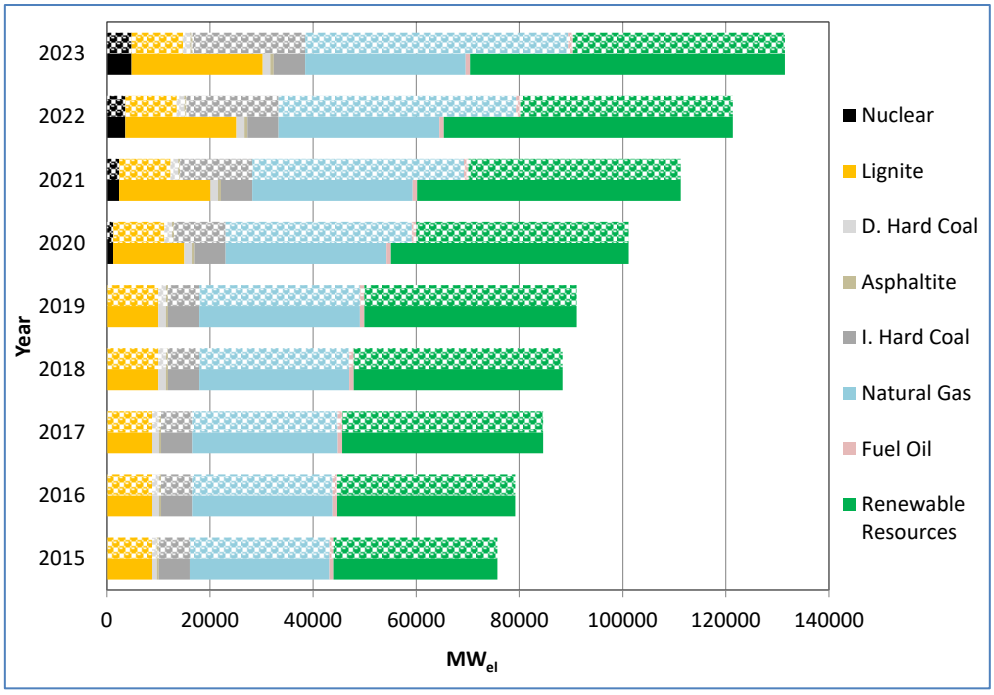

Figure 118- The development of the installed capacities of the power plants w.r.t. the reference (solid bars) and the blue-grey (patterned bars) capacity expansion scenario (own calculation & illustration)

22.2 Reliability Assessments on the Capacity Expansion Scenarios

The system adequacy of each mentioned capacity expansion scenario is assessed for the capability of power plants as a whole to meet power demand at all times with an acceptably high probability. The system adequacy is a particularly important issue; since the uncertainty in electricity supply increases as the share of power generation from intermittent renewable energy resources in total increases. The system adequacy can be assessed by taking into account the capacity credit of the power plants in a power system (International Energy Agency, 2011, p. 190)[177]. According to Freris and Infield (2008, p. 213), the capacity credit of any power plant is defined to be a measure of the ability of any plant to individually contribute to the covering of peak demand in a power system. The capacity credit of a RET can be calculated based on the effective load carrying capacity (ELCC) of that plant (p. 190).

The ELCC of an individual generator is defined as the amount of additional load which can be served at the target reliability level when that generator is added to the system (Leisch & Cochran, 2015). The capacity credit of a RET is calculated as a ratio of ELCC to its nominal capacity[178] to indicate the fraction of its capacity that adds to the system reliability. For example as shown in Figure 119, the addition of 2000 MW_{el} of a RET can meet an increase of 400 MW_{el} of system load at the target reliability level by having an ELCC of 400 MW_{el} or a capacity credit of 20% of its nominal capacity.

The loss of load probability (LOLP) and the loss of load expectation (LOLE) are the two key parameters in the calculation of ELCC (Leisch & Cochran). LOLP is the probability that the load will exceed the available generating capacity during a planning period (i.e. typically 1 year). LOLE is the expected number of hours (i.e. the sum of the LOLPs) in a given period, during which the load will not be met. According to IEA (p. 190), the industry standard for OECD countries is accepted to be an expectation of 0.1 day per year loss of load (i.e. also applied in Figure 119).

[177] See the publication "Harnessing Variable Renewables: A Guide to the Balancing Challenge" for more information.

[178] It is the maximum achievable output of a power plant due to its technical capability.

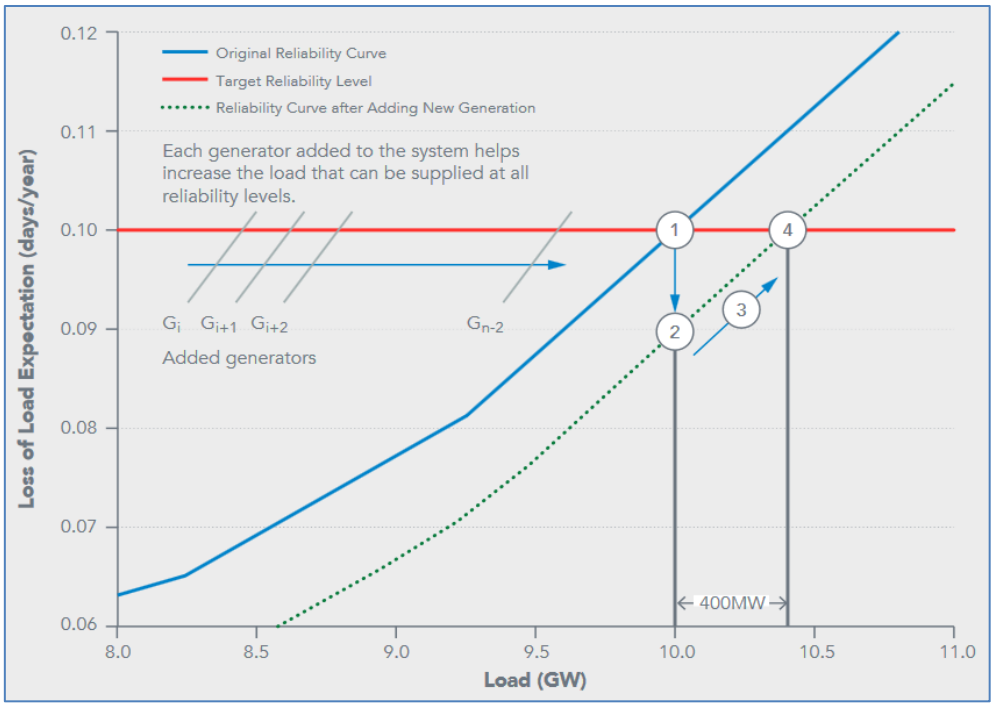

Figure 119- The steps for calculating the ELCC of an added RET to a power system (Leisch & Cochran, 2015)

ELCC can be calculated in four steps (see Figure 119) as follows (Leisch & Cochran):

1. The LOLE of a given set of generators without the new RET is calculated (illustrated by the blue curve). Then, the system load, which can be supplied by the given set of generators (excluding the new RET), is determined while meeting the target reliability level (i.e. the intersection of the blue and red lines).
2. The new RET is added to the previous set of generators and the LOLE for the corresponding level of load is recalculated. After that the recalculated LOLE is lower indicating higher reliability.
3. The system load is gradually increased by adding a constant amount of load (by moving along the green dotted curve resulting from the shifting of the blue curve) and recalculating the LOLE until the LOLE of the system with the added generator reaches the target reliability level.
4. The difference between the load levels corresponding to point 4 and point 1 at a constant LOLE is the ELCC of the added new RET. The corresponding capacity credit is obtained as a ratio of the ELCC to the nominal capacity.

The major parameter affecting the capacity credits of RETs is the correlation of their power output with the power demand. A RET, which can serve load during the times of high power demand, achieves a higher capacity credit than the one operating during the times of low

power demand (Milligan & Porter, 2006, p. 92). The calculation of ELCC requires a comprehensive database based on the following major parameters (Milligan & Porter):

- The nominal capacities, the technical characteristic, the forced outage rates and the maintenance schedules of the generators in the corresponding power system
- Data on hourly power demand for at least one year
- Data on hourly power output by RETs for at least one year
- Forecasts of hourly power demand and output of all generators for the planning period (i.e. synchronized with each other), transmission constraints, etc.

Accordingly, the capacity credits of power plants are specific to power systems; since they mainly depend on the correlation of power plant outputs with the periods of peak demand in power systems (International Energy Agency, p. 191). A study on the capacity credits of power plants, which are specific to the Turkish power system, has not been conducted yet. The capacity credits of power plants can be assessed by using simulation and by probabilistic analysis to estimate the occurrence of the peak load demand and the amount of generated electricity from the RETs (European Wind Energy Association, 2010, p. 80). Any of the corresponding analyses are not conducted during the course of this study due to their marginal benefit to the objective of this study in comparison to the required high effort.

The capacity credits for thermal (including biomass and geothermal as given by TEIAS) and hydropower plants are estimated from the average availabilities of these power plant types during the occurrence of the annual peak load demand[179] in the year 2013 and 2014. Correspondingly, the capacity credits of thermal and hydropower plants are estimated to be 70% and 66% respectively.

The capacity credits for wind and solar PV power plants (i.e. intermittent generators) are handled different from the aforementioned type of power plants; since the corresponding values vary as more of them are installed. Thus, the firm reserve margin is calculated dependent on the cases of the high and the low capacity credits of the intermittent generators. In Figure 120, the estimated capacity credits for wind power plants are displayed according to the published studies in "Harnessing Variable Renewables: A Guide to the Balancing Challenge" by IEA (2011). In the figure, the East United States and the United Kingdom

[179] According to TEIAS, the annual peak load demands occurred on Thursday 29.08.2013 at 3 p.m. and on Thursday 14.08.2014 at 3 p.m. During the former date, the availability of thermal and hydropower plants were 68.1% and 72.6%; whereas during the latter datum, they amount to 71.7% and 60.5% respectively.

(UK) serves as an example for power systems with high capacity credit of wind power plants; whereas the West United States and Germany exemplify the opposite case. It can be inferred from the figure that capacity credit of wind power plants differs from each other dependent on the power system; however it decreases with increasing degree of penetration[180] in all power systems. According to the given information by IEA (p. 191), capacity credit of wind power plants ranges from 6% to 25% at up to 30% wind penetration in different power systems. For this study, it is assumed that the wind power plants in Turkey possess high capacity credit value as in the case of the East United States and the United Kingdom; since Turkey is a peninsula and possesses high wind power potential which is spread around its geography. In the period 2015-2023, the penetration level[181] of wind power is calculated to be in the range of 10% to 32%. Therefore, the high end of the bandwidth given by IEA is taken as the high capacity credit value for the wind power plants in Turkey.

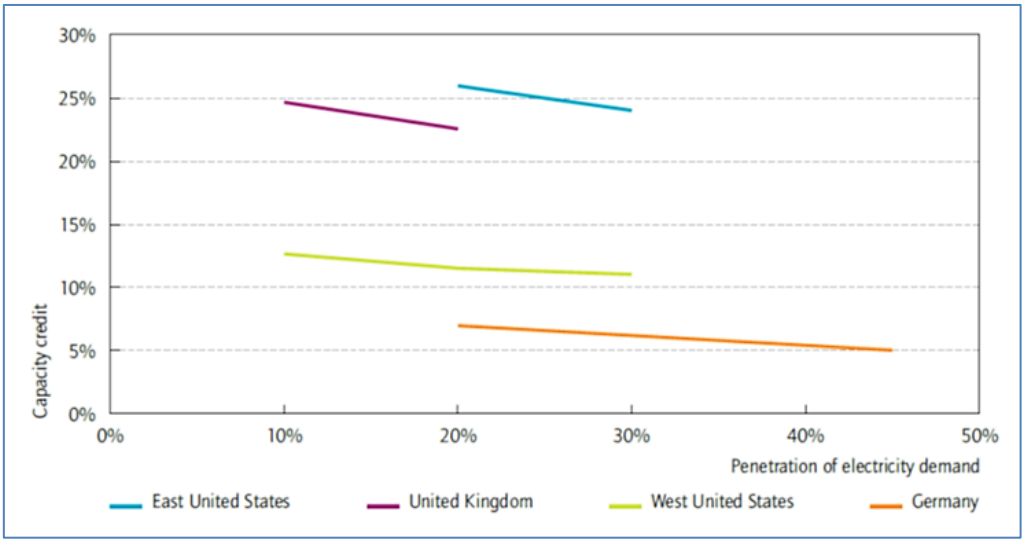

Figure 120- The estimated capacity credit of the wind power plants in the corresponding regions (International Energy Agency, 2011, p. 191)

The capacity credit of wind power plants can be further examined in Figure 121 according to the published studies in "Powering Europe: wind energy and the electricity grid" by European Wind Energy Association. It can be inferred from the figure that the capacity credit of wind power plants can decrease to 5% with their capacity expansion as in the case of Germany. It is also mentioned in the report "World Energy Outlook 2013: Renewable Energy Outlook" (WEO 2013) that in the European Union, it typically falls between 5% and 10% for wind

[180] The level of wind penetration can be measured by taking the ratio of installed capacity of wind power to annual peak load demand in any power system.

[181] For the year 2015, the ratio of installed capacity of wind power (3957 MW_{el}) to annual peak load demand (40919 MW_{el}) is 10%. For the year 2023, the ratio of installed capacity of wind power (20000 MW_{el}) to annual peak load demand (62320 MW_{el}) is 32%.

(International Energy Agency, 2013, p. 215). Therefore, the low capacity credit value for the wind power plants in Turkey is taken as 5% for the analysis.

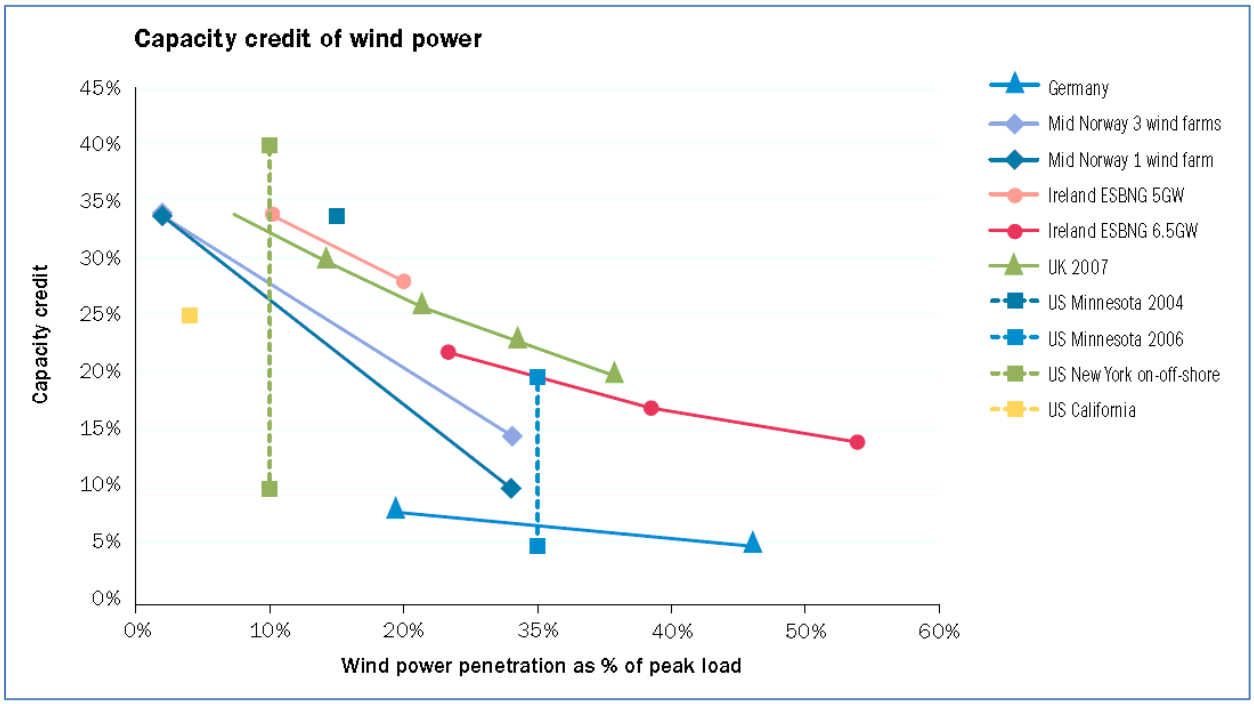

Figure 121- The estimated capacity credit of the wind power plants in the corresponding regions (European Wind Energy Association, 2010, p. 82)

In Figure 122, the capacity credits for solar PV and concentrating solar power[182] (CSP) plants in the Western United States is displayed. It can be inferred from the figure that the corresponding capacity credit values are around 30% for solar PV and 90% for solar CSP at low penetration levels. In contrast to the wind power plants, the change in the capacity credit values for solar PV power plants is negligible with the increasing degree of penetration. Further, it is emphasized by IEA (p. 192) that the capacity credit of solar PV power plants can be higher than 30% in power systems in which the occurrence of annual peak demand and solar PV power generation tend to be well aligned with each other. Accordingly, the high capacity credit value for the solar PV power plants in Turkey is assumed to be 30%; since in Turkey, both annual peak demand and high amount of electricity generation from solar PV power plants occur in the summer months. Finally, the low capacity credit value for the solar PV power plants in Turkey is taken as 0% for the analysis; since in the European Union, it typically falls between 0% and 5% according to WEO 2013 (International Energy Agency, 2013, p. 215).

[182] Note that in this study, concentrating solar power plants are not considered for capacity expansion analysis.

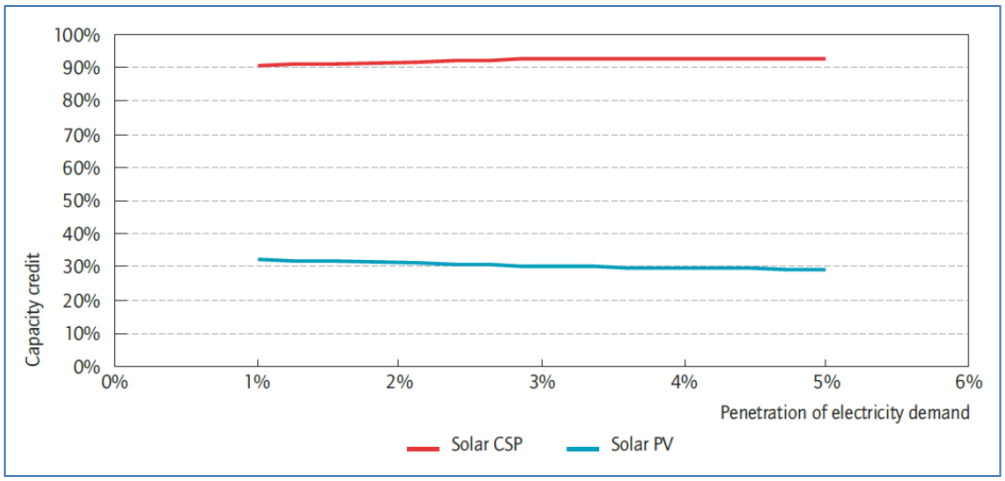

Figure 122- Capacity credits for solar technologies in the Western United States (International Energy Agency, 2011, p. 192)

By using the assumed capacity credits, the firm capacities of all considered power plant types can be measured as fractions of the nominal capacities of those power plant types as expressed below (International Energy Agency, 2011, p. 190):

$$Firm\ Capacity = Nominal\ Installed\ Capacity \cdot Capacity\ Credit \tag{22.2.1}$$

The contribution of all installed power plants in a power system to system adequacy can be measured as follows:

$$Firm\ Reserve\ Margin = \frac{Total\ Firm\ Capacity}{Annual\ Peak\ Demand} \tag{22.2.2}$$

In this study, the firm reserve margin in a considered year is defined to be the ratio of the total (or sum of) firm capacities to the peak demand. The firm reserve margin is calculated for each year considering the development of the annual peak demand, the installed capacities of the power plants in the mentioned scenarios and the assumed capacity credit for each type of power plant. The value of the firm reserve margin is proposed to be indicating the adequate supply of electricity when it is higher than or equal to unity. The firm reserve margin is derived from another measurement so called reserve margin in the report "Security of Supply in Electricity Markets: Evidence and Policy Issues" by IEA (2002, p. 16) as expressed below:

$$Reserve\ Margin = \frac{Total\ Installed\ Capacity - Peak\ Demand}{Total\ Installed\ Capacity} \tag{22.2.3}$$

The reserve margin[183] is defined to be the percentage of installed capacity in excess of peak demand over a year of period. Accordingly, the calculation of the reserve margin ignores the contribution of power plants in meeting the annual peak demand and cannot account for system adequacy.

The development of the firm reserve margin[184] w.r.t. the capacity expansion scenarios is tabulated in Table 61. In the table, the rubrics "High" and "Low" indicate the firm reserve margin which is calculated based on the high and the low capacity credit cases for the intermittent generators.

Table 61- The development of the firm reserve margin w.r.t. the capacity expansion scenarios, and high and low capacity credit cases for intermittent generators (own calculation & illustration)

Year	Reference Scenario		Green Scenario		Grey Scenario		Blue Scenario		Blue-Grey Scenario	
	High	Low	High	Low	High	Low	High	Low	High	Low
2014	1.1	1.1	1.1	1.1	1.1	1.1	1.1	1.1	1.1	1.1
2015	1.2	1.1	1.2	1.1	1.2	1.1	1.2	1.1	1.2	1.1
2016	1.1	1.1	1.1	1.1	1.1	1.1	1.1	1.1	1.1	1.1
2017	1.1	1.1	1.1	1.1	1.1	1.1	1.1	1.1	1.1	1.1
2018	1.1	1.1	1.1	1.1	1.1	1.1	1.1	1.1	1.1	1.1
2019	1.1	1.1	1.1	1.1	1.1	1.1	1.1	1.1	1.1	1.1
2020	1.1	1.1	1.1	1.0	1.1	1.1	1.1	1.1	1.2	1.1
2021	1.2	1.1	1.1	1.0	1.2	1.1	1.2	1.1	1.2	1.2
2022	1.2	1.1	1.1	1.0	1.2	1.1	1.2	1.1	1.3	1.2
2023	1.2	1.1	1.1	1.0	1.2	1.1	1.2	1.1	1.3	1.3

The result of the analysis indicates that the adequate supply of electricity can be achieved according to the capacity expansion of power plants in all mentioned scenarios and cases. This is due to the fact that Turkey possesses a thermally dominated power plant park with large reservoir hydropower plants which can regularly generate electricity. In the period 2014-2019, the magnitude of the firm reserve margin is same in all scenarios w.r.t. both cases; since the year 2014 is the base year and the power plant data for the period 2015-2019 is obtained from TEIAS. In particular, the magnitude of the firm reserve margins for the grey and the blue scenarios are similar in the period 2020-2023; since same amount of RETs is installed in the corresponding period.

In the period 2020-2023, the firm reserve margin calculated w.r.t. the blue-grey scenario is greater than the firm reserve margin calculated w.r.t. the all other scenarios (i.e. true for both

[183] According to IEA (2002, p. 22), the typical engineering targets for reserves are in the order of 18% to 25%.
[184] The annual peak load demand is obtained from the result of the forecasted time series (see Table 36).

cases); whereas the opposite is true for the green scenario. This is due to the fact that the capacity credit of thermal power plants is assumed to be higher than the RETs. Thus, the more thermal power plant is installed; the higher the total firm capacity will be as observed in the blue-grey scenario. The calculated firm reserve margin w.r.t. the green scenario, which is based on the low capacity credit case, is on the verge of adequate electricity supply in the period 2020-2023. In that case, a system inadequacy might take place, if dry hydrological conditions or unexpected events in Turkish power system (e.g. unexpected outage of thermal power plants, abrupt increase in power demand, transmission grid congestions, etc.) were to occur. Nevertheless the assumed low capacity credits are pessimistic values for solar and wind power plants in Turkey (i.e. 0% and 5% respectively), since the capacity credits of intermittent generators are higher, if their power output is correlated (i.e. synchronous) with power demand. Namely, in Turkey, the highest power demand and the highest power output of those power plants occur during summer. Note that the accuracy of the forecasted annual peak load demand, which is utilized in the corresponding calculations, is also a crucial factor affecting the results; since the uncertainty in forecasts rises as the forecast horizon rises. An overestimated peak load demand in the period 2020-2023 should also be taken into account for the assessment of the results due to using time series analysis.

22.3 Technical and Cost Parameters of the Power Plants

The social cost-benefit analysis focuses on the calculation of the social cost of supplying electricity in each year of the period 2015-2023. The social cost of supplying electricity is composed of fixed, variable and external costs. Note that the social cost of supplying electricity depends not only on the mentioned costs but also on the demand for electricity which is approximated in the form of future load duration curves of Turkey in PART B (see Table 49 in Chapter 13). Further, the fixed costs consist of capital and fixed O&M costs. Furthermore, the variable costs consist of fuel and variable O&M costs. Finally, the external costs originate from the environmental and health damages due to supplying electricity. In Table 62, the specific investment, the fixed O&M, the variable O&M costs and the economic lifetime of the thermal power plants are represented. According to the report "World Energy Investment Outlook 2014" by IEA (2014), the represented costs for thermal power plants are assumed to be not changing during the study period; since they are mature technologies. As for the related costs of RETs, the relevant information is provided in Chapter 7 (see Table 9 on p. 52).

Table 62- The cost inputs for thermal power plants (own illustration)

Type of Power Plant w.r.t. Utilized Fuel	Specific Investment Cost[185] [$/kW$_{el}$]	Fixed O&M Cost[186] [$/MW$_{el}$-y]	Variable O&M Cost[187] [$/MWh$_{el}$]	Economic Lifetime[188] [Year]
Nuclear	4167	68,800	6.9	60
Natural Gas	690	29,435	2.7	30
Imported Hard Coal	1165	37,643	3.4	40
Domestic Hard Coal	682	37,643	3.4	40
Lignite	1559	12,133	2.1	40
Asphaltite	2519	12,133	2.1	40
Fuel Oil	1280	357,800	-	40

[185] The specific investment costs of the nuclear and fuel oil fired power plants are obtained from AKKUYU NGS (2013) and Ozcan et al. (2014, p. 2056) respectively. The related specific investment costs for the other ones are calculated according to own research (see APPENDIX H).

[186] The fixed O&M cost of the fuel oil fired power plant is obtained from Ozcan et al. (2014, p. 2056). The related costs for the other ones are taken from the report "Projected Costs of Generating Electricity 2015 Edition" (NEA, IEA, OECD, 2015, p. 111).

[187] The variable O&M costs of other power plants are obtained from NEA, IEA and OECD (p. 111).

[188] The economic life time of power plants is obtained from NEA, IEA and OECD (p. 30).

Note that the represented costs in Table 62 do not include administrative costs[189] (e.g. license fee, grid connection fee, contribution fee) which are paid to the public institutions in Turkey.

The CAPEX[190] of the RETs and thermal power plants are tabulated in Table 9 and Table 62 as specific investment costs of the corresponding power plants respectively. The CAPEX is assumed to be annuitized as fixed investment charges over the corresponding economic life times of all commissioned power plants in the period 2015-2023. In addition, the capital cost of power plants, which are commissioned prior the year 2015 (so called existing power plants), are considered to be sunk costs and therefore, not taken into account for the calculations. The corresponding calculations are carried out as expressed below:

$$The\ Capital\ Cost\ of\ Capaciy\ per\ year = CAPEX \cdot \frac{\rho \cdot (1+\rho)^t}{(1+\rho)^t - 1} \qquad (22.3.1)$$

In Eq. (22.3.1), the terms "t" and "ρ" denote the economic life time of the corresponding power plants and the discount rate respectively. The ρ is considered to be 5%[191] for the analysis. Further, the fixed O&M costs, which constitute taxes and insurance, personnel administration costs, etc., are incurred by all type of power plants independent of their commissioning date. The capital and the fixed O&M costs are both independent of the amount of electricity generated, however they are dependent on the installed capacity of the power plants and consequently must be paid whether running or not. As a result, the more power capacity is commissioned, the more capital and fixed O&M costs are annually incurred.

The variable O&M costs, which include the cost of waste disposal, the cost of unscheduled repairs, etc., are incurred by all type of power plants independent of their commissioning date. The fuel costs indicate the incurred fuel costs due to generation of electricity by thermal power plants in that year. The variable O&M and fuels costs are both dependent on the amount of electricity generated. In addition, the fuel cost of the thermal power plants is also dependent on the type of utilized fuels, efficiency of the power plants and the market price of fuels.

[189] See p. 52 for the related information.

[190] The CAPEX (i.e. capital expenditure) encompasses the costs of erecting the power plant and bringing it to commercial operation and as well as the costs related to interest charges accrued during the construction period.

[191] Detailed information about this assumption is provided in Chapter 7 Assessment of Investments on Renewable Energy Technologies.

In Table 63, the heating values of the resources and their mean specific CO_2 emission factors are represented for generating electricity in Turkey. It can be inferred that imported resources possess quite high calorific values relative to the domestic fossil fuels in Turkey. Further, natural gas and biomass/biogas indicate the least specific CO_2 emission factors. Finally, imported hard coal and domestic types of coal (excluding asphaltite) indicate about the same level of mean specific CO_2 emission factors. Note that the specific CO_2 emission factor of lignite is mentioned to be in the range of 0.71-1.38 t/MWh_{el} and that of hard coal is mentioned to be in the range of 0.92-1.1 t/MWh_{el} by Ari and Köksal (2011, p. 6126). In addition, Ari and Köksal indicated that their results are quite close to those of International Energy Agency for Turkey. Last but not least, Turkey has not set any "Kyoto Target" to reduce the CO_2 emission level and the generators do not incur any costs for the emission of CO_2.

Table 63- The heating value of the resources and the related mean CO_2 emission factors for electricity generation (own illustration)

Type of Resource	Calorific Value[192] [kcal/kg]	Mean Specific CO_2 Emission Factor[193] [t/MWh_{el}]
Natural Gas	12313	0.37
Fuel Oil	9860	0.76
Imported Hard Coal	6100	1.01
Domestic Hard Coal	3300	1.01
Lignite	2000	1.08
Asphaltite	4300	0.46
Geothermal	-	0.94
Biomass/Biogas	-	0.37

In Table 64, the efficiencies for both existing and the commissioned power plants in the period 2015-2023 are tabulated. It can be inferred that the efficiencies of the commissioned power plants are considerably higher than the existing ones.

[192] The calorific values of fuels are obtained from the Turkish Directorate General of Renewable Energy (2016).
[193] The mean specific CO_2 emission factor for geothermal power plants is obtained from Aksoy (2014, p. 599); whereas the others are obtained from Ari and Köksal (2011, p. 6126).

Table 64- The efficiencies of the existing and the commissioned power plants (own illustration)

Type of Power Plant w.r.t. Utilized Fuel	Efficiency of Existing Power Plants[194] [-]	Efficiency of New Power Plants[195] [-]
Nuclear	-	37%
Natural Gas	55%	60%
Imported Hard Coal	41%	46%
Domestic Hard Coal	34%	46%
Lignite	34%	43%
Asphaltite	43%	43%
Fuel Oil	46%	46%

In this study, the domestic market price of the fuels are projected according to the price forecasts in the quarterly report on commodity markets outlook by World Bank Group (2015, p. 41). The calculations are based on the assumption that the change in fuel prices in domestic market (i.e. Δp_{dom}) are perfectly correlated with the price changes in international energy markets (i.e. Δp_{int}). The Δp_{int} equals to the difference between the fuel price in the year $t+1$ and t and divided by $p_{int,t}$ as expressed below:

$$\Delta p_{dom,t+1} = \Delta p_{int,t+1} = \frac{p_{int,t+1} - p_{int,t}}{p_{int,t}} \tag{22.3.2}$$

In Table 65, the calculated changes in forecasted fuel prices according to the World Bank Group are represented. Note that the price change for crude oil is obtained from average spot market price of Brent, Dubai and West Texas Intermediate (WTI), and the natural gas price indicates the spot market price for Europe.

Table 65- The change in the forecasted fuel prices w.r.t. the previous year (own calculation & illustration according to World Bank Group)

Year	Australian Hard Coal [$/ton]	Crude Oil [$/bbl]	Natural Gas [$/MWh$_{th}$]
2016	-14%	-2%	1%
2017	4%	6%	3%
2018	4%	6%	1%
2019	4%	6%	3%
2020	4%	6%	2%
2021	4%	7%	2%
2022	4%	7%	2%
2023	4%	6%	2%

[194] Own data according to the conducted studies during the master thesis of the author.
[195] The data are obtained from NEA, IEA and OECD (2015, pp. 38-39).

Correspondingly, the domestic market price of fuels is projected for the period 2016-2023 by starting from the base year 2015 as represented below:

$$p_{dom,t+1} = p_{dom,t} \cdot (1 + \Delta p_{dom,t+1}) \tag{22.3.3}$$

In Figure 123, the projected domestic price for fuel oil and natural gas are depicted. The provisional domestic fuel oil price for 2015 is given as 637 $/tonne in "Energy Prices and Taxes Quarterly Statistics Fourth Quarter 2015" by IEA (2015, p. 327). The price is for high sulphur fuel oil utilized in power plants and includes taxes (i.e. excise tax for oil products and value added tax). In the same report, the provisional price for domestic natural gas price for 2015 is given as 32.3 $/MWh$_{th}$ (2015, p. 338). The price is for natural gas utilized in power plants and includes all taxes. Note that in this study all given fuel prices are in nominal U.S. dollars.

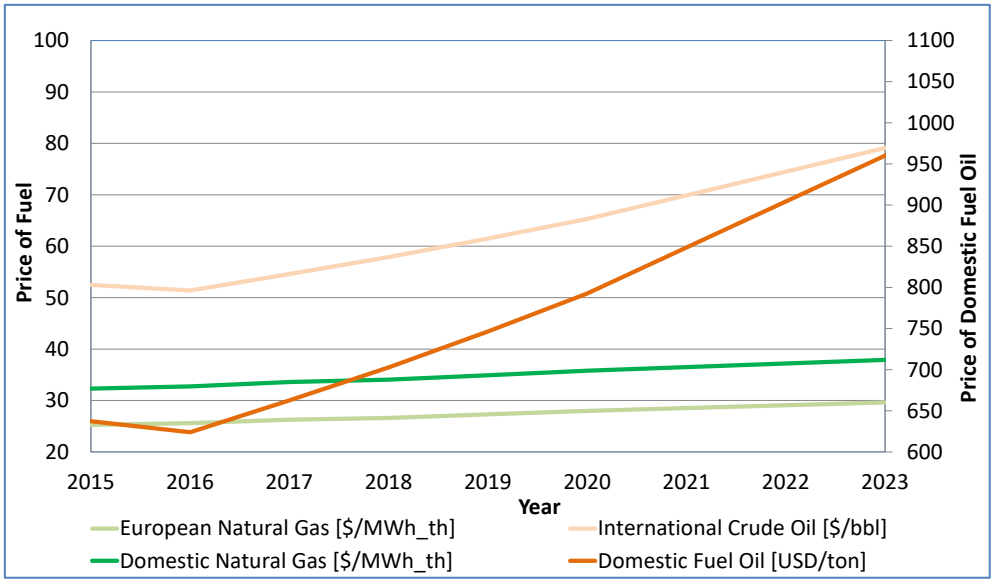

Figure 123- The projected domestic prices for fuel oil and natural gas w.r.t. the changes in forecasted international fuel prices (own calculation & illustration)

In Figure 124, the projected domestic prices for imported hard coal, domestic hard coal, lignite and asphaltite are depicted. The price of imported hard coal, domestic hard coal and lignite are projected according the forecasted spot market price for Australian hard coal by World Bank Group. Further, the price for asphaltite is assumed to be constant; since there is not any international market for it. The price of asphaltite is given 26.9 $/ton (incl. value added tax) and assumed to be constant until the year 2023 according to the report by Is Investment (2012, p. 9). The provisional price for imported hard coal for Turkey in the year

2015 is calculated to be 74.6 $/ton from the report "Coal Trader International" by Platts (2015, p. 7). The price is for steam coal utilized in power plants and includes value added tax. The price of domestic hard coal is given as 66 $/ton (incl. value added tax) by the state hard coal enterprise. The provisional price for lignite for 2015 is given as 31 $/ton by IEA[196]. The price is for lignite utilized in power plants and includes value added tax. Finally, it can be inferred from the figure that the price of domestic types of coal per ton are substantially lower than the price of imported hard coal per ton.

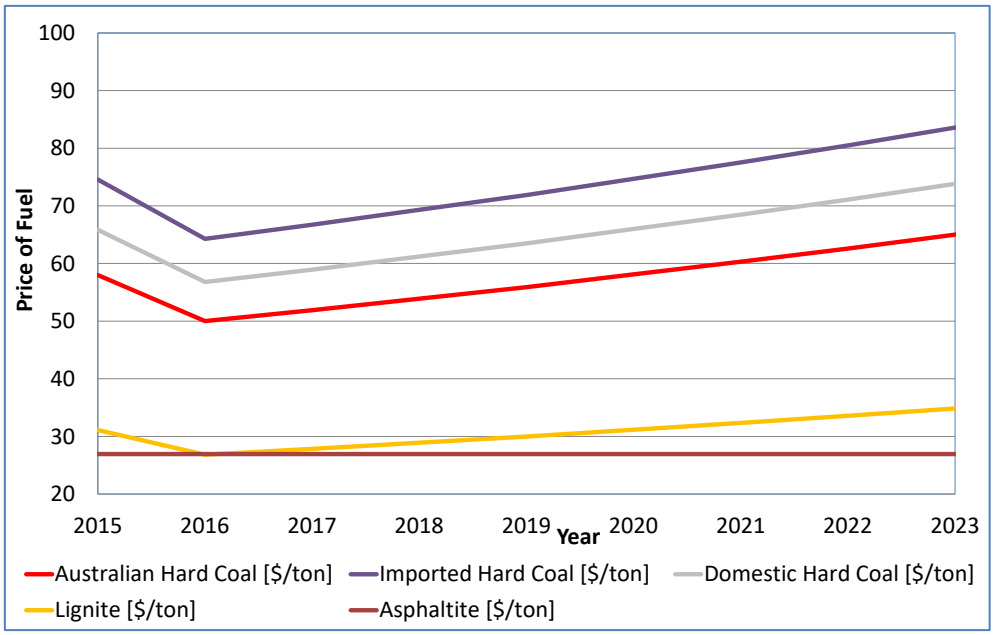

Figure 124- The projected prices of domestic coal types and imported hard coal w.r.t. the international fuel prices (own calculation & illustration)

The fuel cost of the Akkuyu nuclear power plant, including both front-end and waste management costs, is taken as 9.33 $/MWh$_{el}$ according to NEA, IEA and OECD[197]. In this study, it is assumed that the fuel cost of the nuclear power plant does not change in the period 2015-2023. The fuel costs of other thermal power plants are calculated considering the heating value, price of the fuels and the efficiency of the power plants. An example fuel cost calculation for generating 1 MWh$_{el}$ by a new lignite fired power plant in the year 2015 is expressed below:

[196] The relevant information can be found in "Energy Prices and Taxes Quarterly Statistics Fourth Quarter 2015" (2015, p. 327).
[197] The relevant information can be found in "Projected Costs of Generating Electricity 2015 Edition" (NEA, IEA, OECD, 2015, p. 112).

$$2000\ \frac{kcal}{kg}\cdot\frac{0.001163\ kWh}{1\ kcal}\cdot\frac{1000\ kg}{1\ ton}=2326\frac{kWh_{th}}{ton} \quad (22.3.4)$$

$$31.1\frac{\$}{ton}\cdot\frac{1}{2326}\frac{ton}{kWh_{th}}\cdot\frac{1}{43\%}\cdot\frac{1000\ kWh_{el}}{1\ MWh_{el}}=31.1\frac{\$}{MWh_{el}} \quad (22.3.5)$$

In Eq. (22.3.4), the heating value of coal is converted from kcal/kg to kWh_{th}/ton and in Eq. (22.3.5), the cost of coal is converted from \$/ton to \$/MWh_{el}.

The fuel costs per unit amount of electricity generated by the existing power plants are tabulated in Table 66. It can be inferred from the table that the highest fuel cost per MW_{el} generated electricity is calculated to be incurred by the fuel oil fired power plants; whereas the least fuel cost is incurred by the asphaltite fired power plants. Although the domestic hard coal and the lignite are projected to be cheaper than the imported hard coal, the unit fuel cost of electricity generated by the domestic hard coal and the lignite fired power plants are higher than the imported hard coal fired ones. This is due to the relatively low calorific values of the corresponding domestic fuels and relatively low efficiencies of the corresponding power plant types (see Table 63 and Table 64). In addition, the unit fuel cost of the natural gas fired power plants is calculated to be higher than the domestic fossil fuel fired ones. Hence, all considered domestic fossil fuels can compete against natural gas for electricity generation.

Table 66- The fuel cost per unit amount of generated electricity (own calculation & illustration)

Year	Fuel Cost of Existing Thermal Power Plants [\$/MWh_{el}]					
	Lignite	D. Hard Coal	Asphaltite	I. Hard Coal	Natural Gas	Fuel Oil
2015	39.3	50.5	12.5	25.6	58.7	120.8
2016	33.9	43.5	12.5	22.1	59.5	118.3
2017	35.2	45.1	12.5	22.9	61.1	125.6
2018	36.5	46.9	12.5	23.8	61.8	133.2
2019	37.9	48.7	12.5	24.7	63.5	141.5
2020	39.5	50.6	12.5	25.7	65.1	150.3
2021	40.8	52.5	12.5	26.6	66.4	160.9
2022	42.5	54.5	12.5	27.7	67.6	171.4
2023	44.1	56.6	12.5	28.7	68.9	182.0

In Table 67, the fuel costs per unit amount of electricity generated by the commissioned thermal power plants in the period 2015-2023 are tabulated. It can be inferred that the highest fuel cost per MW_{el} generated electricity is calculated to be incurred by the fuel oil fired power plants; whereas the least unit fuel cost is incurred by the Akkuyu nuclear power plant. The ranking of the unit fuel costs for existing power plants is similarly observed for the

commissioned power plants; however the existing power plants (excluding asphaltite and fuel oil fired ones) incur higher fuel costs than the commissioned power plants due to possessing relatively low efficiencies (see Table 64).

Table 67- The fuel cost per unit amount of generated electricity (own calculation & illustration)

Year	Fuel Cost of Commissioned Thermal Power Plants [$/MWh$_{el}$]						
	Nuclear	Lignite	D. Hard Coal	Asphaltite	I. Hard Coal	Natural Gas	Fuel Oil
2015	9.3	31.1	37.3	12.5	22.9	53.8	120.8
2016	9.3	26.8	32.2	12.5	19.7	54.5	118.3
2017	9.3	27.8	33.4	12.5	20.4	56.0	125.6
2018	9.3	28.9	34.7	12.5	21.2	56.7	133.2
2019	9.3	30.0	36.0	12.5	22.0	58.2	141.5
2020	9.3	31.2	37.4	12.5	22.9	59.7	150.3
2021	9.3	32.3	38.8	12.5	23.7	60.8	160.9
2022	9.3	33.6	40.3	12.5	24.7	62.0	171.4
2023	9.3	34.9	41.8	12.5	25.6	63.2	182.0

The external cost of electricity generation is internalized in the total supply cost of electricity to compare the social costs of different technologies based on the different capacity expansion plans. In order to apply the "with-and-without" approach for the aforementioned appraisal; the approximated magnitude of the specific impacts per generated amount of electricity is obtained from Rafaj and Kypreos (2007) and Ecofys (2014) to form a bandwidth w.r.t. the considered type of technologies. The corresponding values are tabulated in Table 68 under the rubrics of "Adjusted ExternE" and "Ecofys" respectively.

Table 68- The specific external costs of power plant types for electricity generation (own illustration according to Rafaj & Kypreos and Ecofys)

Type of Power Plant w.r.t. Utilized Fuel/Resource	Specific External Cost [$/MWh$_{el}$]	
	Adjusted ExternE	Ecofys
Hydropower	1.3	1.3
Wind Power	1.3	5.4
Solar PV	3.9	18.1
Biomass	5.9	22.8
Geothermal	5.9	12.1
Nuclear	6.8	22.9
Natural Gas	13.8	44.1
Lignite[198]	37.4	138.2
Hard Coal/Asphaltite[199]	37.4	122.5
Oil	57.8	112.6

[198] Lignite value for Ecofys indicates the average of maximum and minimum values for EU-28.

[199] This is an assumption based on the fact that its quality is better than lignite and is as good as hard coal (see Table 63).

The set of values for the low end of the bandwidth is obtained from the study "Internalisation of external cost in the power generation sector: Analysis with Global Multi-regional MARKAL[200] model" by Rafaj and Kypreos (2007, p. 842). The tabulated external cost values are the adjusted outcomes of the ExternE Project by the authors and are calculated specific to the Organization for Economic Cooperation and Development (OECD) region which is comprised of the Western Europe, Turkey, Japan, Australia and New Zealand (OOECD). The determinants, which are utilized for scaling the externalities for the period 2010-2050, are as follows:

- A high population density in the corresponding OECD region is assumed.
- The fuel quality is expressed as the content of the Sulphur in coal and oil.
- The Sulphur content in coal, which is assumed to be 1% in all world regions, is mentioned to be the typical average of all different coal types.
- The technology specification w.r.t. installation of the emissions control systems are taken into account.
- The possible improvements in conversion efficiency over the modelled time horizon are considered.
- The external costs are associated with local air pollutants (SO_2, NO_x, particulates) and global climate change (CO_2).
- Both lignite and hard coal fired power plants have flue-gas desulfurization and denitrification systems.
- The external cost of global warming (global warming damage cost) is assumed to be $ 25 per ton of CO_2 emission.

As it is mentioned in Rafaj and Kypreos (2007, p. 832), the economic valuation of the damage is obtained by the willingness-to-pay of the affected individual to avoid a negative impact resulting from electricity generation from a power plant. Further, the external costs are calculated by following the pathways of polluting substances from the release source to the point of damage occurrence (i.e. so called the impact pathway approach). Furthermore, it is mentioned that detailed site-specific characterization of technologies is carried out through a

[200] The analysis were carried out by using the Global MARKAL (Market and Allocation)-Model for five regions such as North America (NAME) and the rest of the OECD (OOECD), the transition-economies of Central & Eastern Europe and the Former Soviet Union, (EEFSU), the developing countries in Asia (ASIA) and Latin America, Africa and the Middle East (LAFM). It is mentioned to be a multi-regional ''bottom-up'' partial equilibrium model of the global energy system with endogenous technological learning, is used to address impacts of internalization of external costs from power production (Rafaj & Kypreos, p. 828)

"bottom-up" approach which enable consideration of every essential stage in different energy chains and comparison between different fuel-cycles and different kinds of burden and impact within a fuel-cycle. Furthermore, the costs of environmental and health damages originate from local pollutants (SO_2, NO_x) and climate change, wastes, occupational health, risk of accidents, noise and other burdens. The mentioned negative impacts are mentioned to be computed by using a so called damage function. Finally, Friedrich and Bickel (2001) state that the results of the ExternE Project are valuable support for decision making but does not replace the decision making process due to existing uncertainties and made assumptions. Note that it is assumed that those costs do not change in the period 2015-2023.

The set of values for the high end of the bandwidth is obtained from the study "Subsidies and costs of EU energy" by Ecofys (2014). The external costs of this study are assessed by utilizing the "External-E tool" which can integrate life cycle assessment (LCA), actual power production data and monetization methodologies to estimate and value total environmental impacts (Ecofys, p. 12). The LCA is defined to be a standardized technique that tracks all material, energy, and pollutant flows of a system from raw material extraction, manufacturing, transport, and construction to operation and end-of-life disposal (The National Renewable Energy Laboratory of the USA, 2016). In addition, the LCA is stated to be assisting in determining environmental burdens from "cradle to grave" (i.e. raw material extraction to waste treatment) and facilitate comparisons of energy technologies. The LCA is carried out for the group of 'reference' power technologies in EU-28[201] countries in three steps as follows (Ecofys, 2014)[202]:

1. In the life cycle inventory analysis, data are collected on the environmental interventions (resource use and emissions to air, water and soil) occurring in the life cycle of the product from cradle to grave.
2. In the life cycle impact assessment (LCIA)[203], those environmental interventions are classified and translated into environmental impacts (i.e. expressed in a single common denominator of impact, e.g. greenhouse gas emissions are converted into carbon dioxide equivalents).

[201] Austria, Belgium, Bulgaria, Croatia, Republic of Cyprus, Czech Republic, Denmark, Estonia, Finland, France, Germany, Greece, Hungary, Ireland, Italy, Latvia, Lithuania, Luxembourg, Malta, Netherlands, Poland, Portugal, Romania, Slovakia, Slovenia, Spain, Sweden and the UK.

[202] See "Subsidies and costs of EU energy: Annex 1-3" for more information.

[203] The LCIA is carried out by utilizing the impact assessment method ReCiPe which is based on the midpoint-endpoint approach (see the mentioned publication in Footnote 202 for more information).

3. At the end of the LCIA, the impacts are monetized according to the damage cost approach which is utilized for valuing the environmental impacts by converting impacts to the damages (end points) as follows:
    - Human health damages
    - Ecosystems and biodiversity
    - Resources and depletion, primarily water, metals and fuels but also including crops, buildings and other assets

The monetization value for climate change is assumed to be 50 €/ton CO_2 equivalent (Ecofys, p. 14). To sum up, the provided results of this study is stated to be approximations based on a set of general assumptions rather than a precise estimate of actual external costs (Ecofys, p. 36). Nonetheless, it is also mentioned that the results indicate an order of magnitude of specific impacts per technology based on the currently best available information. Note that it is assumed that those costs do not change in the period 2015-2023.

23 Techno-Economic Analysis of the Energy Policy 2023

In this chapter, information is provided about the techno-economic analysis, which is carried out by utilizing the capacity expansion model. The techno-economic analysis encompasses the technical and the economic assessments of the energy policy 2023 w.r.t. the alternative capacity expansion scenarios for the period 2015-2023. The technical assessments involve the calculation of the annual amount of electricity generated by all types of power plants and CO_2 emissions caused by thermal, geothermal and biomass power plants. The economic assessments involve the calculation of the social cost of supplying electricity in each year of the mentioned period. In Sections 23.1 and 23.2, theoretical information is given about the definition of welfare and the welfare analysis of electricity market. In Section 23.3, detailed information is provided about the techno-economic calculations.

23.1 Definition of Welfare

Social benefits are defined in Griffin and Steele (1986, p. 46) as the total amount society is willing to pay for a given quantity of goods, holding constant society's level of wellbeing. Further, social costs are defined to be equal to the firm's private costs of production (e.g. capital, labor, and materials) and externally borne costs (e.g. opportunity cost of using a non-renewable resource, impairment of health and damage to property). Hence, the difference between social benefits (i.e. the area OABQ^* in Figure 125) and social costs (i.e. the area OBQ^* in Figure 125) is defined as economic welfare. In Figure 125, the shaded area OAB represents the amount of welfare from output "Q^*" at market price P in a perfectly competitive market. Alternatively, welfare can also be defined as the sum of consumer surplus (i.e. vertically shaded area PAB in Figure 125) and producer surplus (i.e. horizontally shaded area OBP in Figure 125). Consumer surplus is the amount of money that consumers would be willing to pay for a given product minus they are required to pay. Producer surplus is the amount that is paid to producers above and beyond the minimum price required by producers. Thus, any investment that reduces the cost of the product or service process a benefit in savings that increases the consumer plus.

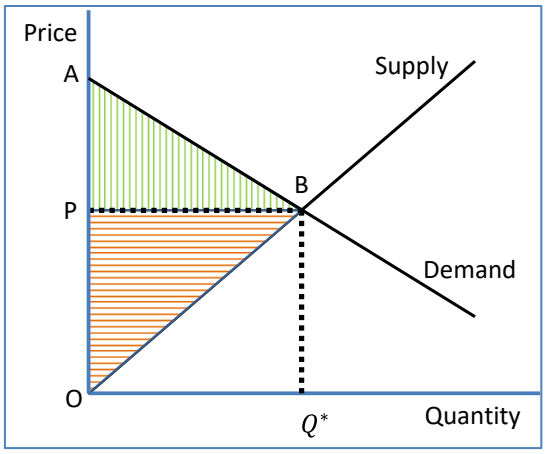

Figure 125- Welfare optimum (own illustration according to Griffin and Steele (1986, p. 51))

Welfare is maximized at the quantity Q^* when the marginal social benefit of the last unit of output equals its marginal social cost (Griffin & Steele, 1986, p. 51). It can be inferred from the figure that the marginal social benefit of the last unit exceeds its marginal social cost at any output below Q^*. In contrast, the marginal social cost of the last unit exceeds its marginal social benefit at any output above Q^*. In the former case, welfare can be increased by raising output; whereas in the latter case, it can be increased by reducing output towards Q^*. As per definition of the economic welfare, empirical quantification of the social costs and the social benefits is required for the welfare analysis. In this study, the purpose is to measure the change in welfare resulting from implementing a policy change. More specifically, implementing a new policy induces opportunity costs[204]; since the scarce resources would have been utilized in alternative energy policies. Correspondingly, the impacts of adoption of a new policy should be assessed relative to alternative policies to appraise whether the resources are efficiently allocated. Thus, a policy should be adopted if it produces greater net social benefits to the society relative to the alternatives.

23.2 Welfare Analysis of Electricity Market

In an electricity market, the market's supply curve is called the merit order curve and is formed by successively adding all of the individual generators' supply curves starting from the technology with the lowest marginal cost[205] (also called variable cost) to the highest one in the generation mix. By using merit order curve, the quantity of capacity supplied by each generator can be determined starting from the origin until the given magnitude of the load

[204] From another point of view, it can also induce savings through avoiding costs w.r.t. the alternatives.

[205] It is the cost of producing one more kilowatt-hour of electricity. It approximately equals to the savings from producing one less kWh (Stoft, 2002, p. 56).

demand is covered. Correspondingly, the market price is set according to the marginal cost of the last dispatched power plant in the merit order (the so called marginal power plant).

In liberalized electricity markets (e.g. the Turkish electricity market), the merit order is formed by the submitted bids of the each individual generator which has to take part in the day-ahead auctions. Accordingly, the system operator utilizes those bids to determine the market price under the given system constraints and the hourly load demands. In this respect, the quantity supplied equals to the quantity demanded and thus, the market is said to have cleared by accomplishing a price so called the market-clearing price (Stoft, 2002, p. 57). It is called a short-run competitive equilibrium through which a market price and a market quantity traded are determined as a result of partial market equilibrium (Stoft, 2002, p. 56). A diagram, similar to the Figure 125, can be constructed to analyze the impact of adoption of energy policy 2023 on economic welfare due to the amount of variable costs[206] avoided/incurred relative to the alternative capacity expansion scenarios.

In Figure 126, representative merit order curves of a reference and an alternative capacity scenario are represented. The merit order curves of the reference and the alternative capacity expansion scenarios are formed by joining the line segments ABCDEF and AGIDEF respectively. The main differences in scenarios are the amount of capacity supplied by lignite and natural gas fired power plants (i.e. domestic vs. imported resource dependency). Namely, the amount of capacity supplied by lignite fired power plants in the reference scenario is higher than the corresponding amount in the alternative scenario (i.e. $x_{lgnt} > x'_{lgnt}$); whereas it is vice versa for the natural gas fired power plants (i.e. $x_{gas} < x'_{gas}$). In both scenarios, the amount of capacity supplied by oil fired power plants are considered to be same (i.e. $x_{oil} = x'_{oil}$). Further, the residual load demand is obtained by subtracting the amount of capacity supplied by RETs from perfectly inelastic hourly load demand. Since the hourly load demand is perfectly inelastic, consumer surplus is infinite. The producer surplus equals to the area of the polygons $pABCDE$ and $pAGIDE$ in the reference and in the alternative scenarios respectively. Although the market clearing price (i.e. p) is same for the two scenarios; the production costs (also the producer surplus) are different due to higher dependency on different type of fuels. Accordingly, the change in welfare can be determined by calculating

[206] They consist of fuel and variable O&M costs. There are no start-up costs to bring the units online, which are in reality added to variable costs.

the difference in total producer cost between the two scenarios. Thus, the change in welfare equals to the area under $AGIDEF$ minus the area under $ABCDEF$ (see Figure 127).

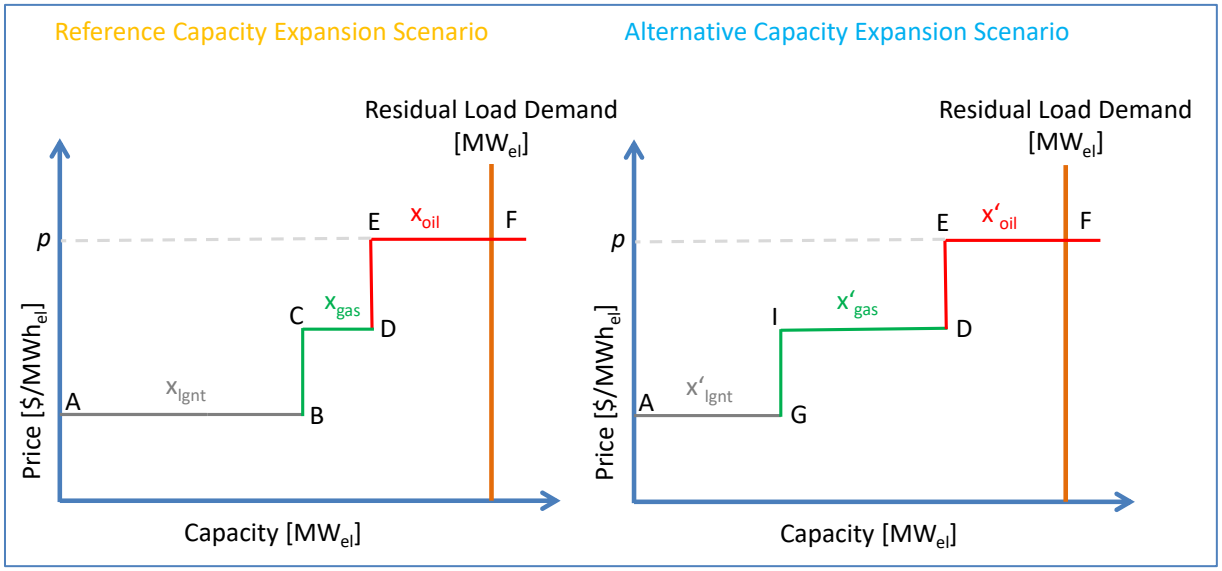

Figure 126- The representative merit order curves of two example capacity expansion scenarios (own illustration)

In Figure 127, the merit order curves are superimposed on each other to indicate the difference in welfare in two scenarios which amounts to the area of the rectangle $IGBC$. Accordingly, the area of the $IGBC$ indicates the amount of savings in variable costs which would have been foregone by utilizing the scarce resources in the alternative capacity expansion scenario.

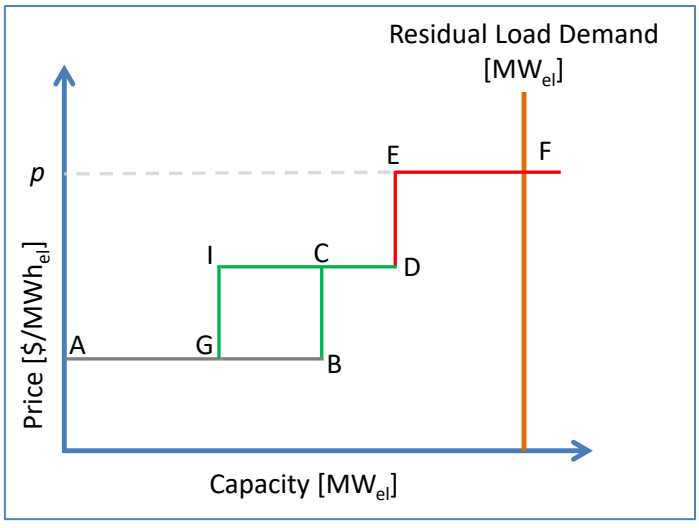

Figure 127- The superimposed merit order curves on each other (own illustration)

In this study, the short equilibrium is considered to be efficient due to the criteria given below for productive efficiency (Stoft, 2002, p. 53):

- The output is produced by the cheapest suppliers and the suppliers are price takers.
- The output is consumed by those most willing to pay for it.
- The right amount is produced and consumed.
- Thus, the production costs have been minimized given total production.

According to the mentioned criteria, welfare has been maximized; since the cost of production is minimized; whereas the value of what is consumed is maximized. Hence, it can be said that the electricity market is efficient due to the fact that the sum of profit and consumer surplus (i.e. welfare) is maximized (Stoft, p. 50). Correspondingly, it is assumed that the short-run profit is enough to cover the fixed costs. In this respect, the short run profits amounts to the normal level of profit (zero) in the long-run competitive equilibrium (Stoft, p. 59).

Note that the approach of short-run market equilibrium disregards the changes in welfare due to the avoided/incurred fixed and external costs. Accordingly, the corresponding costs are exogenously taken into account for the calculation of the net social benefit of adopting energy policy 2023 w.r.t. the alternative scenarios. In this study, long-run market equilibrium cannot be confirmed; since the capacity expansion targets in all scenarios are created in comparison to the energy policy 2023. Hence, only adjustments are carried out for the amount of capacity supplied by thermal power plants; which solely depends on their positions within the corresponding merit order curves and residual load demands. Note that the outputs from RETs are exogenously given to the model according to the annual full load hours represented in Table 52.

23.3 Techno-Economic Calculations

The techno-economic analysis encompasses the technical and the economic assessments of the energy policy 2023 (i.e. reference scenario) w.r.t. the given alternative capacity expansion scenarios for the period 2015-2023. The former involves the calculation of the annual amount of electricity and CO_2 generated by corresponding power plants; whereas the latter involves the calculation of the social cost of supplying electricity in each year of the mentioned period.

The energy output of a thermal power plant type i (E_i) in a year of the period 2015-2023 can be calculated as expressed below:

$$E_i = \int_{D_i}^{D_{i+1}} g^{-1}(z)\, dz \tag{23.3.1}$$

In Eq.(23.3.1), the symbols "D_i" and "g^{-1}"denote the loading point of unit i and the inverse residual load duration curve function which depends on the hourly residual load demand "z" respectively. D_i indicates the load level starting from which the corresponding unit i will generate power according to the merit order of loading. The merit order of loading provides the increasing order of variables cost in which the individual units are expected to be called upon to cover the demand in a power system (i.e. in analogy to the merit order curve). In this manner, the variable cost of electricity generation is minimized. The D_i of unit i is found by summing up the utilized capacities[207] of all units, which are prior to the unit i in the merit order of loading, as expressed below:

$$\begin{Bmatrix} D_1 = 0 & i = 1 \\ D_i = \sum_{j=1}^{i-1} x_j & i = 2, \dots., n+1 \\ D_{n+1} = L^{\bar{p}} & \end{Bmatrix} \tag{23.3.2}$$

It can be inferred from the Eq.(23.3.2) that the difference of two consecutive loading points (e.g. D_i, D_{i+1}) will yield the utilized capacity of unit i (i.e. $x_{i+1} = D_{i+1} - D_i$). The last loading point (D_{n+1}), which corresponds to $L(1)$, equals to the residual peak load demand of the considered year ($L^{\bar{p}}$).

The inverse residual load duration curve function g^{-1} is derived by rescaling the approximating function of each normalized[208] future LDC ($L(t)$[209]). The rescaling of $L(t)$ is carried out according to the difference between the corresponding forecasted annual gross electricity demand (F_{AGD}) and the annual amount of electricity generated by RETs (E_{RET}) as expressed below:

[207] It equals to the availability derated installed capacity of thermal units (i.e. 0.67 for thermal power plants).
[208] See section 12.1 for information on normalization of load duration curves.
[209] Note that "$L(t)$" denotes the 5th degree polynomial function approximating the normalized LDC of a year in the period 2015-2023 (see Chapter 13).

$$g^{-1}(z_t) = L(t) \cdot (F_{AGD} - E_{RET}), \qquad 1 \leq t \leq n \ \wedge \ n = 8760 \ or \ 8784 \tag{23.3.3}$$

In Eq. (23.3.3), the symbol "z_t" denotes the t^{th} hourly load demand in the LDC of the corresponding year. Also, the function "$L(t)$" depends on the duration "t"and the duration t is defined in the range from 0 to 8760 or 8784 hours.

In Figure 128, the allocation of the power plant capacities to a given representative residual load duration curve are displayed in analogy to the mentioned reference and alternative capacity expansion scenarios in Figure 126. It can be inferred from the figure that the annual amount of capacity supplied by lignite fired power plants in the reference scenario is higher than the corresponding amount in the alternative scenario (i.e. $x_{lgnt} > x'_{lgnt}$); whereas it is vice versa for the natural gas fired power plants (i.e. $x_{gas} < x'_{gas}$). In both scenarios, the annual amount of capacity supplied by oil fired power plants are considered to be same (i.e. $x_{oil} = x'_{oil}$). In the figure, the merit order of loading is provided by ranking the thermal power plants w.r.t. their increasing order of variables costs as represented for the same residual load duration curve in both scenarios.

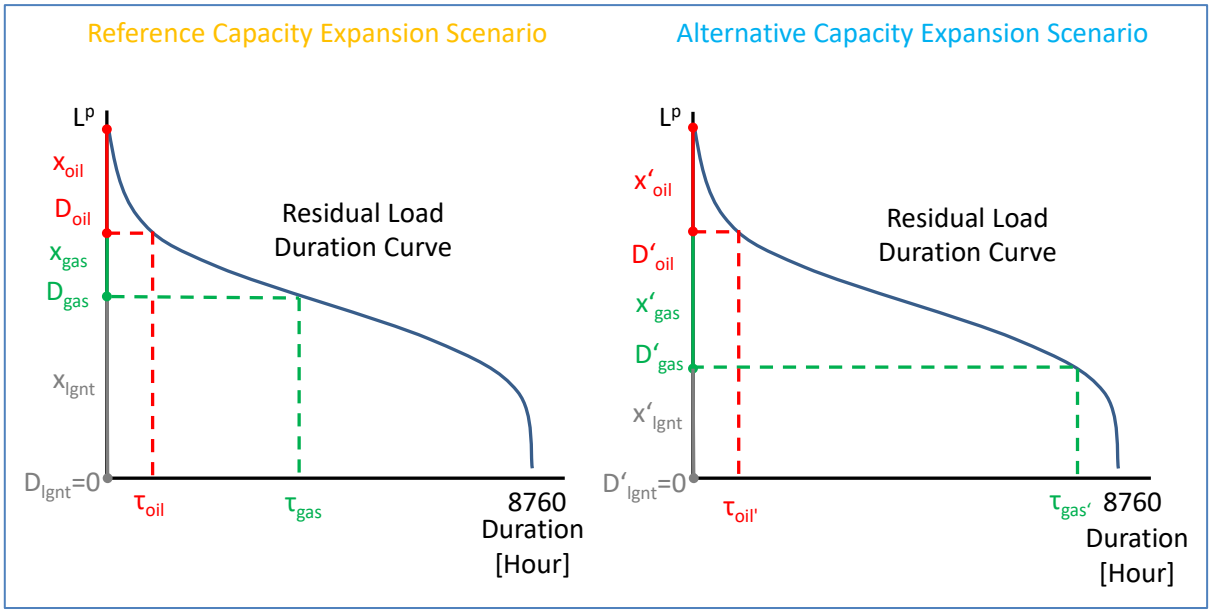

Figure 128- The allocation of capacity to a representative residual load duration curve w.r.t. the capacity expansion scenarios (own illustration)

The annual amount of CO_2 emitted by n type of thermal power plants and also 2 types of RETs (i.e. geothermal and biomass power plants) in a year of the period 2015-2023 can be calculated according to the given CO_2 emission factors (K_i) and the calculated amount of generated electricity as represented below:

$$Q_{CO_2} = \sum_{i=1}^{n+2} K_i \cdot E_i \tag{23.3.4}$$

With regard to economic assessments, the annual social cost of supplying electricity (SC) is composed of fixed, variable and external costs of N type of power plants as expressed below:

$$SC = \sum_{i=1}^{N} FC_i \cdot Cap_i + E_i \cdot (VC_i + EC_i) \tag{23.3.5}$$

In Eq. (23.3.5), the symbols "FC_i", "Cap_i", "VC_i" and "EC_i" denote the fixed cost, installed capacity, variable cost and external cost factor of i^{th} type of power plant for supplying electricity in a year in the period 2015-2023. Note that the fixed costs consist of capital and fixed O&M, and the variable costs consist of fuel and variable O&M costs. The present value of annually incurred social costs in the year 2015, which is discounted w.r.t. the risk free rate of interest "r", is defined to be the total social cost of supplying electricity as indicated below:

$$TSC = \sum_{i=2015}^{2023} \frac{SC_i}{(1+r)^{(i-2015)}} \tag{23.3.6}$$

Thus, the total social cost of supplying electricity is comprised of present value of incurred total costs for capital, fixed O&M, variable O&M, fuel, and externalities. The net social benefit (NSB) of adopting energy policy 2023 is determined by calculating the difference in the total social cost of supplying electricity due to not adopting[210] (TSC') and adopting the energy policy 2023 (TSC) as represented below:

$$NSB = TSC' - TSC \tag{23.3.7}$$

According to Eq. (23.3.7) , if $TSC' > TSC$, the adoption of energy policy 2023 is calculated to be indicating a positive net social benefit. By the same token, if $TSC' < TSC$, a negative net social benefit is indicated due to adopting the energy policy 2023. Correspondingly, the

[210] It means adopting an alternative capacity expansion scenario.

net benefit of adopting energy policy 2023 is measured relative to the savings (i.e. avoided costs) which would have been foregone/gained by utilizing the scarce resources in an alternative capacity expansion scenario. The avoided costs originate from the difference in power plant portfolios considered for the reference scenario and an alternative scenario (e.g., see Figure 128). Therefore, the NSB can also be defined as the sum of total avoided fixed cost ($TFC_{avoided}$), total avoided variable cost ($TVC_{avoided}$) and total avoided external cost ($TEX_{avoided}$) as expressed below:

$$NSB = TFC_{avoided} + TVC_{avoided} + TEX_{avoided} \quad (23.3.8)$$

24 Results of the Technical Analyses

In this chapter, the results of the techno-economic analyses, which involve the calculation of the annual amount of electricity generated by all considered types of power plants, their shares in the total generation of electricity and CO_2 emissions caused by thermal, geothermal and biomass power plants, are represented. In addition, discussions are carried out on the impact of more ambitious utilization of renewable and imported energy resources in the alternative scenarios relative to the reference scenario (i.e. energy policy 2023). The results of the corresponding analyses are summarized in Section 24.5.

The both technical and economic assessments are carried out by using MATLAB® R2011a. The computations are carried out by using a laptop with Intel Core i7 processor 2.20 GHz, 8192MB (1600MHz) memory and operating system of Windows 10. The elapsed time for the preparation of inputs, the techno-economic calculations and the output of results (to Excel® 2010) is about 1 minute for each considered scenario.

24.1 Reference vs. Green Capacity Expansion Scenario

The technical analysis on the reference and the green capacity expansion scenarios is conducted to compare the impact of more ambitious utilization of renewable energy resources for generating electricity. In the green scenario, 15735 MW_{el} more capacity of RETs is considered to be installed instead of installing lignite and asphaltite fired power plants as in the case of the reference scenario.

In Figure 129, the development of the amount of electricity generated by RETs is illustrated w.r.t. the reference (i.e. indicated as solid bars) and the green scenario (i.e. indicated as patterned bars). In the period 2015-2023, the total amount of electricity generated from RETs increases from 86 TWh_{el} to 159 TWh_{el} in the reference scenario and to 195 TWh_{el} in the green scenario. The majority of the electricity is generated by hydropower and wind power plants among the considered RETs. Namely, their total amount of generated electricity increase from 81 TWh_{el} to 142 TWh_{el} in the reference scenario and to 157 TWh_{el} in the green scenario. On the other hand, the share of hydropower and wind power in the total amount of electricity generated by RETs decreases from 94% to 89% in the reference scenario and to 81% in the green scenario. This is due to the fact that the share of solar PV and biomass power in the corresponding total amount increases from 3% to 8% in the reference scenario and to 16% in

the green scenario. Nevertheless, the share of geothermal power in the corresponding total amount is in the range of 3%-4% in both scenarios.

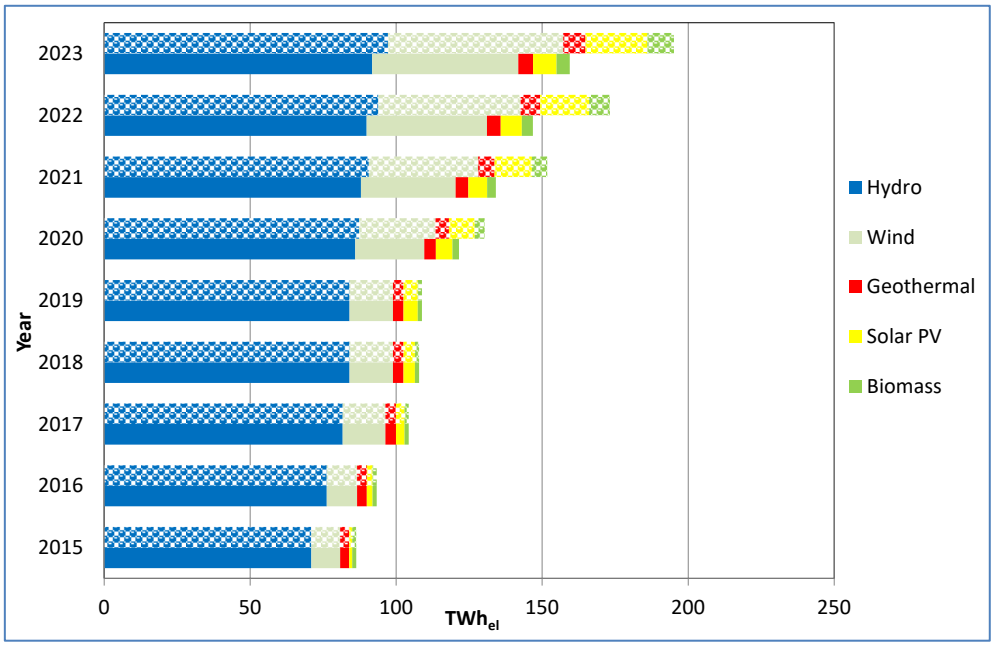

Figure 129- The amount of electricity generated by RETs w.r.t. the reference (solid bars) and the green (patterned bars) capacity expansion scenarios (own calculation & illustration)

In Figure 130, the development of the amount of electricity generated by power plant types is illustrated w.r.t. the reference and the green scenario. In the period 2015-2023, the total amount of electricity generated by all considered types of power plants increases from 270 TWh_{el} to 410 TWh_{el} in both scenarios. In the period 2015-2019, the amount of electricity generated by lignite and asphaltite power plants increases from 55 TWh_{el} to 63 TWh_{el} in both scenarios. In the period 2020-2023, the corresponding amount increases to 150 TWh_{el} in the reference scenario; whereas it stays at 63 TWh_{el} level in the green scenario. With regard to imported resource dependency in the period 2015-2019, the amount of electricity generated by natural gas fired power plants increases from 86 TWh_{el} to 115 TWh_{el} in both scenarios. In the period 2020-2023, the corresponding generation amount gradually decreases to 27 TWh_{el} in the reference scenario and to 78 TWh_{el} in the green scenario. In contrast, the development of the amount of electricity generated by imported hard coal and fuel oil fired power plants, and the nuclear power plant is same in both scenarios. For both scenarios, the common causes for the reduction in the amount of electricity generated by natural gas fired power plants are the commissioning of the nuclear power plant and the capacity expansion of the RETs in the period 2020-2023. More specifically, the corresponding reduction in the reference scenario is higher than the one in the green scenario due to the given reasons below:

- More capacity of lignite and asphaltite fired power plants are installed in the reference scenario relative to the green scenario.
- The mentioned type of power plants displaces natural gas fired power plants for electricity generation due to possessing lower variable costs than the latter.
- They can supply more electricity than the RETs due to being technically capable of operating at higher full load hours than the latter.

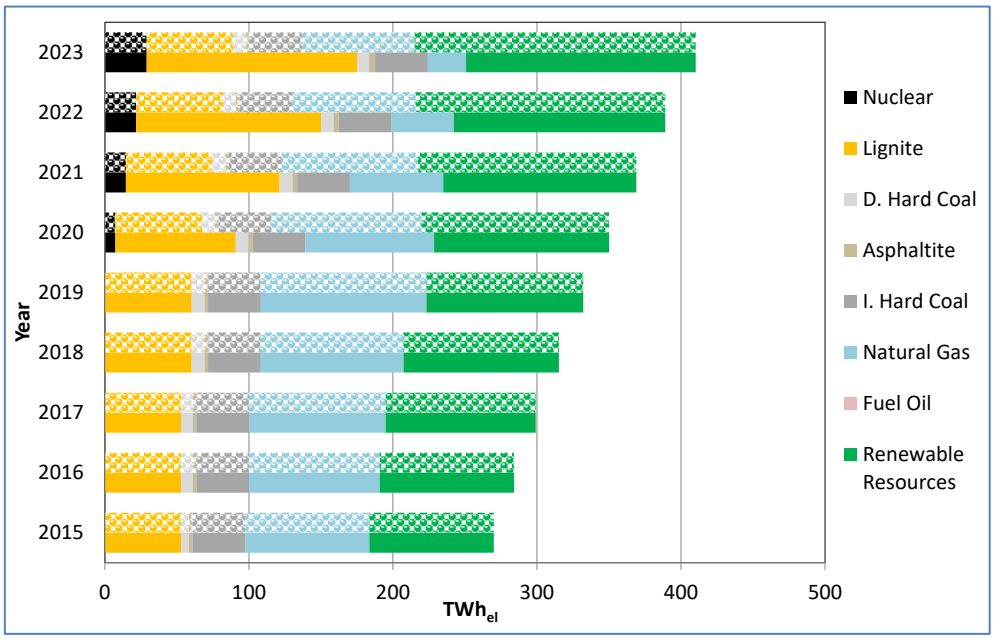

Figure 130- The amount of electricity generated by power plants w.r.t. the reference (solid bars) and the green (patterned bars) capacity expansion scenarios (own calculation & illustration)

The generated amount of electricity by power plants is further analyzed for their shares in the total amount of generated electricity as illustrated in Figure 131. In the figure, power plant types are categorized based on the type of utilized resources such as renewable resources[211], domestic fossil resources[212], natural gas and other imported resources[213]. In the period 2015-2023, the share of RETs in the total amount of generated electricity increases from 32% to 39% in the reference scenario and to 48% in the green scenario. Further, the share of domestic fossil fuel fired power plants in the total amount of generated electricity increases from 23% to 39% in the reference scenario; whereas it decreases from 23% to 17% in the green scenario. Correspondingly, the share of electricity generation from domestic energy resources in the total amount of generated electricity increases from 55% to 78% in the reference scenario and to 65% in the green scenario. Furthermore, the share of natural gas in the total generated

[211] The renewable resources refer to hydropower, wind power, geothermal, solar and biomass resources.
[212] The domestic fossil resources refer to lignite, asphaltite and domestic hard coal.
[213] The other imported resources refer to fuel oil, imported hard coal and nuclear fuel.

amount of electricity decreases from 32% to 6% in the reference scenario and to 19% in the green scenario. Accordingly, the set targets to increase the share of renewable resources and to reduce the share of natural gas are fulfilled by both scenarios. Finally, the share of other imported resources in the total amount of generated electricity increases from 14% to 16% in both scenarios.

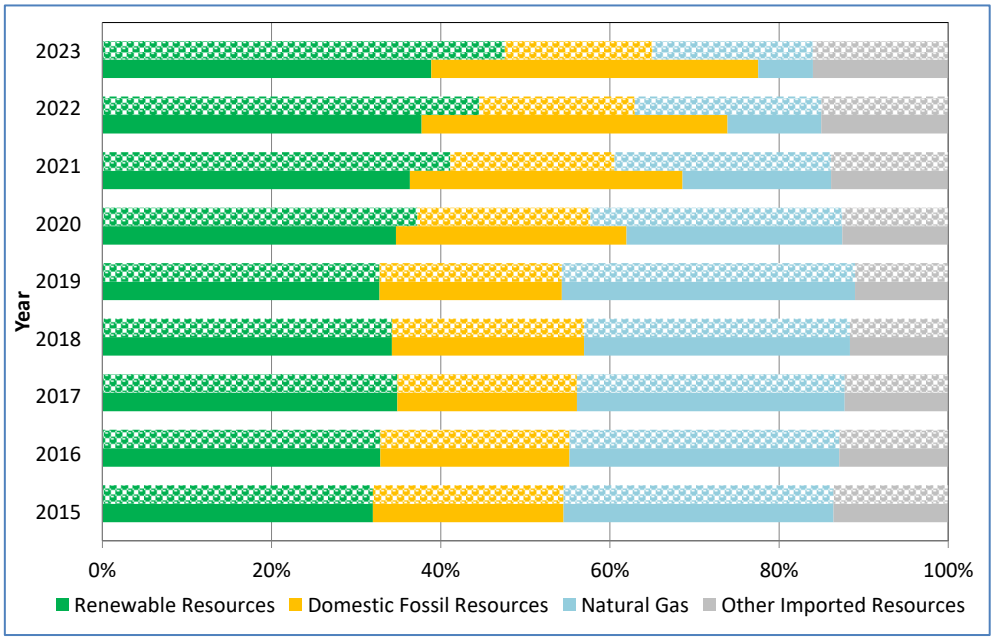

Figure 131- The shares of resources in the total amount of generated electricity w.r.t. the reference (solid bars) and the green (patterned bars) capacity expansion scenarios (own calculation & illustration)

Finally, the generated amount of electricity by power plants is analyzed for the amount of emitted CO_2 as illustrated in Figure 132. In the period 2015-2023, the total amount of CO_2 emissions increases from 136 million ton to 222 million ton in the reference scenario and to 152 million ton in the green scenario. Accordingly, the more ambitious capacity expansion of RETs reduces the level of CO_2 emissions about 30% relative to the reference scenario in the target year 2023. In both scenarios, more than 70% of the CO_2 emissions are caused by the coal fired power plants, especially by the lignite fired ones. More specifically, the total amount of CO_2 emissions by lignite fired power plants increases from 57 million ton to 158 million ton in the reference scenario and to 65 million ton in the green scenario.

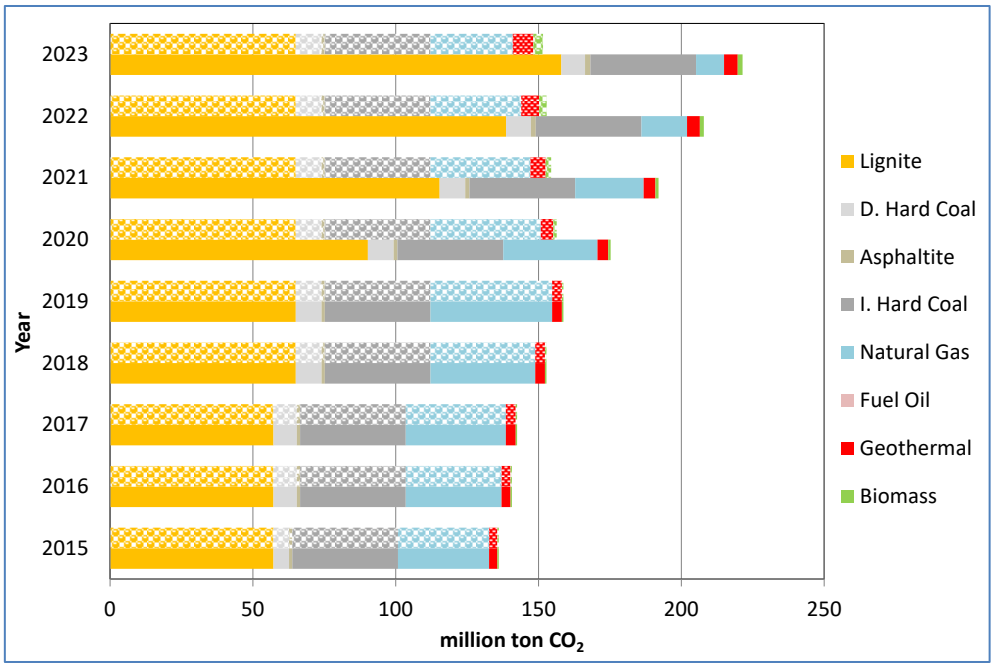

Figure 132- The CO_2 emissions of power plants w.r.t. the reference (solid bars) and the green (patterned bars) capacity expansion scenarios (own calculation & illustration)

24.2 Reference vs. Grey Capacity Expansion Scenario

The technical analysis on the reference and the grey capacity expansion scenarios is conducted to compare the impact of more ambitious utilization of imported hard coal for generating electricity. In the grey scenario, 15735 MW_{el} more capacity of imported hard coal fired power plant is considered to be installed instead of installing lignite and asphaltite fired power plants as in the case of the reference scenario. Hence, the target capacity expansion for RETs is same in both scenarios. In Figure 133, the development of the amount of electricity generated by RETs is illustrated w.r.t. the reference and the grey capacity expansion scenarios.

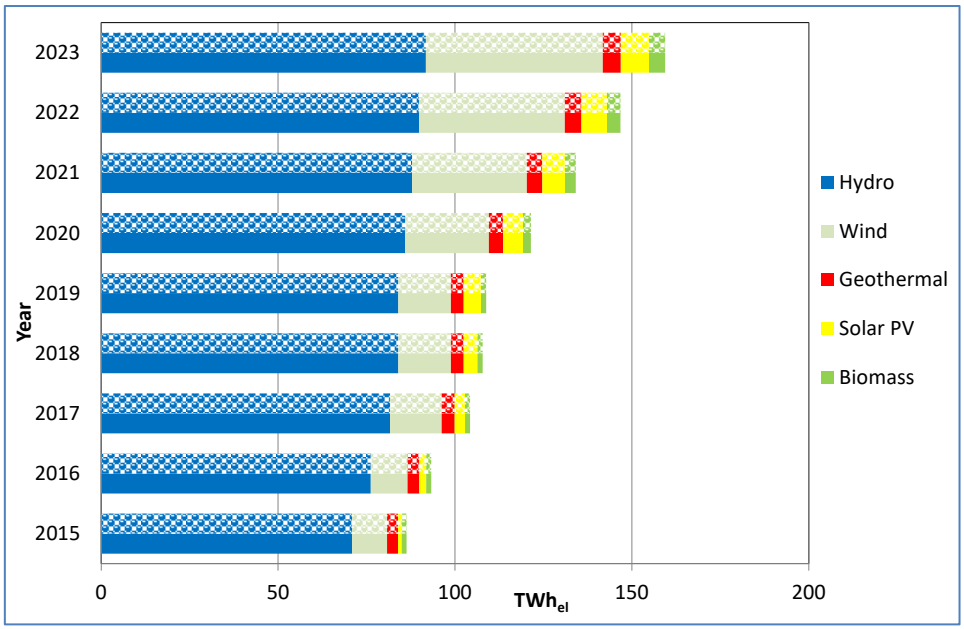

Figure 133- The amount of electricity generated by RETs w.r.t. the reference (solid bars) and the grey (patterned bars) capacity expansion scenarios (own calculation & illustration)

In Figure 134, the development of the amount of electricity generated by power plant types is illustrated w.r.t. the reference and the grey scenario. In the period 2015-2019, the amount of electricity generated by lignite and asphaltite power plants increases from 55 TWh_{el} to 63 TWh_{el} in both scenarios. In the period 2020-2023, the corresponding amount increases to 150 TWh_{el} in the reference scenario; whereas it gradually decreases to 55 TWh_{el} in the grey scenario. The mentioned decrease in the grey scenario is due to the fact that the imported hard coal fired power plants starts to displace lignite fired power plants with the increasing installed capacity of the former; since the variable cost of electricity generation of the former type is lower than the latter type (see Table 62 and Table 67). In the period 2015-2023, the amount of electricity generated by imported hard coal fired power plants stays at 37 TWh_{el} level in the reference scenario; whereas it increases from 37 TWh_{el} to 132 TWh_{el} in the grey scenario. In contrast, the development of the amount of electricity generated by natural gas and fuel oil fired power plants, and the nuclear power plant is same in both scenarios.

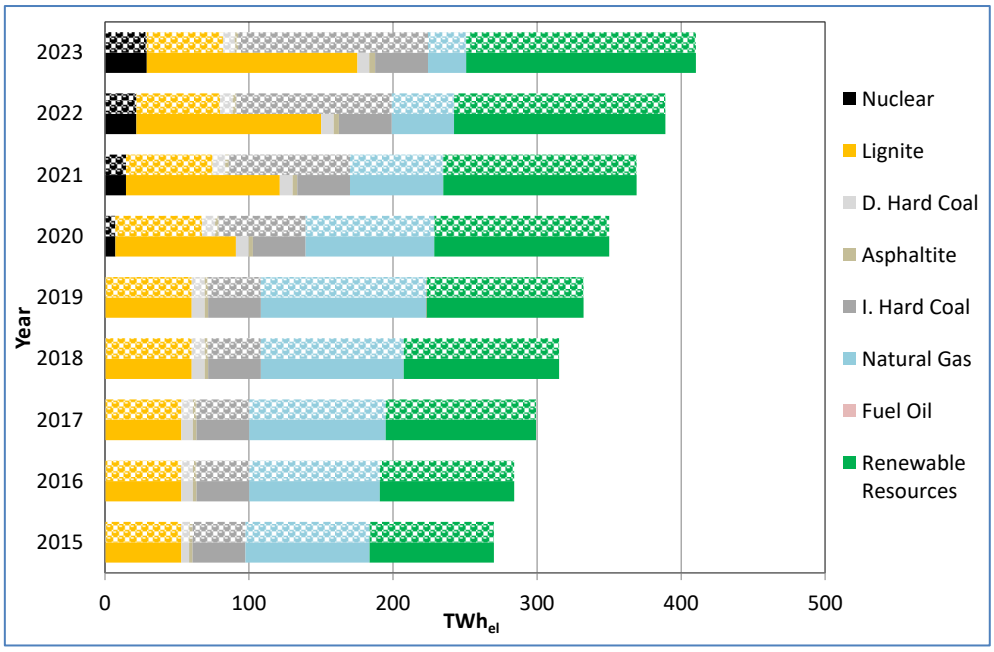

Figure 134- The amount of electricity generated by power plants w.r.t. the reference (solid bars) and the grey (patterned bars) capacity expansion scenarios (own calculation & illustration)

The generated amount of electricity by power plants is further analyzed for their shares in the total amount of generated electricity as illustrated in Figure 135. In the period 2015-2023, the share of RETs in the total amount of generated electricity increases from 32% to 39% in both scenarios. Further, the share of domestic fossil fuel fired power plants in the total amount of generated electricity increases from 23% to 39% in the reference scenario; whereas it decreases from 23% to 15% in the grey scenario. Correspondingly, the share of electricity generation from domestic energy resources in the total amount of generated electricity increases from 55% to 78% in the reference scenario; whereas it decreases from 55% to 54% in the grey scenario. The corresponding decrease in the grey scenario is not only due to the capacity expansion of imported hard coal fired power plants but also due to the previously mentioned displacement of the lignite fired power plants. Furthermore, the share of natural gas in the total generated amount of electricity decreases from 32% to 6% in both scenarios. Accordingly, the set targets to increase the share of renewable energy and to reduce the share of natural gas are fulfilled by both scenarios. Finally, the share of other imported resources in the total amount of generated electricity increases from 14% to 16% in reference scenario and to 39% in the grey scenario.

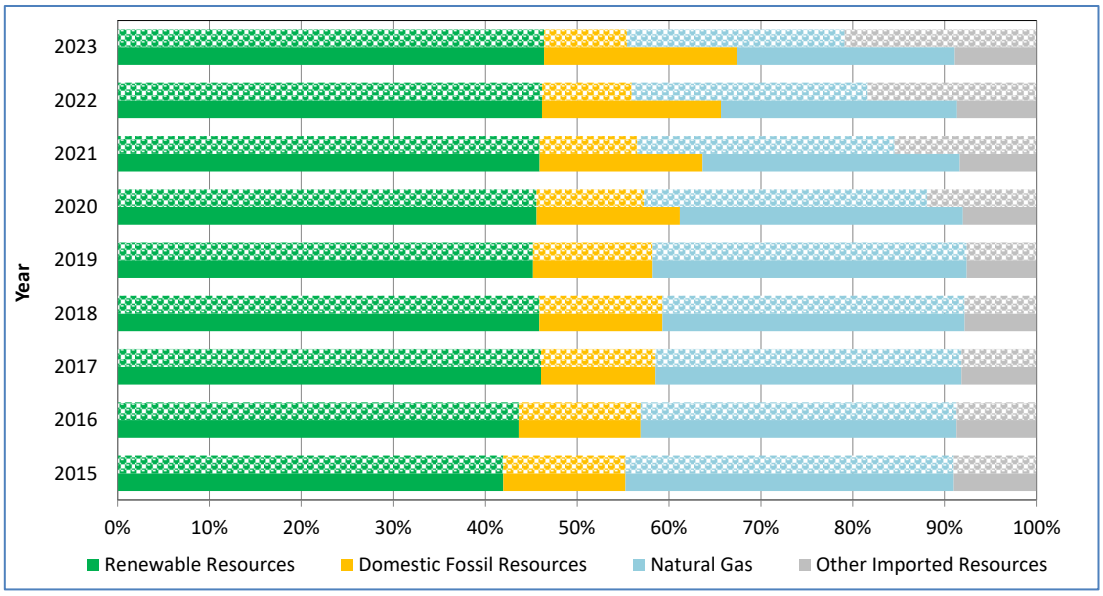

Figure 135- The shares of resources in the total amount of generated electricity w.r.t. the reference (solid bars) and the grey (patterned bars) capacity expansion scenarios (own calculation & illustration)

Finally, the generated amount of electricity by power plants is further analyzed for the amount of emitted CO_2 as illustrated in Figure 136. In the period 2015-2023, the total amount of CO_2 emissions increases from 136 million ton to 222 million ton in the reference scenario and to 216 million ton in the grey scenario. Accordingly, the ambitious capacity expansion of imported hard coal fired plants reduces the level of CO_2 emissions about 3% relative to the reference scenario in the target year 2023. The reduction is due to the CO_2 emission factor of the imported hard coal fired power plants which is slightly less than that of lignite fired ones (see Table 63). In both scenarios, more than 90% of the CO_2 emissions are caused by the coal fired power plants. In particular, the highest share of CO_2 emissions in the total generated amount belongs to the lignite and the imported hard coal fired power plants in the reference and the grey scenarios respectively.

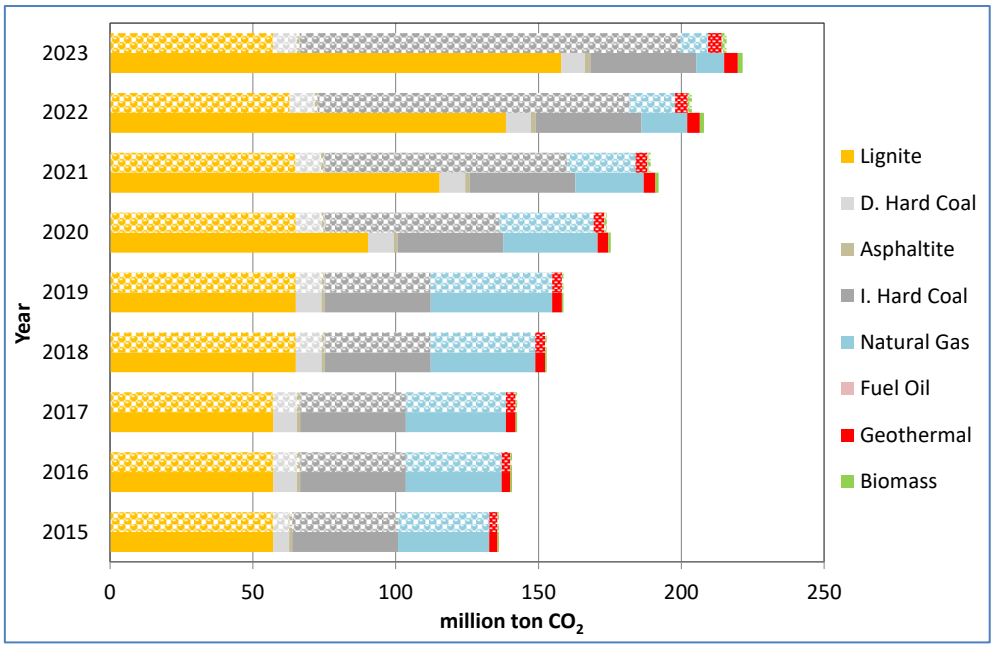

Figure 136- The CO_2 emissions of power plants w.r.t. the reference (solid bars) and the grey (patterned bars) capacity expansion scenarios (own calculation & illustration)

24.3 Reference vs. Blue Capacity Expansion Scenario

The technical analysis on the reference and the blue capacity expansion scenarios is conducted to compare the impact of more ambitious utilization of natural gas for generating electricity. In the blue scenario, 15735 MW_{el} more capacity of natural gas fired power plant is considered to be installed instead of installing lignite and asphaltite fired power plants as in the case of the reference scenario. Hence, the target capacity expansion for RETs is same in both scenarios (see Figure 133).

In Figure 137, the development of the amount of electricity generated by power plant types is illustrated w.r.t. the reference and the blue scenarios. In the period 2015-2019, the amount of electricity generated by lignite and asphaltite power plants increases from 55 TWh_{el} to 63 TWh_{el} in both scenarios. In the period 2020-2023, the corresponding amount increases to 150 TWh_{el} in the reference scenario; whereas it stays at 63 TWh_{el} level in the blue scenario. Further, the amount of electricity generated by natural gas fired power plants increases from 86 TWh_{el} to 115 TWh_{el} in the period 2015-2019 in both scenarios. In the period 2020-2023, the corresponding amount gradually decreases to 27 TWh_{el} in the reference scenario; whereas it varies in the range of 112-113 TWh_{el} in the blue scenario. Finally, the development of the amount of electricity generated by other power plants is same in both scenarios.

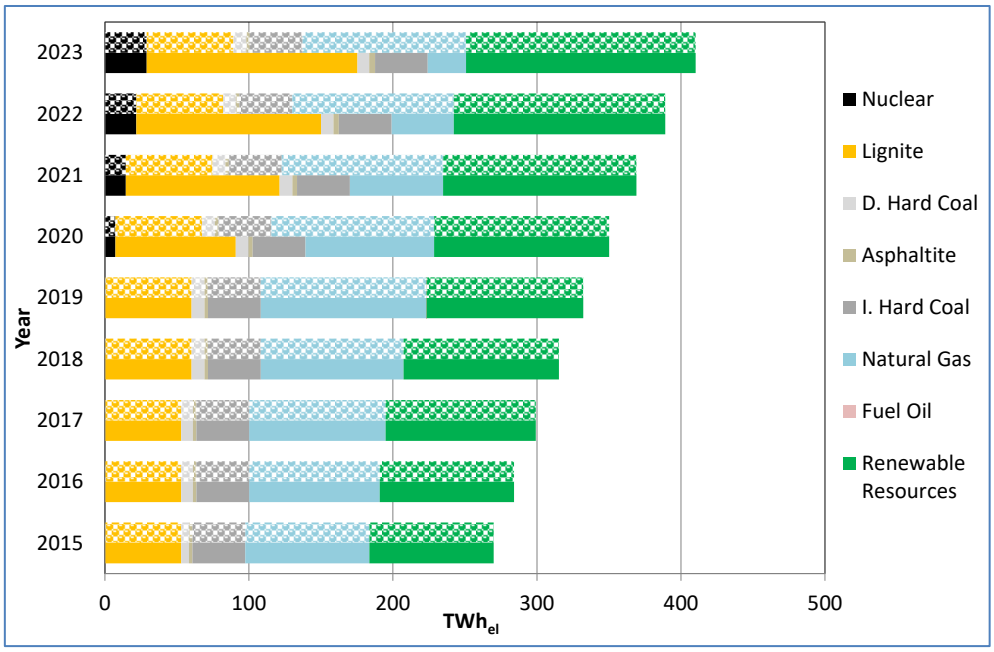

Figure 137- The amount of electricity generated by power plant types w.r.t. the reference (solid bars) and the blue (patterned bars) capacity expansion scenarios (own calculation & illustration)

The generated amount of electricity by power plants is further analyzed for their shares in the total amount of generated electricity as illustrated in Figure 138. In the period 2015-2023, the share of RETs in the total amount of generated electricity increases from 32% to 39% in both scenarios. Further, the share of domestic fossil fuel fired power plants in the total amount of generated electricity increases from 23% to 39% in the reference scenario; whereas it decreases from 23% to 17% in the blue scenario. Correspondingly, the share of electricity generation from domestic energy resources in the total amount of generated electricity increases from 55% to 78% in the reference scenario and to 56% in the blue scenario. Furthermore, the share of natural gas in the total generated amount of electricity decreases from 32% to 6% in the reference scenario and to 28% in the blue scenario. Accordingly, the set targets to increase the share of renewable resources and to reduce the share of natural gas are fulfilled by both scenarios. Finally, the share of other imported resources in the total amount of generated electricity increases from 14% to 16% in both scenarios.

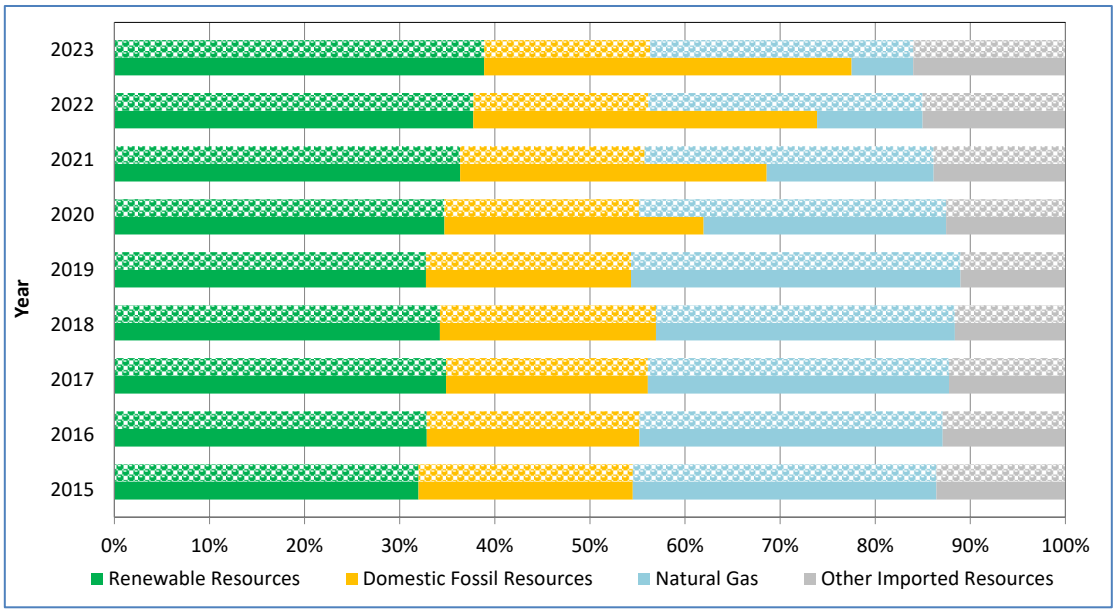

Figure 138- The shares of resources in the total amount of generated electricity w.r.t. the reference (solid bars) and the blue (patterned bars) capacity expansion scenarios (own calculation & illustration)

Finally, the generated amount of electricity by power plant types is analyzed for the amount of emitted CO_2 as illustrated in Figure 139. In the period 2015-2023, the total amount of CO_2 emissions increases from 136 million ton to 222 million ton in the reference scenario and to 161 million ton in the blue scenario. Accordingly, the more ambitious capacity expansion of natural gas fired power plants reduces the level of CO_2 emissions about 27% relative to the reference scenario in the target year 2023. The corresponding reduction is due to the lower CO_2 emission factor of natural gas relative to that of lignite and asphaltite (Table 63). Further, the coal fired power plants cause about 93% of the CO_2 emissions in the reference scenario and about 70% of it in the blue scenario in the year 2023. Finally, the natural gas fired power plants cause about 4% of the CO_2 emissions in the reference scenario and about 26% of it in the blue scenario in the year 2023.

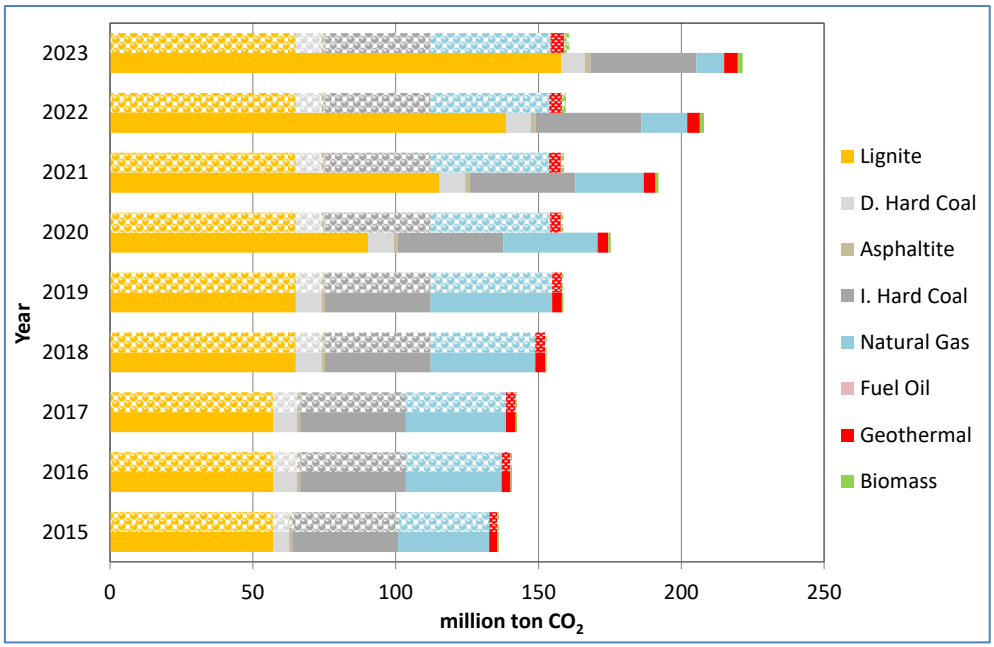

Figure 139- The CO_2 emissions of power plant types w.r.t. the reference (solid bars) and the blue (patterned bars) capacity expansion scenarios (own calculation & illustration)

24.4 Reference vs. Blue-Grey Capacity Expansion Scenario

The technical analysis on the reference and the blue-grey capacity expansion scenarios is conducted to compare the impact of more ambitious utilization of imported hard coal and natural gas for generating electricity. In the blue-grey scenario, 15735 MW_{el} more capacity of imported hard coal and 19865 MW_{el} more capacity of natural gas fired power plants are considered to be installed instead of installing domestic resource based power plants as in the case of the reference scenario.

In Figure 140, the development of the amount of electricity generated by RETs is illustrated w.r.t. the reference and the blue-grey scenario. In both scenarios, the total amount of electricity generated from RETs increases from 86 TWh_{el} to 109 TWh_{el} in the period 2015-2019. In the period 2020-2023, it increases to 159 TWh_{el} in the reference scenario; whereas it stays at 109 TWh_{el} level in the blue-grey scenario.

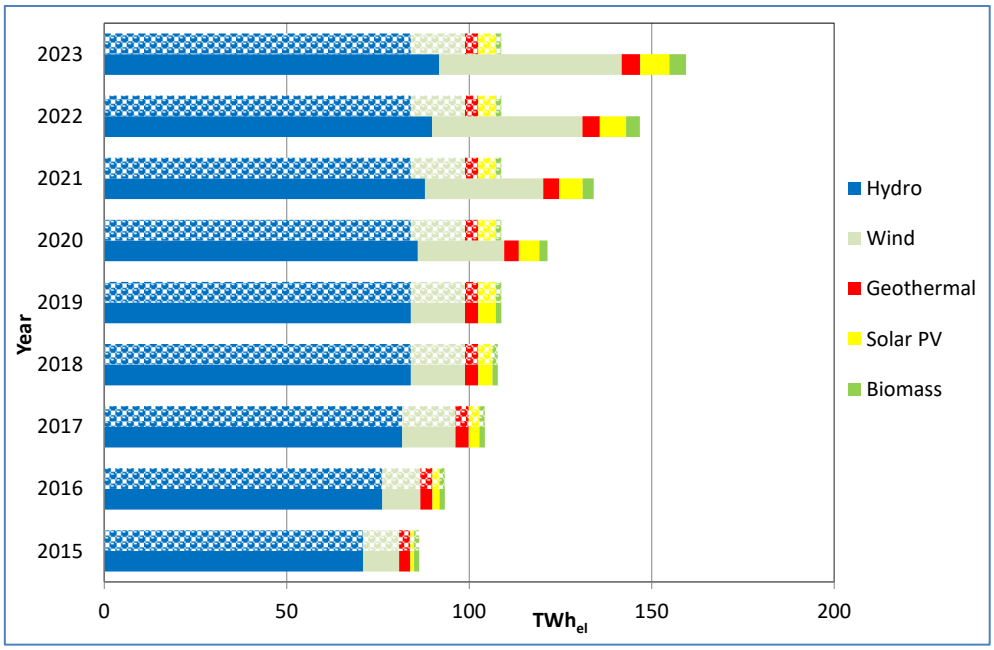

Figure 140- The amount of electricity generated by RETs w.r.t. the reference (solid bars) and the blue-grey (patterned bars) capacity expansion scenarios (own calculation & illustration)

In Figure 141, the development of the amount of electricity generated by power plant types is illustrated w.r.t. the reference and the blue-grey scenarios. In the period 2015-2019, the amount of electricity generated by domestic fossil fuel based power plants increases from 61 TWh_{el} to 72 TWh_{el} in both scenarios. In the period 2020-2023, the corresponding generation amount increases to 159 TWh_{el} in the reference scenario and gradually decreases to 71 TWh_{el} in the blue-grey scenario. The mentioned slight decrease in the blue-grey scenario is due to the fact that the imported hard coal fired power plants starts to displace lignite and domestic hard coal fired power plants with the increasing installed capacity of the former in the period 2020-2023; since the variable cost of electricity generation of the former type is lower than the latter types (see Table 62 and Table 67). Further, the amount of electricity generated by natural gas fired power plants increases from 86 TWh_{el} to 115 TWh_{el} in the period 2015-2019 in both scenarios. In the period 2020-2023, the corresponding generation amount decreases to 27 TWh_{el} in the reference scenario and to 70 TWh_{el} in the blue-grey scenario. The corresponding reduction in the reference scenario is higher than in the blue-grey scenario; since more capacities of lignite and asphaltite fired power plants, and RETs are installed in the reference scenario relative to the blue-grey scenario. Finally, the development of the amount of electricity generated by fuel oil fired power plants and the nuclear power plant is same in both scenarios.

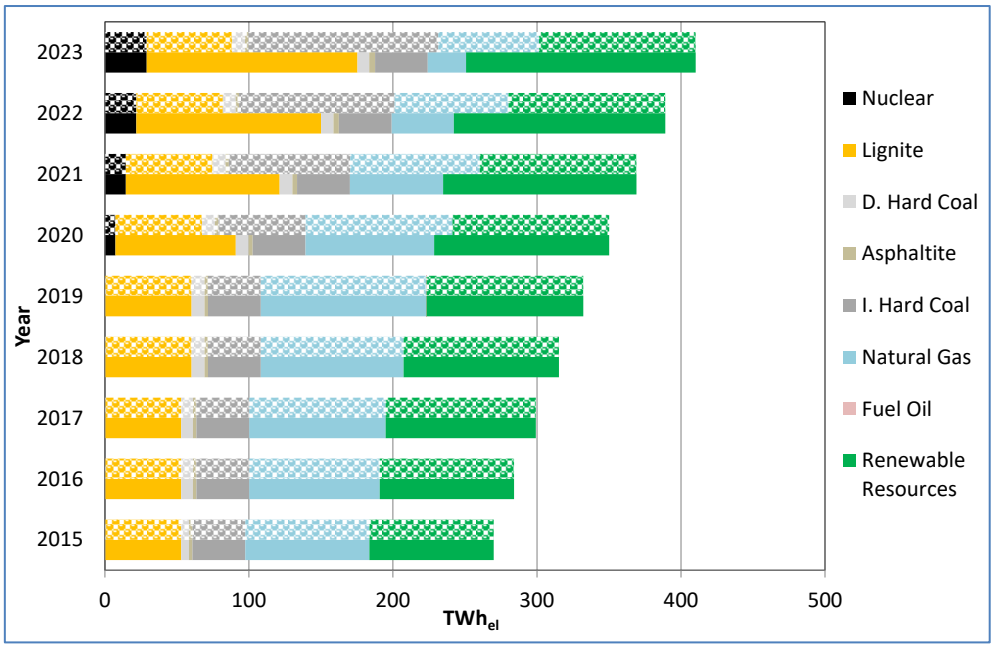

Figure 141- The amount of electricity generated by power plant types w.r.t. the reference (solid bars) and the blue-grey (patterned bars) capacity expansion scenarios (own calculation & illustration)

The generated amount of electricity by power plants is further analyzed for their shares in the total amount of generated electricity as illustrated in Figure 142. In the period 2015-2019, the share of RETs in the total amount of generated electricity is in the range of 32% to 33% in both scenarios. In the period 2020-2023, the corresponding share increases to 39% in the reference scenario; however it decreases to 27% in the blue-grey scenario. Further, the share of domestic fossil fuel fired power plants in the total amount of generated electricity increases from 23% to 39% in the reference scenario; whereas it decreases from 23% to 17% in the blue-grey scenario. Correspondingly, the share of electricity generation from domestic energy resources in the total amount of generated electricity increases from 55% to 78% in the reference scenario; whereas it decreases from 55% to 44% in the blue-grey scenario. Furthermore, the share of natural gas in the total generated amount of electricity decreases from 32% to 6% in the reference scenario and to 17% in the blue-grey scenario. Accordingly, the set targets to increase the share of renewable energy and to reduce the share of natural gas are fulfilled only by the reference scenario; since in the blue-grey scenario, the share of RETs in the total amount of generated electricity is under 30%. Finally, the share of other imported resources in the total amount of generated electricity increases from 14% to 16% in the reference scenario and to 39% in the blue-grey scenario.

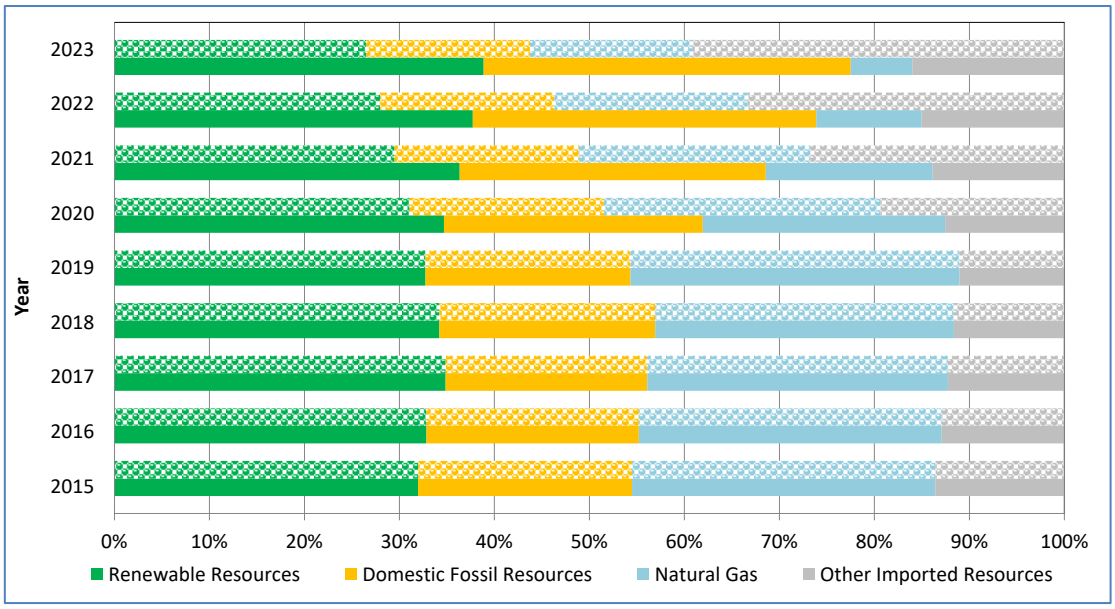

Figure 142- The shares of resources in the total amount of generated electricity w.r.t. the reference (solid bars) and the blue-grey (patterned bars) capacity expansion scenarios (own calculation & illustration)

Finally, the generated amount of electricity by power plants is analyzed for the amount of emitted CO_2 as illustrated in Figure 143. In the period 2015-2023, the total amount of CO_2 emissions increases from 136 million ton to 222 million ton in the reference scenario and to 237 million ton in the blue-grey scenario. Accordingly, the more ambitious capacity expansion of imported resource based power plants increases the level of CO_2 emissions about 7% relative to the reference scenario in the target year 2023. The corresponding increase is mainly due to the installation of imported resource based power plants instead of installing RETs. In both scenarios, more than 87% of the CO_2 emissions are caused by the coal fired power plants. In particular, the highest share of CO_2 emission in the total generated amount belongs to the lignite and the imported hard coal fired power plants in the reference and the grey scenarios respectively.

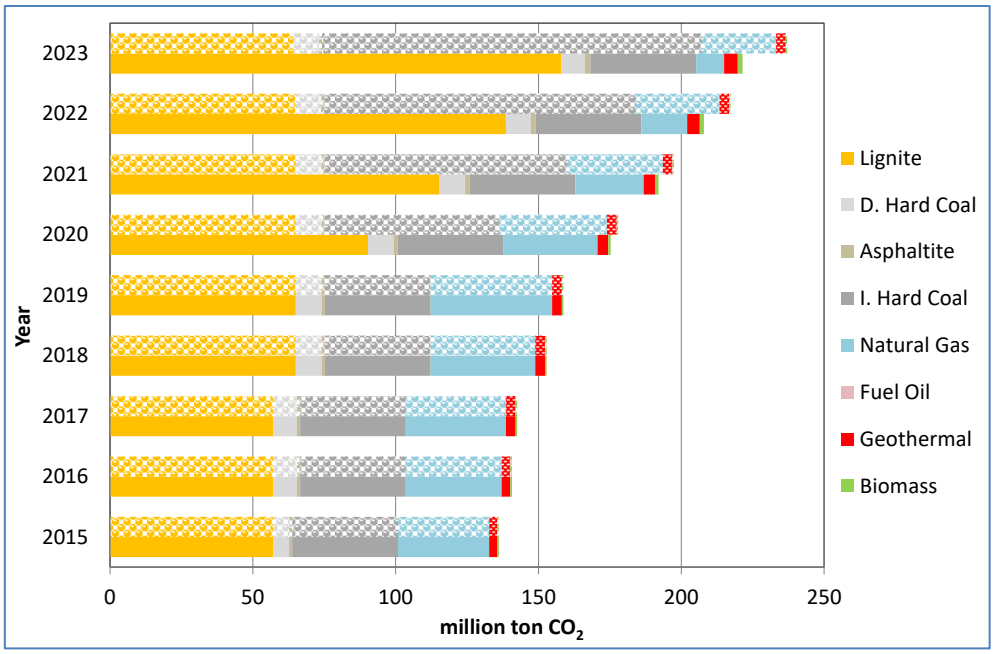

Figure 143- The CO_2 emissions of power plant types w.r.t. the reference (solid bars) and the blue-grey (patterned bars) capacity expansion scenarios (own calculation & illustration)

24.5 A Summary on the Technical Analyses

The main results of the technical analyses for the target year 2023 are tabulated in Table 69. The set target for the year 2023, which is to increase the share of renewable energy to at least 30% of the total electricity generation, is not fulfilled only by the blue-grey scenario (i.e. the imported fossil fuel based capacity expansion). On the other hand, the set target, which is to reduce that of natural gas to at most 30%, is fulfilled by all scenarios. Further, the capacity expansions based on the domestic and the imported hard coal types (i.e. reference and grey scenarios) lead to about the same level of natural gas dependency. Furthermore, the ambitious capacity expansion of RETs (i.e. green scenario) cannot lead to a level of reduction in the natural gas dependency which is as high as the reference scenario due to the low full load hours of operation of RETs. Finally, the green and the blue (i.e. natural gas based capacity expansion) scenarios lead to lower amounts of CO_2 emission in comparison to the other scenarios; whereas the blue-grey scenario indicates the highest amount of CO_2 emissions.

Table 69- The results of the technical assessments w.r.t. the capacity expansion scenarios (own calculation & illustration)

Results	Capacity Expansion Scenarios				
	Reference	Green	Grey	Blue	Blue-Grey
Renewable Share	39%	48%	39%	39%	27%
Natural Gas Share	6%	19%	6%	28%	17%
Domestic Resource Share	78%	65%	54%	56%	44%
CO_2 Emission (million ton)	222	152	216	161	237

25 Results of the Economic Analyses

In this chapter, the results of the techno-economic analyses, which involve the calculation of the total social cost of supplying electricity in the period 2015-2023, are represented for all constructed capacity expansion scenarios. In addition, the total social cost is calculated according to the low end and high end bandwidth of the external costs which are tabulated in Table 68 as Adjusted ExternE and Ecofys values respectively. Thus, the total social cost of each scenario is calculated twice depending on the mentioned low and high cases of specific external costs (i.e. solely varying factor for the same scenario). Finally, discussions are carried out about the tradeoff between the energy policy 2023 and the alternative capacity expansion scenarios in terms of capital, fuel and external costs of electricity generation.

The total social cost of supplying electricity is defined as the present value of annually incurred capital, fixed O&M, variable O&M, fuel, and external costs which are discounted to the year 2015. In particular, the total social cost of supplying electricity is comprised of incurred total capital, total fixed O&M, total variable O&M, total fuel and total external costs. The net social benefit of adopting energy policy 2023 is determined by calculating the difference in the total social cost of supplying electricity due to not adopting and adopting the energy policy 2023. Therefore, it is defined as the sum of total avoided fixed cost, total avoided variable cost and total avoided external cost.

25.1 Reference vs. Green Capacity Expansion Scenario

In this section, the net social benefit of adopting reference scenario is analyzed w.r.t. the green scenario based on the tradeoff between the domestic fossil fuels and the renewable energy resources in terms of capital, fuel and external costs of electricity generation. Namely, the green scenario focuses on presumably reducing both fuel and external costs at the expense of more capital costs in comparison to the reference scenario.

Result based on low specific external costs

In Figure 144, the total social cost of electricity supply w.r.t. the green and the reference scenario is illustrated. In the period 2015-2023, the total social cost of electricity supply amounts to around $202 billion w.r.t. the green scenario and $203.6 billion w.r.t. the reference scenario. Accordingly, the net social benefit of adopting reference scenario is estimated to be $-1.6 billion w.r.t. the green scenario. More specifically, the adoption of the reference

scenario is considered to be beneficial through avoiding $956 million of capital cost, $475 million of fixed O&M cost, $887 million of variable O&M cost, $1.6 billion of fuel cost (i.e. in total $3.9 billion); however it results in negative net social benefit due to incurring additional $5.5 billion of external costs w.r.t. the green scenario. Although it is assumed that the green scenario would lead to reducing both fuel and external costs at the expense of more capital costs, it is observed that it leads to incurring extra fuel costs by generating more electricity from natural gas fired power plants relative to the reference scenario (see section 24.1 for more information). Nevertheless, the mentioned savings due to adopting the reference is more than offset by the high amount of externalities-intensive electricity generation from lignite and asphaltite fired power plants in the reference scenario relative to the green scenario. Thus, the adoption of the reference scenario can lead to foregone savings due to not adopting the green scenario according to the case of low specific external costs.

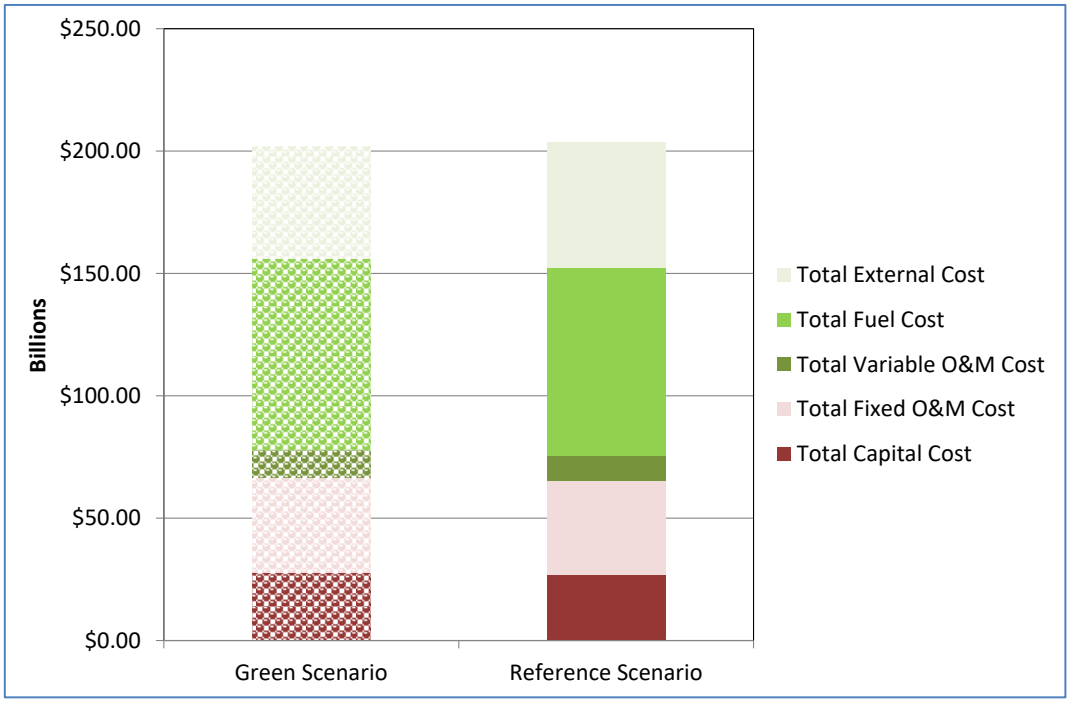

Figure 144- The breakdown of the total social cost of electricity supply (with low specific external costs) in the green (patterned bar) and the reference (solid bar) capacity expansion scenarios (own calculation & illustration)

Result based on high specific external costs

In Figure 145, the total social cost of electricity supply w.r.t. the green and the reference scenario is illustrated for the case of high specific external costs. The only difference between Figure 144 and Figure 145 is the magnitude of the incurred external costs. Accordingly, the total social cost of electricity supply amounts to around $311.1 billion w.r.t. the green scenario and $328.2 billion w.r.t. the reference scenario. Accordingly, the net social benefit of

adopting reference scenario is estimated to be $-17.1 billion w.r.t. the green scenario due to the amplified external costs of lignite and asphaltite fired power plants. Thus, the adoption of the reference scenario, also in this case, can lead to foregone savings due to not adopting the green scenario.

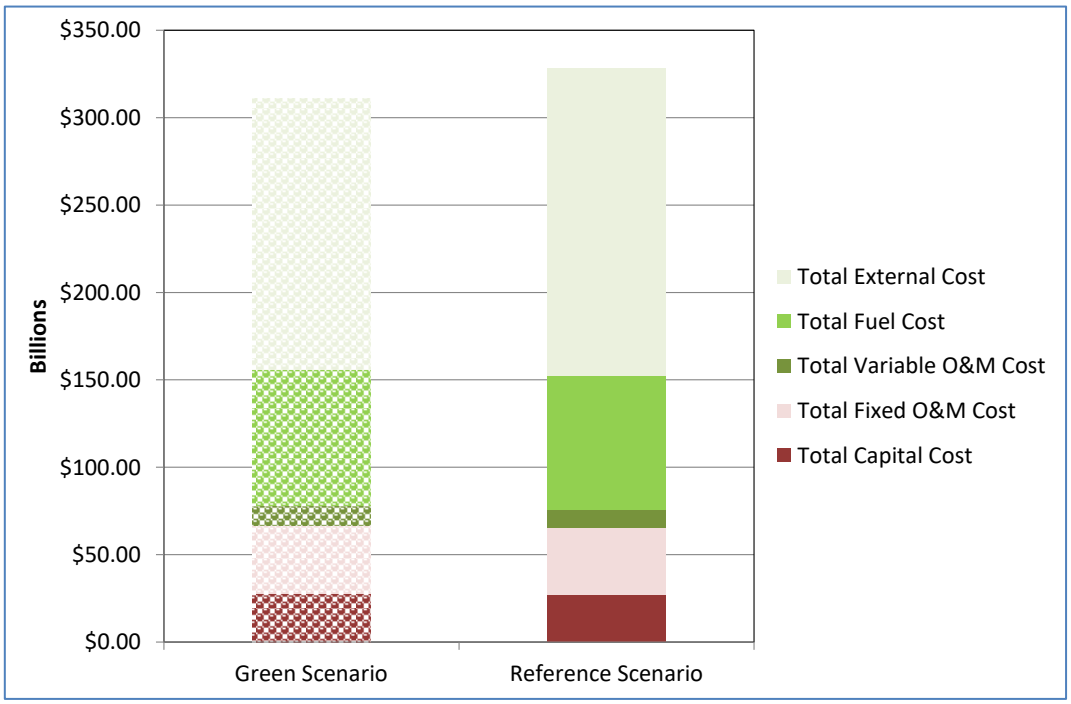

Figure 145- The breakdown of the total social cost of electricity supply (with high specific external costs) in the green (patterned bar) and the reference (solid bar) capacity expansion scenarios (own calculation & illustration)

25.2 Reference vs. Grey Capacity Expansion Scenario

In this section, the net social benefit of adopting reference scenario is analyzed w.r.t. the grey scenario based on the tradeoff between the domestic types of coal and the imported hard coal in terms of capital, fuel and external costs of electricity generation. Namely, the grey scenario focuses on utilizing imported hard coal with high calorific value at the expense of more fuel cost per ton in comparison to the reference scenario.

Result based on low specific external costs

In Figure 146, the total social cost of electricity supply w.r.t. the grey and the reference scenario is illustrated. In the period 2015-2023, the total social cost of electricity supply amounts to around $202.1 billion w.r.t. the grey scenario and $203.6 billion w.r.t. the reference scenario. Accordingly, the net social benefit of adopting reference scenario is estimated to be about $-1.5 billion w.r.t. the grey scenario. More specifically, the adoption of the reference scenario is considered to be beneficial through avoiding $871 million of fixed

O&M cost, $268 million of variable O&M cost (i.e. in total $1.1 billion); however it results in negative net social benefit due to incurring additional $0.8 billion of capital, $1.8 billion of fuel and $86 thousand of external costs[214] w.r.t. the grey scenario (i.e. in total $2.6 billion). Although the high calorific value imported hard is more expensive than per ton lignite, the capital and variable cost of electricity generation by utilizing the former type is lower than the latter type (see Table 62 for specific investment costs, Table 62 and Table 67 for variable costs). Nevertheless, the mentioned savings due to adopting the reference is more than offset by the high amount of capital, fuel and externalities-intensive electricity generation from lignite and asphaltite fired power plants in the reference scenario relative to the grey scenario. Thus, the adoption of the reference scenario can lead to foregone savings due to not adopting the grey scenario according to the case of low specific external costs.

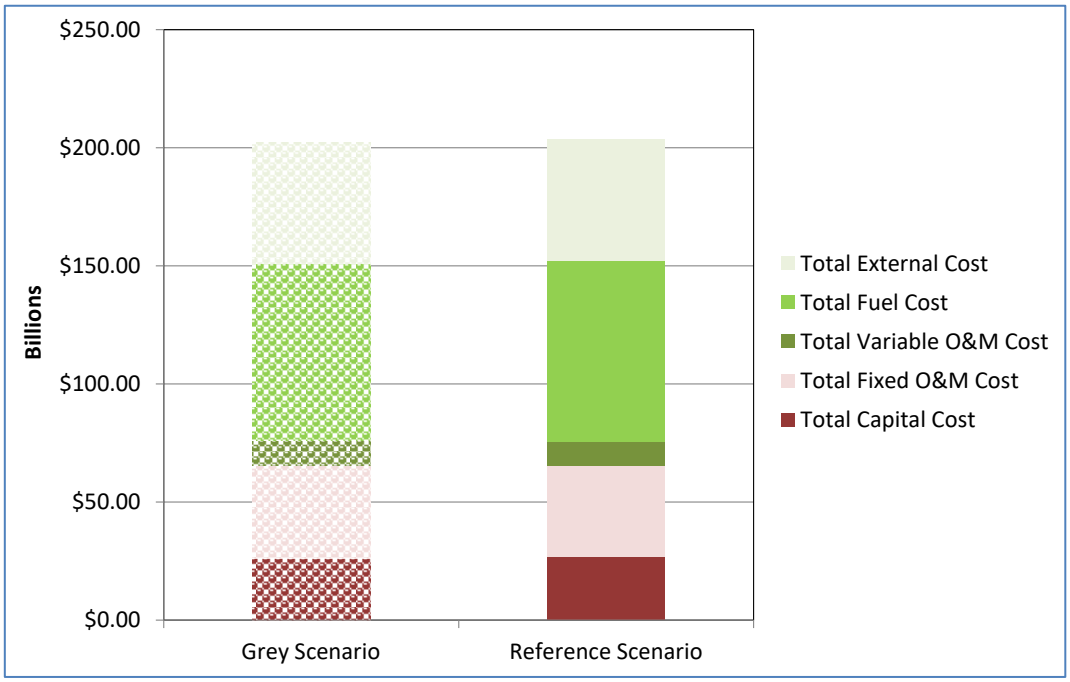

Figure 146- The breakdown of the total social cost of electricity supply (with low specific external costs) in the grey (patterned bar) and the reference (solid bar) capacity expansion scenarios (own calculation & illustration)

Result based on high specific external costs

In Figure 147, the total social cost of electricity supply w.r.t. the grey and the reference scenario is illustrated for the case of high specific external costs. The total social cost of electricity supply amounts to around $323.6 billion w.r.t. the grey scenario and $328.2 billion

[214] The observed lower external cost, in the grey scenario, originates through the slightly more amount of generated electricity from natural gas power plants due to the given capacity expansion path. Note that the specific external cost of lignite, asphaltite and hard coal are same in these calculations and are higher than the one for natural gas.

w.r.t. the reference scenario. Accordingly, the net social benefit of adopting reference scenario is estimated to be $-4.6 billion w.r.t. the grey scenario due to the amplified external costs of lignite and asphaltite fired power plants. Thus, the adoption of the reference scenario, also in this case, can lead to foregone savings due to not adopting the grey scenario.

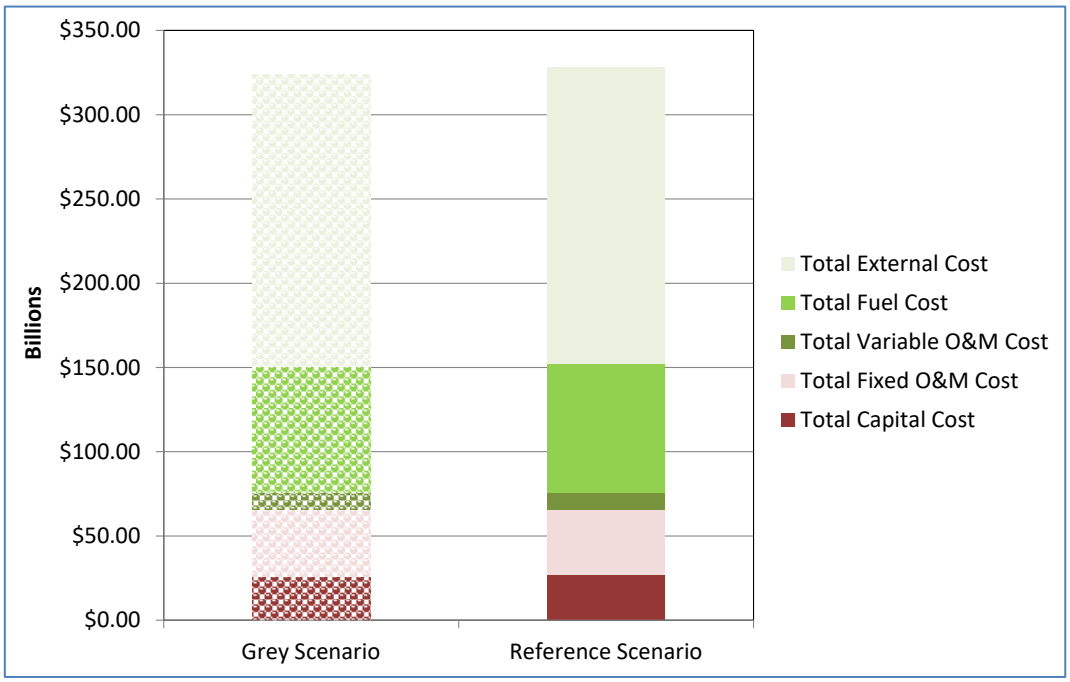

Figure 147- The breakdown of the total social cost of electricity supply (with high specific external costs) in the grey (patterned bar) and the reference (solid bar) capacity expansion scenarios (own calculation & illustration)

25.3 Reference vs. Blue Capacity Expansion Scenario

In this section, the net social benefit of adopting reference scenario is analyzed w.r.t. the blue scenario based on the tradeoff between the domestic types of coal and the natural gas in terms of capital, fuel and external costs of electricity generation. Namely, the blue scenario focuses on presumably reducing capital and external costs at the expense of more fuel costs.

Result based on low specific external costs

In Figure 148, the total social cost of electricity supply w.r.t. the blue and the reference scenario is illustrated. In the period 2015-2023, the total social cost of electricity supply amounts to around $203.8 billion w.r.t. the blue scenario and $203.6 billion w.r.t. the reference scenario. Accordingly, the net social benefit of adopting reference scenario is estimated to be $226 million w.r.t. the blue scenario. More specifically, the adoption of the reference scenario results in positive net social benefit by avoiding $591 million of fixed O&M, $120 million of variable O&M, $5.8 billion of fuel costs (i.e. in total $6.5 billion);

however it leads to incurring additional $1.6 billion of capital and $4.7 billion of external costs (i.e. in total $6.3 billion). Accordingly, the mentioned savings offset the high amount of capital and externalities-intensive electricity generation from lignite and asphaltite fired power plants in the reference scenario relative to the blue scenario. Thus, the adoption of the reference scenario can lead to gains in savings due to not adopting the blue scenario according to the case of low specific external costs.

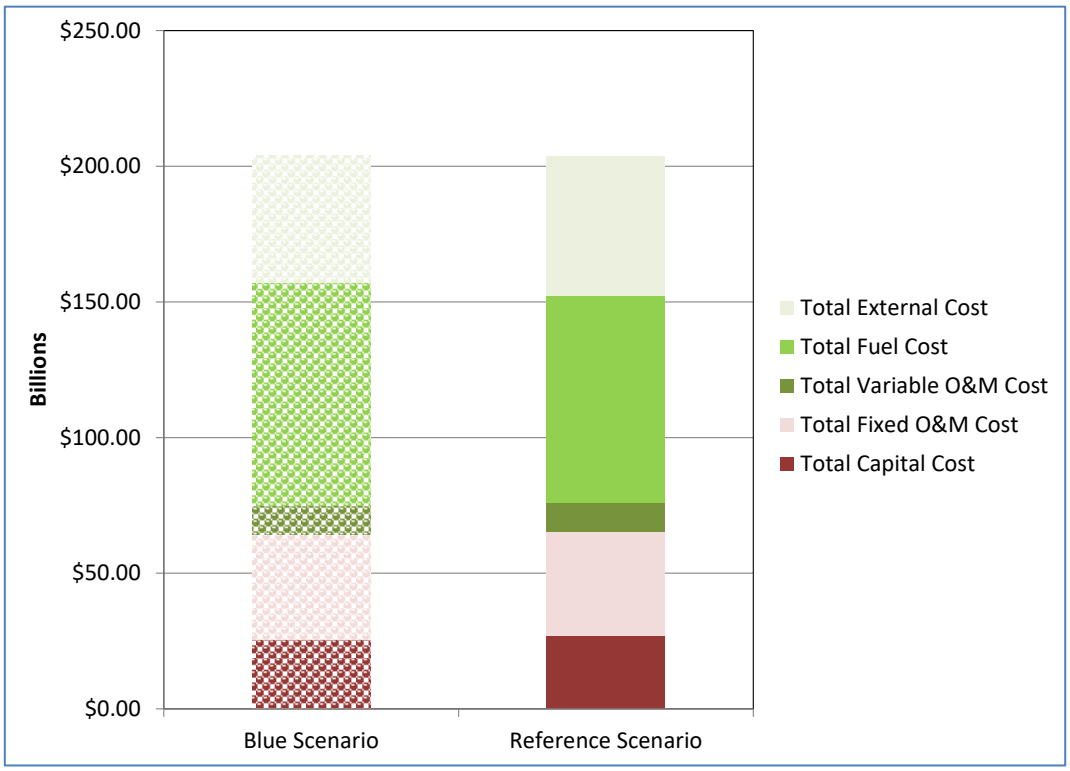

Figure 148- The breakdown of the total social cost of electricity supply (with low specific external costs) in the blue (patterned bar) and the reference (solid bar) capacity expansion scenarios (own calculation & illustration)

Result based on high specific external costs

In Figure 149, the total social cost of electricity supply w.r.t. the blue and the reference scenario is illustrated for the case of high specific external costs. The total social cost of electricity supply amounts to around $314.6 billion w.r.t. the blue scenario and $328.2 billion w.r.t. the reference scenario. Accordingly, the net social benefit of adopting reference scenario is estimated to be $-13.6 billion w.r.t. the blue scenario due to the amplified external costs of lignite and asphaltite fired power plants. Thus, the adoption of the reference scenario can lead to foregone savings due to not adopting the blue scenario.

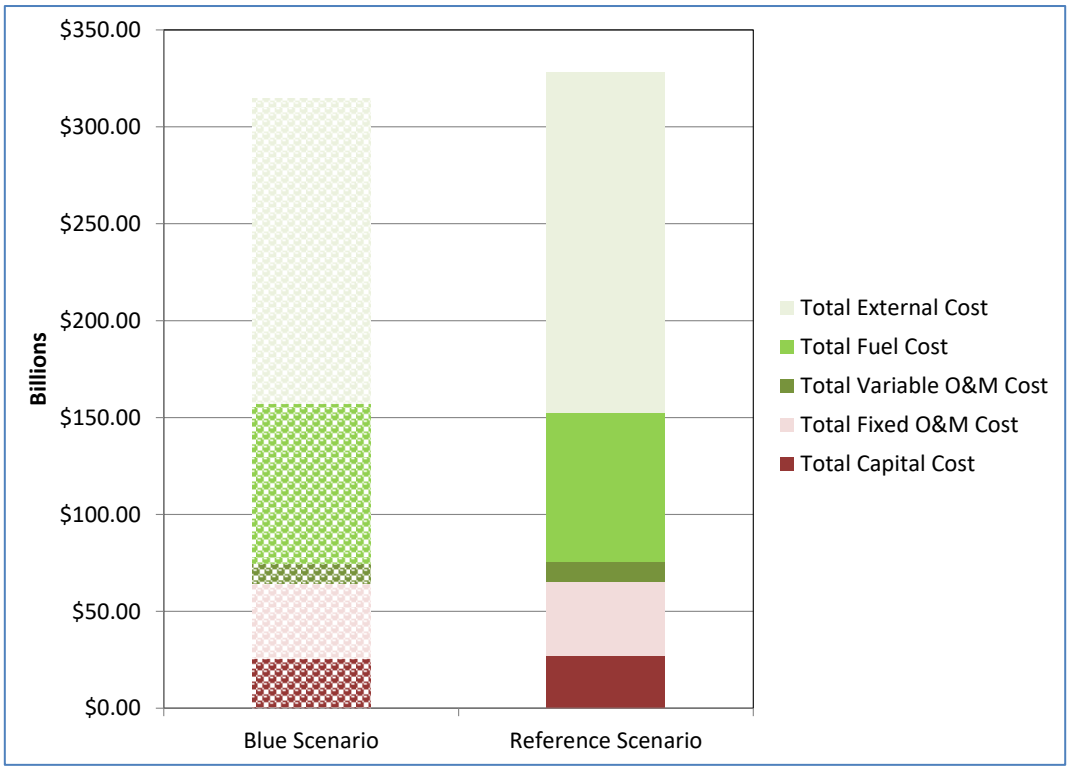

Figure 149- The breakdown of the total social cost of electricity supply (with high specific external costs) in the blue (patterned bar) and the reference (solid bar) capacity expansion scenarios (own calculation & illustration)

25.4 Reference vs. Blue-Grey Capacity Expansion Scenario

In this section, the net social benefit of adopting reference scenario is analyzed w.r.t. the blue-grey scenario based on the tradeoff between the domestic energy resources and the imported fossil fuels in terms of capital, fuel and external costs of electricity generation. The blue-grey scenario focuses on presumably reducing capital costs at the expense of more fuel and external costs for substituting the target capacity expansion of RETs in the reference scenario. In addition, it also focuses on utilizing imported hard coal with high calorific value at the expense of more fuel cost per ton for substituting the target capacity expansion of lignite and asphaltite fired power plants in the reference scenario.

Result based on low specific external costs

In Figure 150, the total social cost of electricity supply w.r.t. the blue-grey and the reference scenario is illustrated. In the period 2015-2023, the total social cost of electricity supply amounts to around $204.6 billion w.r.t. the blue-grey scenario and $203.6 billion w.r.t. the reference scenario. Accordingly, the net social benefit of adopting reference scenario is estimated to be $1 billion w.r.t. the blue-grey scenario. More specifically, the adoption of the reference scenario results in positive net social benefit by avoiding $0.5 billion of fixed

O&M, $4.6 billion of fuel and $1.5 billion external costs (i.e. in total $6.6 billion); however it leads to incurring additional $4.2 billion of capital and $1.4 billion variable O&M costs (i.e. in total $5.6 billion). Accordingly, the mentioned savings offset the high amount of capital-intensive electricity generation from lignite and asphaltite fired power plants in the reference scenario relative to the blue-grey scenario. Thus, the adoption of the reference scenario can lead to gains in savings due to not adopting the blue-grey scenario according to the case of low specific external costs.

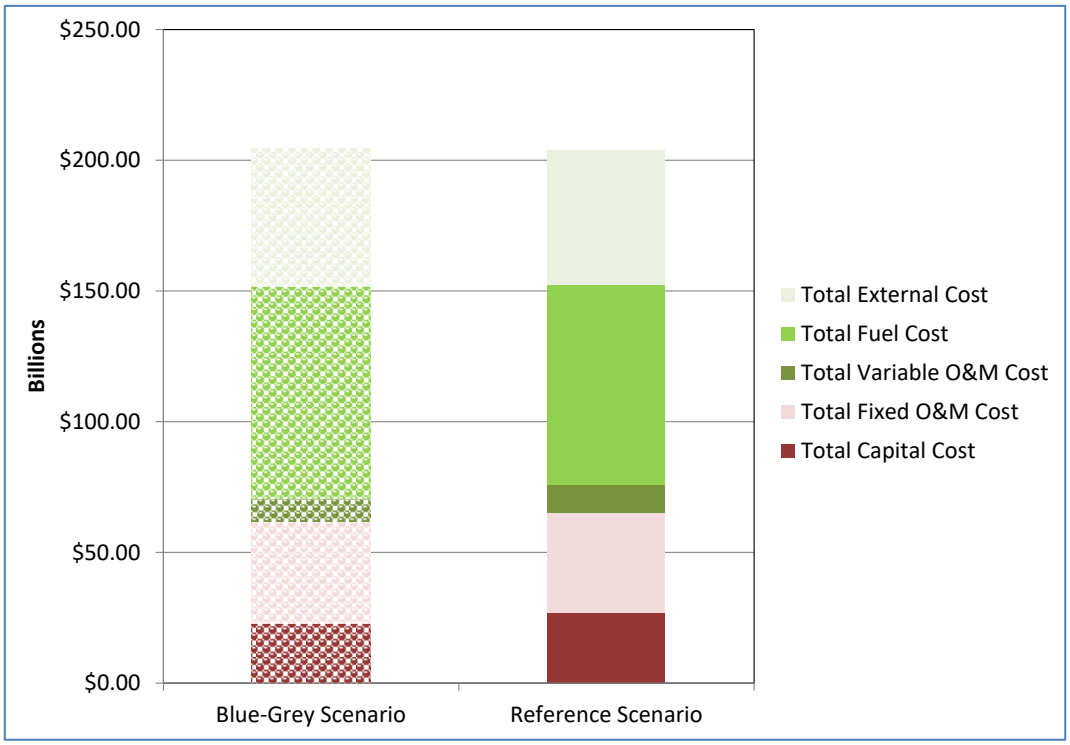

Figure 150- The breakdown of the total social cost of electricity supply (with low specific external costs) in the blue-grey (patterned bar) and the reference (solid bar) capacity expansion scenarios (own calculation & illustration)

Result based on high specific external costs

In Figure 149, the total social cost of electricity supply w.r.t. the blue-grey and the reference scenario is illustrated for the case of high specific external costs. The total social cost of electricity supply amounts to around $ 329.4 billion w.r.t. the blue-grey scenario and $328.2 billion w.r.t. the reference scenario. Accordingly, the net social benefit of adopting reference scenario is estimated to be $1.2 billion w.r.t. the blue-grey scenario due to the savings in fixed O&M, fuel and external costs. Thus, the adoption of the reference scenario, also in this case, can lead to gains in savings due to not adopting the blue-grey scenario.

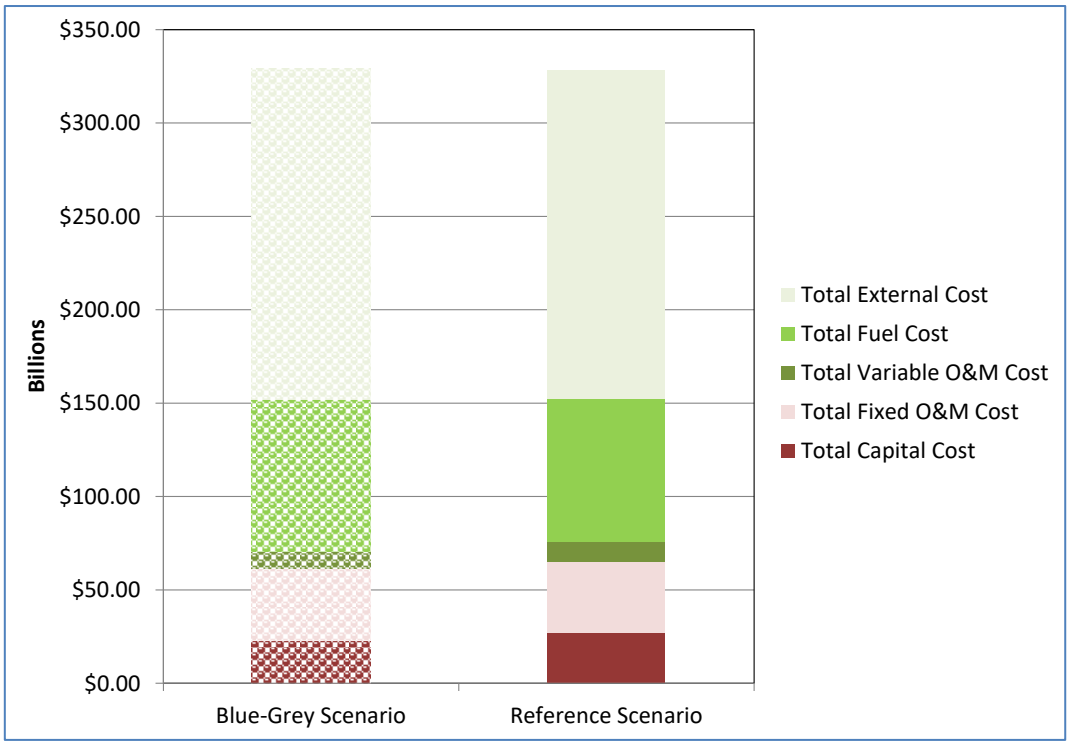

Figure 151- The breakdown of the total social cost of electricity supply (with high specific external costs) in the blue-grey (patterned bar) and the reference (solid bar) capacity expansion scenarios (own calculation & illustration)

25.5 A Summary on the Economic Analyses

The results of the net social benefit analysis of energy policy 2023 (i.e. reference scenario) w.r.t. the alternative capacity expansion scenarios are tabulated in Table 70.

Table 70- The net social benefit of the reference capacity expansion scenario w.r.t. the alternative ones (own calculation & illustration)

Net Benefit w.r.t. Specific External Costs [$ billion]	Capacity Expansion Scenarios			
	Green	Grey	Blue	Blue-Grey
Low Case	-1.6	-1.5	0.2	1
High Case	-17.1	-4.6	-13.6	1.2

The analysis of the reference scenario, which is carried out w.r.t. the green scenario for both low and high cases of specific external costs, indicates that the high amount of externalities-intensive electricity generation from the lignite and the asphaltite fired power plants offsets the savings in fixed and variable costs (see Table 71).

Further, the analysis of the reference scenario w.r.t. the grey scenario indicates that the high amount of capital, fuel and externalities-intensive electricity generation from the mentioned types of power plants offsets the savings in O&M costs (see Table 71). Note that in the low case, the electricity generation is mainly fuel cost intensive (negligible externalities-intensity),

whereas in the high case, it is primarily externalities-intensive and secondarily fuel cost intensive.

Furthermore, the analysis of the reference scenario, which is carried out w.r.t. the blue scenario for the low case of specific external costs, indicates that the savings in O&M and fuel costs offset the high amount of capital and the externalities-intensive electricity generation from the mentioned types of power plants (see Table 71). Most importantly, the resulting net social benefit is negligibly small in magnitude due to the indifference between the specific external costs for hard coal and lignite. In contrast, the same analysis, which is based on the high case of specific external costs, indicates negative net social benefit due to the amplified external costs of the mentioned type of power plants. Therefore, the given value to the environmental and the health impacts of electricity generation is the primary decisive aspect for the net social benefit of domestic types of coal w.r.t. natural gas.

Finally, the analysis of the reference scenario, which is carried out w.r.t. the blue-grey scenario for both low and high cases of specific external costs, indicates that the savings in fixed O&M, fuel and external costs offset the high amount of capital-intensive electricity generation from the mentioned types of power plants (see Table 71).

Table 71- The relative gains (+) and losses (-) for adopting reference scenario w.r.t. the alternative ones (own calculation & illustration)

The Breakdown of Net Social Benefit	Capacity Expansion Scenarios			
	Green	Grey	Blue	Blue-Grey
Capital Cost	+	-	-	-
Fixed O&M Cost	+	+	+	+
Variable O&M Cost	+	+	+	-
Fuel Cost	+	-	+	+
External Cost (Low Case)	-	-	-	+
External Cost (High Case)	-	-	-	+

To sum up, the greatest possible net benefit for the period 2015-2023 can be achieved by the capacity expansion of RETs alone according to the established method of cost-benefit analysis.

26 CONCLUSION OF THE DISSERTATION

The aim of this dissertation is to carry out analyses on the energy policy 2023 regarding the development of the investments in RETs and the net social benefit of the proposed capacity expansion targets for the power plant types. The novelty of this dissertation lies in the developed capacity expansion model, the conducted techno-economic assessments and the aforementioned studies on the investments in RETs, the future LDCs of Turkey and the improved screening curve approach; in order to analyze the energy policy 2023 according to the research objectives and questions. In Sections 26.1 and 26.2, the summaries of the conducted analyses and the obtained results are provided. In Section 26.3, a discussion is carried out on the obtained results and suggestions are made regarding the official targets for the year 2023. In Section 26.4, suggestions are made on the improvements for the limitations regarding the techno-economic analysis for the future works.

26.1 Summary of Methodologies and Analyses

In the first analysis, the development of the investments in RETs is anticipated considering the revenue streams from the FiT scheme and the electricity market, FLHs of operation and cost of capital. Accordingly, the level of FLHs of operation to trigger investment in RETs is quantified w.r.t. the different degrees of flexibilities and discount rates. The results of the analyses are compared with the resource potential related to the FLHs of RETs in Turkey; in order to discuss whether the capacity expansion targets are reachable or not. The novelty of this analysis lies in the application of the NPV and the real option methods to quantify threshold FLHs for the RET investments in Turkey.

In the second analysis, the net social benefit of the energy policy 2023 is appraised by developing a capacity expansion model. The capacity expansion model is developed as a means of quantitative thinking to support appraisal of the energy policy 2023 on well-informed basis and the utilized methods for its development are selected based on the tradeoff between the benefit and the effort in significant contribution to the decision support. The capacity expansion model submits the results of the social cost-benefit analysis by carrying out techno-economic analyses on the given inputs. The inputs related to the technical and the cost parameters of the power plants, the fuel price forecasts and the specific external costs for low and high cases are obtained from official publications and previous studies; whereas the approximations to future LDCs of Turkey and the capacity expansion scenarios are developed

during the course of this dissertation. The novelty of obtaining approximations to future LDCs of Turkey lies in the developed concept and the performed analysis during the course of the approximation analyses.

The constructed scenarios encompass the long-term capacity expansion plans for the period 2015-2023 which is based on the research questions. In the period 2015-2019, the development of the installed capacities of the power plant types is considered to be same for all scenarios according to the given information by TEIAS; whereas all capacity expansion scenarios differ from each other in the period 2020-2023 depending on the proposed targets for the year 2023. Namely, in the reference scenario (i.e. the energy policy 2023), 15735 MW_{el} more capacity of domestic fossil fuel fired power plant and 19865 MW_{el} more capacity of RETs are targeted to be installed in the period 2020-2023 w.r.t. the year 2019. For the green, the grey and the blue scenarios, 15735 MW_{el} more capacity of RETs, imported hard coal and natural gas fired power plants are respectively considered to be installed instead of installing lignite and asphaltite fired power plants as in the case of the reference scenario. With regard to the blue-grey scenario, 15735 MW_{el} more capacity of imported hard coal and 19865 MW_{el} more capacity of natural gas fired power plants are considered to be installed instead of installing domestic resource based power plants as in the case of the reference scenario. In addition, all considered scenarios are assessed for their reliability of supplying electricity by calculating firm reserve margins as a ratio of the total firm capacity to the peak demand.

The capacity expansion scenarios are constructed based on the tradeoff analyses between the reference and the alternative capacity expansion scenarios in terms of capital, fuel and external costs of electricity generation. Namely, the green scenario focuses on presumably reducing both fuel and external costs at the expense of more capital costs in comparison to the reference scenario. Further, the grey scenario focuses on utilizing high calorific value imported hard coal at the expense of more fuel cost per ton in comparison to the reference scenario. Furthermore, the blue scenario focuses on presumably reducing capital and external costs at the expense of more fuel costs in comparison to the reference scenario. Finally, the blue-grey scenario focuses on presumably reducing capital costs at the expense of more fuel and external costs for substituting the target capacity expansion of RETs with natural gas fired power plants. In addition, it also focuses on utilizing imported hard coal with high calorific value at the expense of more fuel cost per ton for substituting the target capacity expansion of lignite and asphaltite fired power plants in the reference scenario.

The techno-economic analysis consists of the technical and the economic assessments of the reference capacity expansion scenario w.r.t. the alternative ones for the period 2015-2023. In particular, the former analysis involves the calculation of the amount of electricity generated by all types of power plants and CO_2 emissions caused by thermal, geothermal and biomass power plants. Further, the latter analysis involves the calculation of the social cost of supplying electricity in each year of the mentioned period. Furthermore, the economic analyses, which are conducted to value the net social benefit of the energy policy 2023, are based on the short-run competitive equilibrium. More specifically, it is assumed that the mentioned equilibrium provides the least cost supply of electricity in the period 2015-2023 for all considered scenarios. Moreover, the corresponding calculations are based on the improved screening curve method regarding existing power plants. Finally, the novelty of that method lies in its efficient and straightforward geometrical solution process to evaluate a static capacity expansion problem considering both existing and candidate power plants in comparison to the previous works for the similar type of improvements.

The benefit of adopting energy policy 2023 is measured relative to the savings which would have been foregone/gained by utilizing the scarce resources in an alternative capacity expansion scenario. In particular, the social cost-benefit analysis on the energy policy 2023 is conducted as a partial equilibrium analysis, is based on the "with-and-without" approach and the established method of cost-benefit analysis.

The net social benefit of adopting energy policy 2023 is analyzed by calculating the difference in the total social cost of supplying electricity in the period 2015-2023 due to not adopting and adopting the energy policy 2023. Further, the total social cost of supplying electricity is defined to be the present value of annually incurred social costs which are discounted to the year 2015. If the total social cost of supplying electricity arising from the latter case is less than the former case, then the adoption of the energy policy 2023 is appraised to be indicating a positive net social benefit. By the same token, if it is vice versa, a negative net social benefit is indicated due to adopting the energy policy 2023. Furthermore, the social cost of supplying electricity is comprised of fixed, variable and external costs. The fixed costs encompass capital and fixed O&M costs. The variable costs encompass fuel and variable O&M costs. Finally, the net social benefit of adopting energy policy indicates the present value of avoided costs (i.e. savings) for capital, fixed O&M, variable O&M, fuel and externalities which are discounted to the year 2015.

26.2 Summary of Results

The analyses on the development of the investments in RETs indicate that the targets for biomass, solar PV and geothermal power plants are anticipated to be reachable under the given assumptions (i.e. including the status quo of the regulations); whereas the achievement of the targets for hydropower and wind power plants are considered to be dependent on the decision of the Turkish government whether the corresponding FiT rates should be increased. Note that the Turkish government has declared that the rates in FiT scheme can be raised; in order to reach the RET capacity expansion targets for the year 2023.

The set target for the year 2023, which is to increase the share of renewable energy to at least 30% of the total electricity generation, is not fulfilled only by the blue-grey scenario. On the other hand, the set target, which is to reduce that of natural gas to at most 30% of the total electricity generation, is fulfilled by all scenarios. In addition, the firm reserve margin calculations indicate that the adequate supply of electricity can be achieved according to the capacity expansion of power plants in all mentioned scenarios.

Further, the ambitious capacity expansion, which is based on the renewable resources in the place of the domestic fossil fuels (i.e. green scenario), cannot lead to a higher level of reduction in the natural gas dependency due to their low FLHs of operation. It leads to incurring extra fuel costs by generating more electricity from natural gas fired power plants; since the fuel cost per unit of generated electricity from natural gas is more expensive than the one from domestic types of coal. Nevertheless, the officially targeted capacity expansion based on the domestic types of coal can lead to foregone savings due to not relying on renewable resources for electricity generation. More specifically, the capacity expansion based on the domestic types of coal is analyzed to be externalities-intensive relative to that based on renewable resources. The greatest possible net benefit for the period 2015-2023 can be achieved in the green scenario among others according to the established method of cost-benefit analysis.

Furthermore, the capacity expansions based on the domestic and imported hard coal (i.e. reference and grey scenarios respectively) lead to about the same level of natural gas dependency. Although the level of natural gas dependency is same in both cases, the officially targeted capacity expansion based on the domestic types of coal can lead to foregone savings due to not relying on imported hard coal for electricity generation. In particular, the

generation of electricity from domestic types of coal is analyzed to be capital, fuel and externalities-intensive relative to that from imported hard coal.

Moreover, the analysis on the net social benefit of domestic coal types w.r.t. natural gas (i.e. blue scenario) indicates that the given value to the environmental and the health impacts of electricity generation is the primary decisive aspect. In particular, a positive net social benefit, which is negligibly small in magnitude, can result due to the indifference between the specific external costs of electricity generation from imported hard coal and lignite. In contrast, a negative social benefit can result due to the higher valuation of the specific external cost of electricity generation from lignite.

Finally, the ambitious capacity expansions based on the renewable energy resources and the natural gas lead to lower amounts of CO_2 emission in comparison to the other scenarios. In contrast, the imported fossil fuel based capacity expansion (i.e. blue-grey scenario) causes the highest amount of CO_2 emission. Last but not least, the officially targeted capacity expansion based on domestic types of coal can not only lead to gains in savings but also to reduction in CO_2 emissions relative to that solely based on imported fossil fuels. More specifically, the savings mainly in fuel and in external costs can offset the high amount of capital-intensive electricity generation from domestic energy resources in the reference scenario relative to that from imported fossil fuels in the blue-grey scenario.

26.3 Discussion on Results

The social cost-benefit analysis of the energy policy 2023 indicates that the targeted capacity expansion of RETs is more beneficial than that of fossil fuel fired power plants. The corresponding comprehensive result is similar to the assessment in NREAP which is limited in scope to the analysis of the impacts of substituting combined cycled gas power plants by RETs. In contrast, the targeted capacity expansion based on domestic coal types are less beneficial than that of imported hard coal and can also be less beneficial than that of natural gas through attaching more value to the health and environmental concerns. Most importantly, the capacity expansion plans, which are based on RETs or imported hard coal in the place of domestic coal types, can provide more benefits to the society by alleviating the natural gas dependency and improving energy policy 2023. On the contrary, the capacity expansion solely dependent on imported energy resources can be the least beneficial alternative for the society.

The ambitious capacity expansion of RETs w.r.t. the energy policy 2023 can lead to more savings in external costs and in the amount of CO_2 emissions at the major expenses of incurring extra capital and extra fuel costs. The extra fuel cost originates from generating more electricity from natural gas fired power plants. Although the increase in electricity generation from natural gas may seem as an increase in imported resource dependency, its share in the total amount of electricity stays under 30% in the target year 2023 and the increase in electricity generation from it solely depends on the increase in the amount of utilized existing capacity of the corresponding power plant type in the period 2020-2023.

The ambitious capacity expansion based on imported hard coal can lead to savings in capital, fuel and external costs relative to that based on domestic types of coal. This is due to the fact that the Turkish lignite resources are low quality coal and has more negative impacts on the environment in comparison to the imported hard coal. In addition, the Turkish government should consider solely relying on imported hard coal rather than forming an energy mix from lignite and imported hard coal. If an energy mix from lignite and imported hard coal were to be proposed, the imported hard coal fired power plants could displace the lignite fired ones as the installed capacity of RETs increases in the period 2020-2023. In that case, the displacement of the lignite fired power plants would mainly induce foregone savings in capital costs.

In conclusion, the Turkish government should review the granted subsidizations to promote investments in RETs and should consider solely relying on the capacity expansion of RETs to achieve the greatest possible net benefit for the period 2015-2023 according to the established method of cost-benefit analysis. The ambitious capacity expansion of RETs cannot endanger the supply reliability of electricity due to the planned capacity expansion of transmission grids and having enough natural gas fired and hydropower plant capacities to backup the intermittent power generation. After this period, Turkey should rely on an energy mix of renewable and fossil fuel resources for the capacity expansion; since the increasing penetration of RETs will require backup capacity for the reliable supply of electricity. The analyses of this study do not provide comprehensive information about the energy policies, global energy market conditions and the magnitude of the externalities of the fossil fuels in the next periods; however the trends of the costs indicate for the future that the imported fossil fuels can be a more beneficial alternative than the domestic fossil fuels. More specifically, it can be deduced from the analyses that the benefits of the domestic fossil fuels are less in comparison to the imported hard coal; whereas their benefits in comparison to the natural gas

are mainly dependent on the tradeoff between the fuel and the external costs. Therefore, the selection of the imported resource type primarily depends on the future energy policies, and on the tradeoff between the fuel and the external costs. If the government adopts the same strategies in the energy policy 2023 for the next periods, imported hard coal can be considered as more beneficial than natural gas; whereas if the government is to be more concerned about the environmental and the health impacts of electricity generation, natural gas can be considered as more beneficial than imported hard coal.

26.4 Suggestions for Future Studies

In this study, the social cost-benefit of energy policy 2023 is measured w.r.t. the alternative scenarios. For future research, an optimal energy mix for the target year 2023 can be proposed by minimizing the total supply cost of electricity. Further, the analysis based on the partial equilibrium can be extended to general equilibrium analysis to consider not only the negative externalities but also the positive externalities related to the supply of electricity. In particular, the increasing productivity of the Turkish electricity sector can lead to positive externalities due to creation of new jobs, reallocation of economic resources and savings in foreign exchanges by reducing imported resource dependency, increasing tax income of the government, etc. Finally, the specific external costs of electricity generation, which are characteristic to Turkey, can be approximated.

BIBLIOGRAPHY

Akkuyu NGS AS. (2013). Akkuyu Nuclear Power Plant-Progress To-date and The Way Forward. Retrieved February 24, 2016, from https://www.iaea.org/NuclearPower/Downloadable/Meetings/2013/2013-02-11-02-14-TM-INIG/20.smirnov.pdf

Aksoy, N. (2014). Power Generation from Geothermal Resources in Turkey. *Renewable Energy, 68*, 595-601.

Alizamir, S., de Véricourt, F., & Sun, P. (2016). Efficient Feed-In-Tariff Policies for Renewable Energy Technologies. *Operations Research, 64*(1), 52-66.

Anderson, D. (1972). Models for Determining Least-Cost Investments in Electricity Supply. *The Bell Journal of Economics and Management Science, 3*(1), 267-299.

Anh, L. N., & Bhattacharyya, S. C. (2011). Integration of Wind Power into the British System in 2020. *Energy*, *36*(10), 5975–5983.

Ari, I., & Koksal, M. A. (2011). Carbon Dioxide Emission from The Turkish Electricity Sector and Its Mitigation Options. *Energy Policy, 39*, 6120–6135.

Atiyas, I., Çetin, T., & Gülen, G. (2012). *Reforming Turkish Energy Markets: Political Economy, Regulation and Competition in the Search for Energy Policy.* New York: Springer Science+Business Media.

Bagdadioglu, N., & Odyakmaz, N. (2009). Turkish electricity reform. *Utilities Policy, 17*, 144–152.

Balat, H. (2008). Contribution of Green Energy Sources to Electrical Power Production of Turkey: A review. *Renewable and Sustainable Energy Reviews, 12*, 1652–1666.

Baldick, R., Park, H., & Lee, D. (2011). Augmented screening curve analysis of thermal generation capacity additions with increased renewables, ancillary services, and carbon prices. (pp. 1-54). Texas: IEEE. Retrieved November 14, 2013, from http://ewh.ieee.org/r10/queensland/v2/lib/exe/fetch.php/chapters:pes:ross_presentation.pdf

Bates, D. M., & Watts, D. G. (1988). *Nonlinear Regression Analysis and Its Applications.* New York: John Wiley & Sohns, Inc.

Batlle, C., & Rodilla, P. (2013). An Enhanced Screening Curves Method for Considering Thermal Cycling Operation Costs in Generation Expansion Planning. *IEEE Transactions on Power Systems, 28*(4), 3683-3691. doi:10.1109/TPWRS.2013.2249540

Bjerksund, P., & Ekern, S. (1990). Managing Investment Opportunities under Price Uncertainty: From "Last Chance" to "Wait and See" Strategies. *Financial Management, 19*(3), 65-83.

Bøckman, T., Fleten, S.-E., Juliussen, E., Langhammer, H., & Revdal, I. (2008). Investment Timing and Optimal Capacity Choice for Small Hydropower Projects. *European Journal of Operational Research, 190*(1), 255–267.

Boomsma, T. K., Meade, N., & Fleten, S.-E. (2012). Renewable Energy Investments under Different Support Schemes: A Real Options Approach. *European Journal of Operational Research*, 225–237.

Borison, A., & Morris, P. (1984). An Efficient Approach to the Optimal Static Geneeration Mix Problem. *IEEE Transactions on Power Apparatus and Systems, PAS-103*(3), 576-580.

Box, G. E., & Jenkins, G. M. (1976). *Time Series Analysis: forecasting and control* (rev. ed.). California: Holden-Day Inc.

Box, G. E., Jenkins, G. M., & Reinsel, G. C. (2008). *Time Series Analysis: Forecasting and Control* (4th ed.). New Jersey: John Wiley & Sons, Inc.

Bradley, R. A., & Srivastava, S. S. (1979). Correlation in Polynomial Regression. *The American Statistician, 33*(1), 11-14.

British Petroleum. (2015, December 11). *Statistical Review 2015.* Retrieved from http://www.bp.com/en/global/corporate/energy-economics/statistical-review-of-world-energy/downloads.html

Brockwell, P. J., & Davis, R. A. (2006). *Time Series: Theory and Methods* (2nd ed.). New York: Springer Science +Business Media, LLC.

Caliskan, M. (2011). *The Wind Energy Potential of Turkey.* Retrieved December 11, 2015, from Directorate General of Meteorology: http://www.tucsa.org/images/yayinlar/sunumlar/mustafa-caliskan.pdf

Chandra, V. (2006). *Fundamentals of Natural Gas: An International Perspective.* Oklahoma: PennWell Corporation.

Colak, I., Bayindir, R., Fulli, G., Tekin, I., Demirtas, K., & Covrig, C.-F. (2014). Smart grid opportunities and applications in Turkey. *Renewable and Sustainable Energy Reviews, 33*, 344-352.

Conejo, A. J., Perez-Arriaga Ignacio J., R. A., & Santamaria, A. (1985). Evaluation of the Impact of Solar Thermal Generation on the Reliability and Economics of an Electrical Utility System. *Proceedings of the Mediterranean Electrotechnical Conference '85: Solar Energy* (pp. 167-173). Madrid: IEEE. Retrieved 11 6, 2013, from http://www.iit.upcomillas.es/aramos/papers/ImpactSolarThermalGeneration.pdf

Connolly, D., Lund, H., Mathiesen, B. V., & Leahy, M. (2010). A review of computer tools for analysing the integration of renewable energy into various energy systems. *Applied Energy, 87*(4), 1059–1082. doi:10.1016/j.apenergy.2009.09.026

Cryer, J. D., & Chan, K.-S. (2008). *Time Series Analysis: With Applications in R* (2nd ed.). New York: Springer Science+Business Media, LLC.

De Jonghe, C., Delarue, E., Belmans, R., & D'haeseleer, W. (2011). Determining optimal electricity technology mix with high level of wind power penetration. *Applied Energy, 88*(6), 2231–2238. doi:10.1016/j.apenergy.2010.12.046

Dilaver, Z., & Hunt, L. C. (2011). Turkish Aggregate Electricity Demand: An Outlook to 2020. *Energy, 36,* 6686-6696.

Directorate General of Mineral Research and Exploration. (2015). *Annual Report 2014.* Retrieved December 12, 2015, from http://www.mta.gov.tr/v2.0/tek_dosyalar/MTA_2014_Faaliyet_Raporu.pdf

Directorate General of Petroleum Affairs. (2015). *Exploration and Production Activities in 2014.* Retrieved December 11, 2015, from http://www.pigm.gov.tr/images/pdf/2015/Exploration-and-Production-Activities-in-2014.pdf

Directorate General of Renewable Energy . (2015, December 12). *Solar Energy Atlas of Turkey.* Retrieved from http://www.eie.gov.tr/MyCalculator/Default.aspx

Directorate General of Renewable Energy. (2015). *Geothermal Energy in Turkey.* Retrieved December 12, 2015, from http://www.eie.gov.tr/yenilenebilir/turkiyede_jeo.aspx

Directorate General of Renewable Energy. (2015, December 12). *Hydropower Potential of Turkey.* Retrieved from http://www.eie.gov.tr/yenilenebilir/h_turkiye_potansiyel.aspx

Directorate General of Renewable Energy. (2016, January 18). *Lower Heating Value of Energy Resources.* Retrieved from http://www.eie.gov.tr/duyurular_haberler/document/SENVER_15_Usul_ve_Esaslar_Ek2.pdf

Dixit, A. (1992). Investment and Hysteresis. *The Journal of Economic Perspectives, 6*(1), 107-132.

Dixit, A. K., & Pindyck, R. S. (1994). *Investment under Uncertainty.* New Jersey: Princeton University Press.

Draper, N. R., & Smith, H. (1981). *Applied Regression Analysis* (2nd ed.). New York: John Wiley & Sons, Inc.

Ecofys. (2014). *Subsidies and costs of EU energy: Annex 1-3.* Ecofys. Retrieved August 16, 2016, from https://ec.europa.eu/energy/sites/ener/files/documents/DESNL14583%20Final%20report%20annexes%201-3%2011%20Nov.pdf

Ecofys. (2014). *Subsidies and costs of EU energy: Final Report.* Ecofys. Retrieved August 14, 2016, from

https://ec.europa.eu/energy/sites/ener/files/documents/ECOFYS%202014%20Subsidies%20and%20costs%20of%20EU%20energy_11_Nov.pdf

Electricity Generation Company. (2015). *Annual Report 2014.* Ankara. Retrieved December 11, 2015, from http://www.euas.gov.tr/Sayfalar/Y%C4%B1ll%C4%B1k-Raporlar.aspx

Elrazaz, Z., Al-Mohawes, N. A., & Mazi, A. A. (1988). Load Duration Curve Forecasting Using Time Series Approach. *Electric Machines & Power Systems, 15*(6), 397-410. doi:10.1080/07313568808909349

Energy Market Regulatory Authority. (2015). *Natural Gas Market Report 2014.* Ankara. doi:http://www3.epdk.org.tr/documents/dogalgaz/rapor_yayin/DPD_RaporYayin2014.pdf

European Commission. (2015). *JRC Geothermal Energy Status Report: Technology, market and economic aspects of geothermal energy in Europe.* Joint Research Centre. Retrieved December 12, 2015, from https://ec.europa.eu/jrc/sites/default/files/jrc_geothermal_report_final.pdf

European Wind Energy Association. (2010). *Powering Europe: wind energy and the electricity grid.* European Wind Energy Association. Retrieved August 8, 2016, from http://www.ewea.org/fileadmin/ewea_documents/documents/publications/reports/Grids_Report_2010.pdf

Export-Import Bank of the United States. (2016, February). *Prior CIRR Rates*. Retrieved February 22, 2016, from http://www.exim.gov/tools-for-exporters/commercial-interest-reference-rates/prior-cirr-rates

Fleten, S.-E., & Ringen, G. (2009). *New Renewable Electricity Capacity under Uncertainty: The Potential in Norway.* Munich Personal RePEc Archive. Retrieved April 14, 2016, from https://mpra.ub.uni-muenchen.de/12857/1/MPRA_paper_12857.pdf

Fleten, S.-E., Maribu, K. M., & Wangensteen, I. (2007). Optimal Investment Strategies in Decentralized Renewable Power Generation under Uncertainty. *Energy, 32*(5), 803–815.

Fox, J. (2008). *Applied Regression Analysis and Generalized Linear Models* (2nd ed.). California: Sage Publications, Inc.

Frank, C. R. (2014). *The Net Benefits of Low and No-Carbon Electricity Technologies.* Washington, D.C.: The Brookings Institution. Retrieved May 27, 2016, from http://www.brookings.edu/~/media/research/files/papers/2014/05/19-low-carbon-future-wind-solar-power-frank/net-benefits-final.pdf

Freris, L., & Infield, D. (2008). *Renewable Energy in Power Systems.* Wiltshire: John Wiley & Sons, Ltd.

Friedrich, R., & Bickel, P. (2001). Estimation of External Costs Using the Impact-Pathway-Approach: Results from the ExternE project series. *TA-Datenbank-Nachrichten, 3*(10). Retrieved August 17, 2016, from http://www.externe.info/externe_2006/frbi01a.pdf

Gallant, A. R. (1975, May). Nonlinear Regression. *The American Statistician, 29*(2), 73-81. Retrieved from http://www.jstor.org/stable/i326386

Georgakaki, A., Tzimas, E., & Peteves, S. D. (2009). *Future Fossil Fuel Electricity Generation in Europe: Options and Consequences.* European Commission Joint Research Center, Institute for Energy. Netherlands: European Commission. Retrieved November 4, 2013, from http://publications.jrc.ec.europa.eu/repository/handle/111111111/6208

Georgiou, P. N. (2016). A bottom-up optimization model for the long-term energy planning of the Greek power supply sector integrating mainland and insular electric systems. *Computers & Operations Research, 66*, 292–312.

Granger, C. W., & Newbold, P. (1977). *Forecasting Economic Time Series.* New York: Academic Press, Inc.

Grausz, S. (2011). *The Social Cost of Coal: Implications for the World Bank.* Climate Advisors. Retrieved February 02, 2016, from http://www.climateadvisers.com/wp-content/uploads/2014/01/2011-10-The-Social-Cost-of-Coal.pdf

Graybill, F. A., & Iyer, H. K. (1994). *Regression Analysis: Concepts and Applications.* Duxbury Press.

Greene, W. H. (2003). *Econometric Analysis* (5th ed.). New Jersey: Prentice Hall.

GRID-Arendal. (2015, December 12). Retrieved from GRID-Arendal A Centre Collaborating with The United Nations Environment Programme (UNEP): http://www.grida.no/graphicslib/detail/hydropower-potential-theoretical-possitibility-for-electricity-generation_1094

Griffin, J. M., & Steele, H. B. (1986). *Energy Economics and Policy* (2nd ed.). Orlando: Academic Press College Divison.

Hach, D., Chyong, C. K., & Spinler, S. (2016). Capacity market design options: A dynamic capacity investment model and a GB case study. *European Journal of Operational Research, 249*(2), 691–705.

Hamilton, J. D. (1994). *Time Series Analysis.* Princeton: Princeton University Press.

Harvey, A. C. (2001). *Forecasting, structural time series models and the Kalman filter.* Cambridge: Cambridge University Press.

Hasan, K., Saha, T., & Eghbal, M. (2012). Emission pricing and locational signal impact on generation portfolio in large scale Queensland network. *Power and Energy Society General Meeting* (pp. 1-8). San Diego: IEEE. doi:10.1109/PESGM.2012.6345173

Herdem, S. (2015, December 4). *Turkey: A New Era For Turkish Energy Market: EPIAs*. Retrieved from modaq: http://www.mondaq.com/turkey/x/384880/Oil+Gas+Electricity/A+New+Era+For+Turkish+Energy+Market+EPIAs

Hillier, F. S., & Liebermann, G. J. (1988). *Operations Research: Einführung* (4 ed.). München: Oldenburg Verlag.

Hirth, L., & Ueckerdt, F. (2013). Redistribution effects of energy and climate policy: The electricity market. *Energy Policy, 62*, 934–947. doi:10.1016/j.enpol.2013.07.055

Hoffman, J. D. (2001). *Numerical Methods for Engineers and Scientists* (2nd ed.). New York: Marcel Dekker, Inc.

Hossain, E., Han, Z., & Poor, V. H. (2012). *Smart Grid Communications and Networking.* Cambridge: Cambridge University Press.

Howells, M. (2011). Presentation on Strategic Energy Investments. (pp. 1-28). Sweden: IAEA. Retrieved from http://www.iaea.org/nuclearenergy/nuclearknowledge/schools/NEM-school/archive/2011/topics/topic1/Strategic_Energy_Investments_2011_Howells.pdf

Huang, D. S. (1970). *Regression and Econometric Methods.* New York: John Wiley & Sons, Inc.

Hyndman, R. J. (2006). Another Look at Forecast-Accuracy Metrics for Intermittent Demand. *FORESIGHT*(4), 43-46. Retrieved September 1, 2015, from http://robjhyndman.com/papers/foresight.pdf

Hyndman, R. J., & Athanasopoulos, G. (2014). *Forecasting: principles and practice.* OTEXTS.COM. Retrieved June 5, 2015, from https://www.otexts.org/book/fpp

International Atomic Energy Agency. (1984). *Expansion Planning for Electrical Generating Systems: A Guidebook.* Vienna: International Atomic Energy Agency in Austria.

International Atomic Energy Agency. (2006). *Computer Manual Series No. 18: Model for Analysis of Energy Demand (MAED-2).* VIENNA: International Atomic Energy Agency. Retrieved December 22, 2014, from http://www-pub.iaea.org/MTCD/publications/PDF/CMS-18_web.pdf

International Energy Agency . (2014). *World Energy Outlook: World Energy Investment Outlook 2014.* Retrieved January 21, 2016, from http://www.worldenergyoutlook.org/weomodel/investmentcosts/

International Energy Agency. (2002). *Security of Supply in Electricity Markets: Evidence and Policy Issues.* Paris: OECD/IEA.

International Energy Agency. (2011). *Harnessing Variable Renewables: A Guide to the Balancing Challenge.* Paris: IEA/OECD.

International Energy Agency. (2011). *World Energy Outlook 2011.* Paris: OECD/IEA. Retrieved January 27, 2016, from https://www.iea.org/publications/freepublications/publication/WEO2011_WEB.pdf

International Energy Agency. (2013). *World Energy Outlook 2013: Renewable Energy Outlook.* Paris: International Energy Agency. Retrieved August 8, 2016, from http://www.worldenergyoutlook.org/media/weowebsite/2013/weo2013_ch06_renewables.pdf

International Energy Agency. (2015). *Energy Prices and Taxes Quarterly Statistics Fourth Quarter 2015.* Paris: International Energy Agency.

International Renewable Energy Agency. (2015). *Renewable Power Generation Costs in 2014.* Bonn: IRENA. Retrieved January 10, 2016, from http://www.irena.org/documentdownloads/publications/irena_re_power_costs_2014_report.pdf

Investment Support and Promotion Agency. (2013, November). Renewable Energy & Environmental Technologies. Retrieved December 13, 2015, from http://www.invest.gov.tr/en-US/infocenter/publications/Documents/ENVIRONMENTAL.TECH.RENEWABLE.INDUSTRY.pdf

Is Investment. (2012, March 13). *Initiating Coverage Park Elek. Madencilik.* Retrieved January 22, 2016

Kaltschmitt, M., & Frick, S. (2006). Status of Geothermal Electricity Generation in Europe: Requirements and Challenges for Power Plant Technology. *Workshop „Electricity Generation from Enhanced Geothermal Systems".* Strasbourg: Institute for Energy and Environmen Leipzig. Retrieved August 2, 2016, from http://engine.brgm.fr/web-offlines/conference-Electricity_generation_from_Enhanced_Geothermal_Systems_-_Strasbourg,_France,_Workshop5/other_contributions/41-slides-0-Status_Geo_Electricity_sf.pdf

Kato, M., Zhou, Y., Kang, C., & Yokoyama, R. (2011). Novel Approach of Modeling Load Duration Curve for Generation Expansion Planning Based on Hill's Function. *IEEJ Transactions on Electrical and Electronic Engineering, 6*, 304–310.

Kennedy, P. (2008). *A Guide to Econometrics* (6th ed.). Massachusetts: Blackwell Publishing.

Kennedy, S. W. (2003). *Dissertation: A Probabilistic Assessment of Large Scale Wind Power Development for Long-Term Energy Resource Planning.* Massachusetts: Harvard University.

Kim, D.-S. (1999). A Standardization Technique to Reduce the Problem of Multicollinearity in Polynomial Regression Analysis. *Bulletin of the International Statistical Institute: The 52nd Session Proceedings, 58*. Retrieved March 27, 2015, from https://www.stat.fi/isi99/proceedings/arkisto/varasto/kim_0574.pdf

Kirchgässner, G., & Wolters, J. (2007). *Introduction to Modern Time Series Analysis.* Heidelberg: Springer-Verlag.

Kong, Z., Wang, L., & Wu, Z. (2011). Application of Fuzzy Soft Set in Decision Making Problems Based on Grey Theory. *Journal of Computational and Applied Mathematics, 236,* 1521–1530.

Koomey, J., Rosenfeld, A. H., & Gadgil, A. (1990a). Conservation screening curves to compare efficiency investments to power plants. *Energy Policy, 18*(8), 774–782. doi:10.1016/0301-4215(90)90030-8

Koomey, J., Rosenfeld, A. H., & Gadgil, A. (1990b). Conservation of Screening Curves to Compare Efficiency. *The Proceedings of the 1990 ACEEE Summer Study on Energy Efficiency in Buildings Asilomar.* California: Center for Building Science at Lawrence Berkeley Laboratory. Retrieved April 4, 2013

Kücükali, S., & Baris, K. (2010). Turkey's Short-Term Gross Annual Electricity Demand Forecast by Fuzzy Logic Approach. *Energy Policy, 38,* 2438–2445.

Kücükdeniz, T. (2010). Long Term Electricity Demand Forecasting: An Alternative Approach with Support Vector. *Istanbul University of Engineering Sciences, 1*, 45-53.

Kumbaroglu, G., Madlener, R., & Demirel, M. (2005). *A Real Options Evaluation Model for the Diffusion Prospects of New Renewable Power Generation Technologies.* Zürich: Centre for Energy Policy and Economics. Retrieved April 14, 2016, from https://www.ethz.ch/content/dam/ethz/special-interest/mtec/cepe/cepe-dam/documents/research/cepe-wp/CEPE_WP35.pdf

Lamont, A. D. (2008). Assessing the long-term system value of intermittent electric generation technologies. *Energy Economics, 30*(3), 1208–1231. doi:10.1016/j.eneco.2007.02.007

Leisch, J., & Cochran, J. (2015, May). Using Wind and Solar to Reliably Meet Electricity Demand. National Renewable Energy Laboratory . Retrieved October 19, 2016, from http://www.nrel.gov/docs/fy15osti/63038.pdf

Levin, N., & Zahavi, J. (1984). Optimal Mix Algorithms with Existing Units. *IEEE Transactions on Power Apparatus and Systems, PAS-103* (5), 954-962. doi:10.1109/TPAS.1984.318698

Levin, N., & Zahavi, J. (1985). Optimal Mix Algorithms with Limited-Energy Plants. *IEEE Transactions on Power Apparatus and Systems, PAS-104*(5), 1131-1139. doi:10.1109/TPAS.1985.323464

Levin, N., Tishler, A., & Zahavi, J. (1983). Time Step vs. Dynamic Optimization of Generation-Capacity-Expansion Programs of Power Systems. *Operations Research, 31*(5), 891-914.

Levin, N., Tishler, A., & Zehavi, Y. (1980). *An Electrical Energy Equilibrium Model: The Dynamic Case.* Tel-Aviv: Tel-Aviv University, Faculty of Management, Leon Recanati Graduate School of Business Administration, Israel Institute of Business Research, 126 PP.

Lewis-Beck, M. S., Bryman, A., & Liao, T. F. (2004). *Encyclopedia of Social Science Research Methods.* California: Sage Publications, Inc.

Madlener, R., & Stoverink, S. (2010). *Power Plant Investments in the Turkish Electricity Sector: A Real Options Approach Taking into Account Market Liberalization.* E.ON Energy Research Center. Retrieved April 14, 2016, from https://www.rwth-aachen.de/global/show_document.asp?id=aaaaaaaaaagvvku

Maybee, J. S., & Uri, N. D. (1978). A Methodology for Forecasting Discrete Approximations to the Load Duration Curve. *Energy Sources, 4*(2), 125-133. doi:10.1080/00908317808908056

Maybee, J. S., & Uri, N. D. (1980). Long-Term Forecasting of Smooth Approximations to the Load Duration Curve. *Applied Mathematical Modelling, 4*(2), 130–132. doi:10.1016/0307-904X(80)90118-3

Maybee, J., Randolph, P., & Uri, N. (1979). Optimal Step Function Approximations to Utility Load Duration Curves. *Engineering Optimization, 4*(2), 89-93. doi:10.1080/03052157908902409

Maybee, S., & Uri, N. D. (1979). Time Series Forecasting of Utility Load Duration Curves. *Electrical Engineering Journal, 4*(1), 4-8. doi:10.1109/CEEJ.1979.6592401

Melikoglu, M. (2013). Vision 2023: Feasibility analysis of Turkey's renewable energy projection. *Renewable Energy, 50*, 570-575.

Milligan, M., & Porter, K. (2006). The Capacity Value of Wind in the United States: Methods and Implementation. *The Electricity Journal, 19*(2), 91-99. Retrieved October 19, 2016, from http://www.science.smith.edu/~jcardell/Courses/EGR325/Readings/CapValu_USA_ElecJrnl.pdf

Mills, T. C. (1990). *Time series techniques for economists.* Cambridge: Cambridge University Press.

Möst, D., Fichtner, W., & Grunwald, A. (2009). *Workshop Energie-systemanalyse: Karlsruhe, 27 November 2008 am KIT Zentrum Energie.* Karlsruhe: Universitätsverlag Karlsruhe. doi:http://dx.doi.org/10.5445/KSP/1000011891

Murphy, F. H., & Weiss, H. J. (1990). An approach to modeling electric utility capacity expansion planning. *Naval Research Logistics, 37*(6), 827–845. doi:10.1002/1520-6750(199012)37:6<827::AID-NAV3220370603>3.0.CO;2-6

Murphy, F. H., Saraf, S., & Soyster, A. L. (1985). The Replication of Multi-year Solutions Using Single Period Models of Electric Utility Capacity Expansion Planning. *IIE Transactions, 17*(4), 396-399. doi:10.1080/07408178508975320

Murphy, F., Sen, S., & Soyster, A. L. (1987). Electric utility expansion planning in the presence of existing capacity: A nondifferentiable, convex programming approach. *Computers & Operations Research, 14*(1), 19–31. doi:10.1016/0305-0548(87)90054-2

Nag, P. K. (2008). *Power Plant Engineering* (3rd ed.). New Delhi: Tata McGraw-Hill Education.

NEA, IEA, OECD. (2015). *Projected Costs of Generating Electricity 2015 Edition.* OECD.

Nelson, C. R. (1973). *Applied Time Series Analysis For Managerial Forecasting.* San Francisco: Holden-Day, Inc.

Nygård, M. T. (2013). *Master Thesis: Investment in Hydropower Plants under Uncertainty.* Department of Industrial Economics and Technology Management. Trondheim: Norwegian University of Science and Technology. Retrieved April 14, 2016, from http://www.diva-portal.org/smash/get/diva2:723982/FULLTEXT01.pdf

Oktay, Z. (2009). Investigation of Coal-Fired Power Plants in Turkey and a Case Study: Can Plant. *Applied Thermal Engineering, 29*, 550–557.

Onar, S. Ç., & Kılavuz, T. N. (2015). Risk Analysis of Wind Energy Investments in Turkey. *Human and Ecological Risk Assessment: An International Journal, 21*(5), 1230-1245.

Ortner, A. (2014). The EU Project: Introduction to the Modelling Framework. *Turkey Regional Workshop.* Vienna: Vienna University of Technology. Retrieved Juli 27, 2016, from http://better-project.net/sites/default/files/Introduction%20to%20the%20modeling%20framework_TUWIEN.pdf

Ozaki, T., & Iino, M. (2001). An Innovation Approach to Non-Gaussian Time Series Analysis. *Journal of Applied Probability, 38*, 78-92.

Özcan, M. (2014). Assessment of Renewable Rnergy Incentive System from Investors' Perspective. *Renewable Energy, 71*, 425-432.

Ozcan, M., Ozturk, S., & Yildirim, M. (2014). Turkey's Long-Term Generation Expansion Planning with The Inclusion of Renewable-Energy Sources. *Computers and Electrical Engineering, 40*, 2050–2061.

Ozturk, H. K., & Ceylan, H. (2005). Forecasting Total and Industrial Sector Electricity Demand Based on Genetic Algorithm Approach: Turkey Case Study. *International Journal of Energy Research, 29*, 829-840. doi:10.1002/er.1092

Ozturk, M., & Yuksel, Y. E. (2016). Energy Structure of Turkey for Sustainable Development. *Renewable and Sustainable Energy Reviews, 53*, 1259–1272.

Parpas, P., & Webster, M. (2014). A stochastic multiscale model for electricity generation capacity expansion. *European Journal of Operational Research, 232*(2), 359–374.

Pindyck, R. S. (1999). The Long-Run Evolution of Energy Prices. *The Energy Journal, 20*(2), 1-27. Retrieved from http://web.mit.edu/rpindyck/www/Papers/Long-Run_Evolution.pdf

Pineda, S., & Morales, J. M. (2016). Capacity expansion of stochastic power generation under two-stage electricity markets. *Computers & Operations Research, 70*, 101–114.

Platts. (2015, June 17). Coal Trader International. *2* . Retrieved January 21, 2016, from https://www.platts.com/im.platts.content/productsservices/products/coaltraderintl.pdf

Polater, H. M. (2013). Long Term Electrical Supply-Demand Balance of Turkey (2013-2023). Retrieved June 23, 2015, from etd.lib.metu.edu.tr/upload/12616134/index.pdf

Rafaj, P., & Kypreos, S. (2007). Internalisation of external cost in the power generation sector: Analysis with Global Multi-regional MARKAL model. *Energy Policy, 35*, 828–843.

Ramos, A., Perez-Arriaga, I., & Bogas, J. (1989). A nonlinear programming approach to optimal static generation expansion planning. *IEEE Transactions on Power Systems, 4*(3), 1140-1146. doi:10.1109/59.32610

Rao, K. S. (2007). *Numerical Methods for Scientists and Engineers* (3rd ed.). New Delhi: Prentice-Hall of India Private Limited.

Ratkowsky, D. A. (1990). *Handbook of Nonlinear Regression Models.* New York: Marcel Dekker, Inc.

Resch, G., Welisch, M., Ortner, A., Totschnig, G., Türk, A., & Steiner, D. (2015). *Bringing Europe and Third countries closer together through renewable Energies: Integrative Assessment of RES cooperation with Third countries (D6.4).* Vienna: Vienna University of Technology (Energy Economics Group). Retrieved Juli 27, 2016, from http://better-project.net/sites/default/files/D6.4%20Integrative%20assessment%20of%20long-term%20prospects%20for%20RES%20cooperation.pdf

Ritz, C., & Streibig, J. C. (2008). *Nonlinear Regression with R.* New York: Springer Science+Business Media, LLC.

Ritzenhofen, I., Birge, J. R., & Spinler, S. (2016). The structural impact of renewable portfolio standards and feed-in tariffs on electricity markets. *European Journal of Operational Research, 255*(1), 224–242.

Sauma, E., Traub, F., & Vera, J. (2015). A Robust optimization approach to assess the effect of delays in the connection-to-the-grid time of new generation power plants over transmission expansion planning. *Annals of Operations Research, 229*(1), 703–741.

Shaalan, H. (2001). Generation of electric power. In Beaty, H. Wayne, & D. G. Fink, *Handbook of Electric Power Calculations* (3rd ed., pp. 167-204). New York: McGraw-Hill.

Shacham, M., & Brauner, N. (1997). Minimizing the Effects of Collinearity in Polynomial Regression. *Industrial & Engineering Chemistry Research, 36*(10), 4405-4412. doi:10.1021/ie970236k

Sheather, S. J. (2009). *A Modern Approach to Regression with R.* New York: Springer Science+Business Media.

Sheridan, B. (2013). Social Cost of Electricity Generation: A Quantification and Comparison between Energy Sources within PJM Interconnection. *Master Thesis*.

Shrestha, G., & Songbo, Q. (2009). Generation Scheduling for a price taker Genco in competitive power markets. *Power Systems Conference and Exposition, 2009* (pp. 1-6). Seattle: IEEE. doi:10.1109/PSCE.2009.4840022

Shumway, R. H., & Stoffer, D. S. (2011). *Time Series Analysis and Its Applications* (3rd ed.). New York: Springer Science+Business Media, LLC.

Sivanandam, S. N., & Paulraj, M. (2009). *Introduction to Artificial Neural Networks.* New Delhi: Vikas Publishing Haus Pvt Ltd.

Sivanandam, S. N., Sumathi, S., & Deepa, N. S. (2007). *Introduction to Fuzzy Logic Using MATLAB.* Berlin: Springer-Verlag.

Spliethoff, H. (2010). *Power Generation from Solid Fuels.* Berlin: Springer-Verlag.

Staffell, I., & Green, R. (2016). Is There Still Merit in the Merit Order Stack? The Impact of Dynamic Constraints on Optimal Plant Mix. *IEEE TRANSACTIONS ON POWER SYSTEMS, 31*(1).

Stoft, S. (2002). *Power System Economics: Designing Markets for Electricity.* New York: John Wiley & Sons Inc.

Stoughton, N., Chen, R., & Lee, S. (1980). Direct Construction of Optimal Generation Mix. *IEEE Transactions on Power Apparatus and Systems, PAS-99*(2), 753-759. doi:10.1109/TPAS.1980.319669

Šúri, M., Huld, T. A., Dunlop, E. D., & Ossenbrink, H. A. (2007). Potential of Solar Electricity Generation in the European Union Member States and Candidate Countries. *Solar Energy, 81*(10), 1295–1305. Retrieved December 12, 2015, from http://re.jrc.ec.europa.eu/pvgis/download/download.htm

Taper, M. L., & Lele, S. R. (2004). *The Nature of Scientific Evidence: Statistical, Philosophical, and Empirical Considerations.* Chicago: University of Chicago Press.

Tewari, J. P. (2003). *Basic Electrical Engineering.* New Delhi: New Age International (P) Limited, Publishers.

The Council of Ministers of the Republic of Turkey. (2009). *Turkey Electricity Energy Market and Supply Security Strategy Paper.* Retrieved 11 21, 2015, from http://weg.ge/wp-content/uploads/2013/05/Turkey-Electricity-Energy-Market-and-Supply-Security-Strategy-Paper-2009.pdf

The Ministry of Energy and Natural Resources. (2014). *National Renewable Energy Action Plan for Turkey.* Retrieved 11 21, 2015, from http://www.eie.gov.tr/duyurular_haberler/document/National_Renewable_Energy_Action_For_Turkey.PDF

The National Renewable Energy Laboratory of the USA. (2016, April 26). Life Cycle Assessments of Energy Technologies. Retrieved August 16, 2016, from http://www.nrel.gov/analysis/sustain_lca_about.html

Tidball, R., Bluestein, J., Rodriguez, N., Knoke, & Stu. (2010). *Cost and Performance Assumptions for Modeling Electricity Generation Technologies.* Colorado: National Renewable Energy Laboratory. Retrieved January 2016, 21, from http://www.nrel.gov/docs/fy11osti/48595.pdf

Turkey Electricity Trading and Contracting Company. (2015). *Sector Report of Year 2014.* Ankara. Retrieved 12 06, 2015, from http://www.tetas.gov.tr/File/?path=ROOT%2f1%2fDocuments%2fSekt%c3%b6r+Raporu%2fSektorRaporu2014.pdf

Turkish Coal Enterprises Institution. (2015). *The Report on Coal Sector (Lignite) 2014.* Ankara. Retrieved December 11, 2015, from http://www.tki.gov.tr/tr/Faaliyet-Raporlarimiz/Kurumsal

Turkish Electricity Transmission Corporation. (2008). *Turkish Electrical Energy 10-Year Generation Capacity Projection (2008 – 2017).* Research Planning and Coordination Department, Ankara. Retrieved December 22, 2014, from http://www.teias.gov.tr/Eng/ApkProjection/CAPACITY%20PROJECTION%202008-2017.pdf

Turkish Electricity Transmission Corporation. (2014). *Turkish Electrical Energy 5-Year Generation Capacity Projection (2014 – 2018).* RESEARCH PLANNING AND COORDINATION DEPARTMENT, Ankara. Retrieved December 22, 2014, from http://www.teias.gov.tr/Eng/ApkProjection/CAPACITY%20PROJECTION%202009-2018.pdf

Turkish Electricity Transmission Corporation. (2015). *Electricity Generation & Transmission Statistics of Turkey.* Retrieved December 22, 2014, from http://www.teias.gov.tr/T%C3%BCrkiyeElektrik%C4%B0statistikleri/istatistik2013/istatistik2013.htm

Turkish Electricity Transmission Corporation. (2015). Turkish Electrical Energy 5-Year Generation Capacity Projection (2015–2019). Ankara. Retrieved February 28, 2016, from http://www.teias.gov.tr/YayinRapor%5CAPK%5Cprojeksiyon%5Cindex.htm

Turkish Hard Coal Enterprise Institution. (2015). *Sectoral Report 2014.* Zonguldak. Retrieved December 11, 2015, from http://www.taskomuru.gov.tr/file/Is_Zekasi_Raporlari/sektor_raporu.pdf

Turkish Statistical Institute. (2014). *National Accounts.* Retrieved December 22, 2014, from http://www.turkstat.gov.tr/UstMenu.do?metod=temelist

Turkish Statistical Institute. (2015). *Environment and Energy.* Retrieved Juni 17, 2015, from http://www.turkstat.gov.tr/UstMenu.do?metod=temelist

Tzimas, E., & Georgakaki, A. (2010). A long-term view of fossil-fuelled power generation in Europe. *Energy Policy, 38*(8), 4252–4264. doi:10.1016/j.enpol.2010.03.055

Ueckerdt, F., Hirth, L., Luderer, G., & Edenhofer, O. (2013). System LCOE: What are the costs of variable renewables? *Energy, 63*, 61–75. doi:10.1016/j.energy.2013.10.072

Uri, N. D. (1977). Research Note: Forecasting the Load Duration Curve. *Applied Mathematical Modelling, 1*(7), 405–407. doi:10.1016/0307-904X(77)90051-8

Uri, N. D. (1979). Mid-Range Forecasting of the Load Duration Curve. *Applied Mathematical Modelling, 3*(5), 379–383. doi:10.1016/S0307-904X(79)80045-1

Uri, N. D., & Maybee, J. S. (1978). Forecasting the Load Duration Curve Using Box-Jenkins Time Series Analysis. *Engineering Optimization, 3*(4), 193-199. doi:10.1080/03052157808902391

Uri, N. D., & Maybee, J. S. (1978). Smooth Approximation and Forecasting of Load Duration Curves. *Electric Power Systems Research, 1*(4), 255–259. doi:10.1016/0378-7796(78)90011-1

Uri, N. D., & Maybee, J. S. (1980). Long-Term Forecasts of Optimal Approximations to the Load Duration Curve. *The Journal of the Operational Research Society, 31*(4), 343-347. doi:10.1057/jors.1980.61

Uri, N. D., & Maybee, J. S. (1980). On the Forecasting of Economically Optimal Approximations to Load Duration Curves. *Engineering Optimization, 4*(4), 199-206. doi:10.1080/03052158008902423

Vespucci, M. T., Bertocchi, M., Pisciella, P., & Zigrino, S. (2015). Two-stage stochastic mixed integer optimization models for power generation capacity expansion with risk measures. *Optimization Methods and Software*, 305-327.

Wei, W. W. (2006). *Time Series Analysis: Univariate and Multivariate Methods* (2nd ed.). Addison-Wesley Publishing Company.

Wetherill, G. B. (1986). *Regression Analysis with Applications.* London: Chapman and Hall.

World Bank Group. (2015). *Commodity Markets Outlook, October 2015.* Washington, DC: World Bank. Retrieved January 16, 2016, from http://pubdocs.worldbank.org/pubdocs/publicdoc/2015/10/22401445260948491/CMO-October-2015-Full-Report.pdf

World Energy Council Turkish Committee. (2007). *Hydraulics and Renewable Energy Study Group Report on Solar Energy in Turkey.* Ankara. Retrieved December 12, 2015, from http://www.dektmk.org.tr/upresimler/2007calismagrubu/gunes_enerjisi_raporu_304.pdf

World Energy Council Turkish Committee. (2014). *Energy Report 2013.* Ankara. Retrieved December 11, 2015 , from http://www.dektmk.org.tr/incele.php?id=MzA2

Yavuzdemir, M., & Gökgöz, F. (2015). Estimating Gross Annual Electricity Demand of Turkey. *International Business Research, 8*(4), 145-154. Retrieved 06 23, 2015, from http://ccsenet.org/journal/index.php/ibr/article/download/44696/25154.

Yılmaz, E. (2014). *On the Uncertainty-Investment Relationship: An Overview with an Application to the Power Plant Investments in Turkish Electricity Sector.* Ankara: Central Bank of the Republic of Turkey. Retrieved April 14, 2016, from http://www.tcmb.gov.tr/wps/wcm/connect/bfc6ce8e-80d7-4a54-b636-e25ef14a7cdb/kapak.pdf?MOD=AJPERES&CACHEID=ROOTWORKSPACEbfc6ce8e-80d7-4a54-b636-e25ef14a7cdb

Zellner, A. (1962). An Efficient Method of Estimating Seemingly Unrelated Regressions and Tests for Aggregation Bias. *Journal of the American Statistical Association, 57*(298), 348-368.

Zhang, T., & Baldick, R. (2015). Consideration of Ancillary Services in Screening Curve Method. *Power & Energy Society General Meeting, 2015 IEEE,* 1-5.

Zhang, T., & Baldick, R. (2016). Consideration of Existing Capacity in Screening Curve Method. *IEEE Transactions on Power Systems, PP*(99), 1-11.

Zhang, T., Baldick, R., & Deetjen, T. (2015). Optimized generation capacity expansion using a further improved screening curve method. *Electric Power Systems Research, 124*, 47–54.

APPENDIX A

Genetic Algorithm (GA) method is introduced by Holland (1965) as a mathematical search technique based on the principles of natural selection and genetic recombination (artificial intelligence). According to Ozturk and Ceylan, GA differs from conventional nonlinear optimization techniques in that they search by maintaining a population (or database) of solutions from which better solutions are created rather than making incremental changes to a single solution to the problem. For more information, see the relevant article.

Grey System Theory (GST) is introduced in early 1980s by Deng (1982). The theory includes white system (system with complete information), grey system (system with incomplete information) and black system (completely unknown system). By using GST, the similarity and dissimilarity among factors in developing dynamic processes are quantitatively analyzed. The theory proposes a dependence to measure the correlation degree of factors; the more similarities develop, the more factors correlate (Kong, Wang, & Wu, 2011, p. 1522). The rolling mechanism is stated to be an efficient technique to increase forecasting accuracy of grey prediction in case of having exponential and chaotic data (Akay & Atak p.1671). For more information, see the relevant article.

The method of artificial neural network (ANN) originates from the studies of the biological nervous system and artificial intelligence (Sivanandam & Paulraj, 2009). The artificial neural network is considered to be functioning in a way similar to the human brain. The function of a neural network is to generate an output pattern when presented with an input pattern. Neural networks consist of nodes connected by adaptable weights storing experimental knowledge from task examples through a process of learning. The ability of the networks to learn means the networks adapting their internal adjustment or weights following exposure to the data (i.e. called training of neuronal networks).

Support Vector Machines (SVM) is based on statistical learning theory and developed by Vapnik and Chervonenkis (Kücükdeniz, p. 47). SVM is stated to be mapping the input data into a higher dimensional feature space through a nonlinear mapping. Subsequently, a linear regression problem is obtained and solved in this feature space.

The Fuzzy Logic Method (FLM) is an artificial intelligence method utilized for dealing with uncertainty through enabling appropriate human reasoning capabilities (introduced by Zadeh, 1965). The fuzzy algorithms depend on a systematic use of linguistic expressions to

characterize the values of variables and relations between them (Kücükali & Baris, p. 2441). On the contrary to the traditional binary set theory describing events those either do or do not occur. FLM uses probability theory to explain if an event will occur, measuring the chance with which a given event is expected to occur (Sivanandam, Sumathi, & Deepa, 2007, p. 2). In FLM, fuzziness describes the ambiguity of an event; whereas randomness describes the uncertainty in the occurrence of an event.

According to Dilaver and Hunt, the structural time series analysis (STSM) decomposes a time series into independent variables, a stochastic trend and a random component. The state space form presentation of an STSM presents the best estimates of the parameters and trend component at a given time. As additional observations are included, the parameters and the unobserved components of the model, such as the trend, are estimated by a combination of a recursive filtering and smoothing process by the Kalman Filter and the maximum likelihood approach.

APPENDIX B

Forecasting Annual Gross Electricity Demand of Turkey in the Period 2015-2025

The summary statistics of the ARIMA(1,2,1) model is represented below. The analytic formulas for the training error measures (i.e. the measure of the quality of the prediction errors) are tabulated below.

ARIMA(1,2,1)
Box Cox transformation: lambda= -0.049

Coefficients:

	ar1	ma1
	0.3558	-0.8482
s.e.	0.1797	0.0969

sigma^2 estimated as 0.0007381: log likelihood=93.69
AIC=-181.38 AICc=-180.76 BIC=-176.09

Training set error measures:

	ME	RMSE	MAE	MPE	MAPE	MASE	ACF1
Training set	-0.7785629	4.308563	2.458468	-0.8738192	2.517793	0.4170107	-0.08534633

(own calculation & illustration)

In the below given table, the symbol "e_i" denotes the i^{th} error ($1 \leq i \leq n \ \wedge \ i \in \mathbb{Z}^+$) and equals to the difference of the i^{th} predicted value ($\hat{Y}_i$) and the i^{th} observed value (Y_i). The symbol "n" denotes the sample size and the symbol"$\bar{e}$" is the mean of errors. Among the error measures, mean absolute scaled error (MASE) is the unfamiliar statistic provided as output in R. The MASE was proposed by Hyndman and Koehler (2006, p. 45) to scale the errors based on the "in-sample mean absolute error" (see the denominator of the formula); in order make the results independent of the scale of the data. A scaled error, which is less than one, indicates a successful prediction by utilizing the corresponding model; whereas higher than one indicates an unsuccessful prediction.

The error measures provided in summary statistics by R and their analytic formulas (own illustration)

Error Measure	Formula	
Mean Absolute Error (ME)	$\frac{1}{n}\sum_{i=1}^{n}(\hat{Y}_i - Y_i)$	(26.4.1)
Root Mean Squared Error (RMSE)	$\sqrt{\frac{1}{n}\sum_{i=1}^{n}(\hat{Y}_i - Y_i)^2}$	(26.4.2)
Mean Absolute Error (MAE)	$\frac{1}{n}\sum_{i=1}^{n}\lvert\hat{Y}_i - Y_i\rvert$	(26.4.3)
Mean Percentage Error (MPE)	$\frac{100\%}{n}\sum_{i=1}^{n}\left(\frac{\hat{Y}_i - Y_i}{Y_i}\right)$	(26.4.4)
Mean Absolute Percentage Error (MAPE)	$\frac{100\%}{n}\sum_{i=1}^{n}\left\lvert\frac{\hat{Y}_i - Y_i}{Y_i}\right\rvert$	(26.4.5)
Scaled Error (q_t)	$\frac{\hat{Y}_i - Y_i}{\frac{1}{n-1}\sum_{i=2}^{n}\lvert Y_i - Y_{i-1}\rvert}$	(26.4.6)
Mean Absolute Scaled Error (MASE)r	$\frac{1}{n}\lvert q_i\rvert$	(26.4.7)
Autocorrelation of errors at lag 1 (ACF1)	$\frac{\sum_{i=1}^{n-1}\frac{(e_i - \bar{e})(e_{i-1} - \bar{e})}{n}}{\sum_{i=1}^{n}\frac{(e_i - \bar{e})^2}{n}}$	(26.4.8)

Forecasting Peak Load Demand of Turkey in the Period 2015-2025

The summary statistics of the ARIMA(1,2,1) model is represented below.

ARIMA(1,2,1)
Box Cox transformation: lambda= 0.203

Coefficients:

	ar1	ma1
	-0.0654	-0.9854
s.e.	0.1591	0.2245

sigma^2 estimated as 0.08251: log likelihood=-9.05
AIC=24.1 AICc=24.71 BIC=29.38

Training set error measures:

	ME	RMSE	MAE	MPE	MAPE	MASE	ACF1
Training set	-126.295	751.6635	432.5634	-1.054082	3.413489	0.4496915	-0.1043665

(own calculation & illustration)

Obtaining Functional Approximations to Load Duration Curves of Turkey for the Period 2015-2025

The summary statistics of the ARIMA(0,0,0)(1,1,1)[6] model is represented below.

ARIMA(0,0,0)(1,1,1)[6]

Coefficients:

	sar1	sma1
	-0.2597	-0.4046
s.e.	0.1562	0.1363

sigma^2 estimated as 9.057e-13: log likelihood=1044.13
AIC=-2082.25 AICc=-2081.95 BIC=-2074.96

Training set error measures:

	ME	RMSE	MAE	MPE	MAPE	MASE	ACF1
Training set	1.3992E-07	9.1954E-07	3.1643E-07	4.688248	11.0597	0.8363211	-0.02530019

(own calculation & illustration)

APPENDIX C

In the below given table, the BIC values of the polynomial approximations to LDCs of Turkey in the period 2000-2014 are tabulated. Note that in the table only for the six of the values marked as bold italic, the BIC values increase as the degree of polynomials is increased.

Years	Degree of Polynomial								
	4th	5th	6th	7th	8th	9th	10th	11th	12th
2000	-130617.6	-135497.4	-136293.6	-140990.3	-141185.0	-145243.3	-145527.5	-151263.7	-151507.7
2001	-135097.3	-137977.0	-138553.9	-142698.5	-142732.0	-145365.8	-145482.5	-148986.3	-149321.1
2002	-126488.3	-129848.6	-130098.2	-133264.2	-133455.0	-136180.3	-136225.1	-139446.9	***-139445.8***
2003	-132254.8	-136048.7	-136651.1	-139180.6	-139221.8	-141828.1	-142100.2	-144433.8	***-144431.1***
2004	-131715.0	-135809.5	-137039.2	-139487.3	***-139478.8***	-142306.5	-142997.4	-145721.1	-145876.8
2005	-135805.9	-140979.1	-143242.4	-145863.2	***-145855.1***	-147736.6	-149300.1	-152288.8	-152300.7
2006	-141272.7	-145402.8	-147398.5	-151608.6	-151623.6	-153916.2	-155513.6	-159080.1	-159301.5
2007	-145727.7	-149095.0	-153117.1	-155825.6	-155937.6	-158145.5	-159831.9	-162887.6	-163624.0
2008	-151595.5	-154870.2	-157989.4	-162223.3	-163219.0	-166412.6	-168124.7	-172372.5	-173744.4
2009	-147263.9	-151329.0	-152925.0	-156531.6	-156790.6	-159237.9	-160044.1	-162484.3	-163320.7
2010	-151713.8	-157828.8	-159252.4	-165166.0	-165186.3	-168288.6	-169069.1	-172149.8	-173354.5
2011	-174666.6	-179828.7	-181152.3	-187827.9	***-187819.0***	-190279.1	-191028.1	-195602.1	-196109.6
2012	-196365.2	-200475.0	-201997.3	-207363.1	***-207355.6***	-212046.2	-212444.2	-217862.9	-219552.5
2013	-205545.8	-212501.1	-216038.2	-220619.4	-221650.9	-223494.2	-226365.6	-230637.9	-232586.8
2014	-206098.0	-213108.1	-214243.8	-220094.8	-220167.2	-223129.9	-224369.8	-227536.1	-229650.9

In the below given table, the BIC values of the nonlinear and linear functional approximations to LDCs of Turkey in the period 2000-2014 are tabulated. Note that in the table only for the six of the values marked as bold italic, the BIC values of 5th degree polynomial approximations are higher than the corresponding values for the inverse of Hill's function.

Years	Type of Function			
	Exponential Function	Logarithmic Function	Inverse of Hill's Function	5th Degree Polynomial
2000	-131750.5	-131284.6	-133006.4	-135497.4
2001	-135173.6	-136696.6	-139121.6	***-137977.0***
2002	-125262.8	-127373.4	-129618.0	-129848.6
2003	-134242.6	-133322.5	-134296.4	-136048.7
2004	-134724.8	-132525.1	-134504.7	-135809.5
2005	-137215.1	-136246.0	-139195.5	-140979.1
2006	-144066.3	-142305.2	-145685.9	***-145402.8***
2007	-146214.9	-146707.4	-153273.4	***-149095.0***
2008	-157184.1	-154775.2	-159519.8	***-154870.2***
2009	-148912.2	-148214.2	-152048.4	***-151329.0***
2010	-146977.3	-152639.8	-155764.5	-157828.8
2011	-174276.5	-175757.1	-178450.7	-179828.7
2012	-198665.9	-198686.3	-201297.4	***-200475.0***
2013	-208173.6	-206835.6	-208442.0	-212501.1
2014	-204601.7	-207706.1	-207591.4	-213108.1

APPENDIX D

Plots of 4th Degree Polynomial Approximations to LDCs of Turkey in the Period 2000-2014

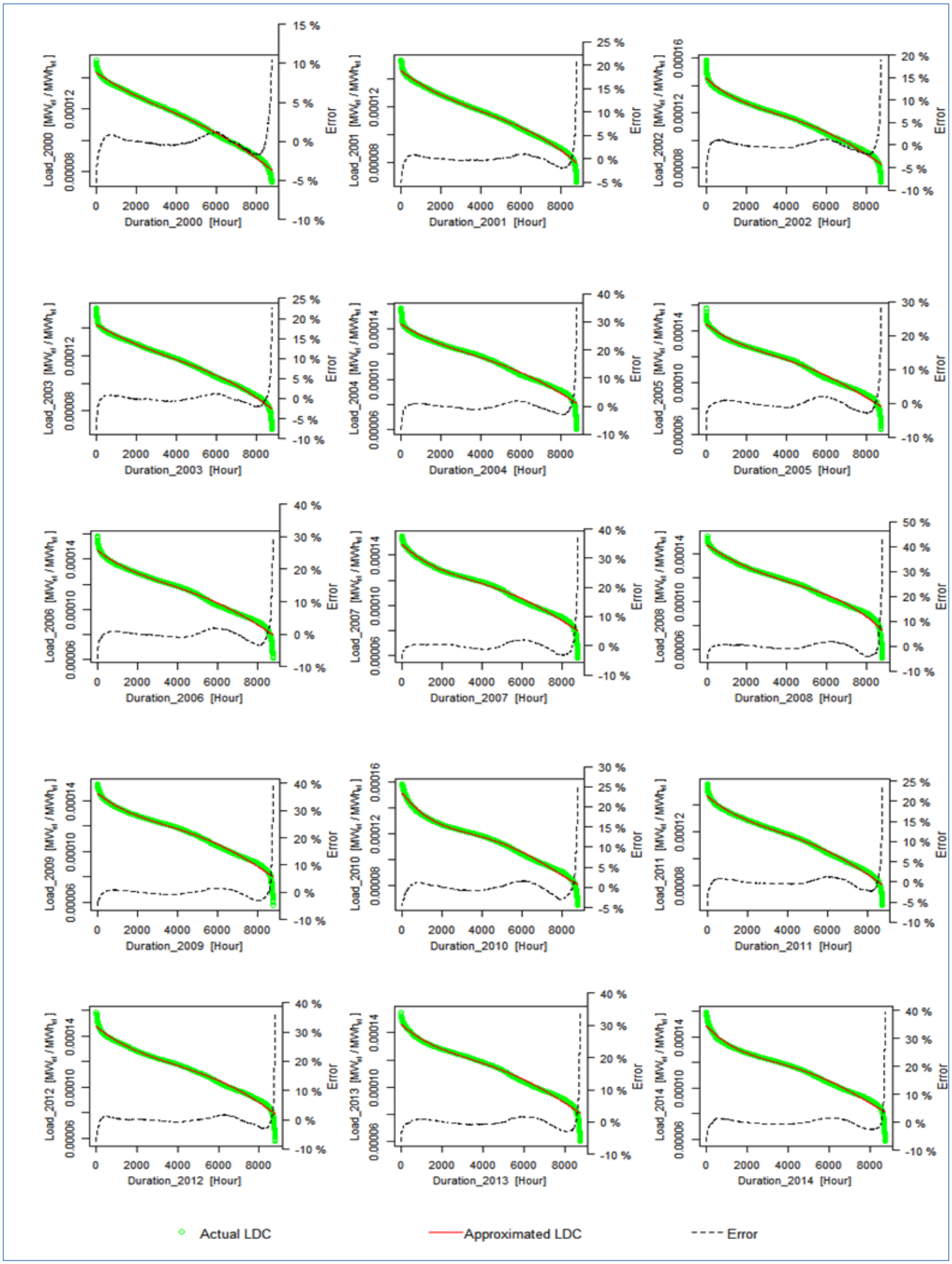

Plots of 5th Degree Polynomial Approximations to LDCs of Turkey in the Period 2000-2014

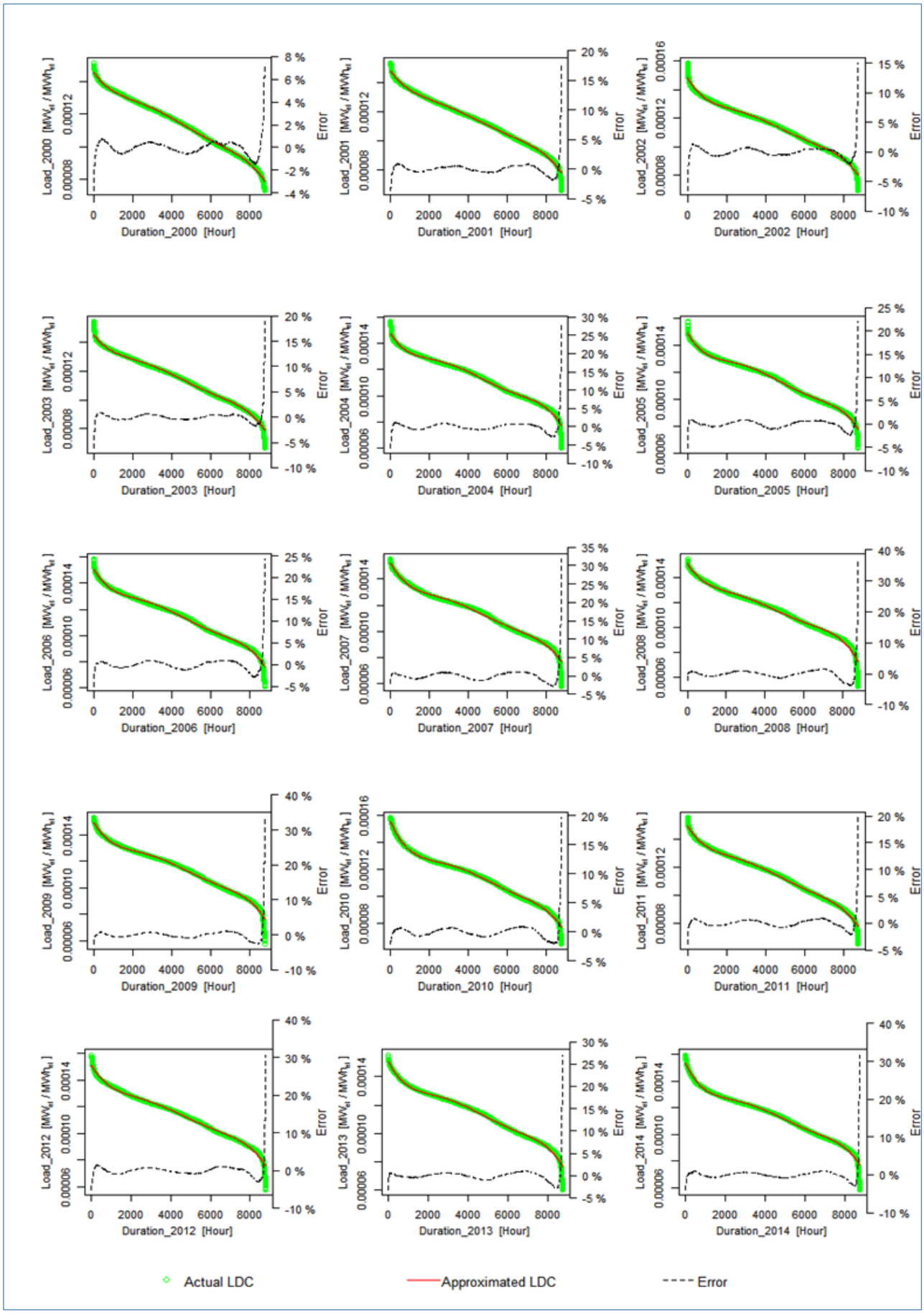

Plots of 6th Degree Polynomial Approximations to LDCs of Turkey in the Period 2000-2014

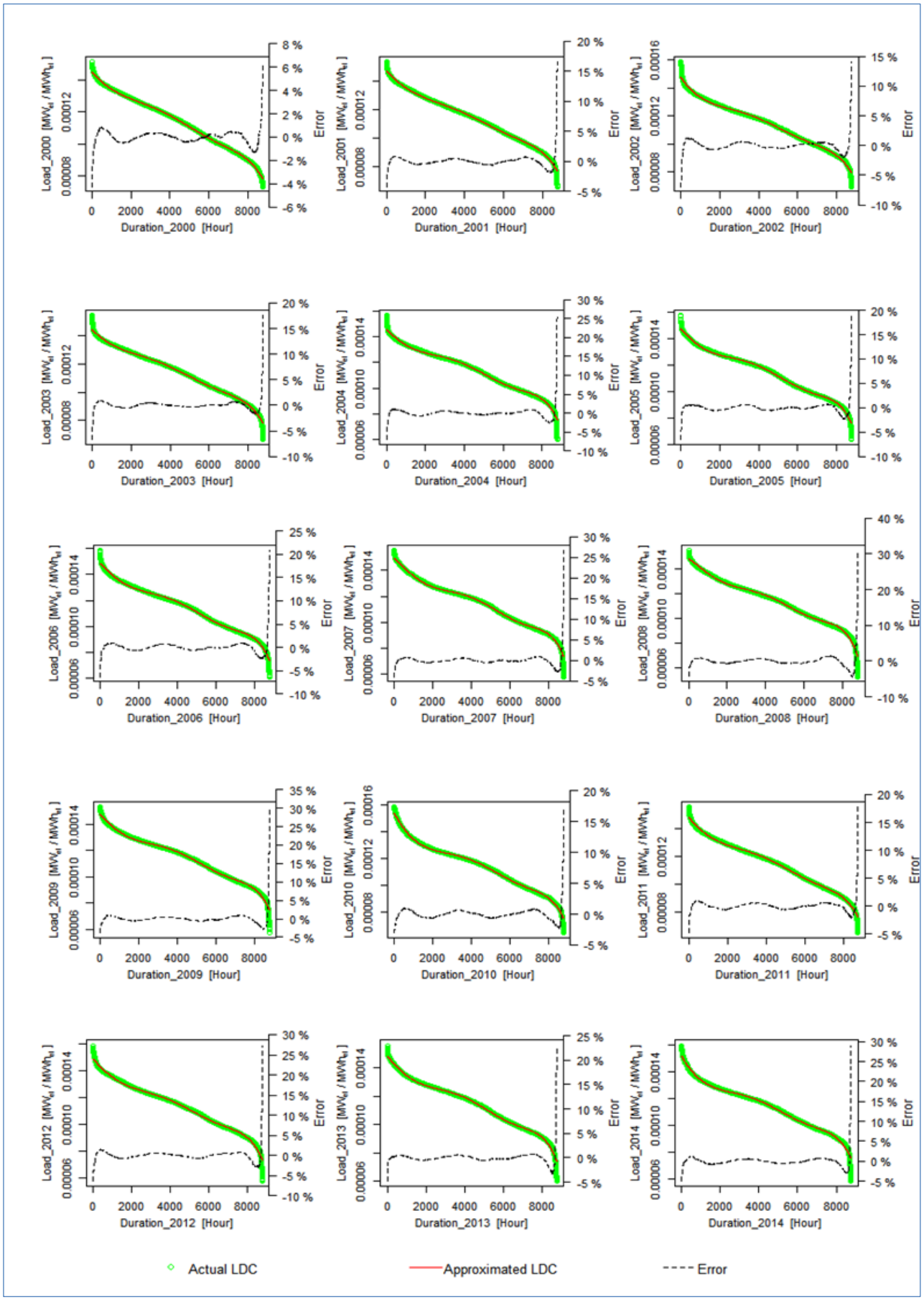

Plots of 7th Degree Polynomial Approximations to LDCs of Turkey in the Period 2000-2014

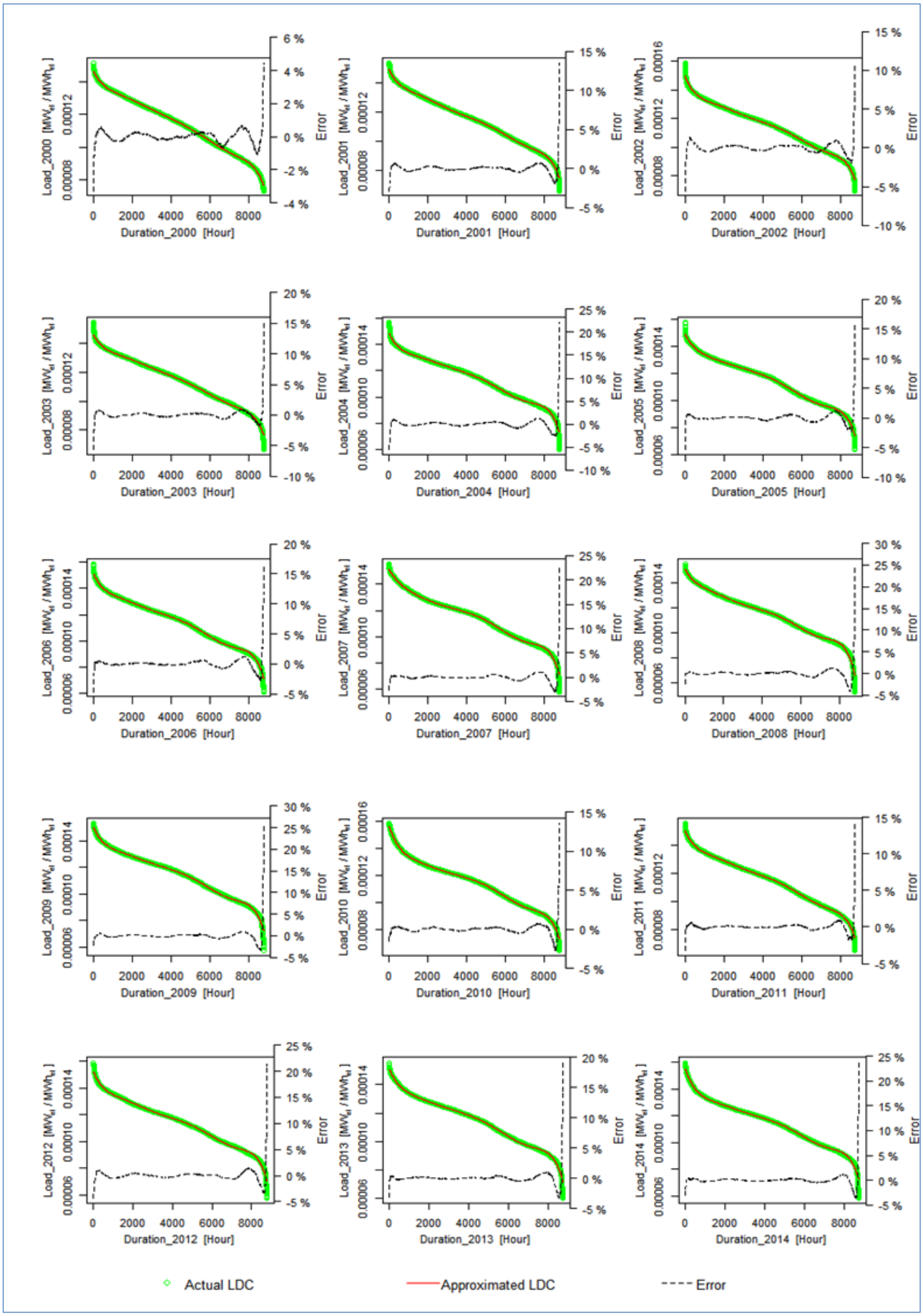

Plots of 8th Degree Polynomial Approximations to LDCs of Turkey in the Period 2000-2014

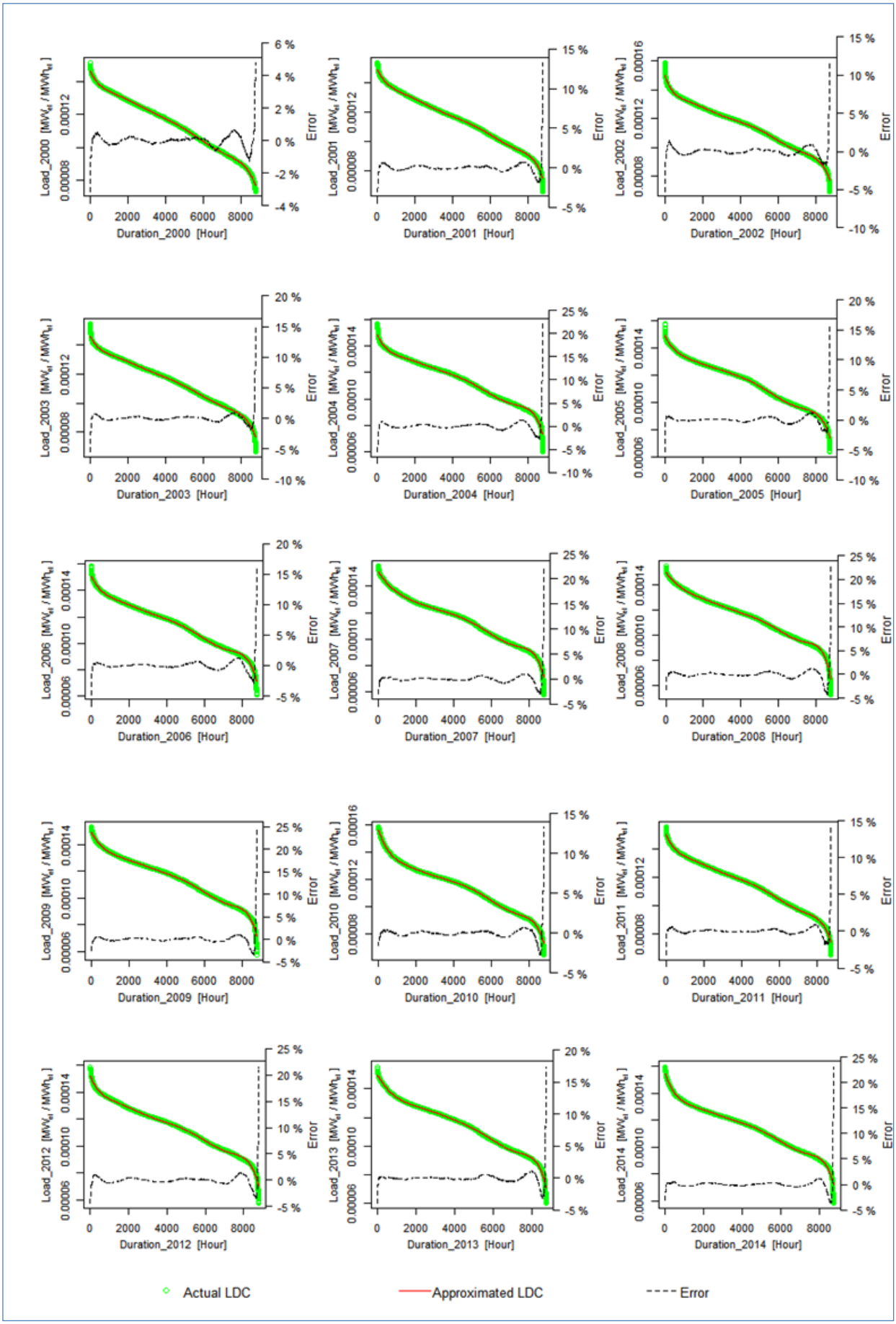

Plots of 9th Degree Polynomial Approximations to LDCs of Turkey in the Period 2000-2014

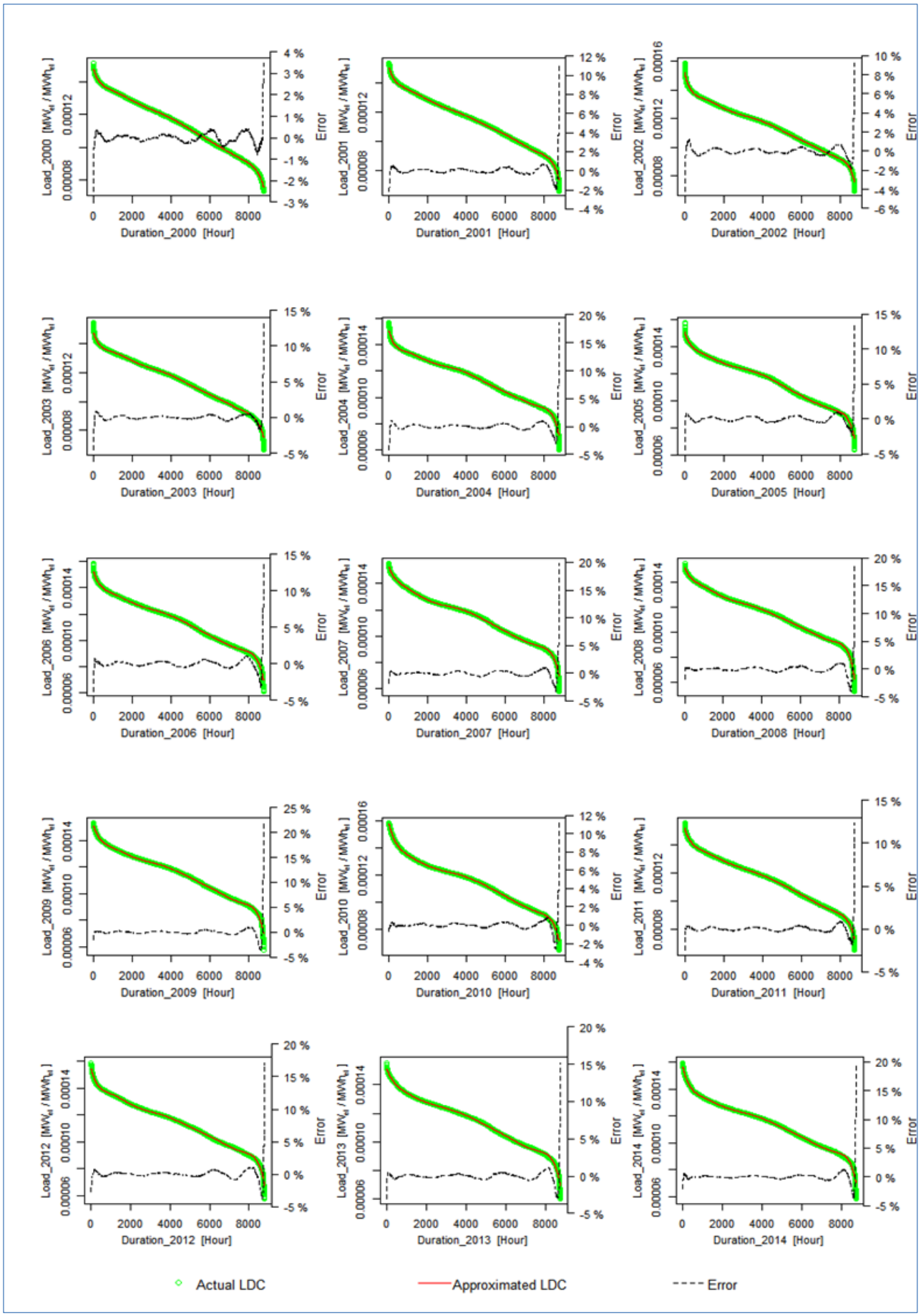

Plots of 10th Degree Polynomial Approximations to LDCs of Turkey in the Period 2000-2014

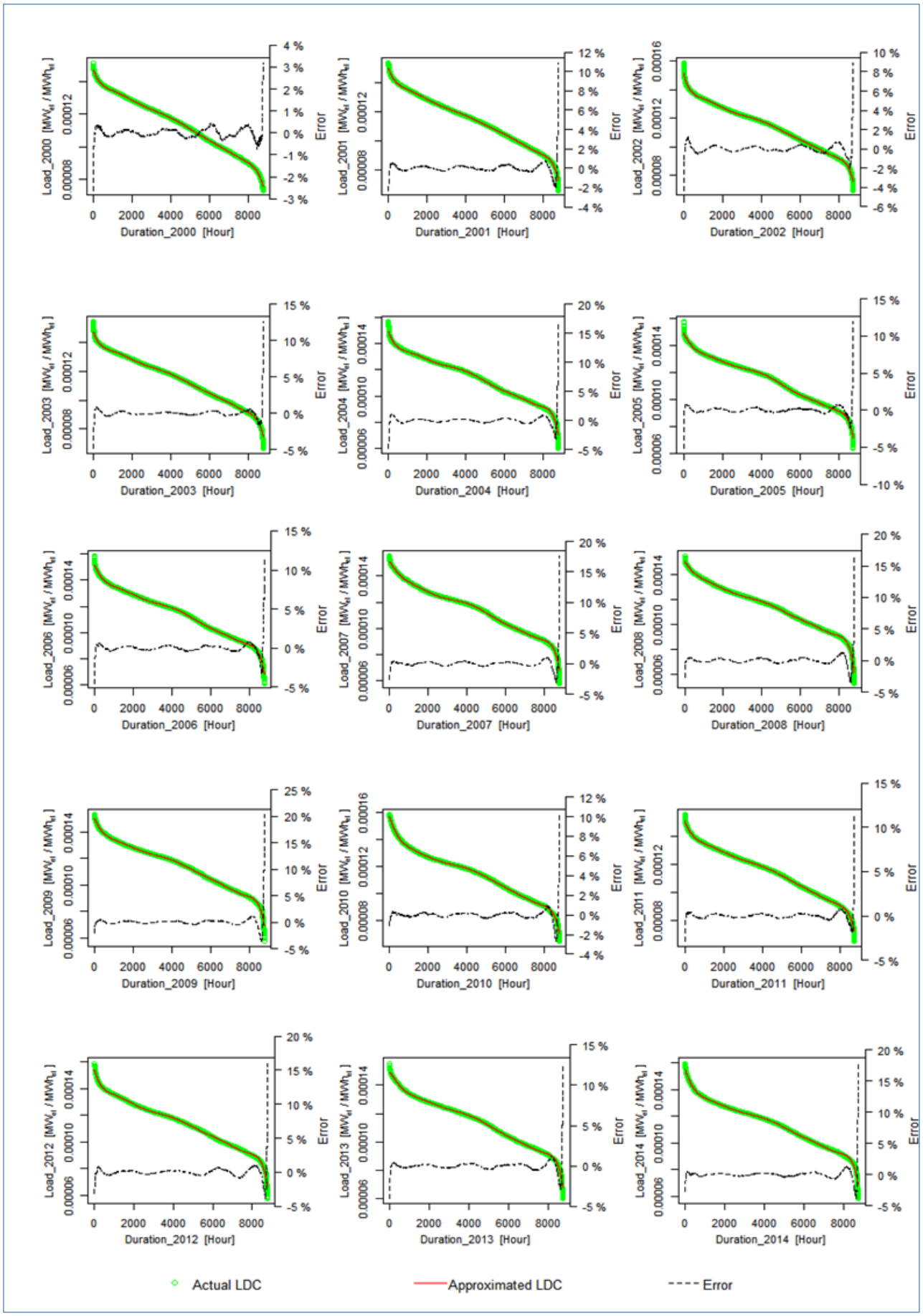

Plots of 11th Degree Polynomial Approximations to LDCs of Turkey in the Period 2000-2014

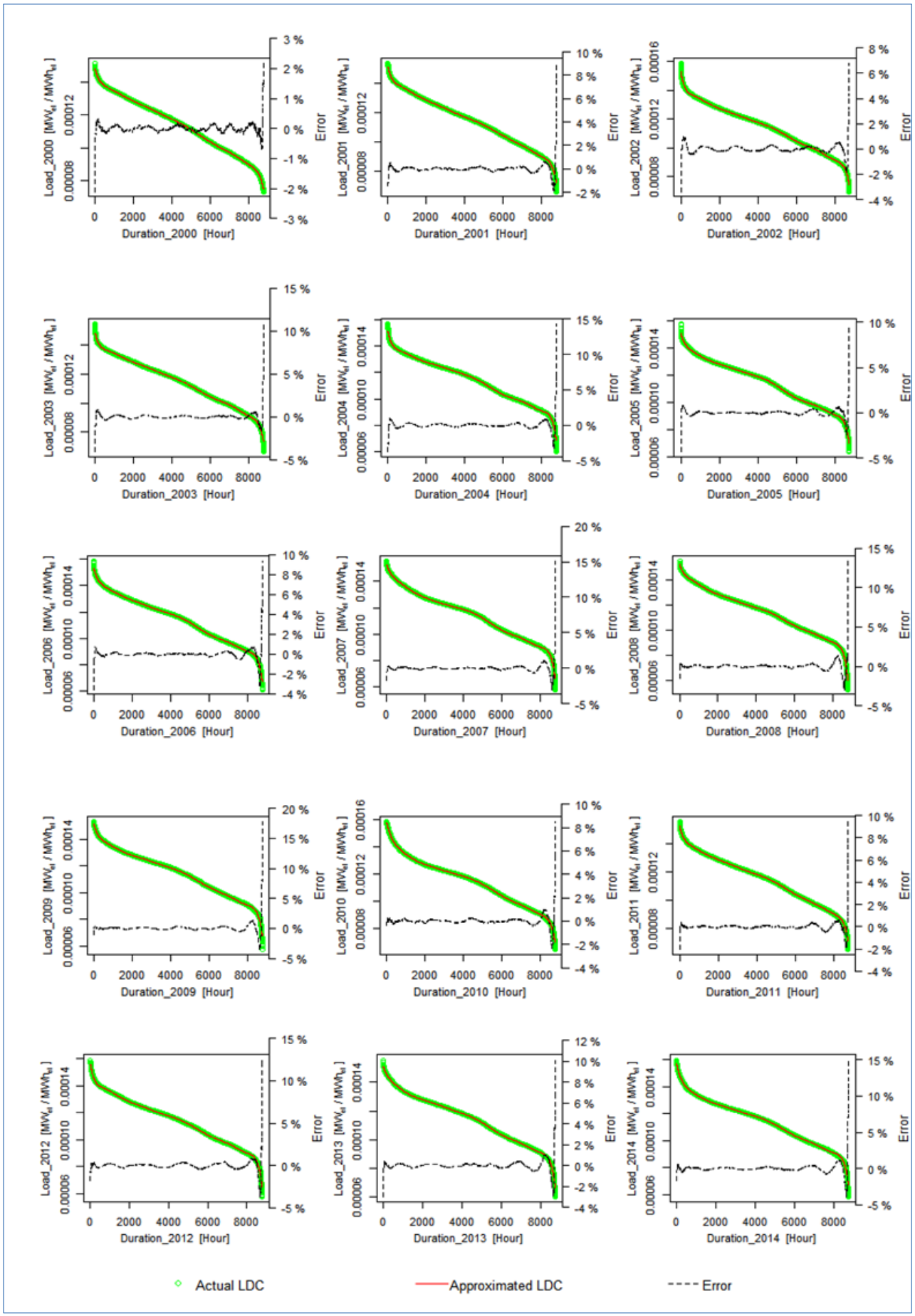

Plots of 12th Degree Polynomial Approximations to LDCs of Turkey in the Period 2000-2014

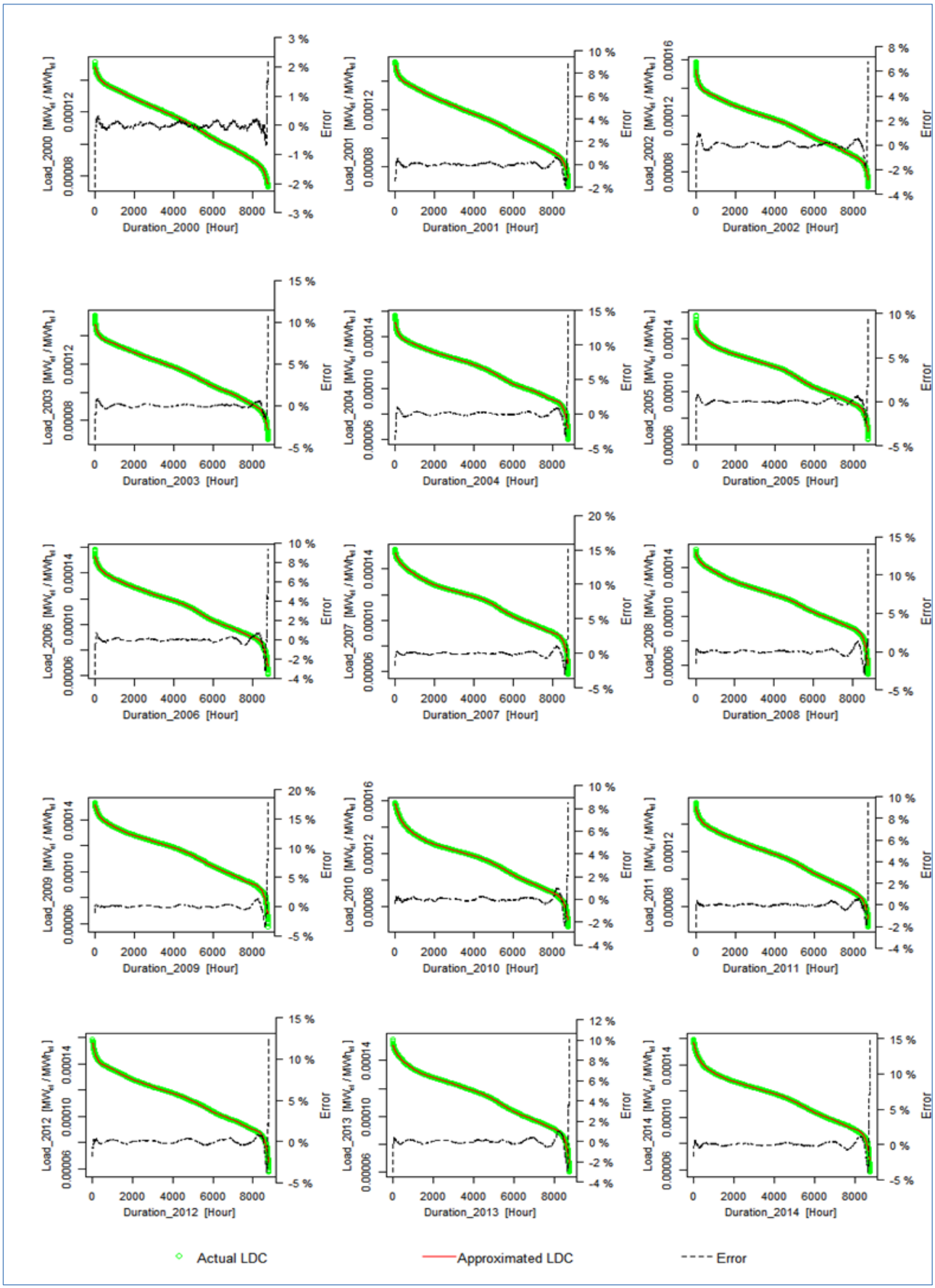

Plots of Exponential Functional Approximations to LDCs of Turkey in the Period 2000-2014

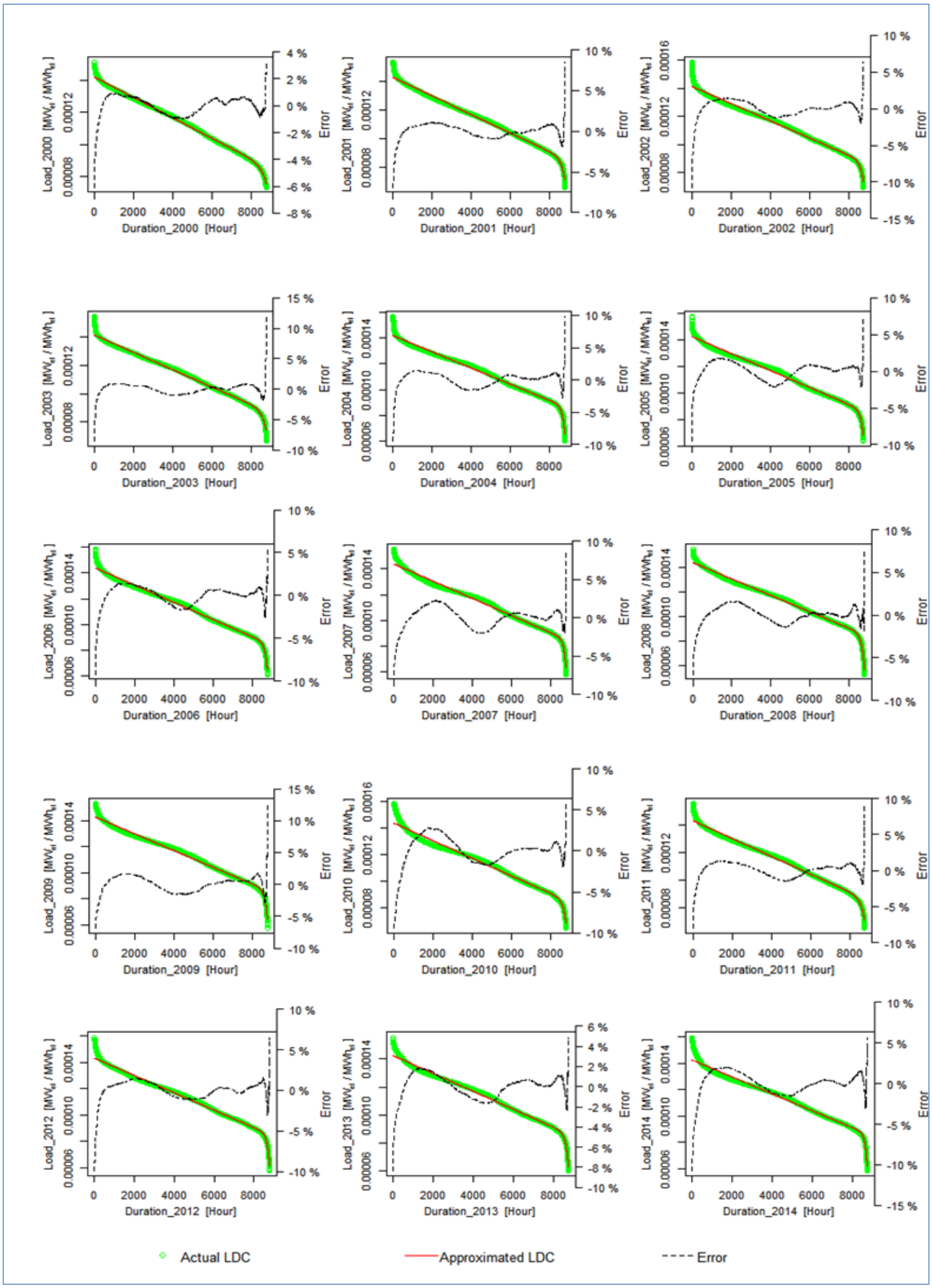

Plots of Logarithmic Functional Approximations to LDCs of Turkey in the Period 2000-2014

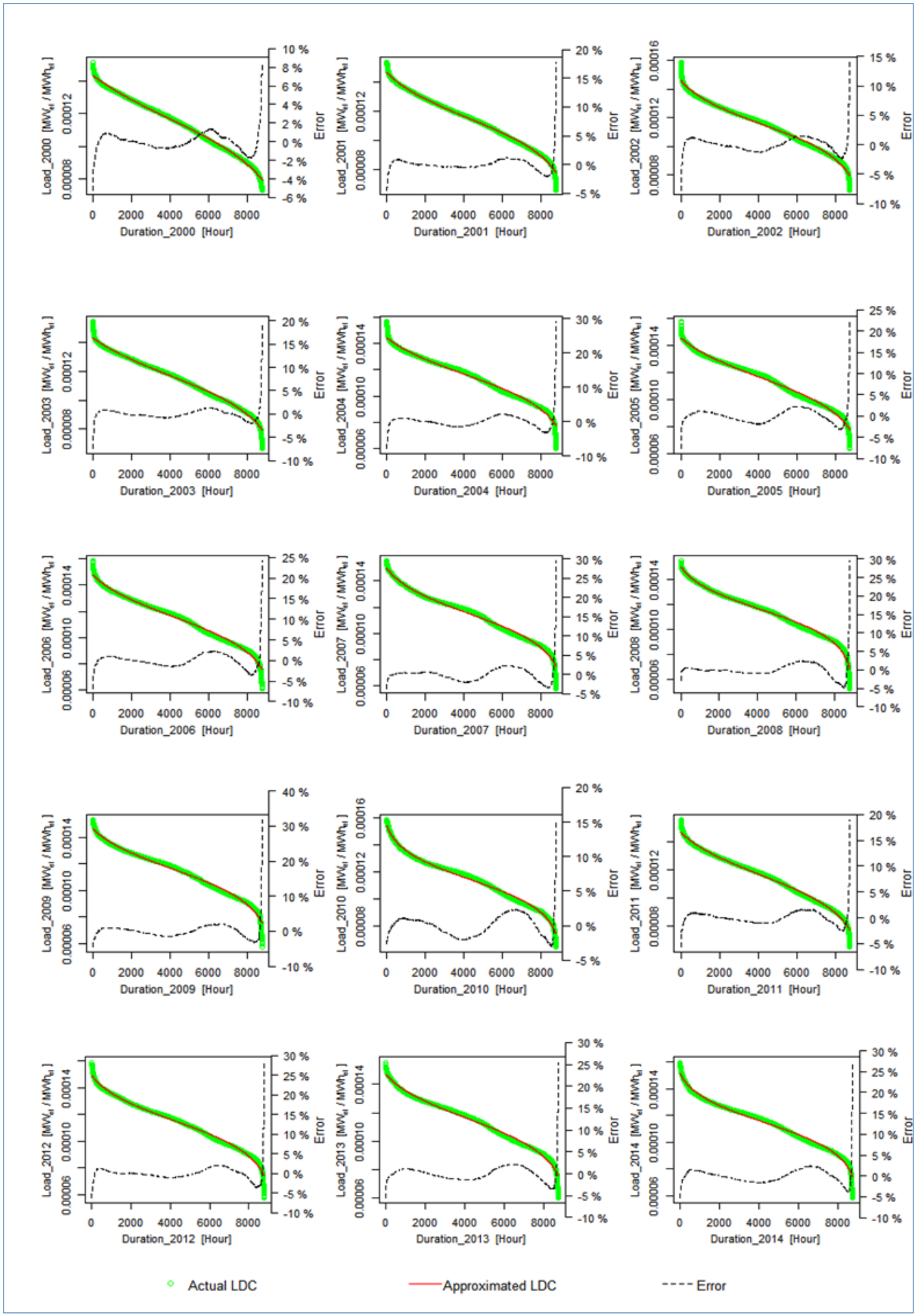

Plots of Approximations to LDCs of Turkey in the Period 2000-2014 Using Inverse of Hill's Function

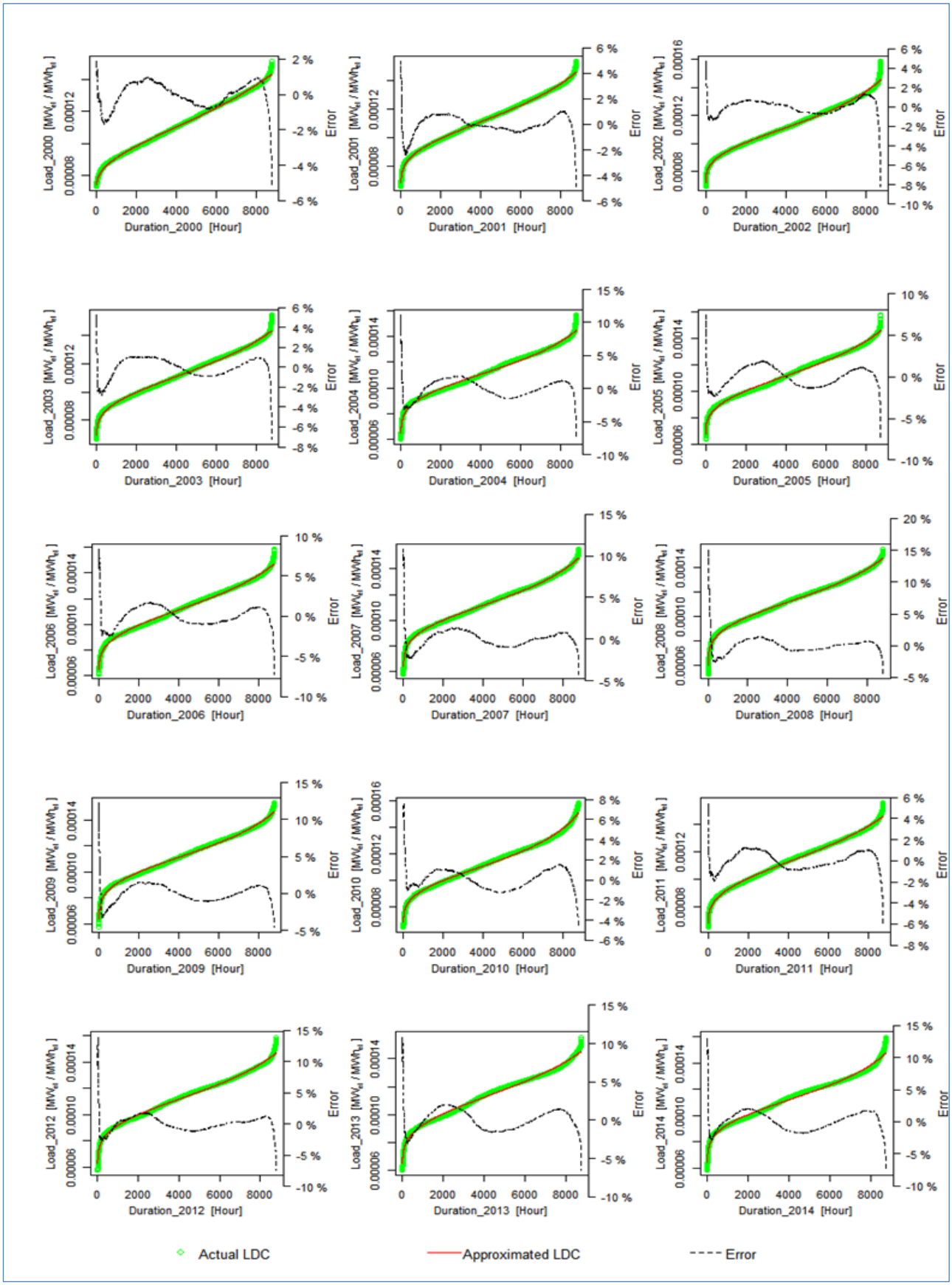

APPENDIX E

Summary Statistics of 4th Degree Polynomial Approximations to LDCs of Turkey in the Period 2000-2014

Year	Parameter	Estimate	Standard Error	t-value	Pr(>|t|)	95% Lower Confidence Limit	95% Upper Confidence Limit
2000	β_0	1.43332282E-04	6.33E-08	2265.49	< 2E-16	1.43208251E-04	1.43456313E-04
	β_1	-9.08304769E-09	1.05E-10	-86.44	< 2E-16	-9.28905567E-09	-8.87703971E-09
	β_2	1.08156890E-12	4.96E-14	21.80	< 2E-16	9.84291219E-13	1.17884658E-12
	β_3	-1.25279710E-16	8.54E-18	-14.67	< 2E-16	-1.42018117E-16	-1.08541303E-16
	β_4	3.20369212E-21	4.82E-22	6.65	< 2E-16	2.25873340E-21	4.14865084E-21
		R^2	Adjusted R^2	F-Statistic	Df (due to $RegSS$)	Df (due to RSS)	Pr>F
	Model	0.9964984	0.9964957	375788.203	4	5282	< 2E-16
Year	Parameter	Estimate	Standard Error	t-value	Pr(>|t|)	95% Lower Confidence Limit	95% Upper Confidence Limit
2001	β_0	1.45861420E-04	7.20E-08	2024.84	< 2E-16	1.45720201E-04	1.46002639E-04
	β_1	-1.10723789E-08	1.19E-10	-93.34	< 2E-16	-1.13049182E-08	-1.08398396E-08
	β_2	1.47625082E-12	5.61E-14	26.33	< 2E-16	1.36633913E-12	1.58616250E-12
	β_3	-1.36209677E-16	9.68E-18	-14.08	< 2E-16	-1.55179980E-16	-1.17239375E-16
	β_4	1.62513461E-21	5.48E-22	2.97	< 2E-16	5.50700525E-22	2.69956870E-21
		R^2	Adjusted R^2	F-Statistic	Df (due to $RegSS$)	Df (due to RSS)	Pr>F
	Model	0.9955853	0.9955821	311437.439	4	5524	< 2E-16
Year	Parameter	Estimate	Standard Error	t-value	Pr(>|t|)	95% Lower Confidence Limit	95% Upper Confidence Limit
2002	β_0	1.45237575E-04	8.90E-08	1632.01	< 2E-16	1.45063112E-04	1.45412038E-04
	β_1	-1.33119414E-08	1.49E-10	-89.33	< 2E-16	-1.36040758E-08	-1.30198070E-08
	β_2	2.77948791E-12	7.06E-14	39.40	< 2E-16	2.64117580E-12	2.91780003E-12
	β_3	-3.58524575E-16	1.22E-17	-29.43	< 2E-16	-3.82410387E-16	-3.34638763E-16
	β_4	1.38818718E-20	6.90E-22	20.11	< 2E-16	1.25285291E-20	1.52352144E-20
		R^2	Adjusted R^2	F-Statistic	Df (due to $RegSS$)	Df (due to RSS)	Pr>F
	Model	0.9925108	0.9925051	174402.822	4	5264	< 2E-16
Year	Parameter	Estimate	Standard Error	t-value	Pr(>|t|)	95% Lower Confidence Limit	95% Upper Confidence Limit
2003	β_0	1.42525976E-04	7.75E-08	1839.43	< 2E-16	1.42374077E-04	1.42677876E-04
	β_1	-8.53042529E-09	1.28E-10	-66.57	< 2E-16	-8.78163971E-09	-8.27921087E-09
	β_2	8.23938975E-13	6.05E-14	13.61	< 2E-16	7.05266038E-13	9.42611912E-13
	β_3	-6.50264545E-17	1.04E-17	-6.23	< 2E-16	-8.54947267E-17	-4.45581823E-17
	β_4	-9.78065199E-22	5.91E-22	-1.65	< 2E-16	-2.13722360E-21	1.81093201E-22
		R^2	Adjusted R^2	F-Statistic	Df (due to $RegSS$)	Df (due to RSS)	Pr>F
	Model	0.9942492	0.9942450	235172.358	4	5441	< 2E-16
Year	Parameter	Estimate	Standard Error	t-value	Pr(>|t|)	95% Lower Confidence Limit	95% Upper Confidence Limit
2004	β_0	1.43539908E-04	1.13E-07	1267.15	< 2E-16	1.43317839E-04	1.43761976E-04
	β_1	-1.03310212E-08	1.88E-10	-55.00	< 2E-16	-1.06992428E-08	-9.96279956E-09
	β_2	1.63523042E-12	8.82E-14	18.54	< 2E-16	1.46234371E-12	1.80811713E-12
	β_3	-2.00289380E-16	1.51E-17	-13.23	< 2E-16	-2.29973698E-16	-1.70605062E-16
	β_4	6.33688114E-21	8.55E-22	7.42	< 2E-16	4.66168485E-21	8.01207743E-21
		R^2	Adjusted R^2	F-Statistic	Df (due to $RegSS$)	Df (due to RSS)	Pr>F
	Model	0.9880840	0.9880755	116109.587	4	5601	< 2E-16
Year	Parameter	Estimate	Standard Error	t-value	Pr(>|t|)	95% Lower Confidence Limit	95% Upper Confidence Limit
2005	β_0	1.45167324E-04	1.06E-07	1370.74	< 2E-16	1.44959711E-04	1.45374936E-04
	β_1	-1.23780886E-08	1.77E-10	-70.04	< 2E-16	-1.27245592E-08	-1.20316179E-08
	β_2	2.57185964E-12	8.32E-14	30.90	< 2E-16	2.40869928E-12	2.73502000E-12
	β_3	-3.61002648E-16	1.43E-17	-25.17	< 2E-16	-3.89116478E-16	-3.32888817E-16
	β_4	1.53259081E-20	8.12E-22	18.87	< 2E-16	1.37333767E-20	1.69184395E-20
		R^2	Adjusted R^2	F-Statistic	Df (due to $RegSS$)	Df (due to RSS)	Pr>F
	Model	0.9895788	0.9895715	136383.505	4	5745	< 2E-16

Year	Parameter	Estimate	Standard Error	t-value	Pr(>|t|)	95% Lower Confidence Limit	95% Upper Confidence Limit
2006	β_0	1.46833734E-04	1.08E-07	1365.44	< 2E-16	1.46622925E-04	1.47044543E-04
	β_1	-1.22669887E-08	1.78E-10	-68.90	< 2E-16	-1.26160125E-08	-1.19179649E-08
	β_2	2.13817661E-12	8.39E-14	25.50	< 2E-16	1.97377261E-12	2.30258061E-12
	β_3	-2.64473338E-16	1.44E-17	-18.30	< 2E-16	-2.92800366E-16	-2.36146311E-16
	β_4	9.14917388E-21	8.18E-22	11.19	< 2E-16	7.54565138E-21	1.07526964E-20
		R^2	Adjusted R^2	F-Statistic	Df (due to $RegSS$)	Df (due to RSS)	Pr>F
	Model	0.9900320	0.9900253	148732.63	4	5990	< 2E-16
Year	Parameter	Estimate	Standard Error	t-value	Pr(>|t|)	95% Lower Confidence Limit	95% Upper Confidence Limit
2007	β_0	1.48480972E-04	1.06E-07	1405.06	< 2E-16	1.48273810E-04	1.48688134E-04
	β_1	-1.52965073E-08	1.74E-10	-87.79	< 2E-16	-1.56380948E-08	-1.49549197E-08
	β_2	3.36004945E-12	8.20E-14	40.96	< 2E-16	3.19924921E-12	3.52084969E-12
	β_3	-4.43453179E-16	1.42E-17	-31.32	< 2E-16	-4.71208578E-16	-4.15697779E-16
	β_4	1.79929455E-20	8.03E-22	22.41	< 2E-16	1.64187287E-20	1.95671623E-20
		R^2	Adjusted R^2	F-Statistic	Df (due to $RegSS$)	Df (due to RSS)	Pr>F
	Model	0.9900731	0.9900667	154018.364	4	6177	< 2E-16
Year	Parameter	Estimate	Standard Error	t-value	Pr(>|t|)	95% Lower Confidence Limit	95% Upper Confidence Limit
2008	β_0	1.47099476E-04	1.21E-07	1218.62	< 2E-16	1.46862845E-04	1.47336107E-04
	β_1	-1.15077000E-08	1.97E-10	-58.41	< 2E-16	-1.18939116E-08	-1.11214884E-08
	β_2	1.28078648E-12	9.22E-14	13.89	< 2E-16	1.09999448E-12	1.46157848E-12
	β_3	-5.66403950E-17	1.58E-17	-3.58	< 2E-16	-8.76620781E-17	-2.56187118E-17
	β_4	-5.10500688E-21	8.93E-22	-5.72	< 2E-16	-6.85560560E-21	-3.35440816E-21
		R^2	Adjusted R^2	F-Statistic	Df (due to $RegSS$)	Df (due to RSS)	Pr>F
	Model	0.9873974	0.9873896	127355.372	4	6502	< 2E-16
Year	Parameter	Estimate	Standard Error	t-value	Pr(>|t|)	95% Lower Confidence Limit	95% Upper Confidence Limit
2009	β_0	1.45715911E-04	1.03E-07	1417.01	< 2E-16	1.45514322E-04	1.45917500E-04
	β_1	-1.27184082E-08	1.70E-10	-75.03	< 2E-16	-1.30507082E-08	-1.23861083E-08
	β_2	2.56971499E-12	7.96E-14	32.27	< 2E-16	2.41363250E-12	2.72579748E-12
	β_3	-3.37662130E-16	1.37E-17	-24.65	< 2E-16	-3.64511376E-16	-3.10812885E-16
	β_4	1.28427330E-20	7.75E-22	16.58	< 2E-16	1.13240434E-20	1.43614226E-20
		R^2	Adjusted R^2	F-Statistic	Df (due to $RegSS$)	Df (due to RSS)	Pr>F
	Model	0.9899633	0.9899569	153475.74	4	6224	< 2E-16
Year	Parameter	Estimate	Standard Error	t-value	Pr(>|t|)	95% Lower Confidence Limit	95% Upper Confidence Limit
2010	β_0	1.51280677E-04	9.53E-08	1586.99	< 2E-16	1.51093807E-04	1.51467547E-04
	β_1	-2.05221151E-08	1.58E-10	-129.78	< 2E-16	-2.08321106E-08	-2.02121196E-08
	β_2	5.57473364E-12	7.44E-14	74.89	< 2E-16	5.42881491E-12	5.72065237E-12
	β_3	-7.80615061E-16	1.28E-17	-60.83	< 2E-16	-8.05771218E-16	-7.55458903E-16
	β_4	3.50736902E-20	7.27E-22	48.22	< 2E-16	3.36477361E-20	3.64996442E-20
		R^2	Adjusted R^2	F-Statistic	Df (due to $RegSS$)	Df (due to RSS)	Pr>F
	Model	0.9914950	0.9914896	186086.717	4	6385	< 2E-16
Year	Parameter	Estimate	Standard Error	t-value	Pr(>|t|)	95% Lower Confidence Limit	95% Upper Confidence Limit
2011	β_0	1.46232608E-04	7.52E-08	1944.81	< 2E-16	1.46085211E-04	1.46380005E-04
	β_1	-1.26076044E-08	1.22E-10	-103.65	< 2E-16	-1.28460399E-08	-1.23691688E-08
	β_2	2.39725107E-12	5.69E-14	42.12	< 2E-16	2.28568973E-12	2.50881240E-12
	β_3	-3.06494828E-16	9.79E-18	-31.32	< 2E-16	-3.25680038E-16	-2.87309618E-16
	β_4	1.13078703E-20	5.54E-22	20.40	< 2E-16	1.02214709E-20	1.23942697E-20
		R^2	Adjusted R^2	F-Statistic	Df (due to $RegSS$)	Df (due to RSS)	Pr>F
	Model	0.9941176	0.9941143	304829.534	4	7215	< 2E-16

Year	Parameter	Estimate	Standard Error	t-value	Pr(>|t|)	95% Lower Confidence Limit	95% Upper Confidence Limit
2012	β_0	1.47301020E-04	9.51E-08	1549.39	< 2E-16	1.47114658E-04	1.47487382E-04
	β_1	-1.30532139E-08	1.51E-10	-86.64	< 2E-16	-1.33485576E-08	-1.27578702E-08
	β_2	2.23373745E-12	6.99E-14	31.95	< 2E-16	2.09670993E-12	2.37076497E-12
	β_3	-2.46095659E-16	1.20E-17	-20.56	< 2E-16	-2.69556203E-16	-2.22635115E-16
	β_4	6.81906237E-21	6.76E-22	10.09	< 2E-16	5.49388444E-21	8.14424031E-21
		R^2	Adjusted R^2	F-Statistic	Df (due to $RegSS$)	Df (due to RSS)	Pr>F
	Model	0.9900664	0.9900616	206686.443	4	8295	< 2E-16
Year	Parameter	Estimate	Standard Error	t-value	Pr(>|t|)	95% Lower Confidence Limit	95% Upper Confidence Limit
2013	β_0	1.46180040E-04	9.42E-08	1551.50	< 2E-16	1.45995349E-04	1.46364731E-04
	β_1	-1.32597251E-08	1.49E-10	-88.82	< 2E-16	-1.35523522E-08	-1.29670981E-08
	β_2	2.78032401E-12	6.93E-14	40.11	< 2E-16	2.64443407E-12	2.91621395E-12
	β_3	-3.74184153E-16	1.19E-17	-31.47	< 2E-16	-3.97491688E-16	-3.50876619E-16
	β_4	1.51315171E-20	6.73E-22	22.47	< 2E-16	1.38117556E-20	1.64512785E-20
		R^2	Adjusted R^2	F-Statistic	Df (due to $RegSS$)	Df (due to RSS)	Pr>F
	Model	0.9891554	0.9891504	198019.923	4	8684	< 2E-16
Year	Parameter	Estimate	Standard Error	t-value	Pr(>|t|)	95% Lower Confidence Limit	95% Upper Confidence Limit
2014	β_0	1.48803382E-04	9.91E-08	1501.75	< 2E-16	1.48609149E-04	1.48997615E-04
	β_1	-1.71988785E-08	1.57E-10	-109.76	< 2E-16	-1.75060493E-08	-1.68917078E-08
	β_2	4.29409637E-12	7.27E-14	59.04	< 2E-16	4.15153424E-12	4.43665851E-12
	β_3	-5.93141916E-16	1.25E-17	-47.56	< 2E-16	-6.17590254E-16	-5.68693578E-16
	β_4	2.59209968E-20	7.06E-22	36.70	< 2E-16	2.45366305E-20	2.73053630E-20
		R^2	Adjusted R^2	F-Statistic	Df (due to $RegSS$)	Df (due to RSS)	Pr>F
	Model	0.9880294	0.9880240	180449.286	4	8745	< 2E-16

Summary Statistics of 5th Degree Polynomial Approximations to LDCs of Turkey in the Period 2000-2014

Year	Parameter	Estimate	Standard Error	t-value	Pr(>|t|)	95% Lower Confidence Limit	95% Upper Confidence Limit
2000	β_0	1.45553736E-04	4.69E-08	3101.40	< 2E-16	1.45461730E-04	1.45645741E-04
	β_1	-1.75698397E-08	1.16E-10	-152.07	< 2E-16	-1.77963406E-08	-1.73433387E-08
	β_2	8.03088767E-12	8.36E-14	96.06	< 2E-16	7.86698881E-12	8.19478654E-12
	β_3	-2.24998796E-15	2.43E-17	-92.55	< 2E-16	-2.29764616E-15	-2.20232976E-15
	β_4	2.75360676E-19	3.05E-21	90.23	< 2E-16	2.69377647E-19	2.81343706E-19
	β_5	-1.23586211E-23	1.38E-25	-89.62	< 2E-16	-1.26289620E-23	-1.20882802E-23
		R^2	Adjusted R^2	F-Statistic	Df (due to $RegSS$)	Df (due to RSS)	Pr>F
	Model	0.9986109	0.9986096	759317.052	5	5281	< 2E-16
Year	Parameter	Estimate	Standard Error	t-value	Pr(>|t|)	95% Lower Confidence Limit	95% Upper Confidence Limit
2001	β_0	1.47988583E-04	6.54E-08	2264.08	< 2E-16	1.47860445E-04	1.48116722E-04
	β_1	-1.90436503E-08	1.58E-10	-120.16	< 2E-16	-1.93543328E-08	-1.87329677E-08
	β_2	8.02271745E-12	1.15E-13	69.90	< 2E-16	7.79769953E-12	8.24773537E-12
	β_3	-2.14776272E-15	3.35E-17	-64.08	< 2E-16	-2.21347021E-15	-2.08205523E-15
	β_4	2.60591062E-19	4.23E-21	61.63	< 2E-16	2.52302296E-19	2.68879828E-19
	β_5	-1.18161963E-23	1.92E-25	-61.56	< 2E-16	-1.21925098E-23	-1.14398829E-23
		R^2	Adjusted R^2	F-Statistic	Df (due to $RegSS$)	Df (due to RSS)	Pr>F
	Model	0.9973817	0.9973793	420765.678	5	5523	< 2E-16
Year	Parameter	Estimate	Standard Error	t-value	Pr(>|t|)	95% Lower Confidence Limit	95% Upper Confidence Limit
2002	β_0	1.48024554E-04	7.63E-08	1939.02	< 2E-16	1.47874896E-04	1.48174212E-04
	β_1	-2.38797521E-08	1.88E-10	-126.88	< 2E-16	-2.42487029E-08	-2.35108013E-08
	β_2	1.14921341E-11	1.37E-13	83.96	< 2E-16	1.12237880E-11	1.17604801E-11
	β_3	-3.03487496E-15	4.00E-17	-75.91	< 2E-16	-3.11325402E-15	-2.95649590E-15
	β_4	3.57933162E-19	5.04E-21	71.06	< 2E-16	3.48058292E-19	3.67808031E-19
	β_5	-1.56717916E-23	2.28E-25	-68.64	< 2E-16	-1.61193645E-23	-1.52242188E-23
		R^2	Adjusted R^2	F-Statistic	Df (due to $RegSS$)	Df (due to RSS)	Pr>F
	Model	0.9960485	0.9960448	265329.796	5	5263	< 2E-16
Year	Parameter	Estimate	Standard Error	t-value	Pr(>|t|)	95% Lower Confidence Limit	95% Upper Confidence Limit
2003	β_0	1.45029201E-04	6.42E-08	2257.40	< 2E-16	1.44903253E-04	1.45155149E-04
	β_1	-1.81550627E-08	1.58E-10	-114.76	< 2E-16	-1.84652007E-08	-1.78449246E-08
	β_2	8.72731595E-12	1.15E-13	75.99	< 2E-16	8.50216683E-12	8.95246508E-12
	β_3	-2.48699729E-15	3.35E-17	-74.26	< 2E-16	-2.55265471E-15	-2.42133986E-15
	β_4	3.09959905E-19	4.22E-21	73.53	< 2E-16	3.01696433E-19	3.18223377E-19
	β_5	-1.41527157E-23	1.91E-25	-74.13	< 2E-16	-1.45269917E-23	-1.37784396E-23
		R^2	Adjusted R^2	F-Statistic	Df (due to $RegSS$)	Df (due to RSS)	Pr>F
	Model	0.9971391	0.9971365	379214.955	5	5440	< 2E-16
Year	Parameter	Estimate	Standard Error	t-value	Pr(>|t|)	95% Lower Confidence Limit	95% Upper Confidence Limit
2004	β_0	1.47387974E-04	0.00	1587.15	< 2E-16	1.47205926E-04	1.47570022E-04
	β_1	-2.48575157E-08	2.28E-10	-109.12	< 2E-16	-2.53040963E-08	-2.44109351E-08
	β_2	1.35314534E-11	1.65E-13	82.10	< 2E-16	1.32083666E-11	1.38545403E-11
	β_3	-3.83553103E-15	4.79E-17	-80.02	< 2E-16	-3.92949138E-15	-3.74157068E-15
	β_4	4.71571343E-19	6.01E-21	78.41	< 2E-16	4.59781242E-19	4.83361444E-19
	β_5	-2.11066860E-23	2.72E-25	-77.73	< 2E-16	-2.16389737E-23	-2.05743983E-23
		R^2	Adjusted R^2	F-Statistic	Df (due to $RegSS$)	Df (due to RSS)	Pr>F
	Model	0.9942685	0.9942634	194292.528	5	5600	< 2E-16
Year	Parameter	Estimate	Standard Error	t-value	Pr(>|t|)	95% Lower Confidence Limit	95% Upper Confidence Limit
2005	β_0	1.49140515E-04	8.02E-08	1859.25	< 2E-16	1.48983263E-04	1.49297767E-04
	β_1	-2.70437798E-08	1.96E-10	-138.21	< 2E-16	-2.74273795E-08	-2.66601802E-08
	β_2	1.45678339E-11	1.41E-13	103.16	< 2E-16	1.42909886E-11	1.48446792E-11
	β_3	-4.03607203E-15	4.11E-17	-98.14	< 2E-16	-4.11669223E-15	-3.95545182E-15
	β_4	4.87433349E-19	5.18E-21	94.16	< 2E-16	4.77284824E-19	4.97581874E-19
	β_5	-2.15089321E-23	2.35E-25	-91.66	< 2E-16	-2.19689748E-23	-2.10488893E-23
		R^2	Adjusted R^2	F-Statistic	Df (due to $RegSS$)	Df (due to RSS)	Pr>F
	Model	0.9957681	0.9957644	270312.649	5	5744	< 2E-16

Year	Parameter	Estimate	Standard Error	t-value	Pr(>|t|)	95% Lower Confidence Limit	95% Upper Confidence Limit
2006	β_0	1.50602074E-04	9.05E-08	1664.82	< 2E-16	1.50424737E-04	1.50779411E-04
	β_1	-2.61687478E-08	2.20E-10	-119.02	< 2E-16	-2.65997797E-08	-2.57377159E-08
	β_2	1.34892250E-11	1.59E-13	85.04	< 2E-16	1.31782712E-11	1.38001789E-11
	β_3	-3.74078428E-15	4.62E-17	-80.98	< 2E-16	-3.83133856E-15	-3.65023001E-15
	β_4	4.55794610E-19	5.82E-21	78.36	< 2E-16	4.44392336E-19	4.67196885E-19
	β_5	-2.03540121E-23	2.64E-25	-77.17	< 2E-16	-2.08710403E-23	-1.98369838E-23
		R^2	Adjusted R^2	F-Statistic	Df (due to $RegSS$)	Df (due to RSS)	Pr>F
	Model	0.9950021	0.9949980	238465.019	5	5989	< 2E-16
Year	Parameter	Estimate	Standard Error	t-value	Pr(>|t|)	95% Lower Confidence Limit	95% Upper Confidence Limit
2007	β_0	1.51968581E-04	9.58E-08	1586.09	< 2E-16	1.51780754E-04	1.52156408E-04
	β_1	-2.79472299E-08	2.31E-10	-121.10	< 2E-16	-2.83996302E-08	-2.74948296E-08
	β_2	1.37237580E-11	1.67E-13	82.26	< 2E-16	1.33966943E-11	1.40508217E-11
	β_3	-3.62442868E-15	4.87E-17	-74.43	< 2E-16	-3.71988911E-15	-3.52896825E-15
	β_4	4.27246461E-19	6.14E-21	69.58	< 2E-16	4.15209569E-19	4.39283353E-19
	β_5	-1.86678041E-23	2.79E-25	-66.98	< 2E-16	-1.92141314E-23	-1.81214768E-23
		R^2	Adjusted R^2	F-Statistic	Df (due to $RegSS$)	Df (due to RSS)	Pr>F
	Model	0.9942503	0.9942457	213593.976	5	6176	< 2E-16
Year	Parameter	Estimate	Standard Error	t-value	Pr(>|t|)	95% Lower Confidence Limit	95% Upper Confidence Limit
2008	β_0	1.51033529E-04	1.11E-07	1354.92	< 2E-16	1.50815011E-04	1.51252047E-04
	β_1	-2.56648551E-08	2.65E-10	-96.72	< 2E-16	-2.61850263E-08	-2.51446839E-08
	β_2	1.27810595E-11	1.90E-13	67.24	< 2E-16	1.24084312E-11	1.31536879E-11
	β_3	-3.57275443E-15	5.52E-17	-64.71	< 2E-16	-3.68099371E-15	-3.46451514E-15
	β_4	4.46160934E-19	6.94E-21	64.26	< 2E-16	4.32550005E-19	4.59771863E-19
	β_5	-2.05426691E-23	3.14E-25	-65.32	< 2E-16	-2.11591677E-23	-1.99261704E-23
		R^2	Adjusted R^2	F-Statistic	Df (due to $RegSS$)	Df (due to RSS)	Pr>F
	Model	0.9923913	0.9923854	169582.2	5	6501	< 2E-16
Year	Parameter	Estimate	Standard Error	t-value	Pr(>|t|)	95% Lower Confidence Limit	95% Upper Confidence Limit
2009	β_0	1.49309929E-04	8.80E-08	1696.31	< 2E-16	1.49137378E-04	1.49482480E-04
	β_1	-2.58866338E-08	2.12E-10	-1.22E+02	< 2E-16	-2.63030628E-08	-2.54702047E-08
	β_2	1.33147566E-11	1.53E-13	8.71E+01	< 2E-16	1.30149279E-11	1.36145853E-11
	β_3	-3.62850541E-15	4.45E-17	-81.49	< 2E-16	-3.71579119E-15	-3.54121963E-15
	β_4	4.35779123E-19	5.61E-21	77.71	< 2E-16	4.24786013E-19	4.46772234E-19
	β_5	-1.92820199E-23	2.54E-25	-75.80	< 2E-16	-1.97807115E-23	-1.87833283E-23
		R^2	Adjusted R^2	F-Statistic	Df (due to $RegSS$)	Df (due to RSS)	Pr>F
	Model	0.9947813	0.9947771	237245.471	5	6223	< 2E-16
Year	Parameter	Estimate	Standard Error	t-value	Pr(>|t|)	95% Lower Confidence Limit	95% Upper Confidence Limit
2010	β_0	1.55153698E-04	7.03E-08	2205.80	< 2E-16	1.55015810E-04	1.55291586E-04
	β_1	-3.46540374E-08	1.70E-10	-203.30	< 2E-16	-3.49881873E-08	-3.43198876E-08
	β_2	1.71421500E-11	1.23E-13	139.20	< 2E-16	1.69007397E-11	1.73835602E-11
	β_3	-4.32916943E-15	3.59E-17	-120.52	< 2E-16	-4.39958723E-15	-4.25875164E-15
	β_4	4.91513824E-19	4.53E-21	108.54	< 2E-16	4.82636639E-19	5.00391010E-19
	β_5	-2.08204185E-23	2.06E-25	-101.30	< 2E-16	-2.12233405E-23	-2.04174965E-23
		R^2	Adjusted R^2	F-Statistic	Df (due to $RegSS$)	Df (due to RSS)	Pr>F
	Model	0.9967380	0.9967355	390142.973	5	6384	< 2E-16
Year	Parameter	Estimate	Standard Error	t-value	Pr(>|t|)	95% Lower Confidence Limit	95% Upper Confidence Limit
2011	β_0	1.49219849E-04	6.28E-08	2375.86	< 2E-16	1.49096729E-04	1.49342968E-04
	β_1	-2.31434029E-08	1.48E-10	-156.28	< 2E-16	-2.34337051E-08	-2.28531007E-08
	β_2	1.09109456E-11	1.06E-13	103.18	< 2E-16	1.07036504E-11	1.11182408E-11
	β_3	-2.90805809E-15	3.07E-17	-94.69	< 2E-16	-2.96826129E-15	-2.84785490E-15
	β_4	3.45677359E-19	3.87E-21	89.38	< 2E-16	3.38095966E-19	3.53258752E-19
	β_5	-1.52584441E-23	1.76E-25	-86.89	< 2E-16	-1.56026693E-23	-1.49142189E-23
		R^2	Adjusted R^2	F-Statistic	Df (due to $RegSS$)	Df (due to RSS)	Pr>F
	Model	0.9971258	0.9971238	500544.159	5	7214	< 2E-16

Year	Parameter	Estimate	Standard Error	t-value	Pr(>|t|)	95% Lower Confidence Limit	95% Upper Confidence Limit
2012	β_0	1.50872331E-04	8.89E-08	1697.80	< 2E-16	1.50698137E-04	1.51046526E-04
	β_1	-2.53675973E-08	2.06E-10	-123.37	< 2E-16	-2.57706538E-08	-2.49645408E-08
	β_2	1.20845372E-11	1.46E-13	83.03	< 2E-16	1.17992269E-11	1.23698474E-11
	β_3	-3.24040982E-15	4.21E-17	-77.03	< 2E-16	-3.32287178E-15	-3.15794786E-15
	β_4	3.90396050E-19	5.28E-21	73.93	< 2E-16	3.80044346E-19	4.00747755E-19
	β_5	-1.74625906E-23	2.39E-25	-73.00	< 2E-16	-1.79315015E-23	-1.69936797E-23
		R^2	Adjusted R^2	F-Statistic	Df (due to $RegSS$)	Df (due to RSS)	Pr>F
	Model	0.9939522	0.9939486	272624.571	5	8294	< 2E-16
Year	Parameter	Estimate	Standard Error	t-value	Pr(>|t|)	95% Lower Confidence Limit	95% Upper Confidence Limit
2013	β_0	1.50505754E-04	7.57E-08	1987.10	< 2E-16	1.50357283E-04	1.50654225E-04
	β_1	-2.80863196E-08	1.75E-10	-160.56	< 2E-16	-2.84292230E-08	-2.77434162E-08
	β_2	1.46305536E-11	1.24E-13	118.22	< 2E-16	1.43879551E-11	1.48731520E-11
	β_3	-3.98174000E-15	3.58E-17	-111.16	< 2E-16	-4.05195591E-15	-3.91152408E-15
	β_4	4.78425178E-19	4.51E-21	106.14	< 2E-16	4.69589227E-19	4.87261128E-19
	β_5	-2.11539594E-23	2.05E-25	-103.30	< 2E-16	-2.15553840E-23	-2.07525348E-23
		R^2	Adjusted R^2	F-Statistic	Df (due to $RegSS$)	Df (due to RSS)	Pr>F
	Model	0.9951346	0.9951318	355189.614	5	8683	< 2E-16
Year	Parameter	Estimate	Standard Error	t-value	Pr(>|t|)	95% Lower Confidence Limit	95% Upper Confidence Limit
2014	β_0	1.53370735E-04	7.96E-08	1925.98	< 2E-16	1.53214637E-04	1.53526834E-04
	β_1	-3.28308903E-08	1.84E-10	-178.78	< 2E-16	-3.31908636E-08	-3.24709170E-08
	β_2	1.67830233E-11	1.30E-13	129.22	< 2E-16	1.65284277E-11	1.70376189E-11
	β_3	-4.39437825E-15	3.76E-17	-116.91	< 2E-16	-4.46805734E-15	-4.32069917E-15
	β_4	5.14030310E-19	4.73E-21	108.69	< 2E-16	5.04759366E-19	5.23301254E-19
	β_5	-2.22855299E-23	2.15E-25	-103.72	< 2E-16	-2.27066906E-23	-2.18643691E-23
		R^2	Adjusted R^2	F-Statistic	Df (due to $RegSS$)	Df (due to RSS)	Pr>F
	Model	0.9946331	0.9946300	324098.392	5	8744	< 2E-16

Summary Statistics of 6th Degree Polynomial Approximations to LDCs of Turkey in the Period 2000-2014

Year	Parameter	Estimate	Standard Error	t-value	Pr(>|t|)	95% Lower Confidence Limit	95% Upper Confidence Limit
2000	β_0	1.44820672E-04	5.01E-08	2890.05	< 2E-16	1.44722436E-04	1.44918909E-04
	β_1	-1.36609847E-08	1.70E-10	-80.13	< 2E-16	-1.39952230E-08	-1.33267465E-08
	β_2	3.44182809E-12	1.74E-13	19.78	< 2E-16	3.10077949E-12	3.78287670E-12
	β_3	-1.36028748E-16	7.52E-17	-1.81	< 2E-16	-2.83461696E-16	1.14041992E-17
	β_4	-1.77665434E-19	1.56E-20	-11.36	< 2E-16	-2.08315154E-19	-1.47015713E-19
	β_5	3.30402567E-23	1.55E-24	21.37	< 2E-16	3.00090843E-23	3.60714291E-23
	β_6	-1.71993646E-27	5.84E-29	-29.46	< 2E-16	-1.83437945E-27	-1.60549348E-27
		R^2	Adjusted R^2	F-Statistic	Df (due to $RegSS$)	Df (due to RSS)	Pr>F
	Model	0.9988071	0.9988057	736797.252	6	5280	< 2E-16
Year	Parameter	Estimate	Standard Error	t-value	Pr(>|t|)	95% Lower Confidence Limit	95% Upper Confidence Limit
2001	β_0	1.47115228E-04	7.13E-08	2064.03	< 2E-16	1.46975499E-04	1.47254956E-04
	β_1	-1.44398315E-08	2.39E-10	-60.51	< 2E-16	-1.49076827E-08	-1.39719804E-08
	β_2	2.60261483E-12	2.44E-13	10.67	< 2E-16	2.12452089E-12	3.08070877E-12
	β_3	3.60120802E-16	1.06E-16	3.40	0.0007	1.52593738E-16	5.67647867E-16
	β_4	-2.79228431E-19	2.21E-20	-12.63	< 2E-16	-3.22555682E-19	-2.35901180E-19
	β_5	4.25099629E-23	2.19E-24	19.37	< 2E-16	3.82071663E-23	4.68127596E-23
	β_6	-2.06657849E-27	8.32E-29	-24.84	< 2E-16	-2.22969363E-27	-1.90346336E-27
		R^2	Adjusted R^2	F-Statistic	Df (due to $RegSS$)	Df (due to RSS)	Pr>F
	Model	0.9976448	0.9976422	389841.289	6	5522	< 2E-16
Year	Parameter	Estimate	Standard Error	t-value	Pr(>|t|)	95% Lower Confidence Limit	95% Upper Confidence Limit
2002	β_0	1.47335538E-04	8.57E-08	1718.94	< 2E-16	1.47167505E-04	1.47503571E-04
	β_1	-2.02286119E-08	2.90E-10	-69.72	< 2E-16	-2.07973999E-08	-1.96598240E-08
	β_2	7.17126884E-12	2.97E-13	24.11	< 2E-16	6.58808063E-12	7.75445704E-12
	β_3	-1.03148063E-15	1.29E-16	-7.98	< 2E-16	-1.28490337E-15	-7.78057891E-16
	β_4	-7.36103963E-20	2.70E-20	-2.73	0.0064	-1.26538081E-19	-2.06827113E-20
	β_5	2.77614062E-23	2.68E-24	10.35	< 2E-16	2.25053006E-23	3.30175117E-23
	β_6	-1.65175940E-27	1.02E-28	-16.26	< 2E-16	-1.85095710E-27	-1.45256170E-27
		R^2	Adjusted R^2	F-Statistic	Df (due to $RegSS$)	Df (due to RSS)	Pr>F
	Model	0.9962375	0.9962332	232211.966	6	5262	< 2E-16
Year	Parameter	Estimate	Standard Error	t-value	Pr(>|t|)	95% Lower Confidence Limit	95% Upper Confidence Limit
2003	β_0	1.44150049E-04	6.99E-08	2062.03	< 2E-16	1.44013003E-04	1.44287095E-04
	β_1	-1.34344481E-08	2.38E-10	-56.33	< 2E-16	-1.39020008E-08	-1.29668953E-08
	β_2	3.18106722E-12	2.44E-13	13.05	< 2E-16	2.70317863E-12	3.65895582E-12
	β_3	7.05510405E-17	1.06E-16	0.67	0.5037	-1.36281550E-16	2.77383631E-16
	β_4	-2.39044489E-19	2.20E-20	-10.88	< 2E-16	-2.82110803E-19	-1.95978174E-19
	β_5	4.09793165E-23	2.18E-24	18.82	< 2E-16	3.67115922E-23	4.52470409E-23
	β_6	-2.09355786E-27	8.24E-29	-25.41	< 2E-16	-2.25506029E-27	-1.93205544E-27
		R^2	Adjusted R^2	F-Statistic	Df (due to $RegSS$)	Df (due to RSS)	Pr>F
	Model	0.9974428	0.9974399	353577.154	6	5439	< 2E-16
Year	Parameter	Estimate	Standard Error	t-value	Pr(>|t|)	95% Lower Confidence Limit	95% Upper Confidence Limit
2004	β_0	1.45606172E-04	9.60E-08	1517.27	< 2E-16	1.45418043E-04	1.45794302E-04
	β_1	-1.54995341E-08	3.24E-10	-47.86	< 2E-16	-1.61344297E-08	-1.48646384E-08
	β_2	2.56383953E-12	3.30E-13	7.78	< 2E-16	1.91753267E-12	3.21014639E-12
	β_3	1.21135990E-15	1.42E-16	8.51	< 2E-16	9.32424587E-16	1.49029521E-15
	β_4	-6.09339469E-19	2.95E-20	-20.62	< 2E-16	-6.67267457E-19	-5.51411482E-19
	β_5	8.71800657E-23	2.92E-24	29.85	< 2E-16	8.14541122E-23	9.29060193E-23
	β_6	-4.10179959E-27	1.10E-28	-37.20	< 2E-16	-4.31794043E-27	-3.88565874E-27
		R^2	Adjusted R^2	F-Statistic	Df (due to $RegSS$)	Df (due to RSS)	Pr>F
	Model	0.9954045	0.9953996	202129.341	6	5599	< 2E-16

Year	Parameter	Estimate	Standard Error	t-value	Pr(>|t|)	95% Lower Confidence Limit	95% Upper Confidence Limit
2005	β_0	1.47127805E-04	7.61E-08	1933.43	< 2E-16	1.46978627E-04	1.47276983E-04
	β_1	-1.66802802E-08	2.54E-10	-65.73	< 2E-16	-1.71777299E-08	-1.61828305E-08
	β_2	2.38254087E-12	2.58E-13	9.22	< 2E-16	1.87589976E-12	2.88918197E-12
	β_3	1.59819553E-15	1.12E-16	14.27	< 2E-16	1.37860957E-15	1.81778148E-15
	β_4	-7.24841437E-19	2.34E-20	-31.02	< 2E-16	-7.70655047E-19	-6.79027827E-19
	β_5	1.00461189E-22	2.32E-24	43.30	< 2E-16	9.59128935E-23	1.05009485E-22
	β_6	-4.63897373E-27	8.79E-29	-52.75	< 2E-16	-4.81136501E-27	-4.46658245E-27
		R^2	Adjusted R^2	F-Statistic	Df (due to $RegSS$)	Df (due to RSS)	Pr>F
	Model	0.9971494	0.9971464	334819.92	6	5743	< 2E-16
Year	Parameter	Estimate	Standard Error	t-value	Pr(>|t|)	95% Lower Confidence Limit	95% Upper Confidence Limit
2006	β_0	1.48427070E-04	8.86E-08	1675.41	< 2E-16	1.48253399E-04	1.48600742E-04
	β_1	-1.49960476E-08	2.95E-10	-50.81	< 2E-16	-1.55746629E-08	-1.44174323E-08
	β_2	4.14807975E-13	3.00E-13	1.38	0.1666	-1.73024839E-13	1.00264079E-12
	β_3	2.29036298E-15	1.30E-16	17.66	< 2E-16	2.03606014E-15	2.54466581E-15
	β_4	-8.40324144E-19	2.70E-20	-31.08	< 2E-16	-8.93320875E-19	-7.87327413E-19
	β_5	1.09974218E-22	2.68E-24	41.00	< 2E-16	1.04716069E-22	1.15232367E-22
	β_6	-4.95552616E-27	1.02E-28	-48.76	< 2E-16	-5.15476584E-27	-4.75628647E-27
		R^2	Adjusted R^2	F-Statistic	Df (due to $RegSS$)	Df (due to RSS)	Pr>F
	Model	0.9964225	0.9964189	277967.866	6	5988	< 2E-16
Year	Parameter	Estimate	Standard Error	t-value	Pr(>|t|)	95% Lower Confidence Limit	95% Upper Confidence Limit
2007	β_0	1.48917933E-04	8.01E-08	1858.19	< 2E-16	1.48760828E-04	1.49075038E-04
	β_1	-1.25200540E-08	2.64E-10	-47.43	< 2E-16	-1.30374879E-08	-1.20026201E-08
	β_2	-4.35322273E-12	2.68E-13	-16.22	< 2E-16	-4.87945826E-12	-3.82698721E-12
	β_3	4.73222445E-15	1.16E-16	40.68	< 2E-16	4.50415330E-15	4.96029560E-15
	β_4	-1.37165628E-18	2.43E-20	-56.49	< 2E-16	-1.41925747E-18	-1.32405510E-18
	β_5	1.62449238E-22	2.41E-24	67.35	< 2E-16	1.57720701E-22	1.67177775E-22
	β_6	-6.89375639E-27	9.15E-29	-75.35	< 2E-16	-7.07310899E-27	-6.71440378E-27
		R^2	Adjusted R^2	F-Statistic	Df (due to $RegSS$)	Df (due to RSS)	Pr>F
	Model	0.9970045	0.9970016	342542.599	6	6175	< 2E-16
Year	Parameter	Estimate	Standard Error	t-value	Pr(>|t|)	95% Lower Confidence Limit	95% Upper Confidence Limit
2008	β_0	1.47783848E-04	1.02E-07	1454.97	< 2E-16	1.47584734E-04	1.47982961E-04
	β_1	-9.27925144E-09	3.32E-10	-27.92	< 2E-16	-9.93079848E-09	-8.62770441E-09
	β_2	-6.28721915E-12	3.36E-13	-18.71	< 2E-16	-6.94612191E-12	-5.62831639E-12
	β_3	5.19475450E-15	1.45E-16	35.81	< 2E-16	4.91036697E-15	5.47914204E-15
	β_4	-1.43300419E-18	3.02E-20	-47.50	< 2E-16	-1.49214016E-18	-1.37386822E-18
	β_5	1.67954278E-22	2.99E-24	56.24	< 2E-16	1.62100284E-22	1.73808272E-22
	β_6	-7.15089277E-27	1.13E-28	-63.34	< 2E-16	-7.37220923E-27	-6.92957631E-27
		R^2	Adjusted R^2	F-Statistic	Df (due to $RegSS$)	Df (due to RSS)	Pr>F
	Model	0.9952952	0.9952908	229176.137	6	6500	< 2E-16
Year	Parameter	Estimate	Standard Error	t-value	Pr(>|t|)	95% Lower Confidence Limit	95% Upper Confidence Limit
2009	β_0	1.47379959E-04	8.96E-08	1645.07	< 2E-16	1.47204335E-04	1.47555584E-04
	β_1	-1.60227123E-08	2.97E-10	-53.98	< 2E-16	-1.66045611E-08	-1.54408635E-08
	β_2	1.79270569E-12	3.01E-13	5.95	< 2E-16	1.20234874E-12	2.38306264E-12
	β_3	1.67824999E-15	1.30E-16	12.90	< 2E-16	1.42314295E-15	1.93335702E-15
	β_4	-7.03203826E-19	2.71E-20	-25.96	< 2E-16	-7.56307942E-19	-6.50099711E-19
	β_5	9.51375072E-23	2.69E-24	35.43	< 2E-16	8.98736041E-23	1.00401410E-22
	β_6	-4.34784503E-27	1.02E-28	-42.76	< 2E-16	-4.54717380E-27	-4.14851626E-27
		R^2	Adjusted R^2	F-Statistic	Df (due to $RegSS$)	Df (due to RSS)	Pr>F
	Model	0.9959666	0.9959627	256066.026	6	6222	< 2E-16

Year	Parameter	Estimate	Standard Error	t-value	Pr(>|t|)	95% Lower Confidence Limit	95% Upper Confidence Limit
2010	β_0	1.53663051E-04	7.31E-08	2102.78	< 2E-16	1.53519797E-04	1.53806305E-04
	β_1	-2.71084845E-08	2.42E-10	-111.87	< 2E-16	-2.75835341E-08	-2.66334349E-08
	β_2	8.31707497E-12	2.46E-13	33.76	< 2E-16	7.83417014E-12	8.79997981E-12
	β_3	-2.57967069E-16	1.07E-16	-2.42	0.0156	-4.66960678E-16	-4.89734590E-17
	β_4	-3.83416818E-19	2.22E-20	-17.26	< 2E-16	-4.26973916E-19	-3.39859720E-19
	β_5	6.71604979E-23	2.20E-24	30.46	< 2E-16	6.28387857E-23	7.14822101E-23
	β_6	-3.34583550E-27	8.35E-29	-40.05	< 2E-16	-3.50961441E-27	-3.18205659E-27
		R^2	Adjusted R^2	F-Statistic	Df (due to $RegSS$)	Df (due to RSS)	Pr>F
	Model	0.9973931	0.9973906	407013.272	6	6383	< 2E-16
Year	Parameter	Estimate	Standard Error	t-value	Pr(>|t|)	95% Lower Confidence Limit	95% Upper Confidence Limit
2011	β_0	1.47918196E-04	6.66E-08	2220.08	< 2E-16	1.47787586E-04	1.48048805E-04
	β_1	-1.67262632E-08	2.15E-10	-77.65	< 2E-16	-1.71485412E-08	-1.63039851E-08
	β_2	3.49132142E-12	2.17E-13	16.11	< 2E-16	3.06655100E-12	3.91609184E-12
	β_3	4.99576555E-16	9.34E-17	5.35	< 2E-16	3.16451080E-16	6.82702031E-16
	β_4	-3.85423047E-19	1.94E-20	-19.82	< 2E-16	-4.23537327E-19	-3.47308767E-19
	β_5	5.82257656E-23	1.93E-24	30.19	< 2E-16	5.44453271E-23	6.20062040E-23
	β_6	-2.79488437E-27	7.31E-29	-38.24	< 2E-16	-2.93817232E-27	-2.65159642E-27
		R^2	Adjusted R^2	F-Statistic	Df (due to $RegSS$)	Df (due to RSS)	Pr>F
	Model	0.9976102	0.9976082	501840.737	6	7213	< 2E-16
Year	Parameter	Estimate	Standard Error	t-value	Pr(>|t|)	95% Lower Confidence Limit	95% Upper Confidence Limit
2012	β_0	1.48886482E-04	9.44E-08	1576.94	< 2E-16	1.48701405E-04	1.49071558E-04
	β_1	-1.57806134E-08	3.00E-10	-52.64	< 2E-16	-1.63682304E-08	-1.51929964E-08
	β_2	1.12856027E-12	2.98E-13	3.78	0.0002	5.43578170E-13	1.71354236E-12
	β_3	1.75754202E-15	1.28E-16	13.75	< 2E-16	1.50697973E-15	2.00810432E-15
	β_4	-6.77288427E-19	2.65E-20	-25.57	< 2E-16	-7.29212427E-19	-6.25364426E-19
	β_5	8.95270857E-23	2.62E-24	34.18	< 2E-16	8.43928019E-23	9.46613694E-23
	β_6	-4.05978058E-27	9.90E-29	-40.99	< 2E-16	-4.25392685E-27	-3.86563432E-27
		R^2	Adjusted R^2	F-Statistic	Df (due to $RegSS$)	Df (due to RSS)	Pr>F
	Model	0.9949711	0.9949675	273464.36	6	8293	< 2E-16
Year	Parameter	Estimate	Standard Error	t-value	Pr(>|t|)	95% Lower Confidence Limit	95% Upper Confidence Limit
2013	β_0	1.48047621E-04	7.21E-08	2053.90	< 2E-16	1.47906325E-04	1.48188918E-04
	β_1	-1.62972202E-08	2.28E-10	-71.39	< 2E-16	-1.67447013E-08	-1.58497391E-08
	β_2	1.16868695E-12	2.27E-13	5.14	< 2E-16	7.23401621E-13	1.61397228E-12
	β_3	2.16559287E-15	9.74E-17	22.23	< 2E-16	1.97463716E-15	2.35654858E-15
	β_4	-8.37287197E-19	2.02E-20	-41.39	< 2E-16	-8.76937001E-19	-7.97637392E-19
	β_5	1.11004195E-22	2.00E-24	55.37	< 2E-16	1.07074185E-22	1.14934205E-22
	β_6	-5.02819307E-27	7.60E-29	-66.15	< 2E-16	-5.17719774E-27	-4.87918839E-27
		R^2	Adjusted R^2	F-Statistic	Df (due to $RegSS$)	Df (due to RSS)	Pr>F
	Model	0.9967650	0.9967627	445845.921	6	8682	< 2E-16
Year	Parameter	Estimate	Standard Error	t-value	Pr(>|t|)	95% Lower Confidence Limit	95% Upper Confidence Limit
2014	β_0	1.51802164E-04	8.70E-08	1743.86	< 2E-16	1.51631527E-04	1.51972802E-04
	β_1	-2.53163190E-08	2.75E-10	-91.95	< 2E-16	-2.58560016E-08	-2.47766363E-08
	β_2	8.20731389E-12	2.74E-13	29.97	< 2E-16	7.67054879E-12	8.74407899E-12
	β_3	-4.79380369E-16	1.17E-16	-4.08	< 2E-16	-7.09503627E-16	-2.49257110E-16
	β_4	-3.23792203E-19	2.44E-20	-13.29	< 2E-16	-3.71568212E-19	-2.76016194E-19
	β_5	6.18665341E-23	2.42E-24	25.61	< 2E-16	5.71313254E-23	6.66017427E-23
	β_6	-3.20170194E-27	9.16E-29	-34.96	< 2E-16	-3.38123428E-27	-3.02216961E-27
		R^2	Adjusted R^2	F-Statistic	Df (due to $RegSS$)	Df (due to RSS)	Pr>F
	Model	0.9952912	0.9952880	308001.427	6	8743	< 2E-16

Summary Statistics of 7th Degree Polynomial Approximations to LDCs of Turkey in the Period 2000-2014

Year	Parameter	Estimate	Standard Error	t-value	Pr(>|t|)	95% Lower Confidence Limit	95% Upper Confidence Limit
2000	β_0	1.46288399E-04	3.63E-08	4032.96	< 2E-16	1.46217288E-04	1.46359509E-04
	β_1	-2.40195136E-08	1.62E-10	-148.67	< 2E-16	-2.43362469E-08	-2.37027803E-08
	β_2	1.99113815E-11	2.20E-13	90.66	< 2E-16	1.94808231E-11	2.03419398E-11
	β_3	-1.07091061E-14	1.31E-16	-81.94	< 2E-16	-1.09653091E-14	-1.04529030E-14
	β_4	3.15503251E-18	3.96E-20	79.71	< 2E-16	3.07744093E-18	3.23262410E-18
	β_5	-5.14812950E-22	6.37E-24	-80.79	< 2E-16	-5.27304496E-22	-5.02321403E-22
	β_6	4.33486724E-26	5.19E-28	83.50	< 2E-16	4.23309240E-26	4.43664209E-26
	β_7	-1.46478538E-30	1.68E-32	-87.04	< 2E-16	-1.49777745E-30	-1.43179331E-30
		R^2	Adjusted R^2	F-Statistic	Df (due to $RegSS$)	Df (due to RSS)	Pr>F
	Model	0.9995101	0.9995095	1538635.22	7	5279	< 2E-16
Year	Parameter	Estimate	Standard Error	t-value	Pr(>|t|)	95% Lower Confidence Limit	95% Upper Confidence Limit
2001	β_0	1.49153432E-04	5.54E-08	2692.16	< 2E-16	1.49044820E-04	1.49262044E-04
	β_1	-2.87212472E-08	2.45E-10	-117.38	< 2E-16	-2.92009478E-08	-2.82415466E-08
	β_2	2.52838564E-11	3.34E-13	75.79	< 2E-16	2.46298372E-11	2.59378755E-11
	β_3	-1.42175013E-14	1.99E-16	-71.38	< 2E-16	-1.46079628E-14	-1.38270398E-14
	β_4	4.32434395E-18	6.05E-20	71.49	< 2E-16	4.20575396E-18	4.44293393E-18
	β_5	-7.15877935E-22	9.76E-24	-73.32	< 2E-16	-7.35018621E-22	-6.96737249E-22
	β_6	6.04633885E-26	7.97E-28	75.82	< 2E-16	5.89001265E-26	6.20266505E-26
	β_7	-2.03712212E-30	2.59E-32	-78.62	< 2E-16	-2.08791959E-30	-1.98632465E-30
		R^2	Adjusted R^2	F-Statistic	Df (due to $RegSS$)	Df (due to RSS)	Pr>F
	Model	0.9988888	0.9988874	708980.357	7	5521	< 2E-16
Year	Parameter	Estimate	Standard Error	t-value	Pr(>|t|)	95% Lower Confidence Limit	95% Upper Confidence Limit
2002	β_0	1.49537560E-04	7.17E-08	2086.27	< 2E-16	1.49397044E-04	1.49678077E-04
	β_1	-3.57586362E-08	3.19E-10	-112.21	< 2E-16	-3.63833515E-08	-3.51339209E-08
	β_2	3.20706367E-11	4.37E-13	73.38	< 2E-16	3.12138482E-11	3.29274252E-11
	β_3	-1.71244674E-14	2.62E-16	-65.33	< 2E-16	-1.76382997E-14	-1.66106350E-14
	β_4	5.02434290E-18	7.98E-20	62.93	< 2E-16	4.86781854E-18	5.18086725E-18
	β_5	-8.13567009E-22	1.29E-23	-63.01	< 2E-16	-8.38877548E-22	-7.88256469E-22
	β_6	6.77890401E-26	1.06E-27	64.22	< 2E-16	6.57195375E-26	6.98585427E-26
	β_7	-2.26362113E-30	3.43E-32	-65.95	< 2E-16	-2.33091115E-30	-2.19633111E-30
		R^2	Adjusted R^2	F-Statistic	Df (due to $RegSS$)	Df (due to RSS)	Pr>F
	Model	0.9979402	0.9979375	364131.135	7	5261	< 2E-16
Year	Parameter	Estimate	Standard Error	t-value	Pr(>|t|)	95% Lower Confidence Limit	95% Upper Confidence Limit
2003	β_0	1.45811145E-04	6.26E-08	2328.39	< 2E-16	1.45688379E-04	1.45933912E-04
	β_1	-2.52494668E-08	2.81E-10	-89.87	< 2E-16	-2.58002547E-08	-2.46986788E-08
	β_2	2.19878125E-11	3.83E-13	57.38	< 2E-16	2.12365720E-11	2.27390530E-11
	β_3	-1.20201823E-14	2.29E-16	-52.58	< 2E-16	-1.24683640E-14	-1.15720005E-14
	β_4	3.57875363E-18	6.94E-20	51.56	< 2E-16	3.44268497E-18	3.71482230E-18
	β_5	-5.87870213E-22	1.12E-23	-52.48	< 2E-16	-6.09828672E-22	-5.65911753E-22
	β_6	4.97493159E-26	9.15E-28	54.39	< 2E-16	4.79560586E-26	5.15425731E-26
	β_7	-1.68875723E-30	2.97E-32	-56.82	< 2E-16	-1.74702287E-30	-1.63049158E-30
		R^2	Adjusted R^2	F-Statistic	Df (due to $RegSS$)	Df (due to RSS)	Pr>F
	Model	0.9983954	0.9983933	483365.824	7	5438	< 2E-16
Year	Parameter	Estimate	Standard Error	t-value	Pr(>|t|)	95% Lower Confidence Limit	95% Upper Confidence Limit
2004	β_0	1.47858118E-04	8.71E-08	1697.18	< 2E-16	1.47687329E-04	1.48028907E-04
	β_1	-3.12085135E-08	3.84E-10	-81.17	< 2E-16	-3.19622698E-08	-3.04547571E-08
	β_2	2.75501526E-11	5.22E-13	52.74	< 2E-16	2.65260142E-11	2.85742911E-11
	β_3	-1.48442713E-14	3.11E-16	-47.71	< 2E-16	-1.54541809E-14	-1.42343617E-14
	β_4	4.45402833E-18	9.43E-20	47.24	< 2E-16	4.26918209E-18	4.63887457E-18
	β_5	-7.45331443E-22	1.52E-23	-49.08	< 2E-16	-7.75102271E-22	-7.15560614E-22
	β_6	6.43852244E-26	1.24E-27	52.03	< 2E-16	6.19592971E-26	6.68111518E-26
	β_7	-2.22575721E-30	4.01E-32	-55.49	< 2E-16	-2.30439515E-30	-2.14711927E-30
		R^2	Adjusted R^2	F-Statistic	Df (due to $RegSS$)	Df (due to RSS)	Pr>F
	Model	0.9970351	0.9970314	268930.687	7	5598	< 2E-16

Year	Parameter	Estimate	Standard Error	t-value	Pr(>|t|)	95% Lower Confidence Limit	95% Upper Confidence Limit
2005	β_0	1.48995435E-04	6.87E-08	2170.12	< 2E-16	1.48860840E-04	1.49130030E-04
	β_1	-2.94698734E-08	3.00E-10	-98.29	< 2E-16	-3.00576608E-08	-2.88820860E-08
	β_2	2.27418579E-11	4.08E-13	55.68	< 2E-16	2.19412300E-11	2.35424858E-11
	β_3	-1.15132917E-14	2.44E-16	-47.17	< 2E-16	-1.19918093E-14	-1.10347741E-14
	β_4	3.42079972E-18	7.42E-20	46.09	< 2E-16	3.27530571E-18	3.56629373E-18
	β_5	-5.83083203E-22	1.20E-23	-48.63	< 2E-16	-6.06587768E-22	-5.59578637E-22
	β_6	5.17599822E-26	9.80E-28	52.82	< 2E-16	4.98388531E-26	5.36811113E-26
	β_7	-1.83850547E-30	3.19E-32	-57.70	< 2E-16	-1.90097103E-30	-1.77603992E-30
		R^2	Adjusted R^2	F-Statistic	Df (due to $RegSS$)	Df (due to RSS)	Pr>F
	Model	0.9981956	0.9981934	453775.94	7	5742	< 2E-16
Year	Parameter	Estimate	Standard Error	t-value	Pr(>|t|)	95% Lower Confidence Limit	95% Upper Confidence Limit
2006	β_0	1.51063002E-04	7.09E-08	2132.11	< 2E-16	1.50924107E-04	1.51201896E-04
	β_1	-3.29446315E-08	3.10E-10	-106.44	< 2E-16	-3.35513790E-08	-3.23378839E-08
	β_2	2.88172437E-11	4.20E-13	68.61	< 2E-16	2.79938298E-11	2.96406576E-11
	β_3	-1.59428722E-14	2.50E-16	-63.67	< 2E-16	-1.64337411E-14	-1.54520033E-14
	β_4	4.91457861E-18	7.60E-20	64.65	< 2E-16	4.76556283E-18	5.06359438E-18
	β_5	-8.37892864E-22	1.23E-23	-68.30	< 2E-16	-8.61942328E-22	-8.13843400E-22
	β_6	7.31972551E-26	1.00E-27	73.05	< 2E-16	7.12329337E-26	7.51615764E-26
	β_7	-2.54637778E-30	3.26E-32	-78.19	< 2E-16	-2.61021628E-30	-2.48253928E-30
		R^2	Adjusted R^2	F-Statistic	Df (due to $RegSS$)	Df (due to RSS)	Pr>F
	Model	0.9982301	0.9982280	482378.408	7	5987	< 2E-16
Year	Parameter	Estimate	Standard Error	t-value	Pr(>|t|)	95% Lower Confidence Limit	95% Upper Confidence Limit
2007	β_0	1.50956051E-04	7.32E-08	2062.30	< 2E-16	1.50812558E-04	1.51099545E-04
	β_1	-2.61954355E-08	3.16E-10	-82.93	< 2E-16	-2.68146537E-08	-2.55762173E-08
	β_2	1.72553686E-11	4.28E-13	40.29	< 2E-16	1.64157266E-11	1.80950106E-11
	β_3	-9.15164725E-15	2.56E-16	-35.82	< 2E-16	-9.65253693E-15	-8.65075758E-15
	β_4	3.01407529E-18	7.76E-20	38.83	< 2E-16	2.86192320E-18	3.16622738E-18
	β_5	-5.60302476E-22	1.25E-23	-44.71	< 2E-16	-5.84867944E-22	-5.35737009E-22
	β_6	5.27188244E-26	1.02E-27	51.49	< 2E-16	5.07118288E-26	5.47258200E-26
	β_7	-1.94275894E-30	3.33E-32	-58.38	< 2E-16	-2.00799789E-30	-1.87751998E-30
		R^2	Adjusted R^2	F-Statistic	Df (due to $RegSS$)	Df (due to RSS)	Pr>F
	Model	0.9980699	0.9980677	456086.842	7	6174	< 2E-16
Year	Parameter	Estimate	Standard Error	t-value	Pr(>|t|)	95% Lower Confidence Limit	95% Upper Confidence Limit
2008	β_0	1.50865313E-04	8.35E-08	1807.71	< 2E-16	1.50701711E-04	1.51028915E-04
	β_1	-2.98699955E-08	3.58E-10	-83.32	< 2E-16	-3.05727650E-08	-2.91672261E-08
	β_2	2.59724101E-11	4.83E-13	53.80	< 2E-16	2.50260809E-11	2.69187393E-11
	β_3	-1.53885546E-14	2.86E-16	-53.78	< 2E-16	-1.59494700E-14	-1.48276391E-14
	β_4	5.03609843E-18	8.65E-20	58.24	< 2E-16	4.86657721E-18	5.20561966E-18
	β_5	-8.93978773E-22	1.39E-23	-64.29	< 2E-16	-9.21239255E-22	-8.66718291E-22
	β_6	8.01545043E-26	1.13E-27	70.78	< 2E-16	7.79346549E-26	8.23743538E-26
	β_7	-2.83715524E-30	3.67E-32	-77.30	< 2E-16	-2.90910642E-30	-2.76520406E-30
		R^2	Adjusted R^2	F-Statistic	Df (due to $RegSS$)	Df (due to RSS)	Pr>F
	Model	0.9975488	0.9975462	377835.057	7	6499	< 2E-16
Year	Parameter	Estimate	Standard Error	t-value	Pr(>|t|)	95% Lower Confidence Limit	95% Upper Confidence Limit
2009	β_0	1.49890190E-04	7.60E-08	1971.53	< 2E-16	1.49741150E-04	1.50039230E-04
	β_1	-3.30790461E-08	3.30E-10	-100.31	< 2E-16	-3.37255196E-08	-3.24325725E-08
	β_2	2.87581897E-11	4.46E-13	64.41	< 2E-16	2.78829653E-11	2.96334140E-11
	β_3	-1.56263321E-14	2.66E-16	-58.78	< 2E-16	-1.61474347E-14	-1.51052295E-14
	β_4	4.75794793E-18	8.06E-20	59.00	< 2E-16	4.59984771E-18	4.91604815E-18
	β_5	-8.04342792E-22	1.30E-23	-61.81	< 2E-16	-8.29852901E-22	-7.78832684E-22
	β_6	6.98204616E-26	1.06E-27	65.69	< 2E-16	6.77368530E-26	7.19040702E-26
	β_7	-2.41685787E-30	3.45E-32	-69.96	< 2E-16	-2.48458046E-30	-2.34913527E-30
		R^2	Adjusted R^2	F-Statistic	Df (due to $RegSS$)	Df (due to RSS)	Pr>F
	Model	0.9977426	0.9977401	392802.582	7	6221	< 2E-16

Year	Parameter	Estimate	Standard Error	t-value	Pr(>|t|)	95% Lower Confidence Limit	95% Upper Confidence Limit
2010	β_0	1.56137506E-04	5.24E-08	2981.50	< 2E-16	1.56034845E-04	1.56240166E-04
	β_1	-4.36923574E-08	2.27E-10	-192.57	< 2E-16	-4.41371325E-08	-4.32475824E-08
	β_2	3.45356524E-11	3.08E-13	112.29	< 2E-16	3.39327612E-11	3.51385436E-11
	β_3	-1.71097191E-14	1.83E-16	-93.27	< 2E-16	-1.74693193E-14	-1.67501188E-14
	β_4	4.94231999E-18	5.57E-20	88.67	< 2E-16	4.83305190E-18	5.05158809E-18
	β_5	-8.10987498E-22	9.00E-24	-90.07	< 2E-16	-8.28639265E-22	-7.93335731E-22
	β_6	6.91270880E-26	7.36E-28	93.90	< 2E-16	6.76840046E-26	7.05701714E-26
	β_7	-2.36332410E-30	2.39E-32	-98.70	< 2E-16	-2.41026256E-30	-2.31638563E-30
		R^2	Adjusted R^2	F-Statistic	Df (due to $RegSS$)	Df (due to RSS)	Pr>F
	Model	0.9989682	0.9989670	882665.233	7	6382	< 2E-16
Year	Parameter	Estimate	Standard Error	t-value	Pr(>|t|)	95% Lower Confidence Limit	95% Upper Confidence Limit
2011	β_0	1.50331138E-04	4.78E-08	3142.26	< 2E-16	1.50237354E-04	1.50424921E-04
	β_1	-3.25404949E-08	2.03E-10	-160.43	< 2E-16	-3.29381143E-08	-3.21428755E-08
	β_2	2.81703858E-11	2.72E-13	103.54	< 2E-16	2.76370516E-11	2.87037200E-11
	β_3	-1.52536026E-14	1.61E-16	-94.53	< 2E-16	-1.55699177E-14	-1.49372874E-14
	β_4	4.57595701E-18	4.89E-20	93.61	< 2E-16	4.48013399E-18	4.67178002E-18
	β_5	-7.58513206E-22	7.88E-24	-96.20	< 2E-16	-7.73969358E-22	-7.43057054E-22
	β_6	6.45666285E-26	6.44E-28	100.23	< 2E-16	6.33038391E-26	6.58294178E-26
	β_7	-2.19642694E-30	2.10E-32	-104.84	< 2E-16	-2.23749698E-30	-2.15535690E-30
		R^2	Adjusted R^2	F-Statistic	Df (due to $RegSS$)	Df (due to RSS)	Pr>F
	Model	0.9990532	0.9990522	1087092.85	7	7212	< 2E-16
Year	Parameter	Estimate	Standard Error	t-value	Pr(>|t|)	95% Lower Confidence Limit	95% Upper Confidence Limit
2012	β_0	1.52154834E-04	7.80E-08	1951.40	< 2E-16	1.52001989E-04	1.52307679E-04
	β_1	-3.68126633E-08	3.25E-10	-113.29	< 2E-16	-3.74496523E-08	-3.61756743E-08
	β_2	3.35777986E-11	4.31E-13	77.85	< 2E-16	3.27323558E-11	3.44232414E-11
	β_3	-1.88083713E-14	2.54E-16	-74.03	< 2E-16	-1.93063979E-14	-1.83103447E-14
	β_4	5.76834780E-18	7.66E-20	75.30	< 2E-16	5.61819113E-18	5.91850447E-18
	β_5	-9.67692823E-22	1.23E-23	-78.60	< 2E-16	-9.91826100E-22	-9.43559546E-22
	β_6	8.28814306E-26	1.00E-27	82.64	< 2E-16	8.09154376E-26	8.48474236E-26
	β_7	-2.82784927E-30	3.25E-32	-86.91	< 2E-16	-2.89163175E-30	-2.76406679E-30
		R^2	Adjusted R^2	F-Statistic	Df (due to $RegSS$)	Df (due to RSS)	Pr>F
	Model	0.9973683	0.9973661	448937.542	7	8292	< 2E-16
Year	Parameter	Estimate	Standard Error	t-value	Pr(>|t|)	95% Lower Confidence Limit	95% Upper Confidence Limit
2013	β_0	1.50433600E-04	6.33E-08	2376.79	< 2E-16	1.50309531E-04	1.50557669E-04
	β_1	-3.15417538E-08	2.63E-10	-119.91	< 2E-16	-3.20573765E-08	-3.10261311E-08
	β_2	2.46636164E-11	3.49E-13	70.67	< 2E-16	2.39795349E-11	2.53476979E-11
	β_3	-1.27343140E-14	2.06E-16	-61.89	< 2E-16	-1.31376569E-14	-1.23309712E-14
	β_4	3.83981338E-18	6.21E-20	61.79	< 2E-16	3.71800037E-18	3.96162639E-18
	β_5	-6.57755364E-22	1.00E-23	-65.72	< 2E-16	-6.77375326E-22	-6.38135403E-22
	β_6	5.83453369E-26	8.17E-28	71.38	< 2E-16	5.67431011E-26	5.99475727E-26
	β_7	-2.06672768E-30	2.66E-32	-77.73	< 2E-16	-2.11884614E-30	-2.01460923E-30
		R^2	Adjusted R^2	F-Statistic	Df (due to $RegSS$)	Df (due to RSS)	Pr>F
	Model	0.9980926	0.9980911	648934.441	7	8681	< 2E-16
Year	Parameter	Estimate	Standard Error	t-value	Pr(>|t|)	95% Lower Confidence Limit	95% Upper Confidence Limit
2014	β_0	1.54953783E-04	7.12E-08	2176.11	< 2E-16	1.54814201E-04	1.55093366E-04
	β_1	-4.54406239E-08	2.96E-10	-153.72	< 2E-16	-4.60200640E-08	-4.48611838E-08
	β_2	3.92065835E-11	3.92E-13	100.02	< 2E-16	3.84382207E-11	3.99749464E-11
	β_3	-2.01335392E-14	2.31E-16	-87.14	< 2E-16	-2.05864667E-14	-1.96806116E-14
	β_4	5.84493033E-18	6.98E-20	83.77	< 2E-16	5.70815800E-18	5.98170266E-18
	β_5	-9.52005598E-22	1.12E-23	-84.72	< 2E-16	-9.74033791E-22	-9.29977405E-22
	β_6	8.03759033E-26	9.18E-28	87.59	< 2E-16	7.85770430E-26	8.21747637E-26
	β_7	-2.72561504E-30	2.99E-32	-91.31	< 2E-16	-2.78412934E-30	-2.66710075E-30
		R^2	Adjusted R^2	F-Statistic	Df (due to $RegSS$)	Df (due to RSS)	Pr>F
	Model	0.9975898	0.9975879	516910.62	7	8742	< 2E-16

Summary Statistics of 8th Degree Polynomial Approximations to LDCs of Turkey in the Period 2000-2014

Year	Parameter	Estimate	Standard Error	t-value	Pr(>|t|)	95% Lower Confidence Limit	95% Upper Confidence Limit
2000	β_0	1.46540349E-04	3.97E-08	3694.48	< 2E-16	1.46462590E-04	1.46618108E-04
	β_1	-2.62998642E-08	2.24E-10	-117.31	< 2E-16	-2.67393858E-08	-2.58603425E-08
	β_2	2.46365056E-11	3.93E-13	62.70	< 2E-16	2.38662523E-11	2.54067590E-11
	β_3	-1.47276713E-14	3.07E-16	-47.90	< 2E-16	-1.53303716E-14	-1.41249710E-14
	β_4	4.88607415E-18	1.26E-19	38.63	< 2E-16	4.63813419E-18	5.13401410E-18
	β_5	-9.26342440E-22	2.93E-23	-31.63	< 2E-16	-9.83762725E-22	-8.68922156E-22
	β_6	9.80688777E-26	3.84E-27	25.55	< 2E-16	9.05432097E-26	1.05594546E-25
	β_7	-5.27668577E-30	2.66E-31	-19.87	< 2E-16	-5.79730881E-30	-4.75606272E-30
	β_8	1.08318191E-34	7.53E-36	14.38	0.0000	9.35528892E-35	1.23083492E-34
		R^2	Adjusted R^2	F-Statistic	Df (due to $RegSS$)	Df (due to RSS)	Pr>F
	Model	0.9995286	0.9995279	1398824.59	8	5278	< 2E-16
Year	Parameter	Estimate	Standard Error	t-value	Pr(>|t|)	95% Lower Confidence Limit	95% Upper Confidence Limit
2001	β_0	1.48975187E-04	6.16E-08	2416.74	< 2E-16	1.48854342E-04	1.49096031E-04
	β_1	-2.71229284E-08	3.46E-10	-78.30	< 2E-16	-2.78019951E-08	-2.64438618E-08
	β_2	2.19903644E-11	6.06E-13	36.27	< 2E-16	2.08017816E-11	2.31789473E-11
	β_3	-1.14182391E-14	4.74E-16	-24.07	< 2E-16	-1.23483834E-14	-1.04880948E-14
	β_4	3.11662296E-18	1.95E-19	15.94	< 2E-16	2.73343234E-18	3.49981358E-18
	β_5	-4.28033734E-22	4.54E-23	-9.43	< 2E-16	-5.16980730E-22	-3.39086738E-22
	β_6	2.20768305E-26	5.96E-27	3.70	0.0002	1.03865731E-26	3.37670879E-26
	β_7	6.45270170E-31	4.14E-31	1.56	0.1190	-1.65924634E-31	1.45646497E-30
	β_8	-7.64642737E-35	1.18E-35	-6.50	< 2E-16	-9.95431460E-35	-5.33854014E-35
		R^2	Adjusted R^2	F-Statistic	Df (due to $RegSS$)	Df (due to RSS)	Pr>F
	Model	0.9988972	0.9988956	624990.949	8	5520	< 2E-16
Year	Parameter	Estimate	Standard Error	t-value	Pr(>|t|)	95% Lower Confidence Limit	95% Upper Confidence Limit
2002	β_0	1.50034919E-04	7.85E-08	1910.56	< 2E-16	1.49880969E-04	1.50188869E-04
	β_1	-4.02435361E-08	4.44E-10	-90.69	< 2E-16	-4.11134951E-08	-3.93735771E-08
	β_2	4.13877580E-11	7.82E-13	52.91	< 2E-16	3.98543985E-11	4.29211175E-11
	β_3	-2.50774433E-14	6.15E-16	-40.80	< 2E-16	-2.62825468E-14	-2.38723397E-14
	β_4	8.46253043E-18	2.54E-19	33.35	< 2E-16	7.96503938E-18	8.96002147E-18
	β_5	-1.63376255E-21	5.90E-23	-27.71	< 2E-16	-1.74934319E-21	-1.51818190E-21
	β_6	1.77211876E-25	7.75E-27	22.86	< 2E-16	1.62016127E-25	1.92407624E-25
	β_7	-9.91097588E-30	5.38E-31	-18.42	< 2E-16	-1.09655200E-29	-8.85643177E-30
	β_8	2.17999295E-34	1.53E-35	14.24	< 2E-16	1.87996932E-34	2.48001657E-34
		R^2	Adjusted R^2	F-Statistic	Df (due to $RegSS$)	Df (due to RSS)	Pr>F
	Model	0.9980167	0.9980137	330867.876	8	5260	< 2E-16
Year	Parameter	Estimate	Standard Error	t-value	Pr(>|t|)	95% Lower Confidence Limit	95% Upper Confidence Limit
2003	β_0	1.46031473E-04	6.97E-08	2095.19	< 2E-16	1.45894837E-04	1.46168110E-04
	β_1	-2.72454407E-08	3.97E-10	-68.56	< 2E-16	-2.80245245E-08	-2.64663570E-08
	β_2	2.61115242E-11	6.97E-13	37.47	< 2E-16	2.47452179E-11	2.74778306E-11
	β_3	-1.55226284E-14	5.45E-16	-28.47	< 2E-16	-1.65913943E-14	-1.44538625E-14
	β_4	5.08741045E-18	2.24E-19	22.68	< 2E-16	4.64769638E-18	5.52712452E-18
	β_5	-9.46840966E-22	5.20E-23	-18.21	< 2E-16	-1.04875059E-21	-8.44931340E-22
	β_6	9.75516454E-26	6.82E-27	14.30	< 2E-16	8.41770631E-26	1.10926228E-25
	β_7	-5.02507720E-30	4.73E-31	-10.63	< 2E-16	-5.95200757E-30	-4.09814683E-30
	β_8	9.50113654E-35	1.34E-35	7.07	< 2E-16	6.86660762E-35	1.21356655E-34
		R^2	Adjusted R^2	F-Statistic	Df (due to $RegSS$)	Df (due to RSS)	Pr>F
	Model	0.9984100	0.9984077	426761.15	8	5437	< 2E-16
Year	Parameter	Estimate	Standard Error	t-value	Pr(>|t|)	95% Lower Confidence Limit	95% Upper Confidence Limit
2004	β_0	1.47847462E-04	9.73E-08	1519.92	< 2E-16	1.47656769E-04	1.48038155E-04
	β_1	-3.11131423E-08	5.46E-10	-57.02	< 2E-16	-3.21827930E-08	-3.00434915E-08
	β_2	2.73528674E-11	9.56E-13	28.61	< 2E-16	2.54784558E-11	2.92272790E-11
	β_3	-1.46765813E-14	7.48E-16	-19.61	< 2E-16	-1.61437274E-14	-1.32094351E-14
	β_4	4.38183156E-18	3.08E-19	14.23	< 2E-16	3.77833781E-18	4.98532531E-18
	β_5	-7.28175453E-22	7.13E-23	-10.22	< 2E-16	-8.67897891E-22	-5.88453014E-22
	β_6	6.21048152E-26	9.34E-27	6.65	< 2E-16	4.37977033E-26	8.04119272E-26
	β_7	-2.06693888E-30	6.46E-31	-3.20	0.0014	-3.33313052E-30	-8.00747244E-31
	β_8	-4.51222013E-36	1.83E-35	-0.25	0.8054	-4.04167941E-35	3.13923538E-35
		R^2	Adjusted R^2	F-Statistic	Df (due to $RegSS$)	Df (due to RSS)	Pr>F
	Model	0.9970352	0.9970309	235274.875	8	5597	< 2E-16

Year	Parameter	Estimate	Standard Error	t-value	Pr(>|t|)	95% Lower Confidence Limit	95% Upper Confidence Limit
2005	β_0	1.48969495E-04	7.67E-08	1942.87	< 2E-16	1.48819183E-04	1.49119807E-04
	β_1	-2.92416799E-08	4.24E-10	-68.91	< 2E-16	-3.00735096E-08	-2.84098501E-08
	β_2	2.22699621E-11	7.43E-13	29.97	< 2E-16	2.08130773E-11	2.37268468E-11
	β_3	-1.11110041E-14	5.83E-16	-19.06	< 2E-16	-1.22536491E-14	-9.96835915E-15
	β_4	3.24690212E-18	2.41E-19	13.50	< 2E-16	2.77536191E-18	3.71844233E-18
	β_5	-5.41578964E-22	5.59E-23	-9.69	< 2E-16	-6.51180315E-22	-4.31977614E-22
	β_6	4.62184974E-26	7.36E-27	6.28	< 2E-16	3.17969011E-26	6.06400937E-26
	β_7	-1.45085714E-30	5.11E-31	-2.84	0.0045	-2.45266124E-30	-4.49053049E-31
	β_8	-1.10616029E-35	1.46E-35	-0.76	0.4473	-3.95926027E-35	1.74693969E-35
		R^2	Adjusted R^2	F-Statistic	Df (due to $RegSS$)	Df (due to RSS)	Pr>F
	Model	0.9981958	0.9981932	397024.816	8	5741	< 2E-16
Year	Parameter	Estimate	Standard Error	t-value	Pr(>|t|)	95% Lower Confidence Limit	95% Upper Confidence Limit
2006	β_0	1.50889621E-04	7.92E-08	1905.83	< 2E-16	1.50734414E-04	1.51044828E-04
	β_1	-3.14350231E-08	4.38E-10	-71.83	< 2E-16	-3.22929126E-08	-3.05771336E-08
	β_2	2.57167928E-11	7.62E-13	33.74	< 2E-16	2.42225090E-11	2.72110767E-11
	β_3	-1.33102409E-14	5.96E-16	-22.35	< 2E-16	-1.44776914E-14	-1.21427904E-14
	β_4	3.77924342E-18	2.45E-19	15.42	< 2E-16	3.29866099E-18	4.25982585E-18
	β_5	-5.67323456E-22	5.69E-23	-9.97	< 2E-16	-6.78845218E-22	-4.55801694E-22
	β_6	3.71078326E-26	7.48E-27	4.96	7.14E-07	2.24496435E-26	5.17660217E-26
	β_7	-2.35739965E-32	5.19E-31	-0.05	0.9638	-1.04103349E-30	9.93885498E-31
	β_8	-7.19501908E-35	1.48E-35	-4.87	1.14E-06	-1.00911109E-34	-4.29892730E-35
		R^2	Adjusted R^2	F-Statistic	Df (due to $RegSS$)	Df (due to RSS)	Pr>F
	Model	0.9982371	0.9982347	423685.809	8	5986	< 2E-16
Year	Parameter	Estimate	Standard Error	t-value	Pr(>|t|)	95% Lower Confidence Limit	95% Upper Confidence Limit
2007	β_0	1.50554416E-04	8.11E-08	1856.07	< 2E-16	1.50395403E-04	1.50713429E-04
	β_1	-2.27329054E-08	4.43E-10	-51.31	< 2E-16	-2.36014503E-08	-2.18643606E-08
	β_2	1.01474762E-11	7.71E-13	13.16	< 2E-16	8.63565179E-12	1.16593006E-11
	β_3	-3.10289563E-15	6.04E-16	-5.14	2.83E-07	-4.28633597E-15	-1.91945529E-15
	β_4	3.99707022E-19	2.49E-19	1.60	0.1086	-8.85251978E-20	8.87939243E-19
	β_5	6.38402374E-23	5.79E-23	1.10	0.2703	-4.96657995E-23	1.77346274E-22
	β_6	-3.06397885E-26	7.62E-27	-4.02	0.0001	-4.55798084E-26	-1.56997686E-26
	β_7	3.88990046E-30	5.30E-31	7.35	2.31E-13	2.85181722E-30	4.92798369E-30
	β_8	-1.66462394E-34	1.51E-35	-11.04	< 2E-16	-1.96031547E-34	-1.36893241E-34
		R^2	Adjusted R^2	F-Statistic	Df (due to $RegSS$)	Df (due to RSS)	Pr>F
	Model	0.9981072	0.9981048	406899.024	8	6173	< 2E-16
Year	Parameter	Estimate	Standard Error	t-value	Pr(>|t|)	95% Lower Confidence Limit	95% Upper Confidence Limit
2008	β_0	1.49576857E-04	8.66E-08	1727.16	< 2E-16	1.49407087E-04	1.49746626E-04
	β_1	-1.88328603E-08	4.72E-10	-39.93	< 2E-16	-1.97574528E-08	-1.79082677E-08
	β_2	3.52567401E-12	8.15E-13	4.33	< 2E-16	1.92799259E-12	5.12335542E-12
	β_3	3.56561297E-15	6.34E-16	5.63	< 2E-16	2.32366659E-15	4.80755936E-15
	β_4	-3.10639925E-18	2.60E-19	-11.95	< 2E-16	-3.61582612E-18	-2.59697238E-18
	β_5	1.04027831E-21	6.01E-23	17.30	< 2E-16	9.22415660E-22	1.15814095E-21
	β_6	-1.77080273E-25	7.88E-27	-22.47	< 2E-16	-1.92528459E-25	-1.61632088E-25
	β_7	1.50934785E-29	5.45E-31	27.67	< 2E-16	1.40241521E-29	1.61628049E-29
	β_8	-5.09954086E-34	1.55E-35	-32.94	< 2E-16	-5.40307076E-34	-4.79601097E-34
		R^2	Adjusted R^2	F-Statistic	Df (due to $RegSS$)	Df (due to RSS)	Pr>F
	Model	0.9978994	0.9978969	385870.301	8	6498	< 2E-16
Year	Parameter	Estimate	Standard Error	t-value	Pr(>|t|)	95% Lower Confidence Limit	95% Upper Confidence Limit
2009	β_0	1.49272791E-04	8.33E-08	1792.70	< 2E-16	1.49109559E-04	1.49436023E-04
	β_1	-2.76909037E-08	4.59E-10	-60.36	< 2E-16	-2.85902732E-08	-2.67915341E-08
	β_2	1.76920781E-11	8.00E-13	22.13	< 2E-16	1.61246622E-11	1.92594940E-11
	β_3	-6.23331423E-15	6.25E-16	-9.97	< 2E-16	-7.45865625E-15	-5.00797222E-15
	β_4	7.09699078E-19	2.57E-19	2.76	0.0058	2.05202928E-19	1.21419523E-18
	β_5	1.59714687E-22	5.97E-23	2.68	0.0075	4.26703546E-23	2.76759019E-22
	β_6	-5.86748135E-26	7.84E-27	-7.48	8.45E-14	-7.40518845E-26	-4.32977426E-26
	β_7	6.55950501E-30	5.44E-31	12.05	< 2E-16	5.49272932E-30	7.62628070E-30
	β_8	-2.55855599E-34	1.55E-35	-16.53	< 2E-16	-2.86203422E-34	-2.25507775E-34
		R^2	Adjusted R^2	F-Statistic	Df (due to $RegSS$)	Df (due to RSS)	Pr>F
	Model	0.9978376	0.9978348	358772.297	8	6220	< 2E-16

Year	Parameter	Estimate	Standard Error	t-value	Pr(>|t|)	95% Lower Confidence Limit	95% Upper Confidence Limit
2010	β_0	1.55994124E-04	5.86E-08	2660.37	< 2E-16	1.55879177E-04	1.56109071E-04
	β_1	-4.24633055E-08	3.21E-10	-132.15	< 2E-16	-4.30932230E-08	-4.18333879E-08
	β_2	3.20155148E-11	5.59E-13	57.24	< 2E-16	3.09191165E-11	3.31119131E-11
	β_3	-1.49682410E-14	4.37E-16	-34.22	< 2E-16	-1.58258134E-14	-1.41106686E-14
	β_4	4.01804543E-18	1.80E-19	22.29	< 2E-16	3.66462988E-18	4.37146099E-18
	β_5	-5.90583093E-22	4.19E-23	-14.11	< 2E-16	-6.72660735E-22	-5.08505450E-22
	β_6	3.97152489E-26	5.51E-27	7.21	6.12E-13	2.89210920E-26	5.05094058E-26
	β_7	-3.06505523E-31	3.82E-31	-0.80	0.4228	-1.05607693E-30	4.43065884E-31
	β_8	-5.86822453E-35	1.09E-35	-5.39	7.31E-08	-8.00261716E-35	-3.73383190E-35
		R^2	Adjusted R^2	F-Statistic	Df (due to $RegSS$)	Df (due to RSS)	Pr>F
	Model	0.9989728	0.9989715	775730.079	8	6381	< 2E-16
Year	Parameter	Estimate	Standard Error	t-value	Pr(>|t|)	95% Lower Confidence Limit	95% Upper Confidence Limit
2011	β_0	1.50328259E-04	5.37E-08	2797.88	< 2E-16	1.50222934E-04	1.50433585E-04
	β_1	-3.25162801E-08	2.89E-10	-112.56	< 2E-16	-3.30825895E-08	-3.19499708E-08
	β_2	2.81213628E-11	4.97E-13	56.53	< 2E-16	2.71462452E-11	2.90964804E-11
	β_3	-1.52122380E-14	3.87E-16	-39.34	< 2E-16	-1.59701961E-14	-1.44542798E-14
	β_4	4.55816679E-18	1.59E-19	28.70	< 2E-16	4.24681543E-18	4.86951815E-18
	β_5	-7.54277703E-22	3.68E-23	-20.48	< 2E-16	-8.26479899E-22	-6.82075507E-22
	β_6	6.40017294E-26	4.84E-27	13.22	< 2E-16	5.45108166E-26	7.34926421E-26
	β_7	-2.15692084E-30	3.36E-31	-6.41	1.50E-10	-2.81604455E-30	-1.49779714E-30
	β_8	-1.12755526E-36	9.58E-36	-0.12	0.9063	-1.99032418E-35	1.76481313E-35
		R^2	Adjusted R^2	F-Statistic	Df (due to $RegSS$)	Df (due to RSS)	Pr>F
	Model	0.9990532	0.9990521	951076.182	8	7211	< 2E-16
Year	Parameter	Estimate	Standard Error	t-value	Pr(>|t|)	95% Lower Confidence Limit	95% Upper Confidence Limit
2012	β_0	1.52106138E-04	8.76E-08	1735.82	< 2E-16	1.51934366E-04	1.52277911E-04
	β_1	-3.64099655E-08	4.64E-10	-78.53	< 2E-16	-3.73188228E-08	-3.55011082E-08
	β_2	3.27724538E-11	7.90E-13	41.51	< 2E-16	3.12246552E-11	3.43202524E-11
	β_3	-1.81345898E-14	6.09E-16	-29.78	< 2E-16	-1.93281628E-14	-1.69410169E-14
	β_4	5.48036024E-18	2.49E-19	22.04	< 2E-16	4.99302454E-18	5.96769595E-18
	β_5	-8.99457270E-22	5.74E-23	-15.68	< 2E-16	-1.01192833E-21	-7.86986211E-22
	β_6	7.38162551E-26	7.51E-27	9.83	< 2E-16	5.90905276E-26	8.85419826E-26
	β_7	-2.19598758E-30	5.20E-31	-4.22	2.43E-05	-3.21521105E-30	-1.17676412E-30
	β_8	-1.79812361E-35	1.48E-35	-1.22	0.2234	-4.69289937E-35	1.09665215E-35
		R^2	Adjusted R^2	F-Statistic	Df (due to $RegSS$)	Df (due to RSS)	Pr>F
	Model	0.9973688	0.9973663	392843.399	8	8291	< 2E-16
Year	Parameter	Estimate	Standard Error	t-value	Pr(>|t|)	95% Lower Confidence Limit	95% Upper Confidence Limit
2013	β_0	1.49410981E-04	6.71E-08	2226.96	< 2E-16	1.49279465E-04	1.49542497E-04
	β_1	-2.31469340E-08	3.54E-10	-65.41	< 2E-16	-2.38405654E-08	-2.24533026E-08
	β_2	7.89256609E-12	6.02E-13	13.10	< 2E-16	6.71189967E-12	9.07323251E-12
	β_3	1.30666723E-15	4.65E-16	2.81	< 2E-16	3.95408909E-16	2.21792555E-15
	β_4	-2.17124395E-18	1.90E-19	-11.42	< 2E-16	-2.54393971E-18	-1.79854819E-18
	β_5	7.69569142E-22	4.40E-23	17.50	< 2E-16	6.83366560E-22	8.55771725E-22
	β_6	-1.31748317E-25	5.77E-27	-22.82	< 2E-16	-1.43063097E-25	-1.20433538E-25
	β_7	1.12189260E-29	4.01E-31	28.01	< 2E-16	1.04336656E-29	1.20041863E-29
	β_8	-3.79146224E-34	1.14E-35	-33.23	< 2E-16	-4.01512162E-34	-3.56780285E-34
		R^2	Adjusted R^2	F-Statistic	Df (due to $RegSS$)	Df (due to RSS)	Pr>F
	Model	0.9983079	0.9983063	640116.603	8	8680	< 2E-16
Year	Parameter	Estimate	Standard Error	t-value	Pr(>|t|)	95% Lower Confidence Limit	95% Upper Confidence Limit
2014	β_0	1.54622478E-04	7.98E-08	1938.01	< 2E-16	1.54466082E-04	1.54778874E-04
	β_1	-4.27224030E-08	4.21E-10	-101.58	< 2E-16	-4.35468290E-08	-4.18979771E-08
	β_2	3.37803976E-11	7.16E-13	47.20	< 2E-16	3.23776314E-11	3.51831638E-11
	β_3	-1.55930408E-14	5.52E-16	-28.24	< 2E-16	-1.66753885E-14	-1.45106930E-14
	β_4	3.90181575E-18	2.26E-19	17.28	< 2E-16	3.45925907E-18	4.34437243E-18
	β_5	-4.90735371E-22	5.22E-23	-9.40	< 2E-16	-5.93074528E-22	-3.88396214E-22
	β_6	1.89552415E-26	6.85E-27	2.77	0.0057	5.52478227E-27	3.23857007E-26
	β_7	1.56643160E-30	4.75E-31	3.29	0.0010	6.34474166E-31	2.49838903E-30
	β_8	-1.22472343E-34	1.35E-35	-9.05	< 2E-16	-1.49013499E-34	-9.59311879E-35
		R^2	Adjusted R^2	F-Statistic	Df (due to $RegSS$)	Df (due to RSS)	Pr>F
	Model	0.9976122	0.9976100	456488.45	8	8741	< 2E-16

Summary Statistics of 9th Degree Polynomial Approximations to LDCs of Turkey in the Period 2000-2014

Year	Parameter	Estimate	Standard Error	t-value	Pr(>|t|)	95% Lower Confidence Limit	95% Upper Confidence Limit
2000	β_0	1.47520256E-04	2.98E-08	4955.25	< 2E-16	1.47461893E-04	1.47578618E-04
	β_1	-3.73476550E-08	2.08E-10	-179.55	< 2E-16	-3.77554404E-08	-3.69398696E-08
	β_2	5.34889943E-11	4.56E-13	117.35	< 2E-16	5.25954105E-11	5.43825780E-11
	β_3	-4.60239007E-14	4.52E-16	-101.88	< 2E-16	-4.69095157E-14	-4.51382857E-14
	β_4	2.24453621E-17	2.41E-19	93.31	< 2E-16	2.19737758E-17	2.29169485E-17
	β_5	-6.55595227E-21	7.47E-23	-87.74	< 2E-16	-6.70244105E-21	-6.40946348E-21
	β_6	1.16923289E-24	1.39E-26	83.82	< 2E-16	1.14188652E-24	1.19657927E-24
	β_7	-1.24850923E-28	1.54E-30	-81.06	< 2E-16	-1.27870425E-28	-1.21831421E-28
	β_8	7.33866787E-33	9.26E-35	79.22	< 2E-16	7.15707004E-33	7.52026570E-33
	β_9	-1.82736215E-37	2.34E-39	-78.17	< 2E-16	-1.87318790E-37	-1.78153639E-37
		R^2	Adjusted R^2	F-Statistic	Df (due to $RegSS$)	Df (due to RSS)	Pr>F
	Model	0.9997816	0.9997812	2683525.67	9	5277	< 2E-16
Year	Parameter	Estimate	Standard Error	t-value	Pr(>|t|)	95% Lower Confidence Limit	95% Upper Confidence Limit
2001	β_0	1.50307163E-04	5.37E-08	2800.18	< 2E-16	1.50201934E-04	1.50412393E-04
	β_1	-4.19779293E-08	3.74E-10	-112.32	< 2E-16	-4.27105833E-08	-4.12452753E-08
	β_2	6.05275270E-11	8.17E-13	74.10	< 2E-16	5.89262784E-11	6.21287756E-11
	β_3	-5.31822489E-14	8.10E-16	-65.69	< 2E-16	-5.47693526E-14	-5.15951452E-14
	β_4	2.65820248E-17	4.32E-19	61.55	< 2E-16	2.57353523E-17	2.74286973E-17
	β_5	-7.96845263E-21	1.35E-22	-59.24	< 2E-16	-8.23213057E-21	-7.70477470E-21
	β_6	1.46062003E-24	2.52E-26	58.01	< 2E-16	1.41125759E-24	1.50998247E-24
	β_7	-1.60389240E-28	2.79E-30	-57.52	< 2E-16	-1.65855512E-28	-1.54922969E-28
	β_8	9.68879932E-33	1.68E-34	57.61	< 2E-16	9.35909031E-33	1.00185083E-32
	β_9	-2.47517712E-37	4.26E-39	-58.15	< 2E-16	-2.55862057E-37	-2.39173366E-37
		R^2	Adjusted R^2	F-Statistic	Df (due to $RegSS$)	Df (due to RSS)	Pr>F
	Model	0.9993162	0.9993151	896149.932	9	5519	< 2E-16
Year	Parameter	Estimate	Standard Error	t-value	Pr(>|t|)	95% Lower Confidence Limit	95% Upper Confidence Limit
2002	β_0	1.51720491E-04	6.68E-08	2270.41	< 2E-16	1.51589486E-04	1.51851496E-04
	β_1	-5.91603008E-08	4.66E-10	-126.92	< 2E-16	-6.00741246E-08	-5.82464771E-08
	β_2	9.08618509E-11	1.02E-12	88.73	< 2E-16	8.88544001E-11	9.28693017E-11
	β_3	-7.89752387E-14	1.02E-15	-77.55	< 2E-16	-8.09717587E-14	-7.69787187E-14
	β_4	3.88443057E-17	5.44E-19	71.35	< 2E-16	3.77769717E-17	3.99116396E-17
	β_5	-1.14166515E-20	1.70E-22	-67.24	< 2E-16	-1.17495059E-20	-1.10837970E-20
	β_6	2.04598767E-24	3.18E-26	64.31	< 2E-16	1.98361679E-24	2.10835855E-24
	β_7	-2.19281288E-28	3.53E-30	-62.20	< 2E-16	-2.26192565E-28	-2.12370012E-28
	β_8	1.29212409E-32	2.13E-34	60.74	< 2E-16	1.25041824E-32	1.33382995E-32
	β_9	-3.22098281E-37	5.39E-39	-59.80	< 2E-16	-3.32656749E-37	-3.11539814E-37
		R^2	Adjusted R^2	F-Statistic	Df (due to $RegSS$)	Df (due to RSS)	Pr>F
	Model	0.9988196	0.9988175	494426.695	9	5259	< 2E-16
Year	Parameter	Estimate	Standard Error	t-value	Pr(>|t|)	95% Lower Confidence Limit	95% Upper Confidence Limit
2003	β_0	1.47526432E-04	6.06E-08	2434.15	< 2E-16	1.47407618E-04	1.47645245E-04
	β_1	-4.40332523E-08	4.26E-10	-103.26	< 2E-16	-4.48692567E-08	-4.31972479E-08
	β_2	6.98313068E-11	9.33E-13	74.82	< 2E-16	6.80015859E-11	7.16610278E-11
	β_3	-6.29235641E-14	9.24E-16	-68.07	< 2E-16	-6.47358326E-14	-6.11112956E-14
	β_4	3.17038097E-17	4.93E-19	64.37	< 2E-16	3.07382400E-17	3.26693795E-17
	β_5	-9.49268592E-21	1.53E-22	-61.96	< 2E-16	-9.79302700E-21	-9.19234485E-21
	β_6	1.72658011E-24	2.87E-26	60.26	< 2E-16	1.67041141E-24	1.78274882E-24
	β_7	-1.87248919E-28	3.17E-30	-59.07	< 2E-16	-1.93463692E-28	-1.81034146E-28
	β_8	1.11380072E-32	1.91E-34	58.29	< 2E-16	1.07634116E-32	1.15126028E-32
	β_9	-2.79742143E-37	4.83E-39	-57.88	< 2E-16	-2.89216898E-37	-2.70267388E-37
		R^2	Adjusted R^2	F-Statistic	Df (due to $RegSS$)	Df (due to RSS)	Pr>F
	Model	0.9990163	0.9990146	613390.765	9	5436	< 2E-16

Year	Parameter	Estimate	Standard Error	t-value	Pr(>|t|)	95% Lower Confidence Limit	95% Upper Confidence Limit
2004	β_0	1.49995299E-04	8.34E-08	1798.23	< 2E-16	1.49831777E-04	1.50158820E-04
	β_1	-5.50080349E-08	5.78E-10	-95.12	< 2E-16	-5.61417766E-08	-5.38742932E-08
	β_2	8.94705996E-11	1.26E-12	70.77	< 2E-16	8.69921945E-11	9.19490047E-11
	β_3	-8.19209965E-14	1.25E-15	-65.49	< 2E-16	-8.43732213E-14	-7.94687718E-14
	β_4	4.20660709E-17	6.65E-19	63.24	< 2E-16	4.07620326E-17	4.33701091E-17
	β_5	-1.27999389E-20	2.06E-22	-62.01	< 2E-16	-1.32045841E-20	-1.23952936E-20
	β_6	2.35760525E-24	3.85E-26	61.23	< 2E-16	2.28212694E-24	2.43308356E-24
	β_7	-2.58192162E-28	4.25E-30	-60.77	< 2E-16	-2.66521320E-28	-2.49863005E-28
	β_8	1.54771381E-32	2.55E-34	60.60	< 2E-16	1.49764205E-32	1.59778557E-32
	β_9	-3.91169950E-37	6.44E-39	-60.71	< 2E-16	-4.03801793E-37	-3.78538107E-37
		R^2	Adjusted R^2	F-Statistic	Df (due to $RegSS$)	Df (due to RSS)	Pr>F
	Model	0.9982124	0.9982095	347210.214	9	5596	< 2E-16
Year	Parameter	Estimate	Standard Error	t-value	Pr(>|t|)	95% Lower Confidence Limit	95% Upper Confidence Limit
2005	β_0	1.50419689E-04	7.19E-08	2091.15	< 2E-16	1.50278676E-04	1.50560702E-04
	β_1	-4.51360818E-08	4.93E-10	-91.62	< 2E-16	-4.61018864E-08	-4.41702771E-08
	β_2	6.35295356E-11	1.08E-12	58.99	< 2E-16	6.14184456E-11	6.56406256E-11
	β_3	-5.58638164E-14	1.07E-15	-52.30	< 2E-16	-5.79579655E-14	-5.37696672E-14
	β_4	2.83956537E-17	5.70E-19	49.83	< 2E-16	2.72784670E-17	2.95128403E-17
	β_5	-8.62141151E-21	1.77E-22	-48.60	< 2E-16	-8.96919905E-21	-8.27362398E-21
	β_6	1.58725434E-24	3.32E-26	47.81	< 2E-16	1.52217673E-24	1.65233196E-24
	β_7	-1.73919790E-28	3.67E-30	-47.33	< 2E-16	-1.81123527E-28	-1.66716053E-28
	β_8	1.04461727E-32	2.22E-34	47.14	< 2E-16	1.00117681E-32	1.08805773E-32
	β_9	-2.65046735E-37	5.61E-39	-47.26	< 2E-16	-2.76039948E-37	-2.54053522E-37
		R^2	Adjusted R^2	F-Statistic	Df (due to $RegSS$)	Df (due to RSS)	Pr>F
	Model	0.9987012	0.9986992	490423.641	9	5740	< 2E-16
Year	Parameter	Estimate	Standard Error	t-value	Pr(>|t|)	95% Lower Confidence Limit	95% Upper Confidence Limit
2006	β_0	1.52513304E-04	7.22E-08	2112.52	< 2E-16	1.52371775E-04	1.52654832E-04
	β_1	-4.90740577E-08	4.92E-10	-99.85	< 2E-16	-5.00375785E-08	-4.81105369E-08
	β_2	7.13798437E-11	1.07E-12	66.84	< 2E-16	6.92864132E-11	7.34732741E-11
	β_3	-6.27958043E-14	1.06E-15	-59.44	< 2E-16	-6.48667444E-14	-6.07248643E-14
	β_4	3.15880309E-17	5.63E-19	56.10	< 2E-16	3.04841779E-17	3.26918838E-17
	β_5	-9.50538561E-21	1.75E-22	-54.22	< 2E-16	-9.84903407E-21	-9.16173715E-21
	β_6	1.74274742E-24	3.28E-26	53.11	< 2E-16	1.67841788E-24	1.80707697E-24
	β_7	-1.91020420E-28	3.63E-30	-52.56	< 2E-16	-1.98145128E-28	-1.83895713E-28
	β_8	1.15147034E-32	2.19E-34	52.51	< 2E-16	1.10848375E-32	1.19445693E-32
	β_9	-2.93809642E-37	5.55E-39	-52.92	< 2E-16	-3.04693138E-37	-2.82926146E-37
		R^2	Adjusted R^2	F-Statistic	Df (due to $RegSS$)	Df (due to RSS)	Pr>F
	Model	0.9987991	0.9987972	553064.312	9	5985	< 2E-16
Year	Parameter	Estimate	Standard Error	t-value	Pr(>|t|)	95% Lower Confidence Limit	95% Upper Confidence Limit
2007	β_0	1.52205501E-04	7.50E-08	2029.95	< 2E-16	1.52058515E-04	1.52352488E-04
	β_1	-4.05253268E-08	5.06E-10	-80.08	< 2E-16	-4.15174016E-08	-3.95332521E-08
	β_2	5.60927499E-11	1.10E-12	51.02	< 2E-16	5.39375311E-11	5.82479686E-11
	β_3	-5.29098874E-14	1.09E-15	-48.57	< 2E-16	-5.50453826E-14	-5.07743923E-14
	β_4	2.84139646E-17	5.82E-19	48.86	< 2E-16	2.72739410E-17	2.95539881E-17
	β_5	-8.94790707E-21	1.81E-22	-49.37	< 2E-16	-9.30323105E-21	-8.59258308E-21
	β_6	1.69027102E-24	3.40E-26	49.77	< 2E-16	1.62369931E-24	1.75684273E-24
	β_7	-1.88927493E-28	3.76E-30	-50.20	< 2E-16	-1.96305221E-28	-1.81549765E-28
	β_8	1.15362009E-32	2.27E-34	50.78	< 2E-16	1.10908463E-32	1.19815555E-32
	β_9	-2.96871800E-37	5.75E-39	-51.59	< 2E-16	-3.08152089E-37	-2.85591512E-37
		R^2	Adjusted R^2	F-Statistic	Df (due to $RegSS$)	Df (due to RSS)	Pr>F
	Model	0.9986776	0.9986756	517881.095	9	6172	< 2E-16

Year	Parameter	Estimate	Standard Error	t-value	Pr(>|t|)	95% Lower Confidence Limit	95% Upper Confidence Limit
2008	β_0	1.51647651E-04	7.50E-08	2022.20	< 2E-16	1.51500643E-04	1.51794658E-04
	β_1	-4.09532245E-08	5.04E-10	-81.18	< 2E-16	-4.19421020E-08	-3.99643471E-08
	β_2	6.01304621E-11	1.09E-12	55.31	< 2E-16	5.79994010E-11	6.22615231E-11
	β_3	-5.73400008E-14	1.07E-15	-53.62	< 2E-16	-5.94361783E-14	-5.52438232E-14
	β_4	3.09450924E-17	5.67E-19	54.54	< 2E-16	2.98327326E-17	3.20574523E-17
	β_5	-9.85978955E-21	1.76E-22	-56.03	< 2E-16	-1.02047859E-20	-9.51479324E-21
	β_6	1.89571551E-24	3.28E-26	57.74	< 2E-16	1.83135030E-24	1.96008071E-24
	β_7	-2.16285794E-28	3.63E-30	-59.66	< 2E-16	-2.23392368E-28	-2.09179220E-28
	β_8	1.34850531E-32	2.18E-34	61.83	< 2E-16	1.30575372E-32	1.39125690E-32
	β_9	-3.53877624E-37	5.51E-39	-64.27	< 2E-16	-3.64671115E-37	-3.43084133E-37
		R^2	Adjusted R^2	F-Statistic	Df (due to $RegSS$)	Df (due to RSS)	Pr>F
	Model	0.9987159	0.9987141	561448.689	9	6497	< 2E-16
Year	Parameter	Estimate	Standard Error	t-value	Pr(>|t|)	95% Lower Confidence Limit	95% Upper Confidence Limit
2009	β_0	1.51042811E-04	7.56E-08	1997.60	< 2E-16	1.50894585E-04	1.51191037E-04
	β_1	-4.69567959E-08	5.15E-10	-91.15	< 2E-16	-4.79667065E-08	-4.59468853E-08
	β_2	6.74599913E-11	1.12E-12	60.22	< 2E-16	6.52638415E-11	6.96561412E-11
	β_3	-6.00702843E-14	1.11E-15	-54.21	< 2E-16	-6.22423570E-14	-5.78982115E-14
	β_4	3.09241077E-17	5.90E-19	52.39	< 2E-16	2.97670715E-17	3.20811439E-17
	β_5	-9.54271091E-21	1.84E-22	-51.97	< 2E-16	-9.90269385E-21	-9.18272798E-21
	β_6	1.79169836E-24	3.44E-26	52.15	< 2E-16	1.72434305E-24	1.85905367E-24
	β_7	-2.00563695E-28	3.80E-30	-52.72	< 2E-16	-2.08021135E-28	-1.93106255E-28
	β_8	1.23062156E-32	2.29E-34	53.63	< 2E-16	1.18563604E-32	1.27560708E-32
	β_9	-3.18509099E-37	5.81E-39	-54.83	< 2E-16	-3.29897584E-37	-3.07120614E-37
		R^2	Adjusted R^2	F-Statistic	Df (due to $RegSS$)	Df (due to RSS)	Pr>F
	Model	0.9985422	0.9985401	473309.311	9	6219	< 2E-16
Year	Parameter	Estimate	Standard Error	t-value	Pr(>|t|)	95% Lower Confidence Limit	95% Upper Confidence Limit
2010	β_0	1.57386682E-04	5.10E-08	3087.85	< 2E-16	1.57286765E-04	1.57486600E-04
	β_1	-5.73225364E-08	3.44E-10	-166.42	< 2E-16	-5.79977656E-08	-5.66473073E-08
	β_2	7.03124724E-11	7.48E-13	94.06	< 2E-16	6.88470783E-11	7.17778665E-11
	β_3	-5.64247338E-14	7.40E-16	-76.28	< 2E-16	-5.78747488E-14	-5.49747187E-14
	β_4	2.73088209E-17	3.94E-19	69.24	< 2E-16	2.65356923E-17	2.80819494E-17
	β_5	-8.07637025E-21	1.23E-22	-65.77	< 2E-16	-8.31711157E-21	-7.83562893E-21
	β_6	1.46830792E-24	2.30E-26	63.86	< 2E-16	1.42323476E-24	1.51338108E-24
	β_7	-1.60296814E-28	2.55E-30	-62.94	< 2E-16	-1.65289565E-28	-1.55304064E-28
	β_8	9.64841836E-33	1.54E-34	62.78	< 2E-16	9.34713354E-33	9.94970318E-33
	β_9	-2.46195505E-37	3.89E-39	-63.26	< 2E-16	-2.53825020E-37	-2.38565990E-37
		R^2	Adjusted R^2	F-Statistic	Df (due to $RegSS$)	Df (due to RSS)	Pr>F
	Model	0.9993688	0.9993679	1122285.34	9	6380	< 2E-16
Year	Parameter	Estimate	Standard Error	t-value	Pr(>|t|)	95% Lower Confidence Limit	95% Upper Confidence Limit
2011	β_0	1.51512786E-04	5.03E-08	3013.23	< 2E-16	1.51414217E-04	1.51611354E-04
	β_1	-4.49372813E-08	3.34E-10	-134.41	< 2E-16	-4.55926698E-08	-4.42818928E-08
	β_2	5.96984899E-11	7.18E-13	83.19	< 2E-16	5.82917148E-11	6.11052650E-11
	β_3	-4.91056991E-14	7.05E-16	-69.65	< 2E-16	-5.04876803E-14	-4.77237180E-14
	β_4	2.35038446E-17	3.74E-19	62.81	< 2E-16	2.27702988E-17	2.42373903E-17
	β_5	-6.82564702E-21	1.16E-22	-58.74	< 2E-16	-7.05344168E-21	-6.59785237E-21
	β_6	1.22077240E-24	2.17E-26	56.20	< 2E-16	1.17819036E-24	1.26335444E-24
	β_7	-1.31599311E-28	2.40E-30	-54.74	< 2E-16	-1.36312249E-28	-1.26886373E-28
	β_8	7.85018561E-33	1.45E-34	54.13	< 2E-16	7.56587524E-33	8.13449598E-33
	β_9	-1.99135818E-37	3.67E-39	-54.22	< 2E-16	-2.06335709E-37	-1.91935927E-37
		R^2	Adjusted R^2	F-Statistic	Df (due to $RegSS$)	Df (due to RSS)	Pr>F
	Model	0.9993274	0.9993265	1190242.95	9	7210	< 2E-16

Year	Parameter	Estimate	Standard Error	t-value	Pr(>|t|)	95% Lower Confidence Limit	95% Upper Confidence Limit
2012	β_0	1.54635706E-04	7.33E-08	2109.61	< 2E-16	1.54492019E-04	1.54779393E-04
	β_1	-6.25695021E-08	4.80E-10	-130.34	< 2E-16	-6.35104906E-08	-6.16285137E-08
	β_2	9.85830860E-11	1.02E-12	96.67	< 2E-16	9.65840618E-11	1.00582110E-10
	β_3	-8.82490687E-14	9.95E-16	-88.73	< 2E-16	-9.01986412E-14	-8.62994962E-14
	β_4	4.44583973E-17	5.25E-19	84.67	< 2E-16	4.34290716E-17	4.54877230E-17
	β_5	-1.33369919E-20	1.62E-22	-82.13	< 2E-16	-1.36553176E-20	-1.30186662E-20
	β_6	2.43512194E-24	3.03E-26	80.49	< 2E-16	2.37582050E-24	2.49442337E-24
	β_7	-2.65610404E-28	3.34E-30	-79.57	< 2E-16	-2.72154142E-28	-2.59066666E-28
	β_8	1.59148541E-32	2.01E-34	79.25	< 2E-16	1.55211813E-32	1.63085270E-32
	β_9	-4.03063927E-37	5.07E-39	-79.46	< 2E-16	-4.13007642E-37	-3.93120212E-37
		R^2	Adjusted R^2	F-Statistic	Df (due to $RegSS$)	Df (due to RSS)	Pr>F
	Model	0.9995286	0.9995279	1398824.59	8	5278	< 2E-16
Year	Parameter	Estimate	Standard Error	t-value	Pr(>|t|)	95% Lower Confidence Limit	95% Upper Confidence Limit
2013	β_0	1.50739673E-04	6.70E-08	2248.70	< 2E-16	1.50608270E-04	1.50871076E-04
	β_1	-3.67772042E-08	4.37E-10	-84.09	< 2E-16	-3.76345027E-08	-3.59199057E-08
	β_2	4.21274921E-11	9.28E-13	45.39	< 2E-16	4.03080785E-11	4.39469058E-11
	β_3	-3.51751855E-14	9.06E-16	-38.84	< 2E-16	-3.69502629E-14	-3.34001080E-14
	β_4	1.81330826E-17	4.79E-19	37.88	< 2E-16	1.71947835E-17	1.90713816E-17
	β_5	-5.72059876E-21	1.48E-22	-38.58	< 2E-16	-6.01126985E-21	-5.42992767E-21
	β_6	1.10304975E-24	2.77E-26	39.85	< 2E-16	1.04878725E-24	1.15731225E-24
	β_7	-1.26857974E-28	3.06E-30	-41.43	< 2E-16	-1.32859791E-28	-1.20856158E-28
	β_8	7.99407773E-33	1.85E-34	43.29	< 2E-16	7.63208450E-33	8.35607095E-33
	β_9	-2.12396930E-37	4.68E-39	-45.41	< 2E-16	-2.21565151E-37	-2.03228709E-37
		R^2	Adjusted R^2	F-Statistic	Df (due to $RegSS$)	Df (due to RSS)	Pr>F
	Model	0.9986327	0.9986313	704341.747	9	8679	< 2E-16
Year	Parameter	Estimate	Standard Error	t-value	Pr(>|t|)	95% Lower Confidence Limit	95% Upper Confidence Limit
2014	β_0	1.56566917E-04	7.49E-08	2091.73	< 2E-16	1.56420193E-04	1.56713642E-04
	β_1	-6.26505553E-08	4.88E-10	-128.34	< 2E-16	-6.36074897E-08	-6.16936209E-08
	β_2	8.37817468E-11	1.04E-12	80.92	< 2E-16	8.17521853E-11	8.58113083E-11
	β_3	-6.88410238E-14	1.01E-15	-68.19	< 2E-16	-7.08200346E-14	-6.68620129E-14
	β_4	3.35254387E-17	5.33E-19	62.85	< 2E-16	3.24797563E-17	3.45711211E-17
	β_5	-9.95731605E-21	1.65E-22	-60.27	< 2E-16	-1.02811654E-20	-9.63346673E-21
	β_6	1.81972899E-24	3.08E-26	59.01	< 2E-16	1.75928375E-24	1.88017423E-24
	β_7	-1.99775410E-28	3.41E-30	-58.58	< 2E-16	-2.06460262E-28	-1.93090557E-28
	β_8	1.20862699E-32	2.06E-34	58.77	< 2E-16	1.16831135E-32	1.24894262E-32
	β_9	-3.09672102E-37	5.21E-39	-59.45	< 2E-16	-3.19882283E-37	-2.99461921E-37
		R^2	Adjusted R^2	F-Statistic	Df (due to $RegSS$)	Df (due to RSS)	Pr>F
	Model	0.9982998	0.9982980	570199.234	9	8740	< 2E-16

Summary Statistics of 10th Degree Polynomial Approximations to LDCs of Turkey in the Period 2000-2014

Year	Parameter	Estimate	Standard Error	t-value	Pr(>|t|)	95% Lower Confidence Limit	95% Upper Confidence Limit
2000	β_0	1.47296947E-04	3.17E-08	4647.10	< 2E-16	1.47234808E-04	1.47359085E-04
	β_1	-3.42867778E-08	2.69E-10	-127.67	< 2E-16	-3.48132818E-08	-3.37602738E-08
	β_2	4.36795020E-11	7.19E-13	60.75	< 2E-16	4.22700591E-11	4.50889448E-11
	β_3	-3.28427881E-14	8.78E-16	-37.39	< 2E-16	-3.45646138E-14	-3.11209624E-14
	β_4	1.31473384E-17	5.85E-19	22.46	< 2E-16	1.20000144E-17	1.42946624E-17
	β_5	-2.72091291E-21	2.33E-22	-11.68	< 2E-16	-3.17746934E-21	-2.26435649E-21
	β_6	1.95798832E-25	5.78E-26	3.39	0.0007	8.25339613E-26	3.09063703E-25
	β_7	2.91566769E-29	9.01E-30	3.24	0.0012	1.14922983E-29	4.68210556E-29
	β_8	-7.45728563E-33	8.58E-34	-8.69	< 2E-16	-9.14002479E-33	-5.77454647E-33
	β_9	6.06978897E-37	4.56E-38	13.31	< 2E-16	5.17549956E-37	6.96407838E-37
	β_{10}	-1.79590958E-41	1.04E-42	-17.33	< 2E-16	-1.99902919E-41	-1.59278996E-41
		R^2	Adjusted R^2	F-Statistic	Df (due to $RegSS$)	Df (due to RSS)	Pr>F
	Model	0.9997933	0.9997929	2552251.53	10	5276	< 2E-16
Year	Parameter	Estimate	Standard Error	t-value	Pr(>|t|)	95% Lower Confidence Limit	95% Upper Confidence Limit
2001	β_0	1.50040023E-04	5.81E-08	2580.27	< 2E-16	1.49926028E-04	1.50154017E-04
	β_1	-3.83648372E-08	4.90E-10	-78.35	< 2E-16	-3.93247329E-08	-3.74049416E-08
	β_2	4.90318143E-11	1.30E-12	37.64	< 2E-16	4.64781229E-11	5.15855058E-11
	β_3	-3.77552867E-14	1.59E-15	-23.77	< 2E-16	-4.08685380E-14	-3.46420354E-14
	β_4	1.56860037E-17	1.06E-18	14.82	< 2E-16	1.36105843E-17	1.77614231E-17
	β_5	-3.46340256E-21	4.22E-22	-8.21	< 2E-16	-4.29074459E-21	-2.63606052E-21
	β_6	3.13715185E-25	1.05E-25	2.99	0.0028	1.07948240E-25	5.19482130E-25
	β_7	2.16514108E-29	1.64E-29	1.32	0.1873	-1.05335478E-29	5.38363695E-29
	β_8	-7.85920990E-33	1.57E-33	-5.01	5.64E-07	-1.09349776E-32	-4.78344219E-33
	β_9	6.92284007E-37	8.37E-38	8.28	< 2E-16	5.28278407E-37	8.56289607E-37
	β_{10}	-2.14455458E-41	1.91E-42	-11.25	< 2E-16	-2.51832871E-41	-1.77078045E-41
		R^2	Adjusted R^2	F-Statistic	Df (due to $RegSS$)	Df (due to RSS)	Pr>F
	Model	0.9993315	0.9993303	824890.104	10	5518	< 2E-16
Year	Parameter	Estimate	Standard Error	t-value	Pr(>|t|)	95% Lower Confidence Limit	95% Upper Confidence Limit
2002	β_0	1.51507136E-04	7.26E-08	2086.59	< 2E-16	1.51364790E-04	1.51649482E-04
	β_1	-5.62386333E-08	6.12E-10	-91.88	< 2E-16	-5.74386214E-08	-5.50386452E-08
	β_2	8.14600002E-11	1.64E-12	49.66	< 2E-16	7.82445012E-11	8.46754992E-11
	β_3	-6.62582645E-14	2.01E-15	-32.93	< 2E-16	-7.02032819E-14	-6.23132471E-14
	β_4	2.98157126E-17	1.35E-18	22.12	< 2E-16	2.71731362E-17	3.24582889E-17
	β_5	-7.67124527E-21	5.39E-22	-14.23	< 2E-16	-8.72828591E-21	-6.61420462E-21
	β_6	1.09043575E-24	1.34E-25	8.11	< 2E-16	8.26924277E-25	1.35394722E-24
	β_7	-6.74056146E-29	2.11E-29	-3.20	0.0014	-1.08686885E-28	-2.61243438E-29
	β_8	-1.73161634E-33	2.01E-33	-0.86	0.3900	-5.68061570E-33	2.21738301E-33
	β_9	4.63065282E-37	1.07E-37	4.31	1.67E-05	2.52370355E-37	6.73760208E-37
	β_{10}	-1.79222224E-41	2.45E-42	-7.31	2.97E-13	-2.27255832E-41	-1.31188617E-41
		R^2	Adjusted R^2	F-Statistic	Df (due to $RegSS$)	Df (due to RSS)	Pr>F
	Model	0.9988314	0.9988292	449431.973	10	5258	< 2E-16
Year	Parameter	Estimate	Standard Error	t-value	Pr(>|t|)	95% Lower Confidence Limit	95% Upper Confidence Limit
2003	β_0	1.47081636E-04	6.46E-08	2275.66	< 2E-16	1.46954930E-04	1.47208342E-04
	β_1	-3.79653282E-08	5.48E-10	-69.22	< 2E-16	-3.90405247E-08	-3.68901317E-08
	β_2	5.03752234E-11	1.46E-12	34.40	< 2E-16	4.75047059E-11	5.32457409E-11
	β_3	-3.67244084E-14	1.79E-15	-20.53	< 2E-16	-4.02307393E-14	-3.32180775E-14
	β_4	1.31726505E-17	1.19E-18	11.04	< 2E-16	1.08326420E-17	1.55126589E-17
	β_5	-1.82680607E-21	4.76E-22	-3.84	0.0001	-2.76016615E-21	-8.93445992E-22
	β_6	-2.25199665E-25	1.18E-25	-1.90	0.0573	-4.57394964E-25	6.99563510E-27
	β_7	1.22511456E-28	1.85E-29	6.61	4.14E-11	8.61907453E-29	1.58832166E-28
	β_8	-1.87157410E-32	1.77E-33	-10.57	< 2E-16	-2.21864542E-32	-1.52450277E-32
	β_9	1.31871856E-36	9.44E-38	13.97	< 2E-16	1.13368646E-36	1.50375066E-36
	β_{10}	-3.64660749E-41	2.15E-42	-16.96	< 2E-16	-4.06819972E-41	-3.22501525E-41
		R^2	Adjusted R^2	F-Statistic	Df (due to $RegSS$)	Df (due to RSS)	Pr>F
	Model	0.9990657	0.9990640	581178.881	10	5435	< 2E-16

Year	Parameter	Estimate	Standard Error	t-value	Pr(>|t|)	95% Lower Confidence Limit	95% Upper Confidence Limit
2004	β_0	1.49046593E-04	8.57E-08	1738.17	< 2E-16	1.48878491E-04	1.49214695E-04
	β_1	-4.21619385E-08	7.19E-10	-58.63	< 2E-16	-4.35717813E-08	-4.07520957E-08
	β_2	4.84546285E-11	1.92E-12	25.28	< 2E-16	4.46973087E-11	5.22119482E-11
	β_3	-2.68418070E-14	2.34E-15	-11.49	< 2E-16	-3.14230612E-14	-2.22605528E-14
	β_4	3.20789062E-18	1.56E-18	2.06	0.0393	1.57460830E-19	6.25832042E-18
	β_5	3.23081645E-21	6.19E-22	5.22	1.86E-07	2.01726110E-21	4.44437180E-21
	β_6	-1.71204862E-24	1.54E-25	-11.15	< 2E-16	-2.01309084E-24	-1.41100641E-24
	β_7	3.85724644E-28	2.39E-29	16.11	< 2E-16	3.38776268E-28	4.32673019E-28
	β_8	-4.63876942E-32	2.28E-33	-20.33	< 2E-16	-5.08600026E-32	-4.19153858E-32
	β_9	2.91076387E-36	1.21E-37	24.01	< 2E-16	2.67308968E-36	3.14843806E-36
	β_{10}	-7.50877017E-41	2.75E-42	-27.27	< 2E-16	-8.04857937E-41	-6.96896097E-41
		R^2	Adjusted R^2	F-Statistic	Df (due to $RegSS$)	Df (due to RSS)	Pr>F
	Model	0.9984221	0.9984193	354031.642	10	5595	< 2E-16
Year	Parameter	Estimate	Standard Error	t-value	Pr(>|t|)	95% Lower Confidence Limit	95% Upper Confidence Limit
2005	β_0	1.49231813E-04	6.87E-08	2172.41	< 2E-16	1.49097146E-04	1.49366479E-04
	β_1	-2.92691842E-08	5.69E-10	-51.41	< 2E-16	-3.03853716E-08	-2.81529967E-08
	β_2	1.30070710E-11	1.52E-12	8.58	< 2E-16	1.00360913E-11	1.59780507E-11
	β_3	1.20655760E-14	1.85E-15	6.52	< 2E-16	8.43744871E-15	1.56937033E-14
	β_4	-1.96478121E-17	1.24E-18	-15.90	< 2E-16	-2.20695801E-17	-1.72260440E-17
	β_5	1.12583140E-20	4.93E-22	22.84	< 2E-16	1.02920715E-20	1.22245564E-20
	β_6	-3.47589615E-24	1.23E-25	-28.34	< 2E-16	-3.71634044E-24	-3.23545186E-24
	β_7	6.29878275E-28	1.92E-29	32.82	< 2E-16	5.92257241E-28	6.67499309E-28
	β_8	-6.70416602E-32	1.83E-33	-36.55	< 2E-16	-7.06374806E-32	-6.34458398E-32
	β_9	3.88482127E-36	9.78E-38	39.72	< 2E-16	3.69307911E-36	4.07656344E-36
	β_{10}	-9.46905973E-41	2.23E-42	-42.48	< 2E-16	-9.90602448E-41	-9.03209498E-41
		R^2	Adjusted R^2	F-Statistic	Df (due to $RegSS$)	Df (due to RSS)	Pr>F
	Model	0.9990119	0.9990102	580256.995	10	5739	< 2E-16
Year	Parameter	Estimate	Standard Error	t-value	Pr(>|t|)	95% Lower Confidence Limit	95% Upper Confidence Limit
2006	β_0	1.51294967E-04	6.92E-08	2184.84	< 2E-16	1.51159217E-04	1.51430717E-04
	β_1	-3.29192029E-08	5.72E-10	-57.59	< 2E-16	-3.40398485E-08	-3.17985574E-08
	β_2	2.00301794E-11	1.52E-12	13.19	< 2E-16	1.70527816E-11	2.30075772E-11
	β_3	6.12580941E-15	1.85E-15	3.30	0.0010	2.49111234E-15	9.76050649E-15
	β_4	-1.70805040E-17	1.24E-18	-13.80	< 2E-16	-1.95061121E-17	-1.46548959E-17
	β_5	1.06060195E-20	4.93E-22	21.49	< 2E-16	9.63862992E-21	1.15734091E-20
	β_6	-3.37367335E-24	1.23E-25	-27.49	< 2E-16	-3.61427129E-24	-3.13307541E-24
	β_7	6.20474578E-28	1.92E-29	32.33	< 2E-16	5.82852840E-28	6.58096317E-28
	β_8	-6.66536713E-32	1.83E-33	-36.36	< 2E-16	-7.02472962E-32	-6.30600464E-32
	β_9	3.88972277E-36	9.77E-38	39.82	< 2E-16	3.69821268E-36	4.08123286E-36
	β_{10}	-9.54046229E-41	2.23E-42	-42.88	< 2E-16	-9.97665732E-41	-9.10426726E-41
		R^2	Adjusted R^2	F-Statistic	Df (due to $RegSS$)	Df (due to RSS)	Pr>F
	Model	0.9990813	0.9990798	650757.079	10	5984	< 2E-16
Year	Parameter	Estimate	Standard Error	t-value	Pr(>|t|)	95% Lower Confidence Limit	95% Upper Confidence Limit
2007	β_0	1.50910777E-04	7.17E-08	2105.87	< 2E-16	1.50770295E-04	1.51051260E-04
	β_1	-2.34911538E-08	5.86E-10	-40.07	< 2E-16	-2.46405322E-08	-2.23417753E-08
	β_2	2.16624687E-12	1.55E-12	1.39	< 2E-16	-8.78749933E-13	5.21124368E-12
	β_3	1.94379057E-14	1.89E-15	10.26	< 2E-16	1.57231548E-14	2.31526566E-14
	β_4	-2.27217919E-17	1.27E-18	-17.96	< 2E-16	-2.52016679E-17	-2.02419160E-17
	β_5	1.22110913E-20	5.05E-22	24.18	< 2E-16	1.12212716E-20	1.32009109E-20
	β_6	-3.69993937E-24	1.26E-25	-29.43	< 2E-16	-3.94635737E-24	-3.45352137E-24
	β_7	6.67069673E-28	1.97E-29	33.90	< 2E-16	6.28498050E-28	7.05641296E-28
	β_8	-7.10133431E-32	1.88E-33	-37.75	< 2E-16	-7.47014653E-32	-6.73252210E-32
	β_9	4.12572288E-36	1.00E-37	41.11	< 2E-16	3.92898392E-36	4.32246185E-36
	β_{10}	-1.00951702E-40	2.29E-42	-44.12	< 2E-16	-1.05436918E-40	-9.64664846E-41
		R^2	Adjusted R^2	F-Statistic	Df (due to $RegSS$)	Df (due to RSS)	Pr>F
	Model	0.9989947	0.9989931	613231.193	10	6171	< 2E-16

Year	Parameter	Estimate	Standard Error	t-value	Pr(>|t|)	95% Lower Confidence Limit	95% Upper Confidence Limit
2008	β_0	1.50325303E-04	7.22E-08	2083.31	< 2E-16	1.50183851E-04	1.50466754E-04
	β_1	-2.37247208E-08	5.88E-10	-40.32	< 2E-16	-2.48783081E-08	-2.25711335E-08
	β_2	6.01068584E-12	1.55E-12	3.88	0.0001	2.97588421E-12	9.04548747E-12
	β_3	1.47901045E-14	1.88E-15	7.88	3.83E-15	1.11104279E-14	1.84697812E-14
	β_4	-1.97532183E-17	1.25E-18	-15.84	< 2E-16	-2.21971042E-17	-1.73093324E-17
	β_5	1.10190506E-20	4.95E-22	22.24	< 2E-16	1.00478580E-20	1.19902433E-20
	β_6	-3.40124607E-24	1.23E-25	-27.68	< 2E-16	-3.64209465E-24	-3.16039748E-24
	β_7	6.21799945E-28	1.92E-29	32.45	< 2E-16	5.84232664E-28	6.59367226E-28
	β_8	-6.70623859E-32	1.83E-33	-36.72	< 2E-16	-7.06426411E-32	-6.34821306E-32
	β_9	3.94763100E-36	9.71E-38	40.65	< 2E-16	3.75724747E-36	4.13801453E-36
	β_{10}	-9.78865021E-41	2.21E-42	-44.35	< 2E-16	-1.02213582E-40	-9.35594224E-41
		R^2	Adjusted R^2	F-Statistic	Df (due to $RegSS$)	Df (due to RSS)	Pr>F
	Model	0.9990143	0.9990128	658374.148	10	6496	< 2E-16
Year	Parameter	Estimate	Standard Error	t-value	Pr(>|t|)	95% Lower Confidence Limit	95% Upper Confidence Limit
2009	β_0	1.50104482E-04	7.77E-08	1933.01	< 2E-16	1.49952255E-04	1.50256709E-04
	β_1	-3.45246296E-08	6.41E-10	-53.87	< 2E-16	-3.57809881E-08	-3.32682711E-08
	β_2	2.81013975E-11	1.70E-12	16.55	< 2E-16	2.47723921E-11	3.14304030E-11
	β_3	-7.37152809E-15	2.07E-15	-3.57	0.0004	-1.14237309E-14	-3.31932524E-15
	β_4	-6.23825581E-18	1.38E-18	-4.53	5.95E-06	-8.93669734E-18	-3.53981427E-18
	β_5	5.80248934E-21	5.48E-22	10.58	< 2E-16	4.72779712E-21	6.87718156E-21
	β_6	-2.11069021E-24	1.36E-25	-15.49	< 2E-16	-2.37774939E-24	-1.84363103E-24
	β_7	4.18291581E-28	2.13E-29	19.64	< 2E-16	3.76550591E-28	4.60032570E-28
	β_8	-4.73077812E-32	2.03E-33	-23.26	< 2E-16	-5.12942920E-32	-4.33212704E-32
	β_9	2.87251781E-36	1.08E-37	26.50	< 2E-16	2.66005483E-36	3.08498079E-36
	β_{10}	-7.27897413E-41	2.47E-42	-29.48	< 2E-16	-7.76300693E-41	-6.79494133E-41
		R^2	Adjusted R^2	F-Statistic	Df (due to $RegSS$)	Df (due to RSS)	Pr>F
	Model	0.9987210	0.9987189	485525.03	10	6218	< 2E-16
Year	Parameter	Estimate	Standard Error	t-value	Pr(>|t|)	95% Lower Confidence Limit	95% Upper Confidence Limit
2010	β_0	1.56759447E-04	5.26E-08	2980.88	< 2E-16	1.56656356E-04	1.56862538E-04
	β_1	-4.91697500E-08	4.29E-10	-114.59	< 2E-16	-5.00109368E-08	-4.83285632E-08
	β_2	4.45405336E-11	1.13E-12	39.28	< 2E-16	4.23175445E-11	4.67635227E-11
	β_3	-2.18677319E-14	1.38E-15	-15.83	< 2E-16	-2.45752446E-14	-1.91602191E-14
	β_4	2.89411048E-18	9.21E-19	3.14	0.0017	1.08863174E-18	4.69958921E-18
	β_5	2.02228054E-21	3.67E-22	5.51	3.83E-08	1.30218090E-21	2.74238017E-21
	β_6	-1.10354981E-24	9.14E-26	-12.07	< 2E-16	-1.28272868E-24	-9.24370937E-25
	β_7	2.48042046E-28	1.43E-29	17.34	< 2E-16	2.20004814E-28	2.76079279E-28
	β_8	-2.97249693E-32	1.37E-33	-21.74	< 2E-16	-3.24052634E-32	-2.70446752E-32
	β_9	1.86308408E-36	7.29E-38	25.55	< 2E-16	1.72012155E-36	2.00604660E-36
	β_{10}	-4.81465379E-41	1.66E-42	-28.96	< 2E-16	-5.14056985E-41	-4.48873773E-41
		R^2	Adjusted R^2	F-Statistic	Df (due to $RegSS$)	Df (due to RSS)	Pr>F
	Model	0.9994421	0.9994412	1142753.82	10	6379	< 2E-16
Year	Parameter	Estimate	Standard Error	t-value	Pr(>|t|)	95% Lower Confidence Limit	95% Upper Confidence Limit
2011	β_0	1.50898999E-04	5.24E-08	2878.10	< 2E-16	1.50796220E-04	1.51001777E-04
	β_1	-3.70910993E-08	4.22E-10	-87.96	< 2E-16	-3.79177231E-08	-3.62644756E-08
	β_2	3.52332334E-11	1.10E-12	31.98	< 2E-16	3.30733706E-11	3.73930962E-11
	β_3	-1.65878137E-14	1.33E-15	-12.46	< 2E-16	-1.91979641E-14	-1.39776633E-14
	β_4	6.54767372E-19	8.83E-19	0.74	0.4586	-1.07704226E-18	2.38657701E-18
	β_5	2.59427341E-21	3.51E-22	7.39	1.69E-13	1.90570805E-21	3.28283877E-21
	β_6	-1.17359243E-24	8.72E-26	-13.45	< 2E-16	-1.34460695E-24	-1.00257791E-24
	β_7	2.48151771E-28	1.36E-29	18.20	< 2E-16	2.21419769E-28	2.74883772E-28
	β_8	-2.87477345E-32	1.30E-33	-22.06	< 2E-16	-3.13019681E-32	-2.61935009E-32
	β_9	1.76114963E-36	6.95E-38	25.34	< 2E-16	1.62493172E-36	1.89736754E-36
	β_{10}	-4.47491521E-41	1.58E-42	-28.25	< 2E-16	-4.78548037E-41	-4.16435005E-41
		R^2	Adjusted R^2	F-Statistic	Df (due to $RegSS$)	Df (due to RSS)	Pr>F
	Model	0.9993944	0.9993936	1189685.53	10	7209	< 2E-16

Year	Parameter	Estimate	Standard Error	t-value	Pr(>|t|)	95% Lower Confidence Limit	95% Upper Confidence Limit
2012	β_0	1.53966290E-04	7.87E-08	1956.66	< 2E-16	1.53812041E-04	1.54120539E-04
	β_1	-5.41206084E-08	6.25E-10	-86.58	< 2E-16	-5.53459525E-08	-5.28952643E-08
	β_2	7.25252924E-11	1.62E-12	44.81	< 2E-16	6.93524416E-11	7.56981431E-11
	β_3	-5.39082648E-14	1.94E-15	-27.76	< 2E-16	-5.77154358E-14	-5.01010938E-14
	β_4	2.04893179E-17	1.28E-18	15.99	< 2E-16	1.79779420E-17	2.30006938E-17
	β_5	-3.50860382E-21	5.07E-22	-6.92	4.79E-12	-4.50223077E-21	-2.51497688E-21
	β_6	-5.18359561E-26	1.25E-25	-0.41	0.6792	-2.97570162E-25	1.93898250E-25
	β_7	1.27302450E-28	1.95E-29	6.52	< 2E-16	8.90343898E-29	1.65570511E-28
	β_8	-2.18223872E-32	1.86E-33	-11.74	< 2E-16	-2.54666100E-32	-1.81781643E-32
	β_9	1.61201675E-36	9.88E-38	16.31	< 2E-16	1.41826484E-36	1.80576865E-36
	β_{10}	-4.58692623E-41	2.25E-42	-20.41	< 2E-16	-5.02741006E-41	-4.14644241E-41
		R^2	Adjusted R^2	F-Statistic	Df (due to $RegSS$)	Df (due to RSS)	Pr>F
	Model	0.9985778	0.9985761	582016.665	10	8289	< 2E-16
Year	Parameter	Estimate	Standard Error	t-value	Pr(>|t|)	95% Lower Confidence Limit	95% Upper Confidence Limit
2013	β_0	1.49213762E-04	6.25E-08	2386.70	< 2E-16	1.49091210E-04	1.49336314E-04
	β_1	-1.76573285E-08	4.94E-10	-35.71	< 2E-16	-1.86265781E-08	-1.66880789E-08
	β_2	-1.67880042E-11	1.28E-12	-13.13	< 2E-16	-1.92952970E-11	-1.42807113E-11
	β_3	4.25328388E-14	1.54E-15	27.69	< 2E-16	3.95221379E-14	4.55435397E-14
	β_4	-3.61931732E-17	1.01E-18	-35.67	< 2E-16	-3.81823080E-17	-3.42040383E-17
	β_5	1.66018556E-20	4.02E-22	41.26	< 2E-16	1.58132063E-20	1.73905049E-20
	β_6	-4.55876472E-24	9.97E-26	-45.71	< 2E-16	-4.75427467E-24	-4.36325477E-24
	β_7	7.69939089E-28	1.56E-29	49.44	< 2E-16	7.39413384E-28	8.00464794E-28
	β_8	-7.83702976E-32	1.49E-33	-52.70	< 2E-16	-8.12851213E-32	-7.54554740E-32
	β_9	4.41206770E-36	7.93E-38	55.65	< 2E-16	4.25666285E-36	4.56747256E-36
	β_{10}	-1.05565371E-40	1.81E-42	-58.40	< 2E-16	-1.09108454E-40	-1.02022288E-40
		R^2	Adjusted R^2	F-Statistic	Df (due to $RegSS$)	Df (due to RSS)	Pr>F
	Model	0.9990185	0.9990174	883321.63	10	8678	< 2E-16
Year	Parameter	Estimate	Standard Error	t-value	Pr(>|t|)	95% Lower Confidence Limit	95% Upper Confidence Limit
2014	β_0	1.55393298E-04	7.67E-08	2025.58	< 2E-16	1.55242918E-04	1.55543679E-04
	β_1	-4.79583772E-08	6.06E-10	-79.10	< 2E-16	-4.91469302E-08	-4.67698242E-08
	β_2	3.85448476E-11	1.57E-12	24.60	< 2E-16	3.54729630E-11	4.16167322E-11
	β_3	-9.19911616E-15	1.88E-15	-4.89	< 2E-16	-1.28856614E-14	-5.51257094E-15
	β_4	-8.16229944E-18	1.24E-18	-6.57	< 2E-16	-1.05972089E-17	-5.72738996E-18
	β_5	7.17040838E-21	4.92E-22	14.56	< 2E-16	6.20516485E-21	8.13565192E-21
	β_6	-2.52434143E-24	1.22E-25	-20.68	< 2E-16	-2.76361426E-24	-2.28506860E-24
	β_7	4.88294186E-28	1.91E-29	25.62	< 2E-16	4.50936327E-28	5.25652044E-28
	β_8	-5.41777272E-32	1.82E-33	-29.77	< 2E-16	-5.77449598E-32	-5.06104946E-32
	β_9	3.23857628E-36	9.70E-38	33.38	< 2E-16	3.04838405E-36	3.42876851E-36
	β_{10}	-8.10002882E-41	2.21E-42	-36.62	< 2E-16	-8.53366152E-41	-7.66639612E-41
		R^2	Adjusted R^2	F-Statistic	Df (due to $RegSS$)	Df (due to RSS)	Pr>F
	Model	0.9985259	0.9985243	591977.965	10	8739	< 2E-16

Summary Statistics of 11th Degree Polynomial Approximations to LDCs of Turkey in the Period 2000-2014

Year	Parameter	Estimate	Standard Error	t-value	Pr(>|t|)	95% Lower Confidence Limit	95% Upper Confidence Limit
2000	β_0	1.48091896E-04	2.00E-08	7404.60	< 2E-16	1.48052688E-04	1.48131104E-04
	β_1	-4.72663348E-08	2.01E-10	-234.58	< 2E-16	-4.76613402E-08	-4.68713295E-08
	β_2	9.36720944E-11	6.45E-13	145.30	< 2E-16	9.24082180E-11	9.49359709E-11
	β_3	-1.14250227E-13	9.49E-16	-120.43	< 2E-16	-1.16109969E-13	-1.12390485E-13
	β_4	8.35185022E-17	7.70E-19	108.41	< 2E-16	8.20081722E-17	8.50288323E-17
	β_5	-3.88739582E-20	3.80E-22	-102.28	< 2E-16	-3.96190531E-20	-3.81288633E-20
	β_6	1.19066562E-23	1.20E-25	99.35	< 2E-16	1.16717077E-23	1.21416047E-23
	β_7	-2.42517854E-27	2.47E-29	-98.29	< 2E-16	-2.47354927E-27	-2.37680782E-27
	β_8	3.24667804E-31	3.30E-33	98.36	< 2E-16	3.18196907E-31	3.31138700E-31
	β_9	-2.74030721E-35	2.76E-37	-99.12	< 2E-16	-2.79450338E-35	-2.68611105E-35
	β_{10}	1.32059452E-39	1.32E-41	100.32	< 2E-16	1.29478734E-39	1.34640170E-39
	β_{11}	-2.76789534E-44	2.72E-46	-101.79	< 2E-16	-2.82120428E-44	-2.71458640E-44
		R^2	Adjusted R^2	F-Statistic	Df (due to $RegSS$)	Df (due to RSS)	Pr>F
	Model	0.9999303	0.9999301	6877119.32	11	5275	< 2E-16
Year	Parameter	Estimate	Standard Error	t-value	Pr(>|t|)	95% Lower Confidence Limit	95% Upper Confidence Limit
2001	β_0	1.51300918E-04	4.60E-08	3288.83	< 2E-16	1.51210731E-04	1.51391104E-04
	β_1	-5.87280718E-08	4.60E-10	-127.63	< 2E-16	-5.96301233E-08	-5.78260203E-08
	β_2	1.27146837E-10	1.46E-12	86.81	< 2E-16	1.24275450E-10	1.30018223E-10
	β_3	-1.65005494E-13	2.15E-15	-76.57	< 2E-16	-1.69229833E-13	-1.60781154E-13
	β_4	1.25929243E-16	1.75E-18	71.80	< 2E-16	1.22491008E-16	1.29367479E-16
	β_5	-6.02673040E-20	8.68E-22	-69.44	< 2E-16	-6.19688475E-20	-5.85657605E-20
	β_6	1.87725654E-23	2.75E-25	68.35	< 2E-16	1.82341739E-23	1.93109569E-23
	β_7	-3.85944149E-27	5.67E-29	-68.02	< 2E-16	-3.97066820E-27	-3.74821477E-27
	β_8	5.19025306E-31	7.62E-33	68.15	< 2E-16	5.04095468E-31	5.33955144E-31
	β_9	-4.38837061E-35	6.40E-37	-68.58	< 2E-16	-4.51382240E-35	-4.26291883E-35
	β_{10}	2.11541101E-39	3.06E-41	69.20	< 2E-16	2.05548383E-39	2.17533818E-39
	β_{11}	-4.43224219E-44	6.33E-46	-69.98	< 2E-16	-4.55641424E-44	-4.30807015E-44
		R^2	Adjusted R^2	F-Statistic	Df (due to $RegSS$)	Df (due to RSS)	Pr>F
	Model	0.9996458	0.9996451	1415647.6	11	5517	< 2E-16
Year	Parameter	Estimate	Standard Error	t-value	Pr(>|t|)	95% Lower Confidence Limit	95% Upper Confidence Limit
2002	β_0	1.53006454E-04	5.80E-08	2638.94	< 2E-16	1.52892789E-04	1.53120119E-04
	β_1	-8.08086485E-08	5.82E-10	-138.85	< 2E-16	-8.19495773E-08	-7.96677196E-08
	β_2	1.76621453E-10	1.87E-12	94.50	< 2E-16	1.72957341E-10	1.80285565E-10
	β_3	-2.22207866E-13	2.77E-15	-80.28	< 2E-16	-2.27634130E-13	-2.16781603E-13
	β_4	1.65399417E-16	2.26E-18	73.12	< 2E-16	1.60964768E-16	1.69834067E-16
	β_5	-7.76736510E-20	1.12E-21	-69.22	< 2E-16	-7.98734734E-20	-7.54738285E-20
	β_6	2.38642200E-23	3.56E-25	67.13	< 2E-16	2.31672782E-23	2.45611618E-23
	β_7	-4.85873179E-27	7.35E-29	-66.11	< 2E-16	-5.00280773E-27	-4.71465585E-27
	β_8	6.48931696E-31	9.87E-33	65.76	< 2E-16	6.29586592E-31	6.68276799E-31
	β_9	-5.45927145E-35	8.29E-37	-65.83	< 2E-16	-5.62184287E-35	-5.29670003E-35
	β_{10}	2.62139456E-39	3.96E-41	66.17	< 2E-16	2.54373440E-39	2.69905471E-39
	β_{11}	-5.47426013E-44	8.21E-46	-66.69	< 2E-16	-5.63516962E-44	-5.31335065E-44
		R^2	Adjusted R^2	F-Statistic	Df (due to $RegSS$)	Df (due to RSS)	Pr>F
	Model	0.9993670	0.9993657	754549.524	11	5257	< 2E-16
Year	Parameter	Estimate	Standard Error	t-value	Pr(>|t|)	95% Lower Confidence Limit	95% Upper Confidence Limit
2003	β_0	1.48291490E-04	5.67E-08	2613.71	< 2E-16	1.48180265E-04	1.48402715E-04
	β_1	-5.76442232E-08	5.73E-10	-100.60	< 2E-16	-5.87675119E-08	-5.65209344E-08
	β_2	1.26359997E-10	1.84E-12	68.81	< 2E-16	1.22760064E-10	1.29959930E-10
	β_3	-1.60741119E-13	2.71E-15	-59.30	< 2E-16	-1.66055296E-13	-1.55426943E-13
	β_4	1.20591533E-16	2.21E-18	54.60	< 2E-16	1.16261552E-16	1.24921513E-16
	β_5	-5.71177453E-20	1.09E-21	-52.26	< 2E-16	-5.92602285E-20	-5.49752620E-20
	β_6	1.77189224E-23	3.46E-25	51.28	< 2E-16	1.70415354E-23	1.83963094E-23
	β_7	-3.64553552E-27	7.13E-29	-51.12	< 2E-16	-3.78533772E-27	-3.50573332E-27
	β_8	4.92220727E-31	9.56E-33	51.47	< 2E-16	4.73474628E-31	5.10966826E-31
	β_9	-4.18628094E-35	8.03E-37	-52.15	< 2E-16	-4.34364541E-35	-4.02891648E-35
	β_{10}	2.03164345E-39	3.83E-41	53.03	< 2E-16	1.95653898E-39	2.10674793E-39
	β_{11}	-4.28620493E-44	7.93E-46	-54.04	< 2E-16	-4.44170107E-44	-4.13070879E-44
		R^2	Adjusted R^2	F-Statistic	Df (due to $RegSS$)	Df (due to RSS)	Pr>F
	Model	0.9993923	0.9993910	812379.03	11	5434	< 2E-16

Year	Parameter	Estimate	Standard Error	t-value	Pr(>|t|)	95% Lower Confidence Limit	95% Upper Confidence Limit
2004	β_0	1.50751162E-04	7.31E-08	2062.14	< 2E-16	1.50607850E-04	1.50894475E-04
	β_1	-6.97295394E-08	7.31E-10	-95.42	< 2E-16	-7.11621616E-08	-6.82969172E-08
	β_2	1.54357596E-10	2.33E-12	66.13	< 2E-16	1.49781450E-10	1.58933743E-10
	β_3	-1.99239486E-13	3.44E-15	-57.97	< 2E-16	-2.05977771E-13	-1.92501201E-13
	β_4	1.52233581E-16	2.79E-18	54.48	< 2E-16	1.46755459E-16	1.57711704E-16
	β_5	-7.33203833E-20	1.38E-21	-53.15	< 2E-16	-7.60249914E-20	-7.06157753E-20
	β_6	2.30773818E-23	4.35E-25	53.03	< 2E-16	2.22242264E-23	2.39305372E-23
	β_7	-4.80748209E-27	8.96E-29	-53.65	< 2E-16	-4.98313810E-27	-4.63182607E-27
	β_8	6.56040970E-31	1.20E-32	54.74	< 2E-16	6.32546111E-31	6.79535829E-31
	β_9	-5.63003112E-35	1.00E-36	-56.11	< 2E-16	-5.82674789E-35	-5.43331435E-35
	β_{10}	2.75312406E-39	4.78E-41	57.64	< 2E-16	2.65948910E-39	2.84675903E-39
	β_{11}	-5.84543158E-44	9.86E-46	-59.27	< 2E-16	-6.03876142E-44	-5.65210175E-44
		R^2	Adjusted R^2	F-Statistic	Df (due to $RegSS$)	Df (due to RSS)	Pr>F
	Model	0.9990308	0.9990289	524209.995	11	5594	< 2E-16
Year	Parameter	Estimate	Standard Error	t-value	Pr(>|t|)	95% Lower Confidence Limit	95% Upper Confidence Limit
2005	β_0	1.50649316E-04	5.76E-08	2616.85	< 2E-16	1.50536459E-04	1.50762173E-04
	β_1	-5.19357657E-08	5.69E-10	-91.33	< 2E-16	-5.30505835E-08	-5.08209479E-08
	β_2	9.98481239E-11	1.81E-12	55.09	< 2E-16	9.62950669E-11	1.03401181E-10
	β_3	-1.29496764E-13	2.67E-15	-48.47	< 2E-16	-1.34734564E-13	-1.24258965E-13
	β_4	1.03060843E-16	2.18E-18	47.33	< 2E-16	9.87920132E-17	1.07329672E-16
	β_5	-5.19795732E-20	1.08E-21	-48.20	< 2E-16	-5.40936107E-20	-4.98655357E-20
	β_6	1.70725114E-23	3.41E-25	50.02	< 2E-16	1.64034319E-23	1.77415909E-23
	β_7	-3.68984690E-27	7.05E-29	-52.33	< 2E-16	-3.82807531E-27	-3.55161849E-27
	β_8	5.19277214E-31	9.46E-33	54.87	< 2E-16	5.00724587E-31	5.37829841E-31
	β_9	-4.57103995E-35	7.95E-37	-57.49	< 2E-16	-4.72691351E-35	-4.41516640E-35
	β_{10}	2.28239437E-39	3.80E-41	60.10	< 2E-16	2.20794486E-39	2.35684388E-39
	β_{11}	-4.92985828E-44	7.87E-46	-62.66	< 2E-16	-5.08410179E-44	-4.77561478E-44
		R^2	Adjusted R^2	F-Statistic	Df (due to $RegSS$)	Df (due to RSS)	Pr>F
	Model	0.9994133	0.9994122	888620.735	11	5738	< 2E-16
Year	Parameter	Estimate	Standard Error	t-value	Pr(>|t|)	95% Lower Confidence Limit	95% Upper Confidence Limit
2006	β_0	1.52834439E-04	5.59E-08	2732.91	< 2E-16	1.52724809E-04	1.52944070E-04
	β_1	-5.73095978E-08	5.50E-10	-104.29	< 2E-16	-5.83868239E-08	-5.62323718E-08
	β_2	1.13153810E-10	1.75E-12	64.81	< 2E-16	1.09731210E-10	1.16576409E-10
	β_3	-1.45206750E-13	2.57E-15	-56.57	< 2E-16	-1.50238281E-13	-1.40175218E-13
	β_4	1.13801091E-16	2.09E-18	54.54	< 2E-16	1.09710413E-16	1.17891769E-16
	β_5	-5.67460505E-20	1.03E-21	-55.02	< 2E-16	-5.87680684E-20	-5.47240327E-20
	β_6	1.84929937E-23	3.26E-25	56.72	< 2E-16	1.78538507E-23	1.91321368E-23
	β_7	-3.97433868E-27	6.73E-29	-59.05	< 2E-16	-4.10628092E-27	-3.84239644E-27
	β_8	5.56891388E-31	9.03E-33	61.67	< 2E-16	5.39189481E-31	5.74593295E-31
	β_9	-4.88538037E-35	7.59E-37	-64.40	< 2E-16	-5.03408608E-35	-4.73667466E-35
	β_{10}	2.43281665E-39	3.62E-41	67.14	< 2E-16	2.36178826E-39	2.50384505E-39
	β_{11}	-5.24413213E-44	7.51E-46	-69.85	< 2E-16	-5.39130877E-44	-5.09695548E-44
		R^2	Adjusted R^2	F-Statistic	Df (due to $RegSS$)	Df (due to RSS)	Pr>F
	Model	0.9994940	0.9994930	1074307.27	11	5983	< 2E-16
Year	Parameter	Estimate	Standard Error	t-value	Pr(>|t|)	95% Lower Confidence Limit	95% Upper Confidence Limit
2007	β_0	1.52411424E-04	6.08E-08	2506.48	< 2E-16	1.52292221E-04	1.52530626E-04
	β_1	-4.71499736E-08	5.92E-10	-79.61	< 2E-16	-4.83110747E-08	-4.59888725E-08
	β_2	9.22321385E-11	1.88E-12	49.17	< 2E-16	8.85548216E-11	9.59094554E-11
	β_3	-1.26962120E-13	2.76E-15	-46.05	< 2E-16	-1.32366851E-13	-1.21557388E-13
	β_4	1.04073295E-16	2.24E-18	46.38	< 2E-16	9.96742135E-17	1.08472377E-16
	β_5	-5.31428141E-20	1.11E-21	-47.84	< 2E-16	-5.53205888E-20	-5.09650394E-20
	β_6	1.75489024E-23	3.52E-25	49.90	< 2E-16	1.68595121E-23	1.82382926E-23
	β_7	-3.80342316E-27	7.27E-29	-52.32	< 2E-16	-3.94591984E-27	-3.66092648E-27
	β_8	5.36281619E-31	9.76E-33	54.93	< 2E-16	5.17143366E-31	5.55419871E-31
	β_9	-4.72871233E-35	8.21E-37	-57.61	< 2E-16	-4.88962546E-35	-4.56779919E-35
	β_{10}	2.36526720E-39	3.92E-41	60.28	< 2E-16	2.28835147E-39	2.44218293E-39
	β_{11}	-5.11872574E-44	8.14E-46	-62.92	< 2E-16	-5.27820164E-44	-4.95924983E-44
		R^2	Adjusted R^2	F-Statistic	Df (due to $RegSS$)	Df (due to RSS)	Pr>F
	Model	0.9993876	0.9993865	915417.261	11	6170	< 2E-16

Year	Parameter	Estimate	Standard Error	t-value	Pr(>|t|)	95% Lower Confidence Limit	95% Upper Confidence Limit
2008	β_0	1.52081803E-04	5.68E-08	2679.41	< 2E-16	1.51970536E-04	1.52193070E-04
	β_1	-5.10308643E-08	5.52E-10	-92.50	< 2E-16	-5.21123675E-08	-4.99493611E-08
	β_2	1.08971072E-10	1.74E-12	62.77	< 2E-16	1.05568053E-10	1.12374091E-10
	β_3	-1.51191295E-13	2.53E-15	-59.65	< 2E-16	-1.56160271E-13	-1.46222319E-13
	β_4	1.22982463E-16	2.05E-18	59.98	< 2E-16	1.18962730E-16	1.27002195E-16
	β_5	-6.21059392E-20	1.01E-21	-61.52	< 2E-16	-6.40848994E-20	-6.01269790E-20
	β_6	2.02503434E-23	3.18E-25	63.68	< 2E-16	1.96270032E-23	2.08736835E-23
	β_7	-4.33145541E-27	6.54E-29	-66.20	< 2E-16	-4.45972295E-27	-4.20318786E-27
	β_8	6.03057658E-31	8.75E-33	68.90	< 2E-16	5.85900557E-31	6.20214758E-31
	β_9	-5.25714413E-35	7.33E-37	-71.71	< 2E-16	-5.40085966E-35	-5.11342859E-35
	β_{10}	2.60382207E-39	3.49E-41	74.56	< 2E-16	2.53536658E-39	2.67227755E-39
	β_{11}	-5.58903218E-44	7.22E-46	-77.45	< 2E-16	-5.73049906E-44	-5.44756530E-44
		R^2	Adjusted R^2	F-Statistic	Df (due to $RegSS$)	Df (due to RSS)	Pr>F
	Model	0.9994876	0.9994867	1151632.27	11	6495	< 2E-16
Year	Parameter	Estimate	Standard Error	t-value	Pr(>|t|)	95% Lower Confidence Limit	95% Upper Confidence Limit
2009	β_0	1.51592301E-04	6.94E-08	2185.83	< 2E-16	1.51456347E-04	1.51728255E-04
	β_1	-5.81286459E-08	6.81E-10	-85.40	< 2E-16	-5.94630132E-08	-5.67942787E-08
	β_2	1.18104550E-10	2.16E-12	54.76	< 2E-16	1.13876422E-10	1.22332677E-10
	β_3	-1.53606895E-13	3.17E-15	-48.51	< 2E-16	-1.59814085E-13	-1.47399705E-13
	β_4	1.20260545E-16	2.57E-18	46.73	< 2E-16	1.15215549E-16	1.25305540E-16
	β_5	-5.93092341E-20	1.27E-21	-46.62	< 2E-16	-6.18033468E-20	-5.68151214E-20
	β_6	1.90322031E-23	4.02E-25	47.31	< 2E-16	1.82436315E-23	1.98207747E-23
	β_7	-4.02489853E-27	8.31E-29	-48.46	< 2E-16	-4.18772553E-27	-3.86207153E-27
	β_8	5.55696330E-31	1.11E-32	49.86	< 2E-16	5.33847197E-31	5.77545463E-31
	β_9	-4.81353007E-35	9.36E-37	-51.41	< 2E-16	-4.99709424E-35	-4.62996591E-35
	β_{10}	2.37230346E-39	4.47E-41	53.04	< 2E-16	2.28461932E-39	2.45998761E-39
	β_{11}	-5.07189123E-44	9.27E-46	-54.72	< 2E-16	-5.25358853E-44	-4.89019394E-44
		R^2	Adjusted R^2	F-Statistic	Df (due to $RegSS$)	Df (due to RSS)	Pr>F
	Model	0.9991367	0.9991352	654145.137	11	6217	< 2E-16
Year	Parameter	Estimate	Standard Error	t-value	Pr(>|t|)	95% Lower Confidence Limit	95% Upper Confidence Limit
2010	β_0	1.57881771E-04	4.50E-08	3510.03	< 2E-16	1.57793594E-04	1.57969947E-04
	β_1	-6.66550963E-08	4.37E-10	-152.65	< 2E-16	-6.75110674E-08	-6.57991253E-08
	β_2	1.11087813E-10	1.38E-12	80.38	< 2E-16	1.08378674E-10	1.13796952E-10
	β_3	-1.30072832E-13	2.03E-15	-64.01	< 2E-16	-1.34056266E-13	-1.26089398E-13
	β_4	9.66049629E-17	1.65E-18	58.39	< 2E-16	9.33613688E-17	9.98485569E-17
	β_5	-4.62642809E-20	8.19E-22	-56.47	< 2E-16	-4.78703282E-20	-4.46582335E-20
	β_6	1.45894239E-23	2.59E-25	56.26	< 2E-16	1.40810300E-23	1.50978178E-23
	β_7	-3.05204737E-27	5.36E-29	-56.94	< 2E-16	-3.15711438E-27	-2.94698036E-27
	β_8	4.18374758E-31	7.20E-33	58.14	< 2E-16	4.04267200E-31	4.32482317E-31
	β_9	-3.60566421E-35	6.05E-37	-59.61	< 2E-16	-3.72424357E-35	-3.48708485E-35
	β_{10}	1.77013796E-39	2.89E-41	61.24	< 2E-16	1.71347570E-39	1.82680022E-39
	β_{11}	-3.77266631E-44	5.99E-46	-62.97	< 2E-16	-3.89011197E-44	-3.65522065E-44
		R^2	Adjusted R^2	F-Statistic	Df (due to $RegSS$)	Df (due to RSS)	Pr>F
	Model	0.9996560	0.9996554	1684854.7	11	6378	< 2E-16
Year	Parameter	Estimate	Standard Error	t-value	Pr(>|t|)	95% Lower Confidence Limit	95% Upper Confidence Limit
2011	β_0	1.52221962E-04	4.16E-08	3658.51	< 2E-16	1.52140399E-04	1.52303525E-04
	β_1	-5.73669610E-08	3.98E-10	-144.05	< 2E-16	-5.81476426E-08	-5.65862793E-08
	β_2	1.11365101E-10	1.25E-12	89.43	< 2E-16	1.08924099E-10	1.13806104E-10
	β_3	-1.39264124E-13	1.82E-15	-76.72	< 2E-16	-1.42822438E-13	-1.35705810E-13
	β_4	1.06271785E-16	1.47E-18	72.32	< 2E-16	1.03391182E-16	1.09152388E-16
	β_5	-5.16197183E-20	7.25E-22	-71.22	< 2E-16	-5.30405553E-20	-5.01988813E-20
	β_6	1.64030996E-23	2.29E-25	71.67	< 2E-16	1.59544551E-23	1.68517441E-23
	β_7	-3.44254178E-27	4.72E-29	-72.90	< 2E-16	-3.53511497E-27	-3.34996859E-27
	β_8	4.71953033E-31	6.33E-33	74.50	< 2E-16	4.59534703E-31	4.84371363E-31
	β_9	-4.05908345E-35	5.32E-37	-76.27	< 2E-16	-4.16341233E-35	-3.95475457E-35
	β_{10}	1.98574271E-39	2.54E-41	78.10	< 2E-16	1.93589926E-39	2.03558615E-39
	β_{11}	-4.21313807E-44	5.27E-46	-79.94	< 2E-16	-4.31645347E-44	-4.10982266E-44
		R^2	Adjusted R^2	F-Statistic	Df (due to $RegSS$)	Df (due to RSS)	Pr>F
	Model	0.9996790	0.9996785	2040674.3	11	7208	< 2E-16

Year	Parameter	Estimate	Standard Error	t-value	Pr(>|t|)	95% Lower Confidence Limit	95% Upper Confidence Limit
2012	β_0	1.56134238E-04	6.19E-08	2521.43	< 2E-16	1.56012853E-04	1.56255622E-04
	β_1	-8.69052508E-08	5.86E-10	-148.24	< 2E-16	-8.80544609E-08	-8.57560408E-08
	β_2	1.94173550E-10	1.82E-12	106.94	< 2E-16	1.90614355E-10	1.97732745E-10
	β_3	-2.48129473E-13	2.63E-15	-94.51	< 2E-16	-2.53275721E-13	-2.42983224E-13
	β_4	1.86515178E-16	2.11E-18	88.35	< 2E-16	1.82377017E-16	1.90653339E-16
	β_5	-8.82519778E-20	1.04E-21	-85.23	< 2E-16	-9.02818407E-20	-8.62221148E-20
	β_6	2.72965492E-23	3.25E-25	83.87	< 2E-16	2.66585401E-23	2.79345582E-23
	β_7	-5.59291377E-27	6.69E-29	-83.61	< 2E-16	-5.72404627E-27	-5.46178126E-27
	β_8	7.51586485E-31	8.94E-33	84.04	< 2E-16	7.34055525E-31	7.69117444E-31
	β_9	-6.36085569E-35	7.49E-37	-84.92	< 2E-16	-6.50768778E-35	-6.21402361E-35
	β_{10}	3.07232046E-39	3.57E-41	86.09	< 2E-16	3.00236658E-39	3.14227435E-39
	β_{11}	-6.45324175E-44	7.38E-46	-87.47	< 2E-16	-6.59786529E-44	-6.30861820E-44
		R^2	Adjusted R^2	F-Statistic	Df (due to $RegSS$)	Df (due to RSS)	Pr>F
	Model	0.9992605	0.9992595	1018099.33	11	8288	< 2E-16
Year	Parameter	Estimate	Standard Error	t-value	Pr(>|t|)	95% Lower Confidence Limit	95% Upper Confidence Limit
2013	β_0	1.50804452E-04	5.33E-08	2826.71	< 2E-16	1.50699873E-04	1.50909030E-04
	β_1	-4.15530823E-08	5.03E-10	-82.66	< 2E-16	-4.25385363E-08	-4.05676283E-08
	β_2	7.18022249E-11	1.56E-12	46.16	< 2E-16	6.87527794E-11	7.48516705E-11
	β_3	-9.90049433E-14	2.25E-15	-43.98	< 2E-16	-1.03417432E-13	-9.45924546E-14
	β_4	8.49628703E-17	1.81E-18	46.87	< 2E-16	8.14096037E-17	8.85161368E-17
	β_5	-4.53501901E-20	8.91E-22	-50.91	< 2E-16	-4.70963694E-20	-4.36040107E-20
	β_6	1.54765378E-23	2.81E-25	55.16	< 2E-16	1.49265275E-23	1.60265481E-23
	β_7	-3.43045604E-27	5.78E-29	-59.35	< 2E-16	-3.54376572E-27	-3.31714636E-27
	β_8	4.90973236E-31	7.75E-33	63.38	< 2E-16	4.75787159E-31	5.06159313E-31
	β_9	-4.37264512E-35	6.51E-37	-67.21	< 2E-16	-4.50017127E-35	-4.24511897E-35
	β_{10}	2.20221672E-39	3.11E-41	70.86	< 2E-16	2.14129513E-39	2.26313831E-39
	β_{11}	-4.78944412E-44	6.44E-46	-74.33	< 2E-16	-4.91574672E-44	-4.66314152E-44
		R^2	Adjusted R^2	F-Statistic	Df (due to $RegSS$)	Df (due to RSS)	Pr>F
	Model	0.9994004	0.9993996	1314722.05	11	8677	< 2E-16
Year	Parameter	Estimate	Standard Error	t-value	Pr(>|t|)	95% Lower Confidence Limit	95% Upper Confidence Limit
2014	β_0	1.57125252E-04	6.99E-08	2249.42	< 2E-16	1.56988327E-04	1.57262177E-04
	β_1	-7.39590983E-08	6.58E-10	-112.44	< 2E-16	-7.52484177E-08	-7.26697788E-08
	β_2	1.34890434E-10	2.03E-12	66.32	< 2E-16	1.30903524E-10	1.38877344E-10
	β_3	-1.63078662E-13	2.94E-15	-55.43	< 2E-16	-1.68845470E-13	-1.57311853E-13
	β_4	1.23530287E-16	2.37E-18	52.15	< 2E-16	1.18887342E-16	1.28173233E-16
	β_5	-6.01592190E-20	1.16E-21	-51.69	< 2E-16	-6.24406210E-20	-5.78778171E-20
	β_6	1.92476399E-23	3.67E-25	52.51	< 2E-16	1.85291081E-23	1.99661716E-23
	β_7	-4.07581172E-27	7.55E-29	-53.98	< 2E-16	-4.22382904E-27	-3.92779440E-27
	β_8	5.64425864E-31	1.01E-32	55.78	< 2E-16	5.44589256E-31	5.84262472E-31
	β_9	-4.90624506E-35	8.50E-37	-57.74	< 2E-16	-5.07281717E-35	-4.73967294E-35
	β_{10}	2.42624793E-39	4.06E-41	59.77	< 2E-16	2.34667599E-39	2.50581987E-39
	β_{11}	-5.20328086E-44	8.42E-46	-61.83	< 2E-16	-5.36824546E-44	-5.03831625E-44
		R^2	Adjusted R^2	F-Statistic	Df (due to $RegSS$)	Df (due to RSS)	Pr>F
	Model	0.9989746	0.9989733	773866.253	11	8738	< 2E-16

Summary Statistics of 12th Degree Polynomial Approximations to LDCs of Turkey in the Period 2000-2014

Year	Parameter	Estimate	Standard Error	t-value	Pr(>|t|)	95% Lower Confidence Limit	95% Upper Confidence Limit
2000	β_0	1.47964316E-04	2.11E-08	7018.39	< 2E-16	1.47922986E-04	1.48005646E-04
	β_1	-4.48151516E-08	2.49E-10	-180.00	< 2E-16	-4.53032463E-08	-4.43270569E-08
	β_2	8.24751891E-11	9.39E-13	87.82	< 2E-16	8.06340436E-11	8.43163346E-11
	β_3	-9.24909145E-14	1.64E-15	-56.37	< 2E-16	-9.57076628E-14	-8.92741661E-14
	β_4	6.08947709E-17	1.60E-18	38.14	< 2E-16	5.77649321E-17	6.40246097E-17
	β_5	-2.47331456E-20	9.55E-22	-25.89	< 2E-16	-2.66057526E-20	-2.28605386E-20
	β_6	6.23955273E-24	3.72E-25	16.79	< 2E-16	5.51097924E-24	6.96812622E-24
	β_7	-9.18917487E-28	9.68E-29	-9.49	< 2E-16	-1.10868590E-27	-7.29149071E-28
	β_8	5.62118928E-32	1.70E-32	3.30	0.0010	2.28506340E-32	8.95731517E-32
	β_9	4.31764385E-36	1.99E-36	2.17	0.0303	4.11022073E-37	8.22426562E-36
	β_{10}	-1.06293208E-39	1.49E-40	-7.14	1.08E-12	-1.35486334E-39	-7.71000814E-40
	β_{11}	7.54250214E-44	6.42E-45	11.74	< 2E-16	6.28333524E-44	8.80166903E-44
	β_{12}	-1.95443976E-48	1.22E-49	-16.07	< 2E-16	-2.19292348E-48	-1.71595604E-48
		R^2	Adjusted R^2	F-Statistic	Df (due to $RegSS$)	Df (due to RSS)	Pr>F
	Model	0.9999335	0.9999334	6611326.21	12	5274	< 2E-16
Year	Parameter	Estimate	Standard Error	t-value	Pr(>|t|)	95% Lower Confidence Limit	95% Upper Confidence Limit
2001	β_0	1.50960919E-04	4.81E-08	3136.63	< 2E-16	1.50866568E-04	1.51055269E-04
	β_1	-5.22594579E-08	5.63E-10	-92.76	< 2E-16	-5.33638844E-08	-5.11550315E-08
	β_2	9.76947396E-11	2.11E-12	46.21	< 2E-16	9.35497933E-11	1.01839686E-10
	β_3	-1.07786366E-13	3.69E-15	-29.20	< 2E-16	-1.15023034E-13	-1.00549698E-13
	β_4	6.63558758E-17	3.60E-18	18.45	< 2E-16	5.93062716E-17	7.34054800E-17
	β_5	-2.29475780E-20	2.16E-21	-10.64	< 2E-16	-2.71741371E-20	-1.87210189E-20
	β_6	3.77531084E-24	8.41E-25	4.49	7.29E-06	2.12673169E-24	5.42388998E-24
	β_7	1.38662426E-28	2.20E-28	0.63	0.5279	-2.91940819E-28	5.69265672E-28
	β_8	-1.95790989E-31	3.87E-32	-5.06	4.44E-07	-2.71717344E-31	-1.19864633E-31
	β_9	4.08520340E-35	4.55E-36	8.98	< 2E-16	3.19333200E-35	4.97707480E-35
	β_{10}	-4.27255909E-39	3.41E-40	-12.53	< 2E-16	-4.94116163E-39	-3.60395655E-39
	β_{11}	2.32910121E-43	1.48E-44	15.78	< 2E-16	2.03978037E-43	2.61842204E-43
	β_{12}	-5.27251158E-48	2.80E-49	-18.80	< 2E-16	-5.82227616E-48	-4.72274701E-48
		R^2	Adjusted R^2	F-Statistic	Df (due to $RegSS$)	Df (due to RSS)	Pr>F
	Model	0.9996672	0.9996664	1380615.42	12	5516	< 2E-16
Year	Parameter	Estimate	Standard Error	t-value	Pr(>|t|)	95% Lower Confidence Limit	95% Upper Confidence Limit
2002	β_0	1.53070078E-04	6.25E-08	2449.82	< 2E-16	1.52947587E-04	1.53192569E-04
	β_1	-8.20374281E-08	7.36E-10	-111.42	< 2E-16	-8.34808377E-08	-8.05940184E-08
	β_2	1.82257587E-10	2.79E-12	65.36	< 2E-16	1.76790525E-10	1.87724649E-10
	β_3	-2.33209462E-13	4.90E-15	-47.61	< 2E-16	-2.42811463E-13	-2.23607461E-13
	β_4	1.76888870E-16	4.79E-18	36.94	< 2E-16	1.67501414E-16	1.86276327E-16
	β_5	-8.48856158E-20	2.88E-21	-29.50	< 2E-16	-9.05261883E-20	-7.92450432E-20
	β_6	2.67661262E-23	1.12E-24	23.82	< 2E-16	2.45629992E-23	2.89692531E-23
	β_7	-5.63296424E-27	2.94E-28	-19.17	< 2E-16	-6.20890236E-27	-5.05702612E-27
	β_8	7.87420433E-31	5.18E-32	15.19	< 2E-16	6.85816185E-31	8.89024680E-31
	β_9	-7.10134346E-35	6.09E-36	-11.66	< 2E-16	-8.29516983E-35	-5.90751710E-35
	β_{10}	3.85941503E-39	4.57E-40	8.45	< 2E-16	2.96434696E-39	4.75448310E-39
	β_{11}	-1.08470933E-43	1.98E-44	-5.49	4.20E-08	-1.47202705E-43	-6.97391614E-44
	β_{12}	1.02173904E-48	3.75E-49	2.72	0.0065	2.85821181E-49	1.75765691E-48
		R^2	Adjusted R^2	F-Statistic	Df (due to $RegSS$)	Df (due to RSS)	Pr>F
	Model	0.9993679	0.9993665	692514.161	12	5256	< 2E-16

Year	Parameter	Estimate	Standard Error	t-value	Pr(>|t|)	95% Lower Confidence Limit	95% Upper Confidence Limit
2003	β_0	1.48234923E-04	6.13E-08	2418.80	< 2E-16	1.48114781E-04	1.48355065E-04
	β_1	-5.65653165E-08	7.24E-10	-78.11	< 2E-16	-5.79849076E-08	-5.51457254E-08
	β_2	1.21430729E-10	2.73E-12	44.44	< 2E-16	1.16073576E-10	1.26787882E-10
	β_3	-1.51160868E-13	4.78E-15	-31.64	< 2E-16	-1.60526407E-13	-1.41795329E-13
	β_4	1.10625542E-16	4.65E-18	23.79	< 2E-16	1.01508639E-16	1.19742445E-16
	β_5	-5.08819250E-20	2.78E-21	-18.27	< 2E-16	-5.63403225E-20	-4.54235275E-20
	β_6	1.52159447E-23	1.08E-24	14.03	< 2E-16	1.30899760E-23	1.73419134E-23
	β_7	-2.97896980E-27	2.83E-28	-10.53	< 2E-16	-3.53354793E-27	-2.42439168E-27
	β_8	3.73153540E-31	4.98E-32	7.49	8.05E-14	2.75472791E-31	4.70834290E-31
	β_9	-2.77590535E-35	5.85E-36	-4.75	2.12E-06	-3.92230881E-35	-1.62950189E-35
	β_{10}	9.69079159E-40	4.38E-40	2.21	0.0270	1.10270059E-40	1.82788826E-39
	β_{11}	3.22783213E-45	1.89E-44	0.17	0.8647	-3.39138892E-44	4.03695535E-44
	β_{12}	-8.76162748E-49	3.60E-49	-2.43	0.0149	-1.58160364E-48	-1.70721854E-49
		R^2	Adjusted R^2	F-Statistic	Df (due to $RegSS$)	Df (due to RSS)	Pr>F
	Model	0.9993929	0.9993916	745356.665	12	5433	< 2E-16
Year	Parameter	Estimate	Standard Error	t-value	Pr(>|t|)	95% Lower Confidence Limit	95% Upper Confidence Limit
2004	β_0	1.50367937E-04	7.79E-08	1929.47	< 2E-16	1.50215160E-04	1.50520715E-04
	β_1	-6.24549320E-08	9.15E-10	-68.27	< 2E-16	-6.42482143E-08	-6.06616497E-08
	β_2	1.21319489E-10	3.44E-12	35.24	< 2E-16	1.14570225E-10	1.28068753E-10
	β_3	-1.35230701E-13	6.01E-15	-22.51	< 2E-16	-1.47009476E-13	-1.23451925E-13
	β_4	8.58079549E-17	5.84E-18	14.69	< 2E-16	7.43594353E-17	9.72564745E-17
	β_5	-3.18554012E-20	3.49E-21	-9.13	< 2E-16	-3.86978957E-20	-2.50129068E-20
	β_6	6.47528269E-24	1.36E-24	4.77	1.86E-06	3.81563989E-24	9.13492550E-24
	β_7	-3.97797727E-28	3.53E-28	-1.13	0.2600	-1.08999227E-27	2.94396820E-28
	β_8	-1.29498088E-31	6.20E-32	-2.09	0.0369	-2.51111394E-31	-7.88478298E-33
	β_9	3.64868617E-35	7.26E-36	5.02	5.19E-07	2.22521452E-35	5.07215782E-35
	β_{10}	-4.21736195E-39	5.42E-40	-7.77	8.94E-15	-5.28076905E-39	-3.15395484E-39
	β_{11}	2.43021980E-43	2.34E-44	10.39	< 2E-16	1.97163102E-43	2.88880857E-43
	β_{12}	-5.71429319E-48	4.43E-49	-12.90	< 2E-16	-6.58276875E-48	-4.84581763E-48
		R^2	Adjusted R^2	F-Statistic	Df (due to $RegSS$)	Df (due to RSS)	Pr>F
	Model	0.9990588	0.9990568	494745.637	12	5593	< 2E-16
Year	Parameter	Estimate	Standard Error	t-value	Pr(>|t|)	95% Lower Confidence Limit	95% Upper Confidence Limit
2005	β_0	1.50542371E-04	6.21E-08	2423.36	< 2E-16	1.50420590E-04	1.50664152E-04
	β_1	-4.99231758E-08	7.21E-10	-69.28	< 2E-16	-5.13358035E-08	-4.85105481E-08
	β_2	9.07298313E-11	2.70E-12	33.54	< 2E-16	8.54271601E-11	9.60325024E-11
	β_3	-1.11808719E-13	4.73E-15	-23.66	< 2E-16	-1.21071918E-13	-1.02545520E-13
	β_4	8.46577709E-17	4.60E-18	18.39	< 2E-16	7.56328655E-17	9.36826763E-17
	β_5	-4.04569160E-20	2.76E-21	-14.66	< 2E-16	-4.58666334E-20	-3.50471985E-20
	β_6	1.24441766E-23	1.08E-24	11.57	< 2E-16	1.03348674E-23	1.45534858E-23
	β_7	-2.45649558E-27	2.81E-28	-8.74	< 2E-16	-3.00722324E-27	-1.90576792E-27
	β_8	2.98846105E-31	4.95E-32	6.04	1.69E-09	2.01773787E-31	3.95918423E-31
	β_9	-1.95876270E-35	5.81E-36	-3.37	0.0008	-3.09868181E-35	-8.18843601E-36
	β_{10}	3.13522129E-40	4.36E-40	0.72	0.4719	-5.40830708E-40	1.16787497E-39
	β_{11}	3.61344948E-44	1.89E-44	1.92	0.0554	-8.29028095E-46	7.30980177E-44
	β_{12}	-1.62460650E-48	3.58E-49	-4.53	5.88E-06	-2.32689949E-48	-9.22313504E-49
		R^2	Adjusted R^2	F-Statistic	Df (due to $RegSS$)	Df (due to RSS)	Pr>F
	Model	0.9994154	0.9994142	817348.247	12	5737	< 2E-16
Year	Parameter	Estimate	Standard Error	t-value	Pr(>|t|)	95% Lower Confidence Limit	95% Upper Confidence Limit
2006	β_0	1.52490074E-04	5.93E-08	2571.36	< 2E-16	1.52373818E-04	1.52606330E-04
	β_1	-5.08793242E-08	6.84E-10	-74.43	< 2E-16	-5.22194160E-08	-4.95392323E-08
	β_2	8.40817606E-11	2.56E-12	32.87	< 2E-16	7.90665021E-11	8.90970191E-11
	β_3	-8.89065984E-14	4.46E-15	-19.94	< 2E-16	-9.76480709E-14	-8.01651259E-14
	β_4	5.52897694E-17	4.34E-18	12.75	< 2E-16	4.67855984E-17	6.37939403E-17
	β_5	-2.01353418E-20	2.60E-21	-7.75	1.08E-14	-2.52288221E-20	-1.50418616E-20
	β_6	3.79362804E-24	1.01E-24	3.75	0.0002	1.80841993E-24	5.77883615E-24
	β_7	-5.83363132E-29	2.64E-28	-0.22	0.8254	-5.76560157E-28	4.59887531E-28
	β_8	-1.42865989E-31	4.66E-32	-3.07	0.0022	-2.34199265E-31	-5.15327128E-32
	β_9	3.40612203E-35	5.47E-36	6.23	5.10E-10	2.33367907E-35	4.47856499E-35
	β_{10}	-3.81579523E-39	4.10E-40	-9.31	< 2E-16	-4.61951908E-39	-3.01207138E-39
	β_{11}	2.18672944E-43	1.77E-44	12.33	< 2E-16	1.83902362E-43	2.53443527E-43
	β_{12}	-5.15514191E-48	3.37E-49	-15.30	< 2E-16	-5.81572192E-48	-4.49456189E-48
		R^2	Adjusted R^2	F-Statistic	Df (due to $RegSS$)	Df (due to RSS)	Pr>F
	Model	0.9995130	0.9995120	1023159.86	12	5982	< 2E-16

Year	Parameter	Estimate	Standard Error	t-value	Pr(>|t|)	95% Lower Confidence Limit	95% Upper Confidence Limit
2007	β_0	1.51752912E-04	6.19E-08	2453.07	< 2E-16	1.51631640E-04	1.51874184E-04
	β_1	-3.48912868E-08	7.08E-10	-49.28	< 2E-16	-3.62791353E-08	-3.35034382E-08
	β_2	3.69787749E-11	2.64E-12	13.99	< 2E-16	3.17983468E-11	4.21592030E-11
	β_3	-2.00235553E-14	4.61E-15	-4.35	1.40E-05	-2.90521637E-14	-1.09949469E-14
	β_4	-7.12049361E-18	4.48E-18	-1.59	0.1124	-1.59119007E-17	1.67091352E-18
	β_5	1.64897557E-20	2.69E-21	6.13	9.19E-10	1.12185082E-20	2.17610033E-20
	β_6	-1.04332447E-23	1.05E-24	-9.95	< 2E-16	-1.24897987E-23	-8.37669065E-24
	β_7	3.65713941E-27	2.74E-28	13.34	< 2E-16	3.11983143E-27	4.19444739E-27
	β_8	-7.97790570E-31	4.83E-32	-16.50	< 2E-16	-8.92555432E-31	-7.03025709E-31
	β_9	1.10884122E-34	5.68E-36	19.52	< 2E-16	9.97499815E-35	1.22018263E-34
	β_{10}	-9.56103637E-39	4.26E-40	-22.45	< 2E-16	-1.03959017E-38	-8.72617099E-39
	β_{11}	4.66509010E-43	1.84E-44	25.31	< 2E-16	4.30374625E-43	5.02643395E-43
	β_{12}	-9.84786362E-48	3.50E-49	-28.11	< 2E-16	-1.05346352E-47	-9.16109201E-48
		R^2	Adjusted R^2	F-Statistic	Df (due to $RegSS$)	Df (due to RSS)	Pr>F
	Model	0.9994572	0.9994561	946528.405	12	6169	< 2E-16
Year	Parameter	Estimate	Standard Error	t-value	Pr(>|t|)	95% Lower Confidence Limit	95% Upper Confidence Limit
2008	β_0	1.51247966E-04	5.53E-08	2734.61	< 2E-16	1.51139542E-04	1.51356389E-04
	β_1	-3.57933058E-08	6.30E-10	-56.77	< 2E-16	-3.70292084E-08	-3.45574032E-08
	β_2	4.10123306E-11	2.33E-12	17.57	< 2E-16	3.64373731E-11	4.55872880E-11
	β_3	-2.07658243E-14	4.03E-15	-5.15	2.73E-07	-2.86753316E-14	-1.28563170E-14
	β_4	-1.16978692E-17	3.90E-18	-3.00	0.0027	-1.93452190E-17	-4.05051944E-18
	β_5	2.17500407E-20	2.32E-21	9.36	< 2E-16	1.71923685E-20	2.63077130E-20
	β_6	-1.32829974E-23	9.02E-25	-14.72	< 2E-16	-1.50520337E-23	-1.15139611E-23
	β_7	4.57110780E-27	2.35E-28	19.47	< 2E-16	4.11096939E-27	5.03124622E-27
	β_8	-9.82807163E-31	4.12E-32	-23.83	< 2E-16	-1.06364280E-30	-9.01971529E-31
	β_9	1.34797244E-34	4.83E-36	27.92	< 2E-16	1.25333524E-34	1.44260964E-34
	β_{10}	-1.14779566E-38	3.61E-40	-31.81	< 2E-16	-1.21852263E-38	-1.07706870E-38
	β_{11}	5.53479089E-43	1.56E-44	35.55	< 2E-16	5.22962631E-43	5.83995547E-43
	β_{12}	-1.15572369E-47	2.95E-49	-39.18	< 2E-16	-1.21355056E-47	-1.09789683E-47
		R^2	Adjusted R^2	F-Statistic	Df (due to $RegSS$)	Df (due to RSS)	Pr>F
	Model	0.9995855	0.9995848	1305118.15	12	6494	< 2E-16
Year	Parameter	Estimate	Standard Error	t-value	Pr(>|t|)	95% Lower Confidence Limit	95% Upper Confidence Limit
2009	β_0	1.50794729E-04	7.00E-08	2153.24	< 2E-16	1.50657442E-04	1.50932015E-04
	β_1	-4.32068262E-08	8.07E-10	-53.55	< 2E-16	-4.47886671E-08	-4.16249853E-08
	β_2	5.07113630E-11	3.02E-12	16.82	< 2E-16	4.48007562E-11	5.66219698E-11
	β_3	-2.32031753E-14	5.25E-15	-4.42	1.01E-05	-3.34986453E-14	-1.29077054E-14
	β_4	-1.51570535E-17	5.11E-18	-2.97	0.0030	-2.51694124E-17	-5.14469456E-18
	β_5	2.53574530E-20	3.06E-21	8.29	< 2E-16	1.93631821E-20	3.13517240E-20
	β_6	-1.49382392E-23	1.19E-24	-12.54	< 2E-16	-1.72733693E-23	-1.26031090E-23
	β_7	5.01953825E-27	3.11E-28	16.15	< 2E-16	4.41028580E-27	5.62879070E-27
	β_8	-1.05963840E-30	5.47E-32	-19.35	< 2E-16	-1.16696266E-30	-9.52314132E-31
	β_9	1.43186372E-34	6.43E-36	22.28	< 2E-16	1.30589600E-34	1.55783145E-34
	β_{10}	-1.20411125E-38	4.81E-40	-25.01	< 2E-16	-1.29848272E-38	-1.10973979E-38
	β_{11}	5.74484164E-43	2.08E-44	27.59	< 2E-16	5.33668418E-43	6.15299910E-43
	β_{12}	-1.18856775E-47	3.95E-49	-30.05	< 2E-16	-1.26609502E-47	-1.11104049E-47
		R^2	Adjusted R^2	F-Statistic	Df (due to $RegSS$)	Df (due to RSS)	Pr>F
	Model	0.9992463	0.9992448	686730.08	12	6216	< 2E-16
Year	Parameter	Estimate	Standard Error	t-value	Pr(>|t|)	95% Lower Confidence Limit	95% Upper Confidence Limit
2010	β_0	1.57261792E-04	4.43E-08	3550.56	< 2E-16	1.57174964E-04	1.57348619E-04
	β_1	-5.52877890E-08	5.05E-10	-109.57	< 2E-16	-5.62769409E-08	-5.42986371E-08
	β_2	5.99924154E-11	1.88E-12	31.90	< 2E-16	5.63053619E-11	6.36794689E-11
	β_3	-3.13487987E-14	3.27E-15	-9.57	< 2E-16	-3.77684309E-14	-2.49291665E-14
	β_4	-5.88340136E-18	3.18E-18	-1.85	0.0647	-1.21261228E-17	3.59320084E-19
	β_5	1.78224873E-20	1.91E-21	9.35	< 2E-16	1.40849674E-20	2.15600072E-20
	β_6	-1.11312593E-23	7.43E-25	-14.99	< 2E-16	-1.25873467E-23	-9.67517191E-24
	β_7	3.79823410E-27	1.94E-28	19.60	< 2E-16	3.41828850E-27	4.17817969E-27
	β_8	-8.05495382E-31	3.41E-32	-23.59	< 2E-16	-8.72435622E-31	-7.38555141E-31
	β_9	1.08945995E-34	4.01E-36	27.18	< 2E-16	1.01087692E-34	1.16804297E-34
	β_{10}	-9.15705385E-39	3.00E-40	-30.48	< 2E-16	-9.74590029E-39	-8.56820742E-39
	β_{11}	4.36388535E-43	1.30E-44	33.58	< 2E-16	4.10914958E-43	4.61862112E-43
	β_{12}	-9.01571324E-48	2.47E-49	-36.52	< 2E-16	-9.49968944E-48	-8.53173705E-48
		R^2	Adjusted R^2	F-Statistic	Df (due to $RegSS$)	Df (due to RSS)	Pr>F
	Model	0.9997155	0.9997149	1867244.83	12	6377	< 2E-16

Year	Parameter	Estimate	Standard Error	t-value	Pr(>|t|)	95% Lower Confidence Limit	95% Upper Confidence Limit
2011	β_0	1.51836463E-04	4.35E-08	3492.51	< 2E-16	1.51751239E-04	1.51921686E-04
	β_1	-5.03923417E-08	4.89E-10	-103.14	< 2E-16	-5.13501162E-08	-4.94345673E-08
	β_2	8.03512276E-11	1.80E-12	44.61	< 2E-16	7.68205533E-11	8.38819019E-11
	β_3	-7.97757566E-14	3.11E-15	-25.63	< 2E-16	-8.58782717E-14	-7.36732415E-14
	β_4	4.48096694E-17	3.01E-18	14.87	< 2E-16	3.89025132E-17	5.07168256E-17
	β_5	-1.33042754E-20	1.80E-21	-7.39	1.57E-13	-1.68310331E-20	-9.77751769E-21
	β_6	1.05446555E-24	7.00E-25	1.51	0.1319	-3.17285355E-25	2.42621645E-24
	β_7	6.40848046E-28	1.82E-28	3.51	4.46E-04	2.83218882E-28	9.98477210E-28
	β_8	-2.57174911E-31	3.21E-32	-8.00	< 2E-16	-3.20159300E-31	-1.94190521E-31
	β_9	4.57776511E-35	3.77E-36	12.14	< 2E-16	3.83842771E-35	5.31710251E-35
	β_{10}	-4.52309119E-39	2.83E-40	-16.00	< 2E-16	-5.07716690E-39	-3.96901549E-39
	β_{11}	2.40333043E-43	1.22E-44	19.65	< 2E-16	2.16357797E-43	2.64308289E-43
	β_{12}	-5.37294180E-48	2.32E-49	-23.12	< 2E-16	-5.82859631E-48	-4.91728729E-48
		R^2	Adjusted R^2	F-Statistic	Df (due to $RegSS$)	Df (due to RSS)	Pr>F
	Model	0.9997012	0.9997007	2009067.64	12	7207	< 2E-16
Year	Parameter	Estimate	Standard Error	t-value	Pr(>|t|)	95% Lower Confidence Limit	95% Upper Confidence Limit
2012	β_0	1.55118541E-04	6.06E-08	2559.37	< 2E-16	1.54999733E-04	1.55237348E-04
	β_1	-6.87851827E-08	6.74E-10	-102.02	< 2E-16	-7.01068478E-08	-6.74635175E-08
	β_2	1.14565217E-10	2.46E-12	46.56	< 2E-16	1.09741874E-10	1.19388561E-10
	β_3	-9.68364298E-14	4.22E-15	-22.97	< 2E-16	-1.05102103E-13	-8.85707570E-14
	β_4	3.13220920E-17	4.05E-18	7.73	1.23E-14	2.33764223E-17	3.92677618E-17
	β_5	7.93782573E-21	2.41E-21	3.30	0.0010	3.22083411E-21	1.26548174E-20
	β_6	-1.10508699E-23	9.32E-25	-11.86	< 2E-16	-1.28768750E-23	-9.22486478E-24
	β_7	4.56708145E-27	2.42E-28	18.88	< 2E-16	4.09296972E-27	5.04119318E-27
	β_8	-1.05597876E-30	4.24E-32	-24.88	< 2E-16	-1.13917538E-30	-9.72782139E-31
	β_9	1.49802814E-34	4.97E-36	30.17	< 2E-16	1.40068841E-34	1.59536787E-34
	β_{10}	-1.29620656E-38	3.71E-40	-34.94	< 2E-16	-1.36893489E-38	-1.22347823E-38
	β_{11}	6.29351143E-43	1.60E-44	39.31	< 2E-16	5.97969873E-43	6.60732412E-43
	β_{12}	-1.31636130E-47	3.03E-49	-43.38	< 2E-16	-1.37584292E-47	-1.25687968E-47
		R^2	Adjusted R^2	F-Statistic	Df (due to $RegSS$)	Df (due to RSS)	Pr>F
	Model	0.9993973	0.9993965	1145215.88	12	8287	< 2E-16
Year	Parameter	Estimate	Standard Error	t-value	Pr(>|t|)	95% Lower Confidence Limit	95% Upper Confidence Limit
2013	β_0	1.49870185E-04	5.17E-08	2900.25	< 2E-16	1.49768889E-04	1.49971480E-04
	β_1	-2.49788337E-08	5.72E-10	-43.68	< 2E-16	-2.60998487E-08	-2.38578188E-08
	β_2	-9.74324434E-13	2.09E-12	-0.47	0.6403	-5.06152626E-12	3.11287739E-12
	β_3	3.94174282E-14	3.58E-15	11.02	< 2E-16	3.24088171E-14	4.64260393E-14
	β_4	-5.72348972E-17	3.44E-18	-16.63	< 2E-16	-6.39812327E-17	-5.04885617E-17
	β_5	4.29492096E-20	2.05E-21	20.98	< 2E-16	3.89370834E-20	4.69613359E-20
	β_6	-1.98008714E-23	7.94E-25	-24.94	< 2E-16	-2.13572556E-23	-1.82444872E-23
	β_7	5.93817058E-27	2.07E-28	28.74	< 2E-16	5.53312978E-27	6.34321137E-27
	β_8	-1.17998148E-30	3.63E-32	-32.46	< 2E-16	-1.25123386E-30	-1.10872910E-30
	β_9	1.54073324E-34	4.26E-36	36.13	< 2E-16	1.45715118E-34	1.62431529E-34
	β_{10}	-1.26994520E-38	3.19E-40	-39.76	< 2E-16	-1.33256269E-38	-1.20732771E-38
	β_{11}	5.98758313E-43	1.38E-44	43.32	< 2E-16	5.71665019E-43	6.25851607E-43
	β_{12}	-1.23021910E-47	2.63E-49	-46.83	< 2E-16	-1.28171777E-47	-1.17872042E-47
		R^2	Adjusted R^2	F-Statistic	Df (due to $RegSS$)	Df (due to RSS)	Pr>F
	Model	0.9995213	0.9995207	1509760.87	12	8676	< 2E-16
Year	Parameter	Estimate	Standard Error	t-value	Pr(>|t|)	95% Lower Confidence Limit	95% Upper Confidence Limit
2014	β_0	1.55856851E-04	6.71E-08	2323.78	< 2E-16	1.55725377E-04	1.55988325E-04
	β_1	-5.14687815E-08	7.42E-10	-69.39	< 2E-16	-5.29227452E-08	-5.00148179E-08
	β_2	3.61794846E-11	2.70E-12	13.39	< 2E-16	3.08813344E-11	4.14776349E-11
	β_3	2.46006799E-14	4.63E-15	5.31	1.12E-07	1.55187084E-14	3.36826515E-14
	β_4	-6.92107491E-17	4.46E-18	-15.52	< 2E-16	-7.79506584E-17	-6.04708399E-17
	β_5	5.94989769E-20	2.65E-21	22.44	< 2E-16	5.43022726E-20	6.46956811E-20
	β_6	-2.85503372E-23	1.03E-24	-27.77	< 2E-16	-3.05659300E-23	-2.65347445E-23
	β_7	8.61633815E-27	2.68E-28	32.20	< 2E-16	8.09185425E-27	9.14082205E-27
	β_8	-1.69909098E-30	4.71E-32	-36.10	< 2E-16	-1.79134645E-30	-1.60683550E-30
	β_9	2.18863322E-34	5.52E-36	39.65	< 2E-16	2.08042140E-34	2.29684505E-34
	β_{10}	-1.77574467E-38	4.14E-40	-42.94	< 2E-16	-1.85680974E-38	-1.69467959E-38
	β_{11}	8.23796847E-43	1.79E-44	46.04	< 2E-16	7.88723095E-43	8.58870599E-43
	β_{12}	-1.66616574E-47	3.40E-49	-48.99	< 2E-16	-1.73283161E-47	-1.59949987E-47
		R^2	Adjusted R^2	F-Statistic	Df (due to $RegSS$)	Df (due to RSS)	Pr>F
	Model	0.9991956	0.9991945	904351.023	12	8737	< 2E-16

Summary Statistics of Exponential Function Approximations to LDCs of Turkey in the Period 2000-2014

Year	Parameter	Estimate	Standard Error	t-value	Pr(>|t|)	95% Lower Confidence Limit	95% Upper Confidence Limit
2000	θ_0	1.42041186E-04	2.71E-08	5250.89	< 2E-16	1.41988155E-04	1.42094217E-04
	θ_1	-1.96739101E-19	1.22E-19	-1.61	0.1077	-4.36460318E-19	4.29821157E-20
	θ_2	3.59870900E-03	7.15E-05	50.36	< 2E-16	3.45861958E-03	3.73879842E-03
	θ_3	-6.33494147E-09	6.08E-12	-1041.27	< 2E-16	-6.34686833E-09	-6.32301462E-09
	Achieved convergence tolerance						
	Model	4.6E-06					
Year	Parameter	Estimate	Standard Error	t-value	Pr(>|t|)	95% Lower Confidence Limit	95% Upper Confidence Limit
2001	θ_0	1.42955914E-04	3.25E-08	4402.05	< 2E-16	1.42892251E-04	1.43019578E-04
	θ_1	-1.42943614E-26	1.44E-26	-0.99	0.3224	-4.26108230E-26	1.40221002E-26
	θ_2	5.51952700E-03	1.16E-04	47.49	< 2E-16	5.29167371E-03	5.74738029E-03
	θ_3	-6.49561047E-09	6.99E-12	-928.69	< 2E-16	-6.50932217E-09	-6.48189877E-09
	Achieved convergence tolerance						
	Model	6.1E-06					
Year	Parameter	Estimate	Standard Error	t-value	Pr(>|t|)	95% Lower Confidence Limit	95% Upper Confidence Limit
2002	θ_0	1.41292191E-04	4.63E-08	3051.87	< 2E-16	1.41201430E-04	1.41382952E-04
	θ_1	-5.93624434E-28	9.55E-28	-0.62	0.5341	-2.46514034E-27	1.27789148E-27
	θ_2	5.87944300E-03	1.85E-04	31.80	< 2E-16	5.51696336E-03	6.24192264E-03
	θ_3	-6.11190786E-09	9.87E-12	-619.11	< 2E-16	-6.13126117E-09	-6.09255455E-09
	Achieved convergence tolerance						
	Model	6.7E-06					
Year	Parameter	Estimate	Standard Error	t-value	Pr(>|t|)	95% Lower Confidence Limit	95% Upper Confidence Limit
2003	θ_0	1.41285272E-04	3.04E-08	4650.27	< 2E-16	1.41225711E-04	1.41344833E-04
	θ_1	-5.98597973E-22	4.17E-22	-1.43	0.1517	-1.41700432E-21	2.19808376E-22
	θ_2	4.29740200E-03	8.03E-05	53.50	< 2E-16	4.13993125E-03	4.45487275E-03
	θ_3	-6.10185660E-09	6.68E-12	-913.01	< 2E-16	-6.11495837E-09	-6.08875483E-09
	Achieved convergence tolerance						
	Model	5.9E-06					
Year	Parameter	Estimate	Standard Error	t-value	Pr(>|t|)	95% Lower Confidence Limit	95% Upper Confidence Limit
2004	θ_0	1.41663384E-04	3.96E-08	3580.99	< 2E-16	1.41585831E-04	1.41740936E-04
	θ_1	-1.31136699E-36	1.87E-36	-0.70	0.4832	-4.97720263E-36	2.35446864E-36
	θ_2	8.17886300E-03	1.63E-04	50.10	< 2E-16	7.85879951E-03	8.49892649E-03
	θ_3	-6.25508115E-09	8.17E-12	-765.37	< 2E-16	-6.27110262E-09	-6.23905967E-09
	Achieved convergence tolerance						
	Model	5.6E-06					
Year	Parameter	Estimate	Standard Error	t-value	Pr(>|t|)	95% Lower Confidence Limit	95% Upper Confidence Limit
2005	θ_0	1.42338503E-04	4.24E-08	3356.73	< 2E-16	1.42255375E-04	1.42421630E-04
	θ_1	-1.40713287E-32	2.08E-32	-0.68	0.4992	-5.48946873E-32	2.67520299E-32
	θ_2	7.12619700E-03	1.70E-04	41.92	< 2E-16	6.79291053E-03	7.45948347E-03
	θ_3	-6.35411973E-09	8.92E-12	-712.00	< 2E-16	-6.37161482E-09	-6.33662464E-09
	Achieved convergence tolerance						
	Model	2.2E-06					
Year	Parameter	Estimate	Standard Error	t-value	Pr(>|t|)	95% Lower Confidence Limit	95% Upper Confidence Limit
2006	θ_0	1.43819544E-04	3.82E-08	3765.05	< 2E-16	1.43744661E-04	1.43894427E-04
	θ_1	-2.03793203E-35	2.72E-35	-0.75	0.4529	-7.36036334E-35	3.28449928E-35
	θ_2	7.88795200E-03	1.53E-04	51.56	< 2E-16	7.58802787E-03	8.18787613E-03
	θ_3	-6.68912772E-09	8.01E-12	-835.37	< 2E-16	-6.70482514E-09	-6.67343029E-09
	Achieved convergence tolerance						
	Model	3.8E-06					

Year	Parameter	Estimate	Standard Error	t-value	Pr(>|t|)	95% Lower Confidence Limit	95% Upper Confidence Limit
2007	θ_0	1.43606777E-04	4.47E-08	3213.84	< 2E-16	1.43519181E-04	1.43694373E-04
	θ_1	-1.59681762E-39	2.96E-39	-0.54	0.5894	-7.39676686E-39	4.20313163E-39
	θ_2	8.97282300E-03	2.13E-04	42.20	< 2E-16	8.55595699E-03	9.38968901E-03
	θ_3	-6.64621109E-09	9.31E-12	-714.13	< 2E-16	-6.66445539E-09	-6.62796680E-09
	Achieved convergence tolerance						
	Model	4.2E-06					
Year	Parameter	Estimate	Standard Error	t-value	Pr(>|t|)	95% Lower Confidence Limit	95% Upper Confidence Limit
2008	θ_0	1.43679171E-04	3.44E-08	4177.44	< 2E-16	1.43611747E-04	1.43746594E-04
	θ_1	-5.12988451E-33	4.22E-33	-1.21	0.2245	-1.34085052E-32	3.14873613E-33
	θ_2	7.27164300E-03	9.43E-05	77.09	< 2E-16	7.08673991E-03	7.45654609E-03
	θ_3	-6.68076710E-09	7.24E-12	-922.45	< 2E-16	-6.69496470E-09	-6.66656951E-09
	Achieved convergence tolerance						
	Model	2.4E-06					
Year	Parameter	Estimate	Standard Error	t-value	Pr(>|t|)	95% Lower Confidence Limit	95% Upper Confidence Limit
2009	θ_0	1.42627353E-04	4.01E-08	3556.89	< 2E-16	1.42548745E-04	1.42705961E-04
	θ_1	-9.14039730E-35	1.21E-34	-0.76	0.4500	-3.28564889E-34	1.45756943E-34
	θ_2	7.72190400E-03	1.52E-04	50.80	< 2E-16	7.42390144E-03	8.01990656E-03
	θ_3	-6.41502534E-09	8.36E-12	-767.65	< 2E-16	-6.43140737E-09	-6.39864330E-09
	Achieved convergence tolerance						
	Model	6.5E-06					
Year	Parameter	Estimate	Standard Error	t-value	Pr(>|t|)	95% Lower Confidence Limit	95% Upper Confidence Limit
2010	θ_0	1.43519796E-04	6.17E-08	2326.96	< 2E-16	1.43398888E-04	1.43640703E-04
	θ_1	-1.44240594E-31	3.19E-31	-0.45	0.6509	-7.68982322E-31	4.80501135E-31
	θ_2	6.85554200E-03	2.54E-04	27.00	< 2E-16	6.35774442E-03	7.35333958E-03
	θ_3	-6.60646358E-09	1.30E-11	-508.62	< 2E-16	-6.63192635E-09	-6.58100080E-09
	Achieved convergence tolerance						
	Model	2.5E-06					
Year	Parameter	Estimate	Standard Error	t-value	Pr(>|t|)	95% Lower Confidence Limit	95% Upper Confidence Limit
2011	θ_0	1.42856124E-04	3.36E-08	4256.14	< 2E-16	1.42790328E-04	1.42921921E-04
	θ_1	-8.51315831E-25	7.68E-25	-1.11	0.2678	-2.35702256E-24	6.54390896E-25
	θ_2	5.06311100E-03	1.04E-04	48.73	< 2E-16	4.85944715E-03	5.26677485E-03
	θ_3	-6.46807480E-09	7.30E-12	-885.49	< 2E-16	-6.48239373E-09	-6.45375587E-09
	Achieved convergence tolerance						
	Model	4.7E-06					
Year	Parameter	Estimate	Standard Error	t-value	Pr(>|t|)	95% Lower Confidence Limit	95% Upper Confidence Limit
2012	θ_0	1.43194068E-04	3.44E-08	4162.30	< 2E-16	1.43126631E-04	1.43261506E-04
	θ_1	-4.99170610E-37	6.26E-37	-0.80	0.4255	-1.72699394E-36	7.28652720E-37
	θ_2	8.30620100E-03	1.44E-04	57.80	< 2E-16	8.02450407E-03	8.58789793E-03
	θ_3	-6.60461229E-09	7.17E-12	-920.70	< 2E-16	-6.61867403E-09	-6.59055056E-09
	Achieved convergence tolerance						
	Model	3.8E-06					
Year	Parameter	Estimate	Standard Error	t-value	Pr(>|t|)	95% Lower Confidence Limit	95% Upper Confidence Limit
2013	θ_0	1.42453398E-04	3.35E-08	4255.29	< 2E-16	1.42387776E-04	1.42519021E-04
	θ_1	-6.59228659E-35	7.65E-35	-0.86	0.3887	-2.15833032E-34	8.39873005E-35
	θ_2	7.76704400E-03	1.33E-04	58.28	< 2E-16	7.50578905E-03	8.02829895E-03
	θ_3	-6.38068298E-09	7.03E-12	-907.17	< 2E-16	-6.39447054E-09	-6.36689542E-09
	Achieved convergence tolerance						
	Model	2.7E-06					
Year	Parameter	Estimate	Standard Error	t-value	Pr(>|t|)	95% Lower Confidence Limit	95% Upper Confidence Limit
2014	θ_0	1.42539279E-04	4.42E-08	3222.32	< 2E-16	1.42452568E-04	1.42625990E-04
	θ_1	-4.12016194E-42	8.30E-42	-0.50	0.6196	-2.03879882E-41	1.21476644E-41
	θ_2	9.66638900E-03	2.31E-04	41.82	< 2E-16	9.21328200E-03	1.01194960E-02
	θ_3	-6.41294444E-09	9.18E-12	-698.74	< 2E-16	-6.43093532E-09	-6.39495355E-09
	Achieved convergence tolerance						
	Model	3.9E-06					

Summary Statistics of Logarithmic Function Approximations to LDCs of Turkey in the Period 2000-2014

Year	Parameter	Estimate	Standard Error	t-value	Pr(>|t|)	95% Lower Confidence Limit	95% Upper Confidence Limit
2000	α_0	1.17596347E-04	8.56E-08	1373.60	< 2E-16	1.17428512E-04	1.17764182E-04
	α_1	-1.79288337E-05	1.10E-07	-162.34	< 2E-16	-1.81453369E-05	-1.77123305E-05
	α_2	2.40472200E+03	4.02E+01	59.75	< 2E-16	2.32582853E+03	2.48361547E+03
	α_3	7.73539100E+03	2.46E+01	314.23	< 2E-16	7.68713112E+03	7.78365088E+03
	Achieved convergence tolerance						
	Model	3.2E-06					
Year	Parameter	Estimate	Standard Error	t-value	Pr(>|t|)	95% Lower Confidence Limit	95% Upper Confidence Limit
2001	α_0	1.15706930E-04	4.44E-08	2605.64	< 2E-16	1.15619877E-04	1.15793984E-04
	α_1	-1.47880006E-05	5.73E-08	-258.18	< 2E-16	-1.49002873E-05	-1.46757139E-05
	α_2	1.17051200E+03	1.65E+01	71.10	< 2E-16	1.13823781E+03	1.20278619E+03
	α_3	8.36221000E+03	1.08E+01	776.46	< 2E-16	8.34109717E+03	8.38332283E+03
	Achieved convergence tolerance						
	Model	2.4E-06					
Year	Parameter	Estimate	Standard Error	t-value	Pr(>|t|)	95% Lower Confidence Limit	95% Upper Confidence Limit
2002	α_0	1.15054360E-04	4.71E-08	2443.92	< 2E-16	1.14962068E-04	1.15146652E-04
	α_1	-1.27273012E-05	5.76E-08	-221.13	< 2E-16	-1.28401355E-05	-1.26144670E-05
	α_2	8.13538100E+02	1.57E+01	51.81	< 2E-16	7.82752345E+02	8.44323855E+02
	α_3	8.51807440E+03	1.09E+01	779.05	< 2E-16	8.49663934E+03	8.53950946E+03
	Achieved convergence tolerance						
	Model	3.2E-06					
Year	Parameter	Estimate	Standard Error	t-value	Pr(>|t|)	95% Lower Confidence Limit	95% Upper Confidence Limit
2003	α_0	1.17413136E-04	7.64E-08	1536.88	< 2E-16	1.17263367E-04	1.17562906E-04
	α_1	-1.53898056E-05	8.86E-08	-173.78	< 2E-16	-1.55634135E-05	-1.52161977E-05
	α_2	1.82610400E+03	3.31E+01	55.25	< 2E-16	1.76130500E+03	1.89090300E+03
	α_3	7.84545500E+03	2.21E+01	355.78	< 2E-16	7.80222555E+03	7.88868445E+03
	Achieved convergence tolerance						
	Model	7.6E-06					
Year	Parameter	Estimate	Standard Error	t-value	Pr(>|t|)	95% Lower Confidence Limit	95% Upper Confidence Limit
2004	α_0	1.16378602E-04	8.64E-08	1347.48	< 2E-16	1.16209288E-04	1.16547916E-04
	α_1	-1.42636935E-05	9.77E-08	-145.96	< 2E-16	-1.44552747E-05	-1.40721122E-05
	α_2	1.34081700E+03	3.32E+01	40.33	< 2E-16	1.27564087E+03	1.40599313E+03
	α_3	8.10690200E+03	2.30E+01	352.91	< 2E-16	8.06186863E+03	8.15193537E+03
	Achieved convergence tolerance						
	Model	7.2E-06					
Year	Parameter	Estimate	Standard Error	t-value	Pr(>|t|)	95% Lower Confidence Limit	95% Upper Confidence Limit
2005	α_0	1.16279797E-04	7.86E-08	1480.18	< 2E-16	1.16125794E-04	1.16433800E-04
	α_1	-1.44411417E-05	9.50E-08	-152.02	< 2E-16	-1.46273664E-05	-1.42549171E-05
	α_2	1.26310400E+03	3.01E+01	41.98	< 2E-16	1.20412521E+03	1.32208279E+03
	α_3	8.19936100E+03	2.01E+01	407.42	< 2E-16	8.15990858E+03	8.23881342E+03
	Achieved convergence tolerance						
	Model	8.9E-06					
Year	Parameter	Estimate	Standard Error	t-value	Pr(>|t|)	95% Lower Confidence Limit	95% Upper Confidence Limit
2006	α_0	1.15938962E-04	6.67E-08	1737.39	< 2E-16	1.15808144E-04	1.16069780E-04
	α_1	-1.47210910E-05	8.17E-08	-180.18	< 2E-16	-1.48812525E-05	-1.45609296E-05
	α_2	1.08694500E+03	2.32E+01	46.85	< 2E-16	1.04146562E+03	1.13242438E+03
	α_3	8.32028100E+03	1.56E+01	531.77	< 2E-16	8.28960851E+03	8.35095349E+03
	Achieved convergence tolerance						
	Model	4.7E-06					

Year	Parameter	Estimate	Standard Error	t-value	Pr(>|t|)	95% Lower Confidence Limit	95% Upper Confidence Limit
2007	α_0	1.15010960E-04	5.10E-08	2253.60	< 2E-16	1.14910915E-04	1.15111005E-04
	α_1	-1.34328156E-05	6.05E-08	-222.02	< 2E-16	-1.35514217E-05	-1.33142094E-05
	α_2	7.09502100E+02	1.48E+01	47.80	< 2E-16	6.80405066E+02	7.38599134E+02
	α_3	8.54787560E+03	1.06E+01	803.00	< 2E-16	8.52700779E+03	8.56874341E+03
	Achieved convergence tolerance						
	Model	9.1E-06					
Year	Parameter	Estimate	Standard Error	t-value	Pr(>|t|)	95% Lower Confidence Limit	95% Upper Confidence Limit
2008	α_0	1.15488136E-04	4.35E-08	2654.45	< 2E-16	1.15402847E-04	1.15573425E-04
	α_1	-1.26104868E-05	4.09E-08	-308.44	< 2E-16	-1.26906341E-05	-1.25303395E-05
	α_2	5.81020300E+02	1.09E+01	53.53	< 2E-16	5.59743003E+02	6.02297597E+02
	α_3	8.42440270E+03	8.72E+00	965.82	< 2E-16	8.40730363E+03	8.44150177E+03
	Achieved convergence tolerance						
	Model	5.0E-06					
Year	Parameter	Estimate	Standard Error	t-value	Pr(>|t|)	95% Lower Confidence Limit	95% Upper Confidence Limit
2009	α_0	1.16265032E-04	6.30E-08	1845.51	< 2E-16	1.16141532E-04	1.16388531E-04
	α_1	-1.36996670E-05	6.87E-08	-199.54	< 2E-16	-1.38342589E-05	-1.35650751E-05
	α_2	1.03787900E+03	2.15E+01	48.30	< 2E-16	9.95757909E+02	1.08000009E+03
	α_3	8.22424600E+03	1.55E+01	532.16	< 2E-16	8.19394972E+03	8.25454228E+03
	Achieved convergence tolerance						
	Model	4.0E-06					
Year	Parameter	Estimate	Standard Error	t-value	Pr(>|t|)	95% Lower Confidence Limit	95% Upper Confidence Limit
2010	α_0	1.14050422E-04	3.43E-08	3328.66	< 2E-16	1.13983254E-04	1.14117589E-04
	α_1	-1.18882523E-05	3.60E-08	-330.11	< 2E-16	-1.19588504E-05	-1.18176543E-05
	α_2	3.08717100E+02	6.34E+00	48.73	< 2E-16	2.96297408E+02	3.21136792E+02
	α_3	8.77403500E+03	5.75E+00	1524.73	< 2E-16	8.76275431E+03	8.78531569E+03
	Achieved convergence tolerance						
	Model	4.4E-06					
Year	Parameter	Estimate	Standard Error	t-value	Pr(>|t|)	95% Lower Confidence Limit	95% Upper Confidence Limit
2011	α_0	1.16099074E-04	4.85E-08	2394.29	< 2E-16	1.16004020E-04	1.16194129E-04
	α_1	-1.46048333E-05	5.88E-08	-248.57	< 2E-16	-1.47200109E-05	-1.44896558E-05
	α_2	1.17263000E+03	1.78E+01	65.72	< 2E-16	1.13765453E+03	1.20760547E+03
	α_3	8.26384800E+03	1.21E+01	684.25	< 2E-16	8.24017318E+03	8.28752282E+03
	Achieved convergence tolerance						
	Model	2.5E-06					
Year	Parameter	Estimate	Standard Error	t-value	Pr(>|t|)	95% Lower Confidence Limit	95% Upper Confidence Limit
2012	α_0	1.15085179E-04	4.09E-08	2811.53	< 2E-16	1.15004939E-04	1.15165418E-04
	α_1	-1.34422215E-05	4.68E-08	-287.12	< 2E-16	-1.35339964E-05	-1.33504466E-05
	α_2	7.33978900E+02	1.23E+01	59.76	< 2E-16	7.09900901E+02	7.58056899E+02
	α_3	8.49209020E+03	9.01E+00	942.01	< 2E-16	8.47441873E+03	8.50976167E+03
	Achieved convergence tolerance						
	Model	4.1E-06					
Year	Parameter	Estimate	Standard Error	t-value	Pr(>|t|)	95% Lower Confidence Limit	95% Upper Confidence Limit
2013	α_0	1.15945493E-04	5.02E-08	2311.36	< 2E-16	1.15847160E-04	1.16043825E-04
	α_1	-1.35239413E-05	5.68E-08	-238.19	< 2E-16	-1.36352392E-05	-1.34126434E-05
	α_2	9.37979400E+02	1.71E+01	54.73	< 2E-16	9.04387004E+02	9.71571796E+02
	α_3	8.31513290E+03	1.23E+01	674.53	< 2E-16	8.29096860E+03	8.33929720E+03
	Achieved convergence tolerance						
	Model	5.4E-06					
Year	Parameter	Estimate	Standard Error	t-value	Pr(>|t|)	95% Lower Confidence Limit	95% Upper Confidence Limit
2014	α_0	1.14614036E-04	3.45E-08	3320.93	< 2E-16	1.14546383E-04	1.14681689E-04
	α_1	-1.19914796E-05	3.78E-08	-317.45	< 2E-16	-1.20655260E-05	-1.19174332E-05
	α_2	4.24441300E+02	8.32E+00	51.01	< 2E-16	4.08132065E+02	4.40750535E+02
	α_3	8.65643020E+03	6.77E+00	1278.60	< 2E-16	8.64315891E+03	8.66970149E+03
	Achieved convergence tolerance						
	Model	7.5E-06					

Summary Statistics of Approximations to LDCs of Turkey in the Period 2000-2014 Using Inverse of Hill's Function

Year	Parameter	Estimate	Standard Error	t-value	Pr(>|t|)	95% Lower Confidence Limit	95% Upper Confidence Limit
2000	b	1.40807952E+04	4.74E+01	297.07	< 2E-16	1.39878731E+04	1.41737172E+04
	c	5.57297456E-05	1.75E-07	317.88	< 2E-16	5.53860573E-05	5.60734340E-05
	m	2.23752492E+00	4.89E-03	457.94	< 2E-16	2.22794623E+00	2.24710361E+00
	Achieved convergence tolerance						
	Model	8.7E-08					
Year	Parameter	Estimate	Standard Error	t-value	Pr(>|t|)	95% Lower Confidence Limit	95% Upper Confidence Limit
2001	b	1.15960814E+04	2.02E+01	574.04	< 2E-16	1.15564798E+04	1.16356829E+04
	c	5.55009617E-05	7.51E-08	739.26	< 2E-16	5.53537823E-05	5.56481411E-05
	m	3.09753883E+00	5.26E-03	588.99	< 2E-16	3.08722903E+00	3.10784863E+00
	Achieved convergence tolerance						
	Model	4.3E-06					
Year	Parameter	Estimate	Standard Error	t-value	Pr(>|t|)	95% Lower Confidence Limit	95% Upper Confidence Limit
2002	b	1.09911617E+04	2.17E+01	507.33	< 2E-16	1.09486902E+04	1.10336332E+04
	c	4.94941693E-05	7.77E-08	636.92	< 2E-16	4.93418285E-05	4.96465102E-05
	m	3.20212962E+00	7.45E-03	429.75	< 2E-16	3.18752220E+00	3.21673705E+00
	Achieved convergence tolerance						
	Model	9.7E-07					
Year	Parameter	Estimate	Standard Error	t-value	Pr(>|t|)	95% Lower Confidence Limit	95% Upper Confidence Limit
2003	b	1.16890475E+04	2.85E+01	409.91	< 2E-16	1.16331442E+04	1.17449507E+04
	c	5.45712553E-05	9.91E-08	550.53	< 2E-16	5.43769292E-05	5.47655814E-05
	m	3.20482514E+00	7.43E-03	431.44	< 2E-16	3.19026275E+00	3.21938754E+00
	Achieved convergence tolerance						
	Model	3.8E-06					
Year	Parameter	Estimate	Standard Error	t-value	Pr(>|t|)	95% Lower Confidence Limit	95% Upper Confidence Limit
2004	b	1.08824199E+04	2.59E+01	420.20	< 2E-16	1.08316496E+04	1.09331903E+04
	c	5.82099294E-05	9.40E-08	619.25	< 2E-16	5.80256515E-05	5.83942073E-05
	m	3.84170486E+00	1.08E-02	357.09	< 2E-16	3.82061419E+00	3.86279552E+00
	Achieved convergence tolerance						
	Model	3.0E-07					
Year	Parameter	Estimate	Standard Error	t-value	Pr(>|t|)	95% Lower Confidence Limit	95% Upper Confidence Limit
2005	b	1.12134243E+04	2.73E+01	411.12	< 2E-16	1.11599538E+04	1.12668947E+04
	c	5.66234134E-05	9.91E-08	571.09	< 2E-16	5.64290434E-05	5.68177833E-05
	m	3.46029097E+00	8.91E-03	388.28	< 2E-16	3.44282025E+00	3.47776169E+00
	Achieved convergence tolerance						
	Model	6.7E-06					
Year	Parameter	Estimate	Standard Error	t-value	Pr(>|t|)	95% Lower Confidence Limit	95% Upper Confidence Limit
2006	b	1.12894469E+04	2.51E+01	449.99	< 2E-16	1.12402653E+04	1.13386286E+04
	c	5.98131847E-05	9.58E-08	624.27	< 2E-16	5.96253581E-05	6.00010113E-05
	m	3.43207359E+00	7.93E-03	432.53	< 2E-16	3.41651840E+00	3.44762879E+00
	Achieved convergence tolerance						
	Model	5.3E-06					
Year	Parameter	Estimate	Standard Error	t-value	Pr(>|t|)	95% Lower Confidence Limit	95% Upper Confidence Limit
2007	b	1.06402293E+04	1.40E+01	760.11	< 2E-16	1.06127879E+04	1.06676707E+04
	c	6.08690066E-05	5.48E-08	1110.31	< 2E-16	6.07615373E-05	6.09764759E-05
	m	3.91190744E+00	6.42E-03	609.55	< 2E-16	3.89932658E+00	3.92448829E+00
	Achieved convergence tolerance						
	Model	6.5E-07					
Year	Parameter	Estimate	Standard Error	t-value	Pr(>|t|)	95% Lower Confidence Limit	95% Upper Confidence Limit
2008	b	1.09447184E+04	1.81E+01	604.58	< 2E-16	1.09092305E+04	1.09802064E+04
	c	6.72655877E-05	7.02E-08	958.16	< 2E-16	6.71279665E-05	6.74032089E-05
	m	4.08878879E+00	7.47E-03	547.11	< 2E-16	4.07413840E+00	4.10343919E+00
	Achieved convergence tolerance						
	Model	8.2E-07					
Year	Parameter	Estimate	Standard Error	t-value	Pr(>|t|)	95% Lower Confidence Limit	95% Upper Confidence Limit
2009	b	1.07379765E+04	1.85E+01	579.75	< 2E-16	1.07016675E+04	1.07742854E+04
	c	6.13616144E-05	6.92E-08	886.91	< 2E-16	6.12259860E-05	6.14972428E-05
	m	4.02374989E+00	8.31E-03	484.32	< 2E-16	4.00746317E+00	4.04003660E+00
	Achieved convergence tolerance						
	Model	4.5E-07					

Year	Parameter	Estimate	Standard Error	t-value	Pr(>|t|)	95% Lower Confidence Limit	95% Upper Confidence Limit
2010	b	1.01930662E+04	1.28E+01	793.28	< 2E-16	1.01678773E+04	1.02182551E+04
	c	5.23029536E-05	5.21E-08	1003.58	< 2E-16	5.22007876E-05	5.24051195E-05
	m	3.60045645E+00	7.23E-03	498.27	< 2E-16	3.58629123E+00	3.61462167E+00
	Achieved convergence tolerance						
	Model	6.7E-06					
Year	Parameter	Estimate	Standard Error	t-value	Pr(>|t|)	95% Lower Confidence Limit	95% Upper Confidence Limit
2011	b	1.21237599E+04	2.79E+01	434.98	< 2E-16	1.20691230E+04	1.21783968E+04
	c	5.96452955E-05	1.00E-07	595.31	< 2E-16	5.94488890E-05	5.98417020E-05
	m	3.13973747E+00	5.99E-03	524.45	< 2E-16	3.12800176E+00	3.15147319E+00
	Achieved convergence tolerance						
	Model	6.8E-06					
Year	Parameter	Estimate	Standard Error	t-value	Pr(>|t|)	95% Lower Confidence Limit	95% Upper Confidence Limit
2012	b	1.11168586E+04	2.14E+01	519.84	< 2E-16	1.10749382E+04	1.11587791E+04
	c	6.30786006E-05	7.99E-08	789.50	< 2E-16	6.29219837E-05	6.32352176E-05
	m	3.78190931E+00	7.64E-03	495.03	< 2E-16	3.76693359E+00	3.79688504E+00
	Achieved convergence tolerance						
	Model	6.0E-06					
Year	Parameter	Estimate	Standard Error	t-value	Pr(>|t|)	95% Lower Confidence Limit	95% Upper Confidence Limit
2013	b	1.16229720E+04	3.15E+01	368.99	< 2E-16	1.15612255E+04	1.16847185E+04
	c	6.22933078E-05	1.11E-07	563.08	< 2E-16	6.20764491E-05	6.25101665E-05
	m	3.60788773E+00	8.81E-03	409.35	< 2E-16	3.59061069E+00	3.62516477E+00
	Achieved convergence tolerance						
	Model	1.8E-06					
Year	Parameter	Estimate	Standard Error	t-value	Pr(>|t|)	95% Lower Confidence Limit	95% Upper Confidence Limit
2014	b	1.05942465E+04	2.18E+01	485.40	< 2E-16	1.05514629E+04	1.06370302E+04
	c	6.05374387E-05	8.11E-08	746.85	< 2E-16	6.03785473E-05	6.06963302E-05
	m	4.04905925E+00	1.03E-02	392.15	< 2E-16	4.02881932E+00	4.06929918E+00
	Achieved convergence tolerance						
	Model	3.2E-06					

APPENDIX F

The direct application of the classical screening curve methodology (TCSCM), without accounting for existing units, has also been carried out by several scholars according to the necessities of the relevant research topics. Murphy et al. (1985) showed a method how an optimal solution of a static model can replicate the first period optimal solution of a dynamic model that can analyze multi-periods. Ramos et al. (1989) introduced a static expansion model based on MINOS optimization code. The introduced model can account for more detailed capital cost analysis, technical minima of thermal units, detailed operation of hydropower units with reservoirs and pumped-storages. Koomey, Rosenfeld, and Gadgil (1990a; 1990b) proposed a simplified methodology to compare supply and demand-size resources. A concept is illustrated to plot demand-side technologies on a screening curve with applications of efficiency investments to power plants. Kennedy (2003) utilizes TCSCM for estimating the social benefit of large-scale wind power production. The static model analyses the social benefit by calculating the difference in the social cost with and without installing wind units to cover the demand. Lamont (2008) examined the marginal value of intermittent technologies by extending the classical screening curve approach. The value of the intermittent technologies is expressed as a function of the average system marginal cost, the capacity factor of the generator, and the covariance between the generator's hourly production and the hourly system marginal cost. Shrestha and Songbo (2009) investigated bidding strategy for generators by the help of TCSCM. It is shown that the probability of a generator's bid being successful should be the range of the capacity factor which makes it the most economical unit. Tzimas and Georgakaki (2010) analyzed the future of the power supply by fossil fuel fired power plants based on a number of scenarios on energy and CO_2 markets, penetration of renewable and nuclear energy technologies. The analyses are carried out by TCSCM taking into account the rate of retirement of the current power plant park, the capacity already planned or under construction and the role of carbon capture and storage technologies. Although the analysis is dynamic, the selected methodology is static. It is assumed that the new capacity, calculated for the fifth year of the planning horizon, is developed gradually year by year throughout the five-year period. De Jonghe, Delarue, Belmans, and D'haeseleer (2011) examined the impact of a high level of wind power penetration on the optimal future power technology mix. The optimal technology mix, determined by TCSCM, is compared to the sensitivity analysis of an extended linear programming model including operational constraints. Baldick et al. (2011) presented an

approach for optimal capacity expansion to include ancillary services for the application of TCSCM. Hasan, Saha, & Eghbal (2012) evaluated the impact of emission price and locational signals on the optimal capacity expansion and electricity price in Queensland network in Australia. The evaluation is made by applying TCSCM based least-cost generation entry along with the `market-based' profit-maximizing power plant investment. Hirth and Ueckerdt (2013) compared the redistribution effects of renewable deployment support schemes and CO_2 pricing by using TCSCM. Through the evaluation process, the screening curves of the technologies, dependent on the level of the assumed CO_2 price, are pivoted and the corresponding load duration curve is reshaped w.r.t. the expansion of renewable energy technologies. Ueckerdt et al. (2013) presented a measure so called "system levelized costs of electricity (LCOE)" as the sum of generation and integration costs per unit of power generated by intermittent renewable power generators (IRPG). The system LCOEs, which are defined to be the marginal economic costs of an additional unit of IRPG, are utilized for determining the optimal and competitive deployment of IRPG. Further, the integration costs of IRPG are the indirect costs such as expenses for grids, balancing services, reserve requirements, and more flexible operation of thermal plants. Finally, the system LCOE is mentioned to be calculated by extending TCSCM to consider power generation costs with and without IRPG. Batlle and Rodilla (2013) analyzed the cost of starts up of cycling operation of thermal units on the capacity expansion by extending the application of TCSCM. Zhang et al. (2015) proposed an improvement to determine the economic maximum time of running at minimum output for thermal power plants. The calculations are based on the comparison between the start-up and the opportunity cost of a thermal unit when running at minimum stable output rather than at full output. Zhang and Baldick (2015) introduced a new approach to analyze the long-term impact of ancillary services on energy mix in a target year. Accordingly, two different models are developed to co-optimize the energy and ancillary services (i.e. by using an improved screening curve approach) and to optimize the generation mix of ancillary services after an energy-only generation mix has already been optimized.

APPENDIX G

The below given data is evaluated as an example by using the geometrical solution process. The example serves as a demonstration of the solution process to guide practitioners during its implementation. The load duration curve is assumed to be linear and is defined by the equation $L(\tau)=1-0.5\tau$. The availability factor is assumed to be equal to 1.

Candidate & Existing Power Plants for Capacity Expansion Planning

Merit Order of Unit	Type of Unit	Variable Cost	Fixed Cost	Installed Capacity
-	-	(€/MW-Year)	(€/MW-Year)	(MW)
1	Candidate	12	130	0
2	Existing	25	0	0.15
3	Existing	38	0	0.1
4	Candidate	44	125	0

The computation steps for the example capacity expansion problem are as follows:

1. Index vectors of candidate and existing units are created. index_new=(1,4), index_existing=(2,3)

2. An index for 1st candidate unit (1) exists.

3. An index for 2nd candidate unit (4) exists.

4. The candidate unit has a positive capacity according to Eq. (19.3.7) as indicated below.

$$130-125 = (25-12)\cdot\frac{1-x_1}{0.5}+(38-25)\cdot\frac{1-x_1-0.15}{0.5}+(44-38)\cdot\frac{1-x_1-0.15-0.10}{0.5}$$

$$\rightarrow x_1 = 0.8141$$

5. The recursion process terminates, since the sum of the utilized capacities until the unit 4 is higher than 1 ($x_1 + x_2 + x_3 = 0.8141 + 0.1500 + 0.1000 = 1.0641$). The reference unit ($\ell$) is 1st unit. The stored resultant capacity expansion at the end of the recursion process is $x_l = 0.8141;\ x_2 = 0.1500;\ x_3 = 0.1000.$

6. The process continues with the analysis according to the scenario 1, 2 and 3 for $x_l > 0$. cusl=(1,4), ncusl=2

6.1 The 1st Iteration of the Scenario 1 for cusl(1)=1:

$x_1 = 1$ and $x_2 = x_3 = x_4 = 0$ $(since\ x_i = 0 \quad \forall i: i > l)$

$$CF_l = 1;\ \ AACC_l = 130 + 12 \cdot 1 = 142;\ \ TTSAT = \frac{130 + 142}{2} \cdot 1 = 136$$

6.2 The 1st Iteration of the Scenario 2 for cusl(1)=1 and eusl(1)=2:

$$x_2 = 0.15;\ \ x_l = 1 - 0.15 = 0.85;\ \ x_3 = x_4 = 0\ (since\ x_i = 0 \quad \forall i: i > 2)$$

$$CF_l = 1;\ CF_2 = \frac{1 - 0.85}{0.5} = 0.3;\ \alpha_2 = 130 + 0.3 \cdot (12 - 25) = 126.1$$

$$AACC_2 = 126.1 + 25 \cdot 0.3 = 133.6;\ AACC_l = 130 + 12 \cdot 1 = 142$$

$$TTSAT = \frac{126.1 + 133.6}{2} \cdot 0.3 + \frac{133.6 + 142}{2} \cdot (1 - 0.3) = 135.415$$

6.3 The 1st Iteration of the Scenario 3 for cusl(1)=1 and eusl(1)=2:

According to the constraint (19.3.42), $x_l = -4 < 0\ \&\ x_2 = 5 > 0.15$. Thus, the result of this scenario is not considered as an expansion alternative, since the non-negativity constraints are not satisfied.

$$(12 - 25) \cdot L^{-1}(D_2) + 130 = 0 \ \ \rightarrow \frac{1 - x_l}{0.5} = 10 \rightarrow x_l = -4 \wedge x_2 = 1 - (-4) = 5$$

6.4 The 2nd Iteration of the Scenario 2 for cusl(1)=1 and eusl(2)=3:

$$x_2 = 0.15;\ \ x_3 = \ 0.1000\ \ x_l = 1 - 0.25 = 0.75;\ \ x_4 = 0\ (since\ x_i = 0 \quad \forall i: i > 3)$$

$$CF_l = 1;\ CF_2 = \frac{1 - 0.75}{0.5} = 0.5;\ CF_3 = \frac{1 - 0.9}{0.5} = 0.2$$

$$\alpha_2 = 130 + 0.5 \cdot (12 - 25) = 123.5;\ \ \alpha_3 = 123.5 + 0.2 \cdot (25 - 38) = 120.9$$

$$AACC_2 = 123.5 + 25 \cdot 0.5 = 136;\ \ AACC_3 = 120.9 + 38 \cdot 0.2 = 128.5;$$

$$AACC_l = 130 + 12 \cdot 1 = 142$$

$$TTSAT = \frac{120.9 + 128.5}{2} \cdot 0.2 + \frac{128.5 + 136}{2} \cdot 0.3 + \frac{136 + 142}{2} \cdot 0.5 = \ 134.115$$

6.5 The 2nd Iteration of the Scenario 3 for cusl(1)=1 and eusl(2)=3:

According to the constraint (19.3.42), $x_l = -1.575 < 0;\ \ x_2 = 0.15\ \&\ x_3 = 2.425 > 0.1$. Thus, the result of this scenario is not considered as an expansion alternative, since the non-negativity constraints are not satisfied.

$$(12 - 25) \cdot L^{-1}(D_2) + (25 - 38) \cdot L^{-1}(D_3) + 130 = 0 \ \ \rightarrow \frac{1 - x_l}{0.5} + \frac{1 - x_l - 0.15}{0.5} = 10$$

$$\rightarrow x_l = -1.575 \wedge\ x_3 = 1 - (-1.575) - 0.15 = 2.425$$

6.6 The 2nd Iteration of the Scenario 1 for cusl(2)=4 :

$x_l = 0.8141;\ x_2 = 0.15;\ \ x_3 = 0.10;\ \ x_4 = \ 1 - 0.8141 - 0.1500 - 0.1000 = -0.0641$

6.7 There is not any existing unit following unit 4, therefore the 3rd and the 4th scenario will not be computed.

7. The scenario 4 and 5 for eusl(1)=2 and eusl(2)=3 will not be computed since cupl=0.

The below given table indicates the result of the example.

The Solution of the Capacity Expansion Problem

Merit Order of Unit	Type of Unit	Utilized Capacity Level	Marginal Value of Capacity (α_i)
-	-	(MW)	(€/MW-Year)
1	Candidate	0.75	-
2	Existing	0.15	123.5
3	Existing	0.1	120.9
4	Candidate	0	-

APPENDIX H

The Installed Capacity and Investment Cost of Combined Cycled Gas Fired Power Plant Projects

Combined Cycle Natural Gas Fired Power Plant	Installed Capacity [MW_{el}]	Specific Investment Cost [$/$kW_{el}$]
CCPP 1	890	745
CCPP 2	882	1083
CCPP 3	835	886
CCPP 4	15	264
CCPP 5	397	673
CCPP 6	1080	891
CCPP 7	850	562
CCPP 8	1148	462
CCPP 9	458	449
CCPP 10	840	881
	Average	690

The Installed Capacity and Investment Cost of Imported Hard Coal Fired Power Plant Projects

Imported Coal Fired Power Plant	Installed Capacity [MW_{el}]	Specific Investment Cost [$/$kW_{el}$]
IHCPP 1	1320	700
IHCPP 2	2000	2584
IHCPP 3	660	1383
IHCPP 4	1960	1020
IHCPP 5	660	1001
IHCPP 6	1200	1000
IHCPP 7	815	541
IHCPP 8	600	683
IHCPP 9	900	1419
IHCPP 10	1580	1320
	Average	1165

The Installed Capacity and Investment Cost of Lignite Fired Power Plant Projects

Lignite Fired Power Plant	Installed Capacity [MW_{el}]	Specific Investment Cost [$/$kW_{el}$]
LPP 1	300	2388
LPP 2	270	1403
LPP 3	250	823
LPP 4	330	554
LPP 5	150	2000
LPP 6	160	2188
	Average	1559

APPENDIX I

Results for the thermal power plants in the reference scenario

Year	Annualized Capital Cost of Thermal Power Plants [$]							Total
	Nuclear	Lignite	D. Hard Coal	Asphaltite	I. Hard Coal	Natural Gas	Fuel Oil	
2015	0	6,178,951	22,263,910	39,639,770	0	63,601,058	9,786,855	141,470,545
2016	0	6,178,951	40,154,553	39,639,770	0	70,532,809	15,688,851	172,194,934
2017	0	6,178,951	40,154,553	39,639,770	0	113,968,776	16,510,648	216,452,698
2018	0	115,219,267	45,521,745	39,639,770	0	154,073,901	16,510,648	370,965,333
2019	0	115,219,267	45,521,745	39,639,770	0	247,697,540	16,510,648	464,588,971
2020	264,284,721	466,510,819	45,521,745	49,623,120	0	247,697,540	16,510,648	1,090,148,593
2021	528,569,442	817,893,238	45,521,745	59,459,656	0	247,697,540	16,510,648	1,715,652,269
2022	792,854,163	1,169,184,789	45,521,745	69,443,005	0	247,697,540	16,510,648	2,341,211,891
2023	1,057,138,884	1,520,476,341	45,521,745	79,279,541	0	247,697,540	16,510,648	2,966,624,699

Year	Fixed O&M Cost of Thermal Power Plants [$]							Total
	Nuclear	Lignite	D. Hard Coal	Asphaltite	I. Hard Coal	Natural Gas	Fuel Oil	
2015	0	224,190,580	42,998,750	9,043,920	310,049,694	1,154,053,152	290,076,059	2,030,412,155
2016	0	224,190,580	63,785,150	9,043,920	310,049,694	1,159,902,688	319,017,630	2,085,989,662
2017	0	224,190,580	63,785,150	9,043,920	310,049,694	1,196,557,248	323,047,469	2,126,674,061
2018	0	249,008,980	70,021,070	9,043,920	310,049,694	1,230,400,992	323,047,469	2,191,572,125
2019	0	249,008,980	70,021,070	9,043,920	310,049,694	1,309,407,712	323,047,469	2,270,578,845
2020	92,818,800	329,301,920	72,790,830	11,785,716	310,049,694	1,316,396,410	323,695,395	2,456,838,765
2021	185,637,600	409,279,214	75,016,530	13,171,410	310,049,694	1,317,158,094	324,086,129	2,634,398,671
2022	278,456,400	489,235,826	75,016,530	14,577,786	310,049,694	1,321,930,984	324,140,535	2,813,407,755
2023	371,275,200	575,127,638	75,684,240	15,963,480	310,049,694	1,326,337,870	324,140,535	2,998,578,657

Year	Variable O&M Cost of Thermal Power Plants [$]							Total
	Nuclear	Lignite	D. Hard Coal	Asphaltite	I. Hard Coal	Natural Gas	Fuel Oil	
2015	0	111,735,026	18,447,207	5,165,242	124,966,942	233,601,721	0	493,916,137
2016	0	111,735,026	27,722,338	5,165,242	124,966,942	245,514,511	0	515,104,059
2017	0	111,735,026	27,722,338	5,165,242	124,966,942	256,652,554	0	526,242,103
2018	0	127,039,446	30,504,878	5,165,242	124,966,942	268,556,792	0	556,233,301
2019	0	127,039,446	30,504,878	5,165,242	124,966,942	311,885,716	7	599,562,232
2020	50,192,698	176,345,189	30,504,878	6,032,493	124,966,942	242,050,520	0	630,092,719
2021	100,385,395	225,387,957	30,303,344	6,886,989	124,966,942	175,501,147	0	663,431,775
2022	150,578,093	270,772,183	29,543,767	7,754,240	124,966,942	117,015,907	0	700,631,132
2023	200,770,790	308,693,371	27,889,098	8,608,737	124,966,942	71,936,061	0	742,865,000

Year	External Cost of Thermal Power Plants [$] (based on low specific external costs)							Total
	Nuclear	Lignite	D. Hard Coal	Asphaltite	I. Hard Coal	Natural Gas	Fuel Oil	
2015	0	1,980,516,566	202,324,201	91,554,527	1,370,605,175	1,189,558,577	0	4,834,559,046
2016	0	1,980,516,566	304,051,453	91,554,527	1,370,605,175	1,250,221,495	0	4,996,949,216
2017	0	1,980,516,566	304,051,453	91,554,527	1,370,605,175	1,306,939,207	0	5,053,666,929
2018	0	2,251,789,238	334,569,629	91,554,527	1,370,605,175	1,367,558,574	0	5,416,077,143
2019	0	2,251,789,238	334,569,629	91,554,527	1,370,605,175	1,588,200,325	40,954	5,636,759,848
2020	49,322,304	3,125,739,363	334,569,629	106,926,645	1,370,605,175	1,232,581,985	0	6,219,745,101
2021	98,644,608	3,995,028,244	332,359,257	122,072,702	1,370,605,175	893,695,879	0	6,812,405,866
2022	147,966,912	4,799,469,025	324,028,417	137,444,820	1,370,605,175	595,874,360	0	7,375,388,710
2023	197,289,216	5,471,626,579	305,880,428	152,590,878	1,370,605,175	366,316,474	0	7,864,308,750

Year	External Cost of Thermal Power Plants [$] (based on high specific external costs)							Total
	Nuclear	Lignite	D. Hard Coal	Asphaltite	I. Hard Coal	Natural Gas	Fuel Oil	
2015	0	7,319,111,500	662,845,259	299,946,738	4,490,313,752	3,801,402,781	0	16,573,620,029
2016	0	7,319,111,500	996,119,412	299,946,738	4,490,313,752	3,995,259,721	0	17,100,751,122
2017	0	7,319,111,500	996,119,412	299,946,738	4,490,313,752	4,176,509,197	0	17,282,000,598
2018	0	8,321,615,072	1,096,101,658	299,946,738	4,490,313,752	4,370,226,962	0	18,578,204,181
2019	0	8,321,615,072	1,096,101,658	299,946,738	4,490,313,752	5,075,318,902	79,803	19,283,375,924
2020	165,995,940	11,551,347,415	1,096,101,658	350,308,165	4,490,313,752	3,938,890,171	0	21,592,957,102
2021	331,991,881	14,763,853,867	1,088,860,139	399,928,983	4,490,313,752	2,855,931,658	0	23,930,880,280
2022	497,987,821	17,736,710,479	1,061,567,022	450,290,411	4,490,313,752	1,904,200,847	0	26,141,070,333
2023	663,983,762	20,220,706,910	1,002,111,416	499,911,229	4,490,313,752	1,170,616,134	0	28,047,643,203

Results for the renewable energy technologies in the reference scenario

Year	Annualized Capital Cost of Renewable Energy Technologies [$]					Total
	Hydro	Wind	Geothermal	Solar PV	Biomass	
2015	428,150,210	43,184,983	31,335,152	72,602,691	2,061,558	577,334,593
2016	748,811,578	69,208,658	37,817,325	144,267,106	2,628,487	1,002,733,154
2017	1,081,452,619	274,580,297	47,290,566	215,012,012	3,751,008	1,622,086,502
2018	1,224,059,952	286,725,945	47,290,566	284,855,798	3,751,008	1,846,683,270
2019	1,224,059,952	286,725,945	47,290,566	353,816,487	3,751,008	1,915,643,959
2020	1,342,051,520	705,150,744	58,113,289	409,427,611	22,267,155	2,537,010,319
2021	1,460,207,193	1,119,391,777	68,681,021	464,346,098	40,598,163	3,153,224,253
2022	1,578,198,761	1,529,374,212	79,288,392	518,585,801	58,639,134	3,764,086,300
2023	1,696,190,329	1,935,372,809	89,645,846	572,160,296	76,605,402	4,369,974,681

Year	Fixed O&M Cost of Renewable Energy Technologies [$]					Total
	Hydro	Wind	Geothermal	Solar PV	Biomass	
2015	1,397,066,775	193,893,000	66,660,000	15,880,320	9,877,680	1,683,377,775
2016	1,500,970,725	202,141,170	70,567,200	30,152,758	9,938,689	1,813,770,542
2017	1,608,756,450	280,513,441	76,545,810	43,847,946	10,155,679	2,019,819,325
2018	1,654,965,525	282,462,772	75,780,352	56,983,265	10,054,122	2,080,246,035
2019	1,654,965,525	279,638,144	75,022,548	69,575,632	9,953,581	2,089,155,430
2020	1,693,198,350	440,635,534	81,908,773	79,174,323	15,072,698	2,309,989,678
2021	1,731,484,350	598,385,012	88,546,208	88,361,236	20,088,437	2,526,865,243
2022	1,769,717,175	752,889,766	95,145,231	97,149,003	24,972,268	2,739,873,442
2023	1,807,950,000	904,289,801	101,501,916	105,549,914	29,786,199	2,949,077,830

Year	Variable O&M Cost of Renewable Energy Technologies [$]					Total
	Hydro	Wind	Geothermal	Solar PV	Biomass	
2015	709,371	252,208,892	30,906	16,701,440	6,990,754	276,641,362
2016	762,129	264,104,043	33,048	31,712,256	7,034,074	303,645,550
2017	816,858	368,134,720	36,210	46,116,347	7,187,793	422,291,928
2018	840,321	372,355,676	36,210	59,931,981	7,116,062	440,280,250
2019	840,321	370,294,850	36,210	73,176,939	7,045,048	451,393,368
2020	859,734	586,132,943	39,933	83,273,598	10,668,533	680,974,741
2021	879,174	799,601,385	43,605	92,937,453	14,219,001	907,680,617
2022	898,587	1,010,674,516	47,328	102,181,780	17,676,253	1,131,478,463
2023	918,000	1,219,510,457	51,000	111,019,498	21,084,179	1,352,583,134

Year	External Cost of Renewable Energy Technologies [$] (based on low specific external costs)					Total
	Hydro	Wind	Geothermal	Solar PV	Biomass	
2015	92,218,230	12,860,250	18,234,540	3,993,600	8,232,624	135,539,244
2016	99,076,770	13,542,750	19,498,320	7,737,600	8,367,144	148,222,584
2017	106,191,540	18,983,250	21,363,900	11,481,600	8,636,184	166,656,474
2018	109,241,730	19,308,250	21,363,900	15,225,600	8,636,184	173,775,664
2019	109,241,730	19,308,250	21,363,900	18,969,600	8,636,184	177,519,664
2020	111,765,420	30,732,000	23,560,470	22,027,200	13,209,864	201,294,954
2021	114,292,620	42,155,750	25,726,950	25,084,800	17,783,544	225,043,664
2022	116,816,310	53,576,250	27,923,520	28,142,400	22,330,320	248,788,800
2023	119,340,000	65,000,000	30,090,000	31,200,000	26,904,000	272,534,000

Year	External Cost of Renewable Energy Technologies [$] (based on high specific external costs)					Total
	Hydro	Wind	Geothermal	Solar PV	Biomass	
2015	91,204,539	53,419,322	37,351,984	18,563,595	31,754,301	232,293,741
2016	97,987,688	56,254,312	39,940,735	35,966,966	32,273,162	262,422,864
2017	105,024,250	78,853,237	43,762,226	53,370,336	33,310,884	314,320,933
2018	108,040,911	80,203,233	43,762,226	70,773,707	33,310,884	336,090,961
2019	108,040,911	80,203,233	43,762,226	88,177,078	33,310,884	353,494,331
2020	110,536,860	127,655,574	48,261,722	102,389,830	50,952,163	439,796,149
2021	113,036,280	175,107,916	52,699,581	116,602,583	68,593,441	526,039,802
2022	115,532,229	222,546,758	57,199,078	130,815,335	86,130,947	612,224,348
2023	118,028,178	269,999,100	61,636,937	145,028,088	103,772,226	698,464,529

Results for the thermal power plants in the green scenario

Year	Annualized Capital Cost of Thermal Power Plants [$]							Total
	Nuclear	Lignite	D. Hard Coal	Asphaltite	I. Hard Coal	Natural Gas	Fuel Oil	
2015	0	6,178,951	22,263,910	39,639,770	0	63,601,058	9,786,855	141,470,545
2016	0	6,178,951	40,154,553	39,639,770	0	70,532,809	15,688,851	172,194,934
2017	0	6,178,951	40,154,553	39,639,770	0	113,968,776	16,510,648	216,452,698
2018	0	115,219,267	45,521,745	39,639,770	0	154,073,901	16,510,648	370,965,333
2019	0	115,219,267	45,521,745	39,639,770	0	247,697,540	16,510,648	464,588,971
2020	264,284,721	115,219,267	45,521,745	39,639,770	0	247,697,540	16,510,648	728,873,692
2021	528,569,442	115,219,267	45,521,745	39,639,770	0	247,697,540	16,510,648	993,158,413
2022	792,854,163	115,219,267	45,521,745	39,639,770	0	247,697,540	16,510,648	1,257,443,134
2023	1,057,138,884	115,219,267	45,521,745	39,639,770	0	247,697,540	16,510,648	1,521,727,855

Year	Fixed O&M Cost of Thermal Power Plants [$]							Total
	Nuclear	Lignite	D. Hard Coal	Asphaltite	I. Hard Coal	Natural Gas	Fuel Oil	
2015	0	224,190,580	42,998,750	9,043,920	310,049,694	1,154,053,152	290,076,059	2,030,412,155
2016	0	224,190,580	63,785,150	9,043,920	310,049,694	1,159,902,688	319,017,630	2,085,989,662
2017	0	224,190,580	63,785,150	9,043,920	310,049,694	1,196,557,248	323,047,469	2,126,674,061
2018	0	249,008,980	70,021,070	9,043,920	310,049,694	1,230,400,992	323,047,469	2,191,572,125
2019	0	249,008,980	70,021,070	9,043,920	310,049,694	1,309,407,712	323,047,469	2,270,578,845
2020	92,818,800	249,345,308	72,790,830	10,379,340	310,049,694	1,316,396,410	323,695,395	2,375,475,777
2021	185,637,600	249,345,308	75,016,530	10,379,340	310,049,694	1,317,158,094	324,086,129	2,471,672,695
2022	278,456,400	249,345,308	75,016,530	10,379,340	310,049,694	1,321,930,984	324,140,535	2,569,318,791
2023	371,275,200	255,280,508	75,684,240	10,379,340	310,049,694	1,326,337,870	324,140,535	2,673,147,387

Year	Variable O&M Cost of Thermal Power Plants [$]							Total
	Nuclear	Lignite	D. Hard Coal	Asphaltite	I. Hard Coal	Natural Gas	Fuel Oil	
2015	0	111,735,026	18,447,207	5,165,242	124,966,942	233,601,721	0	493,916,137
2016	0	111,735,026	27,722,338	5,165,242	124,966,942	245,514,511	0	515,104,059
2017	0	111,735,026	27,722,338	5,165,242	124,966,942	256,652,554	0	526,242,103
2018	0	127,039,446	30,504,878	5,165,242	124,966,942	268,556,792	0	556,233,301
2019	0	127,039,446	30,504,878	5,165,242	124,966,942	311,885,716	7	599,562,232
2020	50,192,698	127,039,446	30,504,878	5,165,242	124,966,942	282,611,663	0	620,480,870
2021	100,385,395	127,039,446	30,504,878	5,165,242	124,966,942	256,120,196	0	644,182,099
2022	150,578,093	127,039,446	30,504,878	5,165,242	124,966,942	232,540,417	0	670,795,019
2023	200,770,790	127,039,446	30,504,878	5,165,242	124,966,942	210,897,965	0	699,345,264

Year	Fuel Cost of Thermal Power Plants [$]							Total
	Nuclear	Lignite	D. Hard Coal	Asphaltite	I. Hard Coal	Natural Gas	Fuel Oil	
2015	0	2,079,086,403	228,611,164	30,622,728	939,909,818	5,020,487,003	0	8,298,717,115
2016	0	1,791,624,296	284,553,685	30,622,728	810,136,747	5,339,402,413	0	8,256,339,869
2017	0	1,858,475,949	295,074,156	30,622,728	840,375,132	5,707,746,316	0	8,732,294,281
2018	0	2,141,594,834	334,883,577	30,622,728	873,133,383	6,019,501,086	0	9,399,735,608
2019	0	2,223,108,824	347,469,071	30,622,728	905,891,634	7,126,904,820	100,273	10,634,097,350
2020	67,673,102	2,312,033,177	361,148,956	30,622,728	941,169,751	6,607,572,135	0	10,320,219,848
2021	135,346,205	2,393,547,167	374,828,840	30,622,728	976,447,867	6,088,750,700	0	9,999,543,508
2022	203,019,307	2,489,881,883	389,055,920	30,622,728	1,014,245,849	5,618,944,000	0	9,745,769,688
2023	270,692,410	2,586,216,599	403,830,196	30,622,728	1,053,303,764	5,177,656,004	0	9,522,321,700

Year	External Cost of Thermal Power Plants [$] (based on low specific external costs)							Total
	Nuclear	Lignite	D. Hard Coal	Asphaltite	I. Hard Coal	Natural Gas	Fuel Oil	
2015	0	1,980,516,566	202,324,201	91,554,527	1,370,605,175	1,189,558,577	0	4,834,559,046
2016	0	1,980,516,566	304,051,453	91,554,527	1,370,605,175	1,250,221,495	0	4,996,949,216
2017	0	1,980,516,566	304,051,453	91,554,527	1,370,605,175	1,306,939,207	0	5,053,666,929
2018	0	2,251,789,238	334,569,629	91,554,527	1,370,605,175	1,367,558,574	0	5,416,077,143
2019	0	2,251,789,238	334,569,629	91,554,527	1,370,605,175	1,588,200,325	40,954	5,636,759,848
2020	49,322,304	2,251,789,238	334,569,629	91,554,527	1,370,605,175	1,439,129,504	0	5,536,970,377
2021	98,644,608	2,251,789,238	334,569,629	91,554,527	1,370,605,175	1,304,228,302	0	5,451,391,479
2022	147,966,912	2,251,789,238	334,569,629	91,554,527	1,370,605,175	1,184,154,155	0	5,380,639,636
2023	197,289,216	2,251,789,238	334,569,629	91,554,527	1,370,605,175	1,073,945,359	0	5,319,753,144

Year	External Cost of Thermal Power Plants [$] (based on high specific external costs)							Total
	Nuclear	Lignite	D. Hard Coal	Asphaltite	I. Hard Coal	Natural Gas	Fuel Oil	
2015	0	7,319,111,500	662,845,259	299,946,738	4,490,313,752	3,801,402,781	0	16,573,620,029
2016	0	7,319,111,500	996,119,412	299,946,738	4,490,313,752	3,995,259,721	0	17,100,751,122
2017	0	7,319,111,500	996,119,412	299,946,738	4,490,313,752	4,176,509,197	0	17,282,000,598
2018	0	8,321,615,072	1,096,101,658	299,946,738	4,490,313,752	4,370,226,962	0	18,578,204,181
2019	0	8,321,615,072	1,096,101,658	299,946,738	4,490,313,752	5,075,318,902	79,803	19,283,375,924
2020	165,995,940	8,321,615,072	1,096,101,658	299,946,738	4,490,313,752	4,598,941,997	0	18,972,915,157
2021	331,991,881	8,321,615,072	1,096,101,658	299,946,738	4,490,313,752	4,167,846,116	0	18,707,815,216
2022	497,987,821	8,321,615,072	1,096,101,658	299,946,738	4,490,313,752	3,784,132,187	0	18,490,097,228
2023	663,983,762	8,321,615,072	1,096,101,658	299,946,738	4,490,313,752	3,431,944,380	0	18,303,905,362

Results for the renewable energy technologies in the green scenario

Year	Annualized Capital Cost of Renewable Energy Technologies [$]					Total
	Hydro	Wind	Geothermal	Solar PV	Biomass	
2015	428,150,210	43,184,983	31,335,152	72,602,691	2,061,558	577,334,593
2016	748,811,578	69,208,658	37,817,325	144,267,106	2,628,487	1,002,733,154
2017	1,081,452,619	274,580,297	47,290,566	215,012,012	3,751,008	1,622,086,502
2018	1,224,059,952	286,725,945	47,290,566	284,855,798	3,751,008	1,846,683,270
2019	1,224,059,952	286,725,945	47,290,566	353,816,487	3,751,008	1,915,643,959
2020	1,424,104,070	824,190,516	76,645,350	635,390,361	49,496,782	3,009,827,080
2021	1,624,230,242	1,356,222,136	105,559,838	913,513,271	94,731,242	4,094,256,729
2022	1,824,356,413	1,882,934,060	134,330,516	1,188,198,625	139,513,414	5,169,333,028
2023	2,024,400,532	2,404,437,236	162,669,660	1,488,981,147	183,900,664	6,264,389,239

Year	Fixed O&M Cost of Renewable Energy Technologies [$]					Total
	Hydro	Wind	Geothermal	Solar PV	Biomass	
2015	1,397,066,775	193,893,000	66,660,000	15,880,320	9,877,680	1,683,377,775
2016	1,500,970,725	202,141,170	70,567,200	30,152,758	9,938,689	1,813,770,542
2017	1,608,756,450	280,513,441	76,545,810	43,847,946	10,155,679	2,019,819,325
2018	1,654,965,525	282,462,772	75,780,352	56,983,265	10,054,122	2,080,246,035
2019	1,654,965,525	279,638,144	75,022,548	69,575,632	9,953,581	2,089,155,430
2020	1,719,785,850	487,234,046	94,984,886	123,830,436	22,747,187	2,448,582,406
2021	1,784,632,763	690,627,000	114,436,912	175,898,207	35,268,731	2,800,863,613
2022	1,849,479,675	889,903,372	133,592,926	225,833,735	47,537,570	3,146,347,278
2023	1,914,300,000	1,085,147,761	152,252,875	279,390,623	59,572,397	3,490,663,656

Year	Variable O&M Cost of Renewable Energy Technologies [$]					Total
	Hydro	Wind	Geothermal	Solar PV	Biomass	
2015	709,371	252,208,892	30,906	16,701,440	6,990,754	276,641,362
2016	762,129	264,104,043	33,048	31,712,256	7,034,074	303,645,550
2017	816,858	368,134,720	36,210	46,116,347	7,187,793	422,291,928
2018	840,321	372,355,676	36,210	59,931,981	7,116,062	440,280,250
2019	840,321	370,294,850	36,210	73,176,939	7,045,048	451,393,368
2020	873,234	648,118,237	46,308	130,241,794	16,100,576	795,380,150
2021	906,161	922,861,193	56,355	185,007,951	24,963,919	1,133,795,579
2022	939,087	1,194,600,725	66,453	237,532,989	33,648,770	1,466,788,023
2023	972,000	1,463,412,548	76,500	293,868,612	42,168,358	1,800,498,017

Year	External Cost of Renewable Energy Technologies [$] (based on low specific external costs)					Total
	Hydro	Wind	Geothermal	Solar PV	Biomass	
2015	92,218,230	12,860,250	18,234,540	3,993,600	8,232,624	135,539,244
2016	99,076,770	13,542,750	19,498,320	7,737,600	8,367,144	148,222,584
2017	106,191,540	18,983,250	21,363,900	11,481,600	8,636,184	166,656,474
2018	109,241,730	19,308,250	21,363,900	15,225,600	8,636,184	173,775,664
2019	109,241,730	19,308,250	21,363,900	18,969,600	8,636,184	177,519,664
2020	113,520,420	33,982,000	27,321,720	34,451,040	19,935,864	229,211,044
2021	117,800,865	48,654,125	33,249,450	49,935,600	31,222,092	280,862,132
2022	122,081,310	63,326,250	39,207,270	65,420,160	42,508,320	332,543,310
2023	126,360,000	78,000,000	45,135,000	82,586,400	53,808,000	385,889,400

Year	External Cost of Renewable Energy Technologies [$] (based on high specific external costs)					Total
	Hydro	Wind	Geothermal	Solar PV	Biomass	
2015	91,204,539	53,419,322	37,351,984	18,563,595	31,754,301	232,293,741
2016	97,987,688	56,254,312	39,940,735	35,966,966	32,273,162	262,422,864
2017	105,024,250	78,853,237	43,762,226	53,370,336	33,310,884	314,320,933
2018	108,040,911	80,203,233	43,762,226	70,773,707	33,310,884	336,090,961
2019	108,040,911	80,203,233	43,762,226	88,177,078	33,310,884	353,494,331
2020	112,272,569	141,155,529	55,966,339	160,140,015	76,895,219	546,429,671
2021	116,505,962	202,101,076	68,108,816	232,117,455	120,427,668	739,260,976
2022	120,739,355	263,046,623	80,312,929	304,094,895	163,960,116	932,153,919
2023	124,971,012	323,998,920	92,455,406	383,889,349	207,544,451	1,132,859,138

Results for the thermal power plants in the grey scenario

Year	Annualized Capital Cost of Thermal Power Plants [$]							Total
	Nuclear	Lignite	D. Hard Coal	Asphaltite	I. Hard Coal	Natural Gas	Fuel Oil	
2015	0	6,178,951	22,263,910	39,639,770	0	63,601,058	9,786,855	141,470,545
2016	0	6,178,951	40,154,553	39,639,770	0	70,532,809	15,688,851	172,194,934
2017	0	6,178,951	40,154,553	39,639,770	0	113,968,776	16,510,648	216,452,698
2018	0	115,219,267	45,521,745	39,639,770	0	154,073,901	16,510,648	370,965,333
2019	0	115,219,267	45,521,745	39,639,770	0	247,697,540	16,510,648	464,588,971
2020	264,284,721	115,219,267	45,521,745	39,639,770	267,521,852	247,697,540	16,510,648	996,395,544
2021	528,569,442	115,219,267	45,521,745	39,639,770	535,043,704	247,697,540	16,510,648	1,528,202,117
2022	792,854,163	115,219,267	45,521,745	39,639,770	802,565,555	247,697,540	16,510,648	2,060,008,689
2023	1,057,138,884	115,219,267	45,521,745	39,639,770	1,070,087,407	247,697,540	16,510,648	2,591,815,262

Year	Fixed O&M Cost of Thermal Power Plants [$]							Total
	Nuclear	Lignite	D. Hard Coal	Asphaltite	I. Hard Coal	Natural Gas	Fuel Oil	
2015	0	224,190,580	42,998,750	9,043,920	310,049,694	1,154,053,152	290,076,059	2,030,412,155
2016	0	224,190,580	63,785,150	9,043,920	310,049,694	1,159,902,688	319,017,630	2,085,989,662
2017	0	224,190,580	63,785,150	9,043,920	310,049,694	1,196,557,248	323,047,469	2,126,674,061
2018	0	249,008,980	70,021,070	9,043,920	310,049,694	1,230,400,992	323,047,469	2,191,572,125
2019	0	249,008,980	70,021,070	9,043,920	310,049,694	1,309,407,712	323,047,469	2,270,578,845
2020	92,818,800	249,345,308	72,790,830	10,379,340	491,757,474	1,316,396,410	323,695,395	2,557,183,557
2021	185,637,600	249,345,308	75,016,530	10,379,340	673,465,254	1,317,158,094	324,086,129	2,835,088,255
2022	278,456,400	249,345,308	75,016,530	10,379,340	855,173,034	1,321,930,984	324,140,535	3,114,442,131
2023	371,275,200	255,280,508	75,684,240	10,379,340	1,036,880,814	1,326,337,870	324,140,535	3,399,978,507

Year	Variable O&M Cost of Thermal Power Plants [$]							Total
	Nuclear	Lignite	D. Hard Coal	Asphaltite	I. Hard Coal	Natural Gas	Fuel Oil	
2015	0	111,735,026	18,447,207	5,165,242	124,966,942	233,601,721	0	493,916,137
2016	0	111,735,026	27,722,338	5,165,242	124,966,942	245,514,511	0	515,104,059
2017	0	111,735,026	27,722,338	5,165,242	124,966,942	256,652,554	0	526,242,103
2018	0	127,039,446	30,504,878	5,165,242	124,966,942	268,556,792	0	556,233,301
2019	0	127,039,446	30,504,878	5,165,242	124,966,942	311,885,716	7	599,562,232
2020	50,192,698	127,039,446	30,504,878	5,165,242	206,047,053	242,064,478	0	661,013,795
2021	100,385,395	126,764,074	30,303,476	5,165,242	287,127,163	175,521,999	0	725,267,349
2022	150,578,093	122,843,781	29,544,029	5,165,242	368,207,274	117,029,912	0	793,368,331
2023	200,770,790	111,457,648	27,889,098	5,165,242	449,287,384	71,936,061	0	866,506,224

Year	Fuel Cost of Thermal Power Plants [$]							Total
	Nuclear	Lignite	D. Hard Coal	Asphaltite	I. Hard Coal	Natural Gas	Fuel Oil	
2015	0	2,079,086,403	228,611,164	30,622,728	939,909,818	5,020,487,003	0	8,298,717,115
2016	0	1,791,624,296	284,553,685	30,622,728	810,136,747	5,339,402,413	0	8,256,339,869
2017	0	1,858,475,949	295,074,156	30,622,728	840,375,132	5,707,746,316	0	8,732,294,281
2018	0	2,141,594,834	334,883,577	30,622,728	873,133,383	6,019,501,086	0	9,399,735,608
2019	0	2,223,108,824	347,469,071	30,622,728	905,891,634	7,126,904,820	100,273	10,634,097,350
2020	67,673,102	2,312,033,177	361,148,956	30,622,728	1,485,438,217	5,636,264,936	0	9,893,181,116
2021	135,346,205	2,388,216,867	371,728,366	30,622,728	2,105,786,720	4,133,693,301	0	9,165,394,187
2022	203,019,307	2,405,398,942	373,702,763	30,622,728	2,773,828,643	2,786,769,082	0	8,573,341,465
2023	270,692,410	2,260,376,356	361,769,128	30,622,728	3,489,761,264	1,727,331,015	0	8,140,552,900

Year	External Cost of Thermal Power Plants [$] (based on low specific external costs)							Total
	Nuclear	Lignite	D. Hard Coal	Asphaltite	I. Hard Coal	Natural Gas	Fuel Oil	
2015	0	1,980,516,566	202,324,201	91,554,527	1,370,605,175	1,189,558,577	0	4,834,559,046
2016	0	1,980,516,566	304,051,453	91,554,527	1,370,605,175	1,250,221,495	0	4,996,949,216
2017	0	1,980,516,566	304,051,453	91,554,527	1,370,605,175	1,306,939,207	0	5,053,666,929
2018	0	2,251,789,238	334,569,629	91,554,527	1,370,605,175	1,367,558,574	0	5,416,077,143
2019	0	2,251,789,238	334,569,629	91,554,527	1,370,605,175	1,588,200,325	40,954	5,636,759,848
2020	49,322,304	2,251,789,238	334,569,629	91,554,527	2,259,870,903	1,232,653,061	0	6,219,759,662
2021	98,644,608	2,246,908,232	332,360,700	91,554,527	3,149,136,631	893,802,060	0	6,812,406,758
2022	147,966,912	2,177,420,575	324,031,287	91,554,527	4,038,402,359	595,945,679	0	7,375,321,339
2023	197,289,216	1,975,600,018	305,880,428	91,554,527	4,927,668,087	366,316,474	0	7,864,308,750

Year	External Cost of Thermal Power Plants [$] (based on high specific external costs)							Total
	Nuclear	Lignite	D. Hard Coal	Asphaltite	I. Hard Coal	Natural Gas	Fuel Oil	
2015	0	7,319,111,500	662,845,259	299,946,738	4,490,313,752	3,801,402,781	0	16,573,620,029
2016	0	7,319,111,500	996,119,412	299,946,738	4,490,313,752	3,995,259,721	0	17,100,751,122
2017	0	7,319,111,500	996,119,412	299,946,738	4,490,313,752	4,176,509,197	0	17,282,000,598
2018	0	8,321,615,072	1,096,101,658	299,946,738	4,490,313,752	4,370,226,962	0	18,578,204,181
2019	0	8,321,615,072	1,096,101,658	299,946,738	4,490,313,752	5,075,318,902	79,803	19,283,375,924
2020	165,995,940	8,321,615,072	1,096,101,658	299,946,738	7,403,685,304	3,939,117,304	0	21,226,462,016
2021	331,991,881	8,303,577,035	1,088,864,868	299,946,738	10,317,056,857	2,856,270,976	0	23,197,708,354
2022	497,987,821	8,046,781,452	1,061,576,428	299,946,738	13,230,428,409	1,904,428,755	0	25,041,149,603
2023	663,983,762	7,300,942,118	1,002,111,416	299,946,738	16,143,799,961	1,170,616,134	0	26,581,400,129

Results for the renewable energy technologies in the grey scenario

Year	Annualized Capital Cost of Renewable Energy Power Plants [$]					Total
	Hydro	Wind	Geothermal	Solar PV	Biomass	
2015	428,150,210	43,184,983	31,335,152	72,602,691	2,061,558	577,334,593
2016	748,811,578	69,208,658	37,817,325	144,267,106	2,628,487	1,002,733,154
2017	1,081,452,619	274,580,297	47,290,566	215,012,012	3,751,008	1,622,086,502
2018	1,224,059,952	286,725,945	47,290,566	284,855,798	3,751,008	1,846,683,270
2019	1,224,059,952	286,725,945	47,290,566	353,816,487	3,751,008	1,915,643,959
2020	1,342,092,546	705,120,984	58,039,161	409,427,611	22,239,925	2,536,920,227
2021	1,460,125,140	1,119,332,555	68,680,280	464,346,098	40,543,976	3,153,028,050
2022	1,578,157,734	1,529,402,493	79,214,998	518,585,801	58,665,010	3,764,026,037
2023	1,696,190,329	1,935,372,213	89,644,378	572,160,296	76,604,857	4,369,972,074

Year	Fixed O&M Cost of Renewable Energy Power Plants [$]					Total
	Hydro	Wind	Geothermal	Solar PV	Biomass	
2015	1,397,066,775	193,893,000	66,660,000	15,880,320	9,877,680	1,683,377,775
2016	1,500,970,725	202,141,170	70,567,200	30,152,758	9,938,689	1,813,770,542
2017	1,608,756,450	280,513,441	76,545,810	43,847,946	10,155,679	2,019,819,325
2018	1,654,965,525	282,462,772	75,780,352	56,983,265	10,054,122	2,080,246,035
2019	1,654,965,525	279,638,144	75,022,548	69,575,632	9,953,581	2,089,155,430
2020	1,693,211,644	440,623,884	81,856,469	79,174,323	15,065,023	2,309,931,343
2021	1,731,457,763	598,361,946	88,546,208	88,361,236	20,073,242	2,526,800,394
2022	1,769,703,881	752,901,184	95,093,967	97,149,003	24,979,789	2,739,827,824
2023	1,807,950,000	904,289,801	101,501,916	105,549,914	29,786,199	2,949,077,830

Year	Variable O&M Cost of Renewable Energy Power Plants [$]					Total
	Hydro	Wind	Geothermal	Solar PV	Biomass	
2015	709,371	252,208,892	30,906	16,701,440	6,990,754	276,641,362
2016	762,129	264,104,043	33,048	31,712,256	7,034,074	303,645,550
2017	816,858	368,134,720	36,210	46,116,347	7,187,793	422,291,928
2018	840,321	372,355,676	36,210	59,931,981	7,116,062	440,280,250
2019	840,321	370,294,850	36,210	73,176,939	7,045,048	451,393,368
2020	859,741	586,117,446	39,908	83,273,598	10,663,101	680,953,794
2021	879,161	799,570,563	43,605	92,937,453	14,208,245	907,639,026
2022	898,580	1,010,689,843	47,303	102,181,780	17,681,577	1,131,499,083
2023	918,000	1,219,510,457	51,000	111,019,498	21,084,179	1,352,583,134

Year	External Cost of Renewable Energy Power Plants [$] (based on low specific external costs)					Total
	Hydro	Wind	Geothermal	Solar PV	Biomass	
2015	92,218,230	12,860,250	18,234,540	3,993,600	8,232,624	135,539,244
2016	99,076,770	13,542,750	19,498,320	7,737,600	8,367,144	148,222,584
2017	106,191,540	18,983,250	21,363,900	11,481,600	8,636,184	166,656,474
2018	109,241,730	19,308,250	21,363,900	15,225,600	8,636,184	173,775,664
2019	109,241,730	19,308,250	21,363,900	18,969,600	8,636,184	177,519,664
2020	111,766,298	30,731,188	23,545,425	22,027,200	13,203,138	201,273,248
2021	114,290,865	42,154,125	25,726,950	25,084,800	17,770,092	225,026,832
2022	116,815,433	53,577,063	27,908,475	28,142,400	22,337,046	248,780,416
2023	119,340,000	65,000,000	30,090,000	31,200,000	26,904,000	272,534,000

Year	External Cost of Renewable Energy Power Plants [$] (based on high specific external costs)					Total
	Hydro	Wind	Geothermal	Solar PV	Biomass	
2015	91,204,539	53,419,322	37,351,984	18,563,595	31,754,301	232,293,741
2016	97,987,688	56,254,312	39,940,735	35,966,966	32,273,162	262,422,864
2017	105,024,250	78,853,237	43,762,226	53,370,336	33,310,884	314,320,933
2018	108,040,911	80,203,233	43,762,226	70,773,707	33,310,884	336,090,961
2019	108,040,911	80,203,233	43,762,226	88,177,078	33,310,884	353,494,331
2020	110,537,728	127,652,199	48,230,904	102,389,830	50,926,220	439,736,881
2021	113,034,545	175,101,166	52,699,581	116,602,583	68,541,555	525,979,430
2022	115,531,361	222,550,133	57,168,259	130,815,335	86,156,890	612,221,980
2023	118,028,178	269,999,100	61,636,937	145,028,088	103,772,226	698,464,529

Results for the thermal power plants in the blue scenario

Year	Annualized Capital Cost of Thermal Power Plants [$]							Total
	Nuclear	Lignite	D. Hard Coal	Asphaltite	I. Hard Coal	Natural Gas	Fuel Oil	
2015	0	6,178,951	22,263,910	39,639,770	0	63,601,058	9,786,855	141,470,545
2016	0	6,178,951	40,154,553	39,639,770	0	70,532,809	15,688,851	172,194,934
2017	0	6,178,951	40,154,553	39,639,770	0	113,968,776	16,510,648	216,452,698
2018	0	115,219,267	45,521,745	39,639,770	0	154,073,901	16,510,648	370,965,333
2019	0	115,219,267	45,521,745	39,639,770	0	247,697,540	16,510,648	464,588,971
2020	264,284,721	115,219,267	45,521,745	39,639,770	0	424,760,996	16,510,648	905,937,148
2021	528,569,442	115,219,267	45,521,745	39,639,770	0	601,824,452	16,510,648	1,347,285,325
2022	792,854,163	115,219,267	45,521,745	39,639,770	0	778,887,908	16,510,648	1,788,633,502
2023	1,057,138,884	115,219,267	45,521,745	39,639,770	0	955,951,364	16,510,648	2,229,981,679

Year	Fixed O&M Cost of Thermal Power Plants [$]							Total
	Nuclear	Lignite	D. Hard Coal	Asphaltite	I. Hard Coal	Natural Gas	Fuel Oil	
2015	0	224,190,580	42,998,750	9,043,920	310,049,694	1,154,053,152	290,076,059	2,030,412,155
2016	0	224,190,580	63,785,150	9,043,920	310,049,694	1,159,902,688	319,017,630	2,085,989,662
2017	0	224,190,580	63,785,150	9,043,920	310,049,694	1,196,557,248	323,047,469	2,126,674,061
2018	0	249,008,980	70,021,070	9,043,920	310,049,694	1,230,400,992	323,047,469	2,191,572,125
2019	0	249,008,980	70,021,070	9,043,920	310,049,694	1,309,407,712	323,047,469	2,270,578,845
2020	92,818,800	249,345,308	72,790,830	10,379,340	310,049,694	1,465,815,970	323,695,395	2,524,895,337
2021	185,637,600	249,345,308	75,016,530	10,379,340	310,049,694	1,615,997,214	324,086,129	2,770,511,815
2022	278,456,400	249,345,308	75,016,530	10,379,340	310,049,694	1,770,189,664	324,140,535	3,017,577,471
2023	371,275,200	255,280,508	75,684,240	10,379,340	310,049,694	1,924,016,110	324,140,535	3,270,825,627

Year	Variable O&M Cost of Thermal Power Plants [$]							Total
	Nuclear	Lignite	D. Hard Coal	Asphaltite	I. Hard Coal	Natural Gas	Fuel Oil	
2015	0	111,735,026	18,447,207	5,165,242	124,966,942	233,601,721	0	493,916,137
2016	0	111,735,026	27,722,338	5,165,242	124,966,942	245,514,511	0	515,104,059
2017	0	111,735,026	27,722,338	5,165,242	124,966,942	256,652,554	0	526,242,103
2018	0	127,039,446	30,504,878	5,165,242	124,966,942	268,556,792	0	556,233,301
2019	0	127,039,446	30,504,878	5,165,242	124,966,942	311,885,716	7	599,562,232
2020	50,192,698	127,039,446	30,504,878	5,165,242	124,966,942	306,500,577	0	644,369,784
2021	100,385,395	127,039,446	30,504,878	5,165,242	124,966,942	303,880,462	0	691,942,366
2022	150,578,093	127,039,446	30,504,878	5,165,242	124,966,942	304,185,858	0	742,440,460
2023	200,770,790	127,039,446	30,504,878	5,165,242	124,966,942	307,589,002	0	796,036,301

Year	Fuel Cost of Thermal Power Plants [$]							Total
	Nuclear	Lignite	D. Hard Coal	Asphaltite	I. Hard Coal	Natural Gas	Fuel Oil	
2015	0	2,079,086,403	228,611,164	30,622,728	939,909,818	5,020,487,003	0	8,298,717,115
2016	0	1,791,624,296	284,553,685	30,622,728	810,136,747	5,339,402,413	0	8,256,339,869
2017	0	1,858,475,949	295,074,156	30,622,728	840,375,132	5,707,746,316	0	8,732,294,281
2018	0	2,141,594,834	334,883,577	30,622,728	873,133,383	6,019,501,086	0	9,399,735,608
2019	0	2,223,108,824	347,469,071	30,622,728	905,891,634	7,126,904,820	100,273	10,634,097,350
2020	67,673,102	2,312,033,177	361,148,956	30,622,728	941,169,751	7,054,968,727	0	10,767,616,440
2021	135,346,205	2,393,547,167	374,828,840	30,622,728	976,447,867	7,015,048,716	0	10,925,841,523
2022	203,019,307	2,489,881,883	389,055,920	30,622,728	1,014,245,849	7,068,565,635	0	11,195,391,323
2023	270,692,410	2,586,216,599	403,830,196	30,622,728	1,053,303,764	7,220,102,504	0	11,564,768,200

Year	External Cost of Thermal Power Plants [$] (based on low specific external costs)							Total
	Nuclear	Lignite	D. Hard Coal	Asphaltite	I. Hard Coal	Natural Gas	Fuel Oil	
2015	0	1,980,516,566	202,324,201	91,554,527	1,370,605,175	1,189,558,577	0	4,834,559,046
2016	0	1,980,516,566	304,051,453	91,554,527	1,370,605,175	1,250,221,495	0	4,996,949,216
2017	0	1,980,516,566	304,051,453	91,554,527	1,370,605,175	1,306,939,207	0	5,053,666,929
2018	0	2,251,789,238	334,569,629	91,554,527	1,370,605,175	1,367,558,574	0	5,416,077,143
2019	0	2,251,789,238	334,569,629	91,554,527	1,370,605,175	1,588,200,325	40,954	5,636,759,848
2020	49,322,304	2,251,789,238	334,569,629	91,554,527	1,370,605,175	1,560,777,848	0	5,658,618,721
2021	98,644,608	2,251,789,238	334,569,629	91,554,527	1,370,605,175	1,547,435,563	0	5,694,598,740
2022	147,966,912	2,251,789,238	334,569,629	91,554,527	1,370,605,175	1,548,990,718	0	5,745,476,199
2023	197,289,216	2,251,789,238	334,569,629	91,554,527	1,370,605,175	1,566,320,377	0	5,812,128,162

Year	External Cost of Thermal Power Plants [$] (based on high specific external costs)							Total
	Nuclear	Lignite	D. Hard Coal	Asphaltite	I. Hard Coal	Natural Gas	Fuel Oil	
2015	0	7,319,111,500	662,845,259	299,946,738	4,490,313,752	3,801,402,781	0	16,573,620,029
2016	0	7,319,111,500	996,119,412	299,946,738	4,490,313,752	3,995,259,721	0	17,100,751,122
2017	0	7,319,111,500	996,119,412	299,946,738	4,490,313,752	4,176,509,197	0	17,282,000,598
2018	0	8,321,615,072	1,096,101,658	299,946,738	4,490,313,752	4,370,226,962	0	18,578,204,181
2019	0	8,321,615,072	1,096,101,658	299,946,738	4,490,313,752	5,075,318,902	79,803	19,283,375,924
2020	165,995,940	8,321,615,072	1,096,101,658	299,946,738	4,490,313,752	4,987,686,498	0	19,361,659,659
2021	331,991,881	8,321,615,072	1,096,101,658	299,946,738	4,490,313,752	4,945,049,336	0	19,485,018,437
2022	497,987,821	8,321,615,072	1,096,101,658	299,946,738	4,490,313,752	4,950,019,055	0	19,655,984,096
2023	663,983,762	8,321,615,072	1,096,101,658	299,946,738	4,490,313,752	5,005,398,434	0	19,877,359,415

Results for the renewable energy technologies in the blue scenario

Year	Annualized Capital Cost of Renewable Energy Power Plants [$]					Total
	Hydro	Wind	Geothermal	Solar PV	Biomass	
2015	428,150,210	43,184,983	31,335,152	72,602,691	2,061,558	577,334,593
2016	748,811,578	69,208,658	37,817,325	144,267,106	2,628,487	1,002,733,154
2017	1,081,452,619	274,580,297	47,290,566	215,012,012	3,751,008	1,622,086,502
2018	1,224,059,952	286,725,945	47,290,566	284,855,798	3,751,008	1,846,683,270
2019	1,224,059,952	286,725,945	47,290,566	353,816,487	3,751,008	1,915,643,959
2020	1,342,092,546	705,120,984	58,039,161	409,427,611	22,239,925	2,536,920,227
2021	1,460,125,140	1,119,332,555	68,680,280	464,346,098	40,543,976	3,153,028,050
2022	1,578,157,734	1,529,402,493	79,214,998	518,585,801	58,665,010	3,764,026,037
2023	1,696,190,329	1,935,372,213	89,644,378	572,160,296	76,604,857	4,369,972,074

Year	Fixed O&M Cost of Renewable Energy Power Plants [$]					Total
	Hydro	Wind	Geothermal	Solar PV	Biomass	
2015	1,397,066,775	193,893,000	66,660,000	15,880,320	9,877,680	1,683,377,775
2016	1,500,970,725	202,141,170	70,567,200	30,152,758	9,938,689	1,813,770,542
2017	1,608,756,450	280,513,441	76,545,810	43,847,946	10,155,679	2,019,819,325
2018	1,654,965,525	282,462,772	75,780,352	56,983,265	10,054,122	2,080,246,035
2019	1,654,965,525	279,638,144	75,022,548	69,575,632	9,953,581	2,089,155,430
2020	1,693,211,644	440,623,884	81,856,469	79,174,323	15,065,023	2,309,931,343
2021	1,731,457,763	598,361,946	88,546,208	88,361,236	20,073,242	2,526,800,394
2022	1,769,703,881	752,901,184	95,093,967	97,149,003	24,979,789	2,739,827,824
2023	1,807,950,000	904,289,801	101,501,916	105,549,914	29,786,199	2,949,077,830

Year	Variable O&M Cost of Renewable Energy Power Plants [$]					Total
	Hydro	Wind	Geothermal	Solar PV	Biomass	
2015	709,371	252,208,892	30,906	16,701,440	6,990,754	276,641,362
2016	762,129	264,104,043	33,048	31,712,256	7,034,074	303,645,550
2017	816,858	368,134,720	36,210	46,116,347	7,187,793	422,291,928
2018	840,321	372,355,676	36,210	59,931,981	7,116,062	440,280,250
2019	840,321	370,294,850	36,210	73,176,939	7,045,048	451,393,368
2020	859,741	586,117,446	39,908	83,273,598	10,663,101	680,953,794
2021	879,161	799,570,563	43,605	92,937,453	14,208,245	907,639,026
2022	898,580	1,010,689,843	47,303	102,181,780	17,681,577	1,131,499,083
2023	918,000	1,219,510,457	51,000	111,019,498	21,084,179	1,352,583,134

Year	External Cost of Renewable Energy Power Plants [$] (based on low specific external costs)					Total
	Hydro	Wind	Geothermal	Solar PV	Biomass	
2015	92,218,230	12,860,250	18,234,540	3,993,600	8,232,624	135,539,244
2016	99,076,770	13,542,750	19,498,320	7,737,600	8,367,144	148,222,584
2017	106,191,540	18,983,250	21,363,900	11,481,600	8,636,184	166,656,474
2018	109,241,730	19,308,250	21,363,900	15,225,600	8,636,184	173,775,664
2019	109,241,730	19,308,250	21,363,900	18,969,600	8,636,184	177,519,664
2020	111,766,298	30,731,188	23,545,425	22,027,200	13,203,138	201,273,248
2021	114,290,865	42,154,125	25,726,950	25,084,800	17,770,092	225,026,832
2022	116,815,433	53,577,063	27,908,475	28,142,400	22,337,046	248,780,416
2023	119,340,000	65,000,000	30,090,000	31,200,000	26,904,000	272,534,000

Year	External Cost of Renewable Energy Power Plants [$] (based on high specific external costs)					Total
	Hydro	Wind	Geothermal	Solar PV	Biomass	
2015	91,204,539	53,419,322	37,351,984	18,563,595	31,754,301	232,293,741
2016	97,987,688	56,254,312	39,940,735	35,966,966	32,273,162	262,422,864
2017	105,024,250	78,853,237	43,762,226	53,370,336	33,310,884	314,320,933
2018	108,040,911	80,203,233	43,762,226	70,773,707	33,310,884	336,090,961
2019	108,040,911	80,203,233	43,762,226	88,177,078	33,310,884	353,494,331
2020	110,537,728	127,652,199	48,230,904	102,389,830	50,926,220	439,736,881
2021	113,034,545	175,101,166	52,699,581	116,602,583	68,541,555	525,979,430
2022	115,531,361	222,550,133	57,168,259	130,815,335	86,156,890	612,221,980
2023	118,028,178	269,999,100	61,636,937	145,028,088	103,772,226	698,464,529

Results for the thermal power plants in the blue-grey scenario

Year	Annualized Capital Cost of Thermal Power Plants [$]							Total
	Nuclear	Lignite	D. Hard Coal	Asphaltite	I. Hard Coal	Natural Gas	Fuel Oil	
2015	0	6,178,951	22,263,910	39,639,770	0	63,601,058	9,786,855	141,470,545
2016	0	6,178,951	40,154,553	39,639,770	0	70,532,809	15,688,851	172,194,934
2017	0	6,178,951	40,154,553	39,639,770	0	113,968,776	16,510,648	216,452,698
2018	0	115,219,267	45,521,745	39,639,770	0	154,073,901	16,510,648	370,965,333
2019	0	115,219,267	45,521,745	39,639,770	0	247,697,540	16,510,648	464,588,971
2020	264,284,721	115,219,267	45,521,745	39,639,770	267,521,852	471,235,230	16,510,648	1,219,933,234
2021	528,569,442	115,219,267	45,521,745	39,639,770	535,043,704	694,772,920	16,510,648	1,975,277,497
2022	792,854,163	115,219,267	45,521,745	39,639,770	802,565,555	918,310,610	16,510,648	2,730,621,760
2023	1,057,138,884	115,219,267	45,521,745	39,639,770	1,070,087,407	1,141,848,301	16,510,648	3,485,966,023

Year	Fixed O&M Cost of Thermal Power Plants [$]							Total
	Nuclear	Lignite	D. Hard Coal	Asphaltite	I. Hard Coal	Natural Gas	Fuel Oil	
2015	0	224,190,580	42,998,750	9,043,920	310,049,694	1,154,053,152	290,076,059	2,030,412,155
2016	0	224,190,580	63,785,150	9,043,920	310,049,694	1,159,902,688	319,017,630	2,085,989,662
2017	0	224,190,580	63,785,150	9,043,920	310,049,694	1,196,557,248	323,047,469	2,126,674,061
2018	0	249,008,980	70,021,070	9,043,920	310,049,694	1,230,400,992	323,047,469	2,191,572,125
2019	0	249,008,980	70,021,070	9,043,920	310,049,694	1,309,407,712	323,047,469	2,270,578,845
2020	92,818,800	249,345,308	72,790,830	10,379,340	491,757,474	1,505,034,450	323,695,395	2,745,821,597
2021	185,637,600	249,345,308	75,016,530	10,379,340	673,465,254	1,694,434,174	324,086,129	3,212,364,335
2022	278,456,400	249,345,308	75,016,530	10,379,340	855,173,034	1,887,845,104	324,140,535	3,680,356,251
2023	371,275,200	255,280,508	75,684,240	10,379,340	1,036,880,814	2,080,890,030	324,140,535	4,154,530,667

Year	Variable O&M Cost of Thermal Power Plants [$]							Total
	Nuclear	Lignite	D. Hard Coal	Asphaltite	I. Hard Coal	Natural Gas	Fuel Oil	
2015	0	111,735,026	18,447,207	5,165,242	124,966,942	233,601,721	0	493,916,137
2016	0	111,735,026	27,722,338	5,165,242	124,966,942	245,514,511	0	515,104,059
2017	0	111,735,026	27,722,338	5,165,242	124,966,942	256,652,554	0	526,242,103
2018	0	127,039,446	30,504,878	5,165,242	124,966,942	268,556,792	0	556,233,301
2019	0	127,039,446	30,504,878	5,165,242	124,966,942	311,885,716	7	599,562,232
2020	50,192,698	127,039,446	30,504,878	5,165,242	206,047,053	276,357,637	0	695,306,953
2021	100,385,395	127,039,446	30,504,878	5,165,242	287,127,163	243,594,574	0	793,816,699
2022	150,578,093	126,785,759	30,330,719	5,165,242	368,207,274	214,221,262	0	895,288,349
2023	200,770,790	125,350,655	30,045,201	5,165,242	449,287,384	189,551,559	0	1,000,170,832

Year	Fuel Cost of Thermal Power Plants [$]							Total
	Nuclear	Lignite	D. Hard Coal	Asphaltite	I. Hard Coal	Natural Gas	Fuel Oil	
2015	0	2,079,086,403	228,611,164	30,622,728	939,909,818	5,020,487,003	0	8,298,717,115
2016	0	1,791,624,296	284,553,685	30,622,728	810,136,747	5,339,402,413	0	8,256,339,869
2017	0	1,858,475,949	295,074,156	30,622,728	840,375,132	5,707,746,316	0	8,732,294,281
2018	0	2,141,594,834	334,883,577	30,622,728	873,133,383	6,019,501,086	0	9,399,735,608
2019	0	2,223,108,824	347,469,071	30,622,728	905,891,634	7,126,904,820	100,273	10,634,097,350
2020	67,673,102	2,312,033,177	361,148,956	30,622,728	1,485,438,217	6,308,493,106	0	10,565,409,286
2021	135,346,205	2,393,547,167	374,828,840	30,622,728	2,105,786,720	5,548,754,122	0	10,588,885,783
2022	203,019,307	2,484,773,694	386,273,083	30,622,728	2,773,828,643	4,915,269,916	0	10,793,787,371
2023	270,692,410	2,550,895,817	396,206,214	30,622,728	3,489,761,264	4,419,278,385	0	11,157,456,816

Year	External Cost of Thermal Power Plants [$] (based on low specific external costs)							Total
	Nuclear	Lignite	D. Hard Coal	Asphaltite	I. Hard Coal	Natural Gas	Fuel Oil	
2015	0	1,980,516,566	202,324,201	91,554,527	1,370,605,175	1,189,558,577	0	4,834,559,046
2016	0	1,980,516,566	304,051,453	91,554,527	1,370,605,175	1,250,221,495	0	4,996,949,216
2017	0	1,980,516,566	304,051,453	91,554,527	1,370,605,175	1,306,939,207	0	5,053,666,929
2018	0	2,251,789,238	334,569,629	91,554,527	1,370,605,175	1,367,558,574	0	5,416,077,143
2019	0	2,251,789,238	334,569,629	91,554,527	1,370,605,175	1,588,200,325	40,954	5,636,759,848
2020	49,322,304	2,251,789,238	334,569,629	91,554,527	2,259,870,903	1,407,282,430	0	6,394,389,031
2021	98,644,608	2,251,789,238	334,569,629	91,554,527	3,149,136,631	1,240,444,694	0	7,166,139,327
2022	147,966,912	2,247,292,600	332,659,501	91,554,527	4,038,402,359	1,090,868,421	0	7,948,744,320
2023	197,289,216	2,221,855,213	329,528,014	91,554,527	4,927,668,087	965,244,102	0	8,733,139,159

Year	External Cost of Thermal Power Plants [$] (based on high specific external costs)							Total
	Nuclear	Lignite	D. Hard Coal	Asphaltite	I. Hard Coal	Natural Gas	Fuel Oil	
2015	0	7,319,111,500	662,845,259	299,946,738	4,490,313,752	3,801,402,781	0	16,573,620,029
2016	0	7,319,111,500	996,119,412	299,946,738	4,490,313,752	3,995,259,721	0	17,100,751,122
2017	0	7,319,111,500	996,119,412	299,946,738	4,490,313,752	4,176,509,197	0	17,282,000,598
2018	0	8,321,615,072	1,096,101,658	299,946,738	4,490,313,752	4,370,226,962	0	18,578,204,181
2019	0	8,321,615,072	1,096,101,658	299,946,738	4,490,313,752	5,075,318,902	79,803	19,283,375,924
2020	165,995,940	8,321,615,072	1,096,101,658	299,946,738	7,403,685,304	4,497,170,165	0	21,784,514,878
2021	331,991,881	8,321,615,072	1,096,101,658	299,946,738	10,317,056,857	3,964,016,570	0	24,330,728,775
2022	497,987,821	8,304,997,492	1,089,843,785	299,946,738	13,230,428,409	3,486,024,421	0	26,909,228,666
2023	663,983,762	8,210,992,183	1,079,584,550	299,946,738	16,143,799,961	3,084,574,132	0	29,482,881,326

Results for the renewable energy technologies in the blue-grey scenario

Year	Annualized Capital Cost of Renewable Energy Power Plants [$]					Total
	Hydro	Wind	Geothermal	Solar PV	Biomass	
2015	428,150,210	43,184,983	31,335,152	72,602,691	2,061,558	577,334,593
2016	748,811,578	69,208,658	37,817,325	144,267,106	2,628,487	1,002,733,154
2017	1,081,452,619	274,580,297	47,290,566	215,012,012	3,751,008	1,622,086,502
2018	1,224,059,952	286,725,945	47,290,566	284,855,798	3,751,008	1,846,683,270
2019	1,224,059,952	286,725,945	47,290,566	353,816,487	3,751,008	1,915,643,959
2020	1,224,059,952	286,725,945	47,290,566	353,816,487	3,751,008	1,915,643,959
2021	1,224,059,952	286,725,945	47,290,566	353,816,487	3,751,008	1,915,643,959
2022	1,224,059,952	286,725,945	47,290,566	353,816,487	3,751,008	1,915,643,959
2023	1,224,059,952	286,725,945	47,290,566	353,816,487	3,751,008	1,915,643,959

Year	Fixed O&M Cost of Renewable Energy Power Plants [$]					Total
	Hydro	Wind	Geothermal	Solar PV	Biomass	
2015	1,397,066,775	193,893,000	66,660,000	15,880,320	9,877,680	1,683,377,775
2016	1,500,970,725	202,141,170	70,567,200	30,152,758	9,938,689	1,813,770,542
2017	1,608,756,450	280,513,441	76,545,810	43,847,946	10,155,679	2,019,819,325
2018	1,654,965,525	282,462,772	75,780,352	56,983,265	10,054,122	2,080,246,035
2019	1,654,965,525	279,638,144	75,022,548	69,575,632	9,953,581	2,089,155,430
2020	1,654,965,525	276,841,762	74,272,323	68,184,120	9,854,045	2,084,117,775
2021	1,654,965,525	274,073,345	73,529,600	66,820,437	9,755,504	2,079,144,411
2022	1,654,965,525	271,332,611	72,794,304	65,484,029	9,657,949	2,074,234,418
2023	1,654,965,525	268,619,285	72,066,361	64,174,348	9,561,370	2,069,386,889

Year	Variable O&M Cost of Renewable Energy Power Plants [$]					Total
	Hydro	Wind	Geothermal	Solar PV	Biomass	
2015	709,371	252,208,892	30,906	16,701,440	6,990,754	276,641,362
2016	762,129	264,104,043	33,048	31,712,256	7,034,074	303,645,550
2017	816,858	368,134,720	36,210	46,116,347	7,187,793	422,291,928
2018	840,321	372,355,676	36,210	59,931,981	7,116,062	440,280,250
2019	840,321	370,294,850	36,210	73,176,939	7,045,048	451,393,368
2020	840,321	368,254,633	36,210	71,714,373	6,974,744	447,820,281
2021	840,321	366,234,818	36,210	70,281,059	6,905,143	444,297,551
2022	840,321	364,235,202	36,210	68,876,410	6,836,237	440,824,380
2023	840,321	362,255,581	36,210	67,499,855	6,768,021	437,399,988

Year	External Cost of Renewable Energy Power Plants [$] (based on low specific external costs)					Total
	Hydro	Wind	Geothermal	Solar PV	Biomass	
2015	92,218,230	12,860,250	18,234,540	3,993,600	8,232,624	135,539,244
2016	99,076,770	13,542,750	19,498,320	7,737,600	8,367,144	148,222,584
2017	106,191,540	18,983,250	21,363,900	11,481,600	8,636,184	166,656,474
2018	109,241,730	19,308,250	21,363,900	15,225,600	8,636,184	173,775,664
2019	109,241,730	19,308,250	21,363,900	18,969,600	8,636,184	177,519,664
2020	109,241,730	19,308,250	21,363,900	18,969,600	8,636,184	177,519,664
2021	109,241,730	19,308,250	21,363,900	18,969,600	8,636,184	177,519,664
2022	109,241,730	19,308,250	21,363,900	18,969,600	8,636,184	177,519,664
2023	109,241,730	19,308,250	21,363,900	18,969,600	8,636,184	177,519,664

Year	External Cost of Renewable Energy Power Plants [$] (based on high specific external costs)					Total
	Hydro	Wind	Geothermal	Solar PV	Biomass	
2015	91,204,539	53,419,322	37,351,984	18,563,595	31,754,301	232,293,741
2016	97,987,688	56,254,312	39,940,735	35,966,966	32,273,162	262,422,864
2017	105,024,250	78,853,237	43,762,226	53,370,336	33,310,884	314,320,933
2018	108,040,911	80,203,233	43,762,226	70,773,707	33,310,884	336,090,961
2019	108,040,911	80,203,233	43,762,226	88,177,078	33,310,884	353,494,331
2020	108,040,911	80,203,233	43,762,226	88,177,078	33,310,884	353,494,331
2021	108,040,911	80,203,233	43,762,226	88,177,078	33,310,884	353,494,331
2022	108,040,911	80,203,233	43,762,226	88,177,078	33,310,884	353,494,331
2023	108,040,911	80,203,233	43,762,226	88,177,078	33,310,884	353,494,331